Nanostructure and Physical Properties of Collagen Biomaterials

Katie Sizeland

2015

Nanostructure and Physical Properties of Collagen Biomaterials

A thesis presented in partial fulfilment of the requirements for the degree of

Doctor of Philosophy

In

Engineering

at Massey University, Manawatu, New Zealand.

Katie Sizeland

2015

Abstract

Collagen is the main structural component of leather, skin, pericardium, and other tissues. All of these biomaterials have a mechanical function and the physical properties are partly a result of the structure of the collagen fibrils. The architecture of the collagen network and how it changes when different chemical and mechanical processes are applied is not fully understood and forms the foundation of this thesis. Synchrotron-based small angle X-ray scattering has been used to quantify aspects of the collagen structure, specifically the orientation index (OI) and D-spacing of the collagen biomaterials investigated. In leather, the nanostructural changes of the collagen network and the strength of the material across a range of different animals, through each stage of the leather-making process, and when model compounds are added or the fat liquor addition is varied has been investigated. Both the D-spacing and fibril orientation were found to change with leather processing. The changes to the thickness of the leather during processing impacts the fibril OI and, once taken into account, the main difference in OI is due to the hydration state of the material with dry materials being less oriented than wet. Model compounds urea, proline, and hydroxyproline were found to increase D-spacing. It was found that as the fat liquor addition is increased, the D-spacing increased. Pure lanolin resulted in a similar increase in D-spacing. The collagen fibril structure and strength of both adult and neonatal pericardium was also investigated. Significant differences were observed with the neonatal tissue having a higher modulus of elasticity and being significantly more aligned than adult pericardium. Neonatal pericardium is advantageously thinner for heart valve applications. This research proves it has the necessary physical properties required. By understanding the hierarchical structure of collagen and its mechanisms for modification when subjected to different chemical and mechanical processes, we gain valuable insight in understanding the performance of leather and skin in biological, medical, and industrial contexts. This will lead to better comprehension of current processes and informs future processing developments.

Acknowledgements

This work has been made possible by a number of people whom I would like to thank.

Thank you to my supervisor and mentor, Professor Richard Haverkamp - without you none of this would have been possible. I greatly appreciate your positive attitude and enthusiastic approach to the projects we have worked on. You inspired me to start my PhD in the first place and you showed me how much fun research can be so thank you.

I would like to thank Mum, Dad, Jacqui, Tom, Nate, and Charlie. Your love and support means the world to me and I couldn't have achieved this without you there every step of the way. Thank you to my friends and everyone who has believed in me and supported me along the way.

I would like to thank the fantastic team on the SAXS/WAXS beamline at the Australian Synchrotron and the ongoing support from Nigel Kirby, Adrian Hawley, and Stephen Mudie. Thanks to you our requests have never been impossible and your knowledge and expertise have been a tremendous help. I am absolutely certain that my PhD and all the research projects I am involved in would not have gone so smoothly without your input. I look forward to continuing to work with you in the future and will continue to try and find any excuse to come back to the synchrotron - it feels like a second home now! Thank you to the New Zealand Synchrotron Group for providing travel funding for the synchrotron trips.

I would like to thank the New Zealand Leather and Shoe Research Association (LASRA) who, supported by the Ministry of Business, Innovation, and Employment on grant number LSRX0801, financially backed this research project. In particular I want to thank Richard Edmonds, Sue Cooper, and Geoff Holmes from LASRA for providing their knowledge and expertise throughout my PhD.

Thank you to Associate Professor Gillian Norris for your input throughout much of this research project.

Table of Contents

List of Figures

List of Tables

LIST OF PUBLICATIONS

Journal Articles

Sizeland, K. H., Edmonds, R. L., Basil-Jones, M. M., Kirby, N., Hawley A., Mudie S. T., & Haverkamp R. G. (2015). Changes to Collagen Structure during Leather Processing. *Journal of Agricultural and Food Chemistry,* 63(9), 2499-2505.

Wells H. C., **Sizeland K. H.,** Kirby N., Hawley A., Mudie S. T., & Haverkamp R. G. (2015). Collagen Fibril Structure and Strength in Acellular Dermal Matrix Materials of Bovine, Porcine, and Human Origin. *ACS Biomaterials*, 1, 1026-1038.

Sizeland K. H., Holmes. G., Edmonds R. L., Kirby N., Hawley A., Mudie, S., & Haverkamp, R. G. (2015). Fatliquor Effects on Collagen Fibril Orientation and D-spacing During Tensile Strain. *Journal of the American Leather Chemists Association*, 110, 355-362.

Kayed H. R., **Sizeland K. H.**, Kirby N., Hawley A., Mudie S. T., & Haverkamp R. G. (2015). Collagen Cross Linking and Fibril Alignment in Pericardium. *RSC Advances,* 5(5), 3611-8.

Wells H. C., **Sizeland K. H.**, Kayed H. R., Kirby N., Hawley A., Mudie S. T., & Haverkamp R. G. (2015). Poisson's Ratio of Collagen Fibrils Measured by Small Angle X-ray Scattering of Strained Bovine Pericardium. *Journal of Applied Physics*, 117(4).

Sizeland K. H., Wells H. C., Norris G. E., Edmonds R. L., Kirby N., Hawley A., Mudie, S., & Haverkamp, R. G. (2015). Collagen D-spacing and the Effect of Fat Liquor Addition. *Journal of the American Leather Chemists Association*, 110(3), 66-71.

Wells, H. C., **Sizeland, K. H.**, Edmonds, R. L., Aitkenhead, W., Kappen, P., Glover, C., Johannessen, B. & Haverkamp, R. G. (2014). Stabilizing Chromium from Leather

Waste in Biochar. *ACS Sustainable Chemistry & Engineering, 2*(7), 1864-1870.

Sizeland, K. H., Wells, H. C., Higgins, J., Cunanan, C. M., Kirby, N., Hawley, A., Mudie, S. T., & Haverkamp, R. G. (2014). Age Dependant Differences in Collagen Alignment of Glutaraldehyde Fixed Bovine Pericardium. *BioMed Research International*.

Sizeland, K. H., Wells, H. C., Basil-Jones, M. M., Edmonds, R. L., & Haverkamp, R. G. (2014). Leather Nanostructure and Performance. *International Leather Maker*, 30-34.

Sizeland, K. H., Basil-Jones, M. M., Edmonds, R. L., Cooper, S. M., Kirby, N. (2013) Collagen Orientation and Leather Strength for Selected Mammals. *Journal of Agricultural and Food Chemistry,* 61, 887-892.

Conference Papers

Sizeland, K. H., Edmonds, R. L., Norris, G. E., Kirby, N., Hawley, A., Mudie, S., & Haverkamp, R. G. (2014). "Modification of collagen d-spacing in skin", *Proceedings of the 28th International Federation of the Societies of Cosmetic Chemists Congress,* (pp. 1222-1235), Palais des Congrès, Paris, France, 27th-30th October, 2014.

Sizeland, K. H., Wells, H. C., Norris, G., Edmonds, R. L. & Haverkamp, R. G. "Collagen D-spacing Modification by Fat Liquor Addition". *Proceedings of the 65th Leather and Shoe Research Association Conference,* Wellington, New Zealand, 13th-14th August, 2014.

Wells, H., **Sizeland, K. H.**, Edmonds, R. L., Aitkenhead, W., Kappen, P., Glover, C., Johannessen, B., & Haverkamp, R. G. 2014. "Biochar and Other Solid Waste Minimisation Options". *Proceedings of the 65th Leather and Shoe Research Association Conference,* Wellington, New Zealand, 13th-14th August, 2014.

Sizeland, K. H., Basil-Jones, M. M., Norris, G. E., Edmonds, R. L. Kirby, N., Hawley, A., & Haverkamp, R. G. "Collagen Alignment and Leather Strength", *Proceedings of*

the International Union of Leather Technologists and Chemists Societies XXXII Congress, (Paper 110), Istanbul, Turkey, 29th-31st May, 2013.

Haverkamp, R. G., Basil-Jones, M. M., **Sizeland, K. H.**, & Edmonds, R. L. "Synchrotron Studies of Leather Structure", *Proceedings of the International Union of Leather Technologists and Chemists Societies XXXII Congress,* (Paper 109), Istanbul, Turkey, 29th-31st May, 2013.

Sizeland, K. H., Basil-Jones, M. M., Edmonds, R. L., & Haverkamp, R. G. "Implications of Synchrotron Analysis for Leather Manufacturing", *Proceedings of the 63rd Annual Leather and Shoe Research Association conference,* (pp. 28-37), Wellington, New Zealand, 16th-17th August, 2012.

Conference Presentations and Posters

Haverkamp, R. G., **Sizeland, K. H.**, Wells, H. C., Kayed, H. R. "Strength in Collagen Materials." *Poster presented at the Materials Research Society Spring Meeting*, San Francisco, USA, 2015.

Haverkamp, R. G., **Sizeland, K. H.**, Wells, H. C., Kayed, H. R., Edmonds, R. L., Kirby, N., Hawley, A., & Mudie, S. "Orientation of Collagen Fibrils in Tissue." *Symposium presented at the 1st Matrix Biology Europe Conference*, Rotterdam, Netherlands, 2015.

Wells, H. C., **Sizeland, K. H.**, Edmonds, R. L., Kirby, N., Hawley, A., Mudie, S., & Haverkamp, R. G. "Poisson Ratio of Collagen Fibrils." *Poster presented at the 1st Matrix Biology Europe Conference, Rotterdam, Netherlands*, 2015.

Sizeland, K. H., Edmonds, R. L., Kirby, N., Hawley, A., Mudie, S., & Haverkamp, R. G. "Chemical Processing and Leather Strength", *Poster presented at the Fourth International Conference on Multifunctional, Hybrid, and Nanomaterials*, Barcelona, Spain, 9th-13th March, 2015.

Sizeland, K. H., Haverkamp, R. G., Wells, H. C., Kayed, H. R., Edmonds, R. L., Kirby, N., Hawley, A., & Mudie, S. "Strength in Collagen Biomaterials", *Poster presented at the Fourth International Conference on Multifunctional, Hybrid, and Nanomaterials*, Barcelona, Spain, 9th-13th March, 2015.

Wells, H. C., **Sizeland, K. H.**, Kayed, H. R., Kirby, N., Mudie, S., & Haverkamp, R. G. "Poisson Ratio of Collagen Fibrils Measured by SAXS", *Poster presented at the Fourth International Conference on Multifunctional, Hybrid, and Nanomaterials*, Barcelona, Spain, 9th-13th March, 2015.

Sizeland, K. H., Basil-Jones, M. M., Edmonds, R. L., Kirby, N., Hawley, A., Mudie, S., & Haverkamp, R. G. "Changes to the Nanostructure of Collagen in Skin During Leather Processing", *Poster presented at the Australian Synchrotron Users Meeting*, Melbourne, Australia, 20th-21st November, 2014.

Sizeland, K. H., Edmonds, R. L., Norris, G. E., Kirby, N., Hawley, A., Mudie, S., & Haverkamp, R. G. "Modification of Collagen Structure in Skin", *Poster presented at the 28th International Federation of Societies of Cosmetic Chemists*, Palais des Congrès, Paris, France, 27th-30th October, 2014.

Sizeland, K. H., Wells, H., Norris, G. E., Edmonds, R. L., & Haverkamp, R. G. "Collagen D-spacing Modification by Fat Liquor Addition", *Symposium presented at the 65th Annual Leather and Shoe Research Association Conference,* Wellington, New Zealand, 13th-14th August, 2014.

Wells, H., **Sizeland, K. H.**, Edmonds, R. L., Aitkenhead, W., Kappen, P., Glover, C., Johannessen, B., & Haverkamp, R. G. "Biochar and Other Solid Waste Minimisation Options", *Symposium presented at the 65th Annual Leather and Shoe Research Association Conference*, Wellington, New Zealand, 13th-14th August, 2014.

Sizeland, K. H., Edmonds, R. L., Norris, G. E., Kirby, N., Hawley, A., Mudie, S. & Haverkamp, R. G. "Effects of Model Compounds on the Nanostructure of Skin", *Poster presented at the 65th Annual Leather and Shoe Research Association Conference*, Wellington, New Zealand, 13th-14th August, 2014.

Wells, H. C., **Sizeland, K. H.**, Edmonds, R. L., Kirby, N., Hawley, A., Mudie, S., & Haverkamp, R. G. "Poisson Ratio of Collagen Fibrils", *Poster presented at the 1st*

Matrix Biology Europe conference (XXIVth FECTS meeting), Rotterdam, Netherlands, 21st-24th June, 2014.

Haverkamp, R. G., Wells, H. C., **Sizeland, K. H.**, Edmonds, R. L., Aitkenhead, W., Kappen, P., Glover, C., & Johannessen, B. "Biochar from Leather - the Fate of Chromium", *Symposium conducted at the 117th Society of Leather Technologists and Chemists Annual Conference*, Northampton, United Kingdom, 26th April, 2014.

Sizeland, K. H., Norris, G. E., Edmonds, R. L., Kirby, N., Hawley, A., & Haverkamp, R. G. "Collagen Fibril Axial Periodicity and the Effects of Polyol Addition", *Poster presented at the 12th International Conference on Frontiers of Polymers and Advanced Materials*, Auckland, New Zealand, 8th-13th December, 2013.

Sizeland, K. H., Norris, G. E., Edmonds, R. L. Kirby, N., Hawley, A., & Haverkamp, R. G. "Polyol Modification of Collagen Fibril Axial Periodicity", *Poster presented at the Australian Synchrotron Users Meeting,* Melbourne, Australia, 21st-22nd November, 2013.

Kayed, H. R., **Sizeland, K. H.**, Kirby, N., Hawley, A., Mudie, S., & Haverkamp, R. G. "Cross Linking Collagen Affects Fibril Orientation", *Poster presented at the Australian Synchrotron Users Meeting,* Melbourne, Australia, 21st-22nd November, 2013.

Sizeland, K. H., Basil-Jones, M. M., Norris, G. E., Edmonds, R. L., Kirby, N., Hawley, A., & Haverkamp, R. G. "Collagen Alignment and Leather Strength", *Poster presented at the 64th Annual Leather and Shoe Research Association Conference,* Wellington, New Zealand, 15th-16th August, 2013.

Sizeland, K. H., Basil-Jones, M. M., Norris, G. E., Edmonds, R. L., Kirby, N., Hawley, A., & Haverkamp, R. G. "Collagen Alignment and Leather Strength", *Poster presented at the International Union of Leather Technologists and Chemists Societies XXXII Congress*, Istanbul, Turkey, 28th-31st June, 2013.

Haverkamp, R. G., Basil-Jones, M. M., **Sizeland, K. H.**, & Edmonds, R. L. "Synchrotron Studies of Leather Structure", *Symposium conducted at the International Union of Leather Technologists and Chemists Societies XXXII Congress*, Istanbul, Turkey, 28th-31st June, 2013.

Sizeland, K. H., Basil-Jones, M. M., Edmonds, R. L. & Haverkamp, R. G. "SAXS of Leather Reveals a Structural Basis for Strength", *Poster presented at the Australian Synchrotron Users Meeting,* Melbourne, Australia. 28th-29th November 2012.

Haverkamp, R. G., Basil-Jones, M. M., **Sizeland, K. H.**, & Edmonds, R. L. "SAXS Structural Studies of Collagen Materials", *Symposium conducted at the Australian Synchrotron Users Meeting*, Melbourne, Australia, 28th-29th November, 2012.

Poddar, D., Ainscough, E. W., Freeman, G. H., Ellis, A., Glover, C. J., Johannessen, B., **Sizeland, K. H.**, Singh, H., Haverkamp, R. G., & Jameson, G. "Preliminary characterization by XAS of Mn hyperaccumulated by probiotic Lactobacillus sp.", *Poster presented at the Australian Synchrotron Users Meeting,* Melbourne, Australia. 28th-29th November, 2012.

Haverkamp, R. G., Basil-Jones, M. M., **Sizeland, K. H.**, & Edmonds, R. L. "Implications of Synchrotron Analysis for Leather Manufacturing", *Symposium conducted at 63rd Annual Leather and Shoe Research Association Conference*, Wellington, New Zealand. 16th-17th August, 2012.

Papers I am Acknowledged in

Beattie, I. R., & Haverkamp, R. G. (2011). Silver and gold nanoparticles in plants: sites for the reduction to metal. *Metallomics*, *3*(6), 628-632.

Luangpipat, T., Beattie, I. R., Chisti, Y., & Haverkamp, R. G. (2011). Gold nanoparticles produced in a microalga. *Journal of Nanoparticle Research*, *13*(12), 6439-6445.

Basil-Jones, M. M., Edmonds, R. L., Cooper, S. M., & Haverkamp, R. G. (2011). Collagen fibril orientation in ovine and bovine leather affects strength: A small angle X-ray scattering (SAXS) study. *Journal of agricultural and food chemistry*, *59*(18), 9972-9979.

Basil-Jones, M. M., Edmonds, R. L., Norris, G. E., & Haverkamp, R. G. (2012). Collagen Fibril Alignment and Deformation during Tensile Strain of Leather: A Small-Angle X-ray Scattering Study. *Journal of agricultural and food chemistry*, *60*(5), 1201-1208.

Owe, L. E., Tsypkin, M., Wallwork, K. S., Haverkamp, R. G., & Sunde, S. (2012). Iridium–ruthenium single phase mixed oxides for oxygen evolution: Composition dependence of electrocatalytic activity. *Electrochimica Acta*, *70*, 158-164.

Haverkamp, R. G. (2013). The Australian Synchrotron - A Powerful Tool for Chemical Research Available to New Zealand Scientists. *Chemistry in New Zealand,* ***76***(1).

Chapter 1: Introduction

1.1 A Perspective on the Leather Industry

Leather is a flexible, strong, biomaterial whose complex architecture is physically defined by the hierarchical structure of collagen. Leather is used in a wide variety of manufacturing applications, including shoes, clothing and upholstery (Commodities and Trade Division, 2010), with high strength being a primary requirement for high-value applications. The shoe industry is the number one customer of the leather industry consuming approximately 80% of the total leather made (Thorstensen, 1993, Russell, 1988, Michel, 2004, Chan et al., 2009, Basil-Jones et al., 2011, Rabinovich, 2001). The majority of shoes are produced using bovine leather as it is a strong material. Ovine leather is far weaker than bovine leather and as such is not used for shoe manufacture. If the physical properties of ovine leather could be improved, it would be suitable for shoes and would lead to a boost in the New Zealand economy.

The physical attributes of leather are largely dependent on the structure of collagen fibres and the interactions among them. With multiple levels of structure, collagen has a hierarchical architecture. The collagen molecule is composed of an amino acid sequence that forms an alpha helix with a left handed twist. It is characterized by the repeating amino acid sequence $(Glycine\text{-}X\text{-}Y)^n$ where the X and Y positions are occupied by a high proportion of the amino acids proline and hydroxyproline respectively, with the most common triplet in collagen being Gly-Pro-Hyp, which accounts for about 10% of the total sequence (Ramshaw et al., 1998). Three of these left handed helices twist together in a right hand manner to form a triple helix, or tropocollagen. Collagen fibrils are assembled from multiples of five staggered tropocollagens with gaps between the end of one tropocollagen and the next responsible for the banding of collagen that is visible with atomic force microscopy or transmitting electron microscopy. This periodicity is known

as the D-spacing and provides an insight into the internal structure of collagen fibrils. Many collagen fibrils make up the structure of a complex biomaterial. The arrangement of the collagen fibrils, particularly the extent of alignment, is an important contributor to the strength of collagen materials.

The structure of collagen is difficult to access by microscopic methods and as such a specific technique for nanoscale investigations is required. Synchrotron based technique small angle X-ray scattering (SAXS) provides a brilliant platform for nanostructure analysis and has been used by researchers since the early to mid-1900's to explore and characterise the structure of collagen (summarised by Gustavson (Gustavson, 1956)). The majority of the work presented in this thesis is based on experimental studies completed using SAXS. Imaging techniques (scanning electron microscopy, transmission electron microscopy, and atomic force microscopy) compliment some experiments and tensile and tear tests have been done alongside SAXS to produce in depth nanostructural analysis and visualisation of the collagen biomaterials.

Collagen is also the main structural component of skin (Fratzl, 2008), some extracellular matrix scaffolds (Floden et al., 2010), and processed pericardium for heart valve repair (Jobsis et al., 2007). Like leather, strength is a requirement for these collagen-based medical materials. Heart valve leaflet replacement with bovine pericardium requires high mechanical strength and a long performance life (Mirnajafi et al., 2010). A greater understanding of these materials may enable processes to be altered to maximise the final physical properties.

1.2 Aims and Objectives

The structure of leather and other extracellular matrix materials can tell us a lot about the material and can relate to the physical properties. This research aims to determine the structure of collagen in different materials and how it adapts and changes when subjected to different processes.

This study follows on from the PhD of Dr. Melissa Basil-Jones. Basil-Jones has shown that small angle X–ray scattering (SAXS) can provide detailed structural information on the amount of fibrous collagen, the microfibril orientation, and the D-spacing of collagen in leather (Basil-Jones et al., 2010). A study of ovine and bovine leather of differing strengths (Basil-Jones et al., 2011) found a statistically significant relationship between tear strength and edge on orientation. This work aims to build on this foundation and use SAXS to investigate the nanostructure of different materials and changes that take place when the material is subjected to mechanical and chemical processes.

The first research aim was to determine if the structure-strength relationship found in ovine and bovine leather extends across a range of selected mammals. In Chapter 3 it is shown that this correlation was indeed found to exist across seven species of mammals with the tear strength of the leathers dependent on the degree to which collagen fibrils are aligned in the plane of the tissue. This research has successfully proven the structure-strength relationship exists among different animals and, with the statistical confidence and diversity of animals investigated, it is suggested that this is a fundamental determinant of strength in tissue.

The second aim of this thesis was to explore the modification of the collagen structure by fat liquoring, a step completed in the leather-making process that involves adding penetrating oils (usually polyols) to leather to achieve high strength and a soft, supple feel. While the fat liquoring process has been carried out by tanners for years it is not known how this process changes the nanostructure of the leather. Chapter 4 details the research done on leather processed with varying amounts of fat liquor and the structural changes observed. It has been proven that the fat liquoring process does indeed alter the collagen fibril network. Chapter 7 continues investigating the effect of fat liquor on the collagen structure by analysing leather under tension.

The third aim of my research was to investigate whether compounds chosen because of their opposite effects on protein solubility change the orientation and D-spacing of the collagen fibrils. This aims to provide insight into how variations in the processing of leather can change the structure of the collagen network.

Chapter 6 portrays how the model compounds urea, proline, and hydroxyproline, were analysed using SAXS. It has been shown they modify the structure of the biomaterial with the D-spacing of the collagen fibrils increasing and the orientation index decreasing.

As hides and skins are processed to produce leather, chemical and physical changes take place that affect the strength and other physical properties of the material. The structural basis of these changes at the level of the collagen fibrils is not fully understood and forms the basis of the fourth objective of my research. In Chapter 5 it is shown that both the D-spacing and fibril orientation change with processing. Much of the OI differences between processing stages was found to be accounted for by the changes in the thickness of the leather. Following a correction for the thickness of the leather the main difference in OI was due to the hydration state of the material with dry materials being less oriented than wet. This understanding is useful for relating structural changes that occur during different stages of processing to the development of the final physical characteristics of leather.

In the percutaneous delivery of heart valves, the size of the device when folded for delivery is important, with thicker material folding into a larger diameter device for insertion. Neonatal pericardium is a thinner material than the adult pericardium that is currently in use which would enable smaller devices to be made that can be inserted through smaller arteries. However the strength of the material must be adequate for a long life of service and the physical properties of neonatal pericardium comparative to adult pericardium have not been adequately investigated and formed the final aim of my research. In Chapter 8 the research shows that neonatal tissue has a higher elastic modulus and has significantly more aligned fibrils. As such the superior strength of neonatal compared with adult tissue supports the use of neonatal bovine pericardium in heterografts.

This research has contributed hugely to the knowledge of the structure of collagen biomaterials. A greater understanding has been gained of how collagen changes and reacts to different mechanical and chemical processes.

Chapter 2: Literature Review

Leather is a complex biomaterial produced from skin. The structure of leather and other tissues such as skin and pericardium is composed primarily of collagen. This network of collagen can be responsible for the physical and aesthetic properties of the biomaterial. The relationships between the collagen architecture and the properties of the biomaterial are not fully understood and may change as a result of different chemical and mechanical processes being applied.

2.1 Skin

Skin is the largest organ of the body, both in surface area and in weight. In humans it covers an area of approximately 2 m^2 and weighs about 4.5-5 kg, about 15% of the total body weight. Ovine skins cover an area of 2.1-3 m^2 and weigh approximately 1.25 kg. The thickness of the skin over most of the body is 1-2 mm, but it can range in thickness from 0.5 mm on the eyelids to 4.0 mm on the heels. The skin functions to protect us against the external environment and is largely responsible for preventing external fluids from penetrating and body fluid from escaping. Skin also has a vital role in thermoregulation and provides sensory information about the environment surrounding it. Skin is a remarkable organ that is capable of relaxation and extension to adapt to the near continuous movement of the body. It is soft, pliable, strong, waterproof, and self-repairing. Skin is part of the integumentary system alongside hair, oil, sweat glands, nails, and sensory receptors. In animals horns, hooves, and claws are included in their integumentary systems. It is composed of the epidermis on the outer surface and the dermis or corium layer underneath, with a dermo-epidermal junction in between. Skin cells follow a life cycle that terminates in 30,000 to 40,000 dead skin cells falling from your body every minute. The structure of the layers and the functions of skin are discussed in this chapter section.

2.1.1 The Epidermis

The epidermis is the outermost layer of the skin and is made up of four principal types of cells, 90% of which are keratinocytes which produce the protein keratin. It contains no blood vessels or nerve endings, rather it obtains nutrients via the diffusion of blood vessels through the dermo-epidermal junction. The epidermis feels strong, flexible, soft, and slightly oily. Other notable cells contained in the epidermis alongside keratinocytes are Merkel cells, melanocytes, and Langerhans cells. Merkel cells are related to the sense of touch. First seen by Langerhans and later named after him, Langerhans cells participate in immune responses against microbes that invade the skin by helping other cells recognise the invader and destroy it (Montagna and Parakkal, 1974). Melanocytes produce pigment and are responsible for the colour of skin and hair. The number of melanocytes varies in different parts of the body but on average there is one melanocyte to every ten keratinocytes in the basal layer.

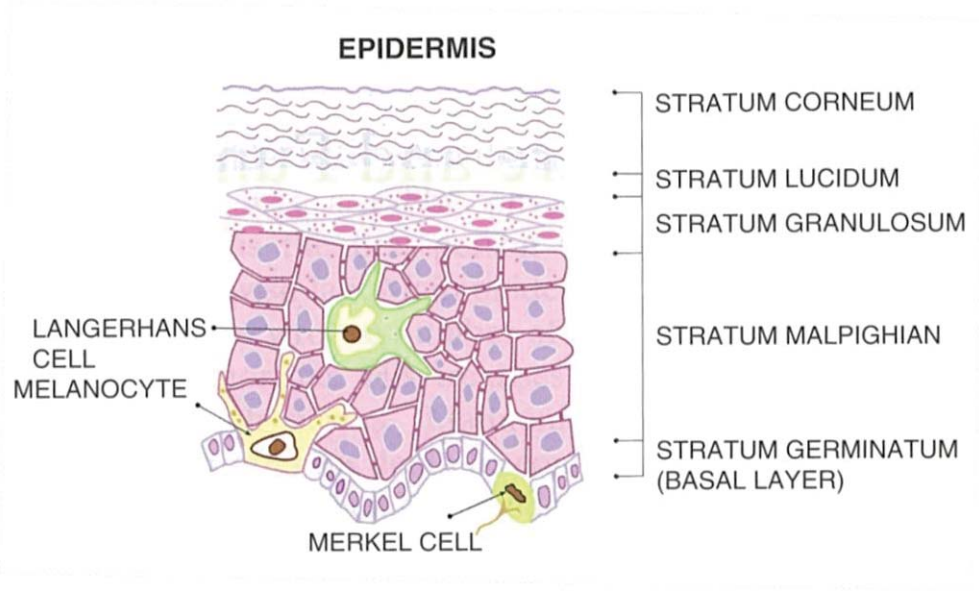

Figure 2.1. Epidermal layers (Zaidi and Lanigan, 2010). Reprinted from Dermatology in Clinical Practice, Z. Zaidi and S. Lanigan, Skin: Structure and Function, pg 2, copyright 2010, with permission from Springer.

The epidermis is comprised of four or five layers, all of which can be seen in Figure 2.1. The four layers of the epidermis of skin found in most parts of the body where skin is thin are as follows, from the surface layer of the skin inward: 1. the *stratum corneum*; 2. the *stratum granulosum*; 3. the *stratum spinosum* or the *stratum malpghian*; and 4. the *stratum basale* (also known as the *stratum germinativum* to indicate its role in forming new cells). In places on the body where friction is experienced the most such as the soles of the feet and the palms of the hands, the skin is thick and there is an additional fifth layer, the *stratum lucidum*. This layer is situated between the stratum corneum and the *stratum granulosum*.

Three processes maintain a healthy epidermis: continuous cell division in the deeper layers with new cells being pushed upwards, effective keratinisation of the cells approaching the surface, and the shedding of keratinised cells from the surface. The entire epidermis is replaced about every six to eight weeks. Histological preparations have shown an ordered structure throughout the epidermis but in particular on the surface layer of the skin, despite the seemingly unorganised rise to the surface of epidermal cells generated in the innermost layer (Christophers, 1971). The cells in the *stratum basale* undergo the mitotic cell division and are then pushed up towards the surface of the skin. With nutrients provided to the cells in the epidermis coming from the dermis, the farther they travel away from the dermis the greater the distance from the nutrients. The cells get flatter, larger, and thinner as they migrate upwards. With the lack of nutrients the cells die and as more cells are continuously divided, the surface layer of the *stratum corneum* is shed and replaced.

The *stratum corneum* is the outermost layer of the skin. It is a dense, relatively hard layer consisting of 25-30 cell layers. The cells have been pushed up from the *stratum granulosum* and are all flattened, dead keratinocytes. The upper layer of cells is shed as more shells are continuously pushed up from the epidermis layers beneath. Cells take approximately 52-75 days to move from the bottom layer of the epidermis, the *stratum basale*, to the top layer of the epidermis, the *stratum corneum*, where they are shed from the skin. The surface layer of the *stratum corneum* is covered with a waxy, waterproof coating of sebum (an oily, fatty

substance) which protects the body by keeping the inner layers hydrated by stopping water loss and stops the entrance of harmful substances into the body.

The second layer from the surface of the skin is the *stratum granulosum*. This layer is composed of diamond-shaped cells that are three to five layers thick. The diamond shape is due to the polyhedral cells moving up from the *stratum spinosum* being flattened a bit. The cells are beginning to die as they are getting farther away from the source of nutrition so this layer is the transition layer between the deeper, active layers below and the layers containing dead cells above.

The *stratum spinosum* is the third layer from the surface of the skin. It is the thickest and strongest layer of the epidermis and consists of 8-10 layers of polyhedral cells that have migrated up from the basal layer. If you try and prepare the skin for microscopic examination these cells will shrink and pull apart. Langerhans cells and the spindles of melanocytes are also present in the *stratum spinosum*.

The basal layer is the innermost layer of the epidermis and is composed of just one layer of cells. It is in this layer that cells undergo division to produce new keratinocytes. The *stratum basale*, dubbed "the cell farm" (Norris and Siegfried, 2011), constantly produces new cells and pushes them up towards the skin surface. A process called keratinisation occurs where the cells accumulate keratin as they move from one epidermal layer to the next. Once the cells are pushed up out of the basal layer they become larger and polyhedral. Alongside the keratinocyte cells, melanocytes and Merkel cells are scattered throughout the basal layer.

The *stratum lucidum* is the extra layer found in thicker skin such as that on the palms of the hands and soles of the feet. This layer, made up of dead, flattened keratinocytes four to six layers thick, lies between the *stratum corneum* and the *stratum granulosum*. This extra layer is thought to add extra toughness to the skin. It is part of the "transit zone" along with the *stratum granulosum* and the *stratum spinosum* that cells pass through before they reach the surface layer of the skin, the *stratum corneum* (Norris and Siegfried, 2011).

2.1.2 The Dermis

The dermis, or the corium, is a tough, elastic, resilient layer of the skin underneath the epidermis. When this layer from animals is dried and treated, it becomes leather (Tortora and Derrickson, 2010). It is several times thicker than the epidermis as shown in Figure 2.2 below and is a matrix of connective tissue that is made up of collagen fibres and elastic fibres embedded in a ground substance (glycosaminoglycans). The collagen fibres are the foundation of the skin's strength and their network imparts remarkable structural integrity and flexibility to the skin. For more on the structure of collagen see section 2.2. Elastic fibres help in the elasticity of the skin and can stretch easily. When the tension is released they resume their original shape. The collagen and elastin fibres are embedded in ground substance which holds water and helps in transporting nutrients, hormones, and fluid molecules through the dermis. The ground substance is a gel containing substances derived from the blood (inorganic ions, blood sugars, blood proteins, water, and urea), proteoglycans, and glycoproteins.

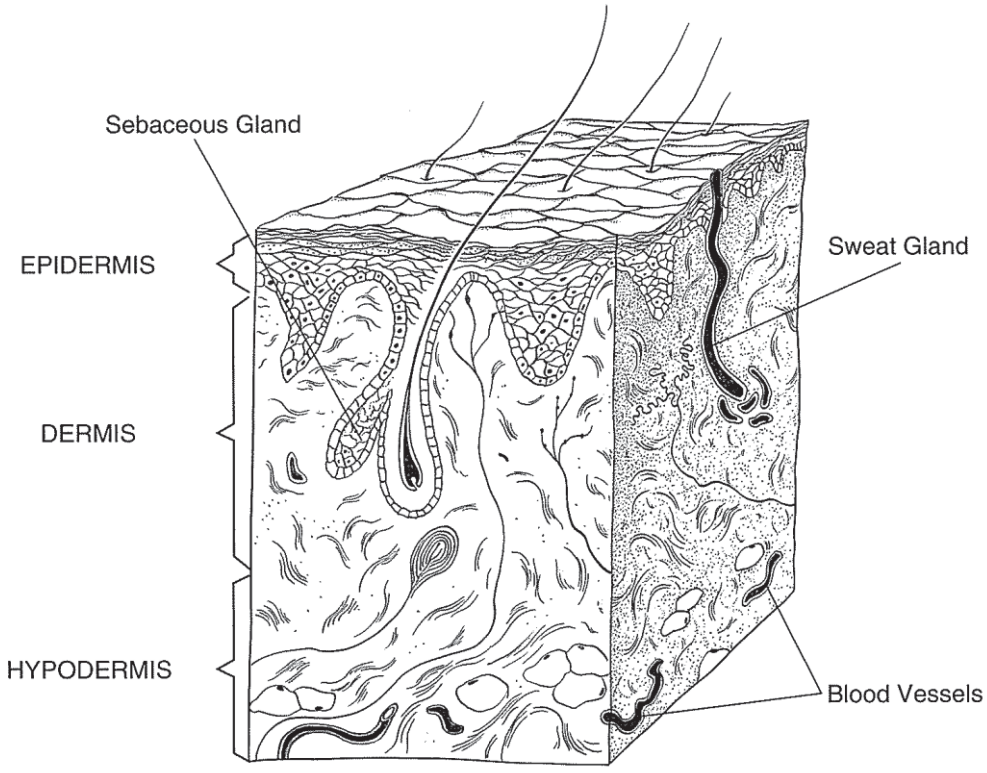

Figure 2.2. Ovine skin anatomy showing the thinner epidermis at the surface and the thicker dermis underneath (Frandson et al., 2013).

The dermis is made up of two parts: the papillary region making up about 20% of the dermis and the reticular region making up approximately 80%. The papillary region acts as the dermo-epidermal junction and the fibres in this dermal region are thin. It provides nutrients to the epidermis and anchors the epidermis to the dermis. The bottom of the epidermis forms an uneven surface with fibres which project downwards into the connective tissue of the dermis. The fibres push into the connective tissue in order to increase the surface area between the epidermis and the dermis so a strong junction is formed between these two layers (Frandson et al., 2013).

The reticular region is a complex and metabolically active layer full of thick, coarse fibres. It functions as the "manufacturing site" as cells and structures in this region produce sebum, hair, nails, and sweat. It is attached to the subcutaneous layer situated underneath the dermis. The collagen fibres in the reticular layer are arranged in a more regular fashion than those in the papillary layer. It is this more regular structure that aids the skin in resisting stretching forces.

Underneath the dermis is the hypodermis or the subcutaneous layer (Figure 2.2). A layer of loose connective tissue and fatty tissue, it enables skin to move without tearing, stores energy, and provides insulation. This hypodermis, or subcutaneous tissue, is known to tanners as flesh by which the skin is connected to the body underneath (Gustavson, 1956).

Sweat glands, hairs, sebaceous glands, arrector pili muscles, blood vessels, lymph vessels, and sensory nerve endings are all structures found in the dermis (all seen in Figure 2.3). Sweat glands are distributed throughout the skin but are more densely found in the soles of the feet, the palms of the hands, the armpits, and the groins. Arrector pili muscles are the smooth muscles in the skin that help in the erection of the hair creating goose bumps that trap warm air near the skin to try and protect against the cold. Blood vessels provide nourishment and can contract when the body needs to retain heat and expand when the body needs to lose heat, shown by a brightening or darkening of the skin's colour. Lymph vessels make up a network throughout the dermis. Sensory nerve endings are found throughout the dermis and transmit sensations such as vibration, warmth, coolness, tickling,

itching, pain, and pressure to the nervous system. Thus the skin is an important organ that relates information about the environment to the body.

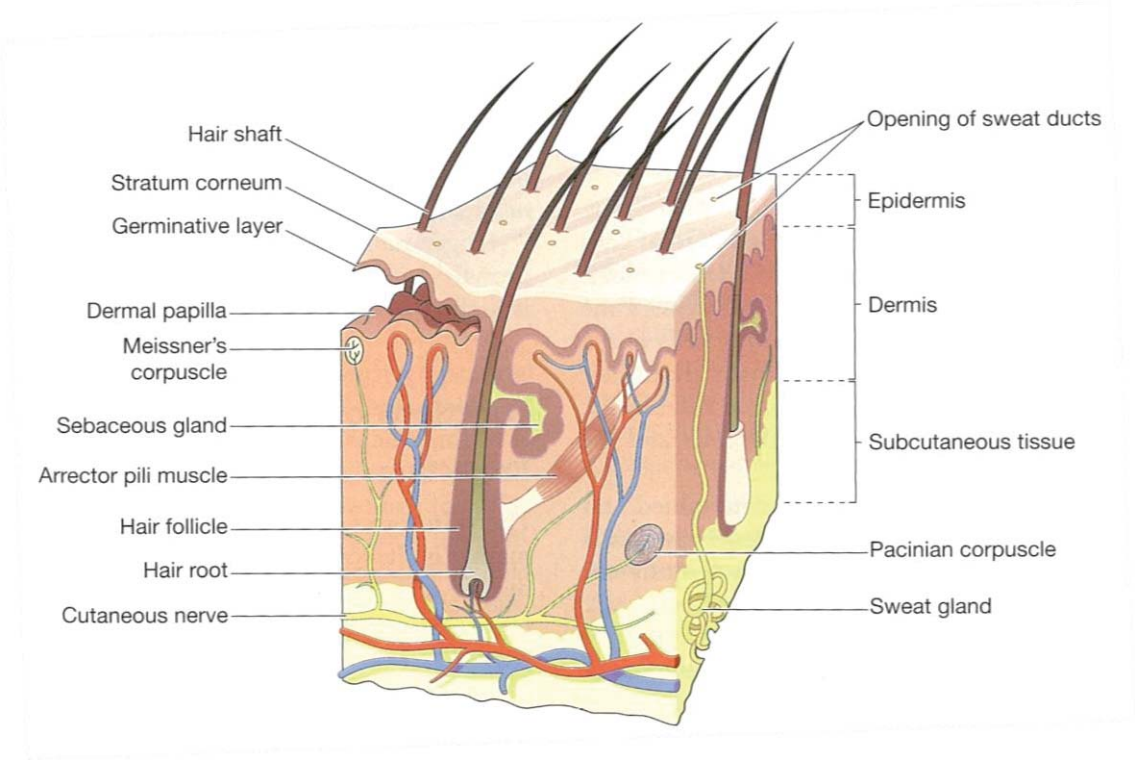

Figure 2.3. Cross section of skin showing the main structures in the dermis (Waugh and Grant, 2006). Reprinted from Ross & Wilson Anatomy and Physiology in Health and Illness, A. Waugh and A. Grant, The Skin, pg 359, copyright 2014, with permission from Elsevier.

The main cells found in the dermis are fibroblasts, macrophages, and mast cells. Fibroblasts are responsible for the formation of the amorphous ground substance and the collagen and elastic fibres. Macrophages take part in the synthesis and degradation of lipids, aid in the protection against viral infection, and dispose of toxic foreign bodies. Mast cells are found throughout the connective tissue and play an important role in the immune system.

2.1.3 Accessory Structures of the Skin

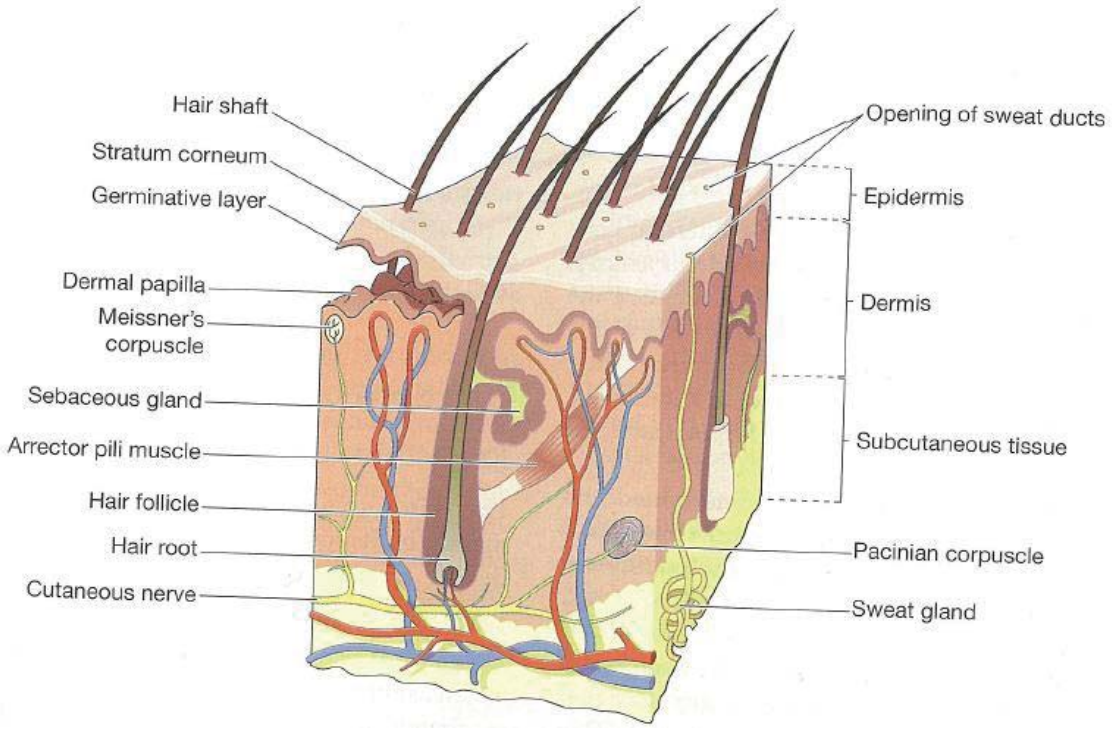

Figure 2.4. Components of the integumentary system. (Tortora and Derrickson, 2010).

The skin is part of the integumentary system. Other components of the integumentary system are accessory structures to the skin that include hair follicles, sebaceous glands, sweat glands, and nails. Apart from nails, these can be found in the dermis and seen in Figure 2.4.

Hair is distributed all over the skin except on the palms and soles. Each hair follicle has a hair shaft and a bulb. The sebaceous gland opens up into the hair follicle and the arrector pili muscle is situated below this gland (Figure 2.5). The hair consists of three layers; from the surface of the hair to the centre of the hair the layers are the medulla layer, the cortex layer, and the cuticle layer. The hair follicle is made up of the external epithelial root sheath and the internal epithelial root sheath. The dermal root sheath is the dense dermis that surrounds the hair follicle. In the tanning process the hair is first removed. A substance that removes the hair is

called a depilatory and it acts by dissolving the hair into a mass that can be easily wiped away. In ovine leather production it is the wool hairs that are removed. Prior to leather processing wool has an oily feel to it. This is imparted by the lanolin, a product of the sebaceous glands.

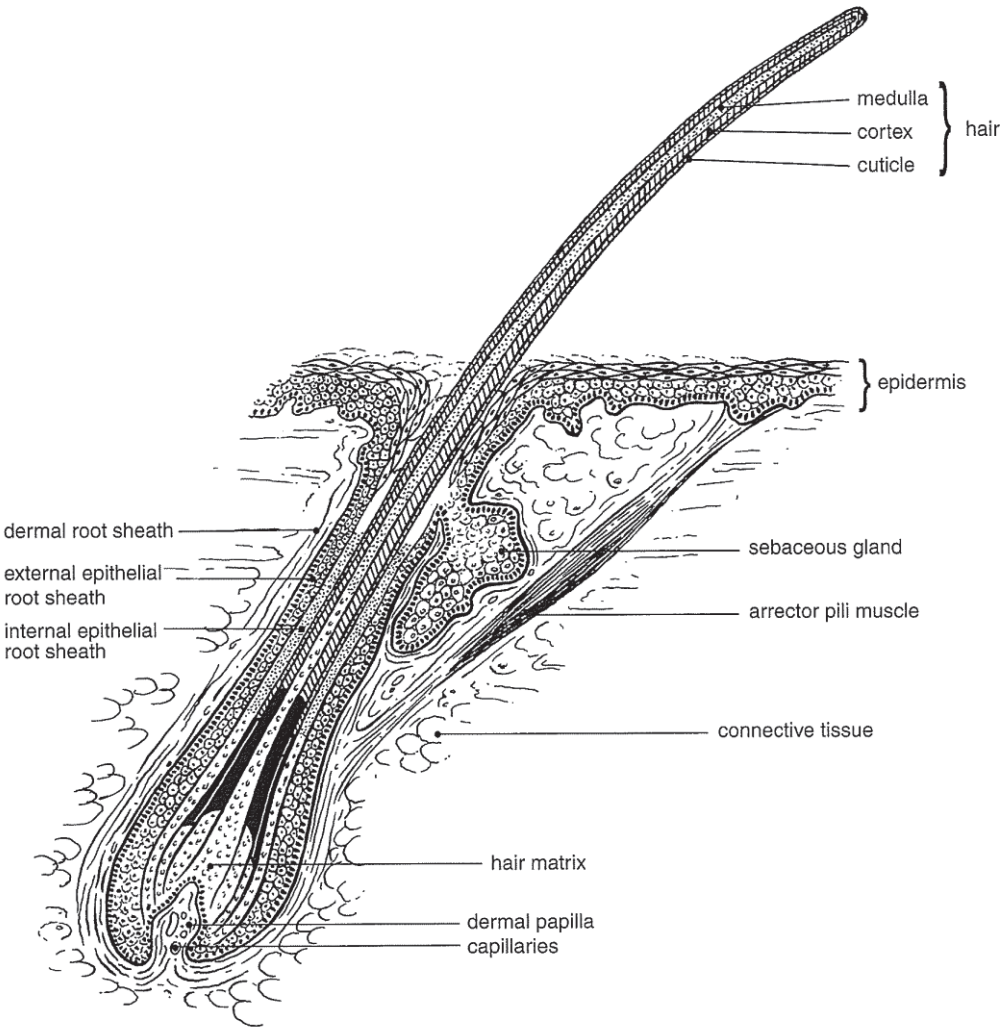

Figure 2.5. Single hair follicle (Frandson et al., 2013).

Mammals have sweat glands that release sweat into the hair follicles or through pores onto the surface of the skin. The sweat helps maintain the body temperature by the process of evaporation of the sweat from the surface of the skin thus cooling down the body. Sebaceous glands open up into the hair follicle and secrete sebum which lubricates the skin preventing it from drying out. Sheep have several

cutaneous pouches that are lined with sebaceous glands. These include: (1) infra-orbital pouches, found at the medial canthus of the eye and larger in rams than in ewes; (2) interdigital pouches on the midline above the hoofs of all four feet; and (3) inguinal pouches near the base of the udder or scrotum (Frandson et al., 2013).

2.1.4 Functions of the Skin

One of the most important functions of the skin is protection. It resists tearing and pressure with its elasticity, and protects the body from injury. Protection comes from the waterproof layer that skin provides, acting as a barrier against invasion by toxic agents. Collagen fibres provide the skin with the strength to resist to mechanical stress. The dermis functions to interact with the epidermis providing it with nourishment. The skin provides a barrier to infection acting as the first line of immunological defense of the body, it prevents the absorption of water from the outside, and loss of water from the inside. It helps regulate the temperature of the body and relays information about the external environment to the body via the sensation of touch. The integumentary system stores blood, with blood vessels in the dermis carrying 8-10% of the total blood flow of a resting adult (Tortora and Derrickson, 2010). In the structure of the skin are Langerhans cells, the first line of defence in the immune system of the body alerting other cells to potentially harmful invaders.

2.2 Collagen

Collagen is an important structural molecule found in abundance throughout the body. It is the main constituent of skin, leather, pericardium, wound healing matrices, and other tissues. Collagen comes in many different forms with each form classed into a "type" and numbered using roman numerals. To be classed as collagen three criteria must be met: 1. It must contribute to the structural integrity of the extracellular matrix; 2. It must form supramolecular aggregates such as networks and fibrils; 3. It must contain at least one triple-helical domain (Karamanos et al., 2012). Found in a diverse range of tissues, the different collagen types have distinctive macro structures. The most commonly occurring fibril-forming collagens (types I, II, III, V, and XI) form the structural basis of skin, tendon, bone, cartilage, and other tissues (Parry and Squire, 2005) (see (Maynes, 2012) for a review of fibril-forming collagen types I, II, and III). Type IV collagen is composed of three polypeptide chains 400 nm in length. Hexagonal networks are formed by collagen type VIII (hexagonal sides of 160 (±15) nm) and collagen type X (hexagonal sides of 100 (±15) nm) (Parry and Squire, 2005). Type VI collagen forms beaded filaments approximately 105 nm long.

The focus of this thesis is on materials composed primarily of type I collagen. The collagen I molecule is prevalent as the basis of many structural components in animals and assembles with a complex hierarchical structure. The collagen molecule is characterized by the repeating amino acid sequence $(Glycine\text{-}X\text{-}Y)^n$. Each polypeptide chain forms an alpha helix with a left handed twist, then three of these left handed helices twist together in a right hand manner to form a triple helix, or tropocollagen. Collagen fibrils are assembled from multiples of five staggered tropocollagens which is responsible for the banding structure of collagen. Fibrils combine to form fibres. Cross links stabilise the structure. Collagen biomaterials are resilient with the inherent strength of the collagen triple helix translated through a number of hierarchical levels to endow that tissue with its specific tough mechanical properties (Stamov and Pompe, 2012). The structure of collagen type I is outlined below to gain an understanding of the molecule at the heart of all investigations completed over the course of this research project.

2.2.1 Amino Acid Structure of Collagen Type I

The primary structure of collagen is its amino acid sequence. In the higher levels of structural organisation three polypeptides form a triple helix around an axis. Glycine must occupy every third position due to steric constraints from the close packing of the three polypeptide chains. This generates collagen's signature amino acid pattern, $(Gly\text{-}X\text{-}Y)^n$. Each polypeptide chain is formed by amino acids linked by covalent peptide bonds (Figure 2.6). The peptide bond is always formed between the amino (NH_2) group of one amino acid and the carboxyl (COOH) group of another amino acid.

The foundation of proteins is built by about twenty different amino acids, each identified by their unique R groups. An R group may be a single hydrogen atom (Glycine) or it may be a large, strongly polar group (Arginine).

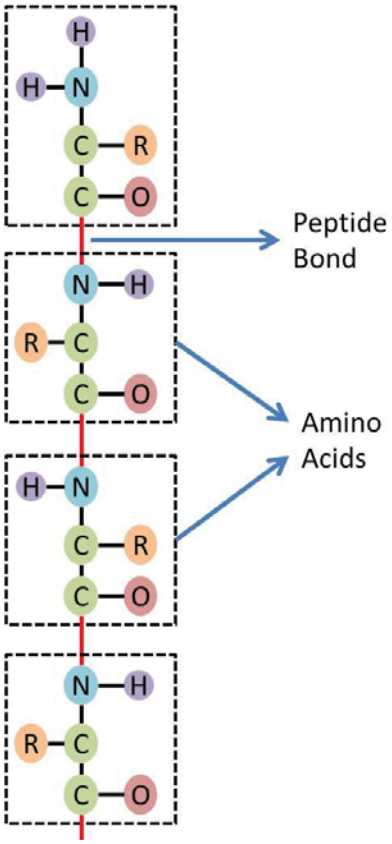

Figure 2.6. Primary structure of collagen is the sequence of amino acids in the polypeptide.

In a collagen molecule there is a significant presence of hydroxyproline and proline, and the Gly- Pro-Hyp triplet makes up about 10% of the molecule. Three specific triplets that contain the proline and hydroxyproline residues contribute to the stability of the collagen molecule in the following order: Gly-Pro-Hyp>Gly-Pro-Y and >Gly-X-Hyp (Segal, 1969).

2.2.2 Alpha Helix Structure of Collagen Type I

The secondary structure concerns how the amino acid sequence is twisted or folded. Common secondary structures are alpha helices and beta pleated sheets. Collagen's secondary structure is an alpha helix with a left hand twist.

The twist of the triple helix is sequence dependent and differs among tissues. Diffraction patterns of rat tail tendon have shown an alpha helix with a 10/3 symmetry (ten units in three turns) (Fraser et al., 1979, Rich and Crick, 1961) while the collagen peptide $(Pro\text{-}Pro\text{-}Gly)_{10}$ has a helix with a proposed 7/2 symmetry (seven units in two turns) (Okuyama et al., 1981). The collagen molecule is not likely to have a uniform twist along its length and may consist of multiple symmetries, for example both 7/2 and 10/3 helical conformations as seen in the section of a collagen molecule shown in Figure 2.7 below.

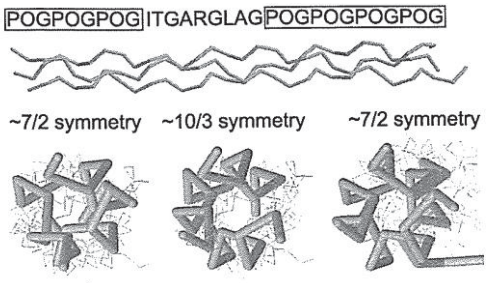

Figure 2.7. Three domains of a peptide showing variation in helical twist (Parry and Squire, 2005). Reprinted from Fibrous Proteins: Coiled-coils, Collagen and Elastomers, D. Parry and J. Squire, Collagen Molecular Structure, pg 311, copyright 2005, with permission from Elsevier.

The proline rings of some of the amino acids restrict the flexibility of the polypeptide chains. The diameter of each collagen molecule is about 14 Å (Maynes, 2012) with 3.6 residues per turn and a 5.4 Å axial repeat.

2.2.3 Tropocollagen Structure of Collagen Type I

The triple helix, or tropocollagen, structure of collagen is its tertiary structure (Figure 2.8). The idea that collagen was supercoiled in a right hand manner into a triple helix around a common axis was initially put together using fibre diffraction analysis and model building (Rich and Crick, 1961). The polypeptide chains are staggered by one residue. To identify each of the collagen molecules they are termed α chains and the chains with different primary structures are numbered with Arabic numerals eg. α1, α2. Type I collagen is composed of two α(I) chains and one α2(I) chain. An α1(I) collagen molecule is composed of 1014 residues and an α2(I) is composed of 1023 residues.

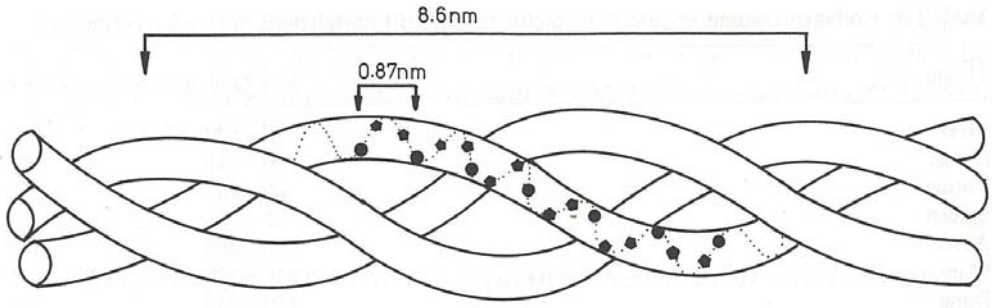

Figure 2.8. The collagen triple helix (Kucharz, 2011). Reprinted from The Collagens: Biochemistry and Pathophysiology, E. Kucharz, Structure, Heterogeneity, and Distribution, pg 7, copyright 1992, with permission from Springer.

Cross links stabilise the triple helix formation and can be intramolecular, linking two α-chains within the same molecule, or intermolecular, the covalent bonds between chains in different molecules. Hydrogen bond cross links in particular play a critical role in the stabilisation of tropocollagens. The triple helix is not an alpha helix due to the fact that not every peptide group participates in hydrogen bonding. Every Gly-X-Y triplet has one strong interchain hydrogen bond between the NH of Gly in one chain and the C=O of the residue in the X position of a neighbouring chain (Rich and Crick, 1961). In addition, when proline does not occupy the X position of the Gly-X-Y peptide triplets, a second interchain hydrogen bond between the NH group of the X position residue and the C=O of the glycine residue is formed mediated by one water molecule (Kramer et al., 1999, Kramer et al., 2000, Emsley et al., 2000). The water molecules involved in these hydrogen bonds form additional hydrogen bonds with hydroxyproline or side chains (all bonds present can be seen in Figure 2.9). As such collagen has a highly ordered hydration network (Suzuki et al., 1980). The first visualisation of the water network that surrounds collagen molecules was accomplished via the determination of the high-resolution structure of a peptide by Bella in 1994 (Bella et al., 1994, Bella et al., 1995). Since then a number of high-resolution structures have confirmed that extended water networks are an inherent feature of all collagen triple-helix peptide crystal structures (Kramer et al., 2000, Kramer et al., 2001, Berisio et al., 2001).

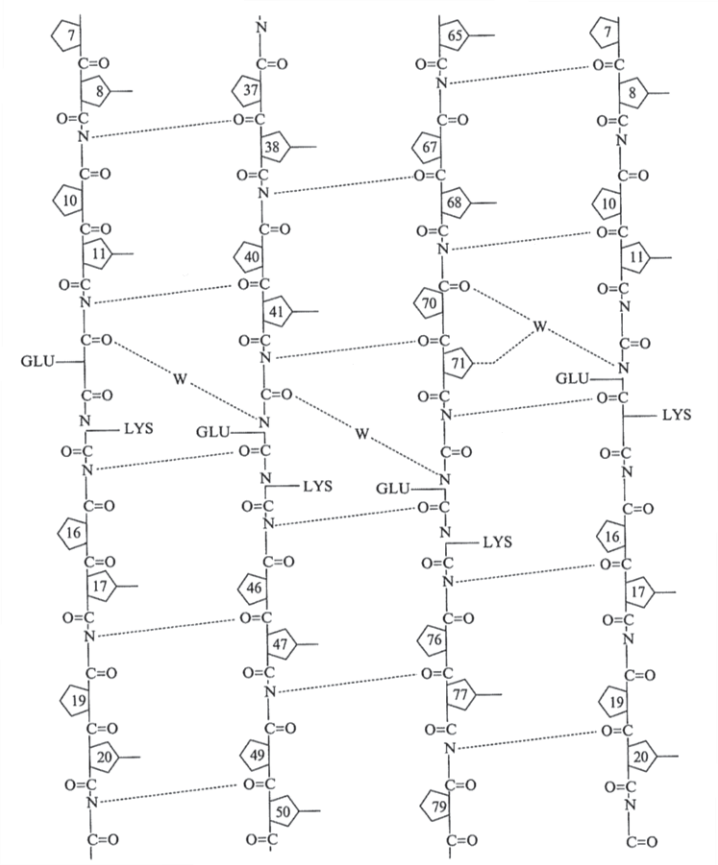

Figure 2.9. Hydrogen bonding network showing the regular pattern of direct hydrogen bonds and how water mediated hydrogen bonds are formed (Parry and Squire, 2005). Reprinted from Fibrous Proteins: Coiled-coils, Collagen and Elastomers, D. Parry and J. Squire, Collagen Molecular Structure, pg 313, copyright 2005, with permission from Elsevier.

2.2.4 Fibril Structure of Collagen Type I

The quaternary structure is the arrangement of tropocollagens relative to one another. A repeat of five staggered tropocollagens forms collagen's quaternary structure. Their staggered arrangement which produces overlaps of adjacent triple helices and gaps between one triple helix and the proceeding triple helix is responsible for the banding of collagen visible with atomic force microscopy

(Figure 2.10 below). The axial periodicity, or D-spacing, is approximately 67 nm and one tropocollagen is about 4.4 D periods long. Studies indicate the exact molecular periodicity of collagen fibrils contains 234.2 amino acids per D repeat (Meek et al., 1979).

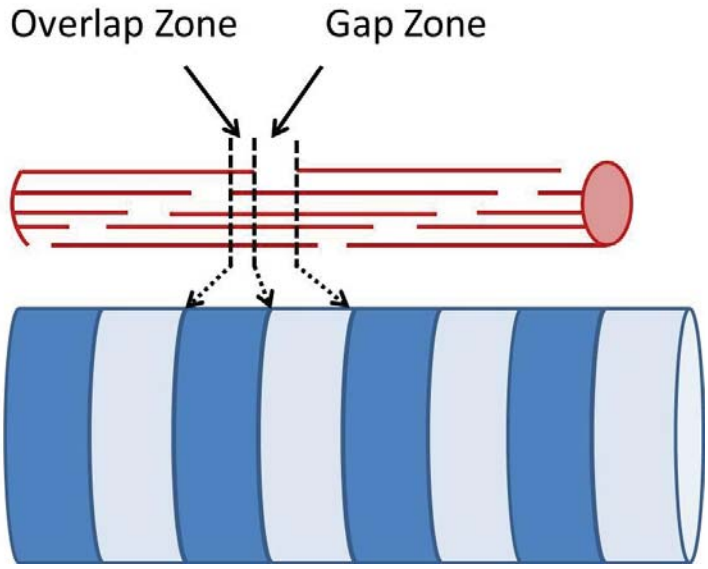

Figure 2.10. Tropocollagens assemble into collagen fibrils with a 67 nm D-spacing that includes an overlap and a gap region (Karamanos et al., 2012).

In some fibrils molecular tilt is present where the tropocollagens are on an angle. In rat tail tendon a tilt of about 5 degrees is present. A tilt of 18 degrees is seen in tissues such as nerve sheaths (Ottani et al., 2001), chordae tendinae (Folkhard et al., 1987a), submucosa (Cameron et al., 2002), and skin (Brodsky et al., 1980). These tissues must resist stresses from a number of directions. They consist of fibrils with uniform diameters that are typically less than 100 nm. This tissues have a shortened axial repeat of 65 nm, where 65 equals 67 cos 18° (where 67 represents the average D-spacing of collagen and 18° is the tilt of the fibrils.

The mechanical stability of the macro structures of collagen rely on intermolecular cross links. Hydrogen bonds between amino acid sidechains and collagen molecule mainchains and those mediated through water bridges are the main stabilizing force of the quaternary structure of arranged tropocollagens (Bella et al., 1995). Interchain water bridges are intrinsically linked to the hydroxyprolines in the

sequence so that high hydroxyproline content will increase the stability of the triple helix (Engel et al., 1977). Water can be regarded as forming a clathrate–like structure around each triple helix and it has a role in maintaining fibril assembly (Bella et al., 1995, Burjanadze, 1992, Rosenbloom et al., 1973).

Within each fibril, the tropocollagen molecules are held together by direct cross links between lysine and allolysine formed as a result of the action of an enzyme lysyl oxidase. The extensive, highly structured hydration shell around the collagen triple helices, along with water bridges between collagen fibrils, have been shown to be critical elements that maintain the macromolecular assemblies of collagen molecules (Bella et al., 1995, Naito et al., 1994, Bella et al., 1994). While the secondary structure remains stable if the water molecules become unavailable to support the hydrogen-bonding network, the mechanical properties of collagen are affected (Gautieri et al., 2011). Hydrophobic residues on the outside of the tropocollagen molecule have also been shown to play an important role in microfibrillar packing by both organizing water structure and through Van der Waals interactions (Usha and Ramasami, 1999).

In each individual fibril there is great strength and elasticity. It is believed that the structure of materials composed of collagen I also requires cross linking of the fibrils. This mechanically couples the fibrils restricting them from sliding past each other in order to achieve high strength (Picu, 2011). The way in which these connections might transmit force between fibrils to resist sliding forces has been modelled (Puxkandl et al., 2002, Cranford and Buehler, 2013, Fessel and Snedeker, 2011, Redaelli et al., 2003, Chan et al., 2009).

2.2.5 Macro Organisation of Collagen

Collagen fibrils form complex networks that can be linked to the physical properties of the tissue. The arrangement of collagen fibrils, particularly the extent of alignment or anisotropy, is an important contributor to the strength of collagen

materials. The structure-function relationship between collagen alignment and mechanical properties has been elucidated for a range of tissue types (Kamma-Lorger et al., 2010, Sellaro et al., 2007, Liao et al., 2007, Gilbert et al., 2008, Purslow et al., 1998). The orientation of collagen measured edge on (alignment in-plane) has been shown to be correlated with strength in a range of mammal skins processed to leather (Basil-Jones et al., 2011, Sizeland et al., 2013).

2.3 Leather

Leather is processed skin consisting primarily of collagen. It is produced on a large scale for shoes, clothing, and upholstery (Commodities and Trade Division, 2010), with high strength being a primary requirement for high-value applications. To produce leather, raw skin goes through hide preservation, dehairing/liming, deliming and bating, pickling, tanning, retanning, fat liquoring, drying, and finishing.

Leather Industry

Skins and hides are the raw materials from which leather is produced. They are by-products of the meat industry and are basic commodities on the world market. Leather usage is outlined below (Table 2.1) with its primary use being for shoe manufacture.

Table 2.1. Leather usage (Thorstensen, 1993).

Item	%
Shoes	56
Garments	9
Work Shoes	10
Handbags	6.5
Leather Goods	6.5
Belts	4
Miscellaneous	8

Skins are often partially processed in order to stop the decomposition of skins and then shipped to another part of the world before the rest of the processing is completed. Sheep (ovine) skins as pickled, salted, and dried sheepskins are available from many parts of the world, including South America, Africa, Australia, and New Zealand. New Zealand is a crucial supplier in the sheepskin industry. It is standard practice to remove wool from the skin as the value of the wool exceeds the value of the skin. While the wool is removed, the old trim practice was to leave hides with the ears, tails, shanks, snouts, and other appendages left on them. Sometimes a tanner would even find hooves and horns attached to the hide. This practice resulted in an economic loss and as a result a new trim system was defined and became the standard of the industry.

2.3.1 Leather Structure

Leather has a micro structure that is comprised of two distinct layers: the grain and the corium. The grain is the outermost layer of the skin and the corium is closest to the flesh of the animal. The structure of the collagen fibrils in the grain layer is generally quite fine in nature and more aligned than in other layers. Below this the corium layer structure has collagen fibrils that are more randomly

orientated. The collagen network is fairly dense and tangled. In addition to the collagen, a network of elastin fibrils is also present which serves to strengthen the hide.

In the tanning industry the skins of large animals, such as full grown cattle and horses, are called 'hides'; the term 'skins' is used when referring to small animals such as sheep, goats, and calves. The term "hide" is never applied to the small animals.

The grain and the corium have significantly different structures (Russell, 1988, Bavinton et al., 1987). Fibril orientation and fibril diameter, particularly in the corium layer, have been shown to be an important factor in the strength of the material (Basil-Jones et al., 2011, Bavinton et al., 1987, Parry et al., 1978, Wells et al., 2013). During the process of making leather, synthetic cross links are introduced that stabilize the molecular structure of the skin and contribute to its physical properties (Folkhard et al., 1987a, Folkhard et al., 1987b, Cuq et al., 2000, Chan et al., 2009).

The D-spacing of the collagen in stronger ovine and bovine leather has been shown to decrease at the interface between the corium and the grain (Basil-Jones et al., 2012). While changes in D-spacing have not been shown to correlate with strength in leather (Basil-Jones et al., 2011) and rat tail tendon (Gonzalez et al., 2014), D-spacing does vary with tissue types (Fang et al., 2012), age (James et al., 1991b, Scott et al., 1981), and chemical treatment (Scott et al., 1981, Ripamonti et al., 1980). It is also possible to observe change in D-spacing when leather is subjected to mechanical stress (Basil-Jones et al., 2012).

Leather is made from skins from different animals. This produces leather with different structural and physical properties. Bovine leather is particularly strong and is the material used for the majority of leather goods manufactured. Sheepskin is very open and porous, has very little structural fibre, and produces very weak leather. Goatskins, compared to sheepskins, have a very tight fibre structure which allows its use in applications that require high flexibility and strength like in the manufacture of gloves and shoes.

If there are heavy fat deposits in cattlehides a change in fibre orientation can occur where the fibres become aligned perpendicular to the surface of the skin. This is called the “vertical fibre defect” and occurs in fat beef cattle such as Herefords. Compared to beef cattle, dairy cattle have very thin hides and their skins contain less fat, are not as thick, and have relatively large surface areas.

2.3.2 Leather Processing

The leather making process is a way of preserving skins to stop decomposition and to provide a strong and flexible material. The process consists of a series of chemical treatments and some mechanical processes. Each of the chemical treatments alters the composition of the original skin, for example, extracting components from the native skin or adding components such as cross linking agents. The chemical treatments used to produce leather from skin and hide may result in changes to the structure of the collagen fibrils and the arrangement of these fibrils. These chemical processes include strong salt solutions, large changes in pH, enzymatic treatments to remove cross links, and new cross links being formed. An overview of tanning chemistry has been presented (Covington, 1997). Some aspects of chemical treatments of skins and the effect on structure they have has been observed previously with liming of skins (increasing the pH with calcium hydroxide) showing a decrease in the D-spacing of collagen (Maxwell et al., 2006). Dehydration of parchment has been shown to result in a decrease in collagen D-spacing from 64.5 to 60.0 nm (Wess and Orgel, 2000). Pickling and retanning agents have been shown to swell collagen fibres at low pH (Bulo et al., 2007). At low ionic strength and non-isoelectric pH charge dependent interactions (screening and selective ion adsorption) are prevalent in maintaining the collagen architecture (Ciferri, 2008) which is also reflected in the greater thermal stability of collagen at low pH (Zanaboni et al., 2000) and in the elastic response of collagen (Grant et al., 2009).

The leather-making process is detailed below.

Hide preservation

The raw material is the skin after it has been removed from the carcass. The raw skin is susceptible to bacterial growth and is in immediate need of some form of preservation to stop the decay. Once the skins have been preserved they can be shipped a great distance or stored before the rest of the leather-making process is continued. As such it is not uncommon for New Zealand to produce sheepskins, United States of America to convert them to leather, and Europe to make the leather into garments. Three methods are used to preserve the skin, salt curing, drying, and brine curing.

The first way of temporarily preserving the skin before tanning is salt curing and is the most common method in Europe, North America, and other temperate climates. The salt acts to slow down bacterial growth by reducing water activity. Salting causes some dehydration of the skins. To salt cure the skins salt packs are created by stacking hides on top of one another with salt spread out in between each hide. The edges are folded to keep the moisture in the salt pack and it is stored in a cool area. Proper salt curing requires 21 days in the pack (Thorstensen, 1993). Following the salt curing process the hides are taken out of the salt packs, the excess salt is shaken off, the hides are inspected and then packaged up ready for shipment. If the salt curing is done properly, the salted hides can keep in a cool storage area for up to a year.

Another method of preservation is drying. It is one of the oldest methods of skin preservation and is simply done by air drying the skin to eliminate the moisture. The skins are spread out on the ground supported by sticks or stones, hung on poles or ropes, or stretched out on a frame and allowed to dry in the shade or the sun. The frame drying is the most common drying method used as the skin shrinks and tightens when it dries allowing easier flat packing of the skins for storage or transportation.

The third method of preservation is brine curing. The skins and hides are chilled, cleaned, and soaked in a saturated brine medium in either vats or raceways for 48 hours until the brine has completely permeated the skin. The hides and skins are then wrung out, inspected, and packaged up for shipment. This method is not as

effective as the salt curing and as such the brine cured hides will only last for 6 months.

Alternatively the hides and skins can be processed through to the chrome tanned (wet blue) stage. This avoids the need for the preservation of the raw material and saves costs on curing and shipping and better preservation of the hides is accomplished.

Dehairing/Liming

The "beamhouse" processes start after the hide has been preserved and includes soaking, fleshing, dehairing/liming, and bating. These leather-making steps remove the salt by soaking and washing the skins (where the skin becomes rehydrated) and treat the skins with an alkali treatment carried out in the presence of sodium sulfide ('liming') combined with suitable enzymes ('bating') which together break down and remove some of the non-fibrous proteins, glycosaminoglycans and other undesirable components. It is also said to 'open up' the structure of the leather to enable better penetration of tanning chemicals in subsequent stages.

Soaking ensures the skins are rehydrated, and makes the skins softer and cleaner. When they arrive at a tannery they usually arrive as cured skins with preservation methods based on the dehydration of the skins. As such the skins must be wet back to hydrate the material using water. Dry skins may need soaking for up to 48 hours to successfully rehydrate.

Dehairing is the process of removing the unwanted hair from the hides and skins and can be done a number of ways. Liming is an dehairing system that has been used for many years. Lime is dissolved in water and applied to the hide. It acts to break down and solubilise the hair keratin. The lime or alkali disrupts hydrogen bonding between fibrils resulting in an opening up of the structure making available more acid and alkaline groups on the skin for future chemical interactions. A painting system, otherwise known as a wool-pulling system, can also be used to remove hair. The skins are washed and painted with a solution of sodium sulfide, lime and sodium sulfide, or sodium sulfide and caustic soda. The

paint is applied to the flesh side of the skin and the skins or hides are piled up and left in a cool place overnight. The skins are laid out the next day and the wool is removed by hand. The remaining hide or skin is then placed in liming solution overnight. Dehairing systems that do not use lime have been considered and trialled by the tanning industry in an attempt to remedy the problems of effluent disposal and stream pollution that comes hand in hand with lime systems but lime based systems are by far the most commonly used practices.

Deliming and Bating

After liming the pH of the hide needs to be lowered for the proceeding processing steps to take place. The pH of hides after liming is about 12. The fibres are swollen from the absorption of lime and alkaline materials. For effective bating a pH that is slightly basic is desired, about pH 7-8. Calcium hydroxide and ammonium salts are used to buffer a solution to pH 7-8 and solubilise the lime. As a more environmentally friendly option sometimes magnesium salts are used. The deliming and the bating procedures are continuous in most tanning operations.

Bating is an enzymatic action for the removal of unwanted hide components. The epidermis, hair, protein degradation products, and the “scud” on the surface of the skin and in the hair follicles and pores are the unwanted components. Bating refers to the action of enzymes on these components. The enzyme activity and the nature of the activity of the enzyme depends on the temperature, amount of added enzyme, and the pH. Conditions are closely monitored during this step.

Pickling

Pickling is the adjustment of the pH of the skin to the level desired for tanning using salt and acid. After the alkaline treatments involved with the liming and bating steps, the skin is acidified in sulfuric acid and sodium chloride. After this stage the skin is referred to as “pickled”. A synthetic, organic cross linking agent and surfactant are often added at this point which may assist with the subsequent chrome tanning stage. Stabilising agents are often added to the pickle to raise the denaturation temperature of the collagen and thus enable skin fat to be removed

more efficiently at higher temperatures. The skins at this stage are called "pretanned". At the end of the pickling stage the skin can be thought of as a purified fibrous network of protein. The curing, soaking, liming, deliming, and bating have all been based on the removal of unwanted components. From here on the processing will be focused on chemical reactions that will produce the wanted physical characteristics of leather, the first step of which is the pickling adjustment of the skin to the desired pH. The tannage to be used in future leather-making steps and the time between pickling and tanning dictates the pH desired at this point. The skins are treated with a solution of water and salt and tumbled before the acid solution is added. Leaving the skin to reach equilibrium overnight, the pH is brought down to pH 3 or lower by the absorption of the acid into the skin. A pH of 2 or lower is needed if there is a wait between the pickling and tanning steps. If the hides and skins are to be tanned immediately the pH is adjusted to 2.5-3. Sufficient salt must be used in the pickling process to prevent swelling.

Tanning

After pickling the hides and skins need to be tanned. Tanning is the treatment of hides and skins for preservation and converts the material into a useful commercial material. Tanning can be completed using either a chrome tan, vegetable tan, or synthetic tan.

Chrome tanning is based on the reaction of the hide with chromium salts to yield a very stable fibrous network which is resistant to bacterial attack and high temperatures. Once chrome tanned the hide is referred to as "wet blue". Chrome tanning must be followed with fatliquoring and is sometimes retanned with a vegetable tan to impart the desired physical qualities of leather. Pickled hides at a pH of 3 or lower are added to a chromium sulfate bath and the chrome tanning salt penetrates into the hide. After this initial absorption of the chromium salt, the pH is raised to allow the chemical reaction between the hide and the chromium salts to complete. The adjoining chains of the fibrils are cross linked together as a result of the chrome tanning.

Vegetable tanning preserves the fibrous network and imparts qualities of fullness and resilience to the leather. It produces leather used for end applications like upholstery and saddlery. Retannage of chrome tanned leather with a vegetable tan is common. Vegetable tannins come from a wide range of plants and can be found in twigs, bark, nuts, leaves, and wood. Vegetable tannins include quebracho, wattle extract (mimosa), myrobalans, gallnuts, gambier, mangrove, hemlock, chestnut, valonia, lignosulfonates (Thorstensen, 1993). The vegetable tanning process relies on a balance of the concentration, pH, and temperature. For example at a high concentration of vegetable tan a greater reaction or fixation will occur between the vegetable tannins and the hide fibres. However at a high concentration the particle size of the tannins is large. An excessive deposition of the tannins on the surface of the skin will occur which blocks the penetration into the hide or skin. Vegetable tanning produces leather with a natural brown colour.

Synthetic tans are much more controllable and predictable than other tanning agents. They are versatile and new "syntans" are being developed for the tanning industry every year. Synthetic tans are often used to obtain specific effects on either the leather processing or the final product for example they can aid in the penetration of dyes or can produce the feel of fullness to the final leather product.

Retanning

Chrome tanned leather tends to be too rigid for most applications so there is normally a second tanning stage using natural vegetable tannins or synthetic tannins to make the final leather feel softer and 'fuller'. After this second tanning stage the skin is called "retanned".

Fat Liquoring

During the processing of skins and hides to leather, efforts are made to optimize the strength, flexibility, and feel of leather. Adding penetrating oils, a process known as fat liquoring, improves leather's texture and flexibility by lubricating the fibres and preventing adhesion between them (Bajza and Vreck, 2001). The initial leather-making processes of liming and bating remove most of the natural oils

from the skin and after tanning the leather does not contain enough lubricants to prevent it from drying into a hard material. Proper lubrication is one of the determining factors in imparting the desired characteristics to the final finished product. Under lubrication will result in hard leather that is prone to cracking. Fatliquoring involves emulsions of oil in a water system that are applied to the leather in a drum. The oil is absorbed into the skin thus lubricating the fibres.

Drying

After fat liquoring, the water is evaporated to dry out the leather. The drying process is an important step in the leather-making process and cannot happen too quickly. Slow drying of leather ensures that as the surface water is evaporated, the water deeper in the skin is drawn to the surface thus the full thickness of the leather dries. Drying under excessive heat causes the surface to dehydrate and the inner part of the skin to retain its moisture as the water does not move fast enough to replace the evaporated surface water. Drying can cause shrinkage as the fibres become closer to one another. To prevent this the leather can be held in an extended position to maximise the final area yield. Drying can be done in air with leathers hung up on ropes, in air whilst being tacked out on boards, on screens held in place by toggles that are placed in a toggling unit (a dryer that can control the temperature and humidity, in a tunnel dryer that controls temperature and humidity with leathers pasted down to large sheets of glass or metal, or in a vacuum dryer where leather is placed on a steel surface and heat is applied under vacuum.

Finishing

The final process is the finishing of the leather. Finishing is not a simple process of painting the surface to cover up any imperfections as it contributes to the leathers' durability and aesthetic qualities. The finishes need to be flexible, adhesive, and durable and leather that has not had a finish applied will lack the feel, texture, and water resistance required for the high end products leather is so well known for. Finishing can comprise of different layers with a top finish needing to stick to the

base coats and the base coat need to stick to the leather to prevent peeling. The finish must be able to withstand a wide range of temperatures and create a uniform colour and appearance through a filling action. Leather coatings can be divided up into four categories – condensation systems, drying oil systems, lacquer systems, and latex systems. Finishing of leather can be done using a combination of these coating systems. Condensation systems involve the formation of a film due to a chemical reaction, usually heat-activated, between components of the coating after application. Drying oil systems form a film when the binder, or film-forming material, and oxygen react leaving a film of polymerized fat molecules. Lacquer systems are based on a film-forming material containing a solvent being deposited onto the leather surface when evaporation occurs. Latex systems contain a binder emulsified in water that is deposited on the leather surface when the water is evaporated or soaked up by the leather

In addition to coatings the leather can be dyed and rubbed to achieve a high gloss finish. Dying can be done by using the tray dying method or a brush dying method. The tray dying method simply involves the immersion of the leather in a shallow tray containing the dye and the brush dying method involves the dye being brushed on to one side of the leather.

Finally, the leather is mechanically softened or 'staked' by rubbing it over an edge to soften the material.

2.4 Pericardium and Heart Valves

Heart valve leaflet replacement with bovine pericardium is an established practice (Nwaejike and Ascione, 2011) using either adult or neonatal pericardium (Paez et al., 2006) and may be performed percutaneously (Cribier et al., 2003). The material requires high mechanical strength and a long performance life (Mirnajafi et al., 2010). The orientation of collagen in pericardium heterograft materials for heart valve leaflets has been shown to affect the stiffness during flexing (Mirnajafi et al., 2005). Greater understanding of the properties of these materials and the

structural basis for these properties is important for improving the serviceability of these replacements.

Pericardium is a fibrous collagen extracellular matrix material with structural similarities to skin and other tissues. The structural differences between neonatal pericardium and adult tissue that give rise to the desirable differences in their physical properties have not been adequately investigated. This thesis presents a study on the comparison of the collagen fibril structure of adult and neonatal bovine pericardium using SAXS. To understand Chapter 8, the structure of the heart, in particular the pericardium and the heart valves, is detailed below.

2.4.1 Structure of the Heart

The heart is responsible for pumping blood around the body. The pumping action squeezes the blood out of the heart and through the blood vessels. The heart is cone shaped and lies behind your sternum on the left hand side. The main structural features of the heart can be seen in Figure 2.11.

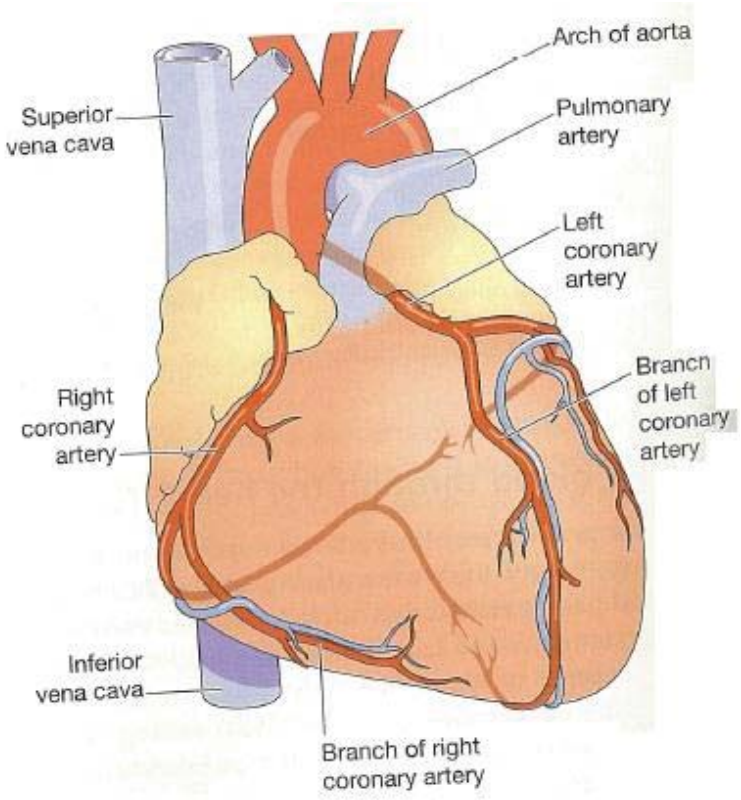

Figure 2.11. Main structural features of the heart (Waugh and Grant, 2006).

The heart is divided into a left side and a right side, each with one ventricle and one atrium. The four chambers are separated by several valves that monitor the flow of the blood and ensures the blood is traveling in the correct direction. The heart wall is made up of three layers of tissue, the myocardium, the endocardium, and the pericardium. The pericardium is a membrane that surrounds and protects the heart and is made up of a fibrous layer and a serous layer. The serous layer of the pericardium is in turn made up of the visceral pericardium, the pericardial cavity, and the parietal pericardium (Figure 2.12). The fibrous pericardium is covered by a layer of mediastinal pleura, or pericardial pleura and this layer together with the serous pericardium and the fibrous pericardium makes up the pericardial sac.

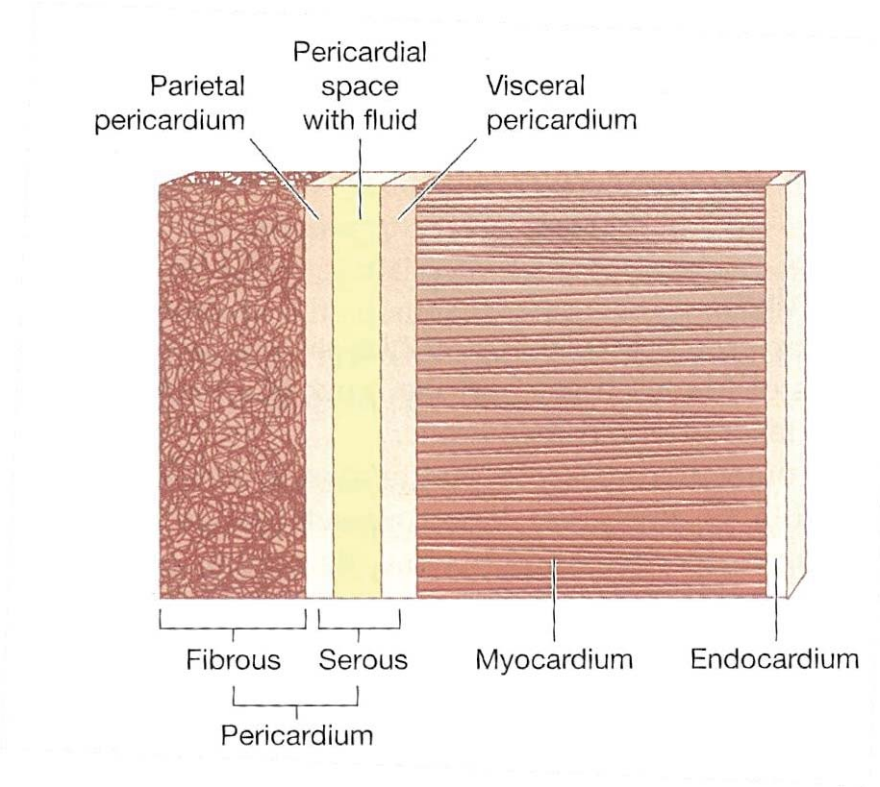

Figure 2.12. Layers of the heart wall (Waugh and Grant, 2006). Reprinted from Ross & Wilson Anatomy and Physiology in Health and Illness, A. Waugh and A. Grant, The Skin, pg 82, copyright 2014, with permission from Elsevier.

The inner layer of the pericardium is the thin, delicate serous layer and the layer of the serous pericardium closest to the heart is the visceral pericardium. It envelops the myocardium layer of the heart wall and lubricates the tissues as the heart beats by secreting fluid into the pericardial cavity. As such the parietal cavity is a space filled with fluid that lies between the visceral and the parietal layers of the pericardium. The parietal pericardium is the outermost layer of the serous pericardium and lines the fibrous layer of the pericardium. This layer also secretes pericardial fluid into the pericardial cavity.

The outer layer of the pericardium is the fibrous pericardium. This layer is a thick, dense, tough layer of fibrous connective tissue that anchors the heart in place by connecting to the sternum and the diaphragm. The fibrous pericardium provides the heart with protection and prevents overstretching of the heart.

2.4.2 Heart Valves

The heart valves both monitor the flow of the blood and are composed of dense connective tissue covered by endocardium. The valves names reflect their location and physical features. The two atrioventricular valves lie between the atrium and the ventricle on each side. The bicuspid valve has two flaps; and the tricuspid valve has three flaps (Figure 2.13). The right atrioventricular valve (tricuspid valve) has three flaps or cusps and the left atrioventricular valve (bicuspid valve) has two cusps.

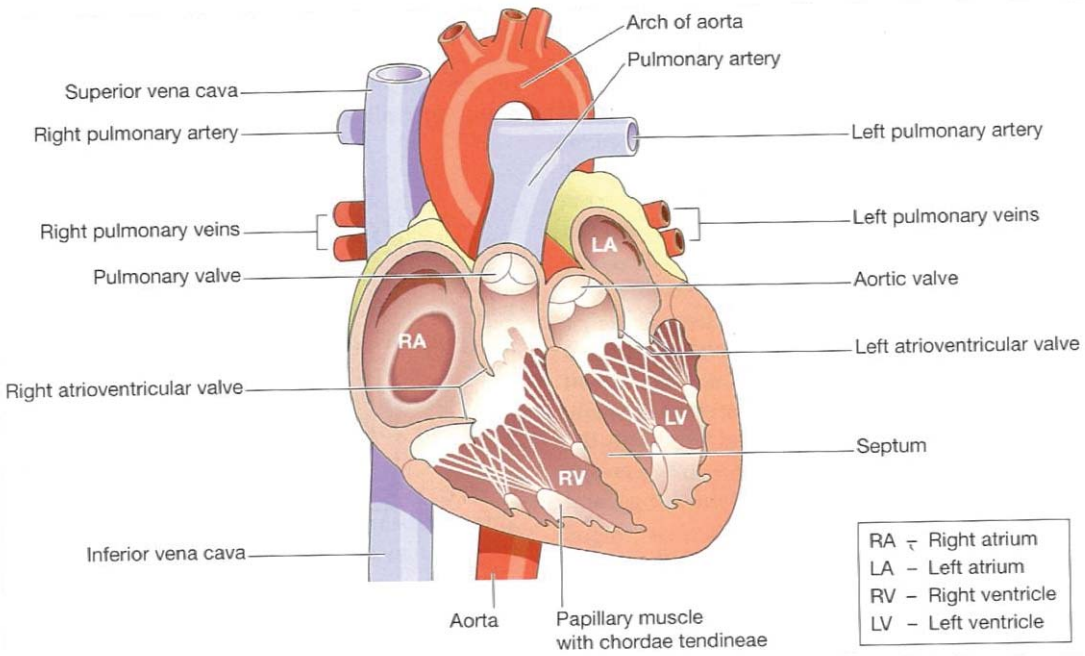

Figure 2.13. Interior of the heart (Waugh and Grant, 2006). Reprinted from Ross & Wilson Anatomy and Physiology in Health and Illness, A. Waugh and A. Grant, The Skin, pg 83, copyright 2014, with permission from Elsevier.

The flow of blood in the heart is one way and it is the role of the heart valves to control this. As such they play a crucial role in the function of the heart. The heart can fail to operate as efficiently as possible if the arteries are compromised or the valves malfunction. The coronary arteries that provide the heart with its own blood supply can clog up and flow of the blood can be slowed greatly. Fixing the

clogging of the arteries has become a common procedure and is an example of successful percutaneous delivery of a device. The surgeons insert a small tube into the blood system that is moved until it is located in the region of the artery that is affected. Balloons are then inflated that push the walls of the artery out, widening the blocked area. These balloons are often replaced with small tubes called stents that are permanently located in the affected area of the artery to keep it wide open for easy blood flow.

Normal function of heart valves occurs when they are able to open and close completely and at the proper times. The heart valve can malfunction if the opening of the valve narrows or the valve fails to close completely. Stenosis occurs if the heart valve opening narrows and the blood flow is restricted, mitral stenosis is when the scar formation from a congenital heart disease causes the narrowing of the valve opening. Insufficiency or incompetence occurs when the valve fails to close completely. Valves can also prolapse causing backflow of the blood. Certain diseases such as rheumatic fever can also damage the valves. A valve needs to be replaced if its malfunction affects daily activities. Valves can be replaced using valves from human donors or pigs and requires open heart surgery. Artificial heart valves have been developed using pericardium and can be inserted percutaneously, thus avoiding open heart surgery (Figure 2.14).

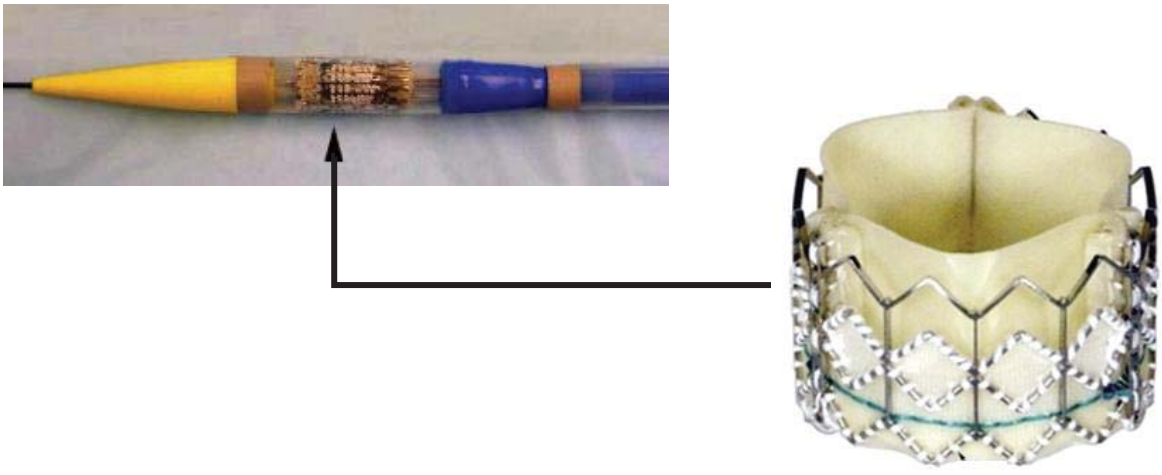

Figure 2.14. Replacement heart valve folded up and inserted via a stent.

2.5 Small Angle X-Ray Scattering for Nanostructural Measurements

The macroscopic properties of many materials are strongly influenced by their nanostructures. In order to understand such structure-property correlations, it is important to venture into characterising the structure and discovering the mechanisms of action of these materials on a very small scale. This requires specialised techniques capable of analysing at a nanoscale level.

The complex architecture of leather is physically defined by a hierarchical structure of collagen where even the quaternary structure is difficult to access by microscopic methods. As such, this fibrous collagen network is a prime example of a material that requires exploration at a nanoscale level. In order to characterise the structure of collagen a number of techniques can be utilised including the following methods:

- Small Angle X-ray Scattering (SAXS) (Kronick and Buechler, 1986, Basil-Jones et al., 2011, Purslow et al., 1998, Liao et al., 2005, Basil-Jones et al., 2012).
- Infra-Red Microscopy (IR)
- Extended X-Ray Absorption Fine Structure (EXAFS)
- X-Ray Absorption Near Edge Structure (XANES)
- Transmission Electron Microscopy (TEM)
- Scanning Electron Microscopy (SEM) (Haines, 1984, Deb Choudhury et al., 2007b, Kielty and Shuttleworth, 1997, Barlow, 1975)
- FTIR Microscopy
- Reflection anisotropy (Schofield et al., 2011)
- Confocal Scanning Optical Microscopy
- Confocal laser scattering (Jor et al., 2011)
- Multiphoton microscopy (Lilledahl et al., 2011)
- Raman polarisation (Falgayrac et al., 2010)
- Anisotropic raman scattering (Janko et al., 2010)
- Small angle light scattering (Billiar and Sacks, 1997)

- Atomic Force Microscopy (AFM) (Deb Choudhury et al., 2007b, Reich et al., 1999, Edmonds et al., 2008, Friedrichs et al., 2007).

These methods allow structures to be defined on a scale that is almost incomprehensible. In an attempt to try and grasp the concept of the length scales being measured, a nanometre can be looked at in relation to something small that is familiar. A single sheet of paper is about 100,000 nanometres thick, a single human hair is approximately 80,000-100,000 nanometres wide and the head of a pin is about 1 million nanometres across (See Figure 2.15 for a larger scale comparison). With these dimensions in mind, it becomes apparent that the capabilities of the techniques listed above to study on a nanoscale level are impressive to say the least.

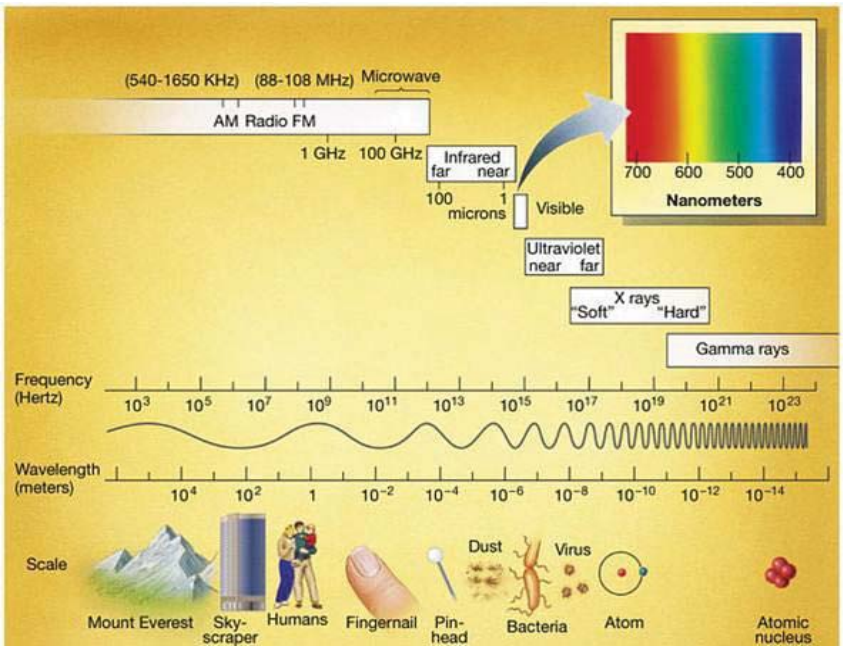

Figure 2.15. Electromagnetic spectrum with real life objects to illustrate scale lengths. Adapted from: http://lasp.colorado.edu/~bagenal/1010/SESSIONS/13.Light.html

Synchrotron based technique small angle X-ray scattering provides a brilliant platform for nanostructure analysis and has been used by researchers since the

early to mid-1900's to explore and characterise the structure of collagen (summarised by Gustavson (Gustavson, 1956)). The majority of the work presented in this thesis is based on experimental studies completed using small angle X-ray scattering. Imaging techniques (transmission electron microscopy and atomic force microscopy) compliment small angle X-ray scattering and have enabled in depth nanostructural analysis and visualisation of the collagen network of leather and other extracellular matrix materials.

Small angle X-ray scattering (SAXS) is a powerful tool for the study of macromolecular structures. SAXS can be used to study the long range order of materials and complex molecules in the size range of 1 – 500 nm. This makes it ideal for the exploration of protein assemblages such as collagen. The high spatial resolution combined with high penetration depth for many materials makes synchrotron X-rays a particularly attractive method to analyse the structure and texture of materials. The fast measuring time, high penetration power, and small wavelength offers the possibility to conduct *in situ* measurements under various sample environments.

SAXS can provide information on macromolecules in solid materials or in solution (Bernado et al., 2007, Tsutakawa et al., 2007, Putnam et al., 2007, Petoukhov and Svergun, 2006). The structural analysis of materials based on the diffraction of X-rays can be used to generate information such as the preferred orientation, a feature that can then be linked to mechanical and other material properties (Burger et al., 2010).

SAXS provides an ideal platform for nanostructure analysis and has previously been used to investigate collagen structure (Cameron et al., 2002, Maxwell et al., 2006, Orgel et al., 2001, Wilkinson and Hukins, 1999) and other collagen rich materials such as tendon (Sasaki and Odajima, 1996a, Sasaki and Odajima, 1996b, Fratzl et al., 1993, James et al., 1991a), bone (Burger et al., 2008a, Burger et al., 2001, Cedola et al., 2006, Burger et al., 2008b, Fratzl et al., 1997, Cedola et al., 2007), cornea (Fratzl and Daxer, 1993), articular cartilage (Mollenhauer et al., 2003, Mollenhauer et al., 2002), and leather (Boote et al., 2002, Sturrock et al., 2004, Basil-Jones et al., 2011, Kronick and Buechler, 1986, Basil-Jones et al., 2012).

Structural studies of collagen under tension have also been conducted (Folkhard et al., 1987b, Misof et al., 1997, Puxkandl et al., 2002, Sasaki et al., 1999).

Over the past decade remarkable progress has been made in SAXS data analysis methods (Svergun and Koch, 2003). The possibilities of the technique have been broadened enabling 3D models to be reconstructed and previously baffling structures to be revealed (Gajda et al., 2013).

Synchrotron radiation is the building block upon which all synchrotron techniques are made from. This section will endeavour to illustrate the concepts of synchrotron radiation and SAXS with a focus on the analysis of collagen matrix materials.

2.5.1 Synchrotron Radiation

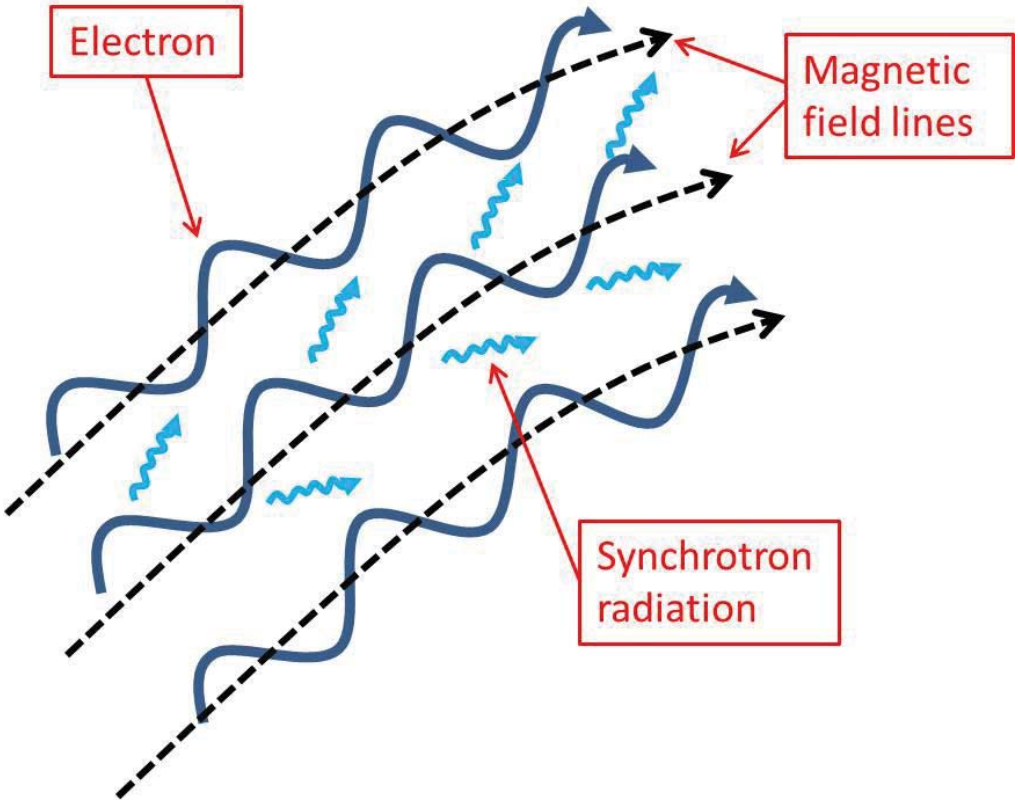

Figure 2.16. Synchrotron radiation emitted from charged particles spiralling in a magnetic field. Adapted from: http://pages.uoregon.edu/jimbrau/BrauImNew/Chap24/6th/24_ 35Figurea-F.jpg

Synchrotron radiation occurs when a charged particle, a proton or an electron, is radially accelerated (Figure 2.16). This happens when the charged particle comes across a magnetic field. The particle is accelerated into a circular, spiral motion that follows the magnetic field and it emits electromagnetic radiation called synchrotron radiation in the process. The acceleration and deflection of the charged particles keeps them in a circular orbit.

In 1947, the radiation was first observed at the General Electric 70MeV Synchrotron in Schenectady, New York and as such was dubbed 'synchrotron radiation' (Elder et al., 1947). Synchrotrons have since evolved with large, particularly expensive facilities built dedicated to producing synchrotron radiation. The Australian Synchrotron, pictured in Figure 2.17, is the closest synchrotron to New Zealand and as such was used for the entirety of the work presented in this thesis. It was built with an initial investment of AU$157 million by the Victorian Government. Additional support totalling AU$50 million was provided by the Australian and New Zealand governments along with universities and major research institutions such as the Australian Nuclear Science and Technology Organisation (ANSTO) and the Commonwealth Scientific and Industrial Research Organisation (CSIRO).

Figure 2.17. The Australian Synchrotron. From: http://adm.monash.edu/records-archives/archives/memo-archive/2004-007/stories/20080305/synchrotron.html

A synchrotron features charged particles that are kept in a closed orbit at constant energy in a ring called a 'storage ring'. It is this large, circular storage ring that denotes the circular shape of most synchrotrons. The basic components of a synchrotron are displayed in Figure 2.18 and the Australian Synchrotron set up is explained in detail below.

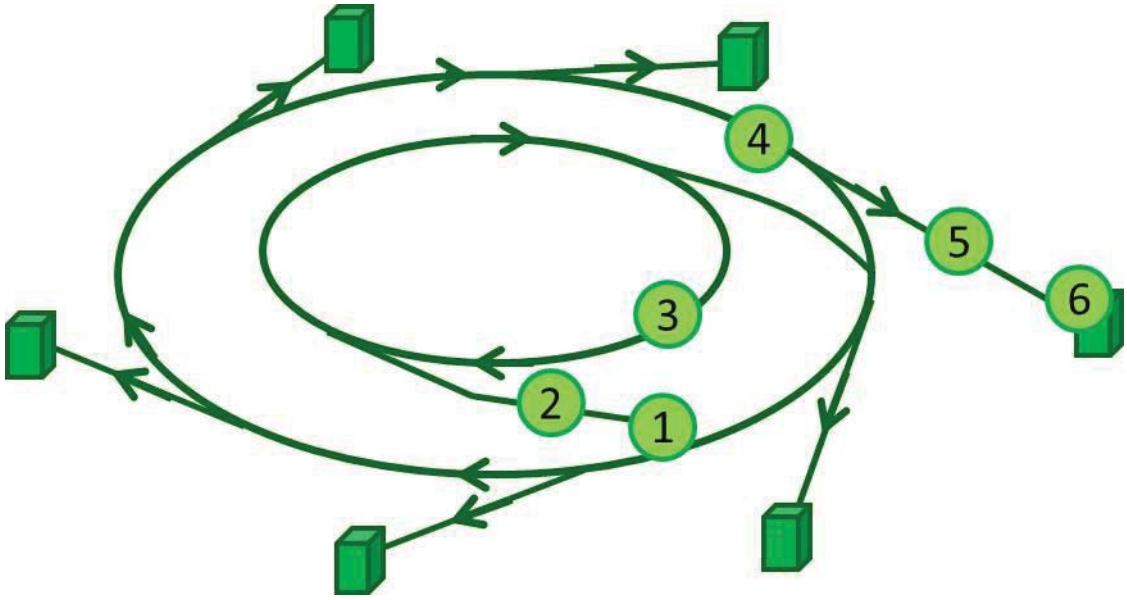

Figure 2.18. Components of a synchrotron: 1) electron gun; 2) linac; 3) booster ring; 4) storage ring; 5) beamline; 6) end station. Adapted from: https://www.synchrotron.org.au/synchrotron-science/how-is-synchrotron-light-created.

Electrons are generated in the centre of a synchrotron by the electron gun. This is done by heating a barium compound cathode to approximately 1000°C. Using 90,000 volts, bunches of electrons are accelerated away from the cathode surface and out of the gun. These charged particles are accelerated by the linear accelerator (linac) to 99.9987% the speed of light and then transferred to the booster ring where their energy is increased to 3GeV. The electrons complete approximately 1 million laps around the booster ring in half a second before they are transferred to the storage ring. The electrons move around the closed orbit for 30-40 hours at a constant energy and continuously produce synchrotron light. A top-up mode is used at the Australian Synchrotron to ensure the number of

circulating electrons remains constant. This is where every two minutes or so more electrons can be injected into the storage ring. Each electron completes 1.4 million laps of the storage ring every second. The storage ring houses bending magnets that are separated by straight sections. When the electrons pass through a bending magnet, the charged particles are forced into a radial motion rather than continuing on a straight path (Figure 2.20). When electrons are deflected they emit electromagnetic radiation, or 'synchrotron radiation/light', producing a beam of synchrotron light at each turn. Each beam of light is 1 million times brighter than the sun and is focused down long pipelines called beamlines. At the end of each beamline is an end station where the synchrotron light encounters the sample.

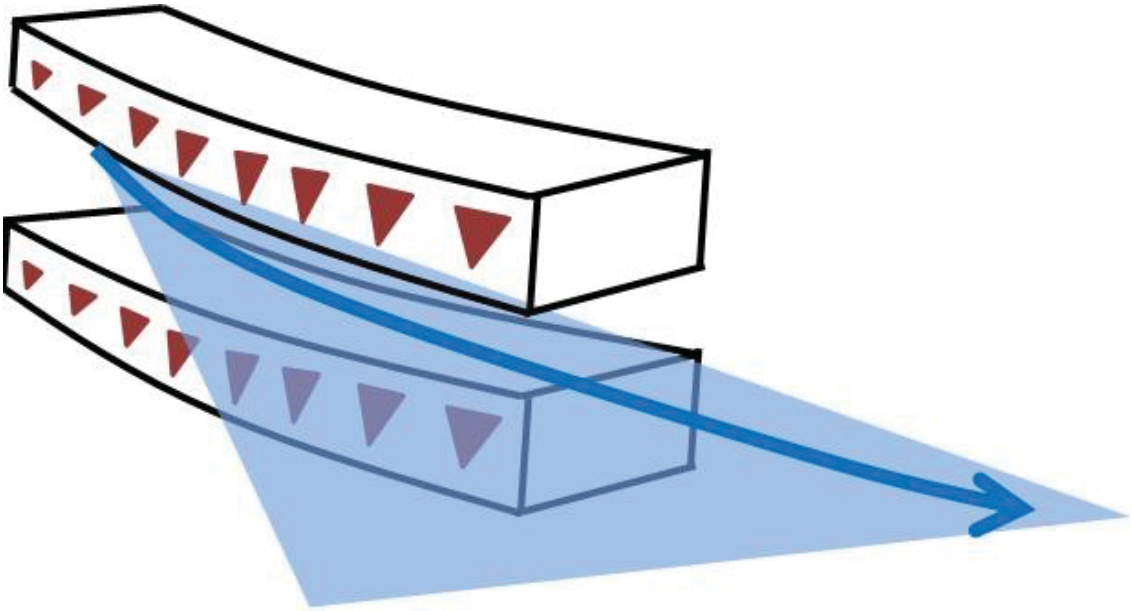

Figure 2.19. A bending magnet changing the path of an electron. Adapted from: https://www.synchrotron.org.au/synchrotron-science/how-is-synchrotron-light-created.

It has been found that special magnetic insertion devices placed in the straight sections of the storage ring significantly increase the intensity of light. Wigglers and undulators are the two types of special magnetic insertion devices that have become key components of storage rings in the past 20 years (Reimers, 2007).

These special magnetic insertion devices are normally a few metres in length and consist of periodic magnetic multipoles. A wiggler (Figure 2.20a) is a multipole magnet that causes the electrons to repeatedly change direction. At each bend, a cone of light is emitted and preceding cones of light superimpose on one another so that the intensity of the light increases with every bend. An undulator (Figure 2.20b) is a series of magnets that are not as strong as those used in a wiggler so the bends in the path of the electron are not as sharp. Cones of light are still emitted at each bend but they only just overlap one another and certain wavelengths are enhanced. The repetitive left and right turns of the electron bunches when passing through a wiggler or an undulator significantly enhances the synchrotron radiation whilst ensuring there is no net deviation from the original direction of travel.

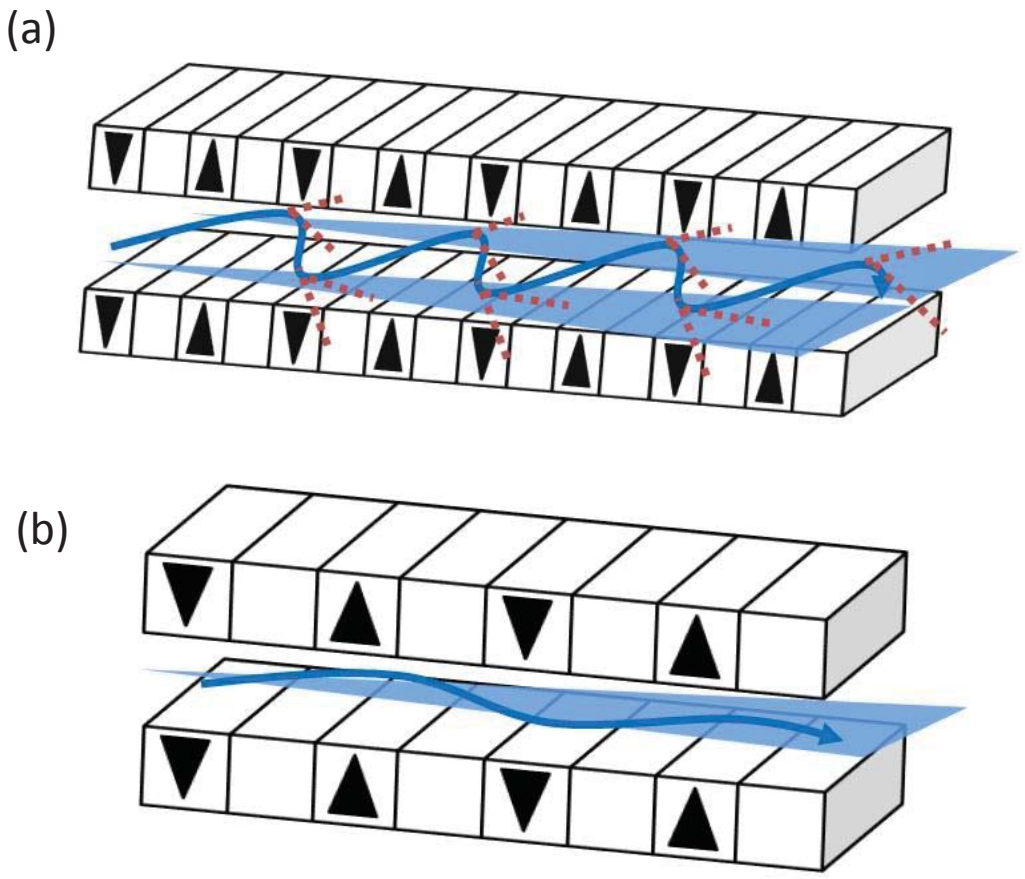

Figure 2.20. (a) a wiggler and (b) an undulator enhancing the intensity of the synchrotron radiation. Adapted from: https://www.synchrotron.org.au/synchrotron-science/how-is-synchrotron-light-created.

2.5.2 General Theory of SAXS

SAXS utilises a narrow beam of monochromatic X-rays and is based on the theory of diffraction. Diffraction is the interference of waves scattered by an object. In the case of X-rays, every electron becomes the source of a scattered wave. The scattered X-ray waves form an interference pattern if the atoms are arranged in a crystal lattice. A two dimensional detector can capture an entire scattering pattern at once (Figure 2.21).

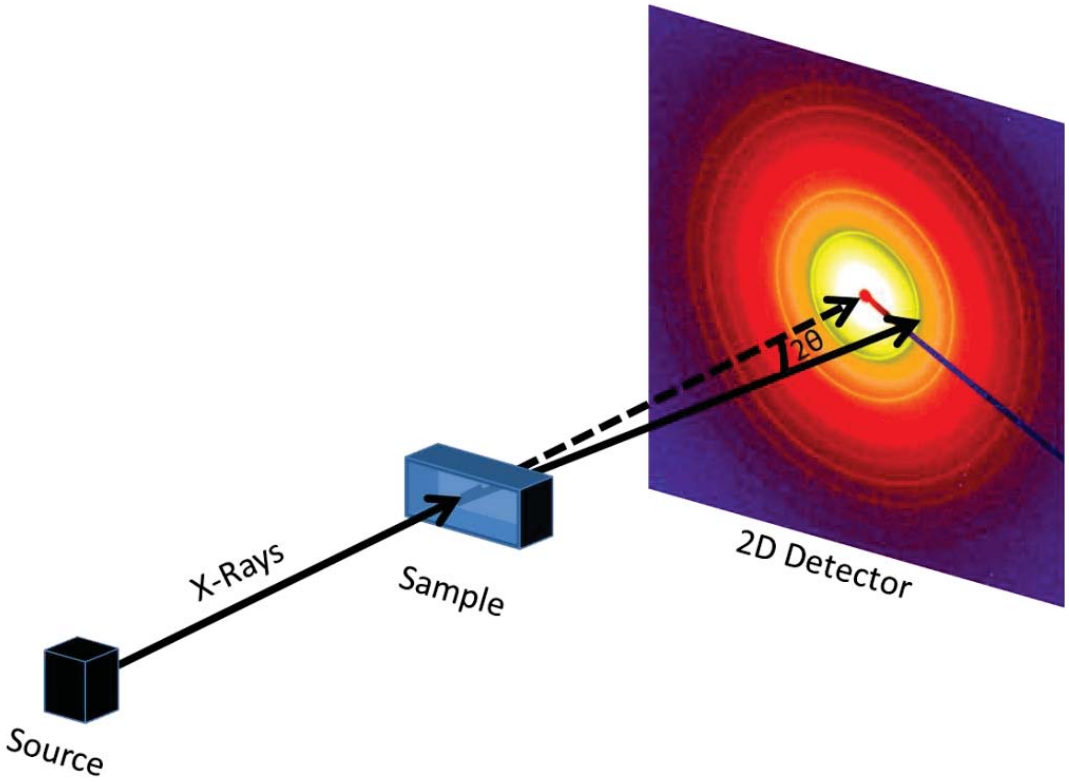

Figure 2.21. Basic SAXS experimental configuration.

The diffraction pattern is dependent on a number of aspects; the incident wave angle, the scattering angle, the crystal structure, and the chemical make-up of the sample. The scattering angle, 2θ, is inversely proportional to the particle size so the larger the distance between two particles or two crystal planes, the smaller the scattering angle (Glatter and Kratky, 1982). SAXS diffraction scans are typically measured at angles less than 10 degrees. This angular scattering range of a few

degrees right down to a few hundredths of a degree enables structural analysis in the particularly topical nanoscale length range (McGuire, 2003).

2.5.3 Bragg's Law

Bragg's Law has formed an integral part of the analysis of collagenous matrix materials presented in this thesis. The origins of the law are presented below to gain more of an understanding of the concepts involved and how it came about.

X-ray diffraction of a crystalline solid was found to produce surprising patterns of reflected X-rays by William Lawrence Bragg and his father William Henry Bragg in 1913 (Thomas, 1990). Bragg explained this pattern by modelling the crystal as a set of parallel planes separated by a constant parameter *d*. Intense peaks, otherwise known as Bragg peaks, occur when scattered waves interfere constructively. Bragg's law describes the condition for constructive interference from successive planes of the crystalline lattice and is illustrated in Figure 2.22 where n is an integer, λ is the wavelength of the incident wave, d is the spacing between the planes in the atomic lattice, and θ is the angle between the incident ray and the scattering planes.

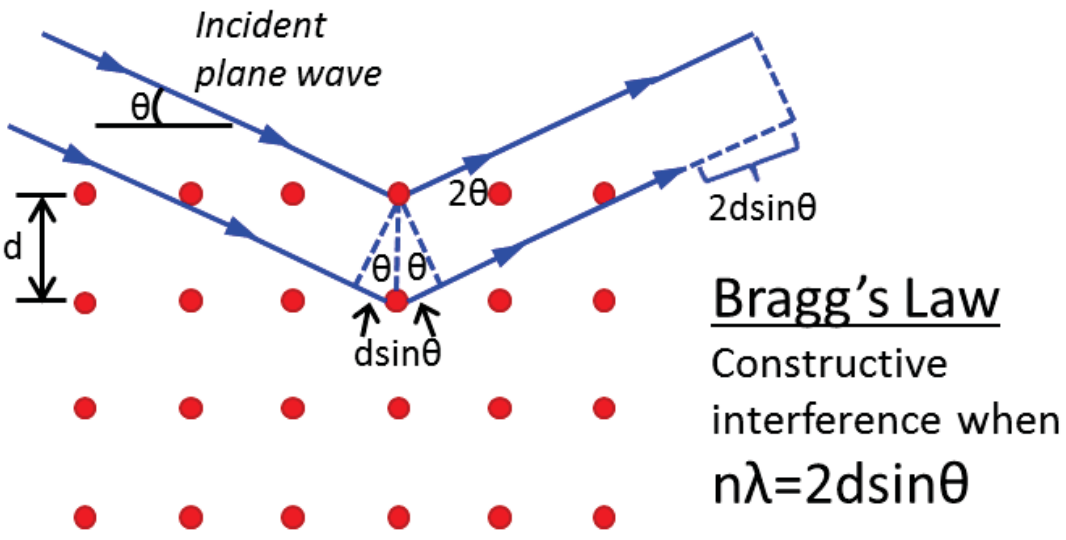

Figure 2.22. Illustration of Bragg's Law.

This illustration (Figure 2.22) showcases a crystalline solid approached by two X-ray beams with identical wavelengths. The beams are scattered off two different atoms with the lower beam traveling an extra distance of 2dsinθ. Constructive interference occurs when this extra length is equal to an integer (n) multiple of the wavelength of the incident X-ray (λ).

The roots of Bragg's law really go back to 1912 when Laue and a small group of scientists made the ground-breaking discovery of X-ray diffraction by crystals. Walter Friedich, Paul Knipping, and Max von Laue submitted a one page report to the Bavarian Academy of Science stating they were "engaged since April 21, 1912 with experiments about the interference of X-rays passing through crystals" (Eckert, 2012). The report laid their claims on the discovery prior to it being formally communicated in a published paper and was backed up by a sketch of the experiment apparatus (Figure 2.23) and some exposures that were sent in with the report.

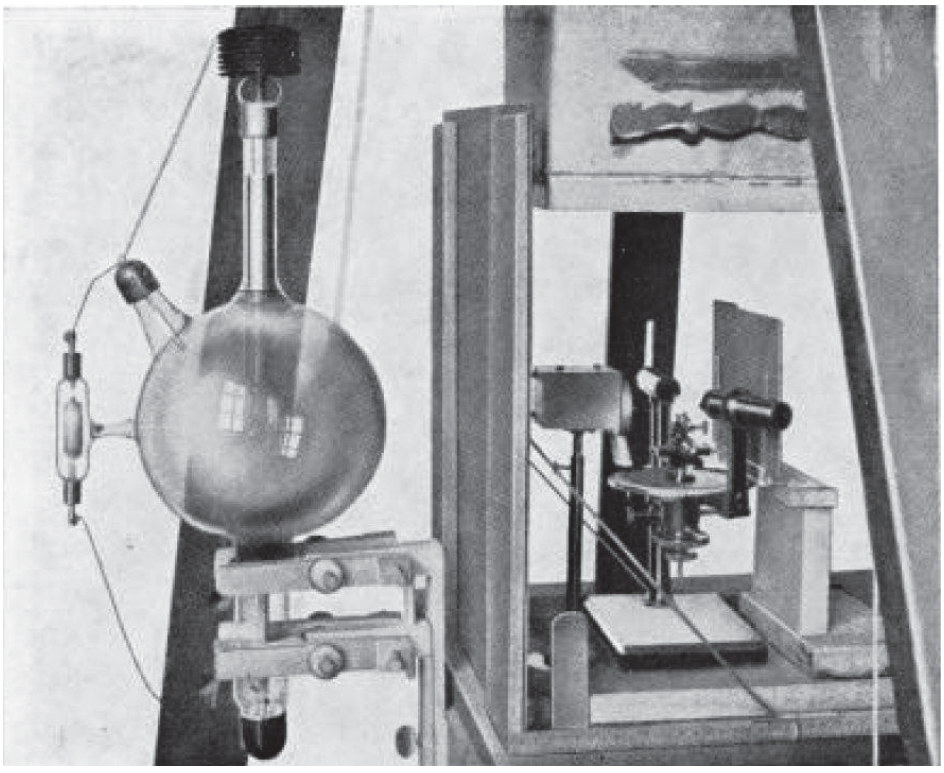

Figure 2.23. Friedich and Knipping's improved experimental set-up (Ewald, 1962). Reprinted from Fifty Years of X-ray Diffraction, P. P. Ewald, Laue's Discovery of X-ray Diffraction by Crystals, pg 41, copyright 1962, with permission from Springer.

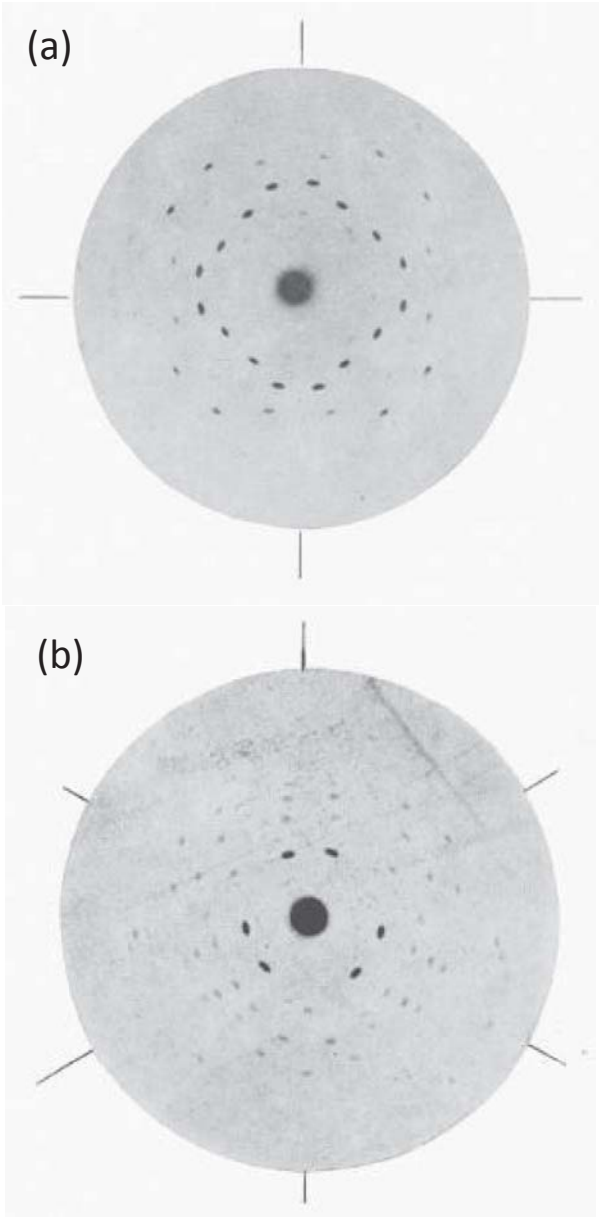

Figure 2.24. Zincblende Laue photographs along (a) four-fold and (b) three-fold axes (Ewald, 1962). Reprinted from Fifty Years of X-ray Diffraction, P. P. Ewald, Laue's Discovery of X-ray Diffraction by Crystals, pg 42, copyright 1962, with permission from Springer.

It was Laue who started to develop a theory based on the assumption that X-rays were electromagnetic radiation. Laue surmised it might be possible for a crystal irradiated with X-rays to give off diffraction effects. On 8th June 1912 at a meeting of the Bavarian Academy, Laue presented an introduction on the theory of diffraction by a three-dimensional lattice (Thomas, 1990). The exciting and truly

ground-breaking discovery quickly gained Max von Laue a Nobel Prize in 1914 for "his discovery of the diffraction of X-rays by crystals" (Nobelprize.org, 2014).

Unfortunately, Laue went wrong when he considered the experimental results from ZnS (Figure 2.24). He fixated on an erroneous notion that the observed effects were associated with X-rays arising in the crystal. Laue also assumed the crystal had a basic cubic structure with one molecule per unit cell. However, despite the flawed assumptions behind his theory, Laue established the wave like nature of X-rays through his explanation of diffraction as the phenomenon causing the observed spots for ZnS.

Sir Lawrence Bragg and his father William Henry Bragg were very much interested in the nature of X-rays and Laue's paper intrigued them. Bragg was able to piece together a collection of several different pieces of knowledge from lectures he had attended that culminated in Bragg's law and provided the answer to Laue's ZnS spots.

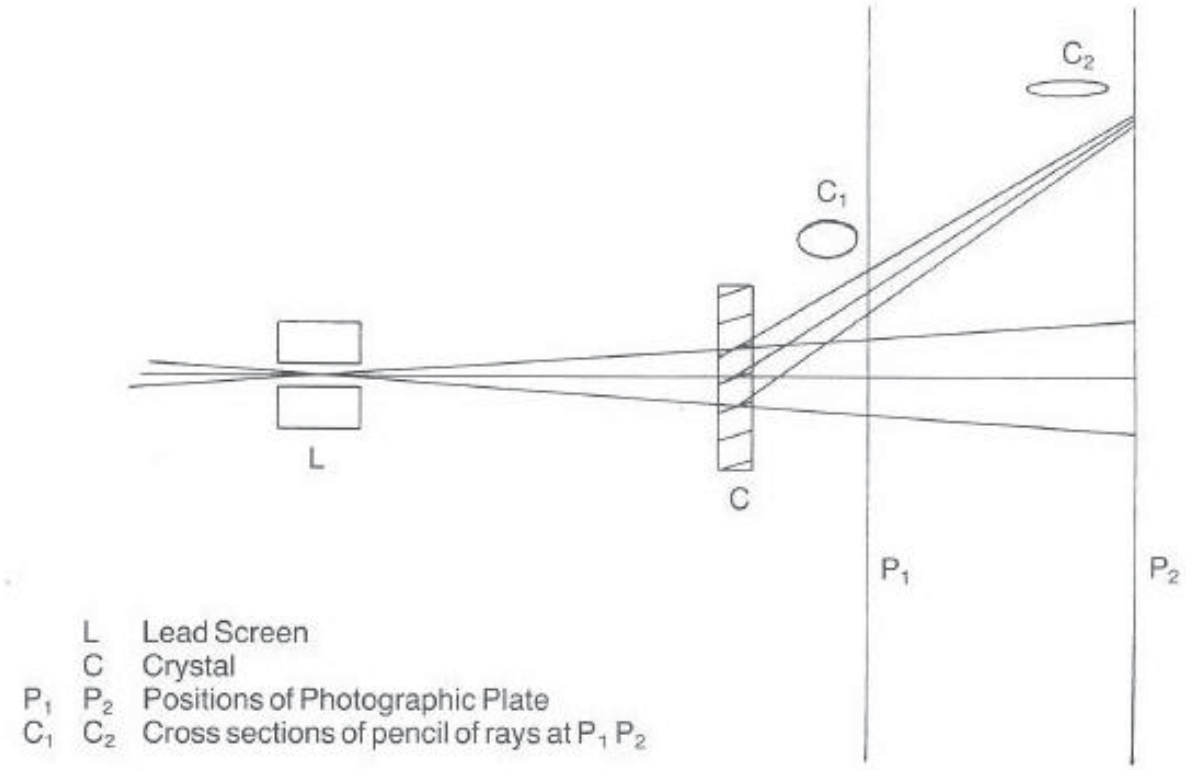

Figure 2.25. Change of shape of X-ray reflections as the photographic plate was moved further away from the crystal (Thomas, 1990).

X-ray reflections were round when the plate was close to the crystal. These reflections that were round became elliptical in the horizontal direction when the photographic plate was moved further away from the crystal (Figure 2.25). Bragg pointed out that an incident cone of X-rays of continuously varying wavelengths that are reflected by lattice planes would come to focus in the vertical direction but would spread out in the horizontal direction (Thomas, 1990).

The idea that sheets of atoms in the crystals reflected formless X-ray pulses came to Bragg. If regarded in such a way then, similar to Wilson's treatment of a diffraction grating (using a diffraction grating white light could be a succession of formless pulses which the lines of a diffraction grating convert into a train of waves (Thomas, 1990)), a wave train would be formed from the pulses reflected from successive equidistant sheets. Since the path difference between the waves of the reflected train is $2d \sin \theta$ where θ is the glancing angle at which the radiation falls on the planes and d is their spacing, it followed immediately that the wavelengths (λ) of the different orders of reflection would be given by $n\lambda=2d\sin\theta$ where n is an integer. Bragg then drew upon the idea that lattices could be both simple cubic or face-centred lattices from a lecture by Gosling on crystal structures. Laue had previously tried to describe the observations of ZnS based on a simple cubic structure. Bragg endeavoured to explain the ZnS diffraction photographs assuming the structure is a face-centred cubic lattice. Everything fell into place. Bragg showed that the Laue pictures were made by a continuous range of X-ray wavelengths, a kind of white radiation, and that X-ray diffraction could be used to get information about the crystal structure. This was the start of X-ray analysis of crystals. Sir Lawrence Bragg and his father were awarded a Nobel Prize in Physics in 1915 for "their services in the analysis of crystal structure by means of X-rays" (Nobelprize.org, 2014).

Bragg's Law made it possible for crystal structures to be explored and defined with collagen being a prime example of this. Collagen fibrils showcase axial periodicity. This d banding pattern includes a gap region and an overlap region in every d spacing period. SAXS patterns of collagen produce Bragg peaks due to this highly repetitive structure. As such it is possible to determine the d spacing of the collagen fibrils from the location of the Bragg peaks.

2.5.4 SAXS of Collagen Biomaterials

SAXS diffraction patterns of fibrous collagen biomaterials such as leather hold information on the arrangement of fibrils within a sample, the axial periodicity of the collagen, and the fibril diameter of the collagen.

Previously, the structure of leather has been investigated using SAXS. Boote et al (Boote et al., 2002) demonstrated that when subjected to increasing amounts of strain the collagen fibrils become more aligned. Sturrock et al (Sturrock et al., 2004) continued on leading to the discovery that the application of biaxial strain during the drying of leather leads to substantial increases in its stiffness. The increase was attributed to a reorientation of the collagen fibrils in planes perpendicular to the surface. Later it was proven that SAXS provides a wealth of useful information that may be used to characterize and compare leathers, skin, and connective tissue. The degree of fibre orientation and the dispersion of the orientation has been quantified in leather (Basil-Jones et al., 2010).

A clear understanding of a nanostructural characteristic of ovine and bovine leather that leads to differences in strength was defined using information extracted from SAXS patterns. A correlation has been found between the tear strength and the orientation of collagen microfibrils in ovine and bovine leather with stronger leather having more fibrils aligned with the surface of the leather, with less cross-over between layers, than weak leather (Basil-Jones et al., 2011). The structural changes of leather when subjected to strain have been defined. Initially an increase in the orientation index was observed as the fibrils reorient under strain. This is followed by a secondary mechanism occurring when the stress is taken up in the individual fibrils showcased by an increase in the D-spacing (Basil-Jones et al., 2012). X-ray measurements have been used to characterise the orientation of collagen microfibrils from various locations on a hide. It was demonstrated that the orientation of collagen fibrils does not vary significantly between different positions in ovine skins which was in contrast to bovine hides (Basil-Jones et al., 2013).

Chapter 3: Collagen Orientation and Leather Strength for Selected Mammals

Collagen materials have a mechanical function, so the manner in which collagen provides them with their strength is of fundamental importance. Previously it has been shown that the orientation of collagen fibrils is correlated with strength; understanding whether this correlation extended across a number of different species formed the basis of this investigation. This study shows that the tear strength of leather across seven species of mammals depends on the degree to which collagen fibrils are aligned in the plane of the tissue. Tear-resistant material has the fibrils contained within parallel planes with little cross-over between the top and bottom surfaces. The orientation index is shown to be linearly related to tear strength such that greater alignment within the plane of the tissue results in stronger material, for example deer leather (Figure 3.1b), while a weaker material has greater cross-over between the planes of the leather as is seen in sheep leather (Figure 3.1a). The statistical confidence and diversity of animals suggests that this is a fundamental determinant of strength in tissue. This insight is valuable in understanding the performance of leather and skin in biological and industrial applications.

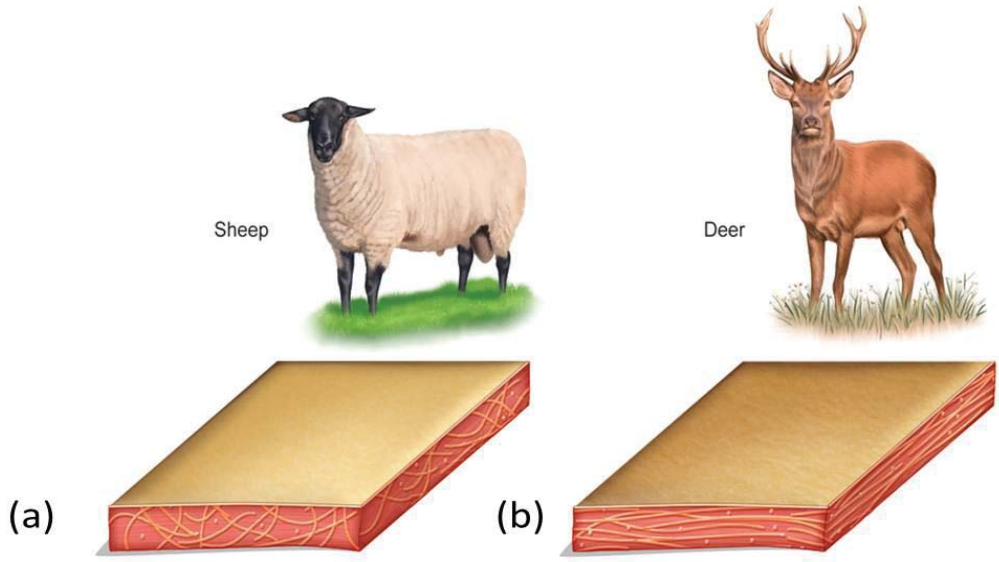

Figure 3.1. Structure-strength relationship of leather: (a) sheep leather with a lower orientation with more cross-over within planes, weaker material; (b) deer

leather with a higher orientation with less cross-over within planes, stronger material (Sizeland et al., 2013).

The following investigation has been published in the Journal of Agricultural and Food Chemistry, Volume 61, Issue 4, pages 887-892 and can be found in Appendix 10.1.

3.1 Introduction

The strength of collagen materials is of crucial importance both in medical and industrial contexts. Collagen is the main structural component of skin (Fratzl, 2008), leather, and some medical scaffolds (Floden et al., 2010). Medical conditions can arise when tissues do not have the required mechanical strength, such as in aneurysms (Lindeman et al., 2010), cervical insufficiency (Oxlund et al., 2010), osteoarthritis (Narhi et al., 2011), and damaged articular cartilage (Stok and Oloyede, 2003). In addition, bone is a composite material in which the structure of collagen is considered important for bone toughness (Zimmermann et al., 2011, Skedros et al., 2006). Strength is also a requirement for collagen-based medical materials such as extracellular matrix scaffolds (Floden et al., 2010) and processed pericardium for heart valve repair (Jobsis et al., 2007). Leather, which is processed skin consisting mostly of collagen, is produced on a large scale for shoes, clothing and upholstery (Commodities and Trade Division, 2010), with high strength being a primary requirement for high-value applications.

Factors that have previously been considered as possibly contributing to the strength of collagenous materials include the amount of collagen present, the molecular structure of the collagen (D-spacing, collagen type), the nature of the cross linking between collagen (Chan et al., 2009), collagen bundle size, and collagen orientation. Of these, much attention has been given to collagen orientation which has been investigated in the cornea (Boote et al., 2011, Kamma-

Lorger et al., 2010), heart valve tissue (Sellaro et al., 2007), pericardium (Liao et al., 2005), bladder tissue (Gilbert et al., 2008), skin (Purslow et al., 1998), and the aorta (Gasser, 2011).

Crimp, the sinuous arrangement of fibre bundles, has been associated with high strength in tendons (Franchi et al., 2007) as well as in heart valves (Joyce et al., 2009), with high crimp resulting in high strength. However, in studies of processed skins of varying strength, crimp was not observed (Basil-Jones et al., 2011).

Collagen orientation has been measured by reflection anisotropy (Schofield et al., 2011), atomic force microscopy (Friedrichs et al., 2007), small angle light scattering (Billiar and Sacks, 1997), confocal laser scattering (Jor et al., 2011), Raman polarization (Falgayrac et al., 2010), anisotropic Raman scattering (Janko et al., 2010), multiphoton microscopy (Lilledahl et al., 2011), and small angle X-ray scattering (SAXS) (Kronick and Buechler, 1986, Basil-Jones et al., 2011, Basil-Jones et al., 2012).

Previously studied was ovine and bovine leather of differing strengths (Basil-Jones et al., 2011) which found a statistically significant relationship between tear strength and edge on orientation. It was speculated that this trend may be of a more general nature. This formed the basis of this investigation and fibril orientation in seven species of mammals was measured to see if this relationship held true.

3.2 Experimental Procedures

3.2.1 Leather Processing and Sampling

The Leather and Shoe Research Association Inc. (LASRA) provided all leather samples for analysis. Samples from ovine skins provided the basis for majority of the work presented in this thesis. The processing method for these skins followed

conventional tanning and beamhouse processes. Specific details of these processes are outlined below along with the selection of the samples.

Ovine pelts were obtained from five-month-old, early season, New Zealand Romney cross lambs. The skins were washed with cold water, dried, and salted. As "salted green" skins they were stored until needed. When needed, after mechanical removal of adhering fat and flesh, conventional lime sulfide paint, comprising 140 g/L sodium sulfide, 50 g/L hydrated lime and 23 g/L pre-gelled starch thickener, was applied to the flesh side of the skin at 400 g/m^2. The residual keratinaceous material was then removed over a period of 16 hours in a 1.2% solution of sodium at 20°C. The pelts were then washed to remove the lime and the pH lowered to 8 with ammonium sulfate, followed by the addition of 0.1% (w/v) Tanzyme (a commercial bate enzyme, Tryptec Biochemicals, Ltd.). This was followed by pickling in a 2% sulfuric acid and 10% sodium chloride solution. Using oxazolidine the pickled pelts were pretanned, degreased with an aqueous surfactant, and then washed. The skins were neutralised in 8% NaCl, 1% disodium phthalate solution (40% active; Feliderm DP, Clariant, UK) and 1% formic acid for 10 min. The running solution was then made up to 5% chrome sulphate (Chromosal B, Lanxess, Germany) and processed for 30 min followed by 0.6% magnesium oxide addition, based on the weight of the skins, to fix the chrome, and processed overnight at 40°C.

The partially processed skins or "wet blue" pelts were then retanned as follows. Wet blue pelts were first neutralised in 1% sodium formate and 0.15% sodium bicarbonate for 1 h. The neutralised wet blue was then washed in two volumes of water and retanned in one volume of water containing 2% synthetic retanning agent (Tanicor PW, Clariant, Germany) and 3% vegetable tanning material (Mimosa, Tanac, Brazil).

Finally, 6% mixed fat liquors were added and the leathers processed at 50°C for 45 minutes. The leather was then fixed by adding 0.5% formic acid and processed for 30 minutes. The leather was drained and washed in three volumes of cold water prior to mechanical softening.

Leather sampling was done using the following procedures. Samples were cut on a flat surface with a sharp scalpel and a ruler using an even downward pressure. It was ensured prior to cutting that the sampling area was free from all obvious defects such as scratches and cuts. All samples were cut from the official sampling position (OSP) on the left or the right side of the backbone, a position defined by Williams (Williams, 2000b) and pictured as the shaded area in Figure 3.2a. Figure 3.2b gives a clear indication as to the location of the OSP in relation to the anatomy of the animal.

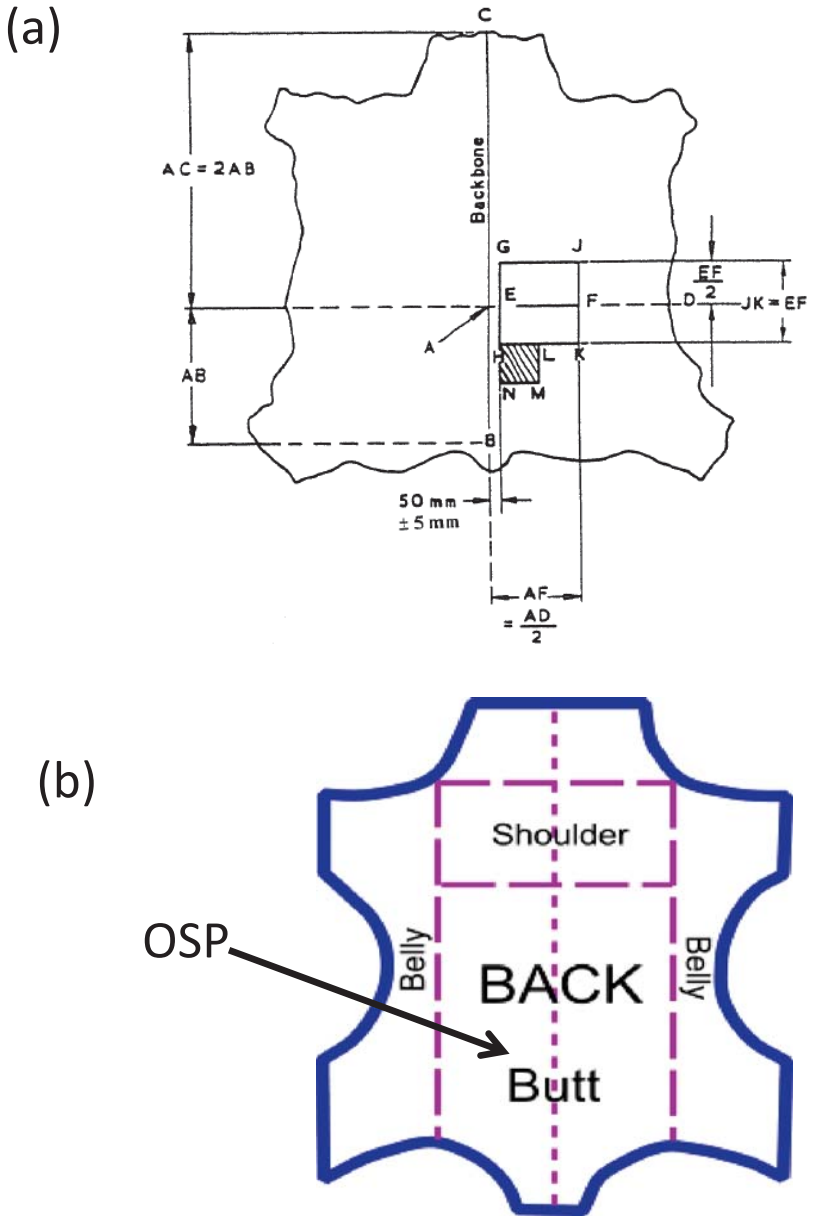

Figure 3.2. Representation of a hide or skin showing the sampling location for whole hides, skins and sides: (a) From Williams (Williams, 2000b) where B is the

root of the tail, AD is a line perpendicular to BC, AC=2AB, AF=FD, JK=EF, GE=EH, HL=LK=HN, and AE=50 mm ± 5 mm; (b) simplification of hide showing the OSP in relation to anatomical features of the animal.

When investigating the nanostructure of the collagen fibril network of leather using synchrotron based SAXS, the samples are placed in the beamline so the full plane of the leather facing the beam is analysed. This provides information on the structure in the x and y directions, but not the z direction. For this work it was important to gain a full three dimensional view of the material. In order to achieve this, samples were cut in different directions from the leather pelts.

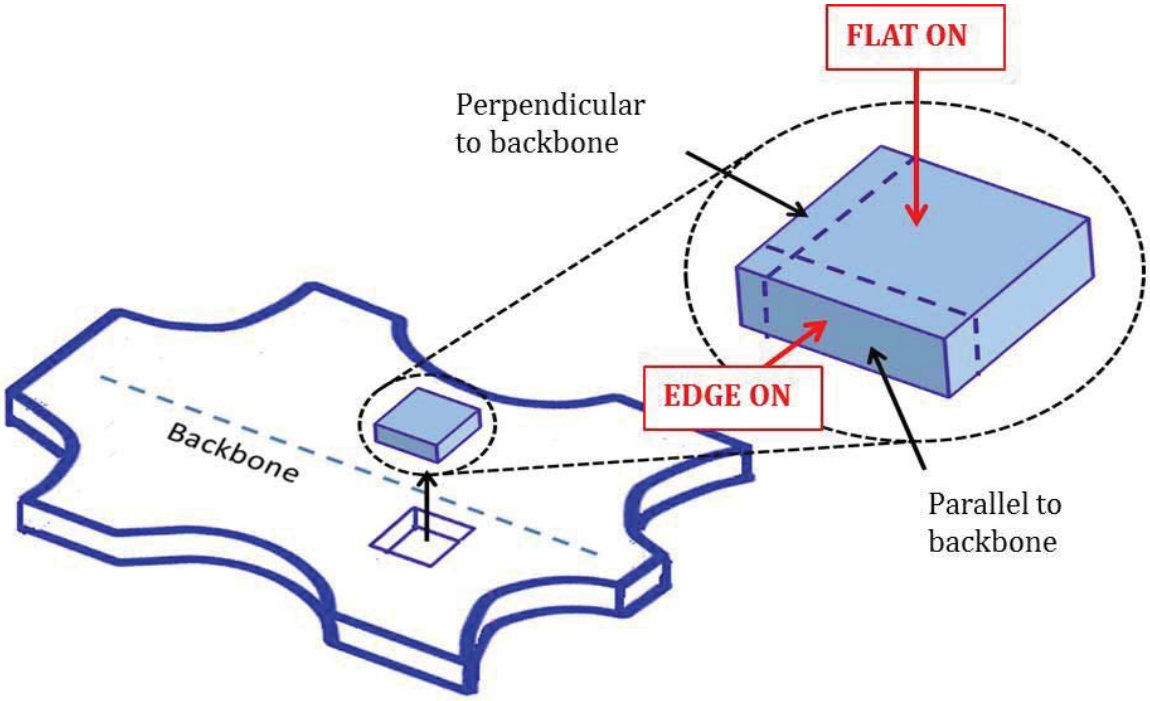

Figure 3.3. Sample cut from the OSP will either be cut as a square for flat on analysis or will be cut along the dotted lines of the square for samples that are parallel or perpendicular to the backbone of the hide.

All samples were cut from the OSP in directions either perpendicular or parallel to the backbone of the hide as shown in Figure 3.3 where the backbone is indicated by the dotted line up the centre of the pelt. These samples were named “edge on”

as when they are placed in the beamline, analysis is done to show the collagen fibrils through the full thickness of the leather. Samples cut for static, edge on analysis measure approximately 1 mm x 30 mm. While the samples may seem thin with a width of 1 mm, the beam size is only 250 x 80 μm so a large sample is not needed to obtain a number of measurements across the leather surface. Majority of measurements are performed through the thickness of the leather to gain structural values for both the corium and grain layers of the sample. It is not necessary to have a wide sample when doing this as the full thickness of the sample can still be analysed. To obtain information in the third dimension, samples need to be analysed from the top surface of the leather. To do this square samples were cut for analysis and placed with the beam pointing perpendicular to the surface of the grain. These samples were named “flat on” and measured approximately 30 mm x 30 mm. For these samples the beam passes through both the grain and the corium layers and allows the structure to be visualised in the z direction. For individual analysis of each layer the square sample was carefully sliced along the intersection of the grain and the corium. The thickness, length, and width of all samples was measured with callipers using a light and consistent force and recorded for future use. Details of all samples were recorded when cut and the samples were stored at room temperature in small, numbered, lidded glass or plastic vials to ensure no information was lost and samples remained unharmed and easily identifiable after transportation (Figure 3.4).

Figure 3.4. An example of the leather samples in plastic and glass vials for storage and transportation.

3.2.2 Small Angle X-Ray Scattering

Small angle X-ray scattering is a technique that is able to provide a wealth of knowledge about macromolecules on the micro scale. As such it is an ideal platform for the nanostructural analysis of collagen based extracellular matrix materials such as leather.

Figure 3.5. SAXS/WAXS beamline at the Australian Synchrotron.

The Australian Synchrotron is a world class facility that provides scientists and researchers with the opportunity to undertake ground breaking research. Ranging from infrared to hard X-rays the Australian synchrotron is a source of highly intense light that can be used across a broad spectrum of research purposes. A research facility of such a high calibre is of course in high demand and beamtime on every single one of the beamlines at the Australian Synchrotron is highly oversubscribed to. Applications for beamtime to analysis fibrous collagen materials on the SAXS/WAXS beamline (pictured in Figure 3.5) have been successful.

At the SAXS beamline each sample was mounted without tension on a custom made plate with a grid of 64 or 132 holes with a 10 mm diameter. Samples were

mounted in two orthogonal directions through the leather; edge on and flat on. Figure 3.6 depicts the direction of the beam for each sample. Edge on samples were fixed to the plate so the full thickness of the leather was subjected to the X-ray beam and measurements were made every 0.25 mm from the grain to the corium. Flat on samples were fixed with the uncut face of the leather directed towards the X-ray beam which was perpendicular to the surface of the leather and four measurements were made per sample in a rectangular grid.

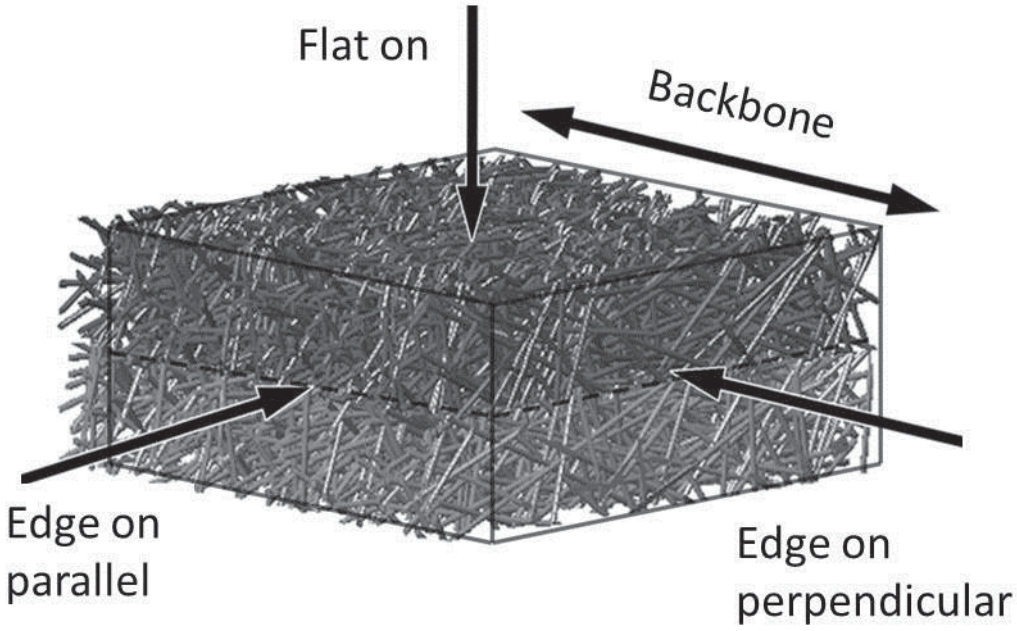

Figure 3.6. Direction of beam on the sample for edge on and flat on sample directions.

Each sample was mounted horizontally across one of the holes and attached to the plate using adhesive tape (Fig 3.7a shows edge on mounted samples). When it was critical that a sample did not dry out and kept its moisture content the sample was placed within one of the holes on the plate and sandwiched in place using kapton tape on both sides of the sample (Fig 3.7b). Kapton tape does not interfere with the diffraction process so has no impact on the results and provides protection to stop the sample from drying out. All plate samples were mounted without tension. Once all the samples are taped in place the plate was attached to a sample stage in the

SAXS beamline. This stage is able to be remotely controlled from outside the beamline hutch and a camera enables the samples to be seen by the beamline user. Static samples only take approximately 10 minutes per sample to collect the diffraction patterns. The remotely controlled sample stage and plate loaded with up to 132 samples is hugely beneficial for maximising the time on the SAXS beamline. If the sample had to be manually changed, the user would have to not only load a new sample into the beamline every time but go through the standard safety procedures required as well, all of which would probably double the allocated time per sample.

(a)

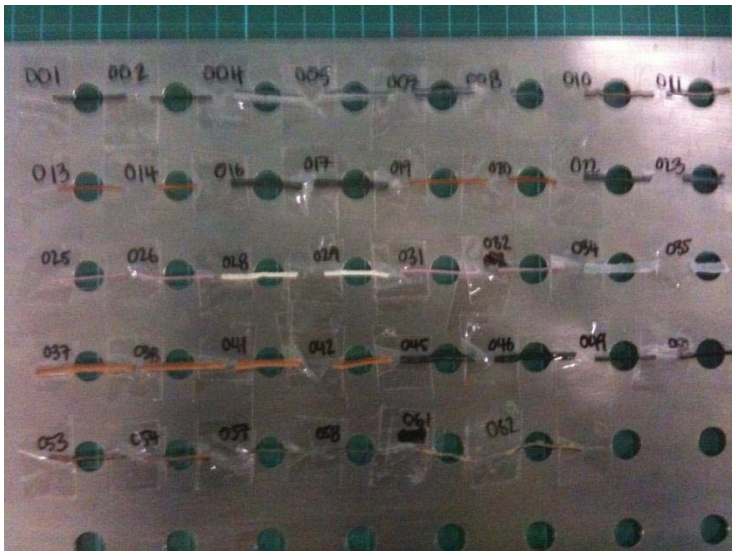

(b)

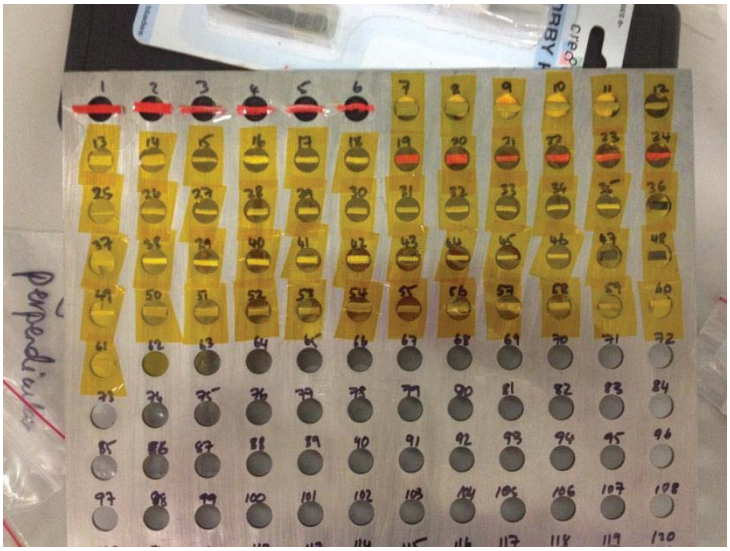

Figure 3.7. (a) edge on samples mounted on the plate ready to be inserted into the beam; (b) wet edge on samples sandwiched between kapton tape on the plate and ready to be inserted into the beam.

Diffraction patterns were recorded on the Australian Synchrotron SAXS/WAXS beamline, using a high-intensity undulator source. An energy resolution of 10^{-4} was obtained from a cryo-cooled Si(111) double-crystal monochromator and the beam size (full width at half maximum [FWHM] focused at the sample) was 250 x 80 µm, with a total photon flux of about 2 x 10^{12} photons s^{-1}. Diffraction patterns were recorded with an X-ray energy of 8 keV using a Pilatus 1M detector with an active area of 170 x 170 mm and a sample-to-detector distance of 3371 mm. Exposure time for the diffraction patterns was 1 second and data processing was carried out using the SAXS15ID software (Cookson et al., 2006).

Diffraction patterns as shown in Figure 3.8a were obtained for each point analysed. These patterns can be integrated to produce intensity plots that display Bragg peaks (Figure 3.8b).

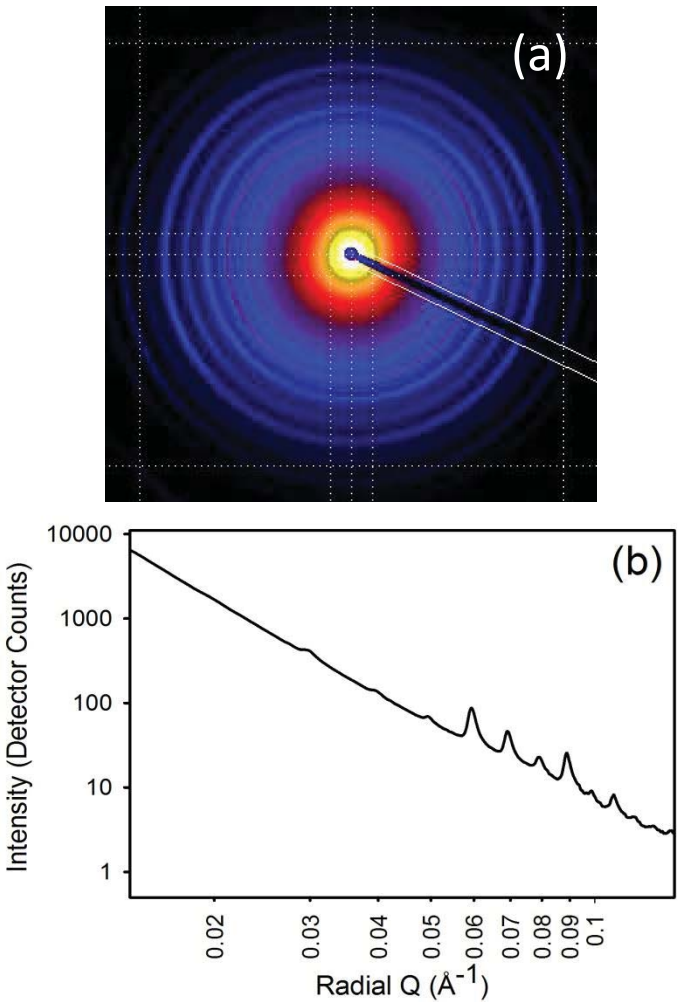

Figure 3.8. (a) SAXS diffraction pattern; (b) plot of intensity versus q.

The diffraction patterns obtained from the SAXS beamline at the Australian Synchrotron hold a surprisingly large amount of information on the structure of the material being analysed. This work focuses on the orientation and the D-spacing of the collagen fibrils. Data was processed using scatterBrainAnalysis (Cookson et al., 2006) and Microsoft Excel. Two important structural aspects of collagen, the orientation index and the D-spacing, are able to be extracted from SAXS diffraction patterns and remain at the centre of the work presented in this thesis.

The orientation index, OI, is defined as (90° – OA)/90°, where OA is the minimum azimuthal angle range, centred at 180°, that contains 50% of the microfibrils (Sacks et al., 1997, Basil-Jones et al., 2010). Using the spread in azimuthal angle of one or more D-spacing diffraction peaks. The peak area is measured above a fitted baseline, at each azimuthal angle. OI provides a measure of the spread of microfibril orientation. An OI approaching 1 indicates that the microfibrils are parallel to each other and the leather surface while an OI of 0 indicates the microfibrils are randomly oriented. The OI was calculated from the spread in azimuthal angle of the most intense Bragg peak which occurs at a q value of around 0.059–0.060 Å. Each OI value presented here represents the average of 14–36 measurements of one sample. For this investigation the sheep and cattle OI averages are derived from 228, 249 and 167 measurements from 15, 14 and 10 samples, respectively and have been reported previously (Basil-Jones et al., 2011). It is not necessary that the samples are highly representative of the particular animal species for general strength-structure relationships to be studied; that there is a range of skins with different strengths is important, although the observed strengths for each species are within industry norms.

The axial periodicity or D-spacing of collagen provides an indication of the nanostructural architecture of collagen microfibrils. The D-spacing is determined for each pattern by taking the central position of a Gaussian curve fitted to one or several of the collagen peaks, dividing these by the peak order (usually from $n = 5$ to $n = 10$), and averaging the resulting values. To do this each of the SAXS diffraction patterns is converted to an ASCII file using scatterBrainAnalysis and this is pasted into an Excel template spreadsheet. The Excel template creates a plot

of intensity versus scattering vector, q (as was shown in Figure 3.8b). The q range to be analysed is manually selected, ensuring the full width of the peak is incorporated. The peak fitting function determines the order of the Bragg peak and the location of it. Standard analysis is based on the 5th to the 9th Bragg peaks.

The scattering vector q can be defined as;

$$q = \frac{4\pi \sin\theta}{\lambda} \qquad \text{(equation 1)}$$

Equation 2 can be rearranged to give λ;

$$\lambda = \frac{4\pi \sin\theta}{q} \qquad \text{(equation 2)}$$

Bragg's law is:

$$n\lambda = 2d \sin\theta \qquad \text{(equation 3)}$$

Substituting equations 2 into equation 3 gives;

$$2d \sin\theta = n\frac{4\pi \sin\theta}{q} \qquad \text{(equation 4)}$$

Dividing equation 4 by 2 sinθ yields;

$$d = \frac{2\pi n}{q}$$

Where n = peak order and d = D-spacing.

The D-spacing was determined for each pattern by taking the central position of several of the collagen peaks, dividing these by the peak order (usually from n = 5 to n = 10) and averaging the resulting values.

3.2.3 Tear Strength Testing

Tear strengths were measured for all samples using standard methods (Williams, 2000a). Samples were cut from the leather at the OSP (Williams, 2000b). The samples were then conditioned at a constant temperature and humidity (20 °C and 65% relative humidity) for 24 h and then tested on an Instron 4467 (Figure 3.9 below).

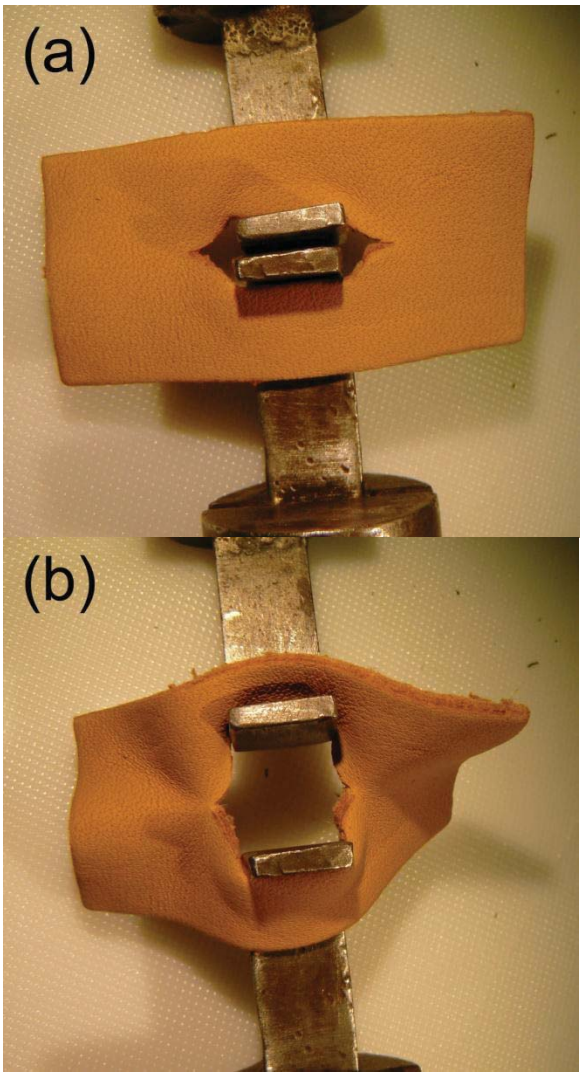

Figure 3.9. Tear test on a leather sample: (a) at start of test; (b) part way through test (Sizeland et al., 2013).

3.3 Results

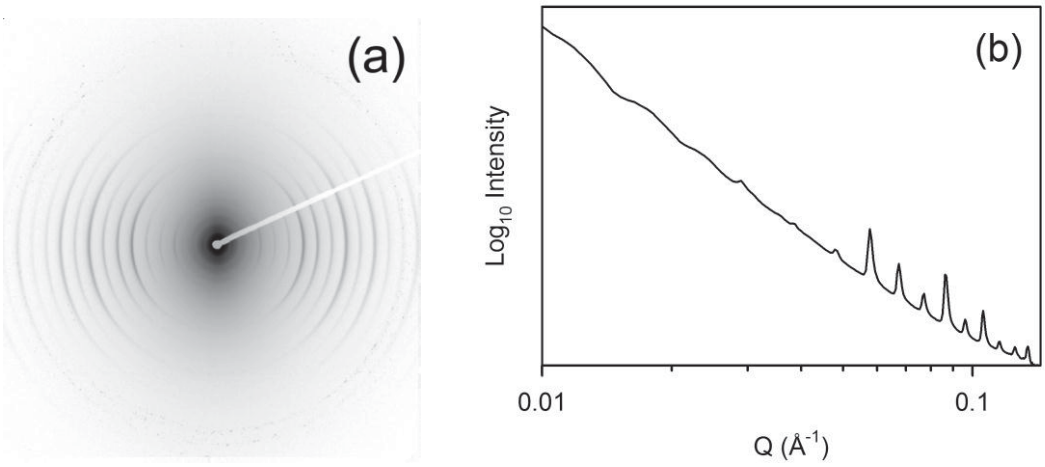

Figure 3.10. SAXS analysis of leather. a) A raw SAXS pattern; b) integrated intensity of a whole pattern (Sizeland et al., 2013).

The SAXS patterns display rings representing the collagen fibril repeating structure (Figure 3.10a). The integrated intensity of the whole pattern enables the position of these peaks to be clearly identified (Figure 3.10b) and from these the D-spacing is determined. The D-spacing varied from 0.628 to 0.653 nm (Figure 3.11) but there is no significant correlation between D-spacing and strength.

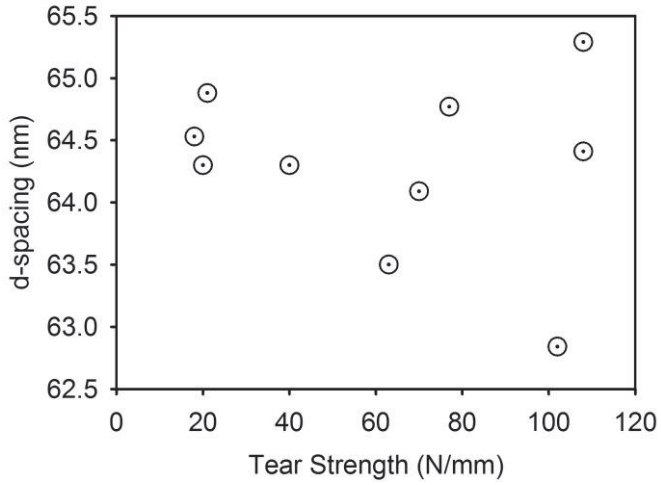

Figure 3.11. Collagen D-spacing and tear strength for leather from different animals (Sizeland et al., 2013).

For any of the rings visible in the SAXS pattern, which correspond to a peak in the meridonal angle, the variation in intensity with azimuthal angle can be plotted (Figure 3.12), which gives a quantitative measure of fibril orientation, represented here as an orientation index (OI).

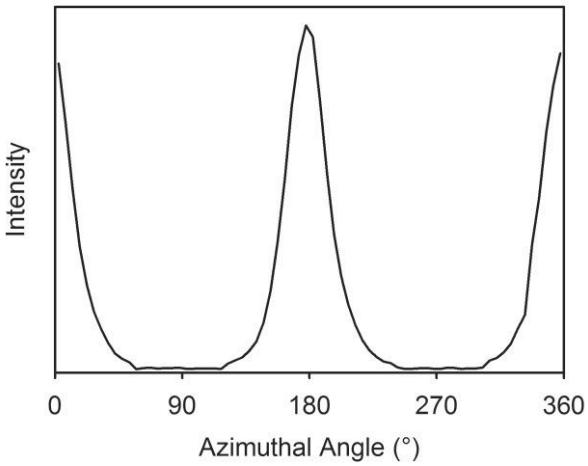

Figure 3.12. Azimuthal variation in intensity at one value of q (one collagen peak) (Sizeland et al., 2013).

There is a large difference in OI between the measurements taken flat on or normal to the leather surface and measurements taken edge on to the leather. The OI normal to the surface is in the range 0.18 – 0.35, with the exception of horse leather (Figure 3.14a), whereas for the edge on measurements the range is 0.41 – 0.63 (Figure 3.14b). Therefore the major component of fibril alignment is planar.

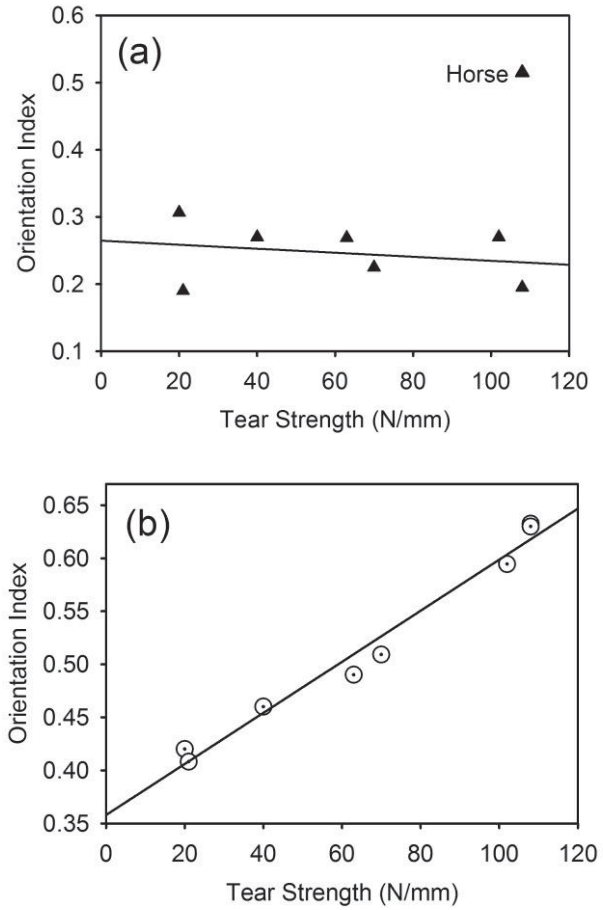

Figure 3.13. Collagen fibril orientation and tear strength for leather from different animals: (a) measured flat on; (b) measured edge on (Sizeland et al., 2013).

There is a strong correlation between tear strength and OI (Table 1; Figure 3.13b) for the edge on measurements, with a least squares fitted slope of 0.0024 mm/N (n = 8, r^2 = 0.98, P < 0.0001). This is a remarkably good correlation. Edge on analysis provides a measure of fibril orientation not frequently accessed. It conveys the degree to which the collagen fibrils are organised in parallel planes as opposed to crossing between the top and the bottom surfaces of the skin.

For the measurements on the flat, if horse leather is excluded as an outlier, then there is little correlation between tear strength and OI (Figure 3.13a) with a least squares fitted slope of 0.0003 mm/N (n = 7, r^2 = 0.06, P = 0.60), suggesting the slight possibility of a negative correlation. This is the more widely used direction of analysis for collagen fibril orientation measurements.

Table 3.1. Leather tear strength compared with orientation index (OI) of collagen fibrils[a].

Animal	Scientific name	Tear strength normalized for thickness (N/mm)	OI measured edge on (average through thickness)
sheep (selected weak)	*Ovis aries*	20	0.420
possum	*Trichosurus vulpecula*	21	0.408
sheep (selected strong)	*Ovis aries*	40	0.460
cattle	*Bos primigenius taurus*	63	0.490
goat	*Capra aegagrus hircus*	70	0.509
water buffalo	*Bubalus bubalis*	102	0.595
deer	*Cervus elaphus*	108	0.630
horse	*Equus ferus caballus*	108	0.633

[a]OI values are the average taken across the thickness of one sample (about 5-10 points) except for sheep and cattle, where these are an average of 6-10 leather samples with 5-10 points for each.

3.4 Discussion

D-spacing. The D-spacing of collagen is known to vary with age (Scott et al., 1981) but it has not been linked with mechanical strength. A link with strength is also not found, therefore supporting the current understanding, although we find a large variation in D-spacing across a large range of strength (Figure 3.11).

Orientation and strength. Collagen orientation shows a strong correlation with tear strength when measured edge on and this relationship is represented in part by existing models. A relationship between fibre alignment and tensile strength has been modelled previously where strength is due to the sum of the components of the fibrils that lie in the direction of force in addition to a component due to the other matrix materials (Bigi et al., 1981). This relationship is represented by Equation. 5.

$$E_z = E_f v_f \int_0^{2\pi} \int_0^{\pi/2} \cos^4 \theta \, F(\theta,\phi) \, d\theta \, d\phi + (1 - v_f) E_m \qquad \text{(equation 5)}$$

Where E_z is the composite Young's modulus of the material in direction z, E_f and E_m are the Young's moduli of the fibres and matrix, v_f is the volume fraction of the fibres and $F(\theta,\phi)$ is the angular distribution function where θ and ϕ are orthogonal.

This model has been applied to just the measured fibrous collagen, neglecting the contribution from matrix materials, to give an orientation index which here this will be called OI′ to distinguish it from the differently formulated OI (Kronick and Sacks, 1991, Kronick and Buechler, 1986) (Equation 6).

$$\text{OI}' = \frac{\int_0^{2\pi} \int_0^{\pi/2} \cos^4 \theta \, F(\theta,\phi) \, d\theta \, d\phi}{\int_0^{2\pi} \int_0^{\pi/2} F(\theta,\phi) \, d\theta \, d\phi} \qquad \text{(equation 6)}$$

OI, calculated here from the angle range representing half of the fibrils, can be converted to the integral of $\cos^4\theta$ by numerical methods (where a Gaussian form to the intensity distribution is assumed). The OI data plotted for the two orthogonal directions shown in Figure 3.13 can then be represented as OI′ where, if the model described above is applicable to this system, it should be proportional to the tensile strength. This results in a plot that also correlates with the tear strength data, however, the correlation is poorer than that obtained with the edge on OI measurements (Figure 3.14). The fit that includes all data is reasonable (n = 8, r^2 = 0.55. P = 0.06) and this fit improves if the horse data point is removed (n = 7,

r^2 = 0.82. P = 0.02). It is not known why horse leather should be an outlier, and this may warrant further investigation. These compare unfavourably with the r^2 of 0.98 for just the OI data edge on. The reason that this three dimensional model is a poorer fit than that of the edge on OI data is considered below.

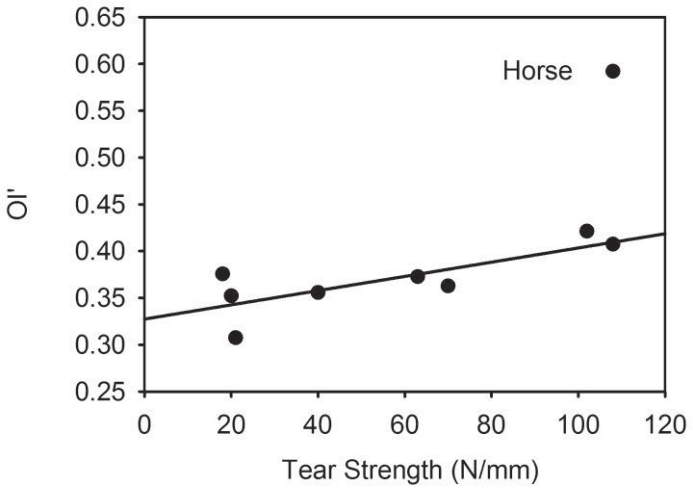

Figure 3.14. Three dimensional modelled OI´ based on normalised integral of $\cos^2\theta \cos^2\phi$ (Sizeland et al., 2013).

Alignment and tear strength – a more complex relationship. Tear strength and tensile strength are related but not identical measures of strength and it is important to understand the difference between these two measures to be able to relate the model in Bigi (Bigi et al., 1981) to the tear strength. The basic assumption of the model outlined in reference (Bigi et al., 1981) is that the strength of collagen is along the axis of the fibrils themselves and that the total strength is the simple sum of these fibrils in the direction of tensile force. This is a good model for tensile strength, however, the more useful measure of strength for practical applications of leather is the tear strength, and this does not directly correlate with tensile strength. Tear strength is perhaps analogous to "toughness" in materials. It is possible for a material to be strong but not tough; for example brittle materials like ceramics are strong but not tough so both aspects need to be considered here.

The ability of leather to resist tear also depends to some extent on the strength perpendicular to the fibril axis which depends on the strength of the cross links

(Chan et al., 2009) or the degree of entanglement, and that strength will be less than the strength of the collagen fibrils. However this appears to be of rather secondary importance compared with fibril alignment. The main component of tear strength for the work presented here is seen to be related to the planar alignment of collagen fibrils. Fibril alignment in the plane has a very strong correlation with tear strength. When the fibrils are not aligned in the plane but instead are perpendicular to the plane (Figure 3.15a) then any tearing force will need to just separate fibres, pulling in the weakest direction. This arrangement is known as vertical fibre defect and occurs sometimes in Hereford cattle (Kronick and Sacks, 1991, Amos, 1958). No samples of this type were included in this study.

When the edge on measurements show the fibrils are rather anisotropic in alignment (Figure 3.15b), then the tear strength is likely to be greater than would be found in the vertical fibre defect structure because now there are fibrils running in the direction of the applied force. Maximum strength is obtained when there is a high degree of alignment in this plane (Figure 3.15c). This trend, depicted from Figure 3.15a to Figure 3.15c below, is what is observed for SAXS measurements over a factor of nearly five in strength (Figure 3.15b); this is a much larger range than has been reported by any other studies.

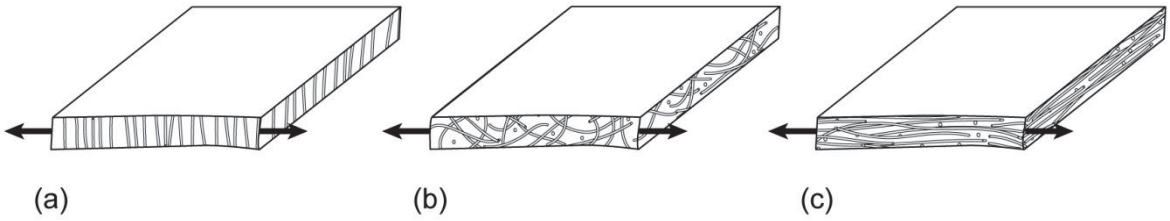

Figure 3.15. The relationship between collagen orientation index (OI) and strength of skin. Edge on measurements with orientation indices that result in leather that is: a) very weak (vertical fibre defect); b) medium strength (low OI); c) strong (high OI). Arrow indicates direction of applied stress in tear measurements (Sizeland et al., 2013).

The reason tear strength does not directly relate to collagen alignment considered in three dimensions (as in Equations 5 and 6) is that tearing is associated with point stresses. To prevent tearing, these point stresses must be resisted. Tearing is used as the industry standard for leather strength because it relates more closely with actual in service performance than with tensile strength. When viewing the tearing process (Figure 3.9), looking flat onto the leather, the points where the tearing will occur are at the two ends of the linear cut hole. In order to resist tearing, the fibres that run at right angles to the two edges to the hole (viewed on the flat) resist this tearing (Figure 3.16a). However, if all the fibres run in this direction then strength may be low due to the failure along shear lines (Figure 3.16b). Therefore, it might be expected that the optimum strength will be associated with a fibre arrangement somewhere between these two extremes, with skin that has a low OI measured in this direction (Figure 3.16c). Hence, this correlation is one where OI is inversely related to strength, which is what is weakly observed for these leathers (Figure 3.13a).

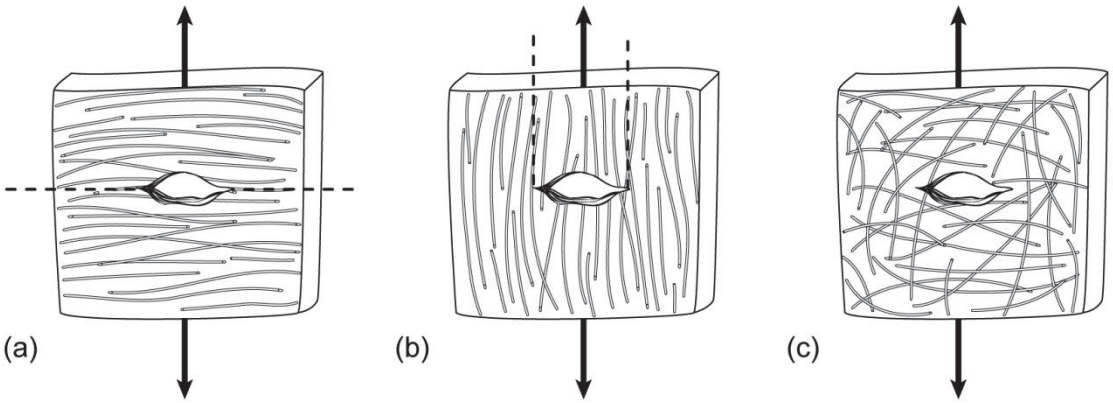

Figure 3.16. The relationship between collagen orientation index (OI) and strength of skin. OI measured on the flat with orientation that results in leather that is a) weak (high OI); b) fairly weak (high OI); c) strong in all directions. Arrow indicates direction of applied stress in tear measurements (Sizeland et al., 2013).

Therefore the existing model for strength, where strength depends on the degree of fibril orientation in the direction of stress considering the three dimensional

structure, does not provide an optimal description of the behaviour of these materials. It does not take into account the fact that, in practice, a tearing process will follow the weakest part of the structure. The consequence of this is that the direction of the tear front is not well defined and a degree of anisotropy when viewed flat on is preferable. The anisotropy, as viewed flat on, enhances the ability to resist point stresses.

These simplified sketches illustrate the mechanism behind the structure–strength relationship that has been measured for the range of animal skins reported here. What is remarkable is the quantitative relationship between tear strength and edge on orientation. The strength range across which this relationship holds is much greater than has previously been demonstrated. The correlation also extends across a wide range of mammals.

There is additional information contained in the SAXS patterns that has not yet been analysed such as the collagen bundle size which is contained in the low Q region of the pattern. This will be addressed in future work. The study will be extended to include a range of animals from other classes and to other tissue types. It is hoped that this work will build a more complete picture of the structural arrangement of collagen materials and will provide insight into the way in which nature constructs these materials for different applications to provide optimum function. It is hoped this will lead to an enhanced understanding of the basis of the hierarchical structure of skin and the reasons for the variations between skin from different positions on one animal, between skin of different species, animal classes, and different tissue types. This study has found a structural motif that is clearly of primary importance in mammals, but it has not yet demonstrated the generalization of this structural motif to other classes or other tissues.

The work is also being extended to develop an understanding of the changes to the collagen fibrils that take place during the processing of leather. Processing can affect the collagen structure, including both the D-period and the fibril orientation. To understand leather as an industrial material it is desirable to understand the structural changes that take place as a result of chemical and physical treatments from skin to finished product.

3.5 Conclusions

In summary, the structure of leather from different mammals has been investigated to attempt to develop a generalized understanding of structure–strength relationships. It has been shown that tear strength of leather is correlated with collagen fibril orientation parallel to the surface of the leather over a large (factor of five) range of strength across seven species of mammals. This has been explained as being due to the strength of the collagen fibrils in their longitudinal axis when suitably arranged to resist the tearing process. This clear demonstration of the structural relationship and consequent insight enables research into other tissues to be better targeted by applying a greater focus to the collagen alignment in plane. It is expected that this highly correlated structure–strength relationship extends to tissues other than those studied here.

Chapter 4: Collagen D-spacing and the Effect of Fat Liquor Addition

The physical properties of leather are partly a result of the structure of the leather's network of type I collagen fibrils. To achieve high strength and a soft, supple feel, penetrating oils (usually polyols) are added to leather during manufacture, and this process is known as fat liquoring. How the collagen structure is modified by fat liquoring (with a lanolin-based fat liquor) is investigated here using synchrotron-based small angle X-ray scattering. The observations of structural changes taking place within collagen fibrils as a result of fat liquoring provides new insight into the nature of fat liquoring and informs future processing developments.

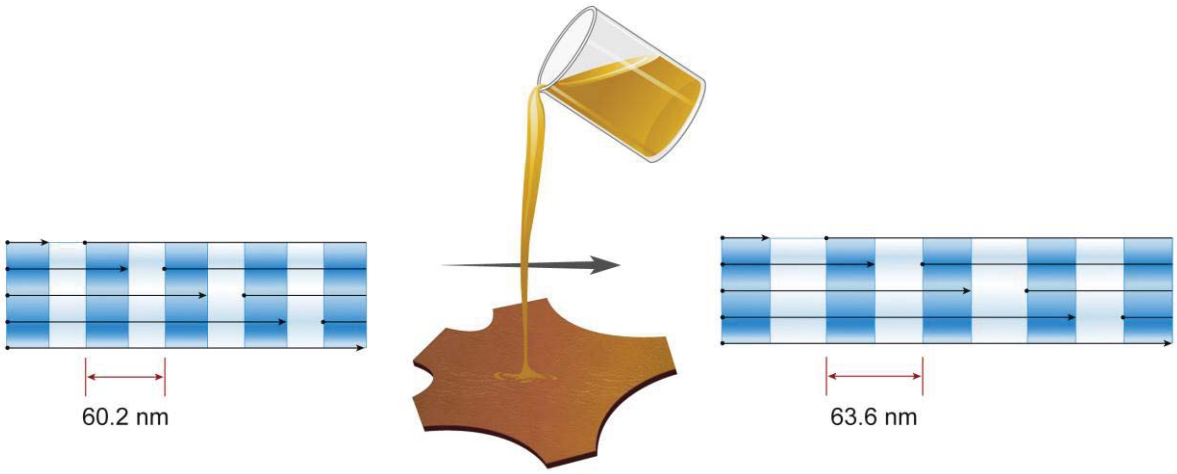

Figure 4.1. Increase in collagen D-spacing when fat liquor is added.

The following investigation has been published in the Journal of American Leather Chemists Association, Volume 110, Issue 3, pages 66-71, and can be found in Appendix 10.1.

4.1 Introduction

Leather is a strong, flexible, complex biomaterial mainly consisting of fibrous type I collagen. Leather is used in a wide variety of manufacturing applications where the physical properties exhibited by the material are important for both strength and aesthetic reasons. The physical attributes of leather are largely dependent on the structure of collagen fibres and the interactions among them (Russell, 1988, Michel, 2004, Chan et al., 2009, Basil-Jones et al., 2011, Rabinovich, 2001). Because leather is processed animal skin, the collagen fibre structure of leather is derived from that of living skin and some other tissues. It is also similar to some collagen-based medical scaffolds (Floden et al., 2010). Fibrous type I collagen accounts for most of leather's complex architecture.

A collagen fibril contains multiple levels of structure. For full details on the structure of collagen please refer to Chapter 2. For this investigation, the structure of collagen is of importance and a brief summary is as follows. The collagen molecule is characterized by the repeating amino acid sequence $(Glycine\text{-}X\text{-}Y)^n$. Each polypeptide chain forms an alpha helix with a left handed twist, then three of these left handed helices twist together in a right hand manner to form a triple helix, or tropocollagen. Hydrogen bonds between amino acid sidechains and collagen molecule mainchains along with hydrogen bonds that are mediated through water bridges are the main stabilizing force of the tropocollagen quaternary structure (Bella et al., 1995). Interchain water bridges are intrinsically linked to the hydroxyprolines in the sequence so that high hydroxyproline content will increase the stability of the triple helix (Engel et al., 1977). In fact, water can be regarded as forming a clathrate–like structure around each triple helix and it has a role in maintaining fibril assembly (Bella et al., 1995, Burjanadze, 1992, Rosenbloom et al., 1973). Collagen fibrils are assembled from multiples of five staggered tropocollagens. Gaps between the end of one tropocollagen and the start of the next result in regions with only 4/5 tropocollagen molecules present. This structure is responsible for the banding of collagen that is visible with atomic force microscopy or transmitting electron microscopy and is the origin of the Bragg diffraction peaks. This spacing is known as the D-spacing and can be measured.

Within each fibril, the tropocollagen molecules are held together by cross links between lysine and allolysine formed as a result of the action of an enzyme lysyl oxidase. The extensive, highly structured hydration shell around the collagen triple helices, along with water bridges between collagen fibrils, have been shown to be critical elements that maintain the macromolecular assemblies of collagen molecules (Bella et al., 1995, Naito et al., 1994, Bella et al., 1994). While the secondary structure remains stable if the water molecules become unavailable to support the hydrogen-bonding network, the mechanical properties of collagen are affected (Gautieri et al., 2011). Hydrophobic residues on the outside of the tropocollagen molecule have also been shown to play an important role in microfibrillar packing by both organizing water structure and through Van der Waals interactions(Usha and Ramasami, 1999).

In terms of microstructure, leather comprises two distinct layers: the 'grain' and the 'corium'. These two layers have significantly different structures (Russell, 1988, Bavinton et al., 1987). Fibril orientation and fibril diameter, particularly in the corium layer, have been shown to be an important factor in the strength of the material (Sizeland et al., 2013, Basil-Jones et al., 2011, Bavinton et al., 1987, Wells et al., 2013, Parry et al., 1978). During the process of making leather, synthetic cross links are introduced that stabilize the molecular structure of the skin and contribute to its physical properties (Folkhard et al., 1987a, Folkhard et al., 1987b, Cuq et al., 2000, Chan et al., 2009). For full details on the structure on leather please refer to Chapter 2.

The D-spacing for stronger ovine and bovine leather has been shown to decrease at the interface between the corium and the grain (Basil-Jones et al., 2012). While changes in D-spacing have not been shown to correlate with strength in leather (Basil-Jones et al., 2011, Sizeland et al., 2013) and rat tail tendon (Gonzalez et al., 2014), D-spacing does vary with tissue types (Fang et al., 2012), animal species (Sizeland et al., 2013), age (James et al., 1991b, Scott et al., 1981), and chemical treatment (Scott et al., 1981, Ripamonti et al., 1980). It is also possible to observe a change in D-spacing when leather is subjected to mechanical stress (Basil-Jones et al., 2012).

During the processing of skins and hides to leather, efforts are made to optimize the strength, flexibility and feel of leather. Adding penetrating oils, a process known as fat liquoring, improves leather's texture and flexibility by lubricating the fibres and preventing adhesion between them (Bajza and Vreck, 2001). However, little is known about how the addition of fat liquor affects the structure of the collagen fibrils themselves.

A study of the addition of fat liquor to leather was completed and possible mechanisms through which the penetrating oil changes the nanostructure of leather have been suggested. With this understanding, it may be possible to manipulate the processing to produce leather of higher strength and with better feel.

4.2 Experimental Procedures

Ovine pelts were obtained from 5-month-old, early season lambs of breeds with "black faces", which may include Suffolk, South Suffolk, and Dorset Down. Conventional beamhouse and tanning processes were used to generate leather as detailed in chapter 3.2.1.

Fat liquoring was carried out using Lipsol EHF (Schill + Seilacher). This product contains a mixture of lanolin, bisulfited fish oil, and 2-methyl-2,4-pentanediol. Lanolin, or wool wax, consists primarily of long chain waxy esters and some hydrolysis and oxidation products of these esters. The fat liquor was added at 0–10% by weight of wet leather prior to drying and mechanical softening. One sample was prepared with just the principal component of the fat liquor, lanolin (Sigma), at a concentration of 8% by weight of wet leather.

Samples for synchrotron-based small angle X-ray scattering (SAXS) analysis were prepared by cutting strips of leather 1 × 30 mm from the official sampling position (OSP) (Williams, 2000b) from pelts of leather processed with 0, 2, 4, 6, 8, and 10%

Lipsol EHF. Full experimental procedures concerning the sampling of leather can be found in Chapter 3.2.1. SAXS analysis of the samples was carried out according to the procedure detailed in Chapter 3.2.2 with measurements made every 0.25 mm through the cross section from the grain to the corium.

The D-spacing of collagen was determined for each spectrum from Bragg's Law by taking the central position of several collagen peaks, dividing these by the peak order (usually from n = 5 to n =10) and averaging the resulting values.

Fibril diameters were calculated from the SAXS data using the Irena software package (Ilavsky and Jemian, 2009) running within Igor Pro. The data was fitted at the wave vector Q, in the range of 0.01 – 0.04 $Å^{-1}$ and at an azimuthal angle which was 90° to the long axis of most of the collagen fibrils. This angle was selected by determining the average orientation of the collagen fibrils from the azimuthal angle for the maximum intensity of the D-spacing diffraction peaks. The "cylinderAR" shape model with an arbitrary aspect ratio of 30 was used for all fitting. Individually optimizing this aspect ratio was not attempted and the unbranched length of collagen fibrils may in practice have a length that exceeds an aspect ratio of 30.

4.3 Results

The SAXS patterns obtained for the different levels of fat liquor clearly show diffraction rings due to the axial periodicity of collagen (Figure 4.2a). Orientation of the collagen fibrils can be seen as the varying intensity of each of these rings around the azimuthal angle and the alignment at right angles to this of the central scattering region. From the integrated intensity of the whole scattering pattern (Figure 4.2b) the position of the diffraction peaks can be measured and from these the D-spacing is determined.

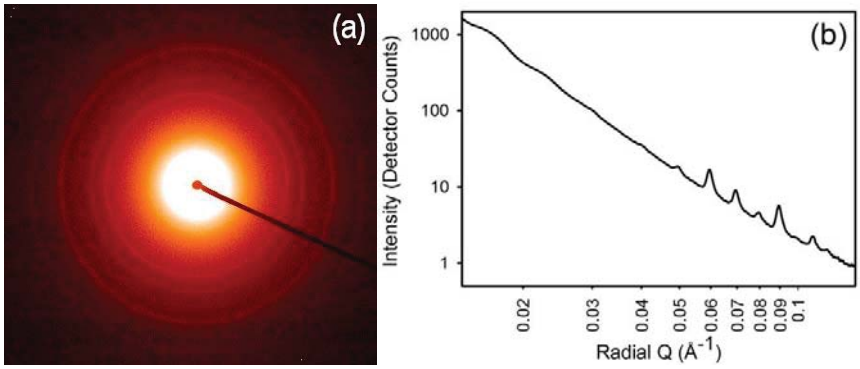

Figure 4.2. Example of SAXS of leather: (a) raw SAXS pattern; (b) integrated intensity profile (Sizeland et al., 2015b).

The addition of fat liquor resulted in an increase in D-spacing of the collagen from 60.2 (σ = 0.47) nm for samples with no fat liquor to 63.6 (σ = 0.43) nm for samples with 10% fat liquor (Figure 4.3). This is an increase of 3.4 nm or 5.6%. The change in D-spacing of the corium and grain layers closely mimicked each other despite structural differences in these layers (Basil-Jones et al., 2010). A strong correlation between D-spacing and the percentage of fat liquor added was found, with a linear fitted slope of 0.34 nm/% and a r^2 value of 0.93 (P = 0.0018 at an alpha of 0.05) (Figure 4.3).

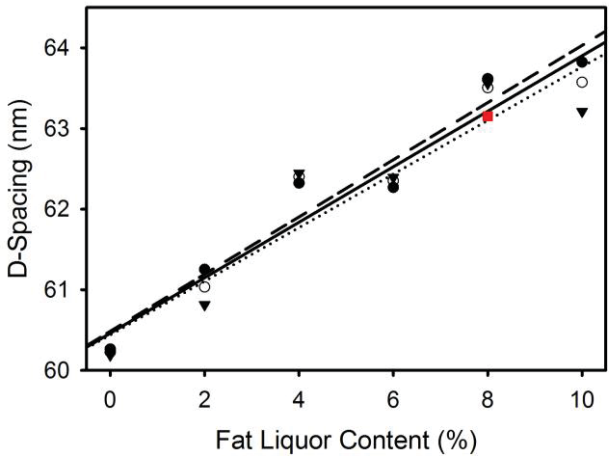

Figure 4.3. Collagen D-spacing versus fat liquor percentage for ovine leather: (●, – – –) corium, (▼, ····) grain, and (○, ——) average. Each point for the corium and grain is taken from the average of about 10 scattering patterns. Pure lanolin at 8% also shown (■) (Sizeland et al., 2015b).

The one sample prepared with 8% lanolin rather than fat liquor had a D-spacing of 63.1 (σ = 0.39) nm, which falls on the regression line in Figure 4.3. This suggests the change in D-spacing may be primarily due to the lanolin content of the fat liquor.

An average fibril diameter of 56.8 (n = 106, σ = 1.3) nm was determined for the leather showing that there was no statistically significant change in the fibril diameter as a result of fat liquor addition.

4.4 Discussion

It was found that the change in collagen D-spacing is proportional to the amount of fat liquor added, with a large change being observed when the greatest amount of fat liquor was added. As pure lanolin had a similar effect, it is not unreasonable to assume that the lanolin component of the fat liquor is causing this change. This increase in D-spacing serves to increase the length (and therefore perhaps the volume) of the collagen fibrils in leather. The equivalent extension in D-spacing by tension applied to leather requires a stress of approximately 3.1 N/mm^2 for strong ovine leather and 0.4 N/mm^2 for weak ovine leather (Basil-Jones et al., 2012).

Fat liquor is considered in the industry to assist in the mechanical properties of leather by "lubricating" the fibril structure, enabling the fibres to slide over one another. This work clearly shows that the fat liquor used in this experiment causes a change in the D-spacing, a fundamental property of fibril structure.

Two possible mechanisms for the change in D-spacing are considered here. One proposition is that the D-spacing increase is caused by an increase in the twist of the tropocollagen helix which would result in a longer tropocollagen and therefore a longer D-spacing in the fibril. However, if an increase in tropocollagen occurred by this mechanism, a significant change in the fibril diameter would be expected.

The diameter was not observed to change and therefore this hypothesis is not supported.

The other option considered is that the observed change is due to an increase in the length of the gaps between two tropocollagen molecules within the fibrils. Collagen fibrils form in a process that controls the registration between adjacent tropocollagen molecules, known as the D-spacing. Inspection of type I tropocollagen maps and interactomes shows that the two regions of the molecule important in fibrillogenesis (residues ~1016-1040, and 776-800) are rich in hydrophobic amino acids and prolines (Di Lullo et al., 2002, Sweeney et al., 2008, Helseth and Veis, 1981, Prockop and Fertala, 1998). Once the tropocollagens are in register, the fibril structure is stabilized by intermolecular hydrogen bonds, often mediated by water, and covalent cross links at the N and C termini of the molecule.

An increase in the D-spacing is indicative of an increase in the axial distance between fibrils and could result in an overall lengthening of the fibril. It could also change the interactions between tropocollagens, whether the interactions are covalent or non-covalent and whether they are mediated through bridging molecules such as water. The fact that it is a direct result of fat liquoring implies that the covalent cross links formed between tropocollagen molecules in the mature fibril, are either nonexistent, are broken during processing of the skin, or that they are flexible enough to allow movement of the tropocollagens relative to one another within the fibril.

Axial periodicity in collagen I is thought to be stabilized by inter-tropocollagen hydrophobic and л-CH2 interactions between the C-terminal region of one tropocollagen and a specific region of a second tropocollagen, driven by the entropic gain from the release of ordered water molecules (Kar et al., 2009). Lanolin is a long chain hydrocarbon ester, made up from a long chain aliphatic lanolin alcohol and fatty acid. Its hydrophobic structure will therefore be relatively rigid allowing it to insert into the hydrophobic regions at the ends of the gap regions between tropocollagen molecules. The relative non-specific nature of hydrophobic interactions is tolerant of movement, and the lanolin will act like

lubricant allowing the tropocollagens to move relative to one another, altering the D-spacing.

It is outside of the scope of this work to elucidate the molecular details of this arrangement. While atomic force microscopy could be used to compare the ratio of the gap and overlap regions among leathers with different levels of fat liquor, obtaining statistically robust sample data could be problematic. It has been shown that there is a range of D-spacing values in any one sample, with different fibril bundles within one piece of tissue having different average D-spacings (Fang et al., 2012). SAXS measurements sample a volume of 80 × 150 × 1000 μm, which might be expected to contain around 3×10^{10} collagen D-spacing units (assuming collagen occupies around 50% of the volume). AFM, however, scans only small areas of a sample at one time, making it difficult to get a representative average D-spacing. Nevertheless, this would be a worthwhile follow-up analysis and could reveal one mechanism by which fat liquor achieves fibril elongation.

4.5 Conclusions

In summary, the structural changes of collagen within leather upon addition of varying amounts of fat liquor have been investigated. It has been shown that as the amount of fat liquor is increased, the D-spacing of the collagen fibrils increased, and that this appears to be due to the lanolin component of the fat liquor. Alternative mechanisms for this increase in D-spacing have been discussed, including an increase in the gap region or an increase in the length of the tropocollagen triple helix. It has been shown that fat liquor does more than lubricate fibres in leather in that it alters the structure of collagen fibrils. The observations of structural changes taking place within collagen fibrils as a result of fat liquoring provides new insight into the nature of fat liquoring and informs future processing developments.

While the focus of this work has been the improved properties of leather, due to the application of lanolin, the changes observed in collagen structure may also occur in raw skin. Mixtures of oils and other chemicals have long been applied to human skin to enhance its appearance and are known as moisturizers. It may be that some of the components of moisturizers increase the D-spacing of collagen in skin, expanding the collagen structure and reducing wrinkles. The effect of a range of other organic additives on collagen structure are currently being investigated as well as the effects of fat liquoring on the nanostructural response of leather when under strain.

Chapter 5: Changes to Collagen Structure During the Processing of Skin to Leather

As hides and skins are processed to produce leather, chemical and physical changes take place that affect the strength and other physical properties of the material. The structural basis of these changes at the level of the collagen fibrils is not fully understood and formed the basis of this investigation. Synchrotron-based small-angle X-ray scattering (SAXS) was used to quantify fibril orientation and D-spacing through eight stages of processing from fresh green ovine skins to staked dry crust leather. Both the D-spacing and fibril orientation changed with processing. The thickness of the leather changed during processing which had an impact on the fibril orientation index (OI); this accounted for much of the OI difference between process stages. After the thickness of the leather was accounted for, the main difference in OI was found to be due to the hydration state of the material with dry materials being less oriented than wet (Figure 5.1). Similarly significant differences in D-spacing were found at different process stages. These were due also to the moisture content, with dry samples having a smaller D-spacing (Figure 5.1). This understanding is useful for relating structural changes that occur during different stages of processing to the development of the final physical characteristics of leather.

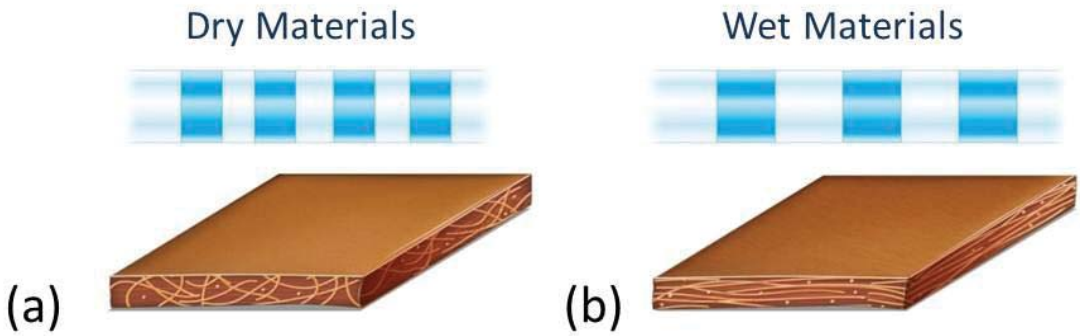

Figure 5.1. D-spacing of collagen fibrils and orientation of collagen fibres: (a) dry materials have a smaller D-spacing and a lower OI; (b) wet materials have a larger D-spacing and a higher OI.

The following investigation has been published in the Journal of Agricultural and Food Chemistry, Volume 63, Issue 9, pages 2499-2505, and can be found in Appendix 10.1.

5.1 Introduction

The leather making process is a way of preserving skins to stop decomposition and to provide a strong and flexible material. For a detailed explanation of the leather making process please refer to Chapter 2. The process consists of a series of chemical treatments and some mechanical processes. Each of the chemical treatments alters the composition of the original skin, for example, extracting components from the native skin or adding components such as cross linking agents. In addition to changes in the chemistry of the collagen, which are well known, it is possible that each of these processes may have an effect on the collagen structure as well, although little information has been presented on this to date.

For this investigation the leather making process was broken down to consist of eight main stages, which are referred to by a variety of names in the industry, but here they have been designated as fresh green, salted, pickled, pretanned, wet blue, retanned, dry crust, and dry crust staked. The “fresh green” is the skin after removal from the carcass. Skins are normally salted as a way of temporarily preserving the skin before tanning. The salt acts to slow down bacterial growth by reducing water activity. Salting causes some dehydration of the skins. The “salted” sample is the skin after salting for preservation. The next stage of the leather making process is the removal of the salt by soaking and washing the skins (where the skin becomes rehydrated) followed by an alkali treatment carried out in the presence of sodium sulfide (‘liming’) combined with suitable enzymes (‘bating’) which together break down and remove some of the non-fibrous proteins, glycosaminoglycans and other undesirable components. It is also said to ‘open up’

the structure of the leather to enable better penetration of tanning chemicals in subsequent stages. After the alkaline treatment stage the skin is typically adjusted back to a lower pH and is acidified in sulfuric acid and sodium chloride. After this stage the skin is referred to here as “pickled”. A synthetic, organic cross linking agent and surfactant are often added at this point which may assist with the subsequent chrome tanning stage. Stabilising agents are often added to the pickle to raise the denaturation temperature of the collagen and thus enable skin fat to be removed more efficiently at higher temperatures. The skins at this stage have been called “pretanned”. After the natural skin fats are removed, the pretanned pelts are tanned using chromium sulfate. The skin after chromium tanning is called “wet blue”. Chrome tanned leather tends to be too rigid for most applications so there is normally a second tanning stage using natural vegetable tannins or synthetic tannins to make the final leather feel softer and ‘fuller’. After this second tanning stage the skin is called “retanned”. At this stage dyes, fat liquors, and modified fats or oils are added to complete the look and feel of the leather. After this ‘fat liquoring’, the leather is dried and is called “dry crust”. The leather is then mechanically softened or ‘staked’ and is referred to here as “dry crust staked”.

Previously it has been shown that small angle X–ray scattering (SAXS) can provide detailed structural information on the amount of fibrous collagen, the microfibril orientation, the D-spacing and the collagen fibril diameter in leather (Basil-Jones et al., 2010, Sturrock et al., 2004, Kronick and Buechler, 1986) and other tissues (Sasaki and Odajima, 1996b, Liao et al., 2005).

The chemical treatments used to produce leather from skin and hide may result in changes to the structure of the collagen fibrils and the arrangement of these fibrils. These chemical processes include strong salt solutions, large changes in pH, enzymatic treatments to remove cross links, and new cross links being formed. An overview of tanning chemistry has been presented (Covington, 1997). Some aspects of chemical treatments of skins and their effect on structure have been observed previously with liming of skins (increasing the pH with calcium hydroxide) showing a decrease in the D-spacing of collagen (Maxwell et al., 2006). Pickling and retanning agents have been shown to swell collagen fibres at low pH (Bulo et al., 2007). At low ionic strength and non-isoelectric pH charge dependent

interactions (screening and selective ion adsorption) are prevalent in maintaining the collagen architecture (Ciferri, 2008) which is also reflected in the greater thermal stability of collagen at low pH (Zanaboni et al., 2000) and in the elastic response of collagen (Grant et al., 2009).

In this investigation, SAXS was used to investigate the changes that take place in the microstructure of leather through the different stages of processing from skin to leather.

5.2 Experimental Procedures

For this investigation an ovine pelt was obtained from a 5-month-old, early season New Zealand Romney cross lamb. Samples were removed from the same skin during several stages of processing. These stages were termed fresh green, salted, pickled, pretanned, wet blue, retanned, dry crust, and dry crust staked. Cross-sections were cut parallel to the backbone and as close together as possible. The samples, except for dry crust and dry crust staked, all had high moisture contents because they were taken during processing.

Conventional beamhouse and tanning processes were used to generate the leather as detailed in Chapter 3.2.1 using oxazolidine as the pretanning agent and chrome as the tanning agent.

Tear strengths of the leathers were tested using standard methods (Williams, 2000a). Samples (strips 1 x 50 mm) were tested on an Instron 4467. For details on tear strength testing please refer back to Chapter 3.

Diffraction patterns were recorded on the Australian Synchrotron SAXS/WAXS beamline utilizing a high-intensity undulator source according to Chapter 3.2.2. All diffraction patterns were recorded with an X-ray energy of 11 keV. The partially processed leather samples were sandwiched between kapton tape before being mounted for X-ray analysis to prevent drying.

SAXS analysis performed whilst stretching a sample was completed as follows. A stretching apparatus was custom built to enable investigation into collagenous materials under tension (Figure 5.2) (Basil-Jones et al., 2012). A linear motor, Linmot PS01, 48 × 240/30 × 180-C (NTI AG, Switzerland), was mounted onto a purpose-built frame with a custom-made clamp fitted to the end of the slider. The clamp was designed not to put a sharp point load on the leather. A L6D aluminium alloy OIML single-point loadcell (Hangzhou Wanto Precision Technology Co., Zhejiang, China) that holds the other end of the sample was attached to a second clamp that was attached to the frame. The slider can be controlled remotely from outside the SAXS beamline hutch. It also enables the sample to be stretched in increments specified by the user as the slider moves the set distance and stops once done.

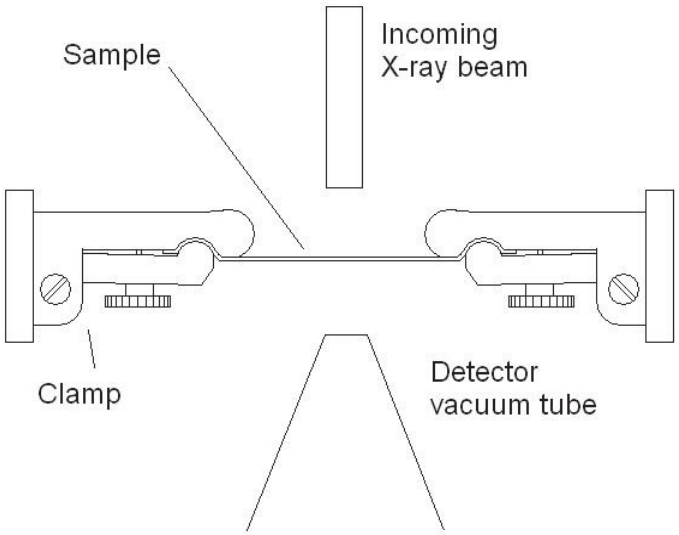

Figure 5.2. Schematic of custom built stretching apparatus (Basil-Jones et al., 2012).

Stretching samples were cut from the official sampling position (OSP) with approximate dimensions of 1 mm by 30 mm. The sample was cut parallel to the backbone. Each leather sample was mounted horizontally between the clamps without tension and then moved into the X-ray beam (Figure 5.3). The sample was straightened out in 1 mm increments until a force was registered by the loadcell.

The slider was then moved back 1 mm so that the sample was not under tension for the initial analysis and diffraction patterns were recorded. Measurements were made edge on through the full thickness of the leather with measurements made every 0.25 mm and the samples analysed from the grain to the corium. The sample was then stretched by 1 mm and was maintained at this extension for 1 minute to stabilise before SAXS diffraction patterns, the extension length, and the force information were recorded. This process of stretching the sample by another 1 mm, stabilising, and then recording data was repeated until the sample failed.

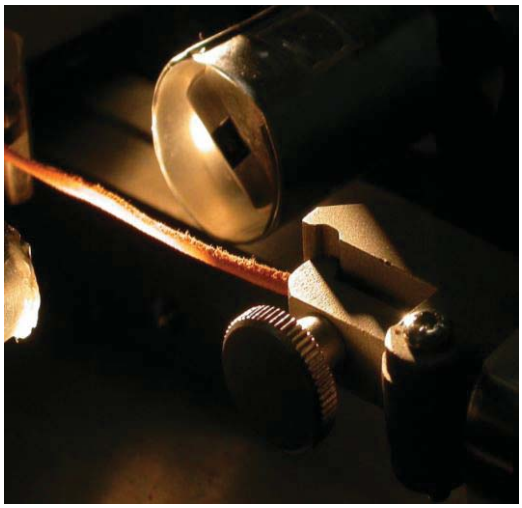

Figure 5.3. Leather sample held by the stretching machine and mounted in the beamline.

Diffraction patterns as shown in Figure 5.4a were obtained for each point analysed. These patterns can be integrated to produce intensity plots that display Bragg peaks (Figure 5.4b).

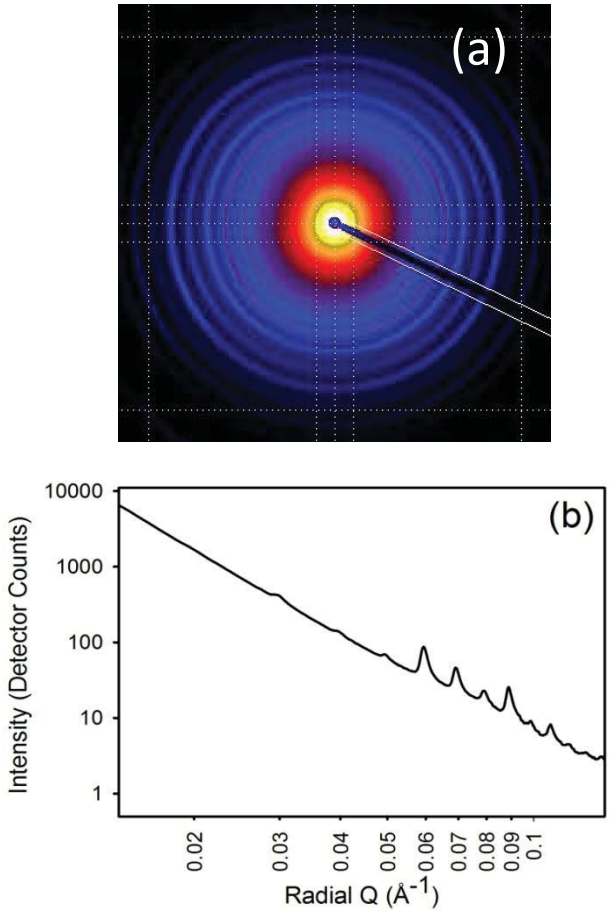

Figure 5.4. (a) SAXS diffraction pattern; (b) plot of intensity versus q.

Orientation index (OI) is defined as (90° – OA)/90° where OA is the azimuthal angle range that contains 50% of the microfibrils centered at 180°. OI is used to give a measure of the spread of microfibril orientation (an OI of 1 indicates the microfibrils are completely parallel to each other; an OI of 0 indicates the microfibrils are completely randomly oriented). The OI is calculated from the spread in azimuthal angle of the most intense D-spacing peak (at around 0.059–0.060 $Å^{-1}$) (Basil-Jones et al., 2011).

The D-spacing was determined from Bragg's Law by taking the centre of a Gaussian curve fitted to the 6th order diffraction peak of an integrated intensity plot for each spectrum.

5.3 Results

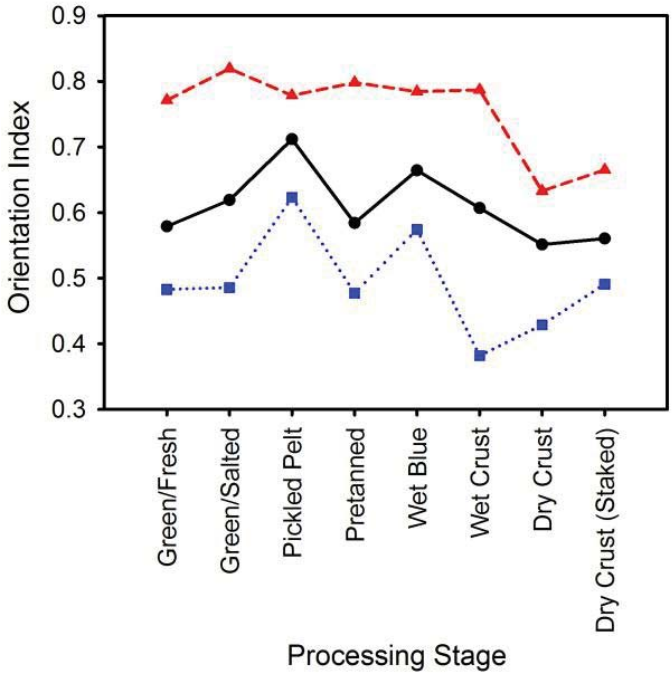

Figure 5.5. Variation in orientation index for all stages of processing: (▲, – – – –) corium, (■, ·····) grain, (●, ———) average (Sizeland et al., 2015a).

Orientation index changes. The OI of the corium region is higher than that of the grain region throughout all the processing stages (Figure 5.5). While there is considerable variation in the OI during processing, the OI of the final staked dry crust leather is fairly similar to that of the fresh green skin so that overall there is not a large change in OI.

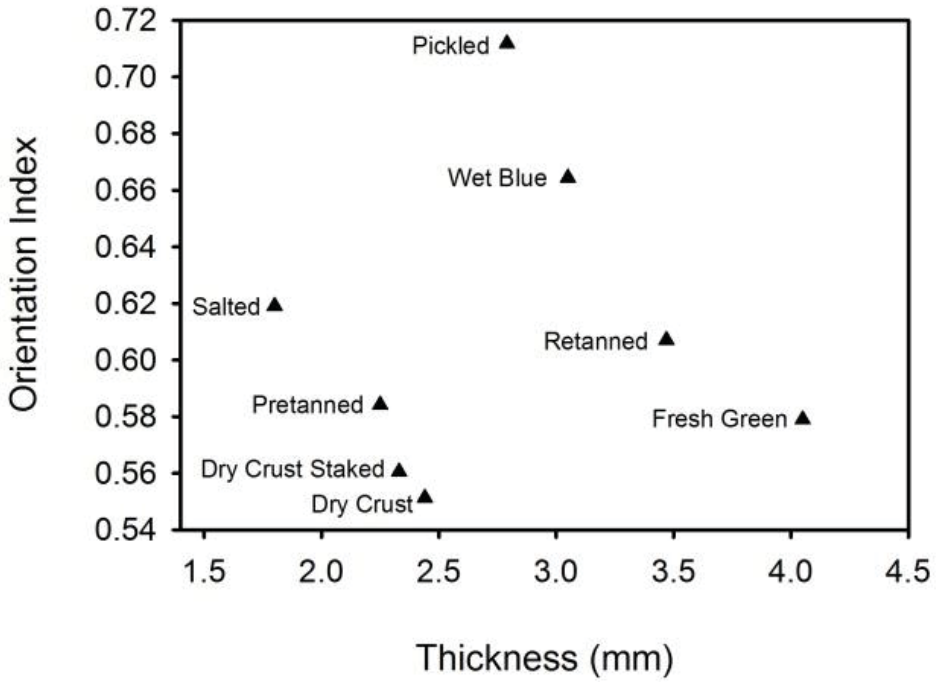

Figure 5.6. Fibril orientation index versus thickness (Sizeland et al., 2015a).

Orientation index and thickness. The thickness of the skin or leather varies by more than a factor of two during processing. With this variation of thickness there is a change in OI (Figure 5.6). The stages appear to be in two groups with the dry samples (salted, pretanned, dry crust, and dry crust staked) in one group of lower OI which decreases with increasing thickness, and the wet samples (pickled, wet blue, retanned, and fresh green) in another group of higher OI that decreases with increasing thickness.

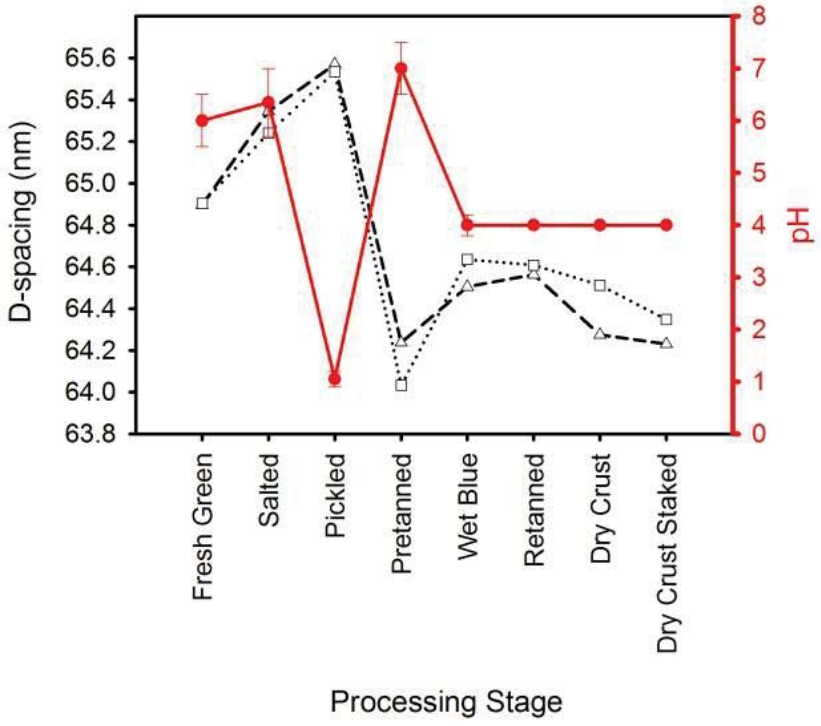

Figure 5.7. Variation in D-spacing and pH between different stages of processing prior to stretching: (Δ, — — —) corium, (□, ·····) grain, (●, ———) pH (Sizeland et al., 2015a).

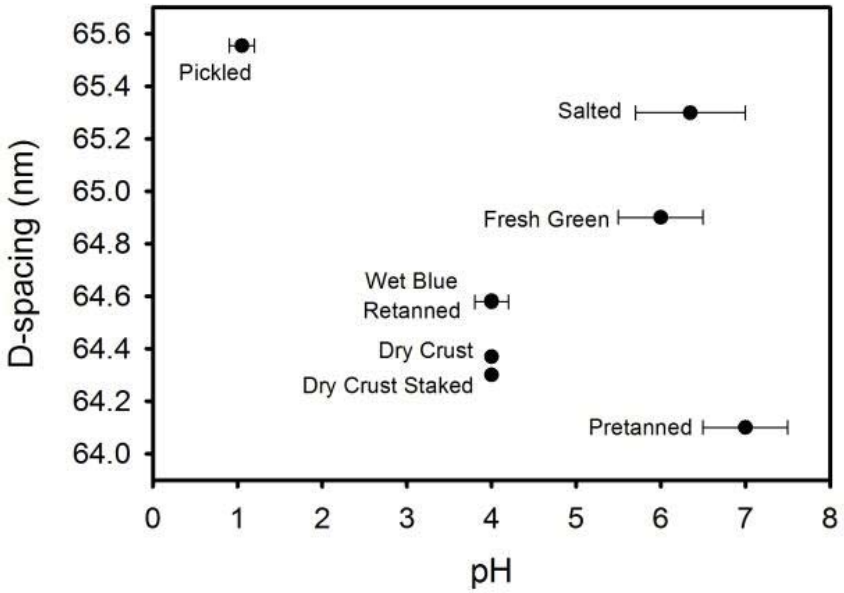

Figure 5.8. Variation of D-spacing with pH (wet blue and retanned points are coincident) (Sizeland et al., 2015a).

D-spacing with processing and pH. Significant changes in the D-spacing of the collagen fibrils with the application of each process step were observed (Figure 5.8). Both the corium and the grain regions of the leather have similar D-spacing and are similarly affected by the processing. The most significant change in D-spacing occurs with pretanning when there is a contraction of the D-spacing of 1.4-1.5 nm (2%). The pH of the solutions in which each process takes place does not appear to correlate with the D-spacing (Figure 5.8). For fresh green and salted skins the pH was measured by a surface probe rather than the process liquor as used in the later stages. Although there is not a correlation of D-spacing with pH, it appears that there is a relationship between D-spacing and the moisture content as three of the dry samples have a lower D-spacing than the wet samples.

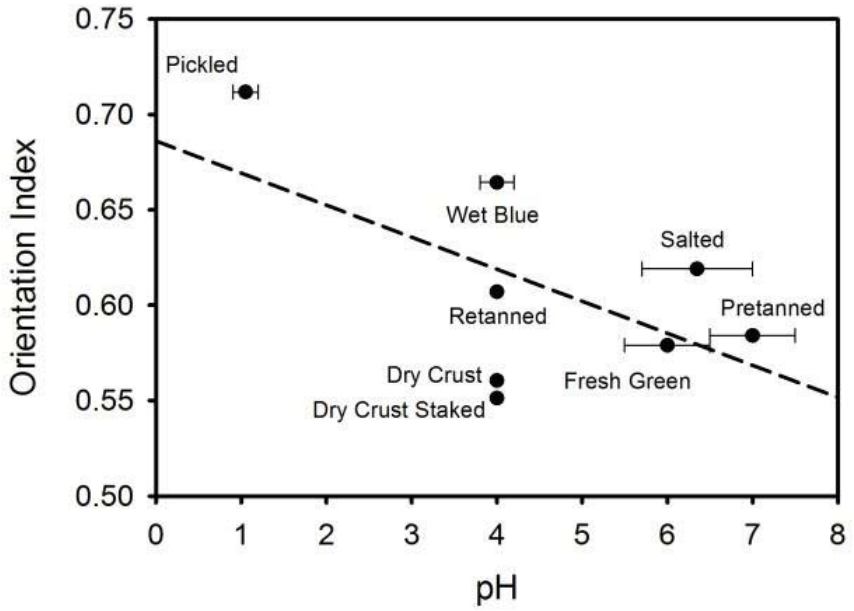

Figure 5.9. Correlation of OI with pH (Sizeland et al., 2015a).

OI and pH. The OI appears to be correlated with pH (Figure 5.9) (Linear regression: $r^2 = 0.335$, $t = -1.74$, $P = 0.133$). However, as discussed later in the chapter it is believed this correlation is not a causal relationship.

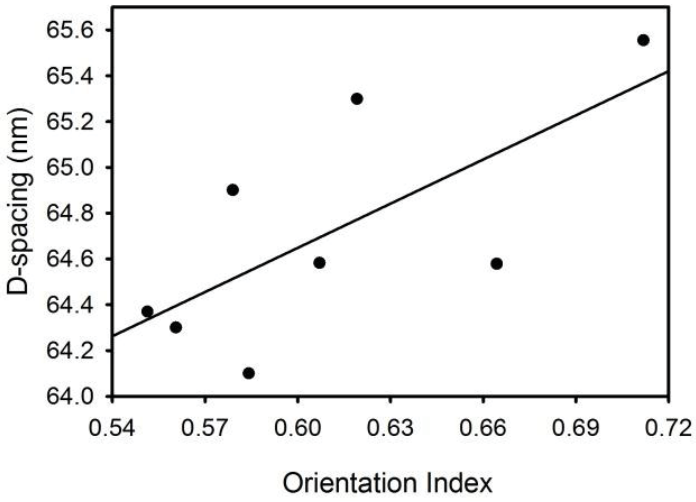

Figure 5.10. D-spacing versus OI for samples of different stages of processing when held without tension (Sizeland et al., 2015a).

D-spacing and OI. A correlation is observed between OI and D-spacing (Figure 5.10). The correlation is statistically significant (Linear regression: $r^2 = 0.485$, t = 2.4, P = 0.055). However, as is discussed later in the chapter it is believed this correlation is not a causal relationship.

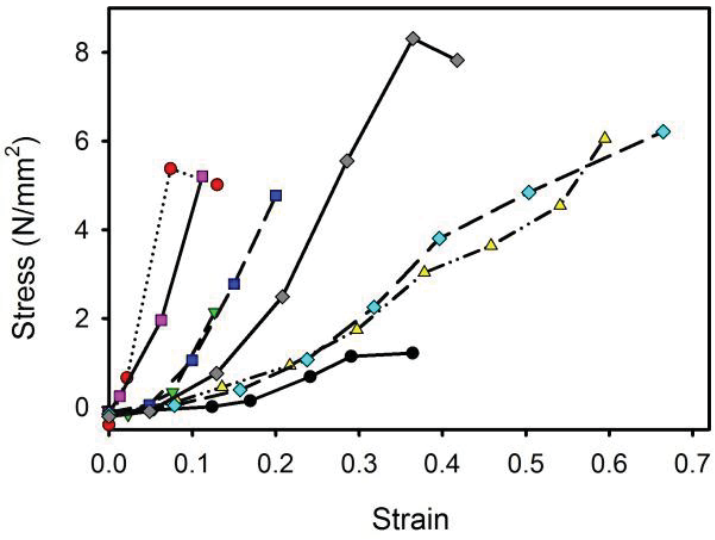

Figure 5.11. Stress strain curves for each process stage, performed *in situ* concurrently with the SAXS measurement (not normalized for sample width or thickness): (●, ————) Fresh green, (●, ·····) salted, (▼, — — — —) pickled, (▲, — ·· — ·· —) pretanned, (■,— —) wet blue, (■, — · — · —) retanned, (♦,— — —) dry crust, (♦, ———) dry crust staked (Sizeland et al., 2015a).

Stress-strain. Stress-strain curves were measured *in situ* at the synchrotron during SAXS data collection (Figure 5.11). The samples were not of a uniform width so an absolute comparison of the modulus of elasticity from these curves is not possible. However, it is possible in a very general way to compare the shapes of the curves. Most of the samples show a toe region, with an initial lower elastic modulus, followed by a linear region.

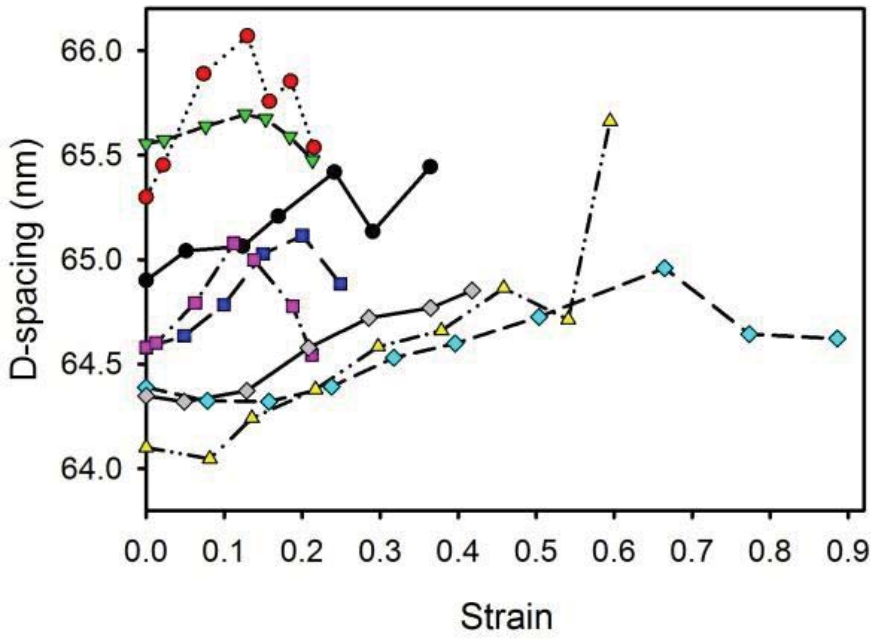

Figure 5.12. Changes in collagen D-spacing as samples of partially processed skin are stretched: (●, ————) Fresh green, (●, ·····) salted, (▼, — — — —) pickled, (▲, — ·· — ·· —) pretanned, (■,— —) wet blue, (■, — · — · —) retanned, (♦,— — —) dry crust, (♦, ———) dry crust staked (Sizeland et al., 2015a).

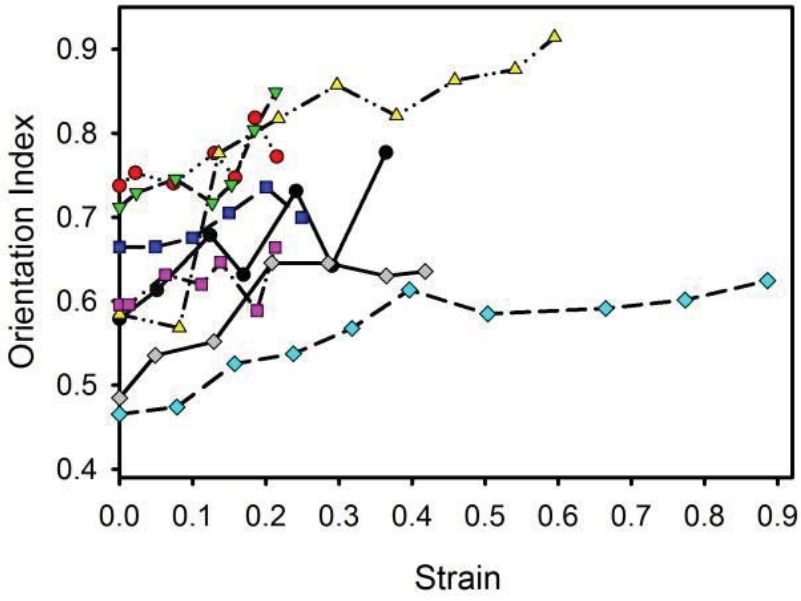

Figure 5.13. Changes in collagen fibril OI as samples of partially processed skin are stretched: (●, ————) Fresh green, (●, ·····) salted, (▼, — — — —) pickled, (▲, — ·· — ·· —) pretanned, (■,— —) wet blue, (■, — · — · —) retanned, (♦,— — —) dry crust, (♦, ————) dry crust staked (Sizeland et al., 2015a).

OI and D-spacing with mechanical stretching. There is an increase in D-spacing as the skin or leather samples are stretched (Figure 5.12). This increase in D-spacing is a measure of the stress being transferred to the individual fibrils causing their length to increase. We also find an increase in OI upon stretching (Figure 5.13) as the collagen fibrils realign in the direction of the applied force (values for the D-spacing and OI changes are tabulated in Tables 5.1 and 5.2). At every stage of the leather making process, a strain applied to the samples resulted in an increase in OI.

Table 5.1. D-spacing changes in processing stages of leather with strain.

Processing Stage	Strain	Initial D-spacing	Maximum D-spacing (nm)	Change in D-spacing (nm)	Change in D-spacing (%)	Change in D-spacing % / strain (%)
Fresh Green	0.36	64.90	65.44	0.54	0.83	2.28
Salted	0.13	65.30	66.07	0.77	1.17	9.01
Pickled	0.13	65.55	65.70	0.14	0.21	1.69
Pretanned	0.59	64.10	65.66	1.56	2.38	4.00
Wet Blue	0.20	64.58	65.12	0.54	0.82	4.12
Retanned	0.11	64.58	65.08	0.50	0.77	6.84
Dry Crust	0.66	64.39	64.96	0.57	0.88	1.32
Dry Crust Staked	0.42	64.35	64.85	0.50	0.78	1.86

Table 5.2. OI changes in processing stages of leather with strain OI.

Processing Stage	Strain	Initial OI*	Final OI	Initial TCOI**	Final TCOI	Change in OI	Change in TCOI
Fresh Green	0.36	0.58	0.78	0.23	0.57	0.20	0.33
Salted	0.13	0.74	0.78	0.50	0.57	0.04	0.07
Pickled	0.13	0.71	0.72	0.45	0.46	0.01	0.01
Pretanned	0.59	0.58	0.91	0.24	0.83	0.33	0.59
Wet Blue	0.20	0.66	0.74	0.37	0.49	0.07	0.12
Retanned	0.11	0.60	0.62	0.26	0.30	0.02	0.04
Dry Crust	0.66	0.47	0.59	0.07	0.25	0.13	0.18
Dry Crust Staked	0.42	0.48	0.64	0.10	0.32	0.15	0.22

* Orientation Index (OI)

** Thickness Corrected Orientation Index (TCOI)

5.4 Discussion

The changes to the structure and arrangement of collagen fibrils in skin during several stages of the chemical processing to form leather have been measured. These build up a picture of what happens in the process of transforming skin to leather.

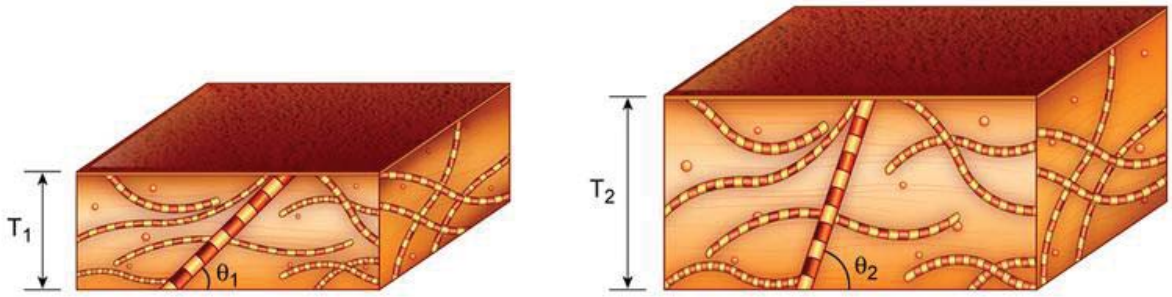

Figure 5.14. Illustration of the change in collagen fibril angle θ to the plane of leather as the thickness T of the leather changes (Sizeland et al., 2015a).

Model of OI change with thickness. During processing of skins to leather the thickness of the material changes substantially, sometimes becoming thicker and at other times becoming thinner. A difference between the thinnest and the thickest stage of a factor of 2.25 was observed. If the collagen fibrils are not lying flat then as the thickness of the leather increases the angle of these fibrils to the plane of leather will increase (Figure 5.14). This will cause a change in OI. Therefore a model for the change in OI with thickness changes has been developed. This enables us to determine how much of the OI change is due just to the change in thickness and how much is due to other factors.

The range of fibre angles in a sample is given by the orientation index OI which is derived from the orientation angle, OA (Basil-Jones et al., 2010). OA is defined as the subtended angle that contains half the fibrils, i.e. it satisfies equation 1.

$$0.5 = \frac{\int_{\theta=-OA/2}^{\theta=OA/2} \theta N d\theta}{\int_{\theta=-90°}^{\theta=90°} \theta N d\theta} \qquad \text{(equation 1)}$$

Where N is the number of fibrils, and θ is the fibre angle (relative to the plane of the leather). In practice this is determined from the SAXS diffraction pattern by the integrated intensity verses azimuthal angle for one of the D-spacing diffraction peaks, equation 2:

$$0.5 = \frac{\int_{\varphi=-OA/2}^{\varphi=OA/2} \varphi I d\varphi}{\int_{\varphi=-90°}^{\varphi=90°} \varphi I d\varphi} \qquad \text{(equation 2)}$$

where *I* is diffraction intensity of a selected D-spacing diffraction peak above a fitted background and φ is the azimuthal angle of the diffracted X-rays.

OI is derived from OA by equation 3.

$$OI = \frac{1 - OA}{OA} \qquad \text{(equation 3)}$$

Therefore, for perfect alignment in the reference direction, which is normally in the plane of a piece of leather or skin, OI = 1, for no alignment or completely isotropic fibrils OI = 0, and for perfect alignment at right angles to the reference direction OI= –1.

If a sample of leather containing a fibre expands in thickness uniformly, and the fibre is at an angle θ_1 from the base (Figure 5.14), then the new angle of the fibre, θ_2, depends on the change in thickness by equation 4.

$$\frac{T_2}{T_1} = \frac{\tan\theta_2}{\tan\theta_1} \qquad \text{(equation 4)}$$

Where T_1 is the original thickness, and T_2 is the new thickness.

Rearranging equation 4 for θ_2 gives the new angle of the fibre after the leather has increased in thickness:

$$\theta_2 = \tan^{-1}\left(\frac{T_2}{T_1}\tan\theta_1\right) \qquad \text{(equation 5)}$$

A transformed OA after stretching can then be calculated. The OA defines the subtended angle of 50% of the fibres. Therefore fibres which have an initial angle from the reference angle of greater than half the OA will, after transformation, still have an angle greater than the transformed OA; fibres which have an initial angle lower than half the OA will, after transformation, still have an angle lower than half the transformed OA. In other words the 50% inside the OA will remain inside the OA, the 50% outside the OA will remain outside the OA. Therefore, it is only necessary to calculate the transformation by equation 5 of the angle that is the OA to calculate the new OA that represents the new fibre distribution.

As an illustration of the extent of this change, for thickness changes similar to those observed here, some values are plotted in Table X below. Note that expanding the thickness sufficiently results in an alignment of fibres vertically (negative OI).

Table 5.3. Calculated change in orientation index of collagen fibrils for different thicknesses of material.

Starting OI	New OI when $T_2/T_1 = 1.5$	New OI when $T_2/T_1 = 2.0$	New OI when $T_2/T_1 = 2.5$
0.00	-0.25	-0.41	-0.52
0.10	-0.16	-0.33	-0.44
0.20	-0.05	-0.23	-0.36
0.30	0.05	-0.13	-0.26
0.40	0.17	-0.01	-0.15
0.50	0.29	0.12	-0.02
0.60	0.42	0.27	0.13
0.70	0.56	0.43	0.31
0.80	0.70	0.61	0.52
0.9	0.85	0.80	0.75
1	1.00	1.00	1.00

It was also considered how the OI might be affected by the area change to the leather, with wet stages generally of larger area than dry stages. This expansion of area would influence the OI in the opposite sense to the thickness change. However the area change of the skin is small, less than 5%, and can be neglected compared with the more than 100% change in the thickness.

With the thickness taken into account the OI now reflects any underlying structural changes that take place during the chemical and mechanical processing of skin through to leather. Therefore the OI for each sample was recalculated using the thinnest sample, the salted skin, as the reference and present the adjusted results in the following analysis.

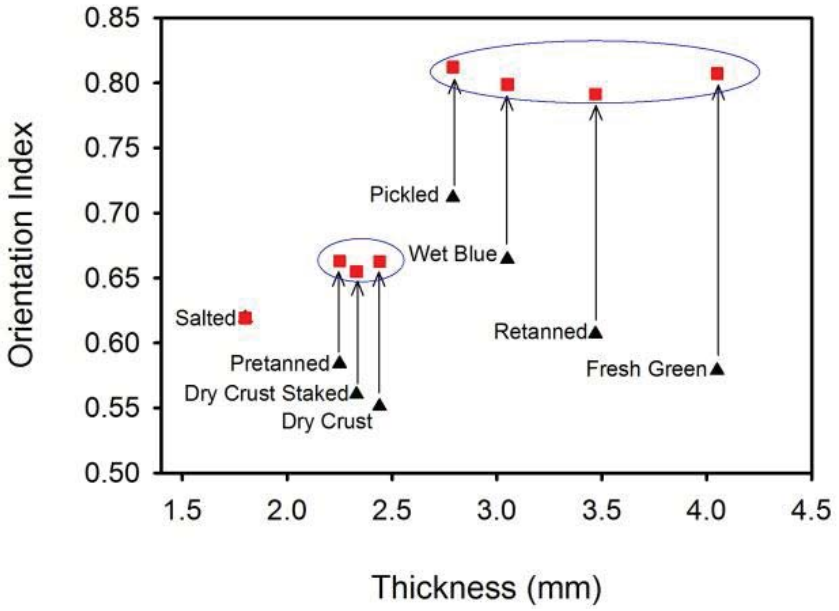

Figure 5.15. Fibril orientation index versus thickness: (▲) measured OI, (■) calculated OI adjusted for thickness changes (relative to salted) (Sizeland et al., 2015a).

OI and water. Once the effect of thickness on the OI is removed it can be seen that the samples fall into two groups (Figure 5.15). There are the fresh green, pickled, wet blue, and retanned materials. These all have a high OI (corrected for thickness relative to salted) of around 0.8. These samples are all wet. The pretanned, dry crust, and dry crust staked all have a corrected OI of around 0.67. These samples are all dry. The salted skin also has a low OI, of 0.62, and it is also a dry sample. Therefore the factor that separates the high OI from the low OI materials is the wetness of the samples. When these collagen materials are dried, the OI decreases. While it might be tempting to ascribe this to a crimping of the collagen fibrils as they dry, which would result in a lower OI, crimping in skin was not observed (unlike in tendon or pericardium (Sizeland et al., 2014) for example). Therefore, although by removing the thickness effect, it has been possible to identify that there is a fundamental change between wet and dry stages but the mechanism of this change has not been determined. It is suggested that a possible mechanism could be the space filling that results from hydration which causes a hindrance to

the movement of fibrils and leads to a higher OI at higher moisture contents. At lower moisture contents there is more space available for fibres to bend and adjust themselves into positions resulting in lower OI.

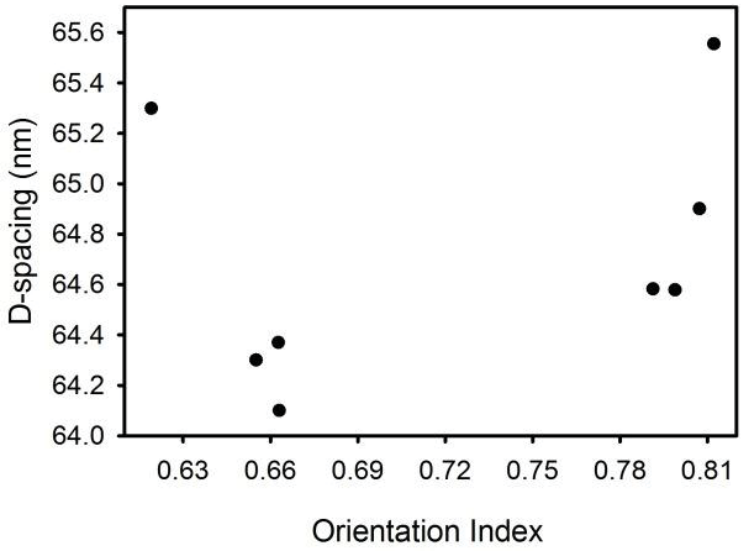

Figure 5.16. D-spacing versus thickness corrected OI for samples of different stages of processing when held without tension.

D-spacing and OI. Once the OI is corrected for thickness effects there is no longer a statistically significant correlation between D-spacing and OI (Figure 5.16) (Linear regression: $r^2 = 0.109$, $t = 0.855$, $P = 0.426$). It is known that the result of straining leather is a straightening or alignment of the fibrils (an increase in OI) and that D-spacing measures the stress applied to individual fibrils (Basil-Jones et al., 2012). A correlation between OI and D-spacing during different stages of processing would have suggested that these were both due to changes in internal strain in leather: when strain is released D-spacing decreases and OI decreases. However, this was not observed here.

D-spacing and water. It was found that the D-spacing is lower in the dry samples by 0.38 nm; wet samples, which include fresh green, pickled, wet blue, and retanned, have an average D-spacing of 64.90 ($\sigma = 0.46$) nm while dry samples, which include salted, pretanned, dry crust, and dry crust staked, have an average

D-spacing of 64.52 (σ = 0.53) nm. Back in the 1940s Bear used X-ray diffraction techniques to show that the hydration state of a sample changes its D-spacing with dry samples at 64 nm and wet samples at 67 nm (Bear, 1944). Since then it has been shown by X-ray diffraction and by atomic force microscopy that the D-spacing is moisture dependent with a reduction in D-spacing on drying (Wess et al., 1998, Kemp et al., 2012, Brodsky et al., 1980, Price et al., 1997). The D-spacing depends on the state of hydration of the fibril and decreases from 67nm for a hydrated fibril, to around 64 nm in air-dried samples (Baer et al., 1988; Bella et al., 1995; Wess and Orgel, 2000). This is believed to be due to the collapse of the gap and overlap regions, and the partial shearing of unit cell contents within the gap region upon loss of water (Wess et al., 1998).

D-spacing and pH. It is perhaps a little surprising that D-spacing is not affected by pH. The D-period is affected by both the length of the tropocollagen units, and by the way these tropocollagen units are assembled into the collagen fibril. The length of these structures is partially determined by the length of the hydrogen bonds between collagen molecules within the tropocollagens and by hydrophobic interactions between tropocollagen units. pH can affect hydrogen bonding which, in collagen and other proteins, relies on a polar interaction between specific functional groups on amino acids (Ciferri, 2008, Zanaboni et al., 2000). Mechanisms for fibril elongation by chemical treatments have previously been discussed (Sizeland et al., 2015a, Sizeland et al., 2014) and it appears that pH does not have an impact here.

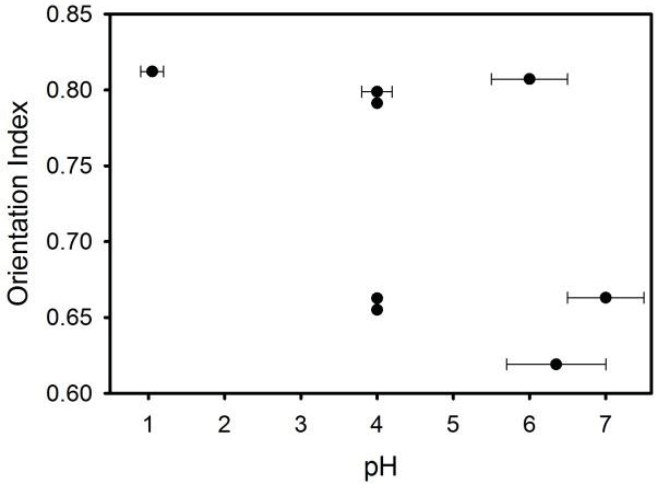

Figure 5.17. Variation of thickness corrected OI with pH.

OI and pH. Once the OI is corrected for thickness it is apparent that there is no correlation between OI and pH (Figure 5.17) (linear regression: regression coefficient = -0.0215, r^2 = 0.488, P = 0.22). These instead fall into two groups: low OI for dry samples and high OI for wet samples, irrespective of the pH conditions.

Response to strain. It was found that when strain was applied to the samples both the OI and D-spacing increased. It has previously been shown that upon stretching of leather collagen fibrils first realign and then lengthen (an increase in the OI followed by an increase in the D-spacing) (Basil-Jones et al., 2012) and that collagen fibrils are very resilient with a high Poisson's ratio (Wells et al., 2014). In pretanned, dry crust, and dry crust staked samples, the OI increased first after the first few increments in strain then the D-spacing increased with the further strain. These samples form a cluster at an OI of approximately 0.67 following thickness correction. The D-spacing of the wet samples (fresh green, pickled, wet blue, and retanned) increased with the first application of strain. These wet samples form a cluster with an OI of about 0.80. Because the dry group has a lower initial OI than the wet samples the fibrils had more realignment potential and therefore a greater change in OI is seen for the dry samples rather than the wet samples which do not have as much opportunity for the fibrils to realign with the direction of the force. Therefore in the wet samples the strain was taken on by the individual collagen fibrils sooner, as shown by the immediate increase in D-spacing.

Cross linking. In the process of treating skin to produce leather, naturally present cross links are removed and new cross links are formed. The natural glycosaminoglycan cross links are removed in the liming and bating stages so that the processed skin, known as pickled, should be largely devoid of cross links. New cross links are added at the pretanned and wet blue stages. While there have been studies on the effects of cross linking on fibril alignment, there have been mixed conclusions drawn about the influence of cross linking. It has been suggested that cross links may stabilize a network structure (with less aligned fibrils) (Deb Choudhury et al., 2007b, Kayed et al., 2015) and that removal of cross links may destabilize the network structure leading to fibrils becoming more aligned (Kayed et al., 2015). However such behavior was not observed here during processing, where much of the cross linking would be expected to be removed by the end of

the pickled stage and then cross links are added by the completion of the wet blue stage.

5.5 Conclusions

Both the D-spacing and fibril orientation changed with processing. It was noted that the thickness of the leather changed during processing which had an impact on the fibril orientation index (OI); this accounted for much of the OI difference between process stages. After recalculation of the OI taking the thickness of the leather into account, the main difference was found to be due to the hydration state of the material with dry materials having a lower OI and wet materials having a higher OI. This shows the change is not a fundamental redistribution of fibrils, but rather due to thickness changes and hydration. Variances were also found in the D-spacing values of the different process stages. These differences were also due to the moisture content, with dry samples having a smaller D-spacing. This understanding may be useful for relating structural changes that occur during different stages of processing to the development of the final physical characteristics of leather.

Chapter 6: Modification of Collagen D-spacing in Skin by Model Compounds

Oils and moisturisers are often added to skin in an attempt to create a smoother, more supple feel. Additives have been shown to modify the collagen fibrils of processed skin, extending the fibril length. If a similar process could take place in living skin it may improve the appearance and strength of skin. Synchrotron-based small angle X-ray scattering has been used to investigate the modification of the collagen structure by model compounds. These model compounds were chosen because of their opposite effects on protein solubility. Urea, which is an osmolyte, is often used to solubilise proteins and is commonly used in skin care products, while the amino acids proline and hydroxyproline are known to precipitate proteins. With the addition of urea, proline and hydroxyproline, the D-spacing of the collagen fibrils increased and the orientation index decreased. The increased D-spacing may be caused by a lengthening of either the direct hydrogen bonds or the water-mediated hydrogen bonds. By understanding the mechanisms for modification of the structure of collagen by fat liquors and other additives valuable insights are gained that will lead to better comprehension of existing skin formulations and the development of new formulations based on more in-depth knowledge about the action of moisturisers and cosmetic products on living skin.

6.1 Introduction

Skin and the much desired smooth, wrinkle-free complexion of youthful skin is an important topic of study for cosmetic science. Collagen I is a major component of skin that contributes to its structure and appearance. In-situ modification of the structure of collagen may be a significant component of the action of skin care cosmetics.

Hydrating or lubricating liquids and gels are added to skin products to achieve a soft, supple feel in both the cosmetics industry and the leather industry. In the leather making process, animal skin is converted to a durable, strong, and flexible material. As leather is the product of processed animal skin, the collagen fibre structure of this complex biomaterial is similar to that of living skin, as well as pericardium and some other tissues. Like skin, Type I collagen accounts for most of the complex architecture of leather, as it does in skin, and it is this fibrous collagen network and the interactions occurring within it that can be held largely accountable for the physical attributes of leather (Russell, 1988, Michel, 2004, Rabinovich, 2001, Chan et al., 2009, Basil-Jones et al., 2011).

Fat liquoring is part of the manufacturing process of leather, whereby penetrating oils are added to achieve the high strength and soft, supple feel of the finished product. These additives have been shown to modify the collagen fibrils and extend the fibril length (Sizeland et al., 2015b). The cosmetic industry is founded in part on the desire of many women (and men) to protect their skin and to avoid the natural signs of aging through the topical application of moisturisers that contain natural oils, fats and other compounds designed to penetrate the dermis. While there has been much research into urea, various peptides and a number of oils and fats (Oikawa et al., 2005, Olsen and Jemec, 1993, Pan et al., 2013, Rawlings and Lombard, 2012) and how they modify the structure of skin and influence skin mechanics, little is known of how they modify the main structural component of skin - the collagen molecules themselves.

The collagen molecule consists of a repeating amino acid sequence, Gly (glycine)-X-Y, which forms an alpha helical polypeptide chain with a left-hand twist. The X and Y positions are occupied by a high proportion of the amino acids proline and hydroxyproline respectively, with the most common triplet in collagen being Gly-Pro-Hyp, which accounts for about 10% of the total sequence (Ramshaw et al., 1998). Three of collagen molecules twist together in a right-hand manner to form a triple helix, or tropocollagen. Hydrogen bonds between side-chains stabilise the tropocollagen quaternary structure along with some covalent cross links. Larger collagen fibrils are assembled from up to five tropocollagens. A part of the fibril contains four tropocollagen molecules and a part contains five, due to staggering

of the tropocollagen molecules. This difference is responsible for the banding of collagen fibrils, visible with atomic force microscopy or transmission electron microscopy, and is known as the D-spacing, which can be measured. Within each fibril, the tropocollagen molecules are held together by cross links (see Reiser (Reiser et al., 1992) for a review on cross links) formed between lysine and allolysine as a result of the action of an enzyme lysyl oxidase (Csiszar, 2001). The D-spacing varies with tissue types, animal species (Sizeland et al., 2013), age (James et al., 1991b), mechanical stress (Basil-Jones et al., 2012) and chemical treatment (Ripamonti et al., 1980).

Within collagen networks, both the D-spacing and the arrangement of the fibrils may vary. One aspect that can be measured relating to the arrangement of the collagen is the orientation and spread in orientation of the fibrils. The relationship between the orientation of fibrils and the mechanical strength has been characterised (Fratzl and Weinkamer, 2007), and the correlation of strength with the orientation of collagen measured edge on (alignment in-plane) has been shown in bovine and ovine skin (Basil-Jones et al., 2011, Basil-Jones et al., 2012) and across a range of mammal species with a strength range of over a factor of five (Sizeland et al., 2013). There may also be a correlation between strength and fibril diameter (Parry et al., 1978, Wells et al., 2013).

Critical elements in maintaining the stability of macromolecular assemblies of collagen are the extensive, highly structured hydration shell and hydrogen bond networks around the collagen triple helices in which hydrogen bonds involving water form bridges between collagen fibrils (Bella et al., 1995, Naito et al., 1994, Bella et al., 1994). Two sets of interchain hydrogen bonds, one direct and one water-mediated, have been detected for a collagen-like peptide (Kramer et al., 1999). Both direct hydrogen bonds and water-mediated hydrogen bonds contribute to collagen stability.

The addition of dissolved amino acids to a protein may affect hydrogen bonding, depending on the amino acid added. Urea, one of the molecules used in this investigation, is an effective denaturant. It has been shown to denature proteins by specifically binding to amide units using hydrogen bonds and by decreasing the

hydrophobic effect by displacing water (Zou et al., 1998). If hydrogen bonds are modified, the triple helices and consequently the collagen fibril structure will be directly impacted.

It is standard practice to add fat liquors to skin during leather processing, however, the effect this has on the structure of collagen has only recently been investigated (Sizeland et al., 2015b). To better understand the influence of the penetrating oils on the molecular structure of collagen, the fibril orientation and axial periodicity of collagen fibrils have been quantified for samples processed with model compounds using synchrotron-based small angle X-ray scattering (SAXS). Three compounds were chosen: urea, known to solubilise proteins, and the amino acids proline and hydroxyproline, both known precipitators of proteins (Record et al., 2013). Here the addition of urea, proline, and hydroxyproline and how they affect the structure of collagen in ovine skin is investigated. In addition, comparisons are made with the effects with that of lanolin, a compound used in many commercial skin preparations, which has previously been seen to modify collagen (Sizeland et al., 2015b).

6.2 Experimental Procedures

Ovine skin from the leather industry was used as a model material to investigate collagen modification by urea (Sigma-Aldrich), hydroxyl-L-proline (Sigma-Aldrich), L-proline (Sigma-Aldrich) and lanolin (Sigma-Aldrich).

Ovine pelts were obtained from 5-month-old, early season, New Zealand Romney cross lambs. The leather was generated using conventional beamhouse and tanning processes as detailed in Chapter 3.2.1.

In conventional beamhouse processing, fat liquors are added after chrome tanning to the wet blue pelts prior to fixing with 0.5% formic acid, washing, drying and mechanical softening. However, to make the samples for this study, the fat liquor

was replaced with urea, L-proline and hydroxyl-L-proline at concentrations of 4% and 7.2% by weight of wet leather. Two further samples were prepared: one with lanolin (Sigma) at a concentration of 8% by weight of wet leather and one with no additives at all.

The samples for SAXS analysis were cut from the official sampling position (OSP) (Williams, 2000b) in strips 1 × 30 mm. Each sample was mounted without tension in the X-ray beam to obtain scattering patterns through the sample's full thickness. Each data point presented here (D-spacing, OI) is the average of 11-17 diffraction patterns recorded every 0.25 mm through the cross-section from the grain to the corium except the sample with no additives, which is the average of 6 patterns. Diffraction patterns were recorded on the Australian Synchrotron SAXS/WAXS beamline as per the method described in Chapter 3.2.2. All diffraction patterns were recorded with an X-ray energy of 11 keV and data processing was carried out using the SAXS15ID software (Cookson et al., 2006).

A measure of the spread in orientation of the microfibrils is given by the orientation index (OI), with an OI of 1 indicating the microfibrils are parallel to each other and an OI of 0 indicating the microfibrils are randomly oriented. OI is defined as (90° – OA)/90°, where OA is the minimum azimuthal angle range that contains 50% of the microfibrils. This measure is based on Sack's method for light scattering (Sacks et al., 1997) but converted to an index (Basil-Jones et al., 2011) using the spread in azimuthal angle of one or more Bragg peaks. The peak used was typically the sixth order peak at approximately 0.055-0.059 $Å^{-1}$ as it is one of the most intense D-spacing peaks. The peak area is measured, above a fitted baseline, at each azimuthal angle.

Bragg's Law was used to determine the D-spacing of collagen by taking the central position of a Gaussian curve fitted to the 6^{th} order diffraction peak of an integrated intensity plot for each spectrum and dividing it by the peak order (for the 6^{th} diffraction peak n = 6).

6.3 Results

SAXS patterns were obtained for the samples processed with no additives, with the model compounds (hydroxyproline, proline and urea) and with lanolin. Diffraction rings that occur due to the axial periodicity displayed by collagen were clearly visible in every spectrum (Figure 6.1a). From the varying intensity around the azimuthal angle of the rings the orientation of the fibrils can be determined. The integrated intensity of the scattering pattern can be plotted (Figure 6.1b) and the D-spacing can be calculated using the central position of the diffraction peak divided by the peak order.

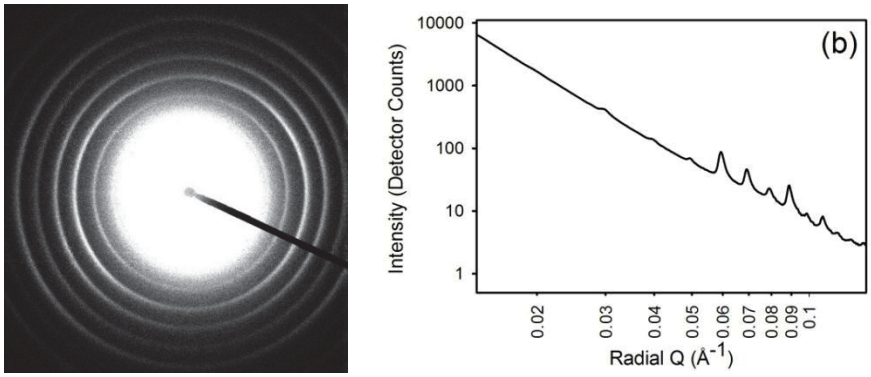

Figure 6.1. Example of SAXS of collagen: (a) SAXS pattern; (b) integrated intensity profile.

The addition of urea, proline and hydroxyproline all result in statistically significant increases in the D-spacing of collagen fibrils (Figure 6.2, for full statistics see Table 6.1). The D-spacing increased from 60.2 (σ = 0.42) nm for samples with no fat liquor or additives up to maximums of 63.4 (σ = 0.25, $P < 0.001$, for $\alpha = 0.05$) nm for urea. When 7.2% urea was added D-spacing increased by 3.2 nm or 5.3%. The D-spacing of leather with 8% lanolin was found to be 63.2 (0.50) nm, an increase of 3.0 nm.

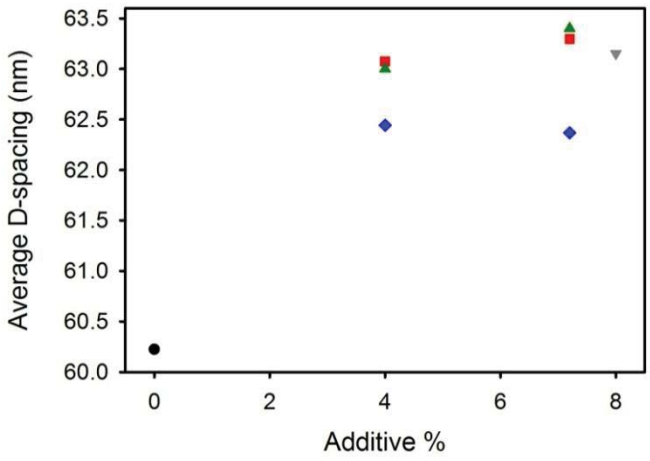

Figure 6.2. Collagen D-spacing versus additive percentage for processed skin: (●) no additives, (▼) lanolin, (♦) hydroxyproline, (■) proline, and (▲) urea. Each point is the average value taken from 11–17 scattering patterns, except the 0% sample, which is the average of 6 patterns.

The OI of the collagen fibrils decreased with the addition of the model compounds (Figure 6.3), with statistically significant decreases occurring with the addition of 4% hydroxyproline, 7.2% hydroxyproline and 4% urea. The OI decreased from 0.59 ($\sigma = 0.05$) for samples with no fat liquor or additives down to 0.44 ($\sigma = 0.12$, $P = 0.0095$ at an alpha of 0.05) for urea. The largest OI change occurred when 4% urea was added, with a decrease of 0.15 nm or 25.3%. The OI of the collagen fibrils in the leather made with 8% lanolin was 0.69 ($\sigma = 0.06$) which, in contrast to the other compounds, is an increase.

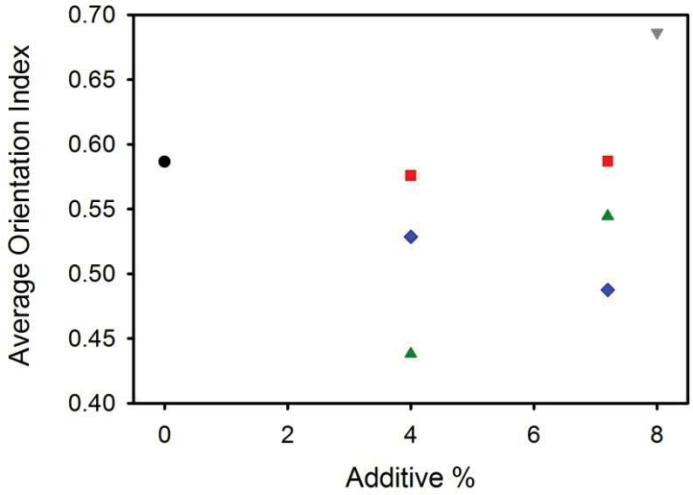

Figure 6.3. Collagen orientation index (OI) versus additive percentage for processed skin: (●) no additives, (▼) lanolin, (♦) hydroxyproline, (■) proline, and (▲) urea. Each point is the average value taken from 11-17 scattering patterns, except the 0 % sample which is the average of six scattering patterns.

Table 6.1. Statistics for orientation index (OI) and D-spacing values when comparing samples with no additives (0%) to samples with added model compounds. All *t*-tests were calculated using an alpha of 0.05.

	Orientation Index comparison				D-spacing comparison			
	Difference in values	Statistical Significance	*t* statistic	*P* value	Difference in values (nm)	Statistical Significance	*t* statistic	*P* value
0% to 4% hydroxyproline	-0.0580	Significant	2.33	0.0307	2.2182	Significant	-13.10	<0.0001
0% to 7.2% hydroxyproline	-0.0992	Significant	4.21	0.0004	2.1416	Significant	-10.54	<0.0001
0% to 4% proline	-0.0107	Not Significant	0.45	0.6600	2.8499	Significant	-18.31	<0.0001
0% to 7.2% proline	0.0005	Not Significant	-0.15	0.9880	3.0729	Significant	-20.48	<0.0001
0% to 4% urea	-0.1486	Significant	2.90	0.0095	2.7751	Significant	-18.79	<0.0001
0% to 7.2% urea	-0.0422	Not Significant	1.69	0.1120	3.1757	Significant	-19.72	<0.0001
0% to 8% lanolin	-0.0998	Significant	-3.36	0.0030	2.9274	Significant	-12.82	<0.0001

6.4 Discussion

It was found that urea, proline, and hydroxyproline changed the collagen fibril OI and D-spacing. Urea and other small organic compounds are present in skin care formulations. As such, any insight as to how such additives might alter the architecture of collagen could benefit the cosmetics industry.

The observed D-spacing increase that the addition of the amino acids produces can be physically equated to a lengthening of the collagen fibrils. The mechanisms coming into play to attain such a lengthening may be due to alterations within the hydrogen bond network.

Both direct hydrogen bonds and water-mediated hydrogen bonds contribute to collagen stability. Firstly, let us consider direct hydrogen bonds. The N-H of glycine and the O=C of the residue in the X position on adjacent polypeptide strands within every tropocollagen are linked by direct hydrogen bonds. There are also hydrogen bonds between the side-chains of the amino acids and main-chain atoms, as well as side-chain–side-chain hydrogen bonds. Urea is known to form hydrogen bonds with peptide groups (Lim et al., 2009). It is therefore possible that the increase in the tropocollagen unit length could be the result of urea breaking some H-bonds within the triple helix, resulting in looser coiling (Bella et al., 1994). This would result in an increase in D-spacing with the effect spread equally over both the gap and the overlap region of the fibril. Interestingly, lanolin had a similar effect. The D-spacing values of collagen after addition of urea at 63.0 (σ = 0.24) nm at 4% concentration and 63.4 (σ = 0.25) nm at 7.2% concentration are similar to those of collagen samples made with 8% lanolin, with a value of 63.2 (σ = 0.50) nm. Lanolin, a long-chain waxy ester, is likely to have a different mechanism based on its hydrophobic properties and its effect on water structure.

Urea was expected to break the water-mediated hydrogen bonds and lengthen the collagen D-spacing. The results showed an increase in the D-spacing as was expected, based on Lim (PNAS 2009) and Record (Record et al., 2013). However, given the protein-precipitating properties of proline (Record et al., 2013), it was expected that proline and hydroxyproline to have the opposite effect, that of

shortening the D-spacing. This was not observed, but rather an extension of the D-spacing was seen (Table 6.1).

The second type of hydrogen bonds to consider is the water-mediated hydrogen bonds. In the presence of hydrophobic molecules, water structure becomes ordered and the number of H-bonds is reduced. In the presence of polar molecules, the number of H-bonds also changes as the polar molecules compete with the water to interact with the tropocollagens. Hydrogen bonds mediated through water bridges within the tropocollagen structure may likewise be affected, resulting in a looser coiling of the triple helix and a concomitant increase in D-spacing. Lanolin, being hydrophobic, could push out the water involved in the water-mediated hydrogen bonds. Without these bonds stabilising the structure of collagen, it may lengthen. As with lanolin, the effect on hydrophobic interactions could explain the structural change to collagen when other compounds are added. Proline has non-polar side chains and is hydrophobic meaning it could act similarly to lanolin by forcing out water molecules due to its hydrophobic nature. Urea has been shown to decrease the hydrophobic effect by displacing water (Zou et al., 1998). If water was displaced by an added molecule the water-mediated hydrogen bonds would be affected and collagen's stabilising hydrogen bonding network would be weakened. Consequently this may be reflected by a lengthening of the collagen D-spacing.

The collagen fibril orientation, or OI, is also affected by the addition of the model compounds. The urea and hydroxyproline decreased the OI of the collagen fibrils (Table 6.1). In contrast, lanolin increases the OI, showing that the addition of lanolin increases the alignment of the fibrils. These observations may reflect the different nature of these two compounds, and a fundamental difference in their mode of activity. Urea exerts its influence through polar interactions and competes with water to make H-bonds with the peptide groups within the collagen structure, essentially affecting the hydration shell around the molecule. Lanolin impacts the collagen structure through hydrophobic interactions ordering the water around the molecule and also affecting the hydration shell. So both lanolin and urea affect water structure. However when these compounds are added to collagen the effect within the fibril and between fibrils is different. Urea disrupts

interactions between fibrils by breaking non-covalent bonds. It is likely that this will result in a decrease in the alignment of parts of or whole fibrils. Conversely, lanolin, because of its structure, can insert itself between fibres, trapping ordered water and allowing the fibres to slide over each other, to increase fibre alignment.

6.5 Conclusions

It was found that the structure of collagen fibrils is modified by treatment with urea, hydroxyproline and lanolin. The change in D-spacing could be caused by either a change in the triple alpha helix structure of tropocollagen or by modifying the bonds between the tropocollagens. Urea lengthens the D-spacing as predicted due to its negative impact on hydrophobic effects through displacement of water and also significantly reduced the OI of the skin. Lanolin had the same effect on D-spacing as urea, it had the opposite effect on the OI to urea. Given that lanolin is a major component of most skin care formulations, understanding how it functions at a molecular level is important for the cosmetic industry. A D-spacing increase was observed for added proline and hydroxyproline. Further investigations of the mechanisms of modification of collagen in skin by urea, proline, hydroxyproline, lanolin, and by extension other organic compounds, may lead to a better understanding of existing skin formulations and their interaction with collagen. Hopefully this knowledge can be extended to the action of moisturisers and cosmetic products on living skin.

Chapter 7: Fat Liquor Effects on Collagen Fibril Orientation and D-spacing in Leather During Tensile Strain

Strength is a very important property of leather and is known to depend on the arrangement of the collagen fibrils within the material. The addition of fat liquor (penetrating oils) is an essential part of the manufacture of leather and enhances the strength and feel of leather. However, the mechanism by which fat liquor leads to increased strength is not understood. Here synchrotron based small angle X-ray scattering (SAXS) is used to monitor the collagen fibril rearrangement and internal strain of leather during tension. Differences in internal structural changes under strain with varying levels of fat liquor are investigated. It is found that when a strain of up to 40-70% was applied to leather, the orientation index of the collagen fibrils changed up to 21.8% and the D-spacing changed by up to 1.8% with no consistent differences at different levels of fat liquor. The extensibility of leather increases by 11.3% with as little as 2% fat liquor addition and the elastic modulus decreases with fat liquor addition but not in proportion to the amount of fat liquor. This change in extensibility is not reflected in differences in OI or D-spacing changes during strain. As reported previously, the fat liquor modifies the D-spacing of collagen. While fat liquor is traditionally considered to lubricate the fibres in leather, here it is shown that this does not to occur at the level of collagen fibrils. This provides an insight in the action of fat liquor in leather manufacture.

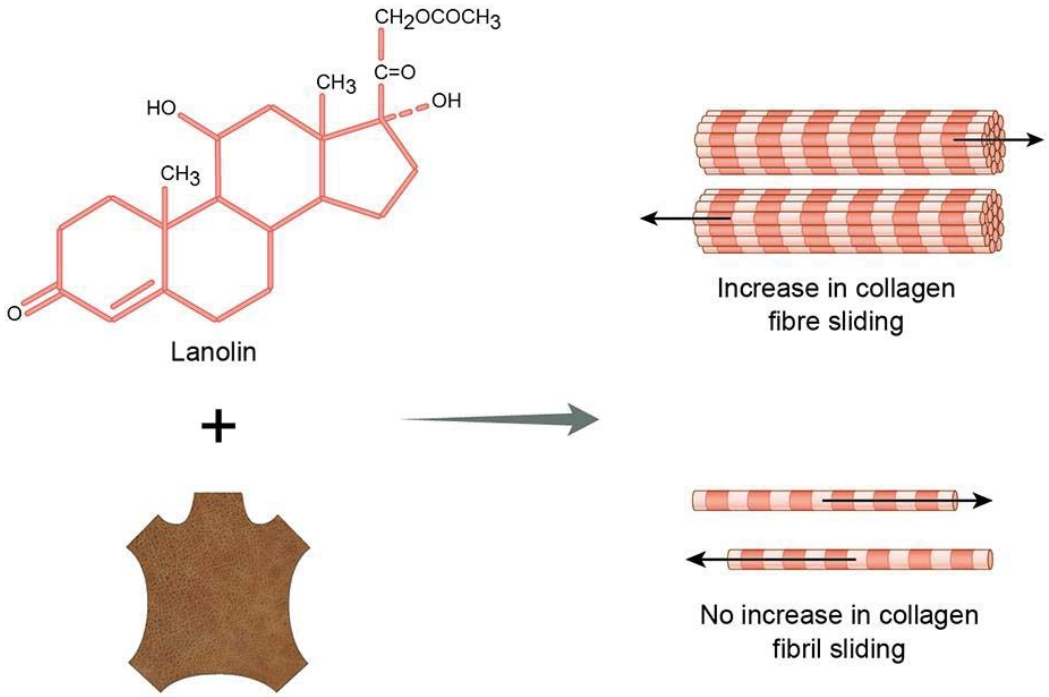

Figure 7.1. Increase in fibre sliding upon stretching of leather after the addition of fat liquor.

7.1 Introduction

The physical properties of leather result from a combination of the native characteristics of the skin or hide from which the leather is prepared and from the chemical and mechanical processing of leather manufacturing. Strength, flexibility, elasticity, and appearance are all important for the applications of leather. The major structural component of leather is type I collagen and it is the mechanical properties of the collagen fibrils (Basil-Jones et al., 2011, Wells et al., 2015, Russell, 1988) and the interactions between the fibrils (Chan et al., 2009, Rabinovich, 2001, Kayed et al., 2015, Deb Choudhury et al., 2007a, Michel, 2004) that make the major contribution to the physical properties of leather.

Interactions between collagen fibrils in leather consist of hydrogen bonding and hydrophobic bonding and cross linking introduced by tanning with chromium salts or tannins. Cross linking agents can alter the strength of the material and the arrangement of collagen fibrils (Kayed et al., 2015).

At a later stage in the processing of skins to leather penetrating oils, known in the industry as fat liquor, is added to improve the feel of the leather and to increase the strength. It is believed that fat liquor acts to lubricate the fibres in leather (Bajza and Vreck, 2001). Recently it has been shown that fat liquor penetrates to the level internal to collagen fibrils and alters the structure of the fibrils, increasing the D-spacing (Sizeland et al., 2015a). This is believed to be a result of shielding of the hydrophobic interaction between individual collagen molecules or tropocollagen units (Sizeland et al., 2014) .

A powerful method to investigate the structure of collagen materials is small angle X–ray scattering (SAXS) which can provide detailed structural information on the microfibril orientation, D-spacing and the collagen fibril diameter in leather and other tissues (Kronick and Buechler, 1986, Kennedy et al., 2004, Goh et al., 2005, Sizeland et al., 2013, Basil-Jones et al., 2010, Wells et al., 2013).

Using SAXS it is possible to characterise the structure of the collagen while tension is being applied. This gives accurate values of the physical properties of the material such as strength, flexibility, extensibility, and elastic modulus which can be compared with the structural measurements to determine if there any correlations between them.

To understand the physical properties of leather, changes to the structure and arrangement of the collagen fibrils during mechanical strain has previously been investigated (Boote et al., 2002, Sturrock et al., 2004, Basil-Jones et al., 2012, Wells et al., 2015). It has been found that with strain of the leather the collagen fibrils first align and then stretch.

This study aims to investigate the effect that fat liquor has on leather during mechanical strain. Is it believed that fat liquor lubricates the fibres in leather and it has been shown that fat liquor penetrates beyond the level of collagen fibrils, so does the fat liquor lubricate at the level of collagen fibrils?

7.2 Experimental Procedures

Ovine pelts were obtained from 5-month-old, early season lambs of breeds with "black faces", which may include Suffolk, South Suffolk, and Dorset Down. Conventional beamhouse and tanning processes were used to generate leather as detailed in Chapter 3.2.1. Fat liquoring was carried out using Lipsol EHF (Schill + Seilacher). This product contains a mixture of lanolin, bisulfited fish oil and 2-methyl-2,4-pentanediol. Lanolin, or wool wax, consists primarily of long chain waxy esters and some hydrolysis and oxidation products of these esters. The fat liquor was added at 0–10% by weight of wet leather prior to drying and mechanical softening.

Samples for synchrotron-based small angle X-ray scattering (SAXS) analysis were prepared by cutting strips of leather 1 × 30 mm from the official sampling position (OSP)(Williams, 2000b) from pelts of leather processed with 0, 2, 4, 6, 8, and 10% Lipsol EHF. Diffraction patterns were recorded on the Australian Synchrotron SAXS/WAXS beamline on static samples as per the experimental procedure detailed in Chapter 3.2.2 using an X-ray energy of 11 keV.

A custom built stretching apparatus was built for in-situ small angle X-ray scattering (SAXS) measurements as described by Basil-Jones (Basil-Jones et al., 2012). SAXS analysis completed whilst stretching a sample was completed by following the method described in Chapter 5.2.

Orientation index (OI) is used to give a measure of the spread of microfibril orientation and can be any number within the range 0–1. An OI of 1 indicates anisotropic microfibrils or fibrils that are completely parallel to each other; an OI of 0 indicates isotropic microfibrils or fibrils that are completely randomly oriented. OI is defined as (90° – OA)/90° where OA is the azimuthal angle range that contains 50% of the microfibrils centered at 180° and is calculated for one of the most intense D-spacing peak (at around 0.059–0.060 $Å^{-1}$) for every diffraction pattern (Basil-Jones et al., 2011).

The D-spacing of collagen was determined for each spectrum from Bragg's Law by taking the central position of several collagen peaks, dividing these by the peak order (usually from n = 5 to n =10) and averaging the resulting values.

Tear strengths of the crust leathers were tested using standard methods (Williams, 2000a). Samples were cut from the leather at the official sampling positions (OSP) (Williams, 2000b). The samples were then conditioned by holding at 20°C and 65% relative humidity for 24 hours then tested on an Instron tensile tester using jaws placed in a standard eye-shaped cut out.

7.3 Results

The offer of fat liquor to the leather ranged up to 10% however the actual uptake of fat liquor was not quite the same as the offer. An analysis of the fat content of the fat liquored leather showed a higher fat content than the nominal offer, with a saturation occurring at 8% offer (Table 7.1).

Table 7.1. Nominal addition of fat liquor and measured content of fat in leather samples.

Nominal Addition of Fat Liquor (%)	Measured Fat Content (%)	Measured fat liquor added (%)
0	1.0	0.0
2	3.8	2.8
4	5.7	4.7
6	8.8	7.8
8	9.8	8.8
10	9.9	8.9

The X-ray scattering patterns recorded for the leather samples show clear diffraction rings (Figure 7.2a and 7.2b) which are due to the collagen d-banding. The integrated intensity for these patterns shows these as well defined peaks from which the d-banding can be identified (Figure 7.2c and 7.2d). The variation in intensity with azimuthal angle (Figure 7.2e) can be used to calculate the orientation index of the collagen fibrils. It can be seen that when the leather is stretched the OI decreases and a portion of the fibrils which are aligned in the direction of the strain become highly stretched with the D-spacing increasing substantially.

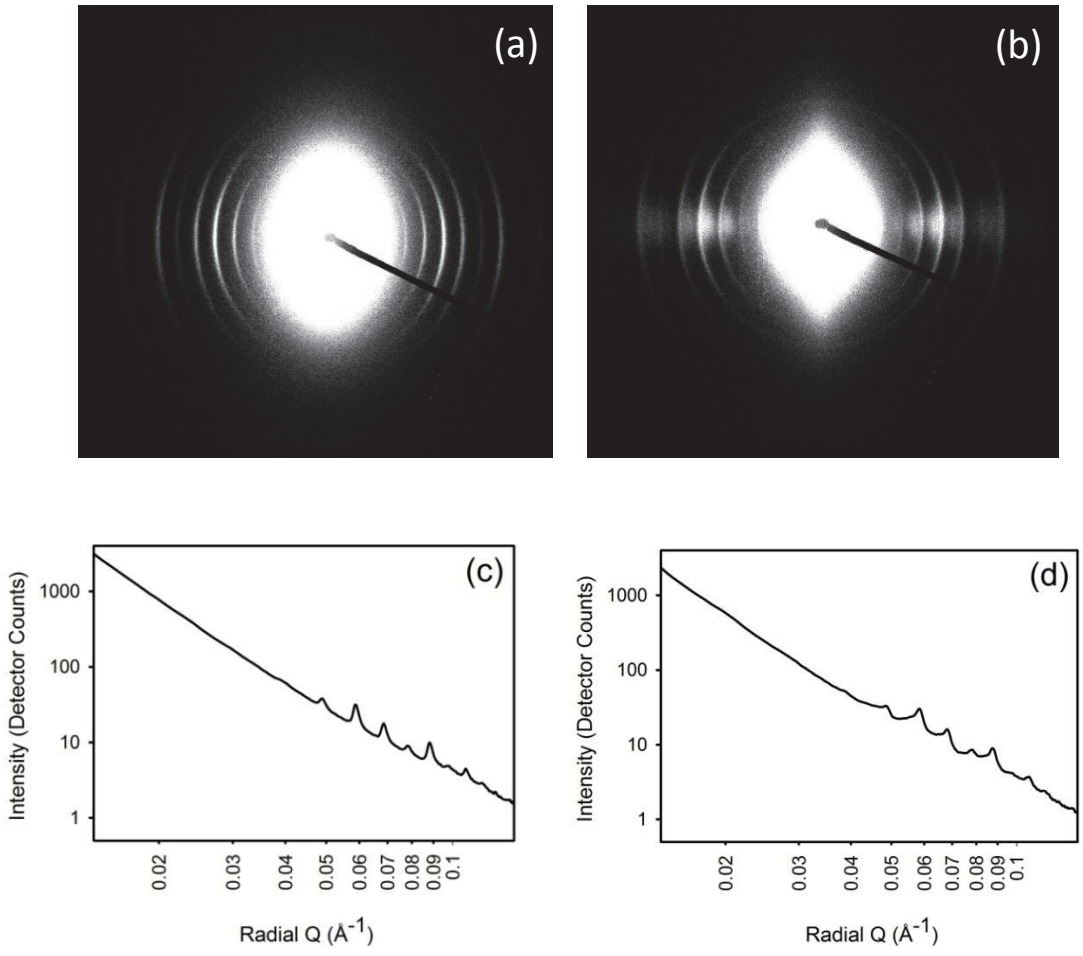

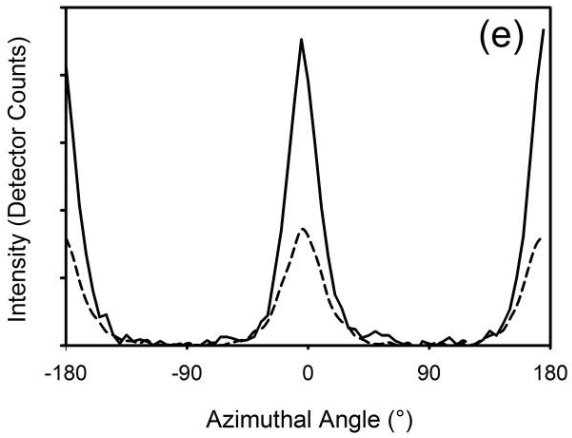

Figure 7.2. Example of SAXS of leather: (a) raw SAXS pattern static; (b) raw SAXS pattern after stretching; (c) integrated intensity profile of static sample; (d) integrated intensity profile of sample after stretching; (e) intensity variation with azimuthal angle for the 5th order diffraction peak (dotted line static, solid line stretched).

When the variation of D-spacing with strain is plotted it becomes apparent that the D-spacing increases with fat liquor content (as reported elsewhere (Sizeland et al., 2015a)) and increases with strain (as seen with ovine leather (Basil-Jones et al., 2012)) (Figure 7.3). There is no difference between 8% and 10% fat liquor offer samples as these had saturated and had the same uptake of fat liquor.

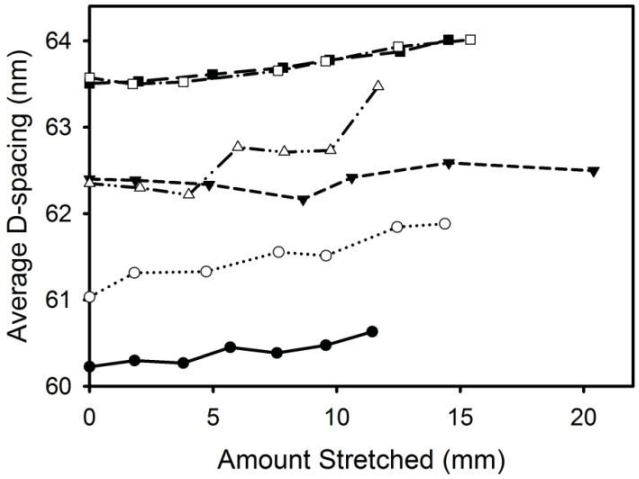

Figure 7.3. Variation in D-spacing with strain and fat liquor content: (●, ——) no fat liquor, (○, ·····) 2% fat liquor, (▼, – – – –) 4% fat liquor, (Δ, – ·· – ·· –) 6% fat liquor, (■, ———) 8% fat liquor, (□, – · – · –) 10% fat liquor.

The OI increases with strain for all samples (Figure 7.4). Samples with more fat liquor have a lower OI than those with less fat liquor (Figure 7.5a). However, when stretched, a sample first has an increase in OI but then the OI measured at maximum strain before the sample breaks does not correlate with fat liquor addition.

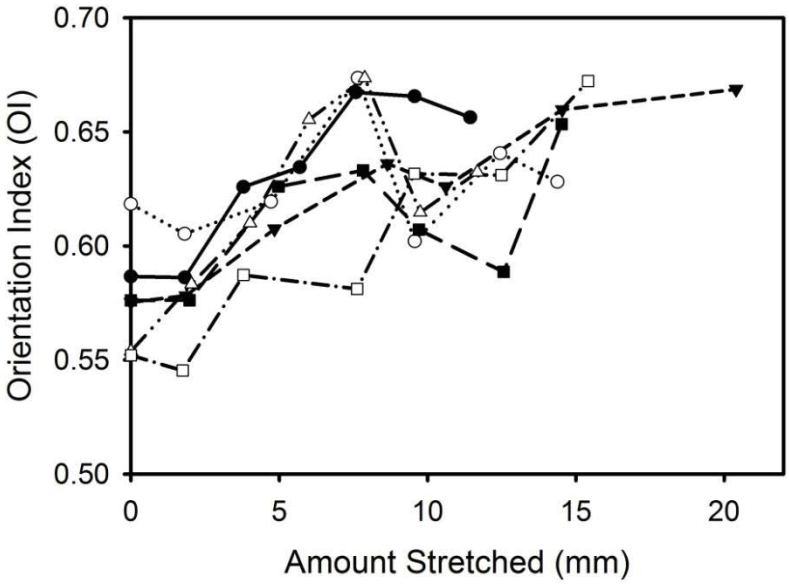

Figure 7.4. Variation in orientation index (OI) with strain and fat liquor content: (●, ——) no fat liquor, (○, ·····) 2% fat liquor, (▼, – – – –) 4% fat liquor, (Δ, – ·· – ·· –) 6% fat liquor, (■, ———) 8% fat liquor, (□, – · – · –) 10% fat liquor.

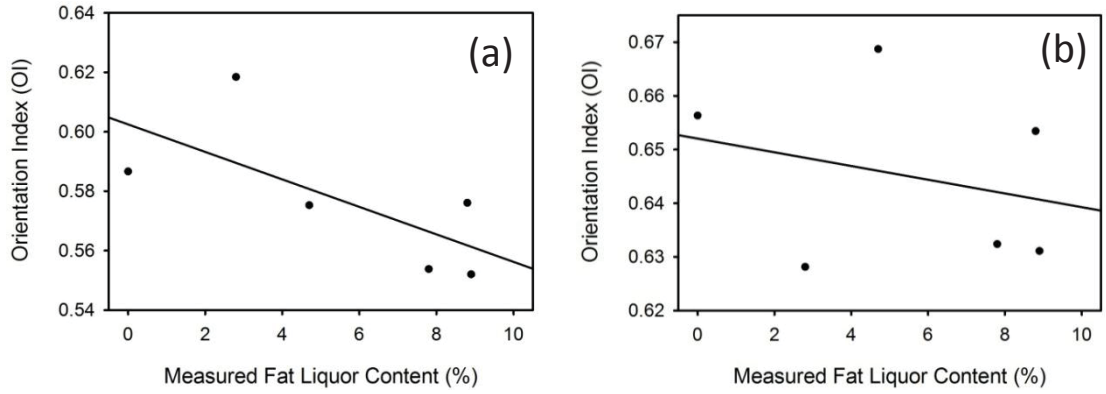

Figure 7.5. Variation of OI with measured fat liquor content: (a) for unstrained leather; (b) for leather strained to maximum, orientation is calculated by taking the average OI of the sample after each stretching increment (from no stretch up to the maximum amount stretched) and averaging these values.

The samples with different fat liquor content do not all stretch the same amount. Therefore a plot of the change in D-spacing and OI at a strain of 0.4 is also shown (Figure 7.6). This provides a fair comparison between the changes that take place to fibril rearrangement and internal fibril stretching for samples under increasing amounts of tension when different levels of fat liquor are present. This shows no trend when stretched with fat liquor content of the sample in either the amount that D-spacing changes or in the OI change with stretching (Figure 7.6)

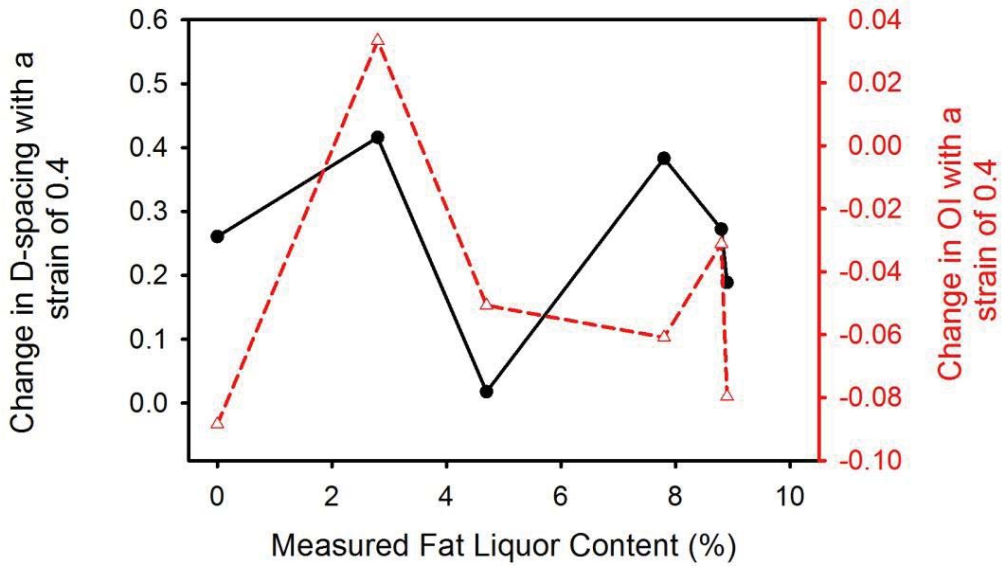

Figure 7.6. Change in OI and D-spacing upon strain to 0.4 for each measured fat liquor content.

The stress-strain curves (Figure 7.7) show that the elasticity varies with fat liquor content. With fat liquor added leather has a longer region of low elastic modulus (material is able to stretch more) before the leather starts to resist stretching. Full stress-strain curves for the small samples measured in-situ during X-ray analysis are shown in Figure 7.7a but these were small samples and must not be over-interpreted. More reliable for elastic modulus measurements were the larger samples measured independently of the SAXS measurements showing the initial drop in elastic modulus with an addition of a small amount of fat liquor followed by a general increase in elastic modulus with further fat liquor additions (Figure

7.7b). The total extensibility of the leather is also shown but does not follow an easily rationalised trend (Figure 7.7c).

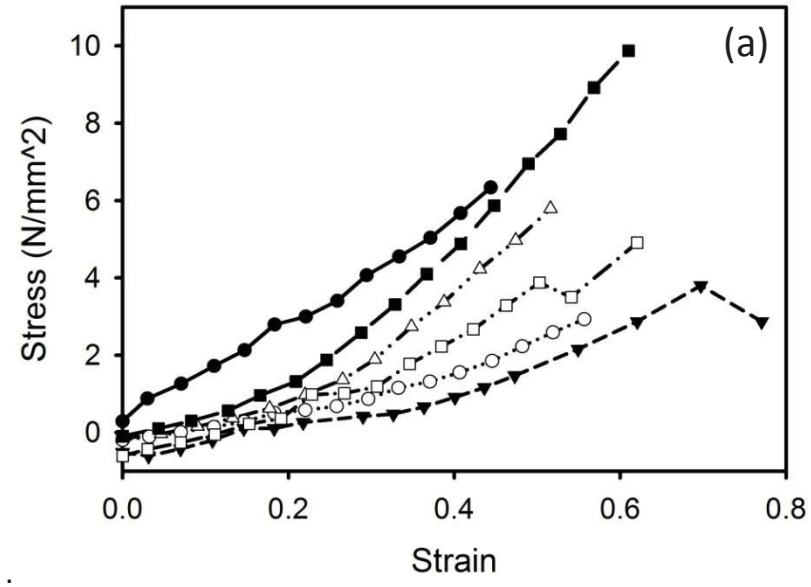

.

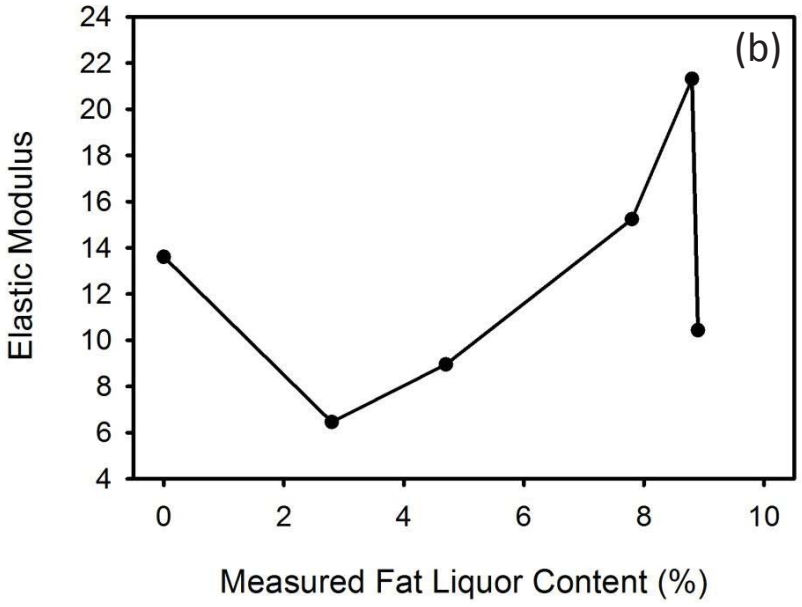

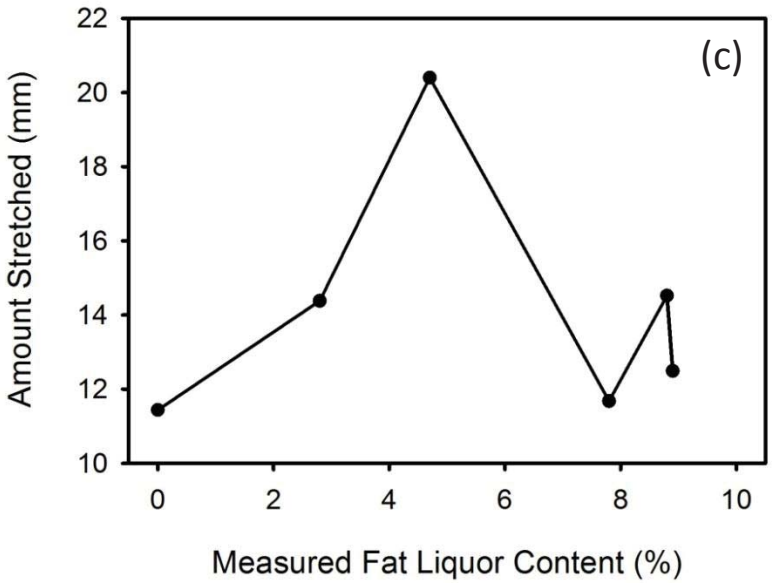

Figure 7.7. (a) Stress-strain on small leather samples recording during SAXS measurements (●, ____) no fat liquor, (○, ·····) 2% fat liquor, (▼, – – – –) 4% fat liquor, (Δ, – ·· – ·· –) 6% fat liquor, (■, ———) 8% fat liquor, (□, – · – · –) 10% fat liquor; (b) Elastic modulus taken from curves in (a); (c) amount stretched by sample versus measured fat liquor content.

The tear force follows a similar trend to the elastic modulus of the samples. There is an initial drop in the tear strength with the addition of a small amount of fat liquor followed by a general increase in tear strength with further fat liquor additions (Figure 7.8). Generally therefore leather is stronger when fat liquor is present.

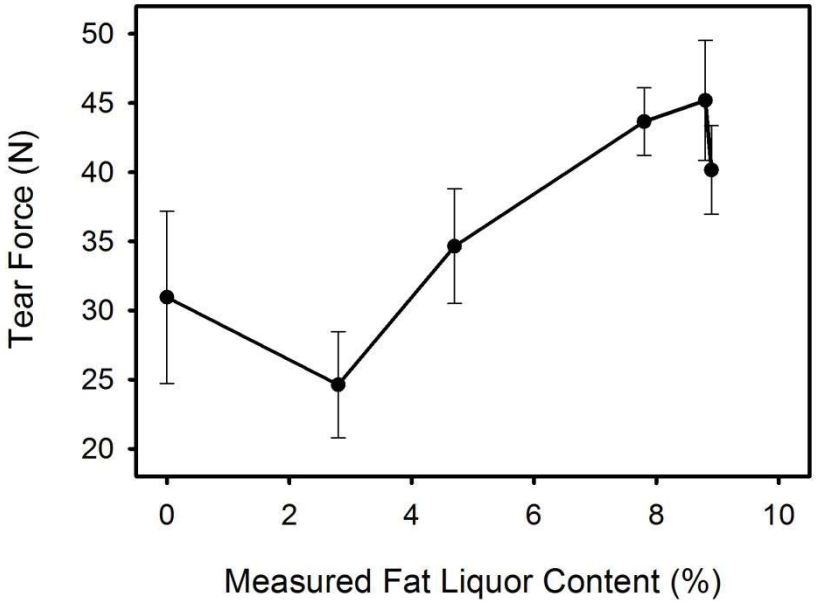

Figure 7.8. Tear force of leather with measured fat liquor content.

The variation of OI through sections of leather with different amounts of fat liquor at different levels of strain (Figure 7.9) show the strain is taken up throughout the thickness of the leather and that this is similar with or without fat liquor added. There is no obviously different mechanism of responding strain with or without fat liquor present.

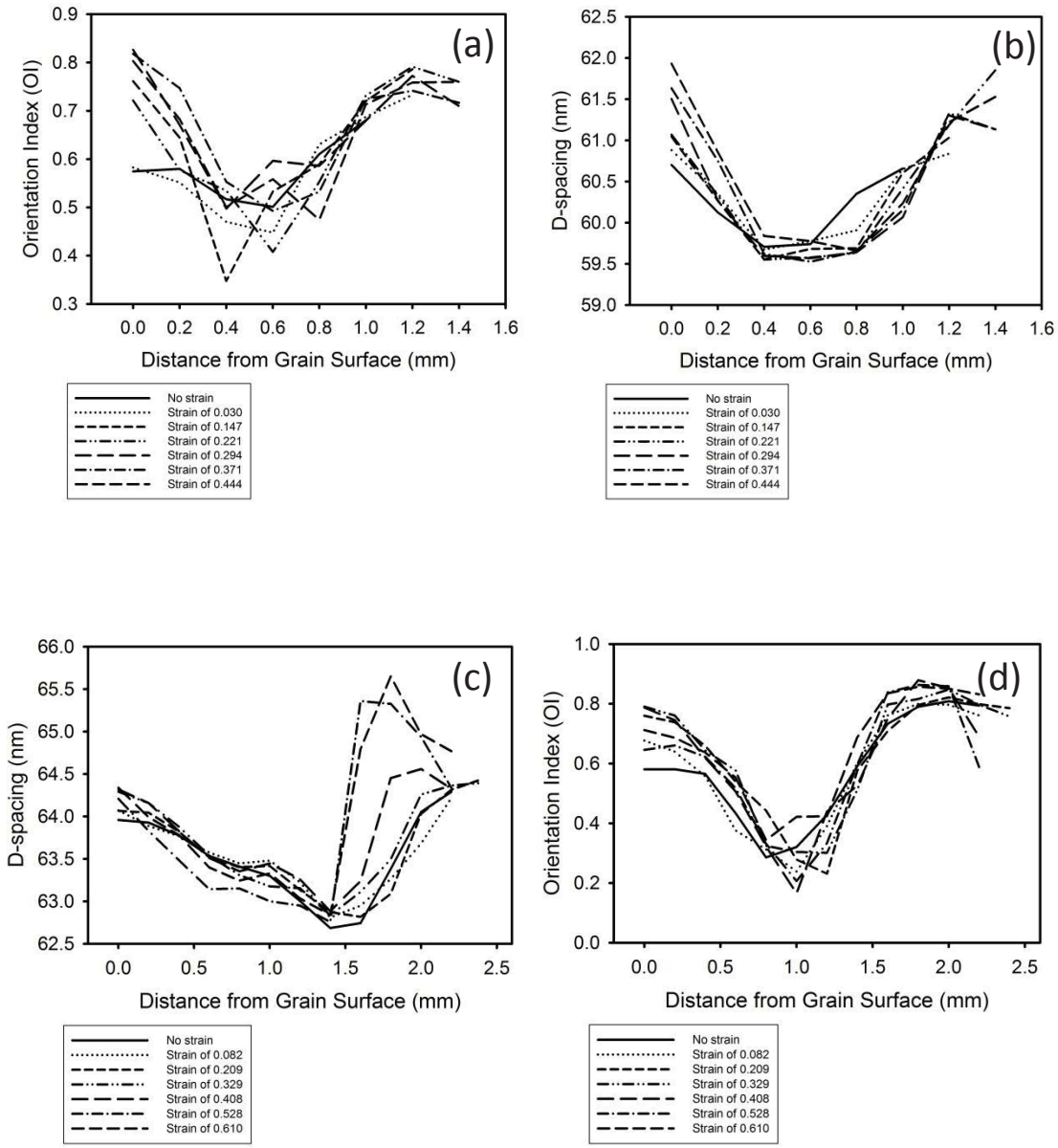

Figure 7.9. Cross sections of leather under strain. No fat liquor (a, b), 8% fat liquor (c, d). Variation of OI with strain (a, c), variation of D-spacing with strain (b, d).

7.4 Discussion

While it can be seen that the fat liquor penetrates to the collagen fibrils and changes some aspect of the structure of the fibrils, the D-spacing, as shown in Chapter 4, there does not appear to be any difference in the change in the orientation of the fibrils during strain with or without fat liquor. Therefore the rearrangement of fibrils in the leather is not greater with fat liquor added than without. In addition, the amount of force individual fibrils experience (evidenced by D-spacing change during stress) is not less with fat liquor than without.

If the fat liquor acted to lubricate the collagen fibrils so that they slide more easily past one another then it would be expected that the OI would change much more with strain when fat liquor is added because as the fibrils slide more easily past each other they would be able to rearrange their positions to become more aligned. If this is the mechanism of action of fat liquor then it would also be expected that once well aligned then the fibrils should be able to stretch more as they are aligned with the direction of force. Neither of these is seen, neither a greater change in OI nor a larger increase in D-spacing. Therefore, there is no evidence of lubrication of the collagen fibrils, even though it is known that the fat liquor penetrates not just to the fibrils but within the fibrils (as evidenced by the change in D-spacing).

From the stress-strain data, and as is well known already, fat liquor does improve the bulk properties of leather and increases the extensibility and decreases the elastic modulus of leather. Therefore fat liquor does have an effect on the leather. Since the lubrication by fat liquor does not appear to occur at the fibril level the mode of action may be lubrication between fibril bundles or fibres which is at a different scale to the fibrils.

Leather takes up strain at a variety of scales, both within the fibril (D-spacing), between fibrils (OI) and at the fibril bundle and fibre level (possibly contributes also to OI). Fat liquor affects the larger scale processes and is important to the properties of finished leather.

7.5 Conclusions

This study has been able to provide more knowledge of the mechanism of action of fat liquor to the elasticity of leather to inform the leather making process. It has been shown leather takes up strain on many levels of the hierarchical structure of collagen and that with the addition of fat liquor the ability of the material to stretch is increased. Lanolin, which was a key component of the fat liquor used here, is commonly used in skin care formulations and as such this knowledge may also apply to skin modified by skin care products.

Chapter 8: Age Dependent Differences in Collagen Alignment of Glutaraldehyde Fixed Bovine Pericardium

Bovine pericardium is used for heart valve leaflet replacement where the strength and thinness are critical properties. Pericardium from neonatal animals (4-7 days old) is advantageously thinner and is considered as an alternative to that from adult animals. In this investigation the structures of adult and neonatal bovine pericardium tissues fixed with glutaraldehyde are characterized by synchrotron-based small angle X-ray scattering (SAXS) and compared with the mechanical properties of these materials. Significant differences are observed between adult and neonatal tissue. It is shown that high alignment in the plane of the tissue provides the mechanism for the increased strength of the neonatal material. The superior strength of neonatal compared with adult tissue (depicted in Figure 8.1) supports the use of neonatal bovine pericardium in heterografts.

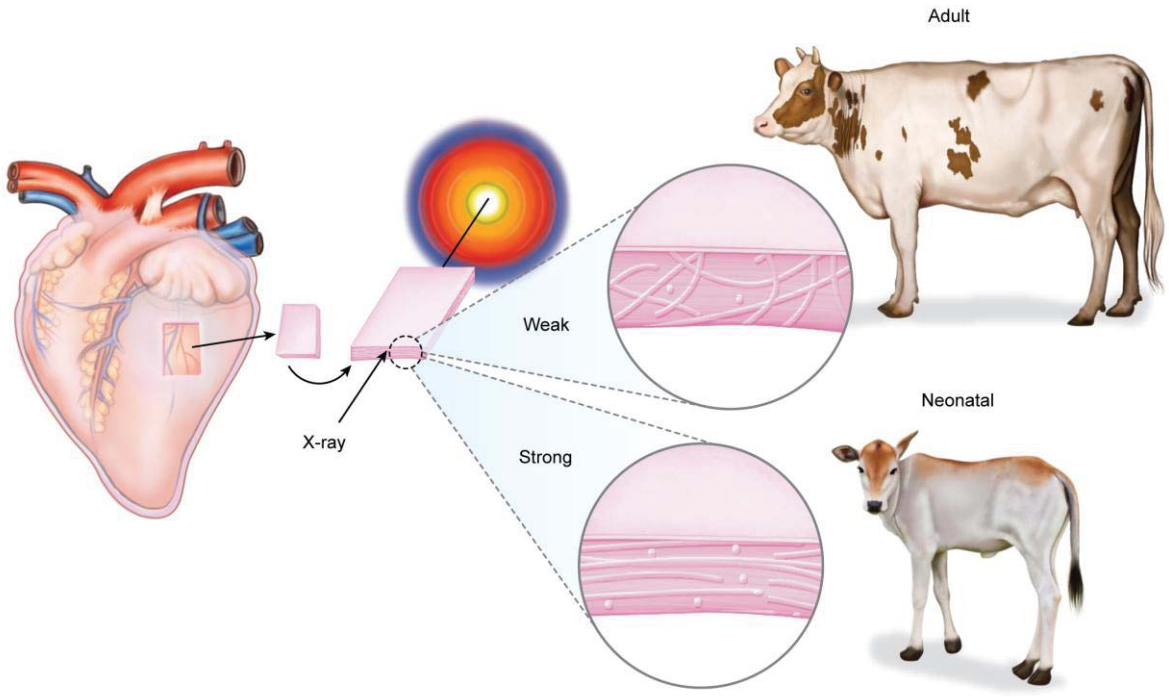

Figure 8.1. Adult pericardium with a lower OI is a weaker material; neonatal pericardium with a higher OI is a stronger material.

The following investigation has been published in the BioMed Research International Journal in 2014, Issue 10, and can be found in Appendix 10.1.

8.1 Introduction

Heart valve leaflet replacement with bovine pericardium is an established practice (Nwaejike and Ascione, 2011) using either adult or calf pericardium (Paez et al., 2006) and may be performed percutaneously (Cribier et al., 2003). It is essential that the mechanical strength and performance of the material is adequate for a long life in service (Mirnajafi et al., 2010). Greater understanding of the properties of these materials and the structural basis for these properties is important for improving the serviceability of these replacements.

Pericardium is a fibrous collagen extracellular matrix material with structural similarities to skin and other tissues. The structure of these collagenous tissues can be characterized by small angle X-ray scattering (SAXS) to yield, for example, quantitative measures of fibril orientation and fibril D-spacing (Liao et al., 2005, Purslow et al., 1998, Basil-Jones et al., 2010). While other methods have been used to study collagen fibril orientation including polarized light microscopy (Julkunen et al., 2010), reflection anisotropy (Schofield et al., 2011), small angle light scattering (Sacks et al., 1997), confocal laser scattering (Jor et al., 2011), Raman polarisation (Falgayrac et al., 2010), and anisotropic Raman scattering (Janko et al., 2010), synchrotron based SAXS has the advantage of excellent non-subjective quantification combined with good spatial resolution.

That there is a function-structure relationship between collagen alignment and mechanical strength is well known (Fratzl and Weinkamer, 2007). The orientation of collagen measured edge on (alignment in-plane) has been shown in bovine and ovine skin to be correlated with strength (Basil-Jones et al., 2011, Basil-Jones et al., 2012). This correlation extends across a range of mammal species with a strength range of over a factor of five (Sizeland et al., 2013). It is the three-dimensional

orientation that is important – simply taking an observation of the fibril orientation normal to the surface of the tissue is not very helpful. Instead, it is necessary to measure the orientation of the fibrils through the thickness of the skin to determine the extent to which they cross between the top and the bottom of the skin layer (Sizeland et al., 2013).

The orientation of collagen in pericardium heterograft materials for heart valve leaflets has been shown to affect the stiffness during flexing (Mirnajafi et al., 2005). In ovine and bovine skin, the orientation of the fibrils in the skin influences the mechanical properties (Sizeland et al., 2013, Basil-Jones et al., 2012).

It has previously been found that pericardium from neonatal calves (4-7 days old) has superior properties for potential application for heart valve repair (Cunanan et al., 2012). Although both adult and calf bovine pericardia are used in heart valve repair, neonatal pericardium has not yet been used for heart valve manufacture. The greater tensile modulus of neonatal pericardium than adult pericardium may enable the thinner neonatal tissue to be used. This would allow a smaller introducer size for percutaneous heart valves. This makes the application of these heart valves possible through diseased femoral arteries which may have reduced diameters (Kroger et al., 2002). Glutaraldehyde cross linked pericardium continues to be the material of choice for heart valve manufacturers and developers. There are several devices on the market and more devices currently in clinical trial that use glutaraldehyde treated tissues.

It is known that collagen tissue properties change with age. Differences have been shown in the thermal stability of tendon collagen between steers aged 24-30 months and bulls aged 5 years old and this has been attributed to increased level of maturity and thermally stable cross links (Willett et al., 2010). Glycation of collagen increases with age and can lead to differences in mechanical properties of the collagen. It has been shown to increase stiffness in connective tissues (Bailey, 2001) and collagen gels (Francis-Sedlak et al., 2009) and increase brittleness in bones(Leeming et al., 2009). Porcine extracellular matrix scaffolds derived from small intestinal submucosa of younger animals and used for *in vivo* remodeling have been studied previously. They were associated with a more constructive, site

appropriate, tissue remodeling response than scaffolds derived from older animals (Sicari et al., 2012). However, specific physical factors causing this difference were not identified.

It has also been found that tissue strength varies with collagen fibril diameter. Larger diameter collagen fibrils are present in stronger tissue. In human aortic valves, the collagen fibril diameter depends on whether the fibrils are from regions of high stress or low stress: larger diameter fibrils (in areas of lower fibril density) result from high stress, suggesting that these larger diameter fibrils provide increased strength (Balguid et al., 2008). Similarly for mouse and rat tendon, fibril diameters increase with loading (Michna, 1984, Biancalana et al., 2010). It is proposed that this is due to the extra mechanical load placed on the tendons on the exercising animals (due to their higher activity levels) stimulating fibril thickening (Biancalana et al., 2010). In bovine leather fibril diameter is found to be only weakly correlated with strength (Wells et al., 2013).

The size distribution of the fibril diameter has also been found to change with age. Fetal tissue has been found to have a unimodal distribution with smaller collagen fibril diameters, whereas older tissue has larger fibrils and may have a unimodal or bimodal size distribution depending on the tissue type and animal (Parry et al., 1978). In studies of equine digital flexor tendons, fibril diameter decreases with exercise, suggesting weakening of tendon with exercise (i.e. fatter fibril is stronger). Unusually, the fibril diameter in these tendons decreases with age, and this is associated with the decrease in strength (PattersonKane et al., 1997b, Cherdchutham et al., 2001).

In the percutaneous delivery of heart valves, the size of the device when folded for delivery is important. Devices made from adult bovine pericardium or porcine pericardium typically require a size 18F to 25F catheter (7.0 – 8.4 mm) (Chiam and Ruiz, 2008). This size is in part dictated by the thickness of the pericardium that is used in the valve, with thicker material folding into a larger diameter device for insertion. A study of 79 patients with peripheral arterial disease found that occluded femoral arteries had an average internal diameter of 4.5 ±1.4 mm with 12 below 3.5 mm (11F on the French catheter scale) (Kroger et al., 2002). These

occluded arteries are significantly smaller than the folded heart valves resulting in difficulties for percutaneous delivery of existing heart valve technology. This provides a motivation to find thinner but sufficiently strong material as a substitute for the existing bovine or porcine pericardium. Neonatal pericardium is one possible option that is investigated here.

The structural differences between neonatal pericardium and adult tissue that give rise to the desirable differences in their physical properties have not been adequately investigated. This study investigates and compares the collagen fibril structure of neonatal and adult bovine pericardium using SAXS. Specifically, the fibril orientation, and the fibril diameter are examined. The use of SAXS at a modern synchrotron facility allows analysis of a small area (250 x 80 μm), enabling quantification of fibril orientation edge on in relatively thin pericardium tissues – a process that is difficult to achieve by other methods.

8.2 Experimental Procedures

Southern Lights Biomaterials Inc. provided all pericardium samples for analysis. The processing method for these pericardia followed conventional procedures and is outlined below along with the selection of the samples.

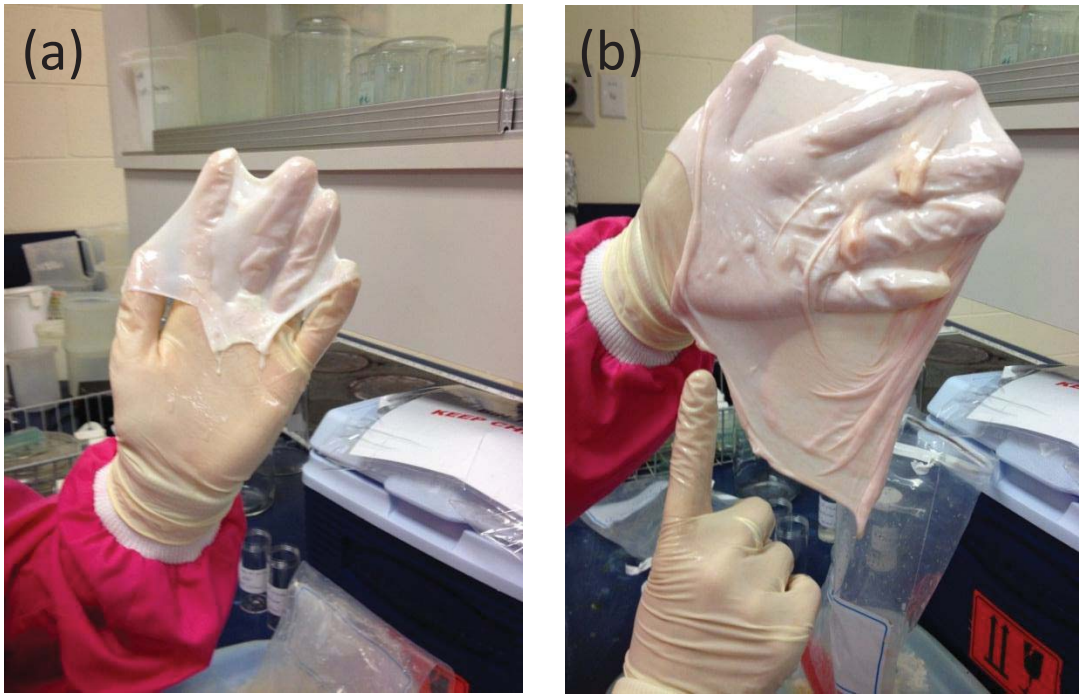

Figure 8.2. (a) neonatal and (b) adult pericardium prior to cutting into a butterfly shape.

Pericardia were selected from 10 neonatal (4 – 7 days old) and 10 adult (18 – 24 months old) cattle (Figure 8.2a and 8.2b above). The fresh pericardia (less than 72 hours post mortem and typically 48 – 72 hours post mortem) were washed several times in PBS buffer (pH 7.4 ± 0.2, 0.01 % NaCl). Neonatal tissue was typically processed closer to 72 hours post mortem due to the logistics of obtaining the samples while adult tissue was typically processed closer to 48 hours post mortem. The tissue was stored at 4 - 7 °C from harvest until the start of washing. Washing in PBS buffer took place at room temperature. The pericardium was then cut and flattened into a "butterfly" shape and held flat with weights around the edge (Figure 8.3) with care taken to ensure there were no air bubbles trapped beneath the material.

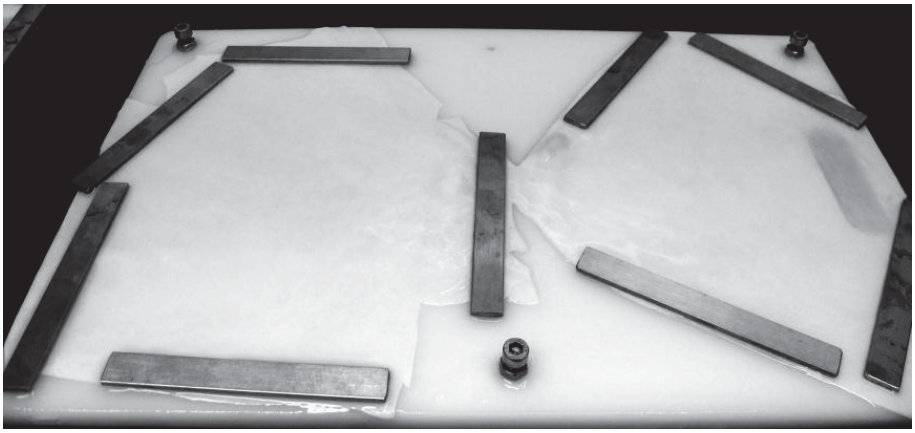

Figure 8.3. Flattened pericardium held with weights around the edge following cutting (Sizeland et al., 2014).

Treatment with glutaraldehyde was performed in several stages at room temperature. First the flat, weighted pericardium was immersed in a tray of 0.625 % glutaraldehyde (in PBS buffer) for 30 minutes. The second stage was immersion in fresh 0.625% glutaraldehyde (in PBS buffer) for 48 hours with the weights removed. For the third stage the solution was changed for fresh 0.625% glutaraldehyde (in PBS buffer) and maintained for a further 48 hours. After this treatment, coupons of 90 mm x 140 mm were cut from the centre of each side of the butterfly. For the SAXS analysis, strips were cut in two directions perpendicular to each other from the centre of coupons. Replicates of each sample were prepared. The thickness of the coupons was measured with callipers using a light and consistent force. Details of all samples were recorded when cut and the samples were stored in small, numbered, lidded glass vials to ensure no information was lost and samples remained unharmed and easily identifiable after transportation. The pericardium samples were stored with enough 0.625% glutaraldehyde PBS solution to keep the material moist until required for other tests. The time between this stage and mechanical or SAXS measurements varied between 1 day and 3 weeks.

In preparation for SAXS analysis, the pericardia were removed from the glutaraldehyde solution in which they had been stored and soaked for at least 1 hour in buffered saline solution. The strips were then mounted between 7-µm-

thick kapton tape to prevent drying during analysis (i.e. retain them in a wet state). The X-ray beam was directed either through the sample perpendicular to the flat surface or through one of two edge mounted samples. This meant that spectra were recorded in each of three orthogonal directions through the tissue for each sample (Figure 8.4).

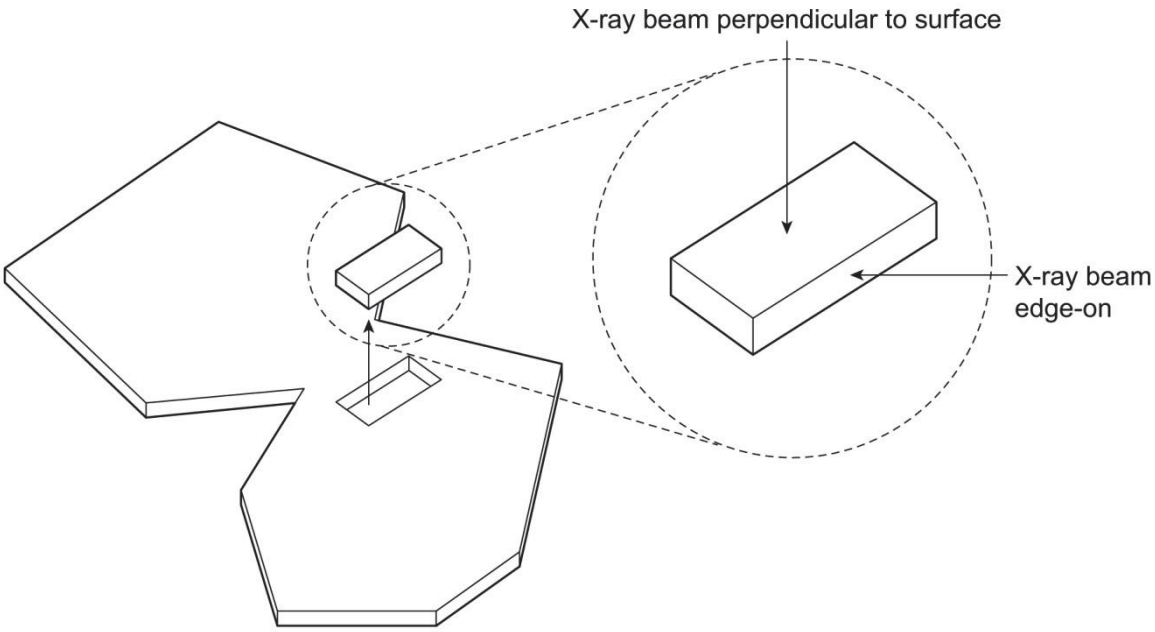

Figure 8.4. Beam direction for SAXS analysis with relation to pericardium butterfly (Sizeland et al., 2014).

For the samples analysed edge on it was necessary to brace the tissue against a stiff plastic strip mount to prevent the pericardium from folding or twisting during analysis. This ensured that there was only one layer of the sample in the path of the X-ray beam throughout all experimental analysis in this direction. All diffraction patterns were recorded at room temperature.

The elastic modulus and ultimate tensile strength were measured uniaxially using an Instron tensile tester on strips of material. For detailed methods on tensile testing please refer to Chapter 3.

Histological cross sections stained with picrosirius red to highlight the collagen were recorded under cross polarized light on one sample of neonatal pericardium and one of adult pericardium (Constant and Mowry, 1968).

Diffraction patterns were recorded on the Australian Synchrotron SAXS/WAXS beamline, utilizing a high-intensity undulator source. Energy resolution of 10^{-4} (e.g. 1 x 10^{-4} Å for 1 Å radiation) was obtained from a cryo-cooled Si(111) double-crystal monochromator and the beam size (FWHM focused at the sample) was 250 x 80 µm, with a total photon flux of about 2 x 10^{12} ph.s^{-1}. All diffraction patterns were recorded with an X-ray energy of 12 keV using a Pilatus 1M detector with an active area of 170 x 170 mm and a sample–to-detector distance of 3371 mm. Exposure time for diffraction patterns was 1 s and data processing was carried out using the SAXS15ID software (Cookson et al., 2006). For full static experimental methods refer to Chapter 3.2.2 and for stretching details see Chapter 5.2.

The orientation index (OI) is used to give a measure of the spread of microfibril orientation and was calculated as detailed in Chapter 3.2.2.

Fibril diameters were calculated from the SAXS data using the Irena software package (Ilavsky and Jemian, 2009) running within Igor Pro as described in Chapter 5.2.

8.3 Results

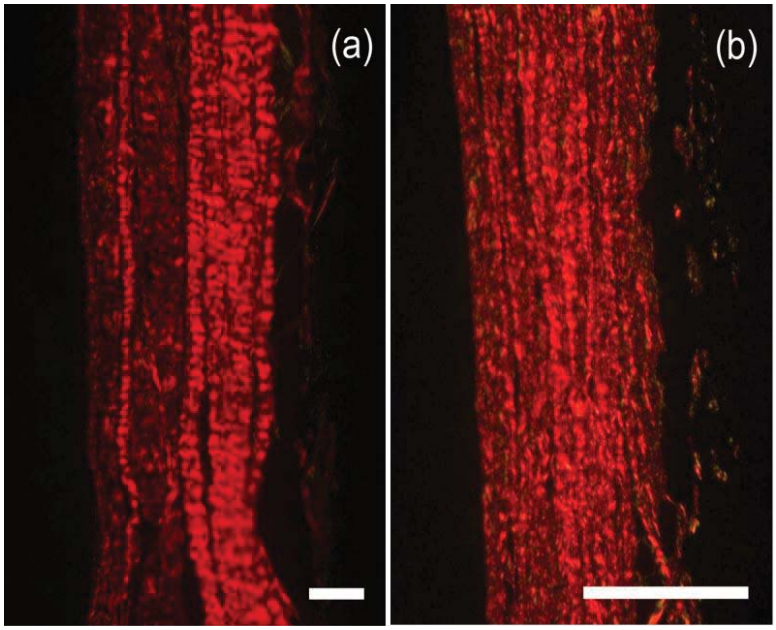

Figure 8.5. Pericardium stained with picrosirius red and imaged through cross polarized light to highlight collagen: a) adult pericardium; b) neonatal pericardium. The parietal side is toward the left, the fibrous side toward the right of each image. Scale bar is 0.1 mm (Sizeland et al., 2014).

Histology. Pericardium stained with picrosirius red highlight differences in the inner and outer layers of the parietal pericardium with more pronounced and larger collagen fibres in the fibrous side of the tissue (Figure 8.5). Differences are apparent between adult and neonatal pericardium with the adult pericardium more clearly differentiated into two layers. The layer on the fibrous side showed a strongly differentiated collagen fibre structure compared with the parietal side of the adult pericardium. By comparison the juvenile pericardium has less differentiation through its thickness.

Thickness. The average thickness was 0.36 (σ = 0.03) mm for adult pericardium and 0.12 (σ = 0.006) mm for neonatal pericardium. The neonatal is therefore one third the thickness of the adult.

Mechanical properties. The elastic modulus of glutaraldehyde fixed neonatal bovine pericardium at both small strain (< 20%) and large strain is found to be very much greater than for glutaraldehyde fixed adult pericardium (Table 8.1).

The ultimate tensile strength is also greater for glutaraldehyde fixed neonatal pericardium rather than adult pericardium (Table 8.1). The strength measured here (standard deviation in parentheses) of 19.1 (σ = 2.2) MPa for adult and 32.9 (σ = 4.1) MPa for neonatal is less than that reported previously for unfixed bovine pericardium of 25-29 MPa and of unfixed porcine pericardium of 22-23 MPa (Paez et al., 2002a, Paez et al., 2002b) but greater than that reported in a different study for calf pericardium at 6-9 months of 11.5 ± 4.6 MPa (Maestro et al., 2006). Here we report the ultimate tensile strength as the tissue property per cross sectional area. The absolute strength of the glutaraldehyde treated adult pericardium is a little higher than the neonatal. However, it is noted that the neonatal pericardium is one third of the thickness of adult pericardium. The strain at failure is much less for neonatal pericardium than adult pericardium. This reflects the higher elastic modulus of the neonatal material compared with adult pericardium and high strength (Table 8.1).

The main objective of this work is to determine why it is that the neonatal pericardium has a higher ultimate tensile strength and a higher tissue modulus. For this purpose the SAXS measurements were used to investigate the structures of these two materials.

Table 8.1. Mechanical properties of adult and neonatal glutaraldehyde fixed bovine pericardium.

Test	Adult (n=13)†	Neonatal (n = 11) †	p†
Small strain (< 0.2) elastic modulus (MPa)	4.8 (2.0)	71.9 (11.6)	<0.0001
Large strain (> 0.2) elastic modulus (MPa)	33.5 (3.2)	83.7 (10.6)	<0.0001
Ultimate tensile strength (MPa)	19.1 (2.2)	32.9 (4.1)	0.0050
Strain at failure	0.80 (0.06)	0.48 (0.03)	0.0002

†Standard error ( ) and p from two tailed t-test comparison of adult and neonatal

SAXS measurements. SAXS patterns of pericardium show clearly the diffraction from collagen fibrils. Two selected SAXS images are shown illustrating a nearly isotropic sample (Figure 8.6a) and a highly oriented sample (Figure 8.6b). The angular position of the bands or rings is due to the D-spacing of the collagen fibrils. The integrated intensity of such a pattern (Figure 8.7) enables the position of each peak of different order to be accurately measured.

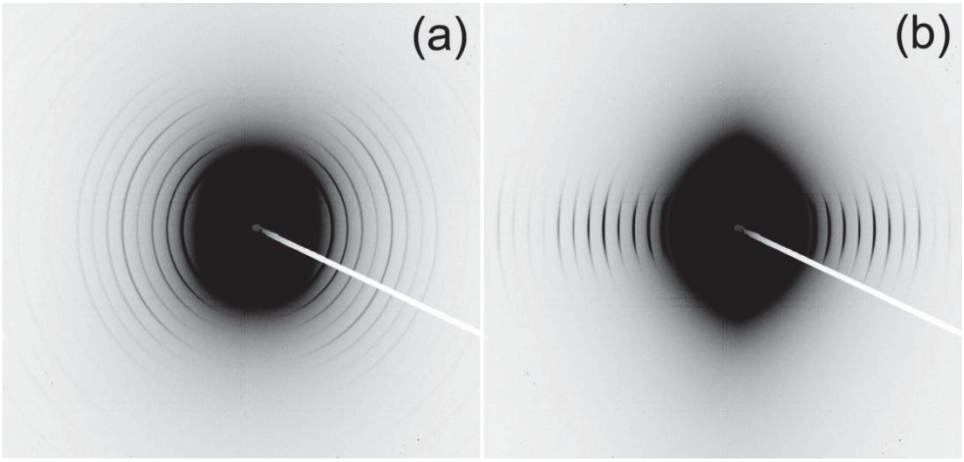

Figure 8.6. SAXS spectra of pericardium: a) a poorly oriented tissue; b) a highly oriented tissue (Sizeland et al., 2014).

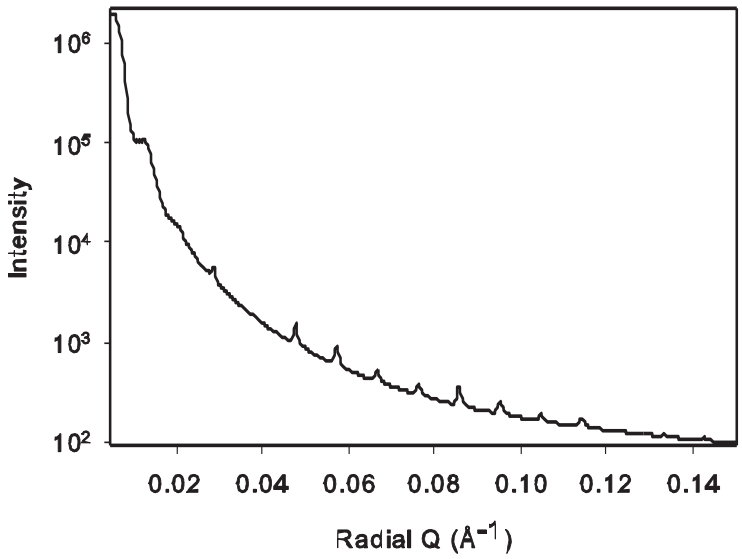

Figure 8.7. SAXS profile of an example bovine pericardium integrated around all azimuthal angles. The sharp peaks due to collagen D-spacing of various orders are visible (order 5 is just below 0.05 $Å^{-1}$, order 6 at just below 0.06 $Å^{-1}$, etc.) (Sizeland et al., 2014).

To obtain a quantitative measure of the orientation of the fibrils, the variation in intensity of one of these collagen peaks is plotted as a function of azimuthal angle (Fig. X below). It is the width of the peak centered at 180° that reflects the orientation index (OI).

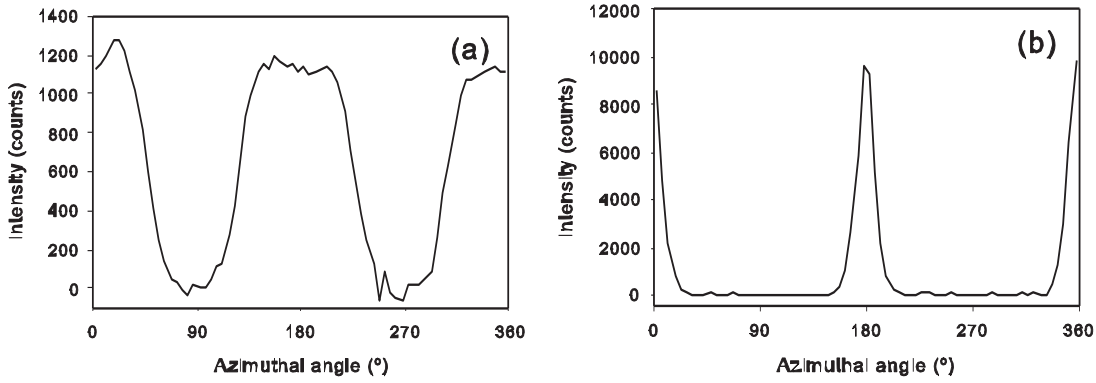

Figure 8.8. Plots of the intensity of a selected collagen peak at varying azimuthal angles for bovine pericardium samples. a) a poorly aligned tissue; b) a highly aligned tissue. The central peak at 180° (and other peaks at 0 and 360°) is the

variation in intensity of collagen D-spacing whereas the lower peaks at 90° and 270° are due to the scattering from the thickness of the fibrils and fibril bundles (Sizeland et al., 2014).

Orientation. The collagen fibril OI measured perpendicular to the surface of the pericardium is very small, indicating a highly isotropic arrangement of fibrils in this direction. There is no statistical difference in alignment between adult tissue (OI = 0.020) and neonatal tissue (OI = 0.071) (t-statistic = 0.794, P = 0.43) (Table 8.2).

In contrast to the perpendicular measurements, edge on the fibrils are more oriented and have a higher OI. The fibrils are therefore approximately in isotropic layers stacked one upon the other. However, there are marked differences between the neonatal and the adult pericardium tissues, and these differences are most noticeable in the degree with which these layers intertwine with each other.

Edge on, the adult pericardium tissue has a significantly lower OI than the neonatal tissue measured both in the vertical and the horizontal directions. Measured in the vertical direction, the adult has an OI of 0.581 (σ = 0.051) compared with the neonatal OI of 0.800 (σ = 0.031). These results are significantly different (t-statistic = 21.5, $P < 0.0001$). Measured in the horizontal direction, the OI of adult pericardium is 0.669 (σ = 0.032) and the OI of neonatal pericardium is 0.763 (σ = 0.106). This shows a significant difference between the two materials (t-statistic = 4.4, $P < 0.0001$). In other words, the fibrils in the neonatal tissue are significantly more aligned within the plane of the tissue than those in the adult tissues.

Table 8.2. Orientation index (OI) for pericardium samples measured perpendicular and edge on to the surface for samples cut vertically or horizontally from the pericardium.

Direction measured	Animal age	OI	Std deviation	No. of pericardia	No. of measurements
Perpendicular	Adult	0.020	0.096	10	42
Perpendicular	Neonatal	0.071	0.152	10	42
Edge on vertical	Adult	0.581	0.051	2	52
Edge on horizontal	Adult	0.669	0.032	2	27
Edge on vertical	Neonatal	0.800	0.031	2	30
Edge on horizontal	Neonatal	0.763	0.106	2	27

Fibril diameter. No statistically significant difference was found in the collagen fibril diameter between neonatal and adult bovine pericardium. Fitting a cylinder model to the SAXS data the adult group (n = 39) gave a mean (with standard deviation) of 47.7 (σ = 3.0) nm while the neonatal group (n = 39) gave 48.4 (σ = 4.5) nm. Comparing the two sample sets there was no significant difference between neonatal and adult (t-statistic = -0.85, P = 0.40).

SAXS cross sections. Pericardium tissue is known to vary throughout its thickness and variation in structure is visible in the histological sections (Figure 8.5). The variation in OI was measured through cross sections of glutaraldehyde fixed pericardium for neonatal and adult tissue.

The OI measured through the thickness of glutaraldehyde fixed pericardium does not show a general change from one side to the other (Figure 8.9). Ovine and bovine leather show a similar flat profile of OI with skin depth (Basil-Jones et al., 2011, Basil-Jones et al., 2012). The flat profile between the two halves of the pericardium is somewhat surprising here as the histology shows two distinct layers. The variability in OI across the sample appears to be larger for the adult than the neonatal tissue. It is proposed that highly aligned collagen fibrils are responsible for high strength and that varied alignment spreads weakness through the thickness of a material. Variability in alignment in the adult pericardium is thus expected to lower the tensile strength of the adult pericardium.

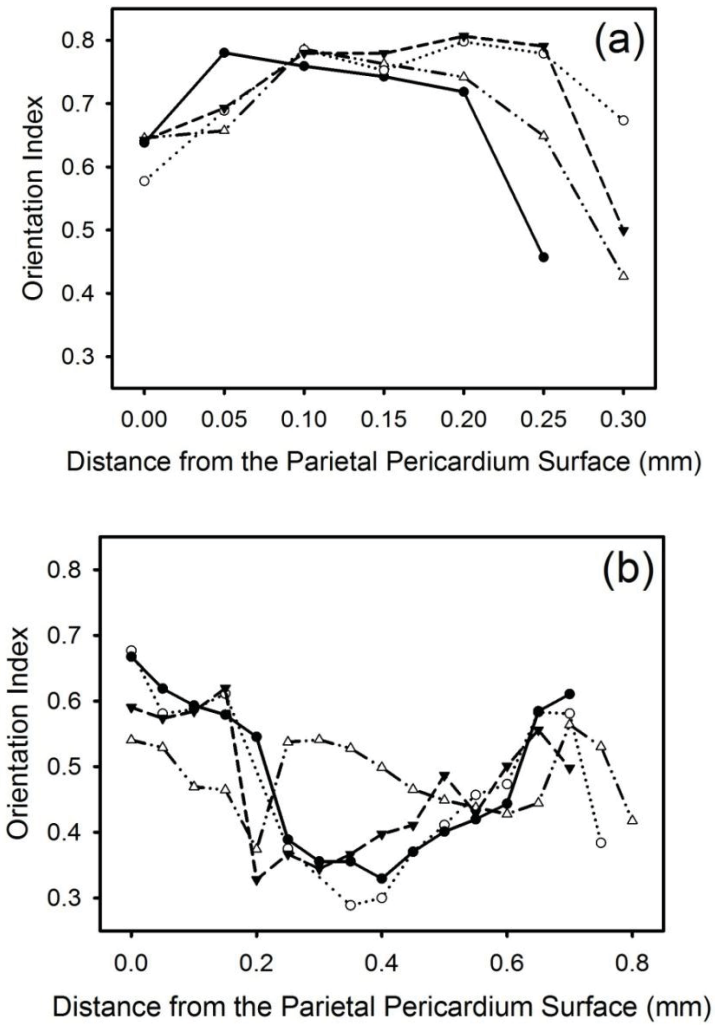

Figure 8.9. Variation of orientation index through the thickness of glutaraldehyde fixed pericardium a) neonatal; b) adult. Each figure shows two profiles for each of two samples (Sizeland et al., 2014).

8.4 Discussion

Adult and neonatal glutaraldehyde fixed pericardium are both useful for constructing bioprosthetic heart valves. However, there are clear differences to be found between the collagen structures in these tissues of different age. These differences are reflected in the orientation of the fibrils.

There was a significant difference observed in the OI between neonatal and adult bovine glutaraldehyde fixed pericardium. For tissue measured edge on, there is a higher OI in the neonatal pericardium than the adult pericardium. This indicates that collagen fibrils are more aligned in the plane of the tissue in the neonatal pericardium. It is in this direction that the main stresses are applied to pericardium under the elastic deformation during normal heart function. Recent studies of human skin reported a difference in SAXS patterns of young and aged skin (no ages given). The intensity of the collagen diffraction peaks and level of anisotropy were both reported to vary. The aged skin has more intense diffraction peaks and is less anisotropic, i.e. has a lower OI, (Cocera et al., 2011) showing a preferential fibril orientation in young individuals that is lost with age. These measurements were taken perpendicular to the skin. The data presented here for bovine pericardium also shows less anisotropy in the older pericardium. However, this difference is most apparent in the edge on measurements rather than the perpendicular ones.

It might be expected that the maximum strength of a tissue composed of collagen would be along the direction in which the collagen fibrils are arranged. Thus, when the collagen is more aligned in the direction in which force is applied the tissue will be stronger. A correlation which supports this concept has been observed for ovine and bovine skin of varying strengths and skin from a range of mammals. In those studies, a higher OI (in the plane of the tissue, but not normal to the plane) was correlated with higher tear strength (Basil-Jones et al., 2011, Sizeland et al., 2013). Therefore the higher OI in edge on measurements of neonatal pericardium should indicate improved tear strength of this tissue in comparison with adult pericardium. This is indeed observed in tensile testing of neonatal and adult bovine pericardium. Neonatal pericardium demonstrated a markedly higher

modulus of elasticity and a higher tensile strength than adult pericardium (Cunanan et al., 2012).

Extending and supporting this concept further, myxomatous and healthy mitral valve leaflets from dogs have been reported to have different degrees of fibril orientation. Myxomatous tissue was found to become less aligned (Hadian et al., 2007) which is a possible contributor to the diminished mechanical performance of this tissue although other changes are present too.

Measured perpendicular, the OI for both the adult and neonatal tissue is very low. The tissues are therefore rather isotropic measured from this direction. This is a very useful property as it may enable material to be cut in any direction from the pericardium for use in heart valve leaflets with minimal differences in mechanical performance.

The greater alignment in the plane of the tissue is thought to be the structural basis for the superior mechanical performance of glutaraldehyde fixed neonatal bovine pericardium. A relationship between fibre alignment and tensile strength has been modelled previously. Strength was found to be due to the sum of the components of the fibrils that lie in the direction of force in addition to a component due to the other matrix materials (Bigi et al., 1981). This model has been applied to just the measured fibrous collagen, neglecting the contribution from other matrix components. A model orientation index is derived which will be called OI′ to distinguish it from the experimentally measured OI (Kronick and Sacks, 1991, Kronick and Buechler, 1986) (Equation. 1).

$$OI' = \frac{\int_0^{2\pi}\int_0^{\pi/2} \cos^4\theta\, F(\theta,\phi)\, d\theta\, d\phi}{\int_0^{2\pi}\int_0^{\pi/2} F(\theta,\phi)\, d\theta\, d\phi} \qquad \text{(equation 1)}$$

Where $F(\theta,\phi)$ is the angular distribution function where θ and ϕ are orthogonal. This model has previously been applied to collagen orientation in leather produced from the skins of a selection of mammals. It was found to be valid across a wide range of strengths, i.e. greater than a factor of 5 (Sizeland et al., 2013).

Some of the apparent non-alignment of fibrils (resulting in a lower OI) could be due to crimp of the collagen fibrils and not only to the variation in whole fibril alignment. However this is not an important consideration in the materials studied. Crimp is observed in the light microscopy sections (Figure 8.5) and would contribute to a decrease in the OI in the direction of SAXS measurements taken edge on. In horse tendon crimp has been found to decrease with age (PattersonKane et al., 1997a), as does the tendon strength, and if there were no other changes to the alignment of collagen in the tendons this would result in an increase in OI with age. This is the opposite of what is observed for the OI change between the neonatal and the adult pericardium. Another consideration which leads us to believe crimp is not an important factor in the measurements reported here is that crimp is generally believed to be associated with strength (Caves et al., 2010). Therefore if the OI measured edge on was only due to crimp this would suggest that the neonatal pericardium, which is stronger, has less crimp and this would contradict the accepted knowledge of the influence of crimp. However, if the differences in OI measured edge on between neonatal and adult pericardium are due to differences in alignment of the collagen fibrils then this relationship would be in agreement with previous studies on skin (treated to produce leather) where a high degree of alignment is correlated with high strength (and crimp is not present) (Sizeland et al., 2013, Basil-Jones et al., 2011).

It is not known if these tissues of different age are affected differently by glutaraldehyde treatment. It has been observed that glutaraldehyde treatment lowers the OI of pericardium (Lee et al., 1989) and it is possible that the neonatal and adult pericardium are affected to a different extent. This possibility is currently being investigated (Sizeland et al., 2013, Basil-Jones et al., 2011).

Changes in fibril diameter were not found to be responsible for differences in strength between neonatal and adult pericardium. This is a little surprising, as fibril diameter is generally believed to affect strength in tendons and age can result in different fibril diameter with typically older tissue having thicker fibrils. However, in tendons the collagen fibrils are more highly aligned than pericardium so perhaps there is less variation in alignment in tendons and therefore factors other than alignment dominate strength differences. On the other hand, in

pericardium (and leather) there is the possibility of significant variation in alignment and therefore alignment may be able to dominate the strength-structure relationship with fibril diameter a less important factor (Wells et al., 2013).

The glutaraldehyde treated neonatal material had a greater modulus of elasticity and greater ultimate tensile strength than the glutaraldehyde treated adult material, and the neonatal material was significantly thinner. This suggests that there may be an advantage in the use of this material in applications such as heart valve leaflets for percutaneous delivery. A thinner tissue is able to be folded to be inserted in a much smaller sized catheter for aortic valve replacement. By using the thinner, but sufficiently strong, neonatal bovine pericardium, it could be possible to reduce the catheter diameter required for the insertion of the folded valve. This is an important consideration for many patients needing such intervention (Kroger et al., 2002, Chiam and Ruiz, 2008).

What has not been determined is the relationship between the collagen fibril alignment in the glutaraldehyde fixed material and in the native material. Treatment of native tissue results in differences in strength, as shown here and elsewhere (Freytes et al., 2004). Cross linking of the collagen fibrils might be expected to have an effect on fibril alignment because the cross linking would place physical constraints on the fibrils. Therefore variation in the degree to which cross linking takes place in different tissues might result in a variable change in alignment. This is the subject of a study currently being undertaken.

8.5 Conclusions

It was found that the glutaraldehyde fixed neonatal tissue has a higher modulus of elasticity (83.7 MPa) than adult pericardium (33.5 MPa) and a higher normalised ultimate tensile strength (32.9 MPa) than adult pericardium (19.1 MPa). Measured edge on to the tissue, the collagen in neonatal pericardium is significantly more aligned (Orientation Index (OI) 0.78) than that in adult pericardium (OI 0.62).

It has been shown that glutaraldehyde fixed neonatal pericardium has a higher elastic modulus and ultimate tensile strength than adult pericardium. Using SAXS it has been shown that there are clear differences in the structure of collagen between neonatal and adult bovine pericardium. The alignment of the collagen in the plane of the tissue is greater in the neonatal pericardium. How this gives a structural understanding of the superior mechanical properties of that material has been described. These findings provide a basis for the potential advantages to using neonatal rather than adult bovine pericardium in heterografts.

Chapter 9: Conclusions

This research set about elucidating how collagen networks in biomaterials react when different chemical and mechanical processes are applied. SAXS has provided the ideal platform for nanostructural analysis of the hierarchical structure of collagen both statically and when under tension.

The structure of leather from different mammals has been investigated to develop a generalized understanding of structure–strength relationships in accordance with the first research aim. Leather from selected mammals has shown tear strengths are correlated with the collagen fibril orientation parallel to the surface of the leather. This has been explained as being due to the strength of the collagen fibrils in their longitudinal axis when suitably arranged to resist the tearing process. This clear demonstration of the structural relationship and consequent insight enables research into other tissues to be better targeted by applying a greater focus to the collagen alignment in plane. It is expected that this highly correlated structure–strength relationship extends to tissues other than those studied here.

Concentrating on the second research aim, this work investigated the structural changes of collagen within leather upon addition of varying amounts of fat liquor. It has been shown that as the amount of fat liquor increased, the D-spacing of the collagen fibrils increased, and that this appears to be due to the lanolin component of the fat liquor. Alternative mechanisms for this increase in D-spacing have been discussed, including an increase in the gap region of a collagen fibril or an increase in the length of the tropocollagens. This work proves that fat liquor does more than lubricate fibres in leather in that it alters the structure of collagen fibrils. This research has shown that leather takes up strain on many levels of the hierarchical structure of collagen and that with the addition of fat liquor the ability of the material to stretch is increased. Lanolin, which was a key component of the fat liquor used here, is commonly used in skin care formulations and as such this knowledge may also apply to skin modified by skin care products. This work has

been able to provide more knowledge of the mechanism of action of fat liquor to the elasticity of leather to inform the leather making process.

The leather manufacturing process has been shown to result in changes in OI. The changes have been proven not to be due to a fundamental redistribution of fibrils, but rather occur as the thickness and the water content change with an increased thickness and also an increased water content (independently of thickness) resulting in a decreased OI. This understanding may be useful for relating structural changes that occur during different stages of processing to the development of the final physical characteristics of leather and sheds light on the fourth objective of my research. For example, if fibril orientation is critical to strength in certain leathers, the structural relationship that should exist between the fresh skin and the final leather is now known and it is possible to seek to maintain this characteristic during processing or to modify it appropriately.

Possible effects on the collagen structure when treated with compounds chosen because of their opposite effects on protein solubility were investigated as per my third research aim. SAXS analysis proved that the structure of collagen fibrils was indeed modified by treatment with urea, hydroxyproline, and lanolin. The change in D-spacing could have been caused by either a change in the triple alpha helix structure of the tropocollagens or by modifying the bonds between the tropocollagens. Urea significantly reduced the OI of the skin and lengthened the collagen D-spacing. The D-spacing increase was predicted due to its negative impact on hydrophobic effects through the displacement of water. Lanolin had the opposite effect on the OI to urea but the same effect on D-spacing. Given that lanolin is a major component of most skin care formulations, understanding how it functions at a molecular level is important for the cosmetic industry. D-spacing increased for leather treated with proline and hydroxyproline. Further investigations of the mechanisms of modification of collagen in skin by urea, proline, hydroxyproline, lanolin, and by extension other organic compounds, may lead to a better understanding of existing skin formulations and their interaction with collagen. Hopefully this knowledge can be extended to the action of moisturisers and cosmetic products on living skin.

Pericardium has been investigated and it has been shown that neonatal pericardium has a higher elastic modulus and higher ultimate tensile strength than adult pericardium. This work highlights that there are clear differences in the structure of collagen between neonatal and adult bovine pericardium. The alignment of the collagen in the plane of the tissue is greater in the neonatal pericardium. It has been described how this gives a structural understanding of the superior mechanical properties of that material. These findings provide a basis for the potential advantages to using neonatal rather than adult bovine pericardium in heterografts for percutaneous heart valve replacements.

This research has significantly contributed to the knowledge of the structure of collagen biomaterials. It has provided a greater understanding as to how collagen changes and reacts when subjected to different mechanical and chemical processes with direct implications in the leather industry. Future research is planned to determine the effect of different tanning agents used in the production of leather on the nanostructure of collagen. The distribution and penetration of these tanning agents will be explored.

Chapter 10: Appendices

Listed below are publications based on my work. This appendix contains copies of my publications and conference presentations.

Outputs based on the research of others have been included.

10.1 Appendix 1: Journal Articles

Sizeland, K. H., Basil-Jones, M. M., Edmonds, R. L., Cooper, S. M., Kirby, N. (2013) Collagen Orientation and Leather Strength for Selected Mammals. *Journal of Agricultural and Food Chemistry,* 61, 887-892.

Wells, H. C., **Sizeland, K. H.**, Edmonds, R. L., Aitkenhead, W., Kappen, P., Glover, C., Johannessen, B. & Haverkamp, R. G. (2014). Stabilizing Chromium from Leather Waste in Biochar. *ACS Sustainable Chemistry & Engineering, 2*(7), 1864-1870.

Sizeland, K. H., Wells, H. C., Higgins, J., Cunanan, C. M., Kirby, N., Hawley, A., Mudie, S. T., & Haverkamp, R. G. (2014). Age Dependant Differences in Collagen Alignment of Glutaraldehyde Fixed Bovine Pericardium. *BioMed Research International*.

Sizeland, K. H., Wells, H. C., Basil-Jones, M. M., Edmonds, R. L., & Haverkamp, R. G. (2014). Leather Nanostructure and Performance. *International Leather Maker*, 30-34.

Sizeland K. H., Wells H. C., Norris G. E., Edmonds R. L., Kirby N., Hawley A., Mudie, S., & Haverkamp, R. G. (2015). Collagen D-spacing and the Effect of Fat Liquor Addition. *Journal of the American Leather Chemists Association*, 110(3), 66-71.

Kayed H. R., **Sizeland K. H.**, Kirby N., Hawley A., Mudie S. T., & Haverkamp R. G. (2015). Collagen Cross Linking and Fibril Alignment in Pericardium. *RSC Advances,* 5(5), 3611-8.

Wells H. C., **Sizeland K. H.**, Kayed H. R., Kirby N., Hawley A., Mudie S. T., & Haverkamp R. G. (2015). Poisson's Ratio of Collagen Fibrils Measured by Small Angle X-ray Scattering of Strained Bovine Pericardium. *Journal of Applied Physics*, 117(4).

Sizeland, K. H., Edmonds, R. L., Basil-Jones, M. M., Kirby, N., Hawley A., Mudie S. T., & Haverkamp R. G. (2015). Changes to Collagen Structure during Leather Processing. *Journal of Agricultural and Food Chemistry,* 63(9), 2499-2505.

Wells H. C., **Sizeland K. H.,** Kirby N., Hawley A., Mudie S. T., & Haverkamp R. G. (2015). Collagen Fibril Structure and Strength in Acellular Dermal Matrix Materials of Bovine, Porcine, and Human Origin. *ACS Biomaterials*, 1, 1026-1038.

Sizeland K. H., Holmes. G., Edmonds R. L., Kirby N., Hawley A., Mudie, S., & Haverkamp, R. G. (2015). Fatliquor Effects on Collagen Fibril Orientation and D-spacing During Tensile Strain. *Journal of the American Leather Chemists Association*, 110, 355-362.

JOURNAL OF AGRICULTURAL AND FOOD CHEMISTRY

Article

pubs.acs.org/JAFC

Collagen Orientation and Leather Strength for Selected Mammals

Katie H. Sizeland,[†] Melissa M. Basil-Jones,[†] Richard L. Edmonds,[‡] Sue M. Cooper,[‡] Nigel Kirby,[§] Adrian Hawley,[§] and Richard G. Haverkamp*,[†]

[†]School of Engineering and Advanced Technology, Massey University, Private Bag 11222, Palmerston North, New Zealand 4442

[‡]Leather and Shoe Research Association of New Zealand, P.O. Box 8094, Palmerston North, New Zealand 4446

[§]Australian Synchrotron, Melbourne, Australia

ABSTRACT: Collagen is the main structural component of leather, skin, and some other applications such as medical scaffolds. All of these materials have a mechanical function, so the manner in which collagen provides them with their strength is of fundamental importance and was investigated here. This study shows that the tear strength of leather across seven species of mammals depends on the degree to which collagen fibrils are aligned in the plane of the tissue. Tear-resistant material has the fibrils contained within parallel planes with little crossover between the top and bottom surfaces. The fibril orientation is observed using small-angle X-ray scattering in leather, produced from skin, with tear strengths (normalized for thickness) of 20−110 N/mm. The orientation index, 0.420−0.633, is linearly related to tear strength such that greater alignment within the plane of the tissue results in stronger material. The statistical confidence and diversity of animals suggest that this is a fundamental determinant of strength in tissue. This insight is valuable in understanding the performance of leather and skin in biological and industrial applications.

KEYWORDS: *collagen, orientation, alignment, leather, strength, SAXS*

INTRODUCTION

The strength of collagen materials is of crucial importance in both medical and industrial contexts. Collagen is the main structural component of skin,[1] leather, and some medical scaffolds.[2] Medical conditions can arise when tissues do not have the required mechanical strength, such as in aneurysms,[3] cervical insufficiency,[4] osteoarthritis,[5] and damaged articular cartilage.[6] In addition, bone is a composite material in which the structure of collagen is considered to be important for bone toughness.[7,8] Strength is also a requirement for collagen-based medical materials such as extracellular matrix scaffolds[2] and processed pericardium for heart valve repair.[9] Leather, which is processed skin consisting mostly of collagen, is produced on a large scale for shoes, clothing, and upholstery,[10] with high strength being a primary requirement for high-value applications.

Factors that have previously been considered as possibly contributing to the strength of collagenous materials include the amount of collagen present, the molecular structure of the collagen (D-spacing, collagen type), the nature of the cross-linking between collagen,[11] collagen bundle size, and collagen orientation. Of these, much attention has been given to collagen orientation. Most collagen tissues are anisotropic, and it is understood that this is a result of the nonuniform requirements for mechanical performance and the consequence of the growth in volume of the animal. Collagen orientation has therefore been investigated in the cornea,[12,13] heart valve tissue,[14] pericardium,[15] bladder tissue,[16] skin,[17] and aorta.[18]

Crimp, the sinuous arrangement of fiber bundles, has been associated with high strength in tendons[19] as well as in heart valves,[20] with high crimp resulting in high strength. However, in studies of skin (leather) of various strengths, crimp was not observed.[21]

Collagen orientation has been measured by reflection anisotropy,[22] atomic force microscopy,[23] small-angle light scattering,[24] confocal laser scattering,[25] Raman polarization,[26] anisotropic Raman scattering,[27] multiphoton microscopy,[28] and small-angle X-ray scattering (SAXS).[21,29,30]

Our recent study of ovine and bovine leathers of differing strengths[21] found a statistically significant relationship between tear strength and edge-on orientation, and we speculated that this trend may be of a more general nature. We have now measured fibril orientation in seven species of mammals to see if this relationship is found more widely. We used SAXS at a modern synchrotron facility, which allows analysis of a small area (250 × 80 μm), and therefore easy measurement of fibril orientation edge-on in tissues that are of limited thickness;[21] such measurements are difficult to make quantitatively by other methods.

EXPERIMENTAL PROCEDURES

Skins were processed to produce leather by the following procedure. After mechanical removal of adhering fat and flesh, conventional lime sulfide paint, comprising 140 g/L sodium sulfide, 50 g/L hydrated lime, and 23 g/L pre-gelled starch thickener, was applied to the flesh side of the skin at 400 g/m^2. The skin was incubated at 20 °C for 16 h and the keratinaceous material manually removed. The skin was then washed to remove the lime, and the pH was lowered to 8 with ammonium sulfate, followed by the addition of 0.1% (w/v) Tanzyme (a commercial bate enzyme). After 75 min at 35 °C, the treated skin was washed and then pickled (20% w/v sodium chloride and 2% w/v sulfuric acid). Pickled pelts were degreased (4% nonionic surfactant; Tetrapol LTN,

Received: October 31, 2012
Revised: December 23, 2012
Accepted: January 8, 2013
Published: January 8, 2013

Shamrock, New Zealand) at 35 °C for 90 min and then washed. The skins were neutralized in 8% NaCl, 1% disodium phthalate solution (40% active; Feliderm DP, Clariant, UK), and 1% formic acid for 10 min. The running solution was then made up to 5% chrome sulfate (Chromosal B, Lanxess, Germany) and processed for 30 min followed by 0.6% magnesium oxide addition, based on the weight of the skins, to fix the chrome, and processed overnight at 40 °C. These wet-blue pelts were neutralized in 1% sodium formate and 0.15% sodium bicarbonate for 1 h and then washed, followed by retanning with 2% synthetic retanning agent (Tanicor PW, Clariant, Germany) and 3% vegetable tanning (mimosa; Tanac, Brazil). Six percent mixed fatliquors were added and the leathers maintained at 50 °C for 45 min, followed by fixing with 0.5% formic acid for 30 min and washing in cold water.

Tear strengths were measured for all samples using standard methods.[31] Samples were cut from the leather at the official sampling position (OSP).[32] The samples were then conditioned at a constant temperature and humidity (20 °C and 65% relative humidity) for 24 h and then tested on an Instron 4467 (Figure 1).

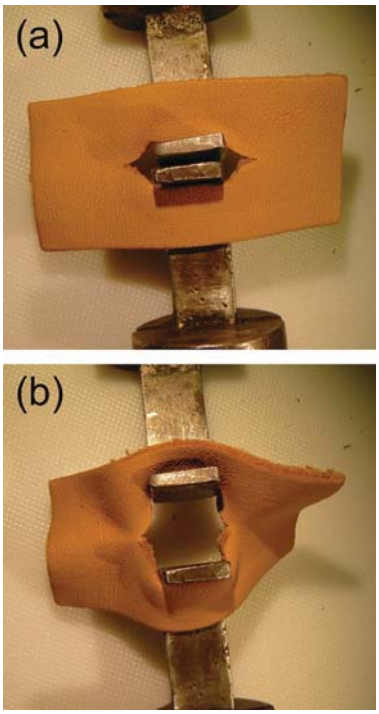

Figure 1. Tear test on a leather sample: (a) at start of test; (b) part way through test.

Samples were prepared for SAXS analysis by cutting strips of leather of 1 × 30 mm from the OSP.[32] Each sample was mounted, without tension, in the X-ray beam to obtain scattering patterns for two orthogonal directions through the leather. For the edge-on analyses measurements were made every 0.25 mm with the samples analyzed from the grain to the corium. For when the beam was directed flat-on (normal to) the surface of the leather, standard samples were cut parallel to the surface, producing a grain sample and a corium sample. These were mounted with the uncut face of the leather directed toward the X-ray beam, and four measurements were made per sample, in a rectangular grid. Diffraction patterns were recorded on the Australian Synchrotron SAXS/WAXS beamline, using a high-intensity undulator source. Energy resolution of 10^{-4} was obtained from a cryocooled Si(111) double-crystal monochromator, and the beam size (fwhm focused at the sample) was 250 × 80 μm, with a total photon flux of about 2×10^{12} ph/s. Diffraction patterns were recorded with an X-ray energy of 8 keV using a Pilatus 1 M detector with an active area of 170 × 170 mm and a sample-to-detector distance of 3371 mm. Exposure time for the diffraction patterns was 1 s, and data processing was carried out using SAXS15ID software.[33]

The orientation index (OI) is defined as (90° − OA)/90°, where OA is the minimum azimuthal angle range, centered at 180°, that contains 50% of the microfibrils.[34,35] OI provides a measure of the spread of microfibril orientation. In the limit, an OI approaching 1 indicates that the microfibrils are parallel to each other and the leather surface, whereas an OI of 0 indicates the microfibrils are randomly oriented. We have calculated the OI from the spread in azimuthal angle of the D-spacing peak, which occurs at around 0.059−0.060 Å^{-1}. Each OI value presented here represents the average of 14−36 measurements of one sample. For edge-on mounted samples these measurements were taken at 0.25 mm intervals from the corium to the grain so that the whole thickness of the sample was covered. For flat-on measurements these were taken on a number of points in a grid pattern. For the sheep and cattle samples the averages are derived from 228, 249, and 167 measurements from 15, 14, and 10 samples, respectively, and have been reported previously.[21]

It is not necessary that the samples are highly representative of the particular animal species for general strength−structure relationships to be studied; that there is a range of skins with different strengths is important, although the observed strengths for each species are within industry norms.

The D-spacing was determined for each pattern by taking the central position of several of the collagen peaks, dividing these by the peak order (usually from n = 5 to n = 10), and averaging the resulting values.

RESULTS

The SAXS patterns display rings representing the collagen fibril repeating structure (Figure 2a). The integrated intensity of the whole pattern enables the position of these peaks to be clearly identified (Figure 2b), and from these the D-spacing is

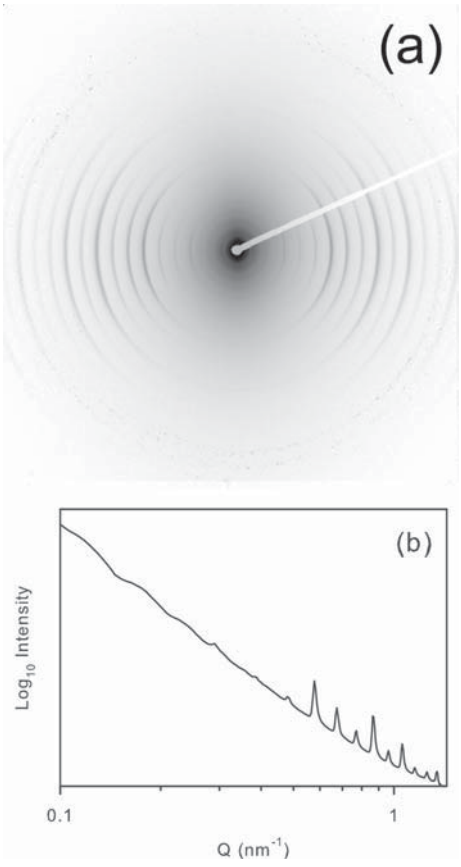

Figure 2. SAXS analysis of leather: (a) raw SAXS pattern; (b) integrated intensity of a whole pattern.

dx.doi.org/10.1021/jf3043067 | J. Agric. Food Chem. 2013, 61, 887−892

determined. The D-spacing varied from 0.628 to 0.653 nm (Figure 3), but there is no significant correlation between D-spacing and strength.

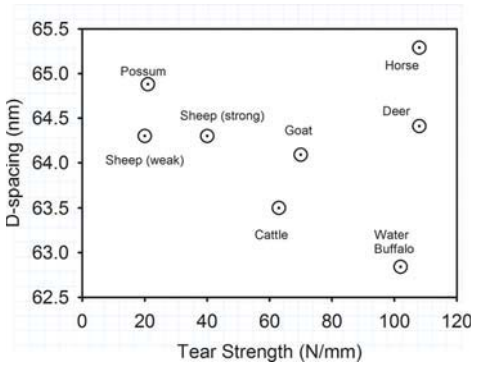

Figure 3. Collagen D-spacing and tear strength for leather from different animals.

For any of the rings visible in the SAXS pattern, which correspond to a peak in the meridional angle, the variation in intensity with azimuthal angle can be plotted (Figure 4), which gives a quantitative measure of fibril orientation, represented here as an OI.

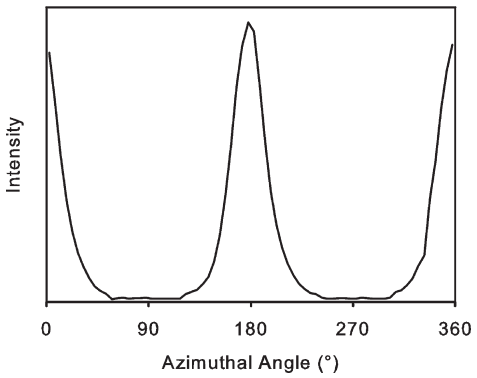

Figure 4. Azimuthal variation in intensity at one value of Q (one collagen peak).

There is a large difference in OI between the measurements taken normal to the leather surface and measurements taken edge-on to the leather. The OI normal to the surface is in the range 0.18−0.35, with the exception of horse leather (Figure 5a), whereas for the edge-on measurements the range is 0.41−0.63 (Figure 5b). Therefore, the major component of fibril alignment is planar.

We find that there is a strong correlation between tear strength and OI (Table 1; Figure 5b) for the edge-on measurements, with a least-squares fitted slope of 0.0024 mm/N ($n = 8$, $r^2 = 0.98$, $P < 0.0001$). This is a remarkably good correlation. Edge-on analysis provides a measure of fibril orientation not frequently accessed. It conveys the degree to which the collagen fibrils are organized in parallel planes as opposed to crossing between the top and bottom surfaces of the skin.

For the measurements on the flat, if we exclude horse leather as an outlier, then there is little correlation between tear strength and OI (Figure 5a) with a least-squares fitted slope of 0.0003 mm/N ($n = 7$, $r^2 = 0.06$, $P = 0.60$), suggesting the slight possibility of a negative correlation. This is the more widely used direction of analysis for collagen fibril orientation measurements.

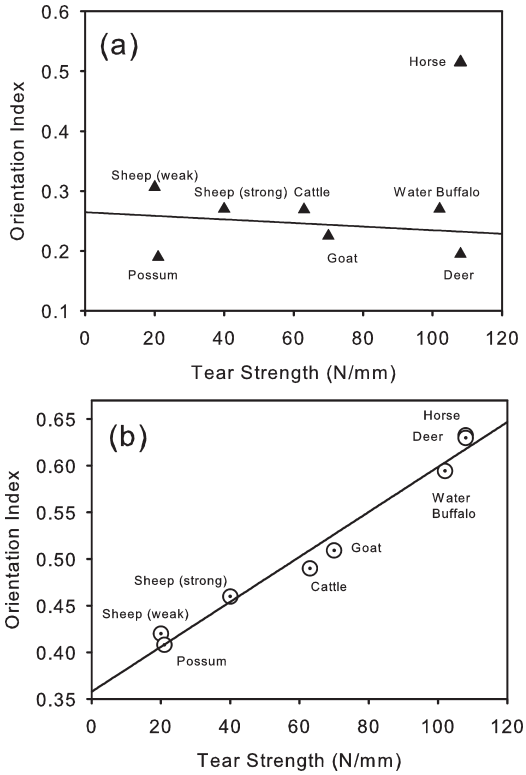

Figure 5. Collagen fibril orientation and tear strength for leather from different animals: (a) measured flat-on; (b) measured edge-on.

Table 1. Leather Tear Strength Compared with Orientation Index (OI) of Collagen Fibrils[a]

animal		tear strength normalized for thickness (N/mm)	OI measured edge-on (average through thickness)
sheep (selected weak)	*Ovis aries*	20	0.420
possum	*Trichosurus vulpecula*	21	0.408
sheep (selected strong)	*Ovis aries*	40	0.460
cattle	*Bos primigenius taurus*	63	0.490
goat	*Capra aegagrus hircus*	70	0.509
water buffalo	*Bubalus bubalis*	102	0.595
deer	*Cervus elaphus*	108	0.630
horse	*Equus ferus caballus*	108	0.633

[a]OI values are the average taken across the thickness of one sample (about 5−10 points) except for sheep and cattle, where these are an average of 6−10 leather samples with 5−10 analysis points for each.

DISCUSSION

D-Spacing. The D-spacing of collagen is known to vary with age,[36] but it has not, to the knowledge of the authors, been linked with mechanical strength. We also do not find a link with strength, therefore supporting the current understanding, although we find a large variation in D-spacing across a large range of strength (Figure 3).

Orientation and Strength. Collagen orientation shows a strong correlation with tear strength when measured edge-on, and this relationship is represented in part by existing models. A relationship between fiber alignment and tensile strength has

dx.doi.org/10.1021/jf3043067 | J. Agric. Food Chem. 2013, 61, 887−892

been modeled previously, where strength is due to the sum of the components of the fibrils that lie in the direction of force in addition to a component due to the other matrix materials.[37] This relationship is represented by eq 1

$$E_z = E_f v_f \int_0^{2\pi} \int_0^{\pi/2} \cos^4 \theta F(\theta, \phi)\, d\theta\, d\phi + (1 - v_f)E_m \quad (1)$$

where E_z is the composite Young's modulus of the material in direction z, E_f and E_m are the Young's moduli of the fibers and matrix, respectively, v_f is the volume fraction of the fibers, and $F(\theta,\phi)$ is the angular distribution function, where θ and ϕ are orthogonal.

This model has been applied to just the measured fibrous collagen, neglecting the contribution from matrix materials, to give an OI, which here we will call OI′ to distinguish it from the differently formulated OI[29,38] (eq 2).

$$OI' = \frac{\int_0^{2\pi} \int_0^{\pi/2} \cos^4 \theta F(\theta, \phi)\, d\theta\, d\phi}{\int_0^{2\pi} \int_0^{\pi/2} F(\theta, \phi)\, d\theta\, d\phi} \quad (2)$$

OI, calculated here from the angle range representing half of the fibrils, can be converted to the integral of $\cos^4\theta$ by numerical methods (where we assume a Gaussian form to the intensity distribution). The OI data plotted for the two orthogonal directions shown in Figure 5 can then be represented as OI′, where, if the model described above is applicable to this system, it should be proportional to the tensile strength. This results in a plot that also correlates with the tear strength data; however, the correlation is poorer than that obtained with the edge-on OI measurements (Figure 6). The fit that includes all data is reasonable ($n = 8$, $r^2 = 0.55$, $P = 0.06$), and this fit improves if the horse data point is removed ($n = 7$, $r^2 = 0.82$, $P = 0.02$). We do not know why horse leather should be an outlier, and this may warrant further investigation. These compare unfavorably with the r^2 of 0.98 for just the OI data edge-on. The reason that this three-dimensional model is a poorer fit than that of the edge-on OI data is considered below.

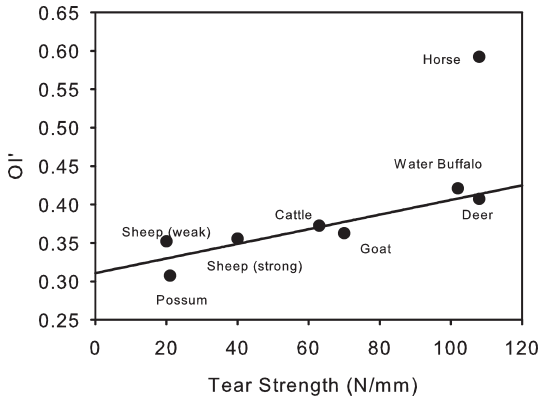

Figure 6. Three-dimensional modeled OI′ based on normalized integral of $\cos^4\theta$.

Alignment and Tear Strength: A More Complex Relationship. Tear strength and tensile strength are related but not identical measures of strength, and it is important to understand the difference between these two measures to be able to relate the model in ref 37 to the tear strength. The basic assumption of the model outlined in ref 37 is that the strength of collagen is along the axis of the fibrils themselves and that the total strength is the simple sum of these fibrils in the direction of tensile force. This is a good model for tensile strength; however, the more useful measure of strength for practical applications of leather is the tear strength, and this does not directly correlate with tensile strength. Tear strength is perhaps analogous to "toughness" in materials.

The ability of leather to resist tear also depends to some extent on the strength perpendicular to the fibril axis, which depends on the strength of the cross-links[11] or the degree of entanglement, and that strength will be less than the strength of the collagen fibrils. However, this appears to be of rather secondary importance compared with fibril alignment. The main component of tear strength for the work presented here is seen to be related to the planar alignment of collagen fibrils. Fibril alignment in the plane has a very strong correlation with tear strength. When the fibrils are not aligned in the plane but instead are perpendicular to the plane (Figure 7a), then any tearing force will need to just separate fibers, pulling in the weakest direction. This arrangement is known as vertical fiber defect and occurs sometimes in Hereford cattle.[38,39] No samples of this type were included in this study.

When the fibrils are rather anisotropic in alignment when measured edge-on (Figure 7b), then the tear strength is likely to be greater than would be found in the vertical fiber defect structure because now there are fibrils running in the direction of the applied force, and maximum strength is obtained when there is a high degree of alignment in this plane (Figure 7c). This trend, depicted in Figure 7 from image a to image c, is what we observe for SAXS measurements over a factor of nearly 5 in strength (Figure 7b), which is a much larger range than has been reported by any other studies.

The reason tear strength does not directly relate to collagen alignment considered in three dimensions (as in eqs 1 and 2) is that tearing is associated with point stresses. To prevent tearing, these point stresses must be resisted. Tearing is used as the industry standard for leather strength because it relates more closely with actual in-service performance than tensile strength. When the tearing process is viewed (Figure 1), looking flat onto

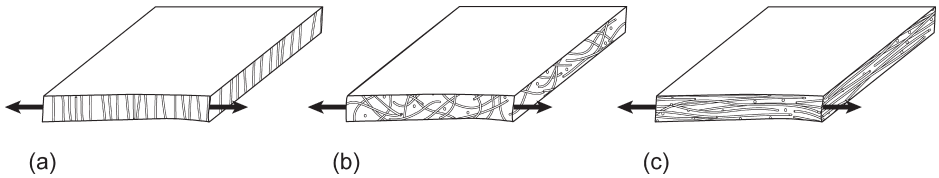

Figure 7. Relationship between collagen orientation index (OI) and strength of skin. OI measured edge-on with orientation that results in leather that is (a) very weak (vertical fiber defect), (b) medium strength (low OI), or (c) strong (high OI). Arrow indicates direction of applied stress in tear measurements.

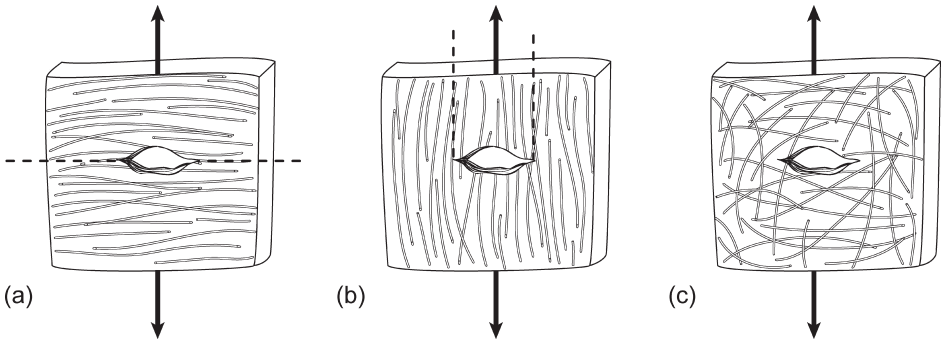

Figure 8. Relationship between collagen orientation index (OI) and strength of skin. OI measured on the flat with orientation that results in leather that is (a) weak (high OI), (b) fairly weak (high OI), (c) strong in all directions. Arrow indicates direction of applied stress in tear measurements. Dashed lines represent probable lines of failure.

the leather, the points where the tearing will occur are at the two ends of the linear cut hole. The fibers that run at right angles to the two edges to the hole (viewed on the flat) resist the tearing process (Figure 8a). However, if all of the fibers run in this direction, then strength may be low due to failure along shear lines (Figure 8b). Therefore, it might be expected that the optimum strength will be associated with a fiber arrangement somewhere between these two extremes, with skin that has a low OI measured in this direction (Figure 8c). Hence, this correlation is one where OI is inversely related to strength, which is what is weakly observed for these leathers (Figure 5a).

Therefore the existing model for strength, where strength depends on the degree of fibril orientation in the direction of stress considering the three-dimensional structure, does not provide an optimal description of the behavior of these materials. It does not take into account the fact that, in practice, a tearing process will follow the weakest part of the structure. The consequence of this is that the direction of the tear front is not well-defined and a degree of anisotropy when viewed flat-on is preferable. The anisotropy, as viewed flat-on, enhances the ability to resist point stresses.

These simplified sketches illustrate the mechanism behind the structure−strength relationship that has been measured for the range of animal skins reported here. What is remarkable is that the relationship between tear strength and edge-on orientation is so quantitative. The strength range across which this relationship holds is much greater than has previously been demonstrated. The correlation also extends across a wide range of mammals.

There is additional information contained in the SAXS patterns that we have not yet analyzed such as the collagen bundle size, which is contained in the low Q region of the pattern. We intend to address this in future work. We are also extending the study to a range of animals from other classes and to other tissue types. We hope, through this work, to build a more complete picture of the structural arrangement of collagen materials and the way in which nature constructs these materials for different applications to provide optimum function. We hope this will lead to an enhanced understanding of the basis of the hierarchical structure of skin and the reasons for the variations between skin from different positions on one animal, between skin of different species, animal classes, and different tissue types. From this study we have found a structural motif that is clearly of primary importance in mammals, but we have not yet demonstrated the generalization of this structural motif to other classes or other tissues.

The work is also being extended to develop an understanding of the changes to the collagen fibrils that take place during the processing of leather. Processing can affect the collagen structure, including both the D-period and the fibril orientation. To understand leather as an industrial material, it is desirable to understand the structural changes that take place as a result of chemical and physical treatments from skin to finished product.

In summary, we have investigated the structure of leather from different mammals to attempt to develop a generalized understanding of structure−strength relationships. We have shown that the tear strength of leather is correlated with collagen fibril orientation parallel to the surface of the leather over a large (factor of 5) range of strengths across seven species of mammals. This has been explained as being due to the strength of the collagen fibrils in their longitudinal axis when suitably arranged to resist the tearing process. This clear demonstration of the structural relationship and consequent insight enables research into other tissues to be better targeted by applying a greater focus to the collagen alignment in plane. We expect that this highly correlated structure−strength relationship extends to tissues other than those studied here.

AUTHOR INFORMATION

Corresponding Author

*E-mail: r.haverkamp@massey.ac.nz.

Funding

This work was supported by the Ministry of Business, Innovation and Employment, New Zealand (Grant LSRX0801). The Australian Synchrotron provided travel funding and accommodation.

Notes

The authors declare no competing financial interest.

ACKNOWLEDGMENTS

This research was undertaken on the SAXS/WAXS beamline at the Australian Synchrotron, Victoria, Australia. David Cookson and Stephen Mudie at the Australian Synchrotron assisted with data collection and processing. Sue Hallas, of Nelson, assisted with editing the manuscript.

REFERENCES

(1) Fratzl, P. *Collagen: Structure and Mechanics*; SpringerScience +Business Media: New York, 2008; Vol. Collagen: Structure and mechanics.

(2) Floden, E. W.; Malak, S.; Basil-Jones, M. M.; Negron, L.; Fisher, J. N.; Byrne, M.; Lun, S.; Dempsey, S. G.; Haverkamp, R. G.; Anderson, I.;

Ward, B. R.; May, B. C. H. Biophysical characterization of ovine forestomach extracellular matrix biomaterials. *J. Biomed. Mater. Res. B* **2010**, *96B*, 67−75.
(3) Lindeman, J. H. N.; Ashcroft, B. A.; Beenakker, J. W. M.; van Es, M.; Koekkoek, N. B. R.; Prins, F. A.; Tielemans, J. F.; Abdul-Hussien, H.; Bank, R. A.; Oosterkamp, T. H. Distinct defects in collagen microarchitecture underlie vessel-wall failure in advanced abdominal aneurysms and aneurysms in Marfan syndrome. *Proc. Natl. Acad. Sci. U.S.A.* **2010**, *107*, 862−865.
(4) Oxlund, B. S.; Ortoft, G.; Bruel, A.; Danielsen, C. C.; Oxlund, H.; Uldbjerg, N. Cervical collagen and biomechanical strength in non-pregnant women with a history of cervical insufficiency. *Reprod. Biol. Endocrin.* **2010**, *8*, 92.
(5) Narhi, T.; Siitonen, U.; Lehto, L. J.; Hyttinen, M. M.; Arokoski, J. P. A.; Brama, P. A.; Jurvelin, J. S.; Helminen, H. J.; Julkunen, P. Minor influence of lifelong voluntary exercise on composition, structure, and incidence of osteoarthritis in tibial articular cartilage of mice compared with major effects caused by growth, maturation, and aging. *Connect. Tissue Res.* **2011**, *52*, 380−392.
(6) Stok, K.; Oloyede, A. A qualitative analysis of crack propagation in articular cartilage at varying rates of tensile loading. *Connect. Tissue Res.* **2003**, *44*, 109−120.
(7) Zimmermann, E. A.; Schaible, E.; Bale, H.; Barth, H. D.; Tang, S. Y.; Reichert, P.; Busse, B.; Alliston, T.; Ager, J. W.; Ritchie, R. O. Age-related changes in the plasticity and toughness of human cortical bone at multiple length scales. *Proc. Natl. Acad. Sci. U.S.A.* **2011**, *108*, 14416−14421.
(8) Skedros, J. G.; Dayton, M. R.; Sybrowsky, C. L.; Bloebaum, R. D.; Bachus, K. N. The influence of collagen fiber orientation and other histocompositional characteristics on the mechanical properties of equine cortical bone. *J. Exp. Biol.* **2006**, *209*, 3025−3042.
(9) Jobsis, P. D.; Ashikaga, H.; Wen, H.; Rothstein, E. C.; Horvath, K. A.; McVeigh, E. R.; Balaban, R. S. The visceral pericardium: macromolecular structure and contribution to passive mechanical properties of the left ventricle. *Am. J. Physiol.−Heart C* **2007**, *293*, H3379−H3387.
(10) Commodities and Trade Division, FAO, United Nations. *World Statistical Compendium for Raw Hides and Skins, Leather and Leather Footwear 1990−2009*; Rome, Italy, 2010.
(11) Chan, Y.; Cox, G. M.; Haverkamp, R. G.; Hill, J. M. Mechanical model for a collagen fibril pair in extracellular matrix. *Eur. Biophys. J.* **2009**, *38*, 487−493.
(12) Boote, C.; Kamma-Lorger, C. S.; Hayes, S.; Harris, J.; Burghammer, M.; Hiller, J.; Terrill, N. J.; Meek, K. M. Quantification of collagen organization in the peripheral human cornea at micron-scale resolution. *Biophys. J.* **2011**, *101*, 33−42.
(13) Kamma-Lorger, C. S.; Boote, C.; Hayes, S.; Moger, J.; Burghammer, M.; Knupp, C.; Quantock, A. J.; Sorensen, T.; Di Cola, E.; White, N.; Young, R. D.; Meek, K. M. Collagen and mature elastic fibre organisation as a function of depth in the human cornea and limbus. *J. Struct. Biol.* **2010**, *169*, 424−430.
(14) Sellaro, T. L.; Hildebrand, D.; Lu, Q. J.; Vyavahare, N.; Scott, M.; Sacks, M. S. Effects of collagen fiber orientation on the response of biologically derived soft tissue biomaterials to cyclic loading. *J. Biomed. Mater. Res. B* **2007**, *80A*, 194−205.
(15) Liao, J.; Yang, L.; Grashow, J.; Sacks, M. S. Molecular orientation of collagen in intact planar connective tissues under biaxial stretch. *Acta Biomater.* **2005**, *1*, 45−54.
(16) Gilbert, T. W.; Wognum, S.; Joyce, E. M.; Freytes, D. O.; Sacks, M. S.; Badylak, S. F. Collagen fiber alignment and biaxial mechanical behavior of porcine urinary bladder derived extracellular matrix. *Biomaterials* **2008**, *29*, 4775−4782.
(17) Purslow, P. P.; Wess, T. J.; Hukins, D. W. L. Collagen orientation and molecular spacing during creep and stress-relaxation in soft connective tissues. *J. Exp. Biol.* **1998**, *201*, 135−142.
(18) Gasser, T. C. An irreversible constitutive model for fibrous soft biological tissue: a 3-D microfiber approach with demonstrative application to abdominal aortic aneurysms. *Acta Biomater.* **2011**, *7*, 2457−2466.
(19) Franchi, M.; Trire, A.; Quaranta, M.; Orsini, E.; Ottani, V. Collagen structure of tendon relates to function. *Sci. World J.* **2007**, *7*, 404−420.
(20) Joyce, E. M.; Liao, J.; Schoen, F. J.; Mayer, J. E.; Sacks, M. S. Functional collagen fiber architecture of the pulmonary heart valve cusp. *Ann. Thorac. Surg.* **2009**, *87*, 1240−1249.
(21) Basil-Jones, M. M.; Edmonds, R. L.; Cooper, S. M.; Haverkamp, R. G. Collagen fibril orientation in ovine and bovine leather affects strength: a small angle X-ray scattering (SAXS) study. *J. Agric. Food Chem.* **2011**, *59*, 9972−9979.
(22) Schofield, A. L.; Smith, C. I.; Kearns, V. R.; Martin, D. S.; Farrell, T.; Weightman, P.; Williams, R. L. The use of reflection anisotropy spectroscopy to assess the alignment of collagen. *J. Phys. D: Appl. Phys.* **2011**, 44.
(23) Friedrichs, J.; Taubenberger, A.; Franz, C. M.; Muller, D. J. Cellular remodelling of individual collagen fibrils visualized by time-lapse AFM. *J. Mol. Biol.* **2007**, *372*, 594−607.
(24) Billiar, K. L.; Sacks, M. S. A method to quantify the fiber kinematics of planar tissues under biaxial stretch. *J. Biomech.* **1997**, *30*, 753−756.
(25) Jor, J. W. Y.; Nielsen, P. M. F.; Nash, M. P.; Hunter, P. J. Modelling collagen fibre orientation in porcine skin based upon confocal laser scanning microscopy. *Skin Res. Technol.* **2011**, *17*, 149−159.
(26) Falgayrac, G.; Facq, S.; Leroy, G.; Cortet, B.; Penel, G. New method for Raman investigation of the orientation of collagen fibrils and crystallites in the Haversian system of bone. *Appl. Spectrosc.* **2010**, *64*, 775−780.
(27) Janko, M.; Davydovskaya, P.; Bauer, M.; Zink, A.; Stark, R. W. Anisotropic Raman scattering in collagen bundles. *Opt. Lett.* **2010**, *35*, 2765−2767.
(28) Lilledahl, M. B.; Pierce, D. M.; Ricken, T.; Holzapfel, G. A.; Davies, C. D. Structural analysis of articular cartilage using multiphoton microscopy: input for biomechanical modeling. *IEEE Trans. Med. Imaging* **2011**, *30*, 1635−1648.
(29) Kronick, P. L.; Buechler, P. R. Fiber orientation in calfskin by laser-light scattering or X-ray-diffraction and quantitative relation to mechanical-properties. *J. Am. Leather Chem. Assoc.* **1986**, *81*, 221−230.
(30) Basil-Jones, M. M.; Edmonds, R. L.; Norris, G. E.; Haverkamp, R. G. Collagen fibril alignment and deformation during tensile strain of leather: a SAXS study. *J. Agric. Food Chem.* **2012**, *60*, 1201−1208.
(31) Williams, J. M. V. IULTCS (IUP) test methods − measurement of tear load-double edge tear. *J. Soc. Leather Technol. Chem.* **2000**, *84*, 327−329.
(32) Williams, J. M. V. IULTCS (IUP) test methods − sampling. *J. Soc. Leather Technol. Chem.* **2000**, *84*, 303−309.
(33) Cookson, D.; Kirby, N.; Knott, R.; Lee, M.; Schultz, D. Strategies for data collection and calibration with a pinhole-geometry SAXS instrument on a synchrotron beamline. *J. Synchrotron Radiat.* **2006**, *13*, 440−444.
(34) Sacks, M. S.; Smith, D. B.; Hiester, E. D. A small angle light scattering device for planar connective tissue microstructural analysis. *Ann. Biomed. Eng.* **1997**, *25*, 678−689.
(35) Basil-Jones, M. M.; Edmonds, R. L.; Allsop, T. F.; Cooper, S. M.; Holmes, G.; Norris, G. E.; Cookson, D. J.; Kirby, N.; Haverkamp, R. G. Leather structure determination by small angle X-ray scattering (SAXS): cross sections of ovine and bovine leather. *J. Agric. Food Chem.* **2010**, *58*, 5286−5291.
(36) Scott, J. E.; Orford, C. R.; Hughes, E. W. Proteoglycan-collagen arrangements in developing rat tail tendon − an electron-microscopical and biochemical investigation. *Biochem. J.* **1981**, *195*, 573−584.
(37) Bigi, A.; Ripamonti, A.; Roveri, N.; Jeronimidis, G.; Purslow, P. P. Collagen orientation by X-ray pole figures and mechanical-properties of media carotid wall. *J. Mater. Sci.* **1981**, *16*, 2557−2562.
(38) Kronick, P. L.; Sacks, M. S. Quantification of vertical-fiber defect in cattle hide by small-angle light-scattering. *Connect. Tissue Res.* **1991**, *27*, 1−13.
(39) Amos, G. L. Vertical fibre in relation to the properties of chrome side leather. *J. Soc. Leather Technol. Chem.* **1958**, *42*, 79−90.

ACS Sustainable Chemistry & Engineering

Research Article

pubs.acs.org/journal/ascecg

Stabilizing Chromium from Leather Waste in Biochar

Hannah C. Wells,[†] Katie H. Sizeland,[†] Richard L. Edmonds,[‡] William Aitkenhead,[‡] Peter Kappen,[§] Chris Glover,[§] Bernt Johannessen,[§] and Richard G. Haverkamp*,[†]

[†]School of Engineering and Advanced Technology, Massey University, Private Bag 11222, Palmerston North 4442, New Zealand

[‡]Leather and Shoe Research Association, P.O. Box 8094, Palmerston North 4446, New Zealand

[§]Australian Synchrotron, 800 Blackburn Road, Clayton, Victoria 3168, Australia

ABSTRACT: Disposal of chrome-tanned leather waste provides an environmental challenge, with land-based methods risking leaching of chromium into the environment. We investigate the production of biochar from leather as an alternative means to dispose of leather waste. Chrome-tanned leather is heated at 500−1000 °C in an environment excluding oxygen to form biochar. The char is leached in 1 M HCl for 15 h, and the leachate is analyzed for Cr to confirm that Cr does not leach from char formed at or above 600 °C. The char is analyzed by X-ray absorption spectroscopy (XAS) for chemical state and structure. X-ray absorption near edge structure (XANES) analysis shows that the leather and biochar contain Cr as a mixture of Cr sulfate and Cr carbide, with the proportion of Cr as carbide increasing from 0% for untreated leather to 88% for char formed at 1000 °C. Modeling of the extended X-ray absorption fine structure (EXAFS) spectra shows that the atomic near-range structure is consistent with that of chromium carbide for the high-temperature samples. Biochar produced from chrome-tanned leather waste contains highly dispersed chromium present as a stable, carbide-like structure (provided sufficiently high temperatures are used). This material, rather than being an environmental problem, may be used for soil remediation and carbon sequestration.

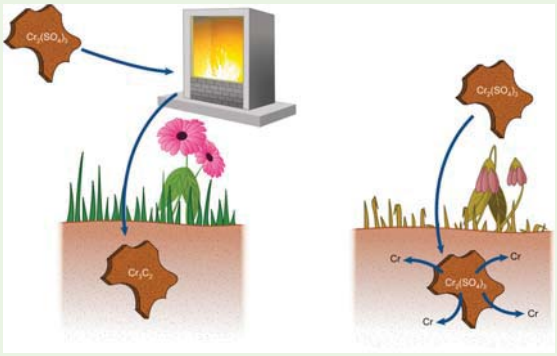

KEYWORDS: *Chromium, Biochar, Leather, XAS, Contaminant, Environment*

INTRODUCTION

Most leather is produced from skins and hides by tanning with chromium salts, normally $Cr_2(SO_4)_3 \cdot xH_2O$. Leather is used in upholstery (car and home), shoes, and clothing, but at the end of the life of these goods, the leather needs to be disposed of in an environmentally benign manner. Leather manufacture and production of goods from leather also produce leather scrap which requires disposal. Annual global leather production is about 6.8 million tonnes,[1] around 80% of which is chrome-tanned.

The main concern in the disposal of leather to landfills is the leaching from leather of Cr. Soluble Cr in a hexavalent oxidation state is considered to be undesirable in the environment,[2,3] and sites where Cr(VI) is present can require remediation.[4]

Current and proposed leather disposal methods include: extraction of Cr before disposal;[5−7] disposal to wetlands for vegetation to absorb the Cr;[8] production of other reconstituted structural materials to bind the Cr in new products;[9,10] and heating leather in an oxidizing environment to create a residue with soluble Cr.[11,12] Cr contained in or on particulates from the burning of coal and biomass (in the presence of oxygen) can produce Cr(VI).[13] Therefore, it is possible that burning leather may also generate Cr(VI), which is undesirable.

It has been proposed that the production of biochar, carbonized organic matter, from waste leather may be a better alternative to other disposal methods.[14] Biochar is produced by heating organic matter in an oxygen deficient environment. The application of leather biochar is a method of sequestering carbon, thereby reducing the amount of carbon that may have otherwise become atmospheric CO_2. Biochar also has the demonstrated benefit of improving agricultural soil productivity.[15] Carbonized leather has previously been considered as a disposal option, with the suggestion of producing an activated carbon product for filtration applications.[16−18]

Ideally, a leather biochar product could be produced that does not leach Cr. Exposing leather that has been "heat stablized" in a nonoxidizing environment to leaching indicates that the material has a low solubility of Cr. Specifically, when leather was stablized at 350 °C or higher in a CO_2 environment, no soluble Cr was detected over a wide pH range in contrast to untreated, chrome-tanned leather.[16] It is also important that the Cr is resistant to oxidation, since both Cr oxidation and reduction between the Cr(III) and Cr(VI) couple[19] can occur in soils, depending on the nature and condition of the soils and

Received: March 24, 2014
Revised: May 12, 2014
Published: June 9, 2014

other factors that control the redox environment. This has led to interest in the analysis of soils for the type of Cr contamination present.[20,21]

The chemical nature of Cr in leather has been characterized: Cr sulfate is used during tanning, and Cr bonds to the leather's collagen[22,23] and is well dispersed. However, the form of Cr present in biochar is unknown, as are its stability and dispersion. In an earlier study of the leaching of leather after heat treatment in a nonoxidizing environment, the chemical state of the Cr was not determined.[16]

The purpose of the work reported here is to investigate the speciation and structure of the Cr in biochar produced from chrome-tanned leather as a function of the heating conditions. It is intended to confirm the earlier reports of decreased solubility of Cr from leather heated in a nonoxidizing environment and determine that the samples being studied here for Cr speciation do in fact exhibit low Cr solubility. Developing an understanding of the nature of entrapment of Cr in leather biochar may enable a prediction of the likely stability of the Cr in the char in the longer term. For the determination of the chemical speciation and structure of Cr, X-ray absorption spectroscopy (XAS) is used and is known to exhibit obvious spectral differences for different oxidation states and chemical environments.

EXPERIMENTAL SECTION

Leather. Standard, commercial chrome-tanned bovine leather was used for all experiments. Raw hides were stripped of hair at 25 °C using 2% w/v sodium hydrosulfide (72% active), 1% w/v sodium sulfide (60% active), 1% hydrated lime, and 0.5% thioglycollic acid (60% active) for 3 h. Next the hides were limed by treating at 28 °C with a solution containing 2% w/v hydrated lime, 1% sodium sulfide (60% active) 0.5% surfactant (nonyl-phenol ethoxylate) for 2 h. Bating followed by treatment with 0.04% (w/w based on hide weight) pancreatic trypsin, followed by tanning with basic Cr sulfate ($Cr_2(SO_4)_3{\cdot}xH_2O$), then retanning with synthetic tannin (Tanicor PW, Clariant), and tara vegetable tannin (Granofin TA, Clariant), followed finally by fatliquoring with a blend of sulfated natural fats.

Pyrolysis Process. The biochar was produced from leather by pyrolysis. The crust leather was stored under ambient conditions prior to pyrolysis. Two pyrolysis reactors were used: a larger unit with no purge gas for the lower-temperature samples (up to 600 °C) and a smaller unit with the sample held under argon for higher-temperature samples (600−1000 °C).

For the larger, lower-temperature reactor, 100 g of leather was placed in a 1 L high-temperature 304 grade stainless-steel reactor. The reactor lid was sealed with a thin layer of potters' clay, and the reactor was flushed with 5 volumes of nitrogen (99.999% pure). The lid contains a nonreturn valve. The reactor was placed in a furnace and heated from ambient to the desired temperature over 1 h, held for 1 h at temperature, and cooled to 100 °C over 3 h before being opened. No control over the atmosphere in the reactor vessel was attempted other than the provision of the nonreturn valve (which resulted in a partial vacuum inside the vessel after cooling).

For the smaller, higher-temperature reactor, 4 g of leather was placed in a 25 mL 304 grade stainless-steel reactor through which a continuous flow of 0.2 L/min argon was passed. The furnace was heated from ambient to the desired temperature and held for 1 h before being rapidly cooled to below 100 °C, at which point the sample was removed; Ar flow was maintained continuously. Three high temperatures were tested, with the following heating and cooling times: heated to 1000 °C over 60 min, held for 60 min, cooled 25 min; heated to 800 °C over 35 min, held for 60 min, cooled 20 min; heated to 600 °C over 50 min, held for 60 min, cooled 5 min. A visual inspection suggested that there was no direct transfer of corrosion product from the stainless steel to the leather char.

Total Chromium Content of Leather and Char. The Cr content of the char and leather samples was measured using a standard industry test method.[24] The leather or char is first ashed in air. The residue is then treated with an oxidizing acid (a mixture of 75% v/v perchloric acid (60%, 25% sulfuric acid (98%)) to convert the Cr to hexavalent Cr. The hexavalent Cr is then reduced back to trivalent Cr using iodine in excess and the excess iodine is back-titrated with potassium thiosulfate. All Cr content is represented as weight percent of Cr, regardless of the chemical form.

Leaching of Chromium. Leachable chromium was measured with duplicate samples of char (5 g) leached in 100 mL of 1 M HCl while shaken for 15 h at room temperature. The char material produced was finely ground prior to leaching. The Cr content of the aqueous HCl leachate was then assessed in duplicate with a Varian 220 SpectrAA using a standard industry test method.[25]

XAS Measurements. X-ray absorption spectra were recorded on the XAS beamline at the Australian Synchrotron, Victoria, Australia. Cr K edge absorption spectra were recorded in transmission mode using a set of flow-through ion chambers supplied with He. The energy was controlled using a fixed exit Si(111) double crystal monochromator. The beam was conditioned using a collimating mirror (Si) and a toroidal focusing mirror (Rh coated). Higher harmonics were rejected using these two mirrors and a flat harmonic rejection mirror (SiO_2). For XAS scans, energy steps of 0.25 eV were employed in the XANES region using 1 s count per step while a step size of 0.035 $Å^{-1}$ was used in the EXAFS region to 14 $Å^{-1}$ with count times up of 6 s per step. The energy resolution was about 1 eV, and the photon flux was in the range 10^{11} to 10^{12} photons s^{-1}. The X-ray beam was about 1.5 × 0.4 mm^2 at the sample. The energy scale was calibrated by simultaneously measuring a Cr foil placed between two downstream ion chambers. Samples were packed in 1 mm thick poly(methyl methacrylate) sample holders. Reference standards were Cr_2O_3 (Prolab), $Cr_2(SO_4)_3{\cdot}xH_2O$ (BDH), $Cr_2(SO_4)_3{\cdot}xH_2O$ (Chromosal B, Lanxess, Germany), $Cr(CO)_6$ (BDH), Cr_3C_2 (Aldrich), and $Cr(O_2C_5H_7)_3$ (Aldrich) all diluted with boron nitride (Aldrich). Data processing was performed with ATHENA[26] and VIPER.[27]

RESULTS AND DISCUSSION

Biochar Formation. Heating leather under a stream of Ar in the small reactor, or in a larger closed vessel with a pressure release valve, resulted in well-formed char that retained the general shape of the leather feedstock, albeit at a smaller size. Weight loss (from ambient moisture) increased with heating temperature, with 62% weight loss being recorded at 300 °C, 73% at 600 °C, 76% at 800 °C, and 79% at 1000 °C. In the small reactor there was a hint of green color (perhaps Cr_2O_3) on the edge of some char that had formed near the outlet of the reactor suggesting that there was some ingress of oxygen near the outlet. These parts of the sample were not used in the analysis because it is believed they are not representative of the sample and they would not form in a larger scale reactor with better environmental control

Leachable Cr. It was found that a small amount of Cr can be leached from leather that has not been heat treated (Table 1), as has been reported previously.[16] After heating of the leather, the leachability of Cr diminishes. At 600 °C where the leather is clearly char very little leaching of Cr could be detected (Table 1). In an earlier leaching study it was found that at 350 °C the Cr was no longer able to be leached from the heated leather.[16] It was therefore sought to understand why Cr has much lower solubility from the charred leather.

XANES. X-ray absorption near edge structure (XANES) is a spectroscopic technique that is element specific and is local bonding sensitive. The technique requires irradiating a sample of interest with X-rays across a range of energy that includes an absorption edge. An inspection of the features of the spectrum

Table 1. Initial Chromium Content and Leachable Chromium of Leather and of Biochar Samples Produced under Various Heat Treatments

sample	initial % Cr (SD)	leachable Cr, as % of initial Cr
leather	0.99 (0.01)	4.67
300 °C[a]	2.60 (0.02)	3.50
600 °C[a]	7.39 (0.04)	0.31
600 °C[b]	11.8 (0.8)	0.08
800 °C[b]	12.5 (0.1)	0.06
1000 °C[b]	15.4 (0.1)	0.03

[a]Larger reaction vessel. [b]Finely ground, from small reaction vessel.

provides information on the bonding of the element of interest. XANES is most often used in a comparative study between spectra of known standards and unknown samples.

Beam Damage. Alteration to the state of Cr is possible in an intense, focused X-ray beam. The likelihood of this was investigated by doing multiple scans on the same spot of a representative sample and observing differences in the XANES spectra (total collection time up to 2 h). From these measurements it was determined that beam damage is negligible under the conditions that the samples are measured.

XANES of Reference Compounds. In the range of reference compounds for which XAS spectra were collected, it is apparent that there are strong differences in all parts of the spectra including the pre-edge region, the edge energy and the postedge region (Figure 1). It was not possible in this instance

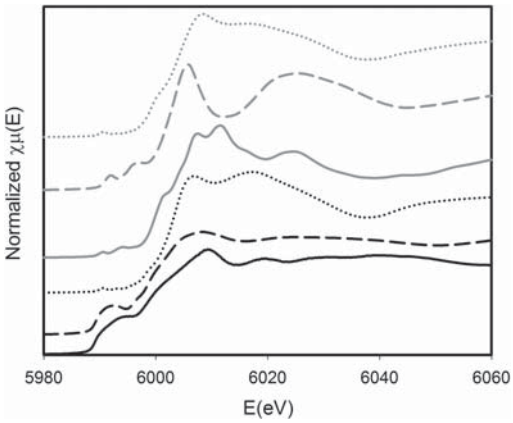

Figure 1. XAS of standards. Cr metal (solid line), Cr_3C_2 (dashed line), $Cr(O_2C_5H_7)_3$ (dotted line), Cr_2O_3 (grey solid line), $CrCO_6$ (grey dashed line), $Cr_2(SO_4)_3$ (grey dotted line).

to analyze any Cr(VI) reference compounds; however, reference spectra are available in the literature[20,28,29] and always show a strong signature pre-edge feature and a large edge shift.

XANES Edge Position and Cr Oxidation State. The energy position of the absorption edge is very sensitive to the oxidation state of the Cr atom that is excited.[28,30] The Cr in Cr_3C_2 is seen to have an effective oxidation state similar to that of Cr metal (Figure 1), and the charge on the Cr in Cr_3C_2 is calculated to be +0.33.[31] One can be confident that there is no Cr(VI) in any of the samples because Cr(VI) has a distinct and sharp pre-edge feature at around 5993.0 eV.[28,29] The feature arises from nonlocal dipole transitions in Cr(VI) compounds, which are tetrahedrally coordinated.[32−34] None of the samples showed this pre-edge feature.

XANES of Leather. The XANES spectrum of dried chrome leather is very similar to that of $Cr_2(SO_4)_3{\cdot}xH_2O$ (Figure 2).

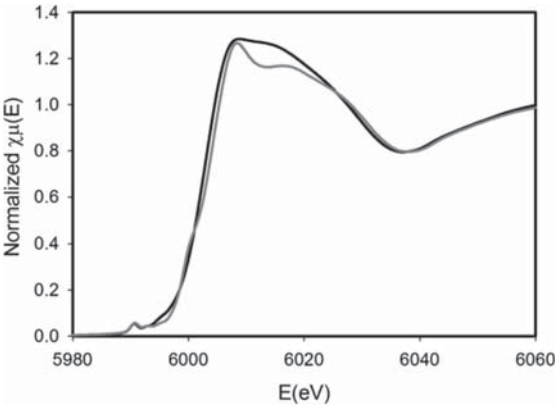

Figure 2. XANES of conditioned chrome tanned leather (solid line) and $Cr_2(SO_4)_3{\cdot}xH_2O$ (grey solid line).

This is the salt that is used in chrome tanning, so clearly some structural aspects of this salt are retained in the tanned leather. Detailed studies on this subject have been reported previously.[22,23]

XANES of Biochar. With heating, changes in leather's XANES spectra are observed from 600 °C, with significant differences with each 200 °C increase to the experimental maximum (Figure 3). The spectrum of the sample heated to 600 °C in the larger vessel appears to be equivalent to that of a sample heated to a lower temperature in the small scale vessel. With heating, a pre-edge peak of 5993.4 eV appears and it increases in intensity after higher temperature treatment. The pre-edge peak that forms in the samples at 600 and 800 °C is in the same position as the peak from the Cr_3C_2 standard but is sharper and is not a good match to the shape of the Cr carbide pre-edge peak (or that of any of the standards) and may reflect a different structure to any of the standards. After treatment at 1000 °C, this peak broadens and begins to look more like the Cr carbide pre-edge feature.

A shift in the absorption edge to a lower energy after heating becomes apparent from 800 °C, with a shift of 0.8 eV, and with a further shift apparent at 1000 °C, yielding a total shift of 1.5 eV from the dry leather or chromium sulfate spectrum. The shape of the postedge spectrum changes consistently with heating.

XANES Linear Fits for Biochar. Using the Athena software,[26] linear combination fitting to normalized $\chi\mu$(E) and to $k^3\chi$(k) were performed. Unconstrained linear combination fitting was attempted using the spectra for $Cr_2(SO_4)_3{\cdot}xH_2O$, Cr metal, Cr_2O_3, and Cr_3C_2 (Figure 4). Dry leather is substituted as a proxy for the $Cr_2(SO_4)_3{\cdot}xH_2O$ spectrum since $Cr_2(SO_4)_3{\cdot}xH_2O$ is the tanning agent used in chrome-tanned leather and the Cr is well dispersed in leather and therefore gave a better XAS at high k than the ground pure compound mixed with BN. The dry leather better reflects the highly dispersed nature of the Cr. The fit range used was 40 eV below to 70 eV above E_0. Best fits were obtained using only two components, dry leather (or $Cr_2(SO_4)_3{\cdot}xH_2O$) and Cr_3C_2 (Figure 5). With an unconstrained fit also containing an initial component of Cr metal or Cr_2O_3, these components do not contribute to the fit. As the treatment temperature increases, the amount of carbide increases. The calculated proportions of

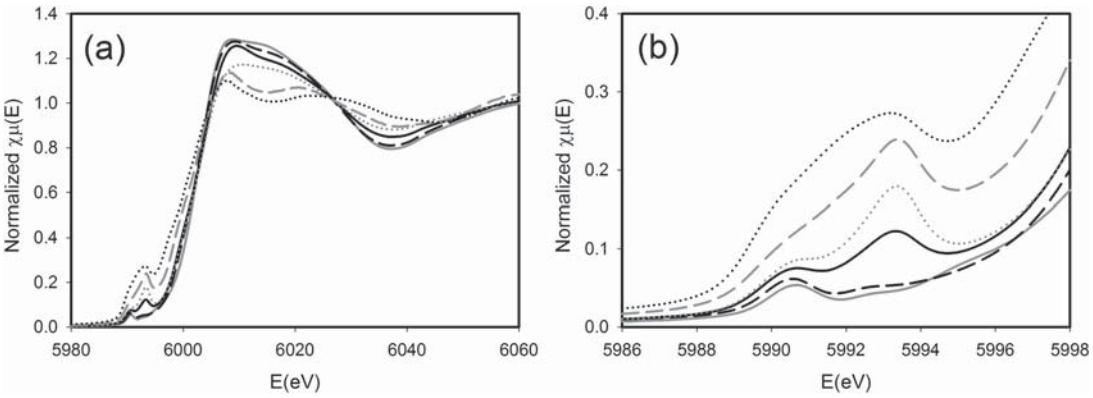

Figure 3. XANES of leather and leather biochar heated to different temperatures. Leather standard (grey solid line); heated in the large vessel at 500 °C (dashed line) or 600 °C (solid line); heated in the small vessel at 600 °C (grey dotted line), 800 °C (grey dashed line), or 1000 °C (dotted line). (a) XANES region. (b) Expanded pre-edge region.

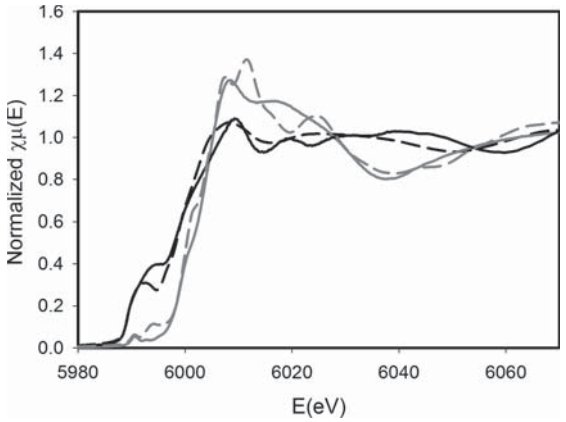

Figure 4. XANES of standards tested for linear combination fit. $Cr_2(SO_4)_3$ (grey solid line), Cr_3C_2 (dashed line), Cr metal (solid line), Cr_2O_3 (grey dashed line).

carbide and Cr sulfate (represented as the dry leather spectrum) are listed in Table 2. Fitting to the $k^3\chi(k)$ spectra gives similar proportions of Cr_3C_2 and $Cr_2(SO_4)_3{\cdot}xH_2O$, as does fitting to the energy spectra.

Chromium Carbide Formation. Thermodynamic considerations suggest that, under high carbon activity and low oxygen activity (as in char formation), Cr metal or Cr carbide may form.[35,36] This occurs at log P_{O2} (bar) below about −16, with the carbides formed at log a_C (carbon activity) above about −2.8 (Cr metal forms at lower a_C).[35] In contrast, during oxy-fuel combustion of coal, Cr(III) in the form of Cr silicate and iron chromite are the dominant species.[37,38] It is not known exactly what conditions prevail in the char formation in the reaction vessels; however, it is expected that P_{O2} is low and a_C is high, and therefore, it is not surprising that Cr carbide is found in the samples.

Fine atmospheric particulates containing Cr, supposed to be from natural and industrial sources, have been found to contain both Cr^0 and Cr carbide using XANES,[39] which demonstrates that Cr carbides are not uncommon in the environment.

It has been reported that carbothermal reduction by pitch of various transition metal oxides, including Cr oxide, forms carbides.[40] In a N_2 atmosphere or an ammonia atmosphere, nitrides may also be formed for most of the metal oxides studied in that report, with the exception of Cr, which did not form nitrides, only carbide.[40] These studies indicate that leather biochar is likely to contain Cr carbide, and not Cr nitride, even if the biochar is formed in the presence of nitrogen. The XANES shows that the Cr changes from the initial, dispersed Cr sulfate to some possibly intermediate compound (which may be a form of carbide) to form a Cr carbide at 1000 °C not dissimilar to Cr_3C_2.

EXAFS of Biochar for Structural Information. Information about the structural environment of the Cr in the leather biochar is obtained from an analysis of the EXAFS range of the data acquired. Data were processed using VIPER,[27] and a Hanning window applied to the Fourier transforms. Theoretical ab initio EXAFS spectra for pairs of atoms were calculated using FEFF6L,[41] with crystal structures from the ATOMS database (Center for Advanced Radiation Sources, University of Chicago). Modeling in k space of the experimental spectra (from selected regions of the Fourier transform) using combinations of EXAFS spectra for these atom pairs was then performed with VIPER.[27] To validate the modeling of the EXAFS data, the spectrum of Cr_2O_3 was used, which is a crystalline material with a relatively simpler structure than Cr_3C_2. The resultant bond lengths are consistent with the crystallographic structure, validating the EXAFS data and fitting and enabling the analysis of the more complex biochar, which XANES has shown to contain a mixture of Cr_3C_2 and other components.

Chromium Carbide. To interpret the EXAFS of the biochar, it is helpful to refer to the literature on EXAFS of Cr carbide. A detailed study of the electronic structure of Cr carbides[31] notes that crystalline Cr_3C_2 belongs to the space group *pnma*, with lattice parameters a = 5.485 Å, b = 2.789 Å, and c = 11.474 Å. Common phases that may form in Cr-based coatings include Cr_3C_2, Cr_7C_3, and $Cr_{23}C_6$. Based on the enthalpies of formation, Cr_3C_2 is the most stable of the Cr carbide phases, followed by Cr_7C_3, with $Cr_{23}C_6$ and Cr_3C equal third.[31] The bonding is described as a combination of metallic, ionic and covalent, in character with a strong proportion of metallic character (e.g., metallicity for Cr_3C_2 is estimated at 15% and is higher for the other Cr carbides). The charge on Cr of Cr_3C_2 is calculated to be $Cr^{+0.33}$.[31] Bond lengths in these compounds[31] and in Cr_3C_2 and Cr doped diamond-like carbon (DLC) films obtained from EXAFS[42] are detailed in Table 3. The bond distances measured in the leather biochar are

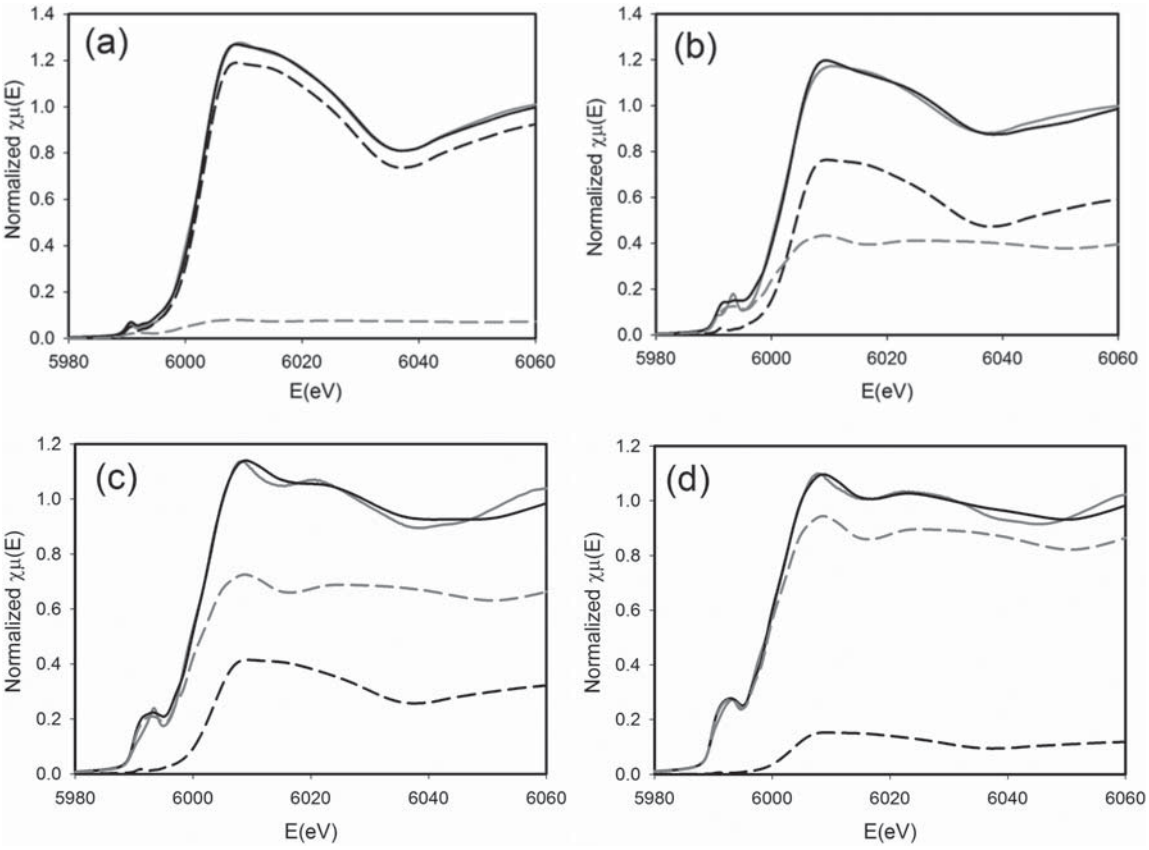

Figure 5. XANES linear combination fit of biochar prepared at (a) 500 °C; (b) 600 °C; (c) 800 °C; and (d) 1000 °C. Cr_3C_2 (grey dashed line), dry leather (dashed line), data (grey solid line), fit (solid line).

Table 2. Chemical Components of Linear Combination Fitting to the XAS Energy Spectrum[a]

	$Cr_2(SO_4)_3{\cdot}xH_2O$ (mol % Cr)	Cr_3C_2 (mol % Cr)	*R* factor ($\times 10^{-4}$), χ^2
biochar 500 °C[b]	93	7	1.7, 0.027
biochar 600 °C[b]	77	23	3.4, 0.051
biochar 600 °C	59	41	5.6, 0.081
biochar 800 °C	35	65	5.8, 0.081
biochar 1000 °C	12	88	2.2, 0.031

[a]Uncertainty in mole percent Cr in $Cr_2(SO_4)_3{\cdot}xH_2O$ and Cr_3C_2 is around ±5%. [b]Larger reaction vessel.

therefore similar to those reported for Cr carbide reported in the literature and to one crystalline compound measured here.

EXAFS of Biochar. There are numerous different atom−atom scattering path lengths in Cr carbide, some of which are quite similar in size. The char formed at 600 °C is too complex a mixture to enable reliable modeling of the EXAFS spectrum. However, the EXAFS spectra of the biochar prepared at 800 and 1000 °C can be fitted with one grouped Cr−C atom pair sets and two grouped Cr−Cr atom pair sets, representing similar atom−atom distances in each group (Figure 6). From the fits, the bond distances shown in Table 4 are obtained. These bond distances are similar to those reported for Cr carbide compounds as listed in Table 3. This EXAFS analysis supports the XANES interpretation and confirms that Cr carbide is formed at higher temperatures.

Stability in the Soil Environment. While it has been found that using acid to produce biochar leachate does not remove Cr from the biochar, long-term stability tests of the material in soil environments were not performed. These would be desirable to ensure the safety of the material for use in agricultural settings. As noted above, oxidation or reduction of

Table 3. Bond Lengths in Cr Carbide Compounds Reported from EXAFS in References 31 and 42

compound	radial distribution peak Cr−C (Å)	radial distribution peak Cr−Cr (Å)	source
Cr_3C	2.12	2.58	31
Cr_3C_2	2.11	2.63	31
Cr_7C_3	2.14	2.58	31
$Cr_{23}C_6$	2.10	2.56	31
Cr_3C_2	2.2	2.7	42
Cr−DLC	2.17−2.25	2.75−2.79	42

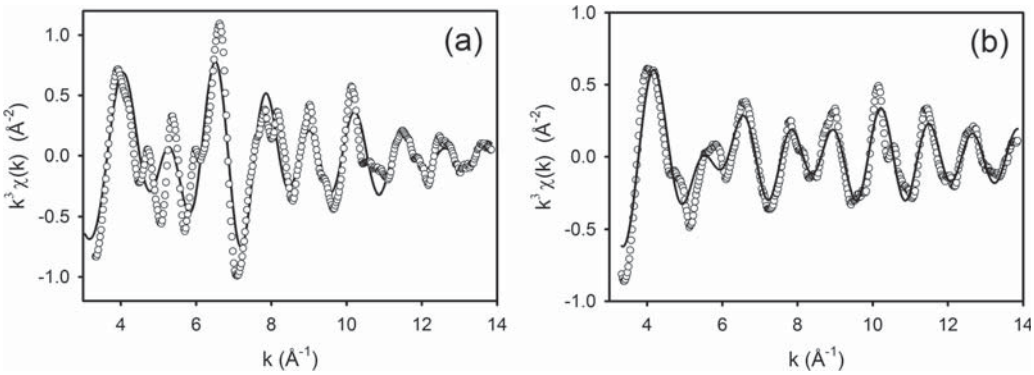

Figure 6. EXAFS of biochar produced at (a) 800 °C and (b) 1000 °C: (circles) $k^3\chi(k)$, (solid line) fitted model.

Table 4. Bond Lengths Obtained from the Modeling of Fourier Transform of EXAFS Spectra of Leather Biochar[a]

sample	Cr−C (Å), coordination number	Cr−Cr (Å), coordination number	Cr−Cr (Å), coordination number
biochar 800 °C	2.07, 3.6	2.58, 0.7	2.94, 3.0
biochar 1000 °C	2.05, 1.7	2.70, 4.3	2.92, 1.8

[a]Six scattering paths were combined for Cr−C, 12 paths for Cr−Cr in total (in two groups).

some Cr compounds can occur in soils, depending on redox environment of the soil[19] and also such oxidation can be facilitated by bacterial action.[43] However, Cr carbide is a very stable material, and is resistant to oxidation or reduction.[44] The charcoal or biochar matrix within which the Cr is contained is also know to be very stable in soils.[45] The addition of charcoal to soil enhances the agricultural productivity of the soil, for example in the traditional terra preta soils from South America[46] but also in more recent studies of soil productivity.[15]

CONCLUSIONS

It has been shown that there may be an environmental benefit in making biochar from chrome-tanned leather waste. The char does not release Cr with acid leaching, unlike untreated leather. It has also been shown that the Cr becomes chemically reduced by a carbothermic reaction on charring at high temperatures forming Cr carbide. Cr carbide is an inherently stable compound and its stability is further enhanced by being highly dispersed in a stable carbon medium. Biochar has the added benefits of enhancing agricultural production from soil and providing long-term sequestration of carbon from the environment. This strategy may turn a large-scale waste into an economic resource.

AUTHOR INFORMATION

Corresponding Author

*E-mail: r.haverkamp@massey.ac.nz.

Notes

The authors declare no competing financial interest.

ACKNOWLEDGMENTS

This research was undertaken on the XAS beamline at the Australian Synchrotron, Victoria, Australia. The NZ Synchrotron Group Ltd is acknowledged for travel funding. Clive Bardell and John Edwards, Massey University, built the high-temperature reactor. The work was supported by Ministry of Business Innovation and Employment grants LSRX0801 and LSRX1202.

REFERENCES

(1) Commodities and Trade Division, F. A. O., United Nations *World statistical compendium for raw hides and skins, leather and leather footwear 1990−2011*; Rome, 2012.

(2) Gao, Y.; Xia, J. Chromium contamination accident in china: viewing environment policy of China. *Environ. Sci. Technol.* **2011**, *45* (20), 8605−8606.

(3) Izbicki, J. A.; Bullen, T. D.; Martin, P.; Schroth, B. Delta Chromium-53/52 isotopic composition of native and contaminated groundwater, Mojave Desert, USA. *Appl. Geochem.* **2012**, *27* (4), 841−853.

(4) James, B. R. The challenge of remediating chromium-contaminated soil. *Environ. Sci. Technol.* **1996**, *30* (6), A248−A251.

(5) Heidemann, E. Disposal and recycling of chrome-tanned materials. *J. Am. Leather Chem. As.* **1991**, *86* (9), 331−333.

(6) Cabeza, L. F.; Taylor, M. M.; DiMaio, G. L.; Brown, E. M.; Mermer, W. N.; Carrio, R.; Celma, P. J.; Cot, J. Processing of leather waste: pilot scale studies on chrome shavings. Isolation of potentially valuable protein products and chromium. *Waste Manage.* **1998**, *18* (3), 211−218.

(7) Beltran-Prieto, J. C.; Veloz-Rodriguez, R.; Perez-Perez, M. C.; Navarrete-Bolanos, J. L.; Vazquez-Nava, E.; Jimenez-Islas, H.; Botello-Alvarez, J. E. Chromium recovery from solid leather waste by chemical treatment and optimization by response surface methodology. *Chem. Ecol.* **2012**, *28* (1), 89−102.

(8) Dotro, G.; Castro, S.; Tujchneider, O.; Piovano, N.; Paris, M.; Faggi, A.; Palazolo, P.; Larsen, D.; Fitch, M. Performance of pilot-scale constructed wetlands for secondary treatment of chromium-bearing tannery wastewaters. *J. Hazard. Mater.* **2012**, *239*, 142−151.

(9) Ashokkumar, M.; Thanikaivelan, P.; Krishnaraj, K.; Chandrasekaran, B. Transforming chromium containing collagen wastes into flexible composite sheets using cellulose derivatives: structural, thermal, and mechanical investigations. *Polym. Composite* **2011**, *32* (6), 1009−1017.

(10) Przepiorkowska, A.; Chronska, K.; Zaborski, M. Chrome-tanned leather shavings as a filler of butadiene-acrylonitrile rubber. *J. Hazard. Mater.* **2007**, *141* (1), 252−257.

(11) Erdem, M. Chromium recovery from chrome shaving generated in tanning process. *J. Hazard. Mater.* **2006**, *129* (1−3), 143−146.

(12) Tahiri, S.; Albizane, A.; Messaoudi, A.; Azzi, M.; Bennazha, J.; Younssi, S. A.; Bouhria, M. Thermal behaviour of chrome shavings and of sludges recovered after digestion of tanned solid wastes with calcium hydroxide. *Waste Manage.* **2007**, *27* (1), 89−95.

(13) Stam, A. F.; Meij, R.; Winkel, H. T.; van Eijk, R. J.; Huggins, F. E.; Brem, G. Chromium speciation in coal and biomass co-combustion products. *Environ. Sci. Technol.* **2011**, *45* (6), 2450−2456.

(14) Aitkenhead, W.; Edmonds, R. L. Biochar: A possibility for solid waste disposal. *Leather Int.* **2013**, *215* (4827), 28−30.
(15) Chan, K. Y.; Van Zwieten, L.; Meszaros, I.; Downie, A.; Joseph, S. Agronomic values of greenwaste biochar as a soil amendment. *Aust. J. Soil Res.* **2007**, *45* (8), 629−634.
(16) Erdem, M.; Ozverdi, A. Leaching behavior of chromium in chrome shaving generated in tanning process and its stabilization. *J. Hazard. Mater.* **2008**, *156* (1−3), 51−55.
(17) Oliveira, L. C. A.; Guerreiro, M. C.; Goncalves, M.; Oliveira, D. Q. L.; Costa, L. C. M. Preparation of activated carbon from leather waste: A new material containing small particle of chromium oxide. *Mater. Lett.* **2008**, *62* (21−22), 3710−3712.
(18) Sekaran, G.; Shanmugasundaram, K. A.; Mariappan, M. Characterization and utilisation of buffing dust generated by the leather industry. *J. Hazard. Mater.* **1998**, *63* (1), 53−68.
(19) Brose, D. A.; James, B. R. Oxidation-reduction transformations of chromium in aerobic soils and the role of electron-shuttling quinones. *Environ. Sci. Technol.* **2010**, *44* (24), 9438−9444.
(20) Kappen, P.; Welter, E.; Beck, P. H.; McNamara, J. M.; Moroney, K. A.; Roe, G. M.; Read, A.; Pigram, P. J. Time-resolved XANES speciation studies of chromium on soils during simulated contamination. *Talanta* **2008**, *75* (5), 1284−1292.
(21) Martin, R. R.; Naftel, S. J.; Sham, T. K.; Hart, B.; Powell, M. A. XANES of chromium in sludges used as soil ameliorants. *Can. J. Chem.* **2003**, *81* (2), 193−196.
(22) Covington, A. D.; Lampard, G. S.; Menders, O.; Chadwick, A. V.; Rafeletos, G.; O'Brien, P. Extanded X-ray absorption fine structure sudies of the role of chromium in leather tanning. *Polyhedron* **2001**, *20*, 461−466.
(23) Reich, T.; Rossberg, A.; Hennig, C.; Reich, G. Characterization of chromium complexes in chrome tannins, leather, and gelatin using extended X-ray absorption fine structure (EXAFS) spectroscopy. *J. Am. Leather Chem. As* **2001**, *96* (4), 133−147.
(24) ISO. *Leather−Chemical determination of chromic oxide content−Part 1: Quantification by titration*; 2007; Vol. ISO 5398-1:2007 (IULTCS/IUC 8-1).
(25) ISO. *Leather−Chemical determination of chromic oxide content−Part 3: Quantification by atomic absorption spectrometry*; 2007; Vol. ISO 5398-3:2007 (IULTCS/IUC 8-3).
(26) Ravel, B.; Newville, M. ATHENA, ARTEMIS, HEPHAESTUS: Data analysis for X-ray absorption spectroscopy using IFEFFIT. *J. Synchrotron Radiat.* **2005**, *12*, 537−541.
(27) Klementev, K. V. Extraction of the fine structure from x-ray absorption spectra. *J. Phys. D Appl. Phys.* **2001**, *34* (2), 209−217.
(28) Pantelouris, A.; Modrow, H.; Pantelouris, M.; Hormes, J.; Reinen, D. The influence of coordination geometry and valency on the K-edge absorption near edge spectra of selected chromium compounds. *Chem. Phys.* **2004**, *300* (1−3), 13−22.
(29) Gardea-Torresday, J. L.; Tiemann, K. J.; Armendariz, V.; Bess-Oberto, L.; Chianelli, R. R.; Rios, J.; Parsons, J. G.; Gamez, G. Characterization of Cr(VI) binding and reduction to Cr(III) by the agricultural byproducts of Avena monida (Oat) biomass. *J. Hazard. Mater.* **2000**, *80* (1−3), 175−188.
(30) Farges, F. Chromium speciation in oxide-type compounds: application to minerals, gems, aqueous solutions and silicate glasses. *Phys. Chem. Miner.* **2009**, *36* (8), 463−481.
(31) Li, Y. F.; Gao, Y. M.; Xiao, B.; Min, T.; Yang, Y.; Ma, S. Q.; Yi, D. W. The electronic, mechanical properties and theoretical hardness of chromium carbides by first-principles calculations. *J. Alloy. Compd.* **2011**, *509* (17), 5242−5249.
(32) de Groot, F.; Vanko, G.; Glatzel, P. The 1s x-ray absorption pre-edge structures in transition metal oxides. *J. Phys.: Condens. Matter* **2009**, *21* (10), DOI: 10.1088/0953-8984/21/10/104207.
(33) Frommer, J.; Nachtegaal, M.; Czekaj, I.; Weng, T. C.; Kretzschmar, R. X-ray absorption and emission spectroscopy of Cr-III (hydr)oxides: analysis of the K-pre-edge region. *J. Phys. Chem. A* **2009**, *113* (44), 12171−12178.
(34) Yamamoto, T. Assignment of pre-edge peaks in K-edge x-ray absorption spectra of 3d transition metal compounds: electric dipole or quadrupole? *X-Ray Spectrom.* **2008**, *37* (6), 572−584.
(35) Chu, W. F.; Rahmel, A. The conversion of chromium-oxide to chromium carbide. *Oxid. Met.* **1981**, *15* (3−4), 331−337.
(36) Grabke, H. J.; Krajak, R.; Paz, J. C. N. On the mechanism of catastrophic carburization - metal dusting. *Corros. Sci.* **1993**, *35* (5−8), 1141−1150.
(37) Jiao, F.; Wijaya, N.; Zhang, L.; Ninomiya, Y.; Hocking, R. Synchrotron-based XANES speciation of chromium in the oxy-fuel fly ash collected from lab-scale drop-tube furnace. *Environ. Sci. Technol.* **2011**, *45* (15), 6640−6646.
(38) Chen, J.; Jiao, F.; Zhang, L.; Yao, H.; Ninomiya, Y. Use of synchrotron XANES and Cr-doped coal to further confirm the vaporization of organically bound Cr and the formation of chromium-(VI) during coal oxy-fuel combustion. *Environ. Sci. Technol.* **2012**, *46* (6), 3567−3573.
(39) Werner, M. L.; Nico, P. S.; Marcus, M. A.; Anastasio, C. Use of micro-XANES to speciate chromium in airborne fine particles in the Sacramento Valley. *Environ. Sci. Technol.* **2007**, *41* (14), 4919−4924.
(40) Eick, B. M.; Youngblood, J. P. Carbothermal reduction of metal-oxide powders by synthetic pitch to carbide and nitride ceramics. *J. Mater. Sci.* **2009**, *44* (5), 1159−1171.
(41) Rehr, J. J.; Deleon, J. M.; Zabinsky, S. I.; Albers, R. C. Theoretical X-ray absorption fine-structure standards. *J. Am. Chem. Soc.* **1991**, *113* (14), 5135−5140.
(42) Singh, V.; Palshin, V.; Tittsworth, R. C.; Meletis, E. I. Local structure of composite Cr-containing diamond-like carbon thin films. *Carbon* **2006**, *44* (7), 1280−1286.
(43) He, J.-Z.; Meng, Y.-T.; Zheng, Y.-M.; Zhang, L.-M. Cr(III) oxidation coupled with Mn(II) bacterial oxidation in the environment. *J. Soils Sediments* **2010**, *10* (4), 767−773.
(44) Sen, S.; Ozdemir, O.; Demirkiran, A. S.; Sen, U.; Yigit, F.; Hashmi, M. S. J. Oxidation kinetics of chromium carbide coating produced on AISI 1040 steel by thermo-reactive deposition method during high temperature in air. *Adv. Mater. Res.* **2012**, *445*, 649−654.
(45) Schmidt, M. W. I.; Torn, M. S.; Abiven, S.; Dittmar, T.; Guggenberger, G.; Janssens, I. A.; Kleber, M.; Kogel-Knabner, I.; Lehmann, J.; Manning, D. A. C.; Nannipieri, P.; Rasse, D. P.; Weiner, S.; Trumbore, S. E. Persistence of soil organic matter as an ecosystem property. *Nature* **2011**, *478* (7367), 49−56.
(46) Glaser, B.; Haumaier, L.; Guggenberger, G.; Zech, W. The 'Terra Preta' phenomenon: a model for sustainable agriculture in the humid tropics. *Naturwissenschaften* **2001**, *88* (1), 37−41.

Hindawi Publishing Corporation
BioMed Research International
Volume 2014, Article ID 189197, 10 pages
http://dx.doi.org/10.1155/2014/189197

Research Article

Age Dependent Differences in Collagen Alignment of Glutaraldehyde Fixed Bovine Pericardium

Katie H. Sizeland,[1] Hannah C. Wells,[1] John Higgins,[2] Crystal M. Cunanan,[3] Nigel Kirby,[4] Adrian Hawley,[4] Stephen T. Mudie,[4] and Richard G. Haverkamp[1]

[1] *School of Engineering and Advanced Technology, Massey University, Palmerston North 4472, New Zealand*
[2] *Southern Lights Biomaterials, Palmerston North 4110, New Zealand*
[3] *Structural Heart Division, Boston Scientific, Los Gatos, CA 95032, USA*
[4] *Australian Synchrotron, Clayton, VIC 3168, Australia*

Correspondence should be addressed to Richard G. Haverkamp; r.haverkamp@massey.ac.nz

Received 17 July 2014; Accepted 2 September 2014; Published 14 September 2014

Academic Editor: Jun Ren

Bovine pericardium is used for heart valve leaflet replacement where the strength and thinness are critical properties. Pericardium from neonatal animals (4–7 days old) is advantageously thinner and is considered as an alternative to that from adult animals. Here, the structures of adult and neonatal bovine pericardium tissues fixed with glutaraldehyde are characterized by synchrotron-based small angle X-ray scattering (SAXS) and compared with the mechanical properties of these materials. Significant differences are observed between adult and neonatal tissue. The glutaraldehyde fixed neonatal tissue has a higher modulus of elasticity (83.7 MPa) than adult pericardium (33.5 MPa) and a higher normalised ultimate tensile strength (32.9 MPa) than adult pericardium (19.1 MPa). Measured edge on to the tissue, the collagen in neonatal pericardium is significantly more aligned (orientation index (OI) 0.78) than that in adult pericardium (OI 0.62). There is no difference in the fibril diameter between neonatal and adult pericardium. It is shown that high alignment in the plane of the tissue provides the mechanism for the increased strength of the neonatal material. The superior strength of neonatal compared with adult tissue supports the use of neonatal bovine pericardium in heterografts.

1. Introduction

Heart valve leaflet replacement with bovine pericardium is an established practice [1] using either adult or calf pericardium [2] and may be performed percutaneously [3]. It is essential that the mechanical strength and performance of the material are adequate for a long life in service [4]. Greater understanding of the properties of these materials and the structural basis for these properties is important for improving the serviceability of these replacements.

Pericardium is a fibrous collagen extracellular matrix material with structural similarities to skin and other tissues. The structure of these collagenous tissues can be characterized by small angle X-ray scattering (SAXS) to yield, for example, quantitative measures of fibril orientation and fibril D-spacing [5–7]. While other methods have been used to study collagen fibril orientation including polarized light microscopy [8], reflection anisotropy [9], small angle light scattering [10], confocal laser scattering [11], Raman polarisation [12], and anisotropic Raman scattering [13], synchrotron based SAXS has the advantage of excellent nonsubjective quantification combined with good spatial resolution.

The fact that there is a function-structure relationship between collagen alignment and mechanical strength is well known [14]. The orientation of collagen measured edge on (alignment in plane) has been shown in bovine and ovine skin to be correlated with strength [15, 16]. This correlation extends across a range of mammal species with a strength range of over a factor of five [17]. It is the three-dimensional orientation that is important: simply taking an observation of the fibril orientation normal to the surface of the tissue is not very helpful. Instead, it is necessary to measure

the orientation of the fibrils through the thickness of the skin to determine the extent to which they cross between the top and the bottom of the skin layer [17].

The orientation of collagen in pericardium heterograft materials for heart valve leaflets has been shown to affect the stiffness during flexing [18]. In ovine and bovine skin, the orientation of the fibrils in the skin influences the mechanical properties [16, 17].

We have previously found that pericardium from neonatal calves (4–7 days old) has superior properties for potential application for heart valve repair [19]. Although both adult and calf bovine pericardia are used in heart valve repair, neonatal pericardium has not yet been used for heart valve manufacture. The greater tensile modulus of neonatal pericardium compared to that of adult pericardium may enable the thinner neonatal tissue to be used. This would allow a smaller introducer size for percutaneous heart valves. This makes the application of these heart valves possible through diseased femoral arteries which may have reduced diameters [20]. Glutaraldehyde crosslinked pericardium continues to be the material of choice for heart valve manufacturers and developers. There are several devices on the market and more devices currently in clinical trial that use glutaraldehyde treated tissues.

It is known that collagen tissue properties change with age. Differences have been shown in the thermal stability of tendon collagen between steers aged 24–30 months and bulls aged 5 years and this has been attributed to increased level of maturity and thermally stable crosslinks [21]. Glycation of collagen increases with age and can lead to differences in mechanical properties of the collagen. It has been shown to increase stiffness in connective tissues [22] and collagen gels [23] and increase brittleness in bones [24]. Porcine extracellular matrix scaffolds derived from small intestinal submucosa of younger animals and used for *in vivo* remodeling have been studied previously. They were associated with a more constructive, site appropriate, tissue remodeling response than scaffolds derived from older animals [25]. However, specific physical factors causing this difference were not identified.

It has also been found that tissue strength varies with collagen fibril diameter. Larger diameter collagen fibrils are present in stronger tissue. In human aortic valves, the collagen fibril diameter depends on whether the fibrils are from regions of high stress or low stress: larger diameter fibrils (in areas of lower fibril density) result from high stress, suggesting that these larger diameter fibrils provide increased strength [26]. Similarly, for mouse and rat tendon, fibril diameters increase with loading [27, 28]. It is proposed that this is due to the extra mechanical load placed on the tendons on the exercising animals (due to their higher activity levels) stimulating fibril thickening [28]. In bovine leather, fibril diameter is found to be only weakly correlated with strength [29].

The size distribution of the fibril diameter has also been found to change with age. Fetal tissue has been found to have a unimodal distribution with smaller collagen fibril diameters, whereas older tissue has larger fibrils and may have a unimodal or bimodal size distribution depending on the tissue type and animal [30]. In studies of equine digital flexor tendons, fibril diameter decreases with exercise, suggesting weakening of tendon with exercise (i.e., fatter fibril is stronger). Unusually, the fibril diameter in these tendons decreases with age, and this is associated with the decrease in strength [31, 32].

In the percutaneous delivery of heart valves, the size of the device when folded for delivery is important. Devices made from adult bovine pericardium or porcine pericardium typically require a size 18 F to 25 F catheter (7.0–8.4 mm) [33]. This size is in part dictated by the thickness of the pericardium that is used in the valve, with thicker material folding into a larger diameter device for insertion. A study of 79 patients with peripheral arterial disease found that occluded femoral arteries had an average internal diameter of 4.5 ± 1.4 mm with 12 below 3.5 mm (11 F on the French catheter scale) [20]. These occluded arteries are significantly smaller than the folded heart valves resulting in difficulties for percutaneous delivery of existing heart valve technology. This provides a motivation to find thinner but sufficiently strong material as a substitute for the existing bovine or porcine pericardium. Neonatal pericardium is one possible option that is investigated here.

The structural differences between neonatal pericardium and adult tissue that give rise to the desirable differences in their physical properties have not been adequately investigated. This study investigates and compares the collagen fibril structure of neonatal and adult bovine pericardium using SAXS. Specifically, the fibril orientation and the fibril diameter are examined. The use of SAXS at a modern synchrotron facility allows analysis of a small area (250 × 80 μm), enabling quantification of fibril orientation edge on in relatively thin pericardium tissues, a process that is difficult to achieve by other methods.

2. Methods

Pericardia were selected from 10 adult (18–24 months old) and 10 neonatal (4–7 days old) cattle. The fresh pericardia (less than 72 hours postmortem and typically 48–72 hours postmortem) were washed several times in PBS buffer (pH 7.4 ± 0.2, 0.01% NaCl). Adult tissue was typically processed closer to 48 hours postmortem while neonatal tissue was processed closer to 72 hours postmortem due to the logistics of obtaining the samples. The tissue was stored at 4–7°C from harvest until the start of washing. Washing in PBS buffer took place at room temperature. The pericardium was then cut and flattened into a "butterfly" shape and held flat with weights around the edge (Figure 1) with care taken to ensure that there were no air bubbles trapped beneath the material.

Treatment with glutaraldehyde was performed in several stages at room temperature. First, the flat, weighted pericardium was immersed in a tray of 0.625% glutaraldehyde (in PBS buffer) for 30 minutes. The second stage was immersion in fresh 0.625% glutaraldehyde (in PBS buffer) for 48 hours with the weights removed. For the third stage the solution was changed for fresh 0.625% glutaraldehyde (in PBS buffer) and maintained for a further 48 hours. After this treatment,

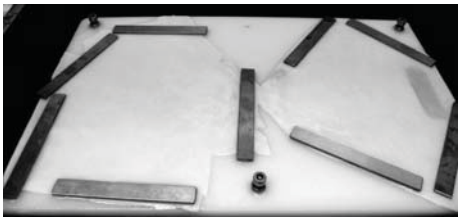

Figure 1: Flattened pericardium, after cutting, held with weights around the edge.

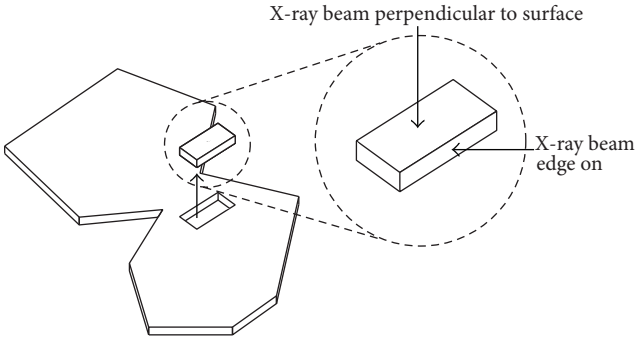

Figure 2: Directions of X-ray analysis of samples.

coupons of 90 mm × 140 mm were cut from the centre of each side of the butterfly. The pericardium was stored with enough 0.625% glutaraldehyde PBS solution to keep the material moist until being required for other tests. The time between this stage and mechanical measurements varied between 1 and 7 days and for the SAXS measurements between 1 and 3 weeks. For the SAXS analysis, strips were cut in two directions perpendicular to each other from the centre of coupons. Replicates of each sample were prepared.

The thickness was measured with callipers using a light and consistent force.

The elastic modulus and ultimate tensile strength were measured uniaxially using an Instron tensile tester on strips of material.

Histological cross-sections stained with picrosirius red to highlight the collagen were recorded under cross-polarized light on one sample of neonatal pericardium and one of adult pericardium [34].

In preparation for SAXS analysis, the pericardia were removed from the glutaraldehyde solution in which they had been stored. After soaking for at least 1 hour in buffered saline solution, the strips were mounted in 7 μm thick Kapton tape to prevent drying during analysis (i.e., retain them in a wet state). The X-ray beam was directed either through the sample perpendicular to the flat surface or through one of two edge mounted samples. This meant that spectra were recorded in each of the three orthogonal directions through the tissue for each sample (Figure 2). For the edge-analysed samples, it was necessary to brace the tissue against a stiff plastic strip mount to prevent the pericardium from folding or twisting during analysis and to ensure that there was only one layer of the sample in the path of the X-ray beam throughout the travel of the beam. All diffraction patterns were recorded at room temperature.

Diffraction patterns were recorded on the Australian Synchrotron SAXS/WAXS beamline, utilizing a high-intensity undulator source. Energy resolution of 10^{-4} (e.g., 1×10^{-4} Å for 1 Å radiation) was obtained from a cryocooled Si(111) double-crystal monochromator and the beam size (FWHM focused at the sample) was 250×80 μm, with a total photon flux of about 2×10^{12} ph·s^{-1}. All diffraction patterns were recorded with an X-ray energy of 12 keV using a Pilatus 1 M detector with an active area of 170 × 170 mm and a sample-to-detector distance of 3371 mm. Exposure time for diffraction patterns was 1 s and data processing was carried out using the SAXS15ID software [35].

The orientation index (OI) is used to give a measure of the spread of microfibril orientation (an OI of 1 indicates the microfibrils are parallel to each other; an OI of 0 indicates the microfibrils are randomly oriented). OI is defined as (90° − OA)/90°, where OA is the minimum azimuthal angle range that contains 50% of the microfibrils. This was based on the method of Sacks for light scattering [10] but converted to an index [15], using the spread in azimuthal angle of, typically, the sixth order peak at approximately 0.055–0.059 Å^{-1}. This peak was selected as it is one of the most intense diffraction peaks. The peak area is measured, above a fitted baseline, at each azimuthal angle.

Fibril diameters were calculated from the SAXS data using the Irena software package [36] running within Igor Pro. The data were fitted at the wave vector, Q, in the range of 0.01–0.04 Å^{-1} and at an azimuthal angle which was 90° to the long axis of most of the collagen fibrils. This angle was selected by determining the average orientation of the collagen fibrils from the azimuthal angle for the maximum intensity of the D-spacing diffraction peaks. The "cylinderAR" shape model with an arbitrary aspect ratio of 30 was used for all fittings. We did not attempt to individually optimize this aspect ratio and the unbranched length of collagen fibrils may in practice have a length that exceeds an aspect ratio of 30.

3. Results

3.1. Histology. Pericardium stained with picrosirius red highlights differences in the inner and outer layers of the parietal pericardium with more pronounced and larger collagen fibres in the fibrous side of the tissue (Figure 3). Differences are apparent between adult and neonatal pericardium with the adult pericardium more clearly differentiated into two layers. The layer on the fibrous side showed a strongly differentiated collagen fibre structure compared with the parietal side of the adult pericardium. By comparison, the juvenile pericardium has less differentiation through its thickness.

3.2. Thickness. The average thickness was 0.36 ($\sigma = 0.03$) mm for adult pericardium and 0.12 ($\sigma = 0.006$) mm for neonatal pericardium. The neonatal is therefore one-third of the thickness of the adult.

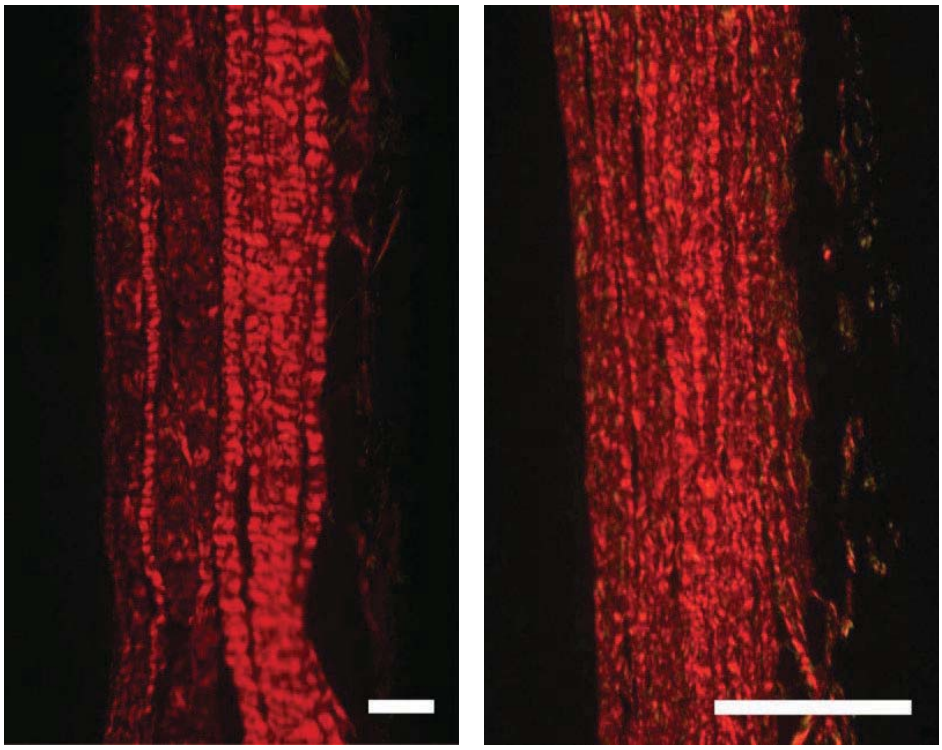

(a) (b)

Figure 3: Pericardium stained with picrosirius red and imaged through cross-polarized light to highlight collagen: (a) adult pericardium; (b) neonatal pericardium. The parietal side is toward the left and the fibrous side toward the right of each image. Scale bar is 0.1 mm.

Table 1: Mechanical properties of adult and neonatal glutaraldehyde fixed bovine pericardium.

Test	Adult ($n = 13$)†	Neonatal ($n = 11$)†	P†
Small strain (<0.2) elastic modulus (MPa)	4.8 (2.0)	71.9 (11.6)	<0.0001
Large strain (>0.2) elastic modulus (MPa)	33.5 (3.2)	83.7 (10.6)	<0.0001
Ultimate tensile strength (MPa)	19.1 (2.2)	32.9 (4.1)	0.0050
Strain at failure	0.80 (0.06)	0.48 (0.03)	0.0002

†Standard error () and P from two-tailed t-test comparison of adult and neonatal pericardium.

3.3. Mechanical Properties. The elastic modulus of glutaraldehyde fixed neonatal bovine pericardium at both small strain (<20%) and large strain is found to be very much greater than for glutaraldehyde fixed adult pericardium (Table 1).

The ultimate tensile strength is also greater for glutaraldehyde fixed neonatal pericardium than for adult pericardium (Table 1). The strength measured here (standard deviation in parentheses) of 19.1 ($\sigma = 2.2$) MPa for adult and 32.9 ($\sigma = 4.1$) MPa for neonatal pericardium is less than that reported previously for unfixed bovine pericardium of 25–29 MPa and of unfixed porcine pericardium of 22-23 MPa [37, 38] but greater than that reported in a different study for calf pericardium at 6–9 months of 11.5 ± 4.6 MPa [39]. We report the ultimate tensile strength as a modulus, that is, tissue property per cross-sectional area. The absolute strength of the glutaraldehyde treated adult pericardium is a little higher than the neonatal. However, it is noted that the neonatal pericardium is one-third of the thickness of adult pericardium. The strain at failure is much less for neonatal pericardium than for adult pericardium. This reflects the higher elastic modulus of the neonatal material compared with adult pericardium and high strength (Table 1).

The main objective of this work is to determine why the neonatal pericardium has a higher ultimate tensile strength and a higher tissue modulus. For this purpose the SAXS measurements were used to investigate the structures of these two materials.

3.4. SAXS Measurements. SAXS patterns of pericardium show clearly the diffraction from collagen fibrils. Two selected SAXS images are shown illustrating a nearly isotropic sample (Figure 4(a)) and a highly oriented sample (Figure 4(b)). The angular position of the bands or rings is due to the D-spacing of the collagen fibrils. The integrated intensity of such a pattern (Figure 5) enables the position of each peak of different order to be accurately measured.

Table 2: Orientation index (OI) for pericardium samples measured perpendicular and edge-on to the surface for samples cut vertically or horizontally from the pericardium.

Direction measured	Animal age	OI	Std deviation	No. of pericardia	No. of measurements
Perpendicular	Adult	0.020	0.096	10	42
Perpendicular	Neonatal	0.071	0.152	10	42
Edge-on vertical	Adult	0.581	0.051	2	52
Edge-on horizontal	Adult	0.669	0.032	2	27
Edge-on vertical	Neonatal	0.800	0.031	2	30
Edge-on horizontal	Neonatal	0.763	0.106	2	27

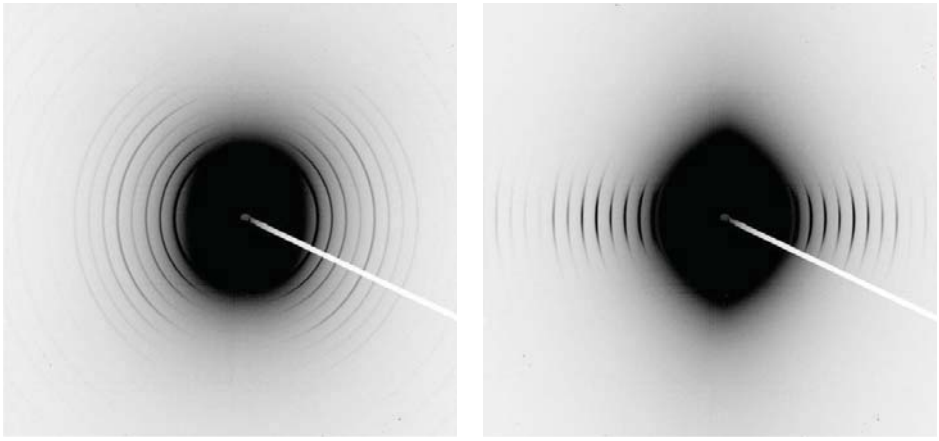

(a) (b)

Figure 4: SAXS spectra of pericardium. (a) A poorly oriented tissue; (b) a highly oriented tissue.

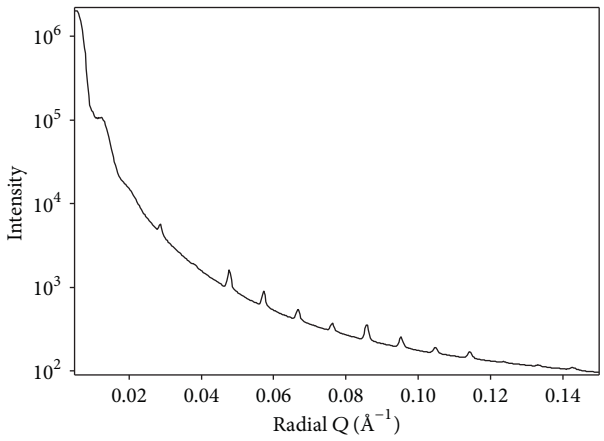

Figure 5: SAXS profile of an example bovine pericardium integrated around all azimuthal angles. The sharp peaks due to collagen D-spacing of various orders are visible (order 5 is just below 0.05 Å^{-1}, order 6 at just below 0.06 Å^{-1}, etc.).

To obtain a quantitative measure of the orientation of the fibrils, the variation in intensity of one of these collagen peaks is plotted as a function of azimuthal angle (Figure 6). It is the width of the peak centered at 180° that reflects the orientation index (OI).

3.5. Orientation. The collagen fibril OI measured perpendicular to the surface of the pericardium is very small, indicating a highly isotropic arrangement of fibrils in this direction. There is no statistical difference in alignment between adult tissue (OI = 0.020) and neonatal tissue (OI = 0.071) (t-statistic = 0.794, $P = 0.43$) (Table 2).

In contrast to the perpendicular measurements, edge on, the fibrils are more oriented and have a higher OI. The fibrils are therefore approximately in isotropic layers stacked one upon the other. However, there are marked differences between the neonatal and the adult pericardium tissues, and these differences are most noticeable in the degree with which these layers intertwine with each other.

Edge on, the adult pericardium tissue has a significantly lower OI than the neonatal tissue measured in both the vertical and the horizontal directions. Measured in the vertical direction, the adult has an OI of 0.581 ($\sigma = 0.051$) compared with the neonatal OI of 0.800 ($\sigma = 0.031$). These results are significantly different (t-statistic = 21.5, $P < 0.0001$). Measured in the horizontal direction, the OI of adult pericardium is 0.669 ($\sigma = 0.032$) and the OI of neonatal pericardium is 0.763 ($\sigma = 0.106$). This shows a significant difference between the two materials (t-statistic = 4.4, $P < 0.0001$). In other words, the fibrils in the neonatal tissue are significantly more aligned within the plane of the tissue than those in the adult tissues.

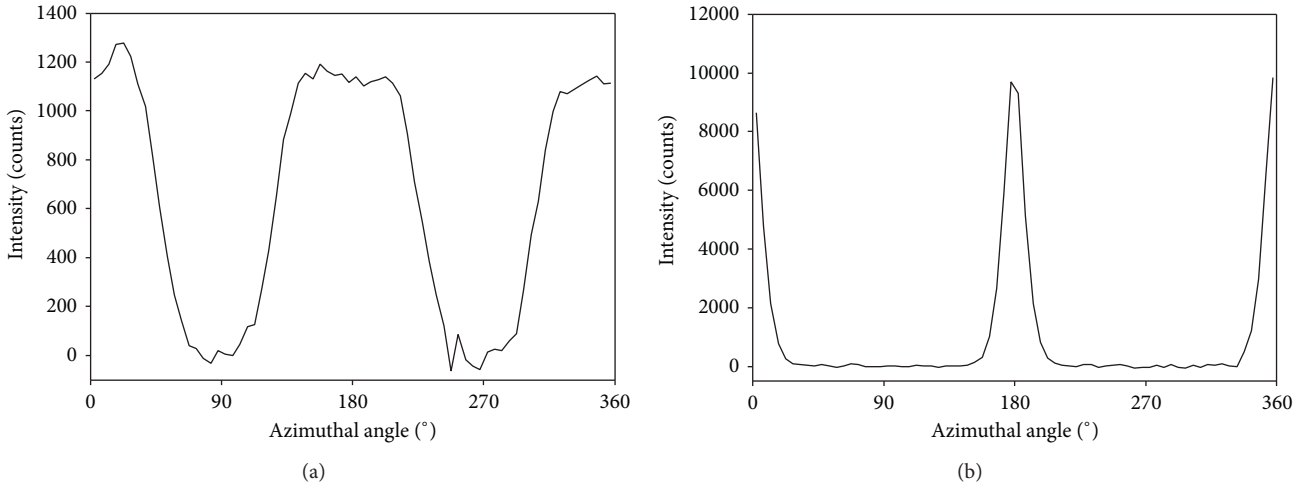

Figure 6: Plots of the intensity of a selected collagen peak at varying azimuthal angles for bovine pericardium samples. (a) A poorly aligned tissue; (b) a highly aligned tissue. The central peak at 180° (and other peaks at 0 and 360°) is the variation in intensity of collagen D-spacing whereas the lower peaks at 90° and 270° are due to the scattering from the thickness of the fibrils and fibril bundles.

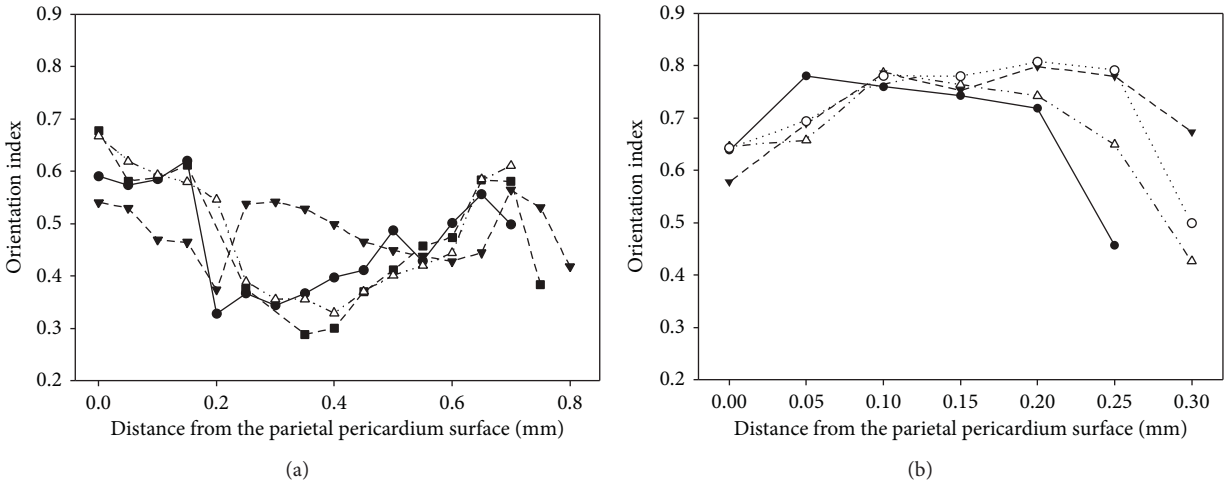

Figure 7: Variation of orientation index through the thickness of glutaraldehyde fixed pericardium: (a) adult; (b) neonatal. Each figure shows two profiles for each of the two samples.

3.6. Fibril Diameter. No statistically significant difference was found in the collagen fibril diameter between neonatal and adult bovine pericardium. Fitting a cylinder model to the SAXS data the adult group ($n = 39$) gave a mean (with standard deviation) of 47.7 ($\sigma = 3.0$) nm while the neonatal group ($n = 39$) gave 48.4 ($\sigma = 4.5$) nm. Comparing the two sample sets there was no significant difference between the neonatal and the adult pericardium (t-statistic = −0.85, $P = 0.40$).

3.7. SAXS Cross-Sections. Pericardium tissue is known to vary throughout its thickness and variation in structure is visible in the histological sections (Figure 3). We have measured the variation in OI through cross-sections of glutaraldehyde fixed pericardium for neonatal and adult tissue.

The OI measured through the thickness of glutaraldehyde fixed pericardium does not show a general change from one side to the other (Figure 7). Ovine and bovine leather show a similar flat profile of OI with skin depth [15, 16]. The flat profile between the two halves of the pericardium is somewhat surprising here as the histology shows two distinct layers. The variability in OI across the sample appears to be larger for the adult than for the neonatal tissue. We propose that highly aligned collagen fibrils are responsible for high strength and that varied alignment spreads weakness through the thickness of a material. Variability in alignment in the adult pericardium is thus expected to lower the tensile strength of the adult pericardium.

4. Discussion

Adult and neonatal glutaraldehyde fixed pericardium are both useful for constructing bioprosthetic heart valves.

However, there are clear differences to be found between the collagen structures in these tissues of different age. These differences are reflected in the orientation of the fibrils.

There was a significant difference observed in the OI between neonatal and adult bovine glutaraldehyde fixed pericardium. For tissue measured edge on, there is a higher OI in the neonatal pericardium than in the adult pericardium. This indicates that collagen fibrils are more aligned in the plane of the tissue in the neonatal pericardium. It is in this direction that the main stresses are applied to pericardium under the elastic deformation during normal heart function. Recent studies of human skin reported a difference in SAXS patterns of young and aged skin (no ages given). The intensity of the collagen diffraction peaks and level of anisotropy were both reported to vary. The aged skin has more intense diffraction peaks and is less anisotropic; that is, it has a lower OI [40], showing a preferential fibril orientation in young individuals that is lost with age. These measurements were taken perpendicularly to the skin. The data presented here for bovine pericardium also shows less anisotropy in the older pericardium. However, this difference is most apparent in the edge-on measurements rather than the perpendicular ones.

It might be expected that the maximum strength of a tissue composed of collagen would be along the direction in which the collagen fibrils are arranged. Thus, when the collagen is more aligned in the direction in which force is applied the tissue will be stronger. A correlation which supports this concept has been observed for ovine and bovine skin of varying strengths and skin from a range of mammals. In those studies, a higher OI (in the plane of the tissue, but not normal to the plane) was correlated with higher tear strength [15, 17]. Therefore the higher OI in edge-on measurements of neonatal pericardium should indicate improved tear strength of this tissue in comparison with adult pericardium. This is indeed observed in tensile testing of neonatal and adult bovine pericardium. Neonatal pericardium demonstrated a markedly higher modulus of elasticity and a higher tensile strength than adult pericardium [19].

Extending and supporting this concept further, myxomatous and healthy mitral valve leaflets from dogs have been reported to have different degrees of fibril orientation. Myxomatous tissue was found to become less aligned [41] which is a possible contributor to the diminished mechanical performance of this tissue although other changes are present too.

Measured perpendicularly, the OI for both adult and neonatal tissue is very low. The tissues are therefore rather isotropic measured from this direction. This is a very useful property as it may enable material to be cut in any direction from the pericardium for use in heart valve leaflets with minimal differences in mechanical performance.

We believe that the greater alignment in the plane of the tissue is the structural basis for the superior mechanical performance of glutaraldehyde fixed neonatal bovine pericardium. A relationship between fibre alignment and tensile strength has been modelled previously. Strength was found to be due to the sum of the components of the fibrils that lie in the direction of force in addition to a component due to the other matrix materials [42]. This model has been applied to just the measured fibrous collagen, neglecting the contribution from other matrix components. A model orientation index is derived which we will call OI' to distinguish it from the experimentally measured OI [43, 44]:

$$\mathrm{OI}' = \frac{\int_0^{2\pi} \int_0^{\pi/2} \cos^4\theta F(\theta,\phi)\, d\theta\, d\phi}{\int_0^{2\pi} \int_0^{\pi/2} F(\theta,\phi)\, d\theta\, d\phi}, \quad (1)$$

where $F(\theta, \phi)$ is the angular distribution function where θ and ϕ are orthogonal. We have previously applied this model to collagen orientation in leather produced from the skins of a selection of mammals. It was found to be valid across a wide range of strengths, that is, greater than a factor of 5 [17].

Some of the apparent nonalignment of fibrils (resulting in a lower OI) could be due to crimp of the collagen fibrils and not only to the variation in whole fibril alignment. However we do not believe this is an important consideration in the materials studied. Crimp is observed in the light microscopy sections (Figure 3) and would contribute to a decrease in the OI in the direction of SAXS measurements taken edge on. In horse tendon crimp has been found to decrease with age [45], as does the tendon strength, and if there were no other changes to the alignment of collagen in the tendons, this would result in an increase in OI with age. This is the opposite of what is observed for the OI change between the neonatal and the adult pericardium. Another consideration which leads us to believe crimp is not an important factor in the measurements reported here is that crimp is generally believed to be associated with strength [46]. Therefore if the OI measured edge on was only due to crimp, this would suggest that the neonatal pericardium, which is stronger, has less crimp and this would contradict the accepted knowledge of the influence of crimp. However, if the differences in OI measured edge on between neonatal and adult pericardium are due to differences in alignment of the collagen fibrils, then this relationship would be in agreement with previous studies on skin (treated to produce leather) where a high degree of alignment is correlated with high strength (and crimp is not present) [15, 17].

We also do not know if these tissues of different age are affected differently by glutaraldehyde treatment. It has been observed that glutaraldehyde treatment lowers the OI of pericardium [47] and it is possible that the neonatal and adult pericardium are affected to a different extent. We are currently investigating this possibility.

We did not find that changes in fibril diameter are responsible for differences in strength between neonatal and adult pericardium. This is a little surprising, as fibril diameter is generally believed to affect strength in tendons and age can result in different fibril diameter with typically older tissue having thicker fibrils. However, in tendons the collagen fibrils are more highly aligned than pericardium so perhaps there is less variation in alignment in tendons and therefore factors other than alignment dominate strength differences. On the other hand, in pericardium (and leather) there is the possibility of significant variation in alignment and therefore

alignment may be able to dominate the strength-structure relationship with fibril diameter being a less important factor [29].

The glutaraldehyde treated adult material had a greater modulus of elasticity and greater ultimate tensile strength than the glutaraldehyde treated neonatal material, while the neonatal material was significantly thinner. This suggests that there may be an advantage in the use of this material in applications such as heart valve leaflets for percutaneous delivery. A thinner tissue is able to be folded to be inserted in a much smaller sized catheter for aortic valve replacement. By using the thinner, but sufficiently strong, neonatal bovine pericardium, it could be possible to reduce the catheter diameter required for the insertion of the folded valve. This is an important consideration for many patients needing such intervention [20, 33].

What we have not determined is the relationship between the collagen fibril alignments in the glutaraldehyde fixed material and in the native material. Treatment of native tissue results in differences in strength, as shown here and elsewhere [48]. Cross-linking of the collagen fibrils might be expected to have an effect on fibril alignment because the cross-linking would place physical constraints on the fibrils. Therefore variation in the degree to which cross-linking takes place in different tissues might result in a variable change in alignment. This is the subject of a study we are currently undertaking.

5. Conclusions

We have shown that glutaraldehyde fixed neonatal pericardium has higher elastic modulus and ultimate tensile strength than adult pericardium. We found, using SAXS, that there are clear differences in the structure of collagen between neonatal and adult bovine pericardium. The alignment of the collagen in the plane of the tissue is greater in the neonatal pericardium. We have described how this gives a structural understanding of the superior mechanical properties of that material. These findings provide a basis for the potential advantages to using neonatal rather than adult bovine pericardium in heterografts.

Conflict of Interests

The authors declare that there is no conflict of interests regarding the publication of this paper.

Acknowledgments

This research was undertaken on the SAXS/WAXS beamline at the Australian Synchrotron, Victoria, Australia. The NZ Synchrotron Group Ltd. is acknowledged for travel funding. Melissa Basil-Jones of Massey University assisted with data collection. Saroja Gurazada of Southern Lights Biomaterials assisted with the pericardium preparation. Sue Hallas of Nelson assisted with editing the paper.

References

[1] N. Nwaejike and R. Ascione, "Mitral valve repair for disruptive acute endocarditis: extensive replacement of posterior leaflet with bovine pericardium," *Journal of Cardiac Surgery*, vol. 26, no. 1, pp. 31–33, 2011.

[2] J. M. García Páez, A. Carrera Sanmartín, E. Jorge Herrero et al., "Durability of a cardiac valve leaflet made of calf pericardium: fatigue and energy consumption," *Journal of Biomedical Materials Research A*, vol. 77, no. 4, pp. 839–849, 2006.

[3] A. Cribier, H. Eltchaninoff, C. Tron et al., "Percutaneous artificial cardiac valves: From animal experimentation to the first human implantation in a case of calcified aortic stenosis," *Archives des Maladies du Coeur et des Vaisseaux*, vol. 96, no. 6, pp. 645–652, 2003.

[4] A. Mirnajafi, B. Zubiate, and M. S. Sacks, "Effects of cyclic flexural fatigue on porcine bioprosthetic heart valve heterograft biomaterials," *Journal of Biomedical Materials Research A*, vol. 94, no. 1, pp. 205–213, 2010.

[5] J. Liao, L. Yang, J. Grashow, and M. S. Sacks, "Molecular orientation of collagen in intact planar connective tissues under biaxial stretch," *Acta Biomaterialia*, vol. 1, no. 1, pp. 45–54, 2005.

[6] P. P. Purslow, T. J. Wess, and D. W. L. Hukins, "Collagen orientation and molecular spacing during creep and stress-relaxation in soft connective tissues," *Journal of Experimental Biology*, vol. 201, no. 1, pp. 135–142, 1998.

[7] M. M. Basil-Jones, R. L. Edmonds, T. F. Allsop et al., "Leather structure determination by small-angle X-ray scattering (SAXS): cross sections of ovine and bovine leather," *Journal of Agricultural and Food Chemistry*, vol. 58, no. 9, pp. 5286–5291, 2010.

[8] P. Julkunen, J. Iivarinen, P. A. Brama, J. Arokoski, J. S. Jurvelin, and H. J. Helminen, "Maturation of collagen fibril network structure in tibial and femoral cartilage of rabbits," *Osteoarthritis and Cartilage*, vol. 18, no. 3, pp. 406–415, 2010.

[9] A. L. Schofield, C. I. Smith, V. R. Kearns et al., "The use of reflection anisotropy spectroscopy to assess the alignment of collagen," *Journal of Physics D: Applied Physics*, vol. 44, Article ID 335302, 2011.

[10] M. S. Sacks, D. B. Smith, and E. D. Hiester, "A small angle light scattering device for planar connective tissue microstructural analysis," *Annals of Biomedical Engineering*, vol. 25, no. 4, pp. 678–689, 1997.

[11] J. W. Y. Jor, P. M. F. Nielsen, M. P. Nash, and P. J. Hunter, "Modelling collagen fibre orientation in porcine skin based upon confocal laser scanning microscopy," *Skin Research and Technology*, vol. 17, no. 2, pp. 149–159, 2011.

[12] G. Falgayrac, S. Facq, G. Leroy, B. Cortet, and G. Penel, "New method for raman investigation of the orientation of collagen fibrils and crystallites in the haversian system of bone," *Applied Spectroscopy*, vol. 64, no. 7, pp. 775–780, 2010.

[13] M. Janko, P. Davydovskaya, M. Bauer, A. Zink, and R. W. Stark, "Anisotropic Raman scattering in collagen bundles," *Optics Letters*, vol. 35, no. 16, pp. 2765–2767, 2010.

[14] P. Fratzl and R. Weinkamer, "Nature's hierarchical materials," *Progress in Materials Science*, vol. 52, no. 8, pp. 1263–1334, 2007.

[15] M. M. Basil-Jones, R. L. Edmonds, S. M. Cooper, and R. G. Haverkamp, "Collagen fibril orientation in ovine and bovine leather affects strength: a small angle X-ray scattering (SAXS) study," *Journal of Agricultural and Food Chemistry*, vol. 59, no. 18, pp. 9972–9979, 2011.

[16] M. M. Basil-Jones, R. L. Edmonds, G. E. Norris, and R. G. Haverkamp, "Collagen fibril alignment and deformation during tensile strain of leather: a small-angle X-ray scattering study," *Journal of Agricultural and Food Chemistry*, vol. 60, no. 5, pp. 1201–1208, 2012.

[17] K. H. Sizeland, M. M. Basil-Jones, R. L. Edmonds et al., "Collagen orientation and leather strength for selected mammals," *Journal of Agricultural and Food Chemistry*, vol. 61, no. 4, pp. 887–892, 2013.

[18] A. Mirnajafi, J. Raymer, M. J. Scott, and M. S. Sacks, "The effects of collagen fiber orientation on the flexural properties of pericardial heterograft biomaterials," *Biomaterials*, vol. 26, no. 7, pp. 795–804, 2005.

[19] C. M. Cunanan, J. J. Higgins, and S. N. Gurazada, "Biomaterials with enhanced properties and devices made therefrom," US Patent Application No. 2012059487, 2012.

[20] K. Kroger, C. Buss, M. Goyen, F. Santosa, and G. Rudofsky, "Diameter of occluded superficial femoral arteries limits percutaneous recanalization: preliminary results," *Journal of Endovascular Therapy*, vol. 9, no. 3, pp. 369–374, 2002.

[21] T. L. Willett, R. S. Labow, I. G. Aldous, N. C. Avery, and J. M. Lee, "Changes in collagen with aging maintain molecular stability after overload: evidence from an in vitro tendon model," *Journal of Biomechanical Engineering*, vol. 132, no. 3, 8 pages, 2010.

[22] A. J. Bailey, "Molecular mechanisms of ageing in connective tissues," *Mechanisms of Ageing and Development*, vol. 122, no. 7, pp. 735–755, 2001.

[23] M. E. Francis-Sedlak, S. Uriel, J. C. Larson, H. P. Greisler, D. C. Venerus, and E. M. Brey, "Characterization of type I collagen gels modified by glycation," *Biomaterials*, vol. 30, no. 9, pp. 1851–1856, 2009.

[24] D. J. Leeming, K. Henriksen, I. Byrjalsen et al., "Is bone quality associated with collagen age?" *Osteoporosis International*, vol. 20, no. 9, pp. 1461–1470, 2009.

[25] B. M. Sicari, S. A. Johnson, B. F. Siu et al., "The effect of source animal age upon the in vivo remodeling characteristics of an extracellular matrix scaffold," *Biomaterials*, vol. 33, no. 22, pp. 5524–5533, 2012.

[26] A. Balguid, N. J. B. Driessen, A. Mol et al., "Stress related collagen ultrastructure in human aortic valves-implications for tissue engineering," *Journal of Biomechanics*, vol. 41, no. 12, pp. 2612–2617, 2008.

[27] H. Michna, "Morphometric analysis of loading-induced changes in collagen- fibril populations in young tendons," *Cell and Tissue Research*, vol. 236, no. 2, pp. 465–470, 1984.

[28] A. Biancalana, L. Veloso, and L. Gomes, "Obesity affects collagen fibril diameter and mechanical properties of tendons in Zucker rats," *Connective Tissue Research*, vol. 51, no. 3, pp. 171–178, 2010.

[29] H. C. Wells, R. L. Edmonds, N. Kirby, A. Hawley, S. T. Mudie, and R. G. Haverkamp, "Collagen fibril diameter and leather strength," *Journal of Agricultural and Food Chemistry*, vol. 61, no. 47, pp. 11524–11531, 2013.

[30] D. A. D. Parry, G. R. G. Barnes, and A. S. Craig, "A comparison of the size distribution of collagen fibrils in connective tissues as a function of age and a possible relation between fibril size distribution and mechanical properties," *Proceedings of the Royal Society of London—Biological Sciences*, vol. 203, no. 1152, pp. 305–321, 1978.

[31] J. C. Patterson-Kane, A. M. Wilson, E. C. Firth, D. A. D. Parry, and A. E. Goodship, "Comparison of collagen fibril populations in the superficial digital flexor tendons of exercised and nonexercised Thoroughbreds," *Equine Veterinary Journal*, vol. 29, no. 2, pp. 121–125, 1997.

[32] W. Cherdchutham, C. K. Becker, E. R. Spek, W. E. Voorhout, and P. R. Van Weeren, "Effects of exercise on the diameter of collagen fibrils in the central core and periphery of the superficial digital flexor tendon in foals," *American Journal of Veterinary Research*, vol. 62, no. 10, pp. 1563–1570, 2001.

[33] P. T. L. Chiam and C. E. Ruiz, "Percutaneous transcatheter aortic valve implantation: assessing results, judging outcomes, and planning trials. the interventionalist perspective," *JACC Cardiovascular Interventions*, vol. 1, no. 4, pp. 341–350, 2008.

[34] V. S. Constantine and R. W. Mowry, "Selective staining of human dermal collagen, II: the use of picrosirius red F3BA with polarization microscopy," *Journal of Investigative Dermatology*, vol. 50, no. 5, pp. 419–423, 1968.

[35] D. Cookson, N. Kirby, R. Knott, M. Lee, and D. Schultz, "Strategies for data collection and calibration with a pinhole-geometry SAXS instrument on a synchrotron beamline," *Journal of Synchrotron Radiation*, vol. 13, no. 6, pp. 440–444, 2006.

[36] J. Ilavsky and P. R. Jemian, "Irena: tool suite for modeling and analysis of small-angle scattering," *Journal of Applied Crystallography*, vol. 42, no. 2, pp. 347–353, 2009.

[37] J. M. G. Páez, E. Jorge, A. Rocha et al., "Mechanical effects of increases in the load applied in uniaxial and biaxial tensile testing. Part II. Porcine pericardium," *Journal of Materials Science: Materials in Medicine*, vol. 13, no. 5, pp. 477–483, 2002.

[38] J. M. García Páez, E. Jorge, A. Rocha et al., "Mechanical effects of increases in the load applied in uniaxial and biaxial tensile testing: part I. Calf pericardium," *Journal of Materials Science: Materials in Medicine*, vol. 13, no. 4, pp. 381–388, 2002.

[39] M. M. Maestro, J. Turnay, N. Olmo et al., "Biochemical and mechanical behavior of ostrich pericardium as a new biomaterial," *Acta Biomaterialia*, vol. 2, no. 2, pp. 213–219, 2006.

[40] M. Cócera, G. Rodríguez, L. Rubio et al., "Characterisation of skin states by non-crystalline diffraction," *Soft Matter*, vol. 7, no. 18, pp. 8605–8611, 2011.

[41] M. Hadian, B. M. Corcoran, R. I. Han, J. G. Grossmann, and J. P. Bradshaw, "Collagen organization in canine myxomatous mitral valve disease: an X-ray diffraction study," *Biophysical Journal*, vol. 93, no. 7, pp. 2472–2476, 2007.

[42] A. Bigi, A. Ripamonti, N. Roveri, G. Jeronimidis, and P. P. Purslow, "Collagen orientation by X-ray pole figures and mechanical properties of media carotid wall," *Journal of Materials Science*, vol. 16, no. 9, pp. 2557–2562, 1981.

[43] P. L. Kronick and M. S. Sacks, "Quantification of vertical-fiber defect in cattle hide by small-angle light scattering.," *Connective Tissue Research*, vol. 27, no. 1, pp. 1–13, 1991.

[44] P. L. Kronick and P. R. Buechler, "Fiber orientation in calfskin by laser-light scattering or X-ray-diffraction and quantitative relation to mechanical-properties," *Journal of the American Leather Chemists Association*, vol. 81, no. 7, pp. 221–230, 1986.

[45] J. C. Patterson-Kane, E. C. Firth, A. E. Goodship, and D. A. D. Parry, "Age-related differences in collagen crimp patterns in the superficial digital flexor tendon core region of untrained horses," *Australian Veterinary Journal*, vol. 75, no. 1, pp. 39–44, 1997.

[46] J. M. Caves, V. A. Kumar, W. Xu, N. Naik, M. G. Allen, and E. L. Chaikof, "Microcrimped collagen fiber-elastin composites," *Advanced Materials*, vol. 22, no. 18, pp. 2041–2044, 2010.

[47] J. M. Lee, S. A. Haberer, and D. R. Boughner, "The bovine pericardial xenograft: I. Effect of fixation in aldehydes without constraint on the tensile viscoelastic properties of bovine pericardium," *Journal of Biomedical Materials Research*, vol. 23, no. 5, pp. 457–475, 1989.

[48] D. O. Freytes, S. F. Badylak, T. J. Webster, L. A. Geddes, and A. E. Rundell, "Biaxial strength of multilaminated extracellular matrix scaffolds," *Biomaterials*, vol. 25, no. 12, pp. 2353–2361, 2004.

Leather nanostructure and performance

Katie H. Sizeland[1], Hannah C. Wells[1], Melissa M. Basil-Jones[1], Richard L. Edmonds[2], Richard G. Haverkamp[1*]

[1]School of Engineering and Advanced Technology, Massey University, Palmerston North, New Zealand; [2]Leather and Shoe Research Association, Palmerston North, New Zealand. *r.haverkamp@massey.ac.nz

One of the very important properties of leather is its mechanical robustness, including the tensile strength, tear resistance and flexibility. If one had a deep understanding of how this natural material achieves these properties, it might be possible to modify and improve aspects of the mechanical performance of leather. Here we describe how we have used some of the most sophisticated tools and techniques available to learn more about the structure of leather at the nanoscale and to relate this structure to the physical properties of leather.

Richard Haverkamp, School of Engineering and Advanced Technology, Massey University

Leather composition

Finished leather is primarily composed of type I collagen but also contains a myriad of other components in smaller quantities such as fats or oils, other proteins such as elastin, and crosslinking agents such as tannins or chrome. Each of these components may make some contribution to the physical properties of the leather. Because the major component of leather is type I collagen, we have focused first on its structure and have investigated how the fibrils of collagen are arranged in leather. We have studied how this arrangement varies among leather that has different physical properties and in leather when it is strained.

Structural analysis of leather via synchrotron based SAXS

The technique we have employed to quantify the collagen structure at the nanoscale is small angle X-ray scattering (SAXS). This technique was invented in the late 1930s. However, only recently has the technique been able to provide the sort of precise and detailed information that is useful for understanding leather structure. This has been possible with the advent of synchrotron-based SAXS. Synchrotrons are large and expensive facilities that cater for a wide range of scientific studies. At the heart of the synchrotron is a ring, typically over 100 metres in diameter (Figure 1), with a stainless steel pipe pumped free of air inside. Bundles of high-energy electrons, contained by a series of magnets (figure 2), circulate inside the ring at close to the speed of light. This travelling bundle of electrons is the source of X-rays of whatever energy you require or of other electromagnetic radiation such as UV, visible light or infrared radiation. For SAXS we use X-rays. To create the X-rays a device called an undulator is placed at one point on the ring. This causes the electrons that pass through to change direction, producing X-rays. These X-rays are directed to the SAXS analysis equipment contained in a radiation-proof hutch where samples to be investigated are placed (Figure 3). The X-ray beam can be tightly focused (0.15 x 0.08mm) and is fired through the piece of leather to be analysed. Most of the X-rays pass straight through but some X-rays are scattered by the structure of the collagen. It is these scattered X-rays that are collected by a detector and the position of these X-rays provides a wealth of information on the dimensions, arrangement and other features of collagen fibrils in the leather.

Figure 1. The Australian Synchrotron, like most synchrotrons, is housed in a round building because the electrons travel in a ring with a large diameter

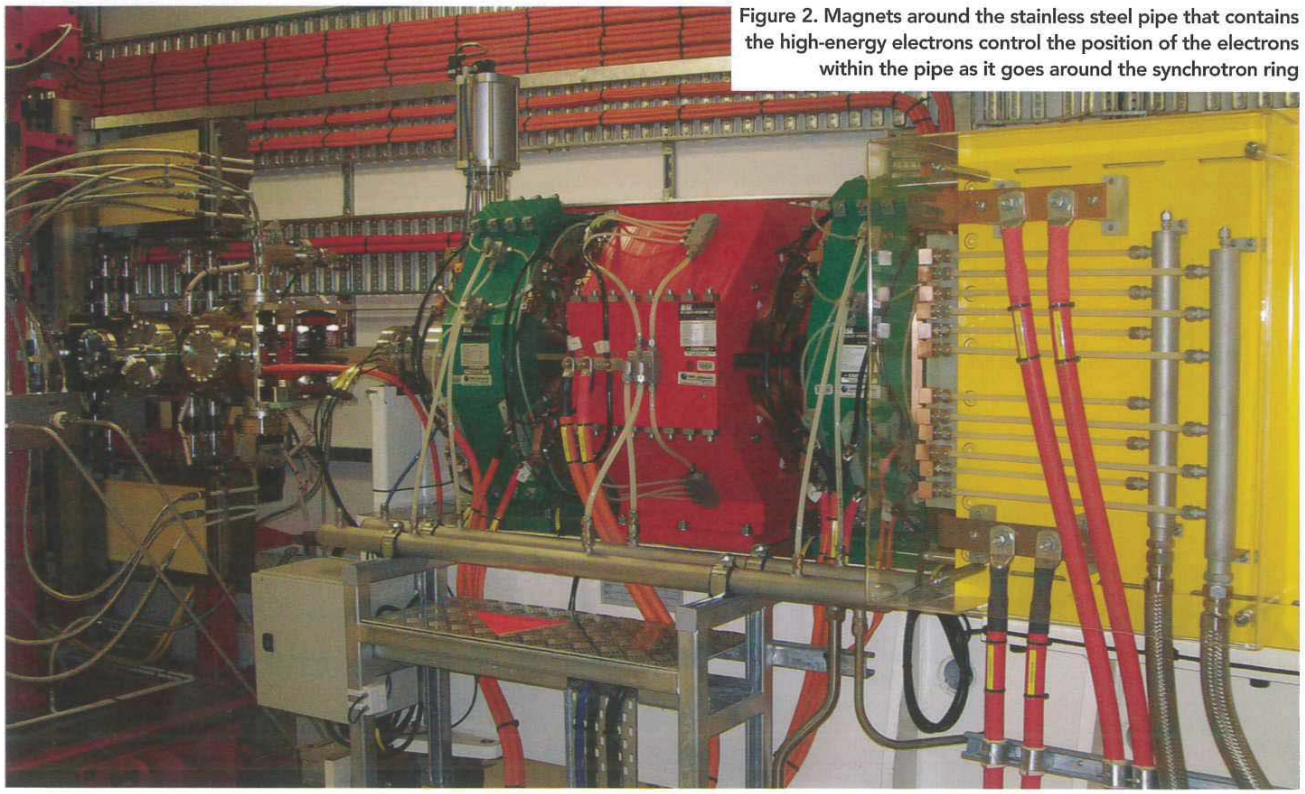

Figure 2. Magnets around the stainless steel pipe that contains the high-energy electrons control the position of the electrons within the pipe as it goes around the synchrotron ring

What we can measure

From SAXS analysis of leather we have been able to extract four useful categories of information on the collagen structure. These are: 1) the average orientation of the collagen fibrils (which direction they are aligned in); 2) the spread of orientation of the fibrils (are they anisotropic or isotropic); 3) an accurate measure of the d-banding in the collagen (and this can tell us about the stress experienced by individual fibrils); and 4) the diameter of the collagen fibrils. Leather is of course a three-dimensional material so measures of orientation can be in three orthogonal directions. By correlating some of these properties with mechanical tests of leather we can infer how changes in the structure of the collagen may affect the mechanical properties.

Collagen fibril orientation and tear strength

We looked at the variety of collagen structural factors we could measure and compared them with tear strength of leather to see if any were correlated. We did find a strong correlation in one of these. The tear strength for leather samples from about 600 ovine and bovine skins or hides (taken from the official sampling position) were measured using standard test methods. The collagen fibril orientations for these samples were measured using SAXS. We can quantify the collagen fibril orientation using an orientation index (OI) where an OI of 1 represents all fibrils are perfectly aligned (anisotropic) whereas an OI of 0 signifies a fully isotropic arrangement[1]. We found that there is a statistically very robust correlation between the tear strength and the fibril alignment in the direction edge on to the leather[2] (Figure 4a). Measured flat on (ie. normal to the leather surface) there is not a strong correlation, it is only the edge on measurements that relate to tear strength. This correlation was also seen for a number of other mammals across a wider tear strength range[3] (Figure 4b). (Note that for the other mammals the figures do not necessarily represent average strength values for the species, but only for the samples we used.) In other words, when the collagen is aligned in parallel planes the result is stronger leather. We have described a model to explain this relationship[3].

What happens to the fibrils when leather is stretched?

It is possible with synchrotron-based SAXS to measure the changes in the structure of the collagen fibrils in leather as a piece of leather is stretched. We built a stretching apparatus to measure the stress-strain on pieces of leather while simultaneously recording SAXS patterns. We found that when leather is stretched the first thing that happens is the fibrils begin to become more aligned in the direction of the applied force (this can be seen by an increase reduction in the OI). After about 15% extension, not much further alignment takes place but instead the individual collagen fibrils start to stretch (with little more alignment taking place)[4]. We can see the stretching because the change in d-spacing of collagen, which is obtained from the SAXS, provides a measure of the force experienced by individual fibrils.

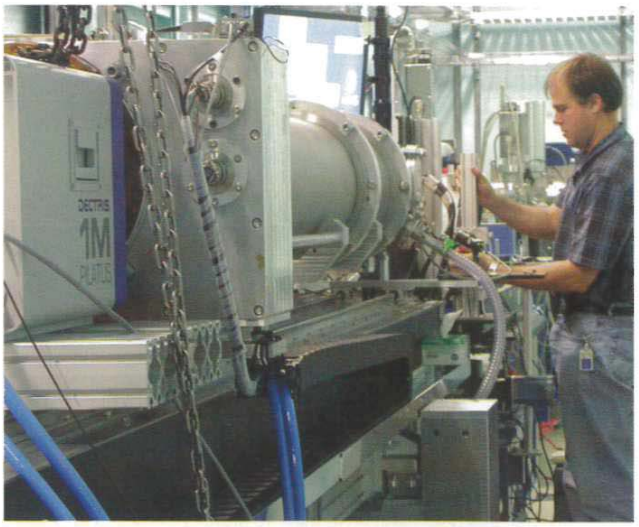

Figure 3. Mounting leather samples for analysis inside the SAXS hutch at the Australian Synchrotron

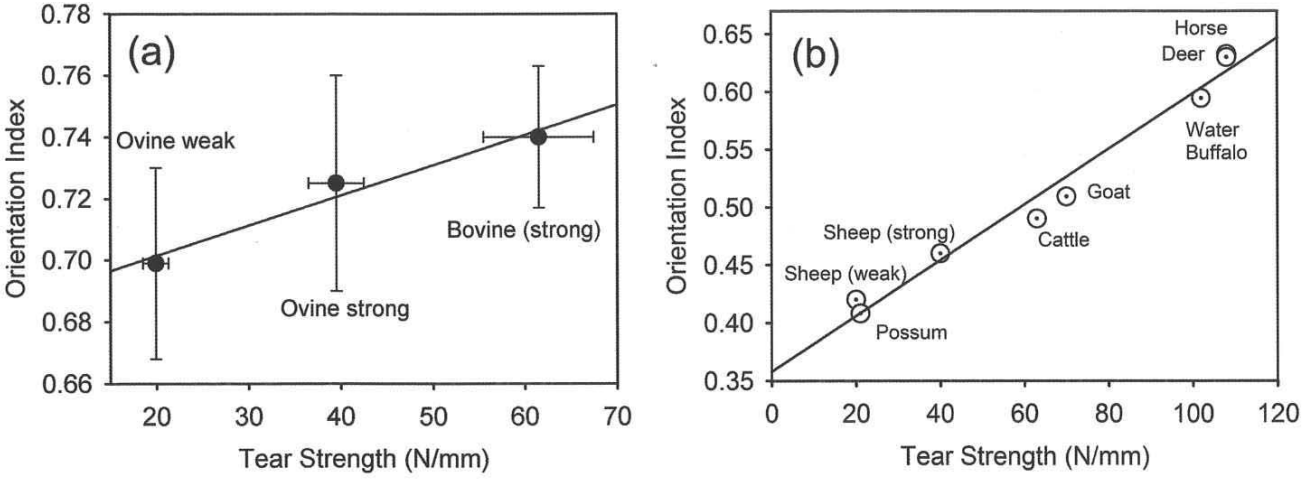

Figure 4. Leather tear strength and collagen fibril orientation. The orientation is measured edge on to the leather: a) Ovine and bovine leather (each point represents the analysis of samples from many skins); b) Other mammals (each point, excluding sheep weak, sheep strong and cattle, represents a sample from one skin). © American Chemical Society. Figure (a) from J. Agric. Food Chem. 59 (18), 9972-9979 (2011); Figure (b) from J Agric Food Chem 61 (4) 887-892 (2013)

Differences through the thickness

We also looked at how the arrangement and structure of collagen fibrils in leather varies through the grain and the corium, both in a relaxed state and when under stress. The fibril orientation changes through the thickness of leather, as one would expect. We also found there are significant differences between bovine and ovine leather and especially between strong ovine leather and weak ovine leather. When strong leather is stretched, the tension is taken up by the fibrils through most of the thickness of the leather (which we can see from the d-spacing natural internal stress gauge), whereas when weak ovine leather is stretched the force is taken up unevenly. Hence it is not surprising that the leather with an uneven load distribution breaks at a lower force.

Fibril diameter and tear strength

There had been some suggestions for materials, such as tendon, that suggested fibril diameter is also important for strength, with larger diameter collagen fibrils resulting in material with higher strength. We have also looked at this using SAXS to measure the fibril diameter and we did find a correlation for bovine leather; however, it was only a weak correlation, and we did not find one for ovine leather[5].

Conclusion

We hope that these fundamental investigations into collagen will ultimately be useful to the craft of leather making. If we understand how the arrangement of collagen differs in different leathers, how collagen behaves under stress, and what chemical processing does to the structure of collagen we may have the ability to control and manipulate these changes to produce improved or more consistent leather products.

Acknowledgements

Major sponsors of this work are the New Zealand Government, Ministry for Business Innovation and Employment (MBIE). This research was undertaken on the SAXS/WAXS beamline at the Australian Synchrotron, Victoria, Australia. The work was assisted by Dr Nigel Kirby, Dr Adrian Hawley and Dr Stephen Mudie of the Australian Synchrotron. The NZ Synchrotron Group Ltd is acknowledged for travel funding. ▫

“ If we understand how the arrangement of collagen differs in different leathers, how collagen behaves under stress, and what chemical processing does to the structure of collagen we may have the ability to control and manipulate these changes to produce improved or more consistent leather products.

Other aspects of leather structure and strength

There are many other aspects of leather structure and processing we can investigate with these techniques. We are now looking into changes to leather structure during processing. For example, when fatliquor is added to leather, what effect does it have on leather structure and how does it lubricate the fibres? How are the dynamics of leather stretching changed by the addition of fatliquor? We have discovered some interesting things and this work will shortly be submitted to the academic literature. What about the changes that take place in the processing of hide or skins to leather through each step of the conventional leather making process? It would be interesting to understand how each of these steps alters the collagen fibril arrangement and structure and why. We have nearly completed this work and are preparing a contribution for publication.

We have also looked in more detail at what happens to collagen fibrils during stretching – how much thinner they get when they are stretched – and what implications this might have for the properties of the materials they form.

Reference: 1. Basil-Jones, M. M.; Edmonds, R. L.; Allsop, T. F.; Cooper, S. M.; Holmes, G.; Norris, G. E.; Cookson, D. J.; Kirby, N.; Haverkamp, R. G., Leather structure determination by small angle X-ray scattering (SAXS): Cross sections of ovine and bovine leather. J. Agric. Food Chem. 2010, 58, 5286-5291.
2. Basil-Jones, M. M.; Edmonds, R. L.; Cooper, S. M.; Haverkamp, R. G., Collagen fibril orientation in ovine and bovine leather affects strength: A small angle X-ray scattering (SAXS) study. J. Agric. Food Chem. 2011, 59, 9972-9979.
3. Sizeland, K. H.; Haverkamp, R. G.; Basil-Jones, M. M.; Edmonds, R. L.; Cooper, S. M.; Kirby, N.; Hawley, A., Collagen Alignment and Leather Strength for Selected Mammals. J. Agric. Food Chem. 2013, 61, 887-892.
4. Basil-Jones, M. M.; Edmonds, R. L.; Norris, G. E.; Haverkamp, R. G., Collagen fibril alignment and deformation during tensile strain of leather: A SAXS study. J. Agric. Food Chem. 2012, 60, 1201-1208.
5. Wells, H. C.; Edmonds, R. L.; Kirby, N.; Hawley, A.; Mudie, S. T.; Haverkamp, R. G., Collagen Fibril Diameter and Leather Strength. J. Agric. Food Chem. 2013, 61, 11524-11531.

Collagen D-spacing and the Effect of Fat Liquor Addition

by

K. H. Sizeland,[a] H.C. Wells,[a] G. E. Norris,[a] R. L. Edmonds,[c] N. Kirby,[d] A. Hawley,[d] S. T. Mudie and R. G. Haverkamp[a]*

[a]*School of Engineering and Advanced Technology, and*

[b]*Institute of Fundamental Science, Massey University,*

Private Bag 11222, Palmerston North 4442, New Zealand

[c]*Leather and Shoe Research Association,*

PO Box 8094, Palmerston North 4446, New Zealand

[d]*Australian Synchrotron,*

800 Blackburn Road, Clayton, VIC 3168, Australia

Abstract

The physical properties of leather are partly a result of the structure of the leather's network of type I collagen fibrils. To achieve high strength and a soft, supple feel, penetrating oils (usually polyols) are added to leather during manufacture, and this process is known as fat liquoring. The modification of the collagen structure by fat liquoring (with a lanolin-based fat liquor) is investigated using synchrotron-based small angle X-ray scattering. The axial periodicity, or D-spacing, of the collagen changes as a result of fat liquoring. With no fat liquor, the D-spacing is 60.2 nm; spacing increases by 6% to 63.6 nm at 10% fat liquor. Pure lanolin results in a similar increase in D-spacing. We discuss mechanisms for fibril elongation brought about by fat liquoring. The observations of structural changes taking place within collagen fibrils as a result of fat liquoring provides new insight into the nature of fat liquoring and informs future processing developments.

Introduction

Leather is a strong, flexible, complex biomaterial mainly consisting of fibrous type I collagen. Leather is used in a wide variety of manufacturing applications where the physical properties exhibited by the material are important for both strength and aesthetic reasons. The physical attributes of leather are largely dependent on the structure of collagen fibers and the interactions among them.[1-5] Because leather is processed animal skin, the collagen fiber structure of leather is derived from that of living skin and some other tissues. It is also similar to some collagen-based medical scaffolds.[6] Fibrous type I collagen accounts for most of leather's complex architecture.

A collagen fibril contains multiple levels of structure. The collagen molecule is characterized by the repeating amino acid sequence $(Glycine\text{-}X\text{-}Y)^n$. Each polypeptide chain forms an alpha helix with a left handed twist, then three of these left handed helices twist together in a right hand manner to form a triple helix, or tropocollagen. Hydrogen bonds between amino acid side chains and collagen molecule main chains and those mediated through water bridges are the main stabilizing force of the tropocollagen quaternary structure.[7] Interchain water bridges are intrinsically linked to the hydroxyprolines in the sequence so that high hydroxyproline content will increase the stability of the triple helix.[8] In fact, water can be regarded as forming a clathrate–like structure around each triple helix and it has a role in maintaining fibril assembly.[7,9,10] Collagen fibrils are assembled from multiples of five staggered tropocollagens. Gaps between the end of one tropocollagen and the next result in regions with only 4/5 tropocollagen molecules present. This structure is responsible for the banding of collagen that is visible with atomic force microscopy or transmitting electron microscopy and is the origin of the Bragg diffraction peaks. This spacing is known as the D-spacing and can be measured. Within each fibril, the tropocollagen molecules are held together by crosslinks between lysine and allolysine formed as a result of the action of an enzyme lysyl oxidase. The extensive, highly structured hydration shell around the collagen triple helices, along with water bridges between collagen fibrils, have been shown to be critical elements that maintain the macromolecular assemblies of collagen molecules.[7,11,12] While the secondary structure remains stable if the water molecules become unavailable to support the hydrogen-bonding network, the mechanical properties of collagen are affected.[13] Hydrophobic residues on the outside of the tropocollagen molecule have also been shown to play an important role in microfibrillar packing by both organizing water structure and through Van der Waals interactions.[14]

*Corresponding author e-mail: r.haverkamp@massey.ac.nz

Manuscript received September 12, 2014, accepted for publication November 12, 2014.

In terms of microstructure, leather comprises two distinct layers: the 'grain' and the 'corium'. These two layers have significantly different structures.[1,15] Fibril orientation and fibril diameter, particularly in the corium layer, have been shown to be an important factor in the strength of the material.[14-18] During the process of making leather, synthetic crosslinks are introduced that stabilize the molecular structure of the skin and contribute to its physical properties.[19-22]

The D-spacing for stronger ovine and bovine leather has been shown to decrease at the interface between the corium and the grain.[23] While changes in D-spacing have not been shown to correlate with strength in leather[4,16] and rat tail tendon,[24] D-spacing does vary with tissue types,[25] animal species,[16] age[26,27] and chemical treatment.[27,28] It is also possible to observe change in D-spacing when leather is subjected to mechanical stress.[23] During the processing of skins and hides to leather, efforts are made to optimize the strength, flexibility and feel of leather. Adding penetrating oils, a process known as fat liquoring, improves leather's texture and flexibility by lubricating the fibers and preventing adhesion between them.[29] However, little is known about how the addition of fat liquor affects the structure of the collagen fibrils themselves.

Here we report a study of the addition of fat liquor to leather in which we attempt to understand how penetrating oil changes the nanostructure of leather. With this understanding, it may be possible to manipulate the processing to produce leather of higher strength and better feel.

Experimental

Ovine pelts were obtained from 5-month-old, early season lambs of breeds with "black faces", which may include Suffolk, South Suffolk, and Dorset Down. Conventional beamhouse and tanning processes were used to generate leather. The pelts were depilated using a caustic treatment comprising sodium sulfide and calcium hydroxide. The residual keratinaceous material was then removed in a solution of sodium sulfide ranging in concentration from 0.8% to 2.4% for 8–16 h at temperatures ranging from 16°C to 24°C. The pelts were then washed and treated with a proteolytic enzyme, either a bacterial enzyme (Tanzyme, Tryptec Biochemicals, Ltd.) or a pancreatic enzyme (Rohapon ANZ, Shamrock, Ltd.), at concentrations ranging from 0.025% to 0.1%, followed by pickling in a 2% sulfuric acid and 10% sodium chloride solution. The pickled pelts were then pretanned using oxazolidine, degreased with an aqueous surfactant, and then tanned using chromium sulfate. The resulting "wet blue" was then retanned using a mimosa vegetable extract.

Fat liquoring was carried out using Lipsol EHF (Schill + Seilacher). This product contains a mixture of lanolin, bisulfited fish oil and 2-methyl-2,4-pentanediol. Lanolin, or wool wax, consists primarily of long chain waxy esters and some hydrolysis and oxidation products of these esters. The fat liquor was added at 0–10% by weight of wet leather prior to drying and mechanical softening. One sample was prepared with just the principal component of the fat liquor, lanolin (Sigma), at a concentration of 8% by weight of wet leather.

Samples for synchrotron-based small angle X-ray scattering (SAXS) analysis were prepared by cutting strips of leather 1 × 30 mm from the official sampling position (OSP)[30] from pelts of leather processed with 0, 2, 4, 6, 8, and 10% Lipsol EHF. Diffraction patterns were recorded on the Australian Synchrotron SAXS/WAXS beamline using a high-intensity undulator source. Each sample was mounted without tension in the X-ray beam to obtain scattering patterns from an edge-on direction. Measurements were made every 0.25 mm through the cross section from the grain to the corium. Energy resolution of 10^{-4} was obtained from a cryo-cooled Si (111) double-crystal monochromator, and the beam size [full width at half maximum (fwhm) focused at the sample] was 250 × 80 μm, with a total photon flux of about 2×10^{12} photons s^{-1}. All diffraction patterns were recorded with an X-ray energy of 11 keV using a Pilatus 1 M detector with an active area of 170 × 170 mm and a sample–detector distance of 3371 mm. Exposure time for diffraction patterns was 1 s, and data processing was carried out using the SAXS15ID software.[31]

The D-spacing of collagen was determined for each spectrum from Bragg's Law by taking the central position of several collagen peaks, dividing these by the peak order (usually from $n = 5$ to $n = 10$) and averaging the resulting values.

Fibril diameters were calculated from the SAXS data using the Irena software package[32] running within Igor Pro. The data were fitted at the wave vector Q, in the range of 0.01 – 0.04 $Å^{-1}$ and at an azimuthal angle which was 90° to the long axis of most of the collagen fibrils. This angle was selected by determining the average orientation of the collagen fibrils from the azimuthal angle for the maximum intensity of the d-spacing diffraction peaks. The "cylinderAR" shape model with an arbitrary aspect ratio of 30 was used for all fitting. We did not attempt to individually optimize this aspect ratio and the unbranched length of collagen fibrils may in practice have a length that exceeds an aspect ratio of 30.

Results

The SAXS patterns obtained for the different levels of fat liquor clearly show diffraction rings due to the axial periodicity of collagen (Figure 1a). Orientation of the collagen fibrils can be seen as the varying intensity of each of these rings around the azimuthal angle and the alignment at right

angles to this of the central scattering region. From the integrated intensity of the whole scattering pattern (Figure 1b) the position of the diffraction peaks can be measured and from these the D-spacing is determined.

The addition of fat liquor resulted in an increase in D-spacing of the collagen from 60.2 (σ = 0.47) nm for samples with no fat liquor to 63.6 (σ = 0.43) nm for samples with 10% fat liquor (Figure 2). This is an increase of 3.4 nm or 5.6%. The change in D-spacing of the corium and grain layers closely mimicked each other despite structural differences in these layers.[33] We find a strong correlation between D-spacing and the percentage of fat liquor added, with a linear fitted slope of 0.34 nm/% and a r^2 value of 0.93 (P = 0.0018 at an alpha of 0.05) (Figure 2).

The one sample prepared with 8% lanolin rather than fat liquor had a D-spacing of 63.1 (σ = 0.39) nm, which falls on the regression line in Fig. 2. This suggests the change in D-spacing may be primarily due to the lanolin content of the fat liquor.

An average fibril diameter of 56.8 (n = 106, σ = 1.3) nm was determined for the leather showing that there was no statistically significant change in the fibril diameter as a result of fat liquor addition.

DISCUSSION

We found that the change in collagen D-spacing is proportional to the amount of fat liquor added, with a large change being observed when the greatest amount of fat liquor was added. As pure lanolin had a similar effect, it is not unreasonable to assume that the lanolin component of the fat liquor is causing this change. This increase in D-spacing serves to increase the length (and therefore perhaps the volume) of the collagen fibrils in leather. The equivalent extension in D-spacing by tension applied to leather requires a stress of approximately 3.1 N/mm^2 for strong ovine leather and 0.4 N/mm^2 for weak ovine leather.[23]

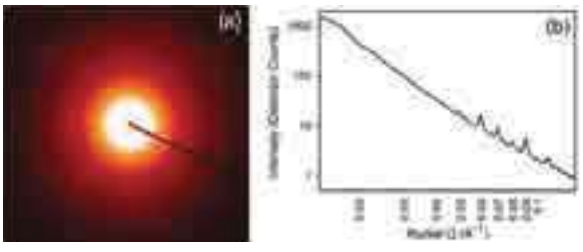

Figure 1. Example of SAXS of leather: (a) raw SAXS pattern; (b) integrated intensity profile.

Fat liquor is considered in the industry to assist in the mechanical properties of leather by "lubricating" the fibril structure, enabling the fibers to slide over one another. This work clearly shows that the fat liquor used in this experiment causes a change in the D-spacing, a fundamental property of fibril structure.

We consider two possible mechanisms for the change in D-spacing. One proposition is that the D-spacing increase is caused by an increase in the twist of the tropocollagen helix, which would result in a longer tropocollagen and therefore a longer D-spacing in the fibril. However, if an increase in tropocollagen occurred by this mechanism, we would expect to also see a significant change in the fibril diameter. The diameter was not observed to change and therefore this hypothesis is not supported.

The other option we considered is that the observed change is due to an increase in the length of the gaps between two tropocollagen molecules within the fibrils. Collagen fibrils form in a process that controls the registration between adjacent tropocollagen molecules, known as the D-spacing. Inspection of type I tropocollagen maps and interactomes shows that the two regions of the molecule important in fibrillogenesis (residues ~1016-1040, and 776-800) are rich in hydrophobic amino acids and prolines.[34-37] Once the tropocollagens are in register, the fibril structure is stabilized by intermolecular hydrogen bonds, often mediated by water, and covalent crosslinks at the N and C termini of the molecule.

An increase in the D-spacing is indicative of an increase in the axial distance between fibrils and could result in an overall lengthening of the fibril. It could also change the interactions between tropocollagens, whether the interactions are covalent

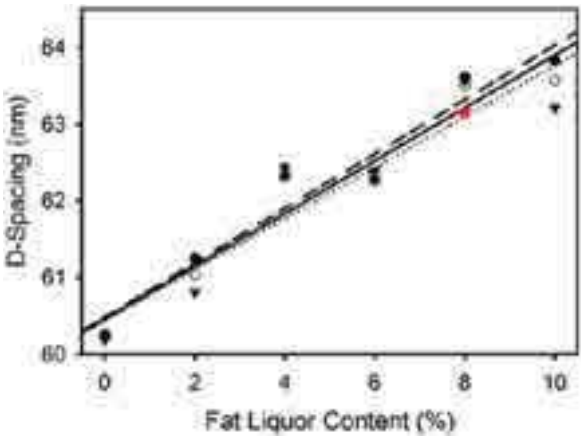

Figure 2. Collagen D-spacing versus fat liquor percentage for ovine leather: (●, -- -- --) corium, (▼, ••••) grain, and (○, - - - - -) average. Each point for the corium and grain is taken from the average of about 10 scattering patterns. Pure lanolin at 8% also shown (■).

or non-covalent and whether they are mediated through bridging molecules such as water. The fact that it is a direct result of fat liquoring implies that the covalent crosslinks formed between tropocollagen molecules in the mature fibril, are either nonexistent, are broken during processing of the skin, or that they are flexible enough to allow movement of the tropocollagens relative to one another within the fibril.

Axial periodicity in collagen I is thought to be stabilized by inter-tropocollagen hydrophobic and л-CH2 interactions between the C-terminal region of one tropocollagen and a specific region of a second tropocollagen, driven by the entropic gain from the release of ordered water molecules.[38] Lanolin is a long chain hydrocarbon ester, made up from a long chain aliphatic lanolin alcohol and fatty acid. Its hydrophobic structure will therefore be relatively rigid allowing it to insert into the hydrophobic regions at the ends of the gap regions between tropocollagen molecules. The relative non-specific nature of hydrophobic interactions is tolerant of movement, and the lanolin will act like lubricant allowing the tropocollagens to move relative to one another, altering the D-spacing.

It is outside of the scope of this work to elucidate the molecular details of this arrangement. While atomic force microscopy could be used to compare the ratio of the gap and overlap regions among leathers with different levels of fat liquor, obtaining statistically robust sample data could be problematic. It has been shown that there is a range of D-spacings in any one sample, with different fibril bundles within one piece of tissue having different average D-spacings.[25] SAXS measurements sample a volume of 80 × 150 × 1000 μm, which might be expected to contain around 3×10^{10} collagen D-spacing units (assuming collagen occupies around 50% of the volume). AFM, however, scans only small areas of a sample at one time, making it difficult to get a representative average D-spacing. Nevertheless, this would be a worthwhile follow-up analysis and could reveal one mechanism by which fat liquor achieves fibril elongation.

Conclusions

In summary, we have investigated the structural changes of collagen within leather upon addition of varying amounts of fat liquor. We have shown that as we increased the amount of fat liquor, the D-spacing of the collagen fibrils increased, and that this appears to be due to the lanolin component of the fat liquor. Alternative mechanisms for this increase in D-spacing have been discussed, including an increase in the gap region or an increase in the length of the tropocollagen triple helix. We have shown that fat liquor does more than lubricate fibers in leather in that it alters the structure of collagen fibrils.

While the focus of this work has been the improved properties of leather, due to the application of lanolin, the changes observed in collagen structure may also occur in raw skin. Mixtures of oils and other chemicals have long been applied to human skin to enhance its appearance and are known as moisturizers. It may be that some of the components of moisturizers increase the D-spacing of collagen in skin, expanding the collagen structure and reducing wrinkles. We are currently investigating the effect of a range of other organic additives on collagen structure as well as the effects of fat liquoring on the nanostructural response of leather when under strain.

Acknowledgements

This work was supported by the Ministry of Business, Innovation and Employment, New Zealand (Grant LSRX0801). The Australian Synchrotron provided travel funding and accommodation. This research was undertaken on the SAXS/WAXS beamline at the Australian Synchrotron, Victoria, Australia who also provided travel funding. Sue Hallas of Nelson assisted with editing.

References

1. Russell, A. E.; Stress-strain relationships in leather and the role of fiber structure. *J. Soc. Leather Technol. Chem.* **72**, 121-134, 1988.
2. Michel, A.; Tanners' dilemma: Vertical fibre defect. *Leather International* **206**, 36-37, 2004.
3. Chan, Y., Cox, G. M., Haverkamp, R. G., and Hill, J. M.; Mechanical model for a collagen fibril pair in extracellular matrix. *Eur. Biophys. J. Biophy. Lett.* **38**, 487-493, 2009.
4. Basil-Jones, M. M., Edmonds, R. L., Cooper, S. M., and Haverkamp, R. G.; Collagen fibril orientation in ovine and bovine leather affects strength: A small angle X-ray scattering (SAXS) study. *J. Agric. Food Chem.* **59**, 9972-9979, 2011.
5. Rabinovich, D.; Seeking soft leathers with a tight grain. *World Leather* **14**, 27-32, 2001.
6. Floden, E. W., Malak, S., Basil-Jones, M. M., Negron, L., Fisher, J. N., Byrne, M., Lun, S., Dempsey, S. G., Haverkamp, R. G., Anderson, I., Ward, B. R., and May, B. C. H.; Biophysical characterization of ovine forestomach extracellular matrix biomaterials. *J. Biomed. Mater. Res. B* **96B**, 67-75, 2010.
7. Bella, J., Brodsky, B., and Berman, H. M.; Hydration structure of a collagen peptide. *Structure* **3**, 893-906, 1995.
8. Engel, J., Chen, H. T., Prockop, D. J., and Klump, H.; Triple Helix Reversible Coil Conversion of Collagen-Like Polytripeptides in Aqueous and Non-Aqueous Solvents - Comparison of Thermodynamic Parameters and Binding of Water to (L-pro-L-pro-gly)N and (L-pro-L-hyp-gly)N. *Biopolymers* **16**, 601-622, 1977.

9. Burjanadze, T. V.; Thermodynamic substantiation of water-bridged collagen structure. *Biopolymers* **32**, 941-949, 1992.
10. Rosenbloom, J., Harsch, M., and Jimenez, S.; Hydroxyproline content determines denaturation temperature of chick tendon collagen. *Arch. Biochem. Biophys.* **158**, 478-484, 1973.
11. Bella, J., Eaton, M., Brodsky, B., and Berman, H. M.; Crystal-structure and molecular-structure of a collagen-like peptide at 1.9-Ångstrom resolution. *Science* **266**, 75-81, 1994.
12. Naito, A., Tuzi, S., and Saito, H.; A high-resolution N-15 solid-state NMR-study of collagen and related polypeptides - the effect of hydration on formation of interchain hydrogen-bonds as the primary source of stability of the collagen-type triple-helix. *Eur. J. Biochem.* **224**, 729-734, 1994.
13. Gautieri, A., Vesentini, S., Redaelli, A., and Buehler, M. J.; Hierarchical Structure and Nanomechanics of Collagen Microfibrils from the Atomistic Scale Up. *Nano Lett.* **11**, 757-766, 2011.
14. Usha, R., and Ramasami, T.; Influence of Hydrogen Bond, Hydrophobic and Electrovalent Salt Linkages on the Transition Temperature, Enthalpy and Activation Energy in Rat Tail Tendon (RTT) Collagen Fibre. *Thermochim. Acta* **338**, 17-25, 1999.
15. Bavinton, J. H., Peters, D. E., and Stephens, L. J. A.; Comparative Morphology of Kangaroo and Bovine Leathers. *J. Am. Leather Chem. Assoc.* **82**, 197-199, 1987.
16. Sizeland, K. H., Haverkamp, R. G., Basil-Jones, M. M., Edmonds, R. L., Cooper, S. M., Kirby, N., and Hawley, A.; Collagen Alignment and Leather Strength for Selected Mammals. *J. Agric. Food Chem.* **61**, 887-892, 2013.
17. Wells, H. C., Edmonds, R. L., Kirby, N., Hawley, A., Mudie, S. T., and Haverkamp, R. G.; Collagen Fibril Diameter and Leather Strength. *J. Agric. Food Chem.* **61**, 11524-11531, 2013.
18. Parry, D. A. D., Barnes, G. R. G., and Craig, A. S.; Comparison of size distribution of collagen fibrils in connective tissues as a function of age and a possible relation between fibril size distribution and mechanical-properties. *P. Roy. Soc. B-Biol. Sci.* **203**, 305-321, 1978.
19. Folkhard, W., Geercken, W., Knorzer, E., Mosler, E., Nemetschek-Gansler, H., Nemetschek, T., and Koch, M. H. J.; Structural dynamic of native tendon collagen. *J. Mol. Biol.* **193**, 405-407, 1987.
20. Folkhard, W., Geercken, W., Knorzer, E., Nemetschek-Gansler, H., Nemetschek, T., and Koch, M. H. J.; Quantitative analysis of the molecular sliding mechanism in native tendon collagen - time-resolved dynamic studies using synchrotron radiation. *Int. J. Biol. Macromol.* **9**, 169-175, 1987.
21. Chan, Y., Cox, G. M., Haverkamp, R. G., and Hill, J. M.; Mechanical model for a collagen fibril pair in extracellular matrix. *Eur. Biophys. J.* **38**, 487-493, 2009.
22. Cuq, M. H., Palevody, C., and Delmas, M.; Fundamental study of cross-linking of collagen with chrome tanning agents in traditional and Cr.A.B processes. *J. Soc. Leather Technol. Chem.* **83**, 233-238, 2000.
23. Basil-Jones, M. M., Edmonds, R. L., Norris, G. E., and Haverkamp, R. G.; Collagen fibril alignment and deformation during tensile strain of leather: A SAXS study. *J. Agric. Food Chem.* **60**, 1201-1208, 2012.
24. Gonzalez, A. D., Gallant, M. A., Burr, D. B., and Wallace, J. M.; Multiscale analysis of morphology and mechanics in tail tendon from the ZDSD rat model of type 2 diabetes. *J. Biomech.* **47**, 681-686, 2014.
25. Fang, M., Goldstein, E. L., Turner, A. S., Les, C. M., Bradford, G. O., Fisher, G. J., Welch, K. B., Rothman, E. D., and Banaszak Holl, M. M.; Type I Collagen DiSpacing in Fibril Bundles of Dermis, Tendon, and Bone: Bridging between Nano- and Micro-Level Tissue Hierachy. *ACS Nano* **6**, 9503-9514, 2012.
26. James, V. J., McConnell, J. F., and Capel, M.; The D-spacing of collagen from mitral heart-valves changes with aging, but not with collagen type-III content. *Biochim. Biophys. Acta* **1078**, 19-22, 1991.
27. Scott, J. E., Orford, C. R., and Hughes, E. W.; Proteoglycan-collagen arrangements in developing rat tail tendon - an electron-microscopical and biochemical investigation. *Biochem. J.* **195**, 573-584, 1981.
28. Ripamonti, A., Roveri, N., Braga, D., Hulmes, D. J. S., Miller, A., and Timmins, P. A.; Effects of pH and ionic-strength on the structure of collagen fibrils. *Biopolymers* **19**, 965-975, 1980.
29. Bajza, Z., and Vreck, I. V.; Fatliquoring agent and drying temperature effects on leather properties. *J. Mater. Sci.* **36**, 5265-5270, 2001.
30. Williams, J. M. V.; IULTCS (IUP) test methods - Sampling. *J. Soc. Leather Technol. Chem.* **84**, 303-309, 2000.
31. Cookson, D., Kirby, N., Knott, R., Lee, M., and Schultz, D.; Strategies for data collection and calibration with a pinhole-geometry SAXS instrument on a synchrotron beamline. *J. Synchrotron Radiat.* **13**, 440-444, 2006.
32. Ilavsky, J., and Jemian, P. R.; Irena: tool suite for modeling and analysis of small-angle scattering. *J. Appl. Crystallogr.* **42**, 347-353, 2009.
33. Basil-Jones, M. M., Edmonds, R. L., Allsop, T. F., Cooper, S. M., Holmes, G., Norris, G. E., Cookson, D. J., Kirby, N., and Haverkamp, R. G.; Leather structure determination by small angle X-ray scattering (SAXS): cross sections of ovine and bovine leather. *J. Agric. Food Chem.* **58**, 5286-5291, 2010.
34. Di Lullo, G. A., Sweeney, S. M., Korkko, J., Ala-Kokko, L., and San Antonio, J. D.; Mapping the ligand-binding sites and disease-associated mutations on the most abundant protein in the human, type I collagen. *J. Biol. Chem.* **277**, 4223-4231, 2002.

35. Sweeney, S. M., Orgel, J. P., Fertala, A., McAuliffe, J. D., Turner, K. R., Di Lullo, G. A., Chen, S., Antipova, O., Perumal, S., Ala-Kokko, L., Forlino, A., Cabral, W. A., Barnes, A. M., Marini, J. C., and Antonio, J. D. S.; Candidate cell and matrix interaction domains on the collagen fibril, the predominant protein of vertebrates. *J. Biol. Chem.* **283**, 21187-21197, 2008.
36. Helseth, D. L., and Veis, A.; Collagen Self-Assembly Invitro - Differentiating Specific Telopeptide-Dependent Interactions Using Selective Enzyme Modification and the Addition of Free Amino Telopeptide. *J. Biol. Chem.* **256**, 7118-7128, 1981.
37. Prockop, D. J., and Fertala, A.; The collagen fibril: The almost crystalline structure. *J. Struct. Biol.* **122**, 111-118, 1998.
38. Kar, K., Ibrar, S., Nanda, V., Getz, T. M., Kunapuli, S. P., and Brodsky, B.; Aromatic Interactions Promote Self-Association of Collagen Triple-Helical Peptides to Higher-Order Structures. *Biochemistry* **48**, 7959-7968, 2009.

RSC Advances

PAPER

View Article Online
View Journal | View Issue

Cite this: *RSC Adv.*, 2015, **5**, 3611

Collagen cross linking and fibril alignment in pericardium

Hanan R. Kayed,[a] Katie H. Sizeland,[a] Nigel Kirby,[b] Adrian Hawley,[b] Stephen T. Mudie[b] and Richard G. Haverkamp*[a]

The influence of natural cross linking by glycosaminoglycan (GAG) on the structure of collagen in animal tissue is not well understood. Neither is the effect of synthetic cross linking on collagen structure well understood in glutaraldehyde treated collagenous tissue for medical implants and commercial leather. Bovine pericardium was treated with chondroitinase ABC to remove natural cross links or treated with glutaraldehyde to form synthetic cross links. The collagen fibril alignment was measured using synchrotron based small angle X-ray scattering (SAXS) and supported by atomic force microscopy (AFM) and histology. The alignment of the collagen fibrils is affected by the treatment. Untreated pericardium has an orientation index (OI) of 0.19 (0.06); the chondroitinase ABC treated material is similar with an OI of 0.21 (0.08); and the glutaraldehyde treated material is less aligned with an OI of 0.12 (0.05). This difference in alignment is also qualitatively observed in atomic force microscopy images. Crimp is not noticeably affected by treatment. It is proposed that glutaraldehyde cross linking functions to bind the collagen fibrils in a network of mixed orientation tending towards isotropic, whereas natural GAG cross links do not constrain the structure to quite such an extent.

Received 17th September 2014
Accepted 5th December 2014

DOI: 10.1039/c4ra10658j

www.rsc.org/advances

1. Introduction

The collagen I molecule is prevalent as the basis of many structural components in animals. It assembles with a complex hierarchical structure. This extracellular matrix forms resilient materials which are mechanically very tough.[1] This toughness is due in part to the highly fibrillar nature of collagen. Polypeptide molecules twist in left handed α-helical chains, and three of these in turn assemble with a right handed twist to form tropocollagens. Collagen fibrils are multiples of five tropocollagen strands thick and of extended length. The fibrils in turn may be assembled into larger fibres and a variety of structural motifs. There is great inherent strength and elasticity in each individual fibril. It is believed that the structure of materials composed of collagen I also require cross linking of the fibrils. This mechanically couples the fibrils restricting them from sliding past each other in order to achieve high strength.[2]

In nature, these cross links between collagen fibrils are provided by proteoglycan bridges, predominantly decoran, forming shape modules.[3,4] These proteoglycan bridges are elastic containing the glycosaminoglycan dermochondan sulfate.[5,6] The way in which these connections might transmit force between fibrils to resist sliding forces has been modelled.[7–11] The energy absorbed by enthalpic transformations in the dermochondan can be significant.[6,12]

It has been found that the tensile elastic modulus of mouse tendon was reduced over much of the stress–strain curve when the natural glycosaminoglycan (GAG) content was lowered by the application of chondroitinase ABC while the ultimate tensile force and ultimate stress were relatively unchanged.[13] However, this is not universally agreed as other work has found no altered mechanical properties in tendon from the removal of GAGs.[14,15]

The GAG cross links associate with the collagen fibril at several different sites but is believed to always be associated with the Gly-Asp-Arg amino acid sequence.[16]

Natural cross linking of collagen also increases with age due to glycation and has been shown to increase stiffness in connective tissues[17] and collagen gels[18] and increase brittleness in bones.[19]

Methods of cross linking other than that found in nature can be used to modify the properties of collagen materials. Cross linking of bovine pericardium with glutaraldehyde either under strain or with no tension has been reported to result in a less extensible and stiffer material which is stronger than the untreated material.[20,21]

However, there is still much to learn about cross linking of collagen and the contribution these cross links make to the structure and mechanical properties of collagen tissues.

The arrangement of collagen fibrils, particularly the extent of alignment or anisotropy, is an important contributor to the

[a]*School of Engineering and Advanced Technology, Massey University, Private Bag 11222, Palmerston North 4442, New Zealand. E-mail: r.haverkamp@massey.ac.nz*
[b]*Australian Synchrotron, 800 Blackburn Road, Melbourne, Australia*

strength of collagen materials. The structure–function relationship between collagen alignment and mechanical properties has been elucidated for a range of tissue types.[22–26] The orientation of collagen measured edge-on (alignment in-plane) has been shown in a range of mammal skins processed to leather to be correlated with strength.[27,28]

Small angle X-ray scattering (SAXS) is a powerful method for measuring the orientation of collagen fibrils in tissue.[26,29,30] Other methods may also be used such as small angle light scattering,[31] confocal laser scattering,[32] reflection anisotropy,[33] and atomic force microscopy.[34]

Bovine pericardium is a suitable material to use as a model in investigating the effect of cross linking, both natural and synthetic, on mechanical properties. Bovine pericardium has an established use for heart valve leaflet replacement.[35,36] The material requires high mechanical strength and a long performance life.[37] The orientation of collagen in pericardium heterograft materials for heart valve leaflets has been shown to affect the stiffness during flexing.[38]

We investigate here the hypothesis that cross links, both natural (GAGs) and synthetic (glutaraldehyde), may constrain the alignment of the collagen fibrils to result in different extents of orientation in collagen tissues which in turn may partially explain the different physical properties of the materials.

2. Methods

2.1 Fresh pericardium samples

Fresh bovine pericardium was obtained from John Shannon and from Southern Lights Biomaterials and stored in phosphate buffered saline (PBS) solution (Lorne Laboratories Ltd). The tissue was rinsed briefly in PBS solution. The tissue was then cut into rectangles of approximate dimensions 40–45 mm × 10 mm with the long axis taken from the long axis of the heart (as shown in Fig. 1). The method of decellularisation was based on Yang *et al.* (2009).[39] The pericardium was washed for 24 h in a 1% octylphenol ethylene oxide condensate (Triton X-100, Sigma), 0.02% EDTA solution made up in PBS. This washing step was conducted under constant agitation at 4 °C. The samples were then rinsed in PBS buffer and stored in PBS. These are what we refer to as "native". Subsequent processing of this material produced glutaraldehyde treated or chondroitinase ABC treated material. All samples were taken from one pericardium and randomly assigned to each treatment method.

2.2 Glutaraldehyde treatment

The Triton treated pericardium was incubated with a 0.6% glutaraldehyde solution made up in PBS buffer at 4 °C for 24 h with constant agitation.[40] It was then stored in a sealed container in the solution of the same composition until SAXS measurements were performed. The total time in storage was 3–5 days.

2.3 Chondroitinase ABC treatment

Removal of GAG cross links was based on the method described by Schmidt *et al.* (1990).[41] The Triton treated pericardium was incubated in 0.125 units of chondroitinase ABC per mL of buffer solution comprising of 0.05 M Tris–HCl, 0.06 M sodium acetate and EDTA-free protease inhibitors (complete, EDTA-free protease inhibitor tablets, Roche Diagnostics, Mannheim, Germany) at approximately 27 °C for 24 h before rinsing and storing in 0.05 M Tris–HCl and 0.06 M sodium acetate buffer in a sealed container at 4 °C.

Care was taken with all handling, cutting and treatment of the samples to not stretch the material as this might cause fibril alignment to change. The data presented here represents a duplication of this experiment with additional care taken in sample selection and handling in the second set of samples and SAXS analysis informed by the experience from the initial experiments.

2.4 GAG assay

An assay for sulfated GAGs was performed in triplicate for each of the sample treatments. GAGs were extracted with 1 mL extraction reagent consisting of a 0.2 M sodium phosphate buffer at pH 6.4, containing 8 mg mL^{-1} sodium acetate, 4 mg mL^{-1} EDTA, 0.8 mg mL^{-1} cysteine HCl and 0.1 mg mL^{-1} papain enzyme (*Carica papaya*, Sigma, Biochemika, enzyme no. 3.4.22.2). Each pericardium sample was incubated at 65 °C for 26 h. These samples were centrifuged and the supernatant containing the extracted GAGs collected. The concentration of GAGs in solution was determined with a Blyscan Sulfated Glycosaminoglycan Assay kit (Bicolor, Carrickfergus, UK). GAGs were precipitated with 1 mL of dye reagent to 20 or 40 μL of supernatant diluted to 100 μL, mechanically inverted for 30 minutes, and then centrifuged. The unbound dye was drained off and 1 mL of Blyscan dissociation reagent was added to the precipitate, left to dissolve for approximately 10 minutes,

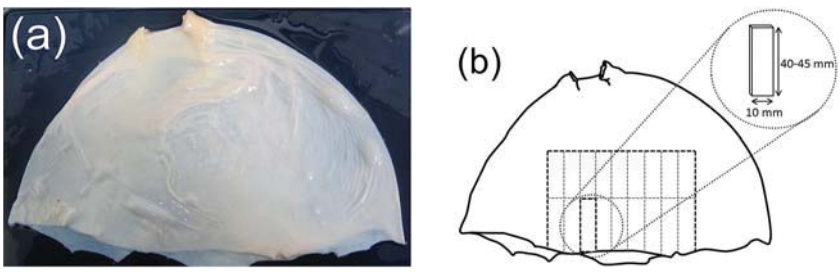

Fig. 1 Pericardium (a) ready to be cut for samples; (b) showing region used and sample size.

and centrifuged. Absorbance was measured at a wavelength of 656 nm and compared with a standard curve.

2.5 SAXS analysis

In preparation for SAXS analysis, the pericardium was removed from the glutaraldehyde and Tris–HCl, sodium acetate buffer solutions in which they had been stored. After soaking for at least 1 h in buffered saline solution (Lorne Laboratories Ltd), pericardium strips were mounted and diffraction patterns recorded while the pericardium was wet. All diffraction patterns were recorded at room temperature.

Diffraction patterns were recorded on the Australian Synchrotron SAXS/WAXS beamline, utilizing a high-intensity undulator source. Energy resolution of 10^{-4} (*e.g.* 1×10^{-4} Å for 1 Å radiation) was obtained from a cryo-cooled Si(111) double-crystal monochromator and the beam size (FWHM focused at the sample) was 250×80 μm, with a total photon flux of about 2×10^{12} ph s^{-1}. All diffraction patterns were recorded with an X-ray energy of 12 keV using a Pilatus 1M detector with an active area of 170×170 mm and a sample-to-detector distance of 3371 mm. Exposure time for diffraction patterns was 1 s and data processing was carried out using the software scatterBrainAnalysis V2.30.[42]

The orientation index (OI) is used to give a measure of the spread of fibril orientation (an OI of 1 indicates the fibrils are parallel to each other; an OI of 0 indicates the fibrils are randomly oriented). OI is defined as $(90° - OA)/90°$, where OA is the minimum azimuthal angle range that contains 50% of the fibrils, based on the method of Sacks for light scattering[43] but converted to an index,[27] using the spread in azimuthal angle of one or more *d*-spacing diffraction peaks. The peak area is measured, above a fitted baseline, at each azimuthal angle.

Four samples were prepared of native material, three with treatment by chondroitinase ABC for 24 h and three with treatment by glutaraldehyde. For each sample one diffraction pattern was recorded at each of nine positions.

From each pattern (an example is shown in Fig. 2) the OI was calculated from the azimuthal spread of the 5th collagen diffraction peak (as seen in Fig. 3 at around 0.05 $Å^{-1}$).

2.6 Atomic force microscopy

Small square sections were cut from the native, chondroitinase ABC and glutaraldehyde treated pericardium samples and mounted onto 12 mm diameter magnetic metal discs with double sided tape. The samples were left to air dry for a few h before being imaged. A Nanoscope E (Veeco) atomic force microscope with a JV scanner was used with *x*–*y* calibration to ±3% completed just prior to imaging. CSG01 cantilevers (NT-MDT, Russia) with a force constant of about 0.05 N m^{-1} were used for contact mode imaging.

2.7 Histology

Samples of pericardium were cut and frozen flat in a Leica CM1850 UV cryogenic microtome at −30 °C before being mounted on microtome disks using embedding medium for frozen tissue specimens. 10 μm thick cross-sections were cut and transferred to glass microscope slides. The mounted sections were stained as per the protocols of the Picrosirius Red Stain Kit (Polysciences, Inc.) before being placed in 70% ethanol for 45 s and left to air dry for several h. Optical images were recorded on a Nikon Eclipse TE2000-U microscope fitted with a Nikon Digital Sight DS-Fi2 camera and cross-polarising filters.

2.8 Tensile properties

Three rectangular sections of pericardium with the long axis of the sections equivalent to the long axis of the heart were cut from each of three pericardium sacs and treated with glutaraldehyde or chondroitinase ABC or left as native tissue. From these, samples were cut using a press knife and stress–strain curves were measured by uniaxial strain using an Instron 4467 with the sample mounted vertically at a rate of 100 mm min^{-1}

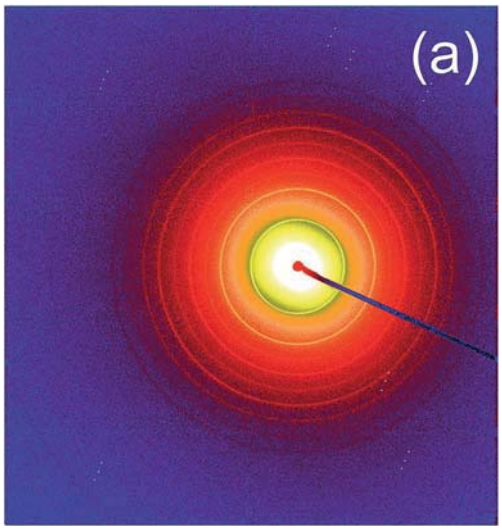

Fig. 2 Representative scattering pattern of pericardium.

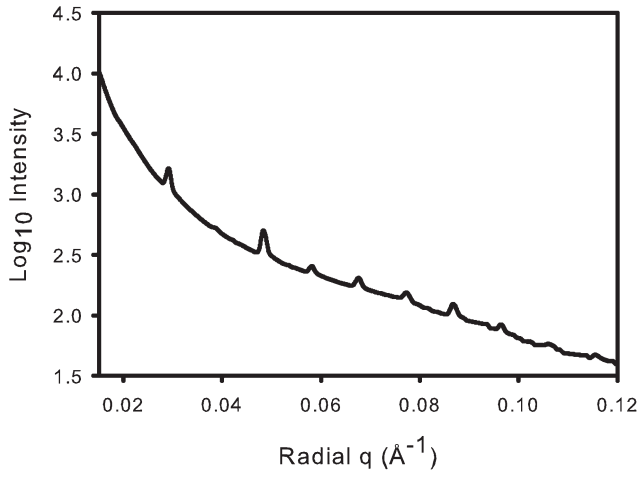

Fig. 3 Representative integrated scattering pattern of pericardium. The sharp peaks are due to diffraction for the *d*-spacing (at different orders).

according to standard ISO 3376:2011. Thickness was measured using method BS EN ISO 2589:2002 but with reduced pressure. Elastic modulus was determined for the linear region of the stress–strain curve.

2.9 Statistical analysis

Statistically significant differences between treatment mean OI values, GAG content and tensile properties were tested for using One Way ANOVA implemented in SigmaPlot 12.0 with a significance level, alpha, of 0.05. If statistical differences were found ($P = <0.001$), pairwise multiple comparisons were performed using the Holm–Sidak method in SigmaPlot 12.0 where the overall significance level used was 0.05. Pairwise comparisons with *P*-values less than 0.05 were considered to be significantly different.

3. Results

3.1 Chondroitinase ABC GAG removal

The GAG assay found that approximately 81% of GAGs were removed with chondroitinase ABC treatment (Fig. 4) which can be considered a success. As expected, glutaraldehyde treatment did not remove the GAGs, showing similar GAG content to the native material. Therefore the chondroitinase treated samples do represent pericardium with most of the GAGs removed.

3.2 Histology

The picrosirius red stained sections of each of the treated samples show a similar level of crimp in each sample type (Fig. 6). Crimp is the wavy structure of collagen fibrils which is typically seen in tendon and pericardium (with a period of 25–45 μm in pericaridum[23]) but not as prominently in skin. The chondroitinase ABC treated sample and native sample are the most similar. The glutaraldehyde treated pericardium has the appearance of a more open structure (which may be because it did not microtome as well) and it has some variation in colour.

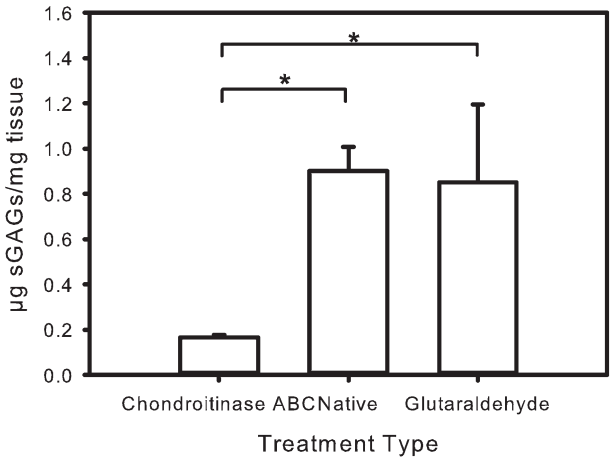

Fig. 4 GAG assay for pericardium for triplicate samples (error bars for 95% confidence intervals). Pairs that are significantly different ($P < 0.001$ for $\alpha = 0.05$) are shown by a *.

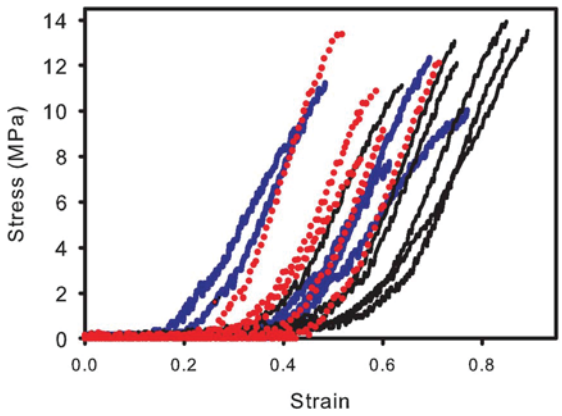

Fig. 5 Stress–strain curves for native pericardium (blue thick lines); chondroitinase ABC treated pericardium (red dotted lines); glutaraldehyde treated pericardium (black thin lines).

While picrosirius red is intended as a specific stain for collagen with type 1 collagen showing as red, other factors can affect birefringence and the resulting colour under cross-polarised filters, such as fibril thickness and the availability of free basic amino acid binding sites. The sulfonic acid groups of the picrosirius red dye molecule bind to the free amino acid residues on collagen, as do the aldehyde groups of glutaraldehyde; therefore binding of glutaraldehyde to these sites will inhibit dye binding and may result in decreased birefringence. The presence of colours other than red in the glutaraldehyde treated samples does not therefore indicate other types of collagen present, but rather, modification to the type I collagen.[44–46]

3.3 Tensile properties

The tensile properties of the pericardia samples had high variability (Fig. 5, Table 1). There is a foot region of variable length followed by an approximately linear region until the material reached its ultimate tensile stress and broke (the failure region is not shown). The chondroitinase treatment perhaps increases the elastic modulus, in agreement with other studies,[17] however with the small sample size this difference cannot be considered statistically significant ($P = 0.043$, $t = -1.9$, for $\alpha = 0.05$). The stress at failure may be higher for glutaraldehyde, also in keeping with other studies,[20,21] but this also cannot be considered statistically significant ($P = 0.012$, $t = -3.1$, for $\alpha = 0.05$). The only statistically significant difference between the mechanical properties of the treatment types is the strain at failure, which is higher for the glutaraldehyde treated material ($P = 0.026$, $t = -2.6$ for $\alpha = 0.05$).

3.4 SAXS

The pericardium gives good scattering patterns with clearly defined diffraction rings due to the *d*-spacing periodicity (Fig. 2). The integrated intensity plots show well defined peaks corresponding to the collagen *D*-period (Fig. 3). The odd numbered peaks have a much higher intensity than the even numbered peaks, a characteristic attributed to a fully hydrated sample.[47] This provides some reassurance that the samples are

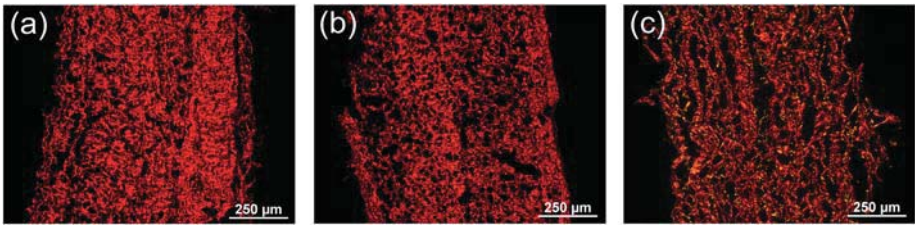

Fig. 6 Picrosirius stained sections of pericardium treated with (a) chondroitinase ABC; (b) native; (c) glutaraldehyde.

maintained in the hydrated state during collection of the diffraction patterns, as intended.

3.5 OI

The distribution of orientation of the fibrils can be seen with a plot of the intensity (we use the peak area) of any of the collagen diffraction peaks (Fig. 7). A narrow peak in this plot is indicative of more highly aligned collagen fibrils, as seen for the native and chondroitinase treated tissue, whereas broader peaks such as that for glutaraldehyde indicate a more isotropic arrangement. This can be quantified as an orientation index, OI. We calculate first an orientation angle (OA) which is defined as the minimum angle which contains 50% of the fibrils.[48] From this the OI is calculated as $(90^\circ - \mathrm{OA})/90^\circ$.

The OI calculated for the three treatments provide different average OI values (Table 2, Fig. 8). There is a statistically significant difference in the OI between the glutaraldehyde treated material and the other two materials but the difference in the OI between the native and chondroitinase treated pericardium does not pass the significance test. Previously we have compared chondroitinase ABC treatment for 48 h and 24 h with diffraction patterns recorded and analysed, however the OI obtained from the 48 h treated samples was not significantly different from that obtained after 24 h, probably indicating that most of the GAGs were removed already by 24 h of treatment (not shown here).

3.6 Atomic force microscopy

Atomic force microscopy provided clear images of collagen fibrils on the fibrous (outer) surface of the pericardium (Fig. 9). AFM provides small area images of a diverse surface so that unbiased selection of images can be difficult. We have selected one image of each material that is generally representative of that sample. The glutaraldehyde treated sample clearly had more of a collagen fibril network with fibrils not so often seen in parallel. In contrast the native material and the pericardium

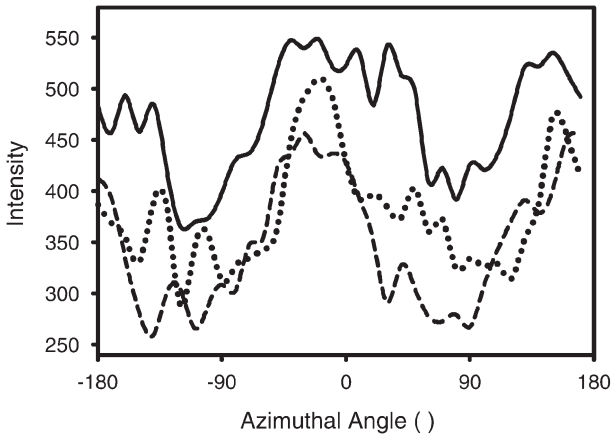

Fig. 7 Representative azimuthal intensity variation plots of the fifth collagen *D*-period diffraction peak for pericardium. The width of the central peak represents the spread in fibril orientation. Solid line, glutaraldehyde; dotted line, native; dashed line, chondroitinase ABC.

treated with chondroitinase ABC contained many aligned collagen fibrils.

4. Discussion

We have found an effect on collagen fibril alignment with cross linking. Native tissue containing GAG cross links has a moderate degree of fibril alignment. When these cross links are removed by treatment with the enzyme chondroitinase ABC the alignment of the fibrils does not show a significant change. When cross links are added, in the form of glutaraldehyde, the alignment of the fibrils decreases, becoming more isotropic with a network like structure forming. These changes do not appear to be associated with a change in crimp. Glutaraldehyde cross links therefore appear to have a direct effect on the arrangement of the collagen fibrils whereas native GAG cross

Table 1 Tensile properties of pericardium (with 95% confidence intervals)

Sample	Elastic modulus in linear region (MPa)	Stress at failure (MPa)	Strain at failure (%)
Native	40 ± 12	10.2 ± 2.2	60 ± 17
Chondroitinase ABC	52 ± 13	10.8 ± 2.7	60 ± 9
Glutaraldehyde	50 ± 6	12.8 ± 1.1	79 ± 10

Table 2 Orientation index obtained for pericardium samples

Sample	Number of diffraction peaks analysed (N)	Mean OI	95% confidence interval
Chondroitinase ABC	27	0.208	0.032
Native	36	0.192	0.021
Glutaraldehyde	27	0.117	0.021

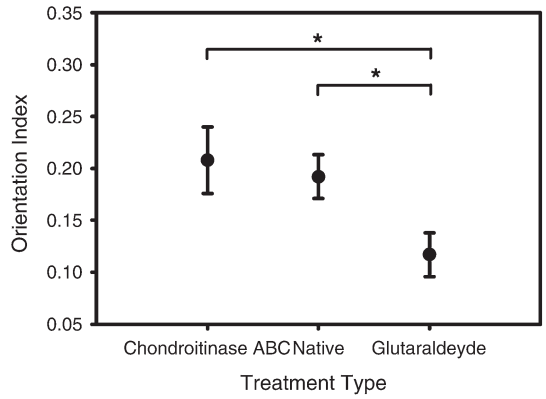

Fig. 8 Orientation index for each of the three levels of cross linking (error bars for 95% confidence intervals). Pairs that are significantly different ($P < 0.001$ for $\alpha = 0.05$) are shown by a *.

links do not have a statistically significant effect on alignment for tissue that is not under any mechanical load.

Glutaraldehyde has long been used as a cross linking agent for collagen, reacting primarily with ε-amino groups of lysine and hydroxylysine located on the outer surface of the triple helix region. Such links have been reported to occur both intramolecularly and intermolecularly depending on the treatment conditions and may involve some polymerisation of the glutaraldehyde to link greater distances.[49–51] Here we have shown that this network structure means not just a cross linked network of collagen but that the collagen fibrils also rearrange into a less aligned, more isotropic network structure under the action of glutaraldehyde cross linking without the application of external force. This chemically induced restructuring results in a decrease in the OI.

We have not specifically investigated the heterogeneity with depth, however the treatment time was ample to enable glutaraldehyde to penetrate the tissue fully.[50] In other work on glutaraldehyde treatment of pericardium, the variation of OI with depth through the glutaraldehyde treated pericardium tissue has been investigated and the OI did not vary greatly throughout the thickness, although a comparison was not been made with untreated pericardium.[52]

In contrast to glutaraldehyde cross links, proteoglycan (containing GAG) cross links are reported to occur solely on the outer surface of collagen fibrils, forming both axially and orthogonally with the majority located orthogonally between adjacent fibrils by the interaction of GAG side chains localised on the surface of collagen fibrils in mature tissues.[53,54] More specifically, it is believed proteoglycan cross links are associated with the gap region of the collagen *d*-spacing, binding to a single tropocollagen molecule.[53,54] We propose that these GAG bridges do not constrain the fibrils in a somewhat unaligned network structure in a higher energy state; these links appear only to form between adjacent fibrils at specific locations. Removal of these links therefore does not result in relaxation of some kind and fibrils do not spontaneously realign into a lower energy state and adopt some sort of preferred alignment. However, we suggest that the removal of the GAG links by chondroitinase ABC may give the potential for fibrils in the treated pericardium to become more easily aligned under tension.

This understanding of structural changes with treatment also has consequences for the preparation of materials for medical applications such as the treatment of bovine pericardium for heart valve repair, or ovine forestomach extracellular matrix material for surgical scaffolds.[55] The modifications imposed on the native tissue due to the processing of the material, sometimes including glutaraldehyde cross linking,

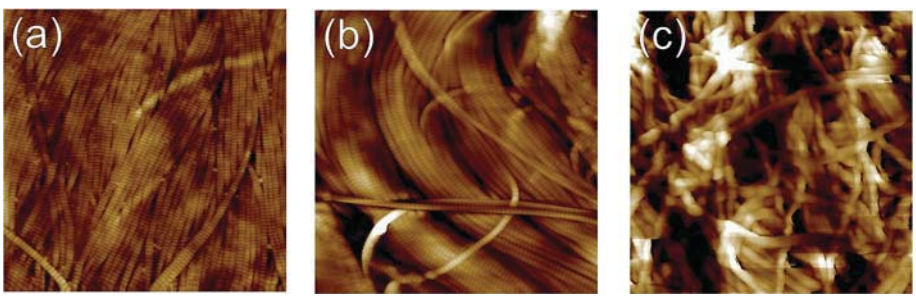

Fig. 9 Atomic force microscopy height images for (a) native bovine pericardium (b) chondroitinase ABC treated pericardium (c) glutaraldehyde treated pericardium. Images are 5 μm square.

may be better understood in terms of the structural changes that lead to altered physical properties. A careful balance of cross linking is then is required to achieve the properties required for in-service applications.

5. Conclusions

We have found that the extent and nature of cross linking present in pericardium has an impact on the collagen fibril orientation. When additional cross links with glutaraldehyde are added the fibrils form more of a network structure. We suggest that formation of cross links *via* glutaraldehyde addition progressively constrains the fibrils into a random network. The relationship between cross linking and fibril alignment provides a perspective on the importance of cross links in determining the structure of tissues. This could have relevance both in the preparation of new biomaterials and in the understanding and treatment of ageing and disorders in human tissues.

Acknowledgements

This research was undertaken on the SAXS/WAXS beamline at the Australian Synchrotron, Victoria, Australia. The NZ Synchrotron Group Ltd is acknowledged for travel funding. John Shannon and Southern Lights Biomaterials supplied the pericardium. Melissa Basil-Jones of Massey University assisted with data collection. Meekyung Ahn assisted with the microtoming and GAG assay, Richard Edmonds assisted with the mechanical tests.

Notes and references

1 D. R. Stamov and T. Pompe, *Soft Matter*, 2012, **8**, 10200–10212.
2 R. C. Picu, *Soft Matter*, 2011, **7**, 6768–6785.
3 J. E. Scott and R. A. Stockwell, *J. Physiol.*, 2006, **574**, 643–650.
4 A. M. Cribb and J. E. Scott, *J. Anat.*, 1995, **187**, 423–428.
5 J. E. Scott, *J. Physiol.*, 2003, **553**, 335–343.
6 R. G. Haverkamp, M. A. K. Williams and J. E. Scott, *Biomacromolecules*, 2005, **6**, 1816–1818.
7 Y. Chan, G. M. Cox, R. G. Haverkamp and J. M. Hill, *Eur. Biophys. J.*, 2009, **38**, 487–493.
8 R. Puxkandl, I. Zizak, O. Paris, J. Keckes, W. Tesch, S. Bernstorff, P. Purslow and P. Fratzl, *Philos. Trans. R. Soc. London*, 2002, **357**, 191–197.
9 S. W. Cranford and M. J. Buehler, *Soft Matter*, 2013, **9**, 1076–1090.
10 G. Fessel and J. G. Snedeker, *J. Theor. Biol.*, 2011, **268**, 77–83.
11 A. Redaelli, S. Vesentini, M. Soncini, P. Vena, S. Mantero and F. M. Montevecchi, *J. Biomech.*, 2003, **36**, 1555–1569.
12 R. G. Haverkamp, A. T. Marshall and M. A. K. Williams, *J. Phys. Chem. B*, 2007, **111**, 13653–13657.
13 S. Rigozzi, A. Stemmer, R. Muller and J. G. Snedeker, *J. Struct. Biol.*, 2011, **176**, 9–15.
14 G. Fessel and J. G. Snedeker, *Matrix Biol.*, 2009, **28**, 503–510.
15 R. B. Svensson, T. Hassenkam, P. Hansen, M. Kjaer and S. P. Magnusson, *Connect. Tissue Res.*, 2011, **52**, 415–421.
16 J. E. Scott, *J. Anat.*, 1995, **187**, 259–269.
17 A. J. Bailey, *Mech. Ageing Dev.*, 2001, **122**, 735–755.
18 M. E. Francis-Sedlak, S. Uriel, J. C. Larson, H. P. Greisler, D. C. Venerus and E. M. Brey, *Biomaterials*, 2009, **30**, 1851–1856.
19 D. J. Leeming, K. Henriksen, I. Byrjalsen, P. Qvist, S. H. Madsen, P. Garnero and M. A. Karsdal, *Osteoporosis Int.*, 2009, **20**, 1461–1470.
20 I. J. Reece, R. Vannoort, T. R. P. Martin and M. M. Black, *Ann. Thorac. Surg.*, 1982, **33**, 480–485.
21 S. E. Langdon, R. Chernecky, C. A. Pereira, D. Abdulla and J. M. Lee, *Biomaterials*, 1999, **20**, 137–153.
22 C. S. Kamma-Lorger, C. Boote, S. Hayes, J. Moger, M. Burghammer, C. Knupp, A. J. Quantock, T. Sorensen, E. Di Cola, N. White, R. D. Young and K. M. Meek, *J. Struct. Biol.*, 2010, **169**, 424–430.
23 T. L. Sellaro, D. Hildebrand, Q. J. Lu, N. Vyavahare, M. Scott and M. S. Sacks, *J. Biomed. Mater. Res., Part A*, 2007, **80A**, 194–205.
24 J. Liao, L. Yang, J. Grashow and M. S. Sacks, *J. Biomech. Eng.*, 2007, **129**, 78–87.
25 T. W. Gilbert, S. Wognum, E. M. Joyce, D. O. Freytes, M. S. Sacks and S. F. Badylak, *Biomaterials*, 2008, **29**, 4775–4782.
26 P. P. Purslow, T. J. Wess and D. W. L. Hukins, *J. Exp. Biol.*, 1998, **201**, 135–142.
27 M. M. Basil-Jones, R. L. Edmonds, S. M. Cooper and R. G. Haverkamp, *J. Agric. Food Chem.*, 2011, **59**, 9972–9979.
28 K. H. Sizeland, R. G. Haverkamp, M. M. Basil-Jones, R. L. Edmonds, S. M. Cooper, N. Kirby and A. Hawley, *J. Agric. Food Chem.*, 2013, **61**, 887–892.
29 M. M. Basil-Jones, R. L. Edmonds, G. E. Norris and R. G. Haverkamp, *J. Agric. Food Chem.*, 2012, **60**, 1201–1208.
30 J. Liao, L. Yang, J. Grashow and M. S. Sacks, *Acta Biomater.*, 2005, **1**, 45–54.
31 K. L. Billiar and M. S. Sacks, *J. Biomech.*, 1997, **30**, 753–756.
32 J. W. Y. Jor, P. M. F. Nielsen, M. P. Nash and P. J. Hunter, *Skin Res. Technol.*, 2011, **17**, 149–159.
33 A. L. Schofield, C. I. Smith, V. R. Kearns, D. S. Martin, T. Farrell, P. Weightman and R. L. Williams, *J. Phys. D: Appl. Phys.*, 2011, **44**, 335302.
34 J. Friedrichs, A. Taubenberger, C. M. Franz and D. J. Muller, *J. Mol. Biol.*, 2007, **372**, 594–607.
35 N. Nwaejike and R. Ascione, *J. Cardiac Surg.*, 2011, **26**, 31–33.
36 J. M. G. Paez, A. C. Sanmartin, E. J. Herrero, I. Millan, A. Cordon, A. Rocha, M. Maestro, R. Burgos, G. Tellez and J. L. Castillo-Olivares, *J. Biomed. Mater. Res., Part A*, 2006, **77**, 839–849.
37 A. Mirnajafi, B. Zubiate and M. S. Sacks, *J. Biomed. Mater. Res., Part A*, 2010, **94**, 205–213.
38 A. Mirnajafi, J. Raymer, M. J. Scott and M. S. Sacks, *Biomaterials*, 2005, **26**, 795–804.
39 M. Yang, C. Z. Chen, X. N. Wang, Y. B. Zhu and Y. J. Gu, *J. Biomed. Mater. Res., Part B*, 2009, **91**, 354–361.

40 P. R. Umashankar, T. Arun and T. V. Kumari, *J. Biomed. Mater. Res., Part A*, 2011, **97**, 311–320.
41 M. B. Schmidt, V. C. Mow, L. E. Chun and D. R. Eyre, *J. Orthop. Res.*, 1990, **8**, 353–363.
42 D. Cookson, N. Kirby, R. Knott, M. Lee and D. Schultz, *J. Synchrotron Radiat.*, 2006, **13**, 440–444.
43 M. S. Sacks, D. B. Smith and E. D. Hiester, *Ann. Biomed. Eng.*, 1997, **25**, 678–689.
44 L. F. Nielsen, D. Moe, S. Kirkeby and C. Garbarsch, *Biotech. Histochem.*, 1998, **73**, 71–77.
45 L. C. U. Junqueira, G. S. Montes and E. M. Sanchez, *Histochemistry*, 1982, **74**, 153–156.
46 D. Dayan, Y. Hiss, A. Hirshberg, J. J. Bubis and M. Wolman, *Histochemistry*, 1989, **93**, 27–29.
47 R. H. Stinson and P. R. Sweeny, *Biochim. Biophys. Acta*, 1980, **621**, 158–161.
48 M. M. Basil-Jones, R. L. Edmonds, T. F. Allsop, S. M. Cooper, G. Holmes, G. E. Norris, D. J. Cookson, N. Kirby and R. G. Haverkamp, *J. Agric. Food Chem.*, 2010, **58**, 5286–5291.
49 L. H. H. O. Damink, P. J. Dijkstra, M. J. A. Van Luyn, P. B. Van Wachem, P. Nieuwenhuis and J. Feijen, *J. Mater. Sci.: Mater. Med.*, 1995, **6**, 460–472.
50 D. T. Cheung, N. Perelman, E. C. Ko and M. E. Nimni, *Connect. Tissue Res.*, 1985, **13**, 109–115.
51 D. T. Cheung and M. E. Nimni, *Connect. Tissue Res.*, 1982, **10**, 201–216.
52 K. H. Sizeland, H. C. Wells, J. J. Higgins, C. M. Cunanan, N. Kirby, A. Hawley and R. G. Haverkamp, *BioMed Res. Int.*, 2014, **2014**, 189197.
53 J. E. Scott and C. R. Orford, *Biochem. J.*, 1981, **197**, 213–216.
54 J. E. Scott, *Biochem. J.*, 1980, **187**, 887–891.
55 E. W. Floden, S. Malak, M. M. Basil-Jones, L. Negron, J. N. Fisher, M. Byrne, S. Lun, S. G. Dempsey, R. G. Haverkamp, I. Anderson, B. R. Ward and B. C. H. May, *J. Biomed. Mater. Res., Part B*, 2010, **96**, 67–75.

JOURNAL OF APPLIED PHYSICS **117**, 044701 (2015)

Poisson's ratio of collagen fibrils measured by small angle X-ray scattering of strained bovine pericardium

Hannah C. Wells,[1] Katie H. Sizeland,[1] Hanan R. Kayed,[1] Nigel Kirby,[2] Adrian Hawley,[2] Stephen T. Mudie,[2] and Richard G. Haverkamp[1,a)]
[1]*School of Engineering and Advanced Technology, Massey University, Private Bag 11222, Palmerston North 4442, New Zealand*
[2]*Australian Synchrotron, 800 Blackburn Road, Clayton, Victoria 3168, Australia*

(Received 26 August 2014; accepted 7 December 2014; published online 26 January 2015)

Type I collagen is the main structural component of skin, tendons, and skin products, such as leather. Understanding the mechanical performance of collagen fibrils is important for understanding the mechanical performance of the tissues that they make up, while the mechanical properties of bulk tissue are well characterized, less is known about the mechanical behavior of individual collagen fibrils. In this study, bovine pericardium is subjected to strain while small angle X-ray scattering (SAXS) patterns are recorded using synchrotron radiation. The change in d-spacing, which is a measure of fibril extension, and the change in fibril diameter are determined from SAXS. The tissue is strained 0.25 (25%) with a corresponding strain in the collagen fibrils of 0.045 observed. The ratio of collagen fibril width contraction to length extension, or the Poisson's ratio, is 2.1 ± 0.7 for a tissue strain from 0 to 0.25. This Poisson's ratio indicates that the volume of individual collagen fibrils decreases with increasing strain, which is quite unlike most engineering materials. This high Poisson's ratio of individual fibrils may contribute to high Poisson's ratio observed for tissues, contributing to some of the remarkable properties of collagen-based materials.
[http://dx.doi.org/10.1063/1.4906325]

I. INTRODUCTION

Type I collagen is a key structural material in animals. It is the main structural component of skin and tendons. Type I collagen is also important in products made from animal skin, or related tissues, such as leather and extracellular matrix scaffolds for surgical applications.[1,2] Type II collagen has a fairly similar fibril structure to type I collagen, although with more branching and cross-linking, and is the main structural component of tissues, such as cartilage, therefore parallels may be drawn between type I and type II collagens. The mechanical properties of collagen-based materials are central to the natural and industrial uses of these materials and have been studied in a variety of tissues.

The bulk mechanical properties of tissues have been well characterised, including measurements of Poisson's ratio. Poisson's ratio, ν, is the ratio of transverse strain $\Delta W/W$ (where W is width of a cube or bar) to longitudinal strain $\Delta L/L$ (where L is the length of a cube or bar) in the loading direction

$$\nu = -\frac{(\Delta W/W)}{\Delta L/L}. \quad (1)$$

For isotropic materials, $\nu > 0.5$ is excluded on theoretical grounds, however, fibrillar collagen is anisotropic. When $\nu > 0.5$ for a material under tension, the volume decreases as the tissue is strained. A wide range of values of ν have been measured for type I and II collagen materials in compression and tension, with many of these giving $\nu > 0.5$. These include tendon under compression[3] with $\nu = 0.8$, spinal dura mater under uniaxial tension $\nu = 0.5$–1.6 depending on the direction of the tissue section taken,[4] bovine articular cartilage in compression[5,6] $\nu = 0.15$–0.20 and 0.16 measured by microindentation,[7] and human patellar cartilage measured in tension[8] $\nu = 0.6$–1.9. The Poisson's ratio in tendon fascicles has been shown to increase with stress[9] up to $\nu = 4$ and in articular cartilage up to $\nu = 1.2$ with increasing strain.[10]

While the mechanical properties of tissue have been well characterized, the mechanical properties of individual collagen fibrils that constitute the tissue are less well known. Collagen fibril diameter has been shown to have some influence on tissue strength.[11,12] In addition, proteogylcan connections between collagen fibrils in tendon subjected to tensile stress have been suggested as contributing to the strength of the tissue.[13,14] Examination of individual collagen fibrils in rat tail tendon with atomic force microscopy can yield an estimate of the Poisson's ratio measured in compression in a transverse direction.[15,16]

Modeling of the crimp present in many collagen tissues, such a tendon and ligament or helical structure of the fibrils, has suggested that these features could explain much of the high Poisson's ratio of the tissue composed of collagen.[17] It has also been suggested that in tendon, the strain may be taken up by sliding of fibrils within the tendon rather than by extension of the collagen fibrils.[18] In leather, where there is

a)r.haverkamp@massey.ac.nz

very little crimp, the reorientation of fibrils may be an important mechanism for absorbing strain.[19,20]

Here, the behavior of individual fibrils of collagen I as strain is applied is studied using small angle X-ray scattering (SAXS) to simultaneously measure the fibril length extension and fibril diameter contraction. Bovine pericardium is used as a model material for this work because it is elastic and strong and has application in medical devices.[21]

II. MATERIALS AND METHODS

Fresh bull (Charolais Cross) pericardium samples were obtained from John Shannon, Wairapara, New Zealand, within 2 h of slaughter. The tissue was cut into rectangles ca. 50 mm × 6 mm, with the long axis aligning with the long axis of the heart. The pericardium was washed for 24 h in a 1% octylphenol ethylene oxide condensate (Triton X-100, Sigma), 0.02% EDTA solution made up in phosphate buffered saline (PBS) (Lorne Laboratories Ltd).[22] The samples were stored in PBS. SAXS diffraction patterns were recorded at room temperature while the pericardium was wet.

For transmission electron microscopy (TEM), samples were fixed with 2% formaldehyde and 3% glutaraldehyde in phosphate buffer, post fixed with 1% OsO_4 and dehydrated using an acetone/water series. The sections were stained with uranyl acetate and then with lead citrate and examined with a Philips CM10 TEM (Philips, Eindhoven, The Netherlands). These show the collagen fibrils with the d-banding visible (Fig. 1).

A stretching apparatus was built as described previously.[19] A linear motor, Linmot PS01 48 × 240/30 × 180-C (NTI AG, Switzerland), was mounted on a purpose-built frame. Clamps to hold the pericardium were fitted between the linear motor and a L6D OIML single-point loadcell (Hangzhou Wanto Precision Technology Co., Zhejiang, China). The pericardium was mounted horizontally without tension. The sample (30 mm between jaws) was stretched in 1 mm increments to take up the slack until a force was just registered by the loadcell, then backed off so that it was not under tension. Diffraction patterns were collected in a 0.5 mm grid of eight points. The sample was stretched in 1 mm increments and maintained for 1 min at each extension to stabilize before SAXS patterns, the extension and the force information were recorded. This process was repeated until the sample failed, with the interval between strain increments around 8–13 min.

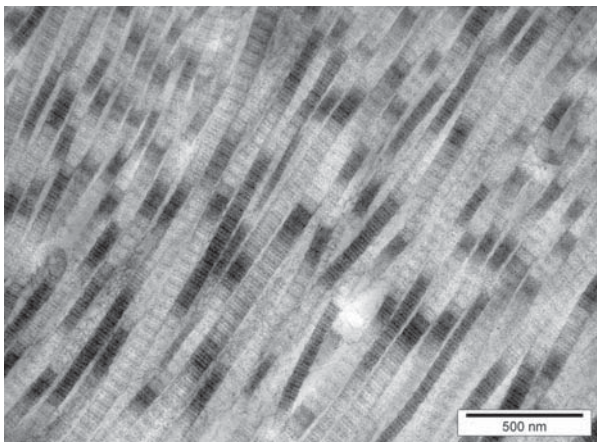

FIG. 1. Transmission electron microscopy of pericardium.

The diffraction patterns were recorded on the Australian Synchrotron SAXS/WAXS beamline which uses a high-intensity undulator source. An X-ray energy of 12 keV was used with energy resolution of 10^{-4} (e.g., 1×10^{-4} for 1 radiation) from a cryo-cooled Si(111) double-crystal monochromator with a beam size (FWHM focused at the sample) of $250 \times 80\ \mu$m, and a total photon flux of about 2×10^{12} ph s^{-1}. A Pilatus 1 M detector with an active area of 170×170 mm and a sample-to-detector distance of 3371 mm was used. Exposure time was 1 s and data processing was carried out using the SAXS15ID software.[23] Each data point presented is the average from of a minimum of eight diffraction patterns recorded on a grid of positions on the sample.

Fibril diameters were calculated from the SAXS data using the Irena software package[24] running within Igor Pro. The data were fitted at the wave vector Q, in the range of 0.01–0.04 $Å^{-1}$ and at an azimuthal angle which was 90° to the long axis of most of the collagen fibrils. This angle was selected by determining the average orientation of the collagen fibrils from the azimuthal angle for the maximum intensity of the d-spacing diffraction peaks. The "cylinder AR" shape model with an arbitrary aspect ratio of 30 was used for all fitting. We did not attempt to individually optimize this aspect ratio and the unbranched length of collagen fibrils may in practice have a length that exceeds an aspect ratio of 30.

The d-spacing was determined from the position of the centre of a Gaussian curve fitted to the 9th order diffraction peak taken from the integrated intensity plots from the azimuthal range from 45° to 135°. The orientation index (OI) is defined by

$$OI = (90^\circ - OA)/90^\circ, \tag{2}$$

where OA (orientation angle) is the minimum azimuthal angle range that contains 50% of the fibrils, based on the method of Sacks for light scattering[25] but converted to an index,[26] using the spread in azimuthal angle of one or more d-spacing diffraction peaks. The OI is used to give a measure of the spread of fibril orientation (an OI of 1 indicates the fibrils are parallel to each other; 0 indicates the fibrils are randomly oriented).

III. RESULTS AND DISCUSSION

The integrated intensity plots show well-defined peaks corresponding to the collagen d-period (Fig. 2). The odd numbered peaks have a much higher intensity than the even numbered peaks, a characteristic attributed to a fully hydrated sample.[27] At right angles to the direction of alignment, the d-peaks are not as apparent, and the scattering results from the fibril diameter distribution. The diffraction that is no longer present at an azimuthal angle rotated by 90° is due to the d-banding, while the broader features that remain or enhanced are due to the fibril diameter or fibrillar spacing.

The stress-strain curve recorded from the *in-situ* stretching is shown in Fig. 3. The maximum strain obtained before

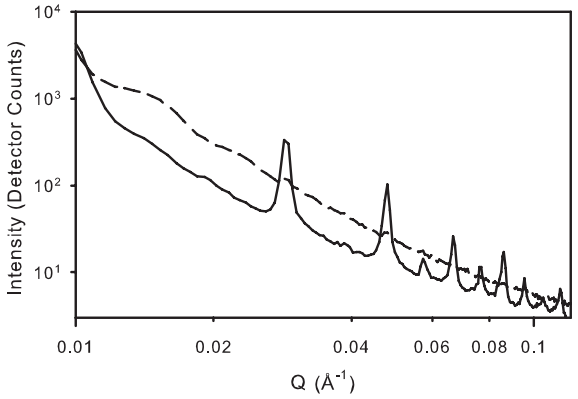

FIG. 2. Representative integrated scattering pattern of pericardium. Solid line—at an azimuthal angle segment centered 90°, which is used for assessing d-spacing; dashed line—at an azimuthal angle segment centered on 0°, which is used for fibril diameter.

rupture was 25%. The time dependency of the stress-strain curve was not considered as it has been found not to affect elastic properties[4] and the time between each data point was approximately constant.

There are two stages in the structural changes at the collagen fibril level we observe. In the first stage (up to a strain, fractional change in length, of about 0.09), we observe is a decrease in collagen fibril diameter with a small increase in d-spacing and a large increase in OI. During this stage, the strain is taken up by reorientation of the fibrils. Pericardium has a marked crimp so that a portion of the observed OI can be due to crimp. It is trivial to show that the shape of the curve from which the OI is derived, if the crimp takes a sinusoidal shape, should have the form

$$I = A\sin(\phi)\cos(\phi), \tag{3}$$

where I is the diffraction peak intensity, ϕ is the azimuthal angle, and A is the magnitude of the crimp. It has been shown elsewhere that, during biaxial strain crimp is maintained,[28] therefore we believe the change in OI is largely due to fibril reorientation rather than straightening of crimp.

During the second stage of strain, there is no significant change in the OI but the d-spacing increases markedly (fibril length) and the fibril diameter decreases (Fig. 4). The

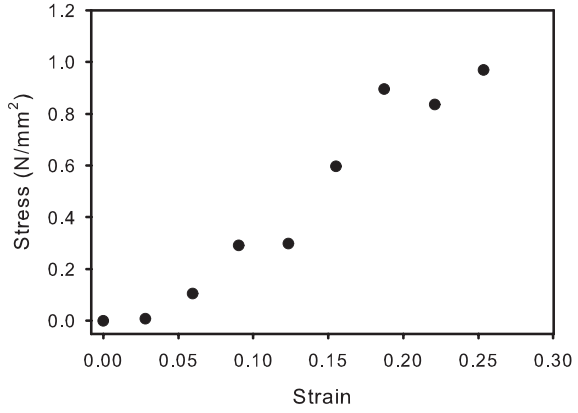

FIG. 3. Stress-strain curve measured on pericardium during *in situ* SAXS measurements.

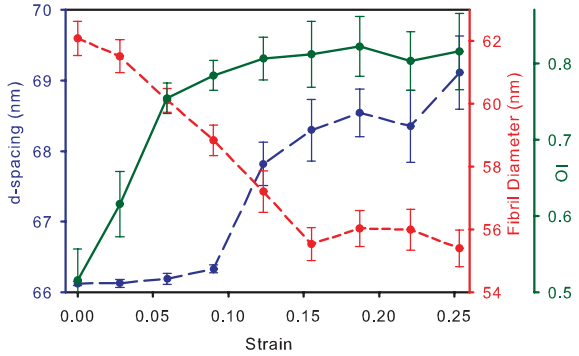

FIG. 4. d-spacing (long dash, blue), fibril diameter (short dash, red), and OI (solid, green) changes with increasing strain. Lines are a guide for the eye only.

d-spacing can be thought of as an internal strain gauge for the collagen fibrils with an increase in d-spacing, indicating an increase in stress on the fibril. At a tissue strain above 0.15, the fibrils continue to stretch but there is a decrease in fibril diameter plateaus. From the unstrained state to the maximum strain state, the d-spacing increases from 66.13 nm to 69.12 nm, a change of 2.99 nm or 4.5%. The OI increases from 0.53 to 0.75 (at a strain of 0.09) and then is stable at around 0.80 at higher strain values (Fig. 4). Fibril diameter decreases from 62.1 nm for the unstretched collagen to 55.4 nm at the maximum strain experienced (Fig. 4), a decrease in 6.7 nm or 10.8%. At first, while the fibril diameter changes, there is little change in d-spacing, then at higher strain, as the fibril diameter decreases, the d-spacing increases.

During this second stage of strain, the change in d-spacing strain (fibril strain) is about 30% of the whole tissue strain. This shows that the strain in the tissue is taken up partly by the strain in the collagen fibrils, as has been observed with light scattering[28] and partly by the tissue strain being transferred to interfibrillar sliding or rearrangement of the fibrils. By contrast, in weak ovine leather (data taken from published work[19]), our calculations of fibril strain versus leather strain give 10% d-spacing strain to whole tissue strain for leather. The collagen fibrils in leather are less aligned than in pericardium, allowing more possibility for realignment. For rat tail tendon, this ratio is 40% for the second (linear) region of the strain curve,[29] perhaps reflecting the high alignment of collagen in tendon.

From the d-spacing change and fibril diameter change, we calculate the Poisson's ratio. Since ν is defined for a cube, we correct the ratio by $\sqrt{\pi}/2$ to account for the approximately cylindrical shape of the collagen fibril (in order to retain the property that a Poisson's ratio of 0.5 represents a material in which the volume does not change with strain). So that the equivalent Poisson's ratio, ν', can be calculated for a rod with diameter D by

$$\nu' = -\frac{\sqrt{\pi}/2(\Delta D/D)}{\Delta L/L}. \tag{4}$$

For collagen in bovine pericardium, at low strain, the Poisson's ratio appears to have a very high value (15–27), but for strain above 0.09, the Poisson's ratio is in the range 2.1–2.8. For the total strain (from 0 to 0.25), the change in

d-spacing and diameter gives $\nu' = 2.1 \pm 0.7$ (these values of ν' can be calculated from Fig. 4). The $\nu' > 0.5$ could be due to tighter packing within the fibril under strain, which may include compression of hydrogen bonding in the fibril, microfibril, or tropocollagen. The extension of the fibrils with increasing strain has previously been ascribed largely to the sliding of the tropocollagen within the fibrils, resulting in an increase in the gap region, rather than to the extension of the tropocollagen molecules that constitute the fibrils.[30] We note that the stress-strain curve does not show a marked foot region, it does not exhibit a low Young's modulus at low strain, which suggests that an entropic straightening of the fibrils may not be a major factor in the strain of the material.

We can know, because of the evidence provided by the OI, that this Poisson's ratio we measure must be due largely to stretching of the fibrils and not to changes in crimp. A straightening of crimp must result in an increase in OI (as can be derived from the relationship represented by (2)), and there was no large increase in OI after the first 0.05 strain and therefore there must be no change in crimp above 0.05 strain.

Using data from a recently published atomic force microscope study on tendon,[31] we calculate $\nu' = 1.9$ (tendon was stretched by 15%), similar to the value we find from our measurements.

IV. CONCLUSIONS

While it has previously been shown that bulk materials based on collagen may have $\nu > 0.5$, we have provided experimental evidence that the collagen fibrils also may have $\nu' > 0.5$. Therefore, this property of collagen fibrils may contribute to the bulk properties of the tissue.

Previously, it has been proposed that much of the high Poisson's ratio of tendon and cartilage is due to the volume loss from fluid exudation[32] although specific attempts to measure this have not always shown water to be exuded.[10,33] We now demonstrate that there is a contribution to the high Poisson's ratio of the tissue from the high Poisson's ratio of the collagen fibrils. This does not exclude the possibility that water is exuded from the fibrils.

ACKNOWLEDGMENTS

This research was undertaken on the SAXS/WAXS beamline at the Australian Synchrotron, Victoria, Australia. The NZ Synchrotron Group Ltd., is acknowledged for travel funding. Melissa Basil-Jones assisted with data collection. John Shannon of Wairarapa supplied the pericardium. Jordan Taylor of the Manawatu Microscopy Centre assisted with TEM. Sue Hallas of Nelson assisted with the editing. The anonymous reviewers are thanked for their input.

[1]E. Floden, S. Malak, M. Basil-Jones, L. Negron, J. Fisher, M. Byrne, S. Lun, S. Dempsey, R. Haverkamp, I. Anderson, B. Ward, and B. May, J. Biomed. Mater. Res. B **96B**, 67–75 (2011).
[2]M. W. Clemens, J. C. Selber, J. Liu, D. M. Adelman, D. P. Baumann, P. B. Garvey, and C. E. Butler, Plastic Reconstr. Surg. **131**, 71–79 (2013).
[3]V. W. T. Cheng and H. R. C. Screen, J. Mater. Sci. **42**, 8957–8965 (2007).
[4]C. Persson, S. Evans, R. Marsh, J. L. Summers, and R. M. Hall, Ann. Biomed. Eng. **38**, 975–983 (2010).
[5]J. S. Jurvelin, M. D. Buschmann, and E. B. Hunziker, J. Biomech. **30**, 235–241 (1997).
[6]P. Kiviranta, J. Rieppo, R. K. Korhonen, P. Julkunen, J. Toyras, and J. S. Jurvelin, J. Orthop. Res. **24**, 690–699 (2006).
[7]G. J. Miller and E. F. Morgan, Osteoarthritis Cartilage **18**, 1051–1057 (2010).
[8]D. M. Elliott, D. A. Narmoneva, and L. A. Setton, J. Biomech. Eng. **124**, 223–228 (2002).
[9]S. P. Reese and J. A. Weiss, J. Biomech. Eng. **135**, 034501 (2013).
[10]L. Edelsten, J. E. Jeffrey, L. V. Burgin, and R. M. Aspden, Soft Matter **6**, 5206–5212 (2010).
[11]D. A. D. Parry, G. R. G. Barnes, and A. S. Craig, Proc. R. Soc. London, Ser. B **203**, 305–321 (1978).
[12]H. C. Wells, R. L. Edmonds, N. Kirby, A. Hawley, S. T. Mudie, and R. G. Haverkamp, J. Agric. Food Chem. **61**, 11524–11531 (2013).
[13]A. M. Cribb and J. E. Scott, J. Anat. **187**, 423–428 (1995).
[14]R. G. Haverkamp, M. A. K. Williams, and J. E. Scott, Biomacromolecules **6**, 1816–1818 (2005).
[15]M. P. E. Wenger and P. Mesquida, Appl. Phys. Lett. **98**, 163707 (2011).
[16]M. Minary-Jolandan and M.-F. Yu, Biomacromolecules **10**, 2565–2570 (2009).
[17]S. P. Reese, S. A. Maas, and J. A. Weiss, J. Biomech. **43**, 1394–1400 (2010).
[18]H. R. C. Screen, D. L. Bader, D. A. Lee, and J. C. Shelton, Strain **40**, 157–163 (2004).
[19]M. M. Basil-Jones, R. L. Edmonds, G. E. Norris, and R. G. Haverkamp, J. Agric. Food Chem. **60**, 1201–1208 (2012).
[20]K. H. Sizeland, M. M. Basil-Jones, R. L. Edmonds, S. M. Cooper, N. Kirby, A. Hawley, and R. G. Haverkamp, J. Agric. Food Chem. **61**, 887–892 (2013).
[21]K. H. Sizeland, H. C. Wells, J. J. Higgins, C. M. Cunanan, N. Kirby, A. Hawley, and R. G. Haverkamp, BioMed Res. Int. **2014**, 189197.
[22]M. Yang, C. Z. Chen, X. N. Wang, Y. B. Zhu, and Y. J. Gu, J. Biomed. Mater. Res. B **91B**, 354–361 (2009).
[23]D. Cookson, N. Kirby, R. Knott, M. Lee, and D. Schultz, J. Synchrotron. Radiat. **13**, 440–444 (2006).
[24]J. Ilavsky and P. R. Jemian, J. Appl. Crystallogr. **42**, 347–353 (2009).
[25]M. S. Sacks, D. B. Smith, and E. D. Hiester, Ann. Biomed. Eng. **25**, 678–689 (1997).
[26]M. M. Basil-Jones, R. L. Edmonds, S. M. Cooper, and R. G. Haverkamp, J. Agric. Food Chem. **59**, 9972–9979 (2011).
[27]R. H. Stinson and P. R. Sweeny, Biochim. Biophys. Acta **621**, 158–161 (1980).
[28]M. S. Sacks, Trans. ASME J. Biomech. Eng. **125**, 280–287 (2003).
[29]P. Fratzl, K. Misof, I. Zizak, G. Rapp, H. Amenitsch, and S. Bernstorff, J. Struct. Biol. **122**, 119–122 (1998).
[30]N. Sasaki and S. Odajima, J. Biomech. **29**, 1131–1136 (1996).
[31]S. Rigozzi, R. Muller, A. Stemmer, and J. G. Snedeker, J. Biomech. **46**, 813–818 (2013).
[32]S. Adeeb, A. Ali, N. Shrive, C. Frank, and D. Smith, Comput. Methods Biomech. **7**, 33–42 (2004).
[33]K. G. Helmer, G. Nair, M. Cannella, and P. Grigg, Trans. ASME J. Biomech. Eng. **128**, 733–741 (2006).

JOURNAL OF AGRICULTURAL AND FOOD CHEMISTRY

Article

pubs.acs.org/JAFC

Changes to Collagen Structure during Leather Processing

Katie H. Sizeland,[†] Richard L. Edmonds,[‡] Melissa M. Basil-Jones,[†] Nigel Kirby,[§] Adrian Hawley,[§] Stephen Mudie,[§] and Richard G. Haverkamp*,[†]

[†]School of Engineering and Advanced Technology, Massey University, Private Bag 11222, Palmerston North, New Zealand

[‡]Leather and Shoe Research Association, Palmerston North 4442, New Zealand

[§]Australian Synchrotron, 800 Blackburn Road, Clayton, Melbourne, Australia

Supporting Information

ABSTRACT: As hides and skins are processed to produce leather, chemical and physical changes take place that affect the strength and other physical properties of the material. The structural basis of these changes at the level of the collagen fibrils is not fully understood and forms the basis of this investigation. Synchrotron-based small-angle X-ray scattering (SAXS) is used to quantify fibril orientation and D-spacing through eight stages of processing from fresh green ovine skins to staked dry crust leather. Both the D-spacing and fibril orientation change with processing. The changes in thickness of the leather during processing affect the fibril orientation index (OI) and account for much of the OI differences between process stages. After thickness is accounted for, the main difference in OI is due to the hydration state of the material, with dry materials being less oriented than wet. Similarly significant differences in D-spacing are found at different process stages. These are due also to the moisture content, with dry samples having a smaller D-spacing. This understanding is useful for relating structural changes that occur during different stages of processing to the development of the final physical characteristics of leather.

KEYWORDS: *leather, collagen, small angle X-ray scattering, orientation*

INTRODUCTION

The leather-making process is a way of preserving skins to stop decomposition and to provide a strong and flexible material. The process consists of a series of chemical treatments and some mechanical processes. Each of the chemical treatments alters the composition of the original skin, for example, extracting components from the native skin or adding components such as cross-linking agents. In addition to changes in the chemistry of the collagen, which are well-known, it is possible that each of these processes may have an effect on the collagen structure as well, although little information has been presented on this to date.

The leather-making process consists of eight main stages, which are referred to by a variety of names in the industry, but here these are designated as fresh green, salted, pickled, pretanned, wet blue, retanned, dry crust, and dry crust staked. The "fresh green" is the skin after removal from the carcass. Skins are normally salted as a way of temporarily preserving the skin before tanning. The salt acts to slow bacterial growth by reducing water activity. Salting causes some dehydration of the skins. The "salted" is the skin after salting for preservation. The next stage of the leather-making process is the removal of the salt by soaking and washing the skins (where the skin becomes rehydrated) followed by an alkali treatment carried out in the presence of sodium sulfide ("liming") combined with suitable enzymes ("bating"), which together break down and remove some of the nonfibrous proteins, glycosaminoglycans, and other undesirable components. It is also said to "open up" the structure of the leather to enable better penetration of tanning chemicals in subsequent stages. After the alkaline treatment stage, the skin is typically adjusted back to a lower pH and is acidified in sulfuric acid and sodium chloride. After this stage the skin is referred to as "pickled". A synthetic, organic cross-linking agent and surfactant are often added at this point, which may assist with the subsequent chrome tanning stage. Stabilizing agents are often added to the pickle to raise the denaturation temperature of the collagen and thus enable skin fat to be removed more efficiently at higher temperatures. The skins at this stage are called "pretanned". After the natural skin fats are removed, the pretanned pelts are tanned using chromium sulfate. The skin after chromium tanning is called "wet blue". Chrome-tanned leather tends to be too rigid for most applications, so there is normally a second tanning stage using natural vegetable tannins or synthetic tannins to make the final leather feel softer and "fuller". After this second tanning stage, the skin is called "retanned". At this stage dyes, fat liquors, and modified fats or oils are added to complete the look and feel of the leather. After this "fat liquoring", the leather is dried and is called "dry crust". The leather is then mechanically softened or "staked" and is referred to here as "dry crust staked".

Previously it has been shown that small-angle X-ray scattering (SAXS) can provide detailed structural information on the microfibril orientation, the D-spacing, and the collagen fibril diameter in leather[1−3] and other tissues.[4,5]

The chemical treatments used to produce leather from skin and hide may result in changes to the structure of the collagen fibrils and the arrangement of these fibrils. These chemical processes include strong salt solutions, large changes in pH,

Received: December 30, 2014
Revised: February 4, 2015
Accepted: February 6, 2015
Published: February 6, 2015

enzymatic treatments to remove cross-links, and new cross-links being formed. An overview of tanning chemistry has been presented.[6] Some aspects of chemical treatments of skins and their effect on structure have been observed previously with liming of skins (increasing the pH with calcium hydroxide) showing a decrease in the D-spacing of collagen.[7] Dehydration of parchment has been shown to result in a decrease in collagen D-spacing from 64.5 to 60.0 nm.[8] Pickling and retanning agents have been shown to swell collagen fibers at low pH.[9] At low ionic strength and nonisoelectric pH, charge-dependent interactions (screening and selective ion adsorption) are prevalent in maintaining the collagen architecture,[10] which is also reflected in the greater thermal stability of collagen at low pH[11] and in the elastic response of collagen.[12]

In this work, we use SAXS to investigate the changes that take place in the microstructure of leather through the different stages of processing from skin to leather. The structural basis of these changes at the level of the collagen fibrils is not fully understood and forms the basis of this investigation.

EXPERIMENTAL PROCEDURES

Ovine pelts were obtained from 5-month-old, early-season New Zealand Romney cross lambs. Samples were removed from the same skin during several stages of processing at or near the "official sampling position" (OSP).[13] These stages were termed fresh green, salted, pickled, pretanned, wet blue, retanned, dry crust, and dry crust staked. Cross sections were cut parallel to the backbone and as close together as possible. The samples, except for dry crust and dry crust staked, all had high moisture contents because these were taken during processing.

Conventional beamhouse and tanning processes were used to generate the leather. A pelt was depilated using a caustic treatment, and then the residual keratinaceous material was removed. The pelt was washed, pretanned, and degreased using 4% (w chemical/w limed leather for all percent chemical additions unless otherwise stated) Tetrapol LTN (Shamrock Group) and 2% Zoldine ZE (The Dow Co.). Sodium formate was added followed by sodium bicarbonate, which was gradually added to increase the pH to 7.5−8. The pickled pelt was then chrome tanned.

The resulting "wet blue" pelt was first neutralized, then washed, and retanned using 2% w/w synthetic retanning agent (Tanicor PW, Clariant, Germany) and 3% w/w vegetable tanning material (mimosa, Tanac, Brazil). Fat liquor was added at a concentration of 6% by weight of wet leather and the leather processed at 50 °C for 45 min. Finally, the leather was fixed by the addition of 0.5% w/w formic acid and processed for 30 min followed by draining and washing.

Tear strengths of the leathers were tested using standard methods.[14,15] Samples (strips 1 × 50 mm) were tested on an Instron 4467. "Dry" samples were conditioned at 23 °C and 50% relative humidity for 24 h before testing following the standard method.[16] "Wet" samples were in contact with free liquid up to the point at which they were tested.

Diffraction patterns were recorded on the Australian Synchrotron SAXS/WAXS beamline, utilizing a high-intensity undulator source. Energy resolution of 10^{-4} was obtained from a cryo-cooled Si (111) double-crystal monochromator, and the beam size (fwhm focused at the sample) was 250 × 80 μm, with a total photon flux of about 2 × 10^{12} ph s^{-1}. All diffraction patterns were recorded with an X-ray energy of 11 keV using a Pilatus 1 M detector with an active area of 170 × 170 mm and a sample-to-detector distance of 3371 mm. Exposure time for diffraction patterns was 1 s, and data processing was carried out using SAXS15ID software.[17] The partially processed leather samples were sandwiched between kapton tape to prevent drying and mounted for X-ray analysis.

A custom-built stretching apparatus was built for in situ SAXS measurements as described elsewhere.[18] Strips of leather, 1 × 30 mm, cut from the OSP, were mounted horizontally without tension and without slack, with a measured separation between the jaws, typically of 15 mm. SAXS patterns were taken through the full thickness of the sample and the force and extension information recorded. The sample was stretched by 1 mm and was maintained at this extension for 1 min before patterns were recorded. This process was repeated with the sample stretched a further 1 mm each time until the sample failed.

Orientation index (OI) is defined as (90° − OA)/90°, where OA is the azimuthal angle range that contains 50% of the microfibrils centered at 180°. OI is used to give a measure of the spread of microfibril orientation (an OI of 1 indicates the microfibrils are completely parallel to each other; an OI of 0 indicates the microfibrils are completely randomly oriented). The OI is calculated from the spread in azimuthal angle of the most intense D-spacing peak (at around 0.059−0.060 $Å^{-1}$).[19]

The D-spacing was determined from Bragg's law by taking the center of a Gaussian curve fitted to the sixth-order diffraction peak of an integrated intensity plot for each spectrum.

RESULTS

Orientation Index Changes. The OI of the corium region is higher than that of the grain region throughout all of the processing stages (Figure 1). Whereas there is considerable variation in the OI during processing, the OI of the final staked dry crust leather is fairly similar to that of the fresh green skin so that overall there is not a large change in OI.

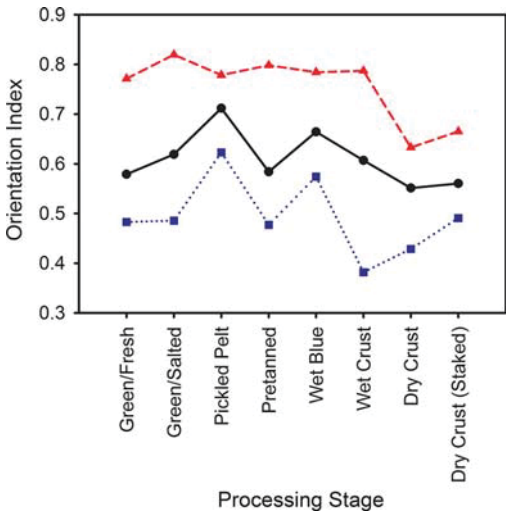

Figure 1. Variation in orientation index for all stages of processing: (red triangles) corium; (blue squares) grain; (black circles) average.

Orientation Index and Thickness. The thickness of the skin or leather varies by a factor of >2 during processing. With this variation of thickness there is a change in OI (Figure 2). The stages appear to be in two groups with the dry samples (salted, pretanned, dry crust, and dry crust staked) in one group of lower OI, which decreases with increasing thickness, and the wet samples (pickled, wet blue, retanned, and fresh green) in another group of higher OI that decreases with increasing thickness.

D-Spacing with Processing and pH. Significant changes are observed in the D-spacing of the collagen fibrils with the application of each process step (Figure 3). Both the corium and the grain regions of the leather have similar D-spacings and are similarly affected by the processing. The most significant change in D-spacing occurs with pretanning, when there is a contraction of the D-spacing of 1.4−1.5 nm (2%). The pH of the solutions in which each process takes place does not appear

DOI: 10.1021/jf506357j
J. Agric. Food Chem. 2015, 63, 2498−2505

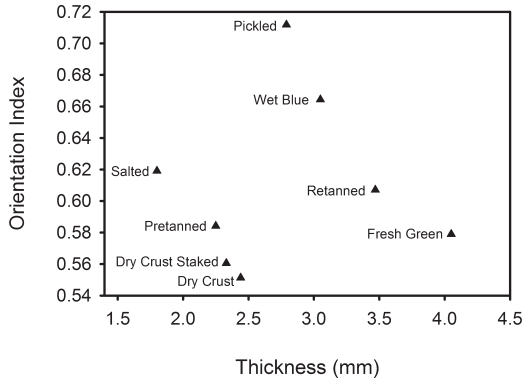

Figure 2. Fibril orientation index versus thickness.

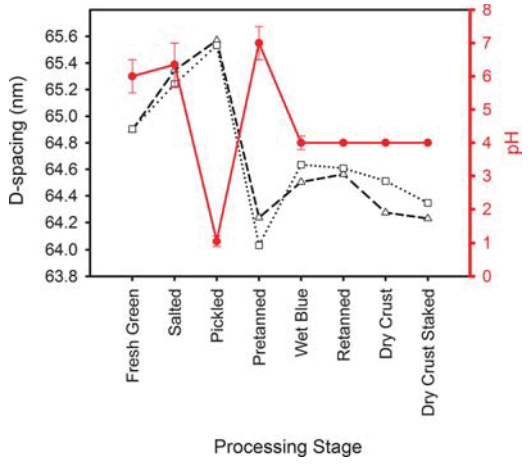

Figure 3. Variation in D-spacing and pH between different stages of processing prior to stretching: (triangles) corium; (squares) grain; (circles) pH.

to correlate with the D-spacing (Figure 4). For fresh green and salted skins the pH was measured by a surface probe rather

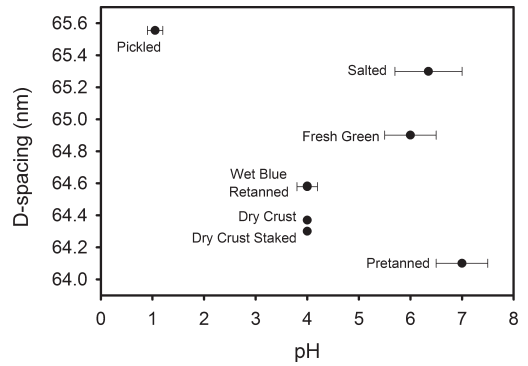

Figure 4. Variation of D-spacing with pH (wet blue and retanned points are coincident).

than the process liquor as used in the later stages. Although there is not a correlation of D-spacing with pH, it appears that there is a relationship between D-spacing and the moisture content. The three dry samples have a lower D-spacing than the wet samples.

Orientation Index and pH. The OI appears to be correlated with pH (Figure 5) (linear regression: $r^2 = 0.335$, $t = -1.74$, $P = 0.133$). However, as discussed later in the paper, we believe this correlation is not a causal relationship.

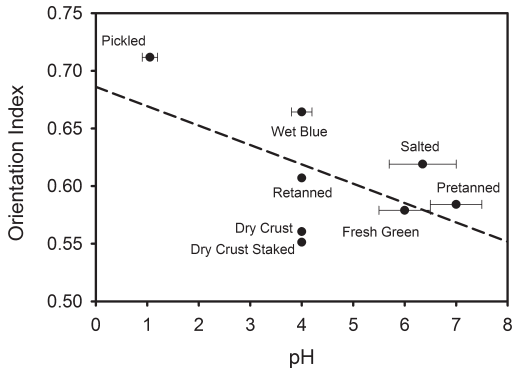

Figure 5. Correlation of OI with pH.

D-Spacing and Orientation Index. A correlation is observed between OI and D-spacing (Figure 6). The

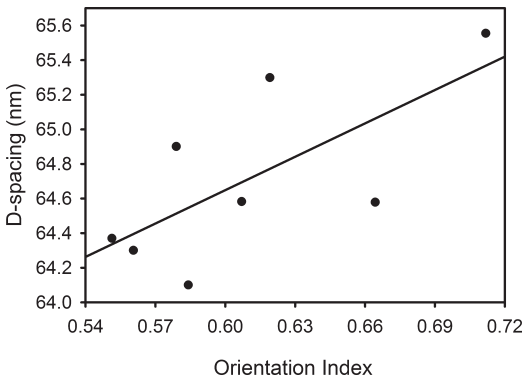

Figure 6. D-spacing versus OI for samples of different stages of processing when held without tension.

correlation is statistically significant (linear regression: $r^2 = 0.485$, $t = 2.4$, $P = 0.055$). However, as is discussed later in the paper, we believe this correlation is not a causal relationship.

Stress–Strain. Stress–strain curves were measured in situ at the synchrotron during SAXS data collection (Figure 7). The samples were not of a uniform width, so an absolute comparison of the modulus of elasticity from these curves is not possible. However, it is possible in a very general way to compare the shapes of the curves. Most of the samples show a toe region, with an initial lower elastic modulus, followed by a linear region.

Orientation Index and D-Spacing with Mechanical Stretching. There is an increase in D-spacing as the skin or leather samples are stretched (Figure 8). This increase in D-spacing is a measure of the stress being transferred to the individual fibrils, causing their length to increase. An increase in OI on stretching is also found (Figure 9) as the collagen fibrils realign in the direction of the applied force (values for the D-spacing and OI changes are found in the Supporting Information). At every stage of the leather processing, a strain applied to the samples results in an increase in OI.

DOI: 10.1021/jf506357j
J. Agric. Food Chem. 2015, 63, 2499−2505

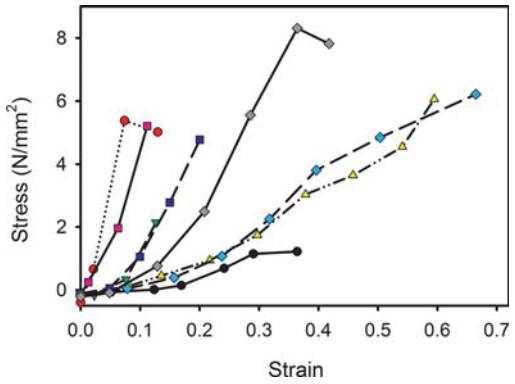

Figure 7. Stress−strain curves for each process stage, performed in situ concurrently with the SAXS measurement (not normalized for sample width or thickness): (black circles) fresh green; (red circles) salted; (green downward triangles) pickled; (yellow upward triangles) pretanned; (magenta squares) wet blue; (blue squares) retanned; (turquoise diamonds) dry crust; (gray diamonds) dry crust staked.

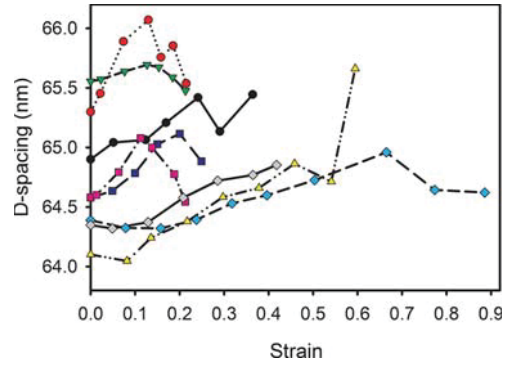

Figure 8. Changes in collagen D-spacing as samples of partially processed skin are stretched: (black circles) fresh green; (red circles) salted; (green downward triangles) pickled; (yellow upward triangles) pretanned; (blue squares) wet blue; (magenta squares) retanned; (turquoise diamonds) dry crust; (gray diamonds) dry crust staked.

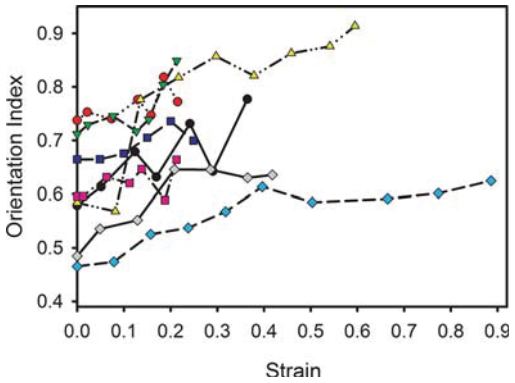

Figure 9. Changes in collagen fibril OI as samples of partially processed skin are stretched: (black circles) fresh green; (red circles) salted; (green downward triangles) pickled; (yellow upward triangles) pretanned; (blue squares) wet blue; (magenta squares) retanned; (turquoise diamonds) dry crust; (gray diamonds) dry crust staked.

DISCUSSION

We have measured the changes to the structure and arrangement of collagen fibrils in skin during several stages of the chemical processing to form leather. These build a picture of what happens in the process of transforming skin to leather.

Model of Orientation Index Change with Thickness. At the different stages of the processing of skin to leather, the thickness of the skin varies, at times becoming thicker and at other times thinner. The variation in thickness amounted to a factor of 2.25. If the collagen fibrils are not lying flat, then as the thickness of the leather increases, the angle of these fibrils to the plane of leather will increase (Figure 10). This will cause a

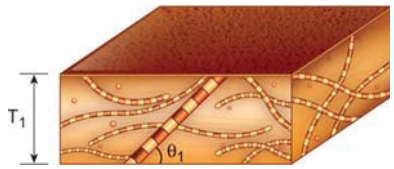

Figure 10. Illustration of the change in collagen fibril angle θ_1 to the plane of leather as the thickness T_1 of the leather changes.

change in OI. We have therefore developed a model for the change in OI with thickness changes. This enables us to determine how much of the OI change is due just to the change in thickness and how much is due to other factors.

The range of fiber angles in a sample is given by the OI, which is derived from the orientation angle, OA.[1] OA is defined as the subtended angle that contains half the fibrils; that is, it satisfies eq 1.

$$0.5 = \frac{\int_{\theta=-\mathrm{OA}/2}^{\theta=\mathrm{OA}/2} \theta N \, \mathrm{d}\theta}{\int_{\theta=-90^\circ}^{\theta=90^\circ} \theta N \, \mathrm{d}\theta} \quad (1)$$

N is the number of fibrils, and θ is the fiber angle (relative to the plane of the leather). In practice, this is determined from the SAXS diffraction pattern by the integrated intensity versus azimuthal angle for one of the D-spacing diffraction peaks, eq 2:

$$0.5 = \frac{\int_{\phi=-\mathrm{OA}/2}^{\phi=\mathrm{OA}/2} \phi I \, \mathrm{d}\phi}{\int_{\phi=-90^\circ}^{\phi=90^\circ} \phi I \, \mathrm{d}\phi} \quad (2)$$

I is the diffraction intensity of a selected D-spacing diffraction peak above a fitted background, and φ is the azimuthal angle of the diffracted X-rays.

OI is derived from OA by eq 3.

$$\mathrm{OI} = \frac{1 - \mathrm{OA}}{\mathrm{OA}} \quad (3)$$

Therefore, for perfect alignment in the reference direction, which is normally the plane of a piece of leather or skin, OI = 1; for no alignment or completely isotropic fibrils, OI = 0; and for perfect alignment at right angles to the reference direction, OI = −1.

If a sample of leather containing a fiber expands in thickness uniformly, and the fiber is at an angle θ_1 from the base (Figure 10), then the new angle of the fiber, θ_2, depends on the change in thickness by eq 4.

$$\frac{T_2}{T_1} = \frac{\tan \theta_2}{\tan \theta_1} \quad (4)$$

T_1 is the original thickness, and T_2 is the new thickness.

Rearranging eq 4 for θ_2 gives the new angle of the fiber after the leather has increased in thickness:

DOI: 10.1021/jf506357j
J. Agric. Food Chem. 2015, 63, 2499−2505

$$\theta_2 = \tan^{-1}\left(\frac{T_2}{T_1}\tan\theta_1\right) \quad (5)$$

It is then possible to calculate a transformed OA after stretching. The OA defines the subtended angle of 50% of the fibers. Therefore, fibers that have an initial angle from the reference angle of greater than half the OA will, after transformation, still have an angle greater than the transformed OA; fibers that have an initial angle lower than half the OA will, after transformation, still have an angle lower than half the transformed OA. In other words, the 50% inside the OA will remain inside the OA, the 50% outside the OA will remain outside the OA. Therefore, it is only necessary to calculate the transformation by eq 5 of the angle that is the OA to calculate the new OA that represents the new fiber distribution.

As an illustration of the extent of this change, for thickness changes similar to those observed here, some values are listed in Table 1. Note that expanding the thickness sufficiently results in an alignment of fibers vertically (negative OI).

Table 1. Calculated Change in Orientation Index of Collagen Fibrils for Different Thicknesses of Material

	new OI when		
starting OI	T_2/T_1 = 1.5	T_2/T_1 = 2.0	T_2/T_1 = 2.5
0.00	−0.25	−0.41	−0.52
0.10	−0.16	−0.33	−0.44
0.20	−0.05	−0.23	−0.36
0.30	0.05	−0.13	−0.26
0.40	0.17	−0.01	−0.15
0.50	0.29	0.12	−0.02
0.60	0.42	0.27	0.13
0.70	0.56	0.43	0.31
0.80	0.70	0.61	0.52
0.9	0.85	0.80	0.75
1	1.00	1.00	1.00

We did also consider how the OI might be affected by the area change to the leather, with wet stages generally of larger area than dry stages. This expansion of area would influence the OI in the opposite sense to the thickness change. However, the area change of the skin is small, <5%, and can be neglected compared with the >100% change in the thickness.

With the thickness taken into account, the OI now reflects any underlying structural changes that take place during the chemical and mechanical processing of skin to leather. The OI has therefore been recalculated for each sample using the thinnest sample, the salted skin, as the reference, and the adjusted results are presented in the following analysis.

Orientation Index and Water. Once the effect of thickness on the OI is removed, it can be seen that the samples fall into two groups (Figure 11). There are the fresh green, pickled, wet blue, and retanned materials. These all have a high OI (corrected for thickness relative to salted) of around 0.8. These samples are all wet. The pretanned, dry crust, and dry crust staked all have a corrected OI of around 0.67. These samples are all dry. The salted skin also has a low OI, of 0.62, and it is also a dry sample. Therefore, the factor that separates the high OI from the low OI materials is the wetness of the samples. When these collagen materials are dried, the OI decreases. Although it might be tempting to ascribe this to a crimping of the collagen fibrils as the materials dry, which would result in a lower OI, crimping in not observed in skin (unlike in tendon or pericardium,[20] for example). Therefore, by removing the thickness effect, we have been able to identify that there is a fundamental change between wet and dry stages, but we have not determined the mechanism of this change. It is suggested that a possible mechanism could be the space filling that results from hydration creates a hindrance to the movement of fibrils and leads to a higher OI at higher moisture contents. At lower moisture contents there is more space available for fibers to bend and adjust themselves into positions resulting in lower OI.

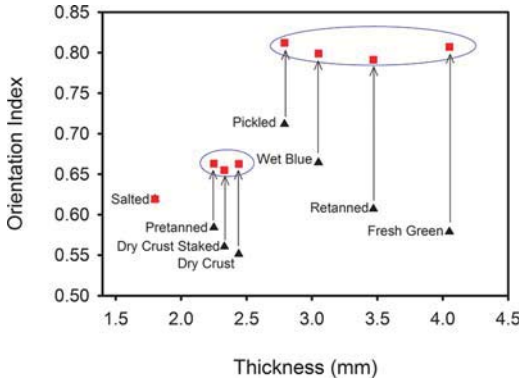

Figure 11. Fibril orientation index versus thickness: (black triangles) measured OI; (red squares) calculated OI adjusted for thickness changes (relative to salted).

D-Spacing and Orientation Index. Once the OI is corrected for thickness effects, there is no longer a statistically significant correlation between D-spacing and OI (Supporting Information, Figure S1) (linear regression: $r^2 = 0.109$, $t = 0.855$, $P = 0.426$). It is known that the result of straining leather is a straightening or alignment of the fibrils (an increase in OI) and that D-spacing measures the stress applied to individual fibrils.[18] A correlation between OI and D-spacing during different stages of processing would have suggested that these were both due to changes in internal strain in leather: when strain is released, D-spacing decreases and OI decreases. However, this was not observed here.

D-Spacing and Water. It was found that the D-spacing is lower in the dry samples by 0.38 nm; wet samples, which include fresh green, pickled, wet blue, and retanned, have an average D-spacing of 64.90 (σ = 0.46) nm, whereas dry samples, which include salted, pretanned, dry crust, and dry crust staked, have an average D-spacing of 64.52 (σ = 0.53) nm. It has previously been shown by X-ray diffraction and by atomic force microscopy that the D-spacing is moisture dependent with a reduction in D-spacing on drying.[8,21−24] This is believed to be due to the collapse of the gap and overlap regions and the partial shearing of unit cell contents within the gap region upon loss of water.[21]

D-Spacing and pH. It is perhaps a little surprising that D-spacing is not affected by pH. The D-period is affected both by the length of the tropocollagen units and by the way these tropocollagen units are assembled into the collagen fibril. The length of these structures is partially determined by the length of the hydrogen bonds between collagen molecules within the tropocollagens and by hydrophobic interactions between tropocollagen units. pH can affect hydrogen bonding, which, in collagen and other proteins, relies on a polar interaction between specific functional groups on amino acids.[10,11]

DOI: 10.1021/jf506357j
J. Agric. Food Chem. 2015, 63, 2499−2505

Mechanisms for fibril elongation by chemical treatments have previously been discussed,[20,25] and it appears that pH does not have an impact here.

Orientation Index and pH. Once the OI is corrected for thickness, it is apparent that there is no correlation between OI and pH (Supporting Information, Figure S2) (linear regression: r^2−0.0215, t = 0.488, P = 0.22). These instead fall into two groups: low OI for dry samples and high OI for wet samples, irrespective of the pH conditions.

Response to Strain. We found that when strain was applied to the samples, both the OI and D-spacing increased. It has previously been shown that upon stretching of leather, collagen fibrils first realign and then lengthen (an increase in the OI followed by an increase in the D-spacing)[18] and that collagen fibrils are very resilient with a high Poisson's ratio.[26] In pretanned, dry crust, and dry crust staked samples, the OI increased first after the first few increments in strain, and then the D-spacing increased with the further strain. These samples form a cluster at an OI of approximately 0.67 following thickness correction. The D-spacing of the wet samples (fresh green, pickled, wet blue, and retanned) increased with the first application of strain. These wet samples form a cluster with an OI of about 0.80. It is possible for the dry group to undergo more realignment with strain than the wet group because the dry samples have a lower OI initially and therefore more scope for change. Therefore, in the wet samples, because less realignment is possible, the strain was taken on by the individual collagen fibrils sooner, as shown by the immediate increase in D-spacing.

Cross-Linking. In the process of treating skin to produce leather, naturally present cross-links are removed and new cross-links are formed. The natural glycosaminoglycan cross-links are removed in the liming and bating stages so that the processed skin, known as pickled, should have fewer cross-links. New cross-links are added at the pretanned and wet blue stages. Although there have been studies on the effects of cross-linking on fibril alignment, there have been mixed conclusions drawn about the influence of cross-linking. It has been suggested that cross-links may stabilize a network structure (with fewer aligned fibrils)[27,28] and that removal of cross-links may destabilize the network structure, leading to fibrils becoming more aligned.[28] However, such behavior is not observed here during processing, where some of the cross-linking would be expected to be removed by the end of the pickled stage, and then cross-links are added by the completion of the wet blue stage.

We have found that although processing results in changes in OI, this is not a fundamental redistribution of fibrils but is rather a decrease in OI that occurs as the thickness increases and also (independently of thickness) as the water content increases. This understanding may be useful for relating structural changes that occur during different stages of processing to the development of the final physical characteristics of leather. For example, if fibril orientation is critical to strength in certain leathers, the structural relationship that should exist between the fresh skin and the final leather is now known, and it is possible to seek to maintain this characteristic during processing or modify it appropriately.

■ ASSOCIATED CONTENT

Ⓢ Supporting Information

Detailed tables of D-spacing changes in processing stages of leather with strain, OI changes in processing stages of leather with strain OI, and variation of D-spacing with OI and pH. This material is available free of charge via the Internet at http://pubs.acs.org.

■ AUTHOR INFORMATION

Corresponding Author

*(R.G.H.) E-mail: r.haverkamp@massey.ac.nz.

Funding

The New Zealand Synchrotron Group provided travel funding. The work was supported by a grant from the Ministry of Business, Innovation, and Employment.

Notes

The authors declare no competing financial interest.

■ ACKNOWLEDGMENTS

This research was undertaken on the SAXS/WAXS beamline at the Australian Synchrotron, Victoria, Australia. Sue Hallas of Nelson assisted with editing.

■ REFERENCES

(1) Basil-Jones, M. M.; Edmonds, R. L.; Allsop, T. F.; Cooper, S. M.; Holmes, G.; Norris, G. E.; Cookson, D. J.; Kirby, N.; Haverkamp, R. G. Leather structure determination by small angle X-ray scattering (SAXS): cross sections of ovine and bovine leather. *J. Agric. Food Chem.* **2010**, *58*, 5286−5291.

(2) Sturrock, E. J.; Boote, C.; Attenburrow, G. E.; Meek, K. M. The effect of the biaxial stretching of leather on fibre orientation and tensile modulus. *J. Mater. Sci.* **2004**, *39*, 2481−2486.

(3) Kronick, P. L.; Buechler, P. R. Fiber orientation in calfskin by laser-light scattering or X-ray-diffraction and quantitative relation to mechanical-properties. *J. Am. Leather Chem. Assoc.* **1986**, *81*, 221−230.

(4) Sasaki, N.; Odajima, S. Stress-strain curve and youngs modulus of a collagen molecule as determined by the x-ray diffaction technique. *J. Biomech.* **1996**, *29*, 655−658.

(5) Liao, J.; Yang, L.; Grashow, J.; Sacks, M. S. Molecular orientation of collagen in intact planar connective tissues under biaxial stretch. *Acta Biomater.* **2005**, *1*, 45−54.

(6) Covington, A. D. Modern tanning chemistry. *Chem. Soc. Rev.* **1997**, *26*, 111−126.

(7) Maxwell, C. A.; Wess, T. J.; Kennedy, C. J. X-ray diffraction study into the effects of liming on the structure of collagen. *Biomacromolecules* **2006**, *7*, 2321−2326.

(8) Wess, T. J.; Orgel, J. P. Changes in collagen structure: drying, dehydrothermal treatment and relation to long term deterioration. *Thermochim. Acta* **2000**, *365*, 119−128.

(9) Bulo, R. E.; Siggel, L.; Molnar, F.; Weiss, H. Modeling of bovine type-I collagen fibrils: interaction with pickling and retanning agents. *Macromol. Biosci.* **2007**, *7*, 234−240.

(10) Ciferri, A. Charge-dependent and charge-independent contributions to ion-protein interaction. *Biopolymers* **2008**, *89*, 700−709.

(11) Zanaboni, G.; Rossi, A.; Onana, A. M. T.; Tenni, R. Stability and networks of hydrogen bonds of collagen triple helical structure: influence of pH and chaotropic nature of three anions. *Matrix Biol.* **2000**, *19*, 511−520.

(12) Grant, C. A.; Brockwell, D. J.; Radford, S. E.; Thomson, N. H. Tuning the elastic modulus of hydrated collagen fibrils. *Biophys. J.* **2009**, *97*, 2985−2992.

(13) IULTCS. *Leather − Chemical, physical and Mechanical and Fastness Tests − Sampling Location*; ISO: Geneva, Switzerland, 2002; ISO 2418:2002.

(14) Williams, J. M. V. IULTCS (IUP) test methods − Measurement of tear load-double edge tear. *J. Soc. Leather Technol. Chem.* **2000**, *84*, 327−329.

(15) IULTCS. *Leather − Physical and Mechanical Tests − Determination of Tear Load−- Part 2: Double Edge Tear*; ISO: Geneva, Switzerland, 2002; BS EN ISO 3377-2:2002(E).

DOI: 10.1021/jf506357j
J. Agric. Food Chem. 2015, 63, 2499−2505

(16) IULTCS. *Leather – Physical and Mechanical Tests – Sample Preparation and Conditioning*; ISO: Geneva, Switzerland, 2012; ISO 2419:2012.
(17) Cookson, D.; Kirby, N.; Knott, R.; Lee, M.; Schultz, D. Strategies for data collection and calibration with a pinhole-geometry SAXS instrument on a synchrotron beamline. *J. Synchrotron Radiat.* **2006**, *13*, 440–444.
(18) Basil-Jones, M. M.; Edmonds, R. L.; Norris, G. E.; Haverkamp, R. G. Collagen fibril alignment and deformation during tensile strain of leather: a SAXS study. *J. Agric. Food Chem.* **2012**, *60*, 1201–1208.
(19) Basil-Jones, M. M.; Edmonds, R. L.; Cooper, S. M.; Haverkamp, R. G. Collagen fibril orientation in ovine and bovine leather affects strength: a small angle X-ray scattering (SAXS) study. *J. Agric. Food Chem.* **2011**, *59*, 9972–9979.
(20) Sizeland, K. H.; Wells, H. C.; Higgins, J. J.; Cunanan, C. M.; Kirby, N.; Hawley, A.; Haverkamp, R. G. Age dependant differences in collagen fibril orientation of glutaraldehyde fixed bovine pericardium. *BioMed. Res. Int.* **2014**, *2014*, No. 189197.
(21) Wess, T. J.; Purslow, P. P.; Kielty, C. M. X-ray diffraction studies of fibrillin-rich microfibrils: effects of tissue extension on axial and lateral packing. *J. Struct. Biol.* **1998**, *122*, 123–127.
(22) Kemp, A. D.; Harding, C. C.; Cabral, W. A.; Marini, J. C.; Wallace, J. M. Effects of tissue hydration on nanoscale structural morphology and mechanics of individual type I collagen fibrils in the Brtl mouse model of Osteogenesis Imperfecta. *J. Struct. Biol.* **2012**, *180*, 428–438.
(23) Brodsky, B.; Eikenberry, E. F.; Cassidy, K. An unusual collagen periodicity in skin. *Biochim. Biophys. Acta* **1980**, *621*, 162–166.
(24) Price, R. I.; Lees, S.; Kirschner, D. A. X-ray diffraction analysis of tendon collagen at ambient and cryogenic temperatures: role of hydration. *Int. J. Biol. Macromol.* **1997**, *20*, 23–33.
(25) Sizeland, K. H.; Wells, H. C.; Norris, G. E.; Edmonds, R. L.; Kirby, N.; Hawley, A.; Mudie, S.; Haverkamp, R. G. Collagen D-spacing and the effect of fat liquor addition. *J. Am. Leather Chem. Assoc.* **2015**, *110*, 66–71.
(26) Wells, H. C.; Sizeland, K. H.; Kayed, H. R.; Kirby, N.; Hawley, A.; Mudie, S. T.; Haverkamp, R. G. Poisson's ratio of collagen fibrils measured by SAXS of strained bovine pericardium. *J. Appl. Phys.* **2015**, *117*, No. 044701.
(27) Deb Choudhury, S.; Haverkamp, R. G.; DasGupta, S.; Norris, G. E. Effect of oxazolidine E on collagen fibril formation and stabilization of the collagen matrix. *J. Agric. Food Chem.* **2007**, *55*, 6813–6822.
(28) Kayed, H. R.; Sizeland, K. H.; Kirby, N.; Hawley, A.; Mudie, S. T.; Haverkamp, R. G. Collagen cross linking and fibril alignment in pericardium. *RSC Adv.* **2015**, *5*, 3611–3618.

DOI: 10.1021/jf506357j
J. Agric. Food Chem. 2015, 63, 2499–2505

ACS Biomaterials SCIENCE & ENGINEERING

Article

pubs.acs.org/journal/abseba

Collagen Fibril Structure and Strength in Acellular Dermal Matrix Materials of Bovine, Porcine, and Human Origin

Hannah C. Wells,[†] Katie H. Sizeland,[†] Nigel Kirby,[‡] Adrian Hawley,[‡] Stephen Mudie,[‡] and Richard G. Haverkamp*[,†]

[†]School of Engineering and Advanced Technology, Massey University, Private Bag 11222, Palmerston North, New Zealand

[‡]Australian Synchrotron, 800 Blackburn Road, Clayton, Melbourne, Victoria, Australia

ABSTRACT: Strength is an important characteristic of acellular dermal matrix (ADM) materials used for surgical scaffolds. Strength depends on the material's structure, which may vary with the source from which the product is produced, including species and animal age. Here, variations in the physical properties and structures of ADM materials from three species are investigated: bovine (fetal and neonatal), porcine, and human materials. Thickness normalized, the bovine materials have a similar strength (tear strength of 75−124 N/m) to the human material (79 N/m), and these are both stronger than the porcine material (43 N/m). Thickness-normalized tensile strengths were similar among all species (18−34 N/mm^2 for bovine although higher in fetal material, 18 N/mm^2 for human and 21 N/mm^2 for porcine). Structure is investigated with synchrotron-based small-angle X-ray scattering (SAXS) for collagen fibril orientation index (OI) and scanning electron microscopy (SEM). SEM reveals a more open structure in bovine ADM than in the porcine and human material. A correlation is found between OI and thickness-normalized tear strength in neonatal bovine material measured with the X-rays edge-on to the sample, but this relationship does not extend across species. The collagen fibril arrangement, viewed perpendicular to the surface, varies between species, with the human material having a unimodal distribution and rather isotropic (OI 0.08), the porcine being strongly bimodal and rather highly oriented (OI 0.61), the neonatal bovine between these two extremes with a bimodal distribution tending toward isotropic (OI 0.14−0.21) and the fetal bovine material being bimodal and less isotropic than neonatal (OI 0.24). The OI varies less through the thickness of the porcine and human materials than through the bovine materials. The similarities and differences in structure may inform the suitability of these materials for particular surgical applications.

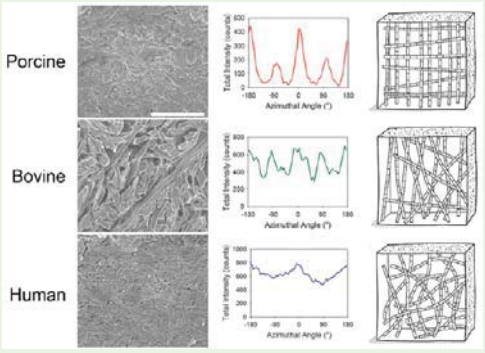

KEYWORDS: *collagen, scaffold, ADM, ECM, strength, orientation*

INTRODUCTION

Scaffold materials are required when a tissue is being reinforced or replaced in a number of reconstructive surgical procedures. These materials must meet a range of requirements such as being immunologically compatible with the body, be readily incorporated into living tissue, have sufficient strength to perform the task, and have appropriate elastic properties. These scaffold materials may be synthesized from a variety of materials[1] or produced by decellurization of native materials. Extracellular matrix materials (ECM) derived from a wide variety of tissues have been successfully used a scaffolds.[2] ECM materials derived from dermal tissues are commercially available and are produced from a variety of species including porcine, bovine, and human dermal tissue. The physical properties of materials manufactured from different source materials differ, yet there is an incomplete understanding of these differences and the structural characteristics that lead to the differences in strength.

The mechanical properties of collagen tissue materials are due in part to the highly fibrillar nature of type I collagen[3,4] and the tissue's ability to respond to imposed stresses.[5] Factors that have been considered as contributing to the strength of collagenous tissue materials include the structure of the collagen (*d*-spacing, collagen type), the nature of the cross-linking between collagen, collagen fibril diameter and collagen orientation. The fibril arrangement can be described in terms of orientation direction and spread. Collagen orientation (quantified as orientation index, OI) has been investigated in the cornea,[6] heart valve tissue,[7] pericardium,[8,9] bladder tissue,[10] skin,[11] aorta,[12] ovine forestomach derived scaffold materials,[13] and leather made from animal skins.[14] The arrangement of collagen fibrils in most tissues is anisotropic due to the nonuniform requirements for mechanical performance. It has been shown that leather's tear strength is correlated with collagen fibril orientation as measured by SAXS with the X-ray beam edge-on to the sample. Specifically, when the collagen fibrils are arranged in parallel or almost-parallel sheets (i.e., have a high OI), the leather is stronger,[15,16] although OI is also affected by the swelling of the material.[17] This relationship was observed in a large sample of ovine and bovine

Received: July 21, 2015
Accepted: September 3, 2015
Published: September 3, 2015

DOI: 10.1021/acsbiomaterials.5b00310
ACS Biomater. Sci. Eng. 2015, 1, 1026−1038

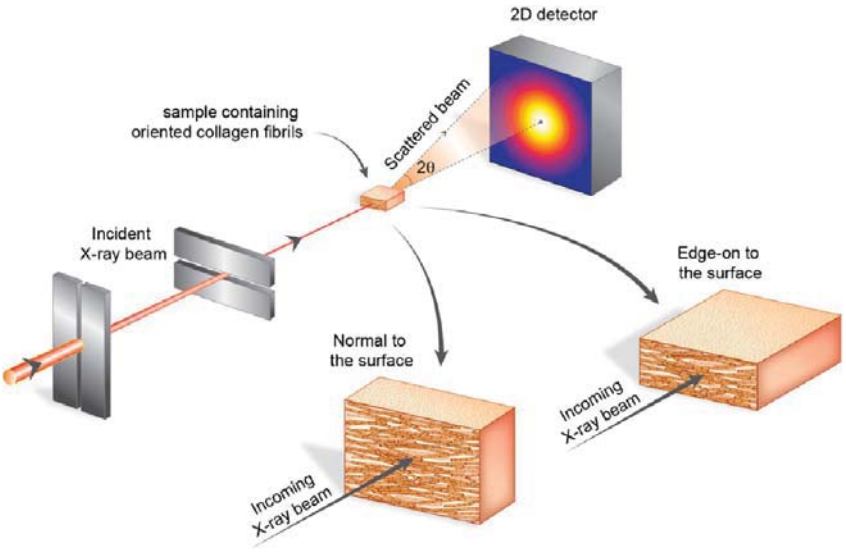

Figure 1. Experimental setup for SAXS analysis.

skins, including bovine pericardium,[8] and across seven species of mammals over a large range of strength (factor of 5). The relationship between OI and strength has been explained as being due to the high strength of the collagen fibrils in their longitudinal axis when suitably arranged to resist the tearing process.[16]

d-Spacing in collagen varies with animal age,[18,19] animal species[16] and tissue type,[20] and the tissue's chemical treatment including water and fat content.[19,21−24] However, there does not appear to be a relationship between *d*-spacing and the strength of leather[15,16] or rat tail tendon.[25]

Collagen fibril diameter may be correlated with strength in some materials. For example, in human aortic valves, regions of high stress may contain larger-diameter fibrils;[26] in mouse tendon, fibril diameter increases with loading;[27] and in bovine leather, higher strength material has larger fibril diameters.[28] Fibril diameter may also increase with age.[29]

Here, we investigate the structure of acellular dermal matrix (ADM) materials, how it differs between bovine, porcine and human materials, and how it changes with age in bovine materials. We attempt to develop an understanding of how ADM structure influences the physical properties of the materials.

EXPERIMENTAL SECTION

Source Material. Commercial ADM materials included Strattice Firm porcine ADM (LifeCell Corporation, US), Alloderm human ADM (LifeCell Corporation, US) and a range of SurgiMend bovine ADM (TEI Biosciences, US), including bovine third trimester fetal ADM and neonatal ADM (animals less than 5 months old) with thicknesses of approximately 1.7, 2.0, 3.0, and 4.0 mm. The Strattice and Alloderm materials were already hydrated whereas the SurgiMend materials required hydrating with distilled water prior to SAXS analysis or tensile testing.

Synchrotron SAXS. Diffraction patterns were recorded on the Australian Synchrotron SAXS/WAXS beamline, using a high-intensity undulator source. Energy resolution of 10^{-4} was obtained from a cryo-cooled Si(111) double-crystal monochromator and the beam size (fwhm focused at the sample) was 250 × 80 μm, with a total photon flux of about 2×10^{12} ph.s^{-1}. All diffraction patterns were recorded with an X-ray energy of 12 keV using a Pilatus 1 M detector with an active area of 170 × 170 mm and a sample-to-detector distance of 3371 mm. Exposure time for diffraction patterns was 1−5 s and initial data processing was carried out using Scatterbrain software.[30]

SAXS analysis was carried out in two directions through the samples. The X-ray beam was either passed through the flat surface of the sample normal to the surface (here referred to as normal) or edge-on to the sample (here referred to as edge-on or cross sections) (Figure 1). For the edge-on measurements, because it is known that structure varies through the thickness of a sample, structure was analyzed at intervals of typically 0.15 mm through the whole thickness of each sample.

Fibril Diameter. Fibril diameters were calculated from the SAXS data using the Irena software package[31] running within Igor Pro. The data were fitted at the wave vector, *Q*, in the range of 0.01−0.04 Å^{-1} and at an azimuthal angle which was 92.5° (over a 5° segment) to the long axis of most of the collagen fibrils. This azimuthal angle of the long axis of the collagen fibrils was determined as the position for the maximum intensity with azimuthal angle of the *d*-spacing diffraction peaks. The "cylinderAR" shape model with an arbitrary aspect ratio of 30 was used for all fitting. We did not attempt to individually optimize this aspect ratio, and the unbranched length of collagen fibrils may in practice exceed an aspect ratio of 30.

***d*-Spacing.** The *d*-spacing was determined from the position of the center of a Gaussian curve fitted to the fifth order diffraction peak taken from the integrated intensity from the azimuthal range from 45 to 135°.

Orientation Index. The OI is a quantification of the spread of microfibril orientation, with 1 indicating parallel microfibrils and 0 indicating randomly oriented microfibrils. OI is defined as (90° − OA)/90°, where OA, the orientation angle, is the minimum azimuthal angle range that contains 50% of the microfibrils[32] converted to an index,[15] using the spread in azimuthal angle of one or more *d*-spacing diffraction peaks. The peak area is measured, above a fitted baseline, at each azimuthal angle.

In many of the diffraction patterns, particularly those measured with the X-ray beam perpendicular to the surface, two peaks were observed in the plot of intensity versus azimuthal angle. In such patterns, an OA calculated using the minimum angle centered on one of these peaks is large and depends on the spacing between the two peaks, therefore not reflecting accurately the isotropy of the collagen fibrils. So, an alternative method to measure the OA was used: the intensities of 5° intervals of azimuthal angle were ranked and sufficient of these were summed to give 50% of the total intensity over a 180° range, where the total angle covered by the summed intervals becomes the OA. When there is only one peak in the intensity versus azimuthal angle plot, this method gives the same OA as when the OA is calculated by summing the area starting at the center of the peak.[15] Another way of describing this is that the OA for one peak is equivalent to 0.675 of the standard deviation of a

DOI: 10.1021/acsbiomaterials.5b00310
ACS Biomater. Sci. Eng. 2015, 1, 1026−1038

Gaussian (if the peak were approximately Gaussian in shape). When there are two peaks, the standard method of finding a combined standard deviation from two Gaussians to obtain a single OI value would not give a good measure of anisotropy since it depends on the separation of the two Gaussians. A more useful way would be to combine the two Gaussians after shifting them so that they are superimposed. This is effectively what the method used here achieves in a numerical way that is not reliant on Gaussian distributions.

Mechanical Testing. Tear strength[33] and tensile strength[34] were measured using standard methods on an Instron device. Two samples were tested for each of tear strength and tensile strength, with the samples taken orthogonally, and the values averaged.

Electron Microscopy. Samples of ADM materials were cut into small cube-shaped pieces and fixed for over 8 h at room temperature in Modified Karnovsky's fixative containing 3% glutaraldehyde and 2% formaldehyde in 0.1 M phosphate buffer (pH 7.2). The samples were then washed three times for 10−15 min in phosphate buffer (0.1 M, pH 7.2) before being dehydrated in a graded series of ethanol washes (25, 50, 75, 95, and 100%), each dehydration stage being 10−15 min long, followed by a final 100% ethanol wash for 1 h. Samples were critical-point (CP) dried using the Polaron E3000 series II critical point drying apparatus with liquid CO_2 as the CP fluid and 100% ethanol as the intermediary fluid. They were then mounted on to aluminum stubs and sputter coated with gold using the Baltec SCD 050 sputter coater. The samples were viewed in the FEI Quanta 200 environmental scanning electron microscope at an accelerating voltage of 20 kV.

RESULTS

Tear Test. Tear tests were performed in two orthogonal directions for each sample, one test in each direction. The results of these tests have been averaged and are listed in Table 1. The nature of the tearing, once tearing starts, is similar for all the samples.

Table 1. Tear Test Results for ADM Materials

sample	thickness (mm)	force at rupture (N)	σ (for force at rupture, N)	thickness-normalized force at rupture (N/mm)
bovine fetal	0.98	76.1	9.0	78.0
bovine neonatal 1.7	1.67	127.0	0.6	76.0
bovine neonatal 2.0	2.01	172.0	11.7	85.6
bovine neonatal 3.0	3.02	227.0	22.8	75.1
bovine neonatal 4.0	3.98	494.3	0.4	124.2
porcine	1.69	73.0	7.9	43.2
human	1.01	79.5	5.9	79.0

The neonatal bovine ADM materials are the strongest on an absolute scale, followed by the human, the fetal bovine and then the porcine material. On a thickness-normalized scale, the fetal bovine material is the strongest followed by the thicker neonatal bovine materials, with the thinner neonatal bovine having a lower strength in the same range as the human ADM. The lowest strength material on a thickness-normalized basis is the porcine ADM. This may be a partial explanation for the higher intraoperative device failures observed for the porcine cohort in study of porcine and bovine matrix for abdominal wall reconstruction.[35]

Table 2. Tensile Test Results for ADM Materials

sample	thickness[a] (mm)	average force at rupture (N)	σ (for force at rupture, N)	cross-section normalized force at rupture (N/mm^2)
bovine fetal	0.97	381[b]		39.3[b]
bovine neonatal 1.7	1.76	415	111	23.8
bovine neonatal 2.0	2.01	451	147	22.4
bovine neonatal 3.0	3.04	561	6	18.5
bovine neonatal 4.0	4.06	> 963[c]		> 23.7[c]
porcine	1.57	328	7	21.0
human	1.11	201	120	17.7

[a]Some of the thicknesses vary a little from the values in Table 1 but represent the thickness as measured on the cut samples used in each of these tests. [b]Only one test, but see text. [c]Sample was not taken to failure.

Table 3. Strain (approximate) of different sample types

sample	strain at 10 N/mm^2 stress
bovine neonatal 1.7	0.48
bovine neonatal 2.0	0.54
bovine neonatal 3.0	0.47
bovine neonatal 4.0	0.30
porcine	0.31
human	0.45

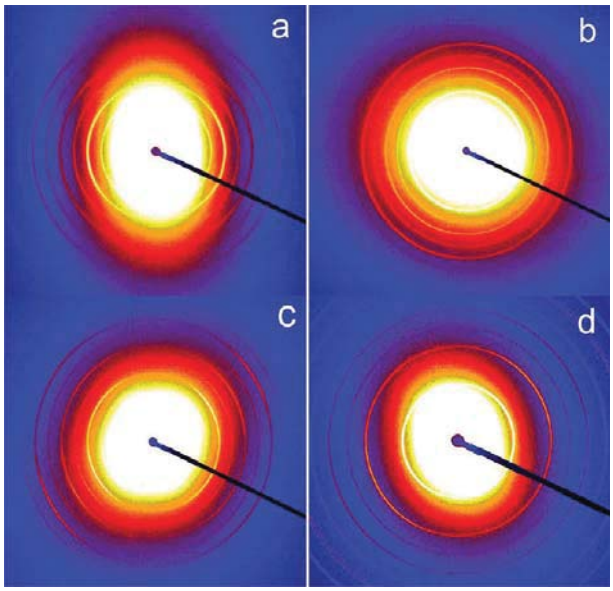

Figure 2. Examples of scattering patterns taken with the X-ray beam edge-on to the samples: (a) fetal bovine; (b) 3 mm thick neonatal bovine; (c) porcine; (d) human ADM materials.

Tensile Test. Tensile tests were performed in two orthogonal directions for each sample, one test in each direction and the averages are listed in Table 2. In the bovine samples, strength increases with thickness; however, the fetal material was the strongest on a thickness-normalized basis. Although not

DOI: 10.1021/acsbiomaterials.5b00310
ACS Biomater. Sci. Eng. 2015, 1, 1026−1038

Table 4. Orientation Index for Collagen from SAXS Measured with the X-ray Beam Edge-on

sample	OI (X-rays edge-on)	σ	no. of measurements
bovine fetal	0.43	0.08	24
bovine neonatal 1.7	0.27	0.06	22
bovine neonatal 2.0	0.32	0.13	22
bovine neonatal 3.0	0.31	0.11	25
bovine neonatal 4.0	0.45	0.15	29
porcine	0.40	0.05	29
human	0.23	0.08	24

Table 5. Orientation Index for Collagen from SAXS Measured with the X-ray Beam Perpendicular to the Surface

sample	OI (X-rays perpendicular)	σ	no. of measurements
bovine fetal	0.24	0.04	18
bovine neonatal 1.7	0.21	0.06	9
bovine neonatal 2.0	0.20	0.07	9
bovine neonatal 3.0	0.14	0.03	9
bovine neonatal 4.0	0.19	0.05	9
porcine	0.61	0.05	9
human	0.08	0.06	9

presented here, a large number of measurements have been made by others on these materials which confirms that the bovine fetal material typically has a higher cross-section-normalized tensile strength than bovine neonatal material.[36]

Extensibility. Extensibility can be approximated as the strain at a force of 10 N/mm^2 on a sample cross section (which is similar to an inverse of elastic modulus over the complete extension range but not thickness normalized). The test results show that the 1.7, 2.0, and 3.0 mm bovine neonatal and human materials are the most extensible, whereas the porcine and 4.0 mm neonatal bovine are the least extensible at this level of force (Table 3).

Small-Angle X-ray Scattering. The SAXS diffraction patterns (Figure 2) can be analyzed in different ways to get structural information on the collagen. The patterns provide information on the structure of the fibrils (*d*-spacing and fibril diameter) and on the arrangement of these fibrils (OI).

Collagen Fibril Orientation Index (OI). Collagen fibril orientation was measured with the X-ray beam edge-on to the ADM materials and perpendicular to the face of the ADM. The OI measured for each material is listed in Tables 4 and 5.

A pairwise multiple comparison of the edge-on measurements (Dunn Method) gave significant differences ($P < 0.05$) between human and both the bovine and porcine ADM materials; between porcine with both human and bovine materials; and between fetal bovine and neonatal bovine. No significant difference in OI was seen when comparing neonatal bovine with either porcine or human.

A pairwise multiple comparison of the flat-on measurements (Dunn Method) gave significant differences ($P < 0.05$) between human and the porcine ADM materials; porcine and both the bovine and human.

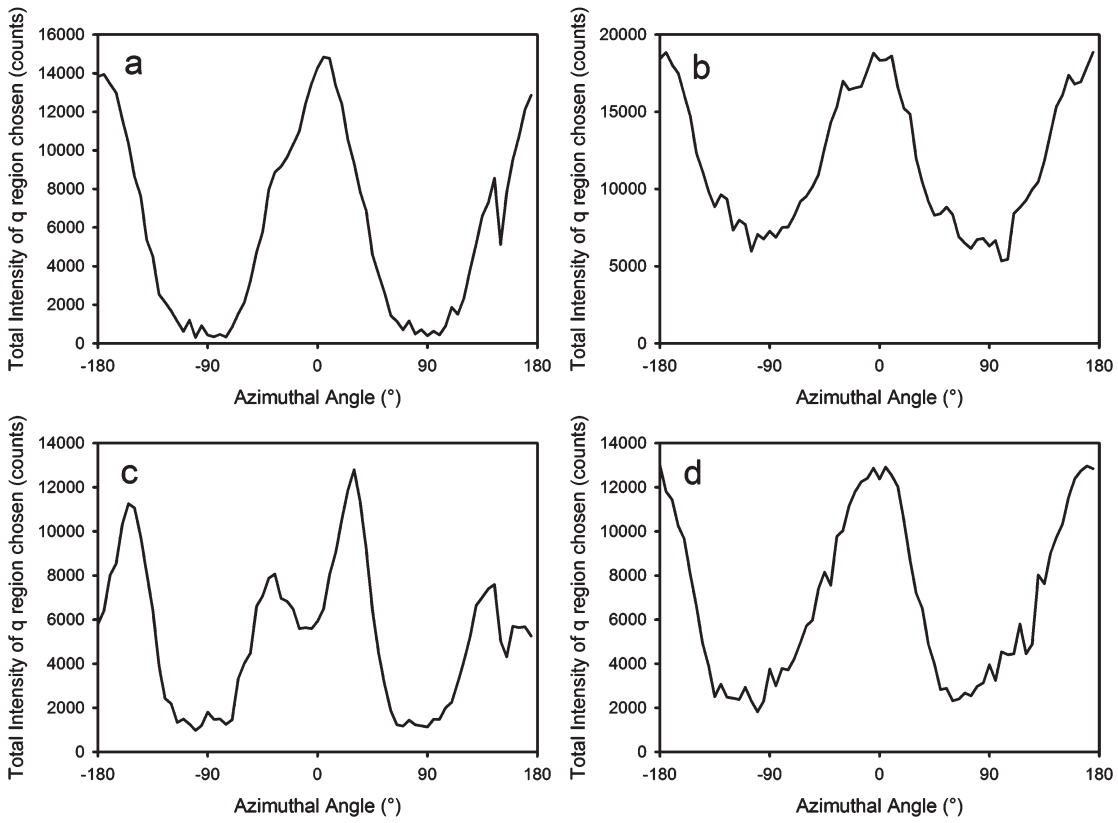

Figure 3. Variation in intensity of the 5th diffraction peak with azimuthal angle (measured with the X-ray beam edge-on to the surface) to illustrate the nature of the fibril orientation: (a) fetal bovine ADM material; (b) 3 mm thick neonatal bovine; (c) porcine; (d) human. These plots correspond with the diffraction patterns in Figure 2.

DOI: 10.1021/acsbiomaterials.5b00310
ACS Biomater. Sci. Eng. 2015, 1, 1026−1038

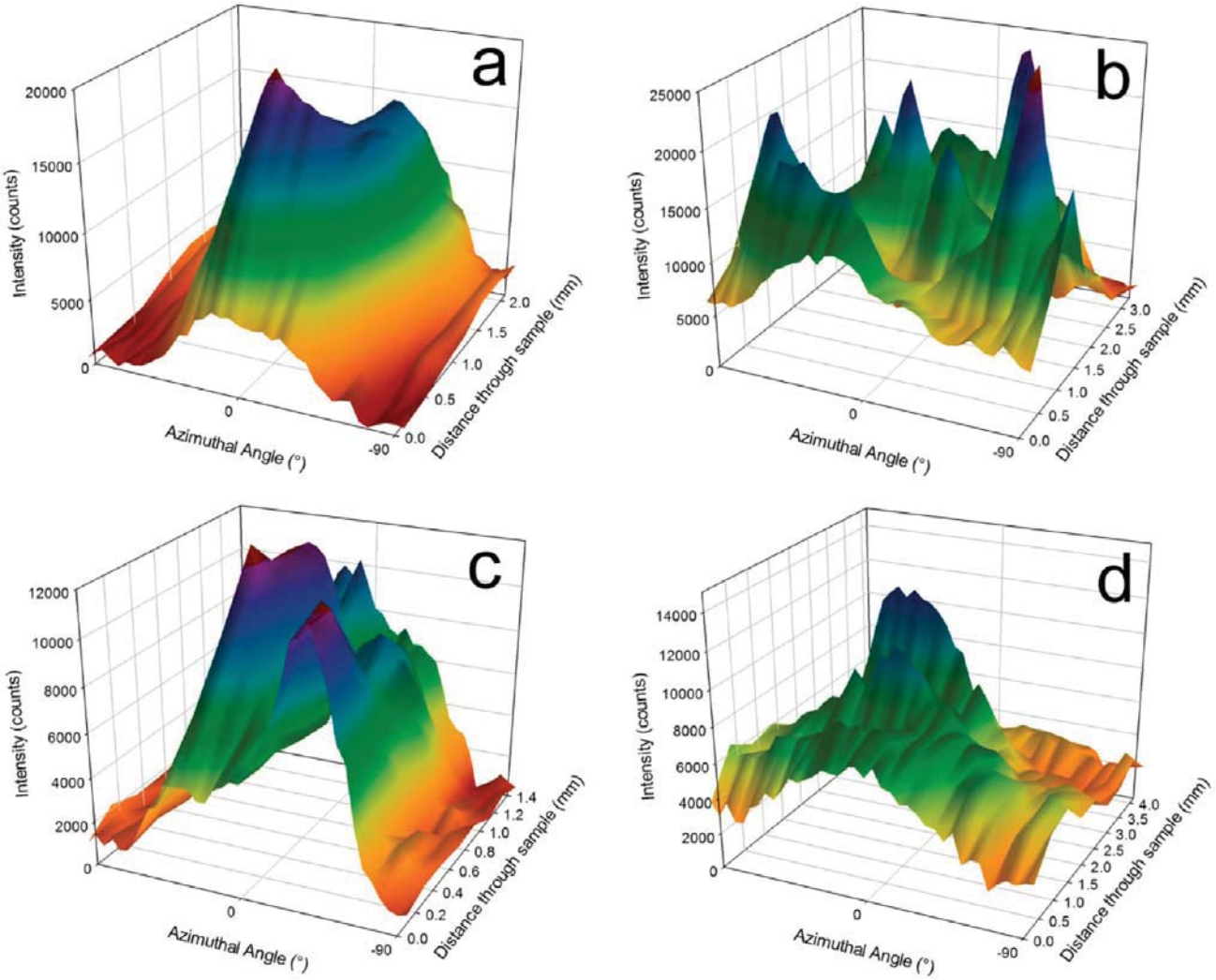

Figure 4. Variation in intensity of the 5th diffraction peak with azimuthal angle (measured with the X-ray beam edge-on to the surface) and distance through the sample (equivalent to a series of plots of the type in Figure 3) to illustrate the nature of the fibril orientation through the sample thickness: a) fetal bovine ADM material; (b) 3 mm thick neonatal bovine; (c) porcine; (d) human. These plots are just for 90° either side of the origin to simplify the images because the information is duplicated in the region for 90 to 180° and −90 to −180°.

Detail of Fibril Orientation. The OI presented for each of the materials is calculated from plots of diffraction intensity for the fifth or sixth *d*-spacing diffraction peak (Figures 3−5); however, the calculation reduces complex information to just one number. More detail of the collagen fibril orientation and the differences between different sample types can be obtained from plots of diffraction intensity (for any of the *d*-spacing diffraction peaks) with azimuthal angle. An analysis of the three-dimensional structure requires at least two diffraction patterns normal to each other. Plots are provided for diffraction intensity versus azimuthal angle with the X-rays edge-on (Figures 3 and 4) and perpendicular (Figure 5) to the plane of the ADM material.

Fibril Orientation (X-rays edge-on). The distribution of orientation of the collagen fibrils in the dermal ECM materials is apparent from the diffraction intensity versus azimuthal angle plots. Single plots at just one point in a section of the ADM are shown in Figure 3. The way the diffraction intensity varies with azimuthal angle gives an indication of how the collagen fibrils are arranged. Where there is only one peak (within a 180° range) and the curve approaches the baseline, there is only one preferred direction of orientation and the spread of fibril direction is around this angle. Examples of this are the edge-on measurements for fetal bovine ADM material (Figure 3a) and to a lesser extent edge-on measurements for neonatal bovine ADM (Figure 3b) and human ADM materials (Figure 3d). Where there are two peaks in this plot, there are two preferred directions of orientation of the collagen fibrils, as seen in the porcine ADM with X-rays edge-on (Figure 3c). When the curve remains considerably above the baseline, the collagen fibril distribution is tending toward isotropic.

Fibril Orientation Sections (X-rays Edge-on). The distribution of orientation of the collagen fibrils and the variation of fibril orientation through the thickness of the ECM materials can be shown with plots of diffraction peak intensity versus azimuthal angle at points at different positions on a cross section of the material representing different depths (Figure 4). These are essentially compilations of plots such as in Figure 3 but with just a −90° to 90° range for simplicity. There is some variation in the fibril arrangement with depth. The bovine, especially fetal, and human materials tend to be a little more highly oriented with

DOI: 10.1021/acsbiomaterials.5b00310
ACS Biomater. Sci. Eng. 2015, 1, 1026−1038

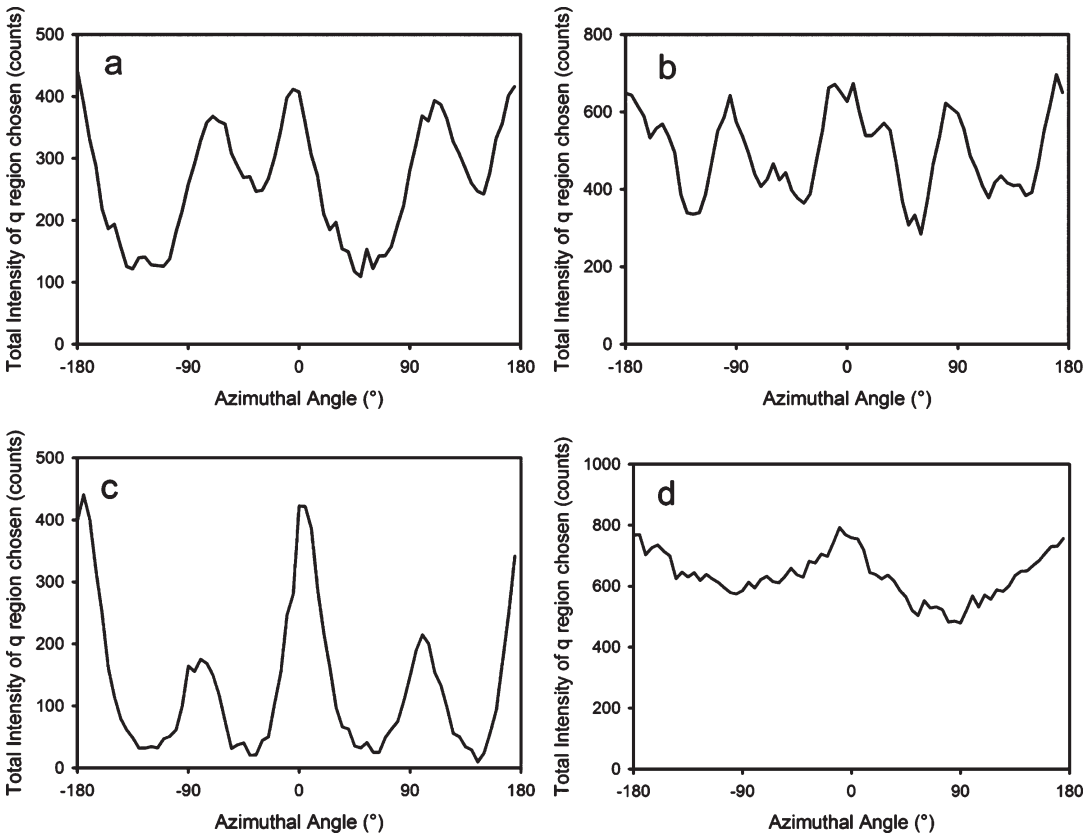

Figure 5. Variation in intensity of the 5th diffraction peak with azimuthal angle (measured with the X-ray beam perpendicular to the surface) to illustrate the nature of fibril orientation: (a) fetal bovine ADM material; (b) 3 mm thick neonatal bovine; (c) porcine; (d) human.

increasing depth. The porcine is highly oriented throughout the thickness, although the direction of orientation changes with depth.

Fibril Orientation (X-rays Normal). Measurements with the X-ray beam perpendicular to the surface reveal differences in fibril orientation between sample types (Figure 5). When the curve remains a long way above the baseline this indicates a tendency toward an isotropic distribution of the collagen fibrils, The fetal bovine ADM material has two well-defined peaks of similar intensity (Figure 5a), as does the neonatal bovine (Figure 5b) although with greater spread and both remaining well above the baseline. The porcine material also has two peaks (Figure 5c), but these are more separate than those of the bovine material (roughly 90° to each other), with one direction dominant, and the curve approaches close to the baseline, showing that the material is far from isotropic. The plots of the human ADM material (Figure 5d) reveal that the fibrils barely exhibit a preferred orientation and are not bimodally distributed.

OI Cross-Sections of ADM. The cross sections through the thickness of the ADM materials (Figure 6) show a variation in OI through the thickness of the bovine materials which, unsurprisingly, is similar to that observed in bovine leather.[37] The fetal bovine material (Figure 6a) is similar to the neonatal material (Figure 6b–e). In the porcine (Figure 6f) and human (Figure 6g) materials, OI varies less through the samples.

Fibril Diameter. Average collagen fibril diameters for each of the sample types calculated from X-ray edge-on measurements are listed in Table 6. A pairwise multiple comparison (Dunn Method) gave significant differences ($P < 0.05$) between porcine and both the human and bovine as well as between human and both the porcine and bovine (except neonatal 3.0). The fetal bovine is not statistically different from the neonatal bovine.

Fetal collagen (rat tail tendon) has been reported to have smaller fibril diameters than collagen from mature animals[29] but we do not observe a difference in collagen fibril diameter between fetal and neonatal bovine ADM materials.

***d*-Spacing.** Average *d*-spacing for the collagen fibrils for each of the sample types is listed in Table 7. A pairwise multiple comparison (Dunn Method) gave significant differences ($P < 0.05$) between human and both the bovine and porcine; porcine and the bovine (except 4.0 mm); porcine and human; but not between fetal bovine and the neonatal bovine.

***d*-Spacing Cross-Sections of ADM.** The *d*-spacing variation through the cross sections is similar for all samples except for the 4 mm neonatal bovine material (Figure 7). The variation between sections is greater for the human, porcine and 4 mm neonatal bovine than for the thinner bovine samples.

Correlation of OI and Strength. Based on measurements with the X-ray beam edge-on to the sample, a statistically significant correlation was found only between OI and tear strength (Figure 8); tensile strength is not significantly correlated with OI (Figure 8 right). These findings are consistent with observations for leather.[15]

For the OI versus tear strength and OI versus tensile strength measured with the X-ray beam perpendicular to the samples there is no statistically significant correlation (Figure 9).

Fibril Diameter and Strength. Fibril diameter has been shown to correlated with tear strength in bovine leather.[28] In collagen grown in tissue culture, larger fibril diameters are associated with higher strength.[38] However, in the bovine

DOI: 10.1021/acsbiomaterials.5b00310
ACS Biomater. Sci. Eng. 2015, 1, 1026−1038

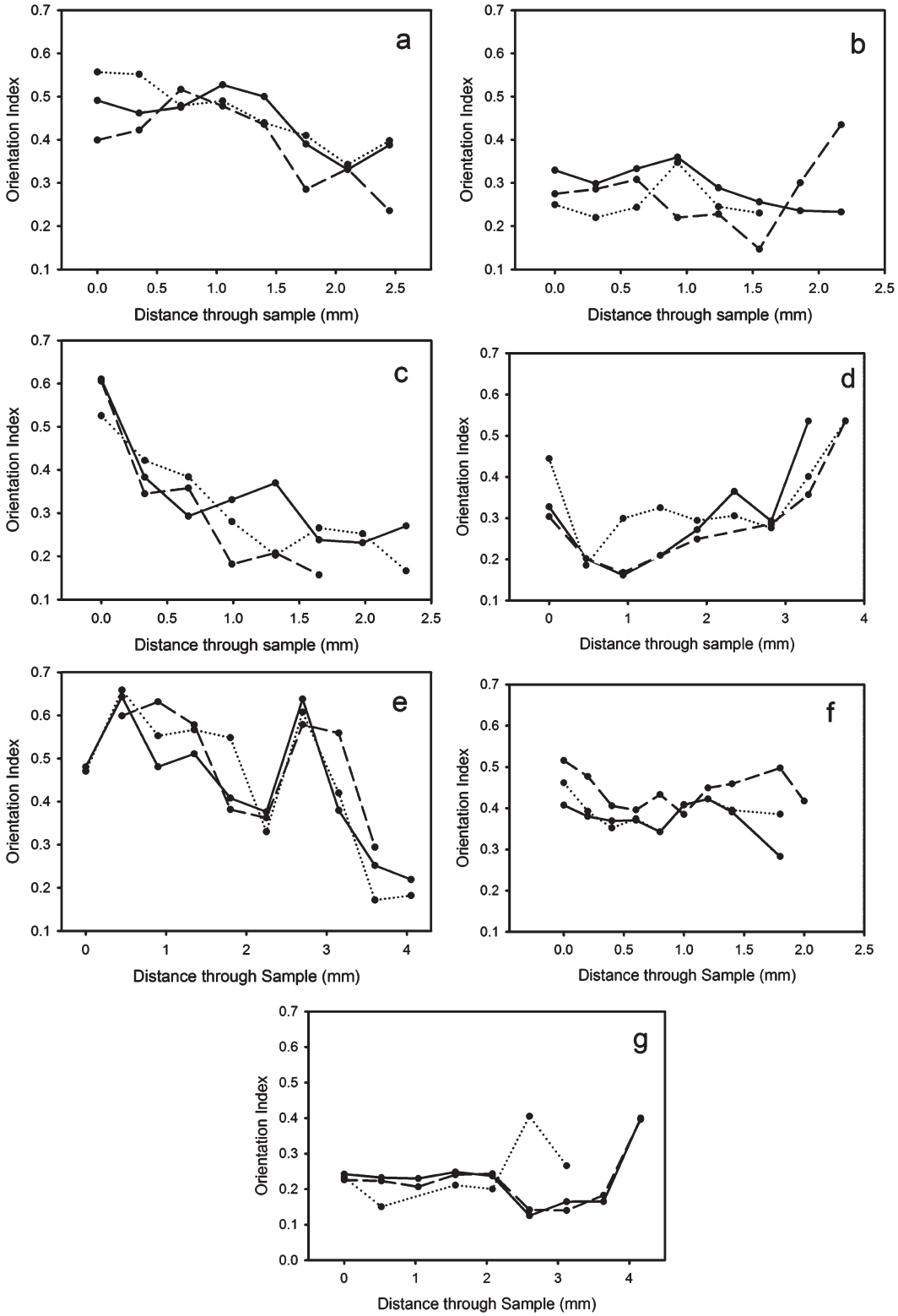

Figure 6. Variation in OI through the thickness of the materials: (a) fetal bovine ADM material; (b) 1.7 mm thick neonatal bovine; (c) 2 mm thick neonatal bovine; (d) 3 mm thick neonatal bovine; (e) 4 mm thick neonatal bovine; (f) porcine; (g) human.

neonatal material we analyzed here, there is no statistically significant correlation between fibril diameter and strength (Figure 10). There is also no correlation in the material of the other species investigated (Figure 10).

SEM Images. The SEM images show structural differences between the bovine, porcine and human ADM (Figures 11 and 12). The bovine material has a more open structure than the porcine and human material, which have a much finer texture.

DOI: 10.1021/acsbiomaterials.5b00310
ACS Biomater. Sci. Eng. 2015, 1, 1026−1038

Table 6. Average Diameter of Collagen Fibrils from SAXS Analysis

sample	fibril diameter (nm)	variance σ	no. of measurements
bovine fetal	58.6	1.3	28
bovine neonatal 1.7	58.3	1.7	26
bovine neonatal 2.0	60.8	1.9	26
bovine neonatal 3.0	57.1	2.5	29
bovine neonatal 4.0	56.0	8.2	32
porcine	61.1	2.1	28
human	55.2	2.7	30

Table 7. Average *d*-Spacing for Collagen from SAXS Analysis (on Hydrated Materials)

sample	*d*-spacing	no. of measurements
bovine fetal	64.00	24
bovine neonatal 1.7	64.13	22
bovine neonatal 2.0	63.95	23
bovine neonatal 3.0	64.01	25
bovine neonatal 4.0	64.23	29
porcine	64.20	28
human	64.60	25

DISCUSSION

Strength from Structure. Collagen structure, as determined by SAXS, is related to the tear strength of the materials. The tear strength differences among bovine pericardium materials are correlated with differences in the collagen fibril orientation index of those materials (Figure 8a). In stronger samples, the fibrils are oriented in a planar manner parallel to the surface of the material (Figure 13b); in weaker materials, fibrils are less oriented in the planar direction (Figure 13a). Orientation direction, as measured with the X-ray beam perpendicular to the plane of the sheets of ADM (Figure 14), does not however have a strong relationship to strength. This has also been seen in leather produced from bovine hides.[15] However, in the ADM materials here, although this relationship was evident in the bovine materials, fibril orientation is not correlated with strength across species. Therefore, although tear strength might be predictable for given OI in bovine materials, this OI will not be associated with the same strength in porcine or human ADM materials. In contrast, studies on leather of seven mammals found a good correlation between OI measured edge-on and strength (although no correlation was found for alligator leather).[15,16] However, we are not able to confirm whether such an OI–strength relationship holds within a selection of porcine or human ADM materials because we did not analyze a range of samples from the two relevant species.

Model for Strength. The relationship between fibril direction and strength has been modeled previously and it can be shown that the strength is due to the sum of the vector components of the fibrils that lie in the direction of force.[8,16,39] A model orientation index is derived which we will call OÍ to distinguish it from the experimentally measured OI eq 1.

$$\mathrm{OI}' = \frac{\int_0^{2\pi}\int_0^{\pi/2} \cos^4\theta F(\theta,\varphi)\mathrm{d}\theta\mathrm{d}\varphi}{\int_0^{2\pi}\int_0^{\pi/2} F(\theta,\varphi)\mathrm{d}\theta\mathrm{d}\varphi} \quad (1)$$

Where $F(\theta,\phi)$ is the angular distribution function where θ and ϕ are fibril angles orthogonal to each other. We have previously applied this model to collagen orientation in leather produced from the skins of a selection of mammals where it was found to be valid across a wide range of strength[16] and also in collagen in bovine pericardium.[8] Other factors that prevent notch growth during tearing are also important.[5]

Distribution of Fibril Orientation with X-rays Normal. The collagen fibril distribution, as measured with the X-rays normal to the surface, perhaps may influence the properties of the materials in service. Although there is no correlation between tear strength and fibril orientation measured with X-rays normal to the surface (Figure 8b), as also seen with leather,[15] elastic properties may vary with fibril direction when the ADM is not isotropic in this dimension. The materials from the different species have different distributions for fibril orientation. A material with an isotropic distribution might be expected to have uniform mechanical properties in all directions (e.g., human and bovine ADM material) whereas one that has a strong unimodal distribution might be expected to behave quite differently in the direction of the orientation compared with a direction at right angles to the orientation. With a bimodal distribution (e.g., as in porcine or fetal bovine ADM materials), the properties would be expected to be more complex but differ in different directions. Other researchers have found that the elastic properties of fetal bovine material are significantly different parallel to the spine (stronger) compared to those perpendicular to the spine (weaker but more elastic).[36] These differences in mechanical properties with direction, if identified for each piece of the material, perhaps could be used to advantage in the selection of materials in specific surgical cases. A detailed study of directional mechanical properties was not part of this study.

***d*-Spacing and Fibril Diameter.** While there are differences between species for both *d*-spacing and fibril diameter, these differences do not appear to be correlated with strength or elasticity. It is known that *d*-spacing decreases with dehydration;[19,21−24] however, for these measurements, the samples were fully hydrated to reflect the state they would be used in surgical application.

Tight or Open Structure. The SEM cross-sections show that there are differences in the structure of the different materials. The bovine materials have the most open structure, with porosity between the fibers, whereas the human and porcine materials are tighter and more compact. At higher magnification, the human ADM looks slightly similar to the bovine material but with a finer texture with some minor porosity between the fibers visible. It may be that a more open structure helps with the integration of the ADM material in vivo,[40] but further, detailed investigation is required.

Variation through Material Thickness. Both the OI (Figures 4 and 6) and *d*-spacing (Figure 7) vary through the thickness of the ADM materials. In the porcine and human ADM material, OI varies less with thickness than do the bovine materials. For other bovine dermal materials, this variation has been well documented;[37] however, the same information is not available for porcine and human ADM. The human material investigated here may, in fact, not reflect a full-thickness dermal material; if so, any measured variation with thickness would be less than for full-thickness material. The *d*-spacing variation through each cross-section is similar for all samples.

Strength. The tear test provides a measure of the toughness of the ADM material and the results are a useful indicator of the in-service stresses and where failure by tearing or bursting is most likely to occur. The neonatal bovine ADM materials are the strongest of the material types in the tear test on an absolute scale, followed by the human, the fetal bovine and then the

DOI: 10.1021/acsbiomaterials.5b00310
ACS Biomater. Sci. Eng. 2015, 1, 1026−1038

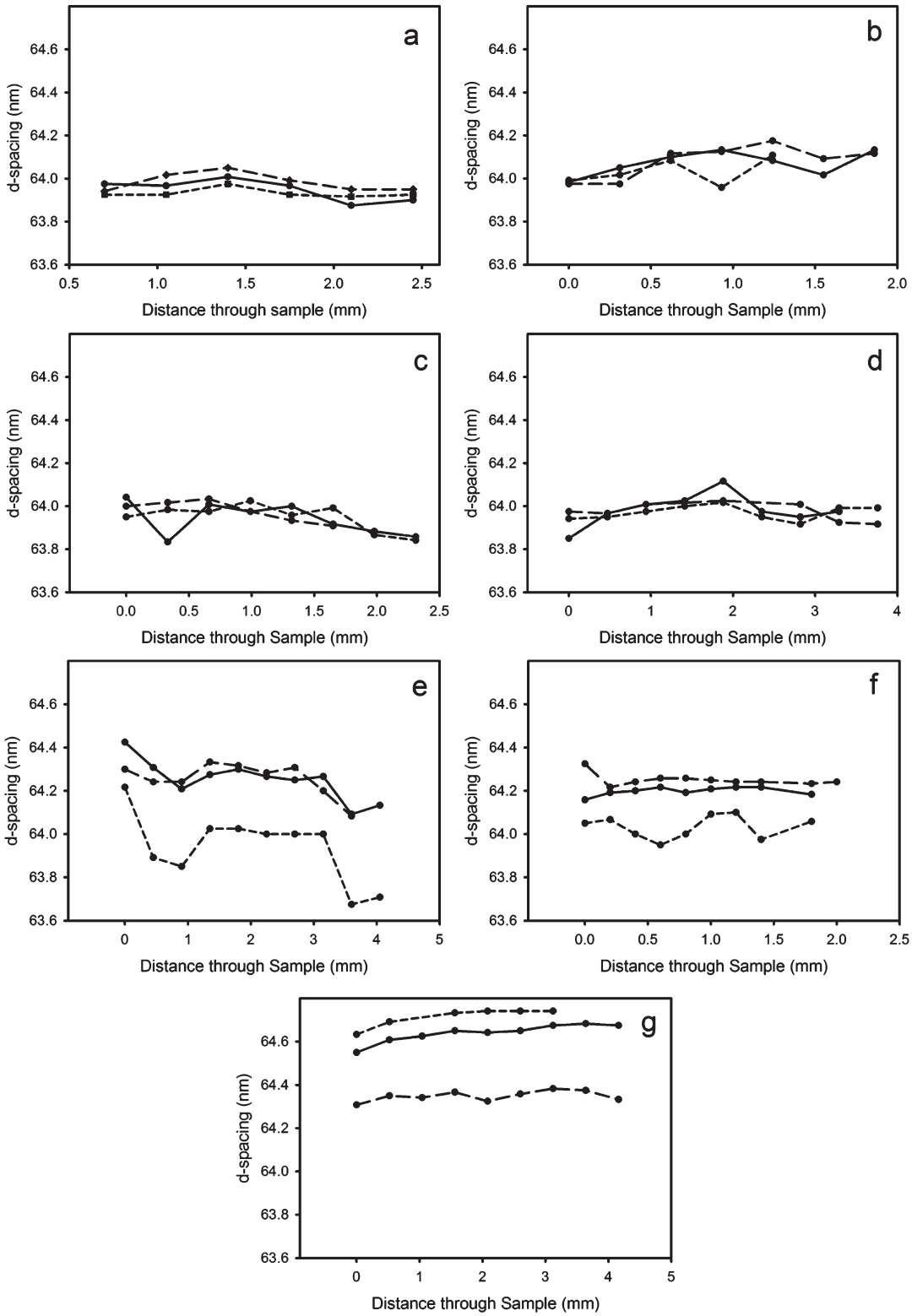

Figure 7. Variation in *d*-spacing through the thickness of ADM materials: (a) fetal bovine, (b) 1.7 mm thick neonatal bovine; (c) 2 mm thick neonatal bovine; (d) 3 mm thick neonatal bovine; (e) 4 mm thick neonatal bovine; (f) porcine; (g) human.

porcine material. The thickness of a surgical scaffold material is also important, partially for aesthetic reasons, and a thin but strong material may be desirable. Therefore, thickness-normalized strength is also a useful measure of the relative merits of different materials. On a thickness-normalized scale, the fetal bovine material is the strongest and its fibers are the most oriented, which perhaps is a general feature of fetal materials (and note that younger bovine pericardium was found to be stronger

DOI: 10.1021/acsbiomaterials.5b00310
ACS Biomater. Sci. Eng. 2015, 1, 1026−1038

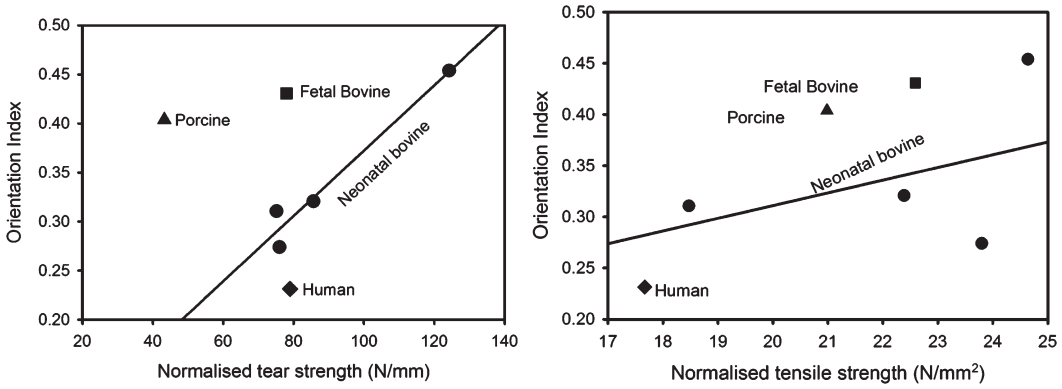

Figure 8. Tear (left) and tensile (right) strength and OI for ADM materials measured with the X-ray beam edge-on to the samples. Line for linear correlation for just the neonatal bovine ADM of varying thickness (tear $r^2 = 0.97$, $P = 0.002$ for $\alpha = 0.05$; tensile $r^2 = 0.44$, $P = 0.22$ for $\alpha = 0.05$).

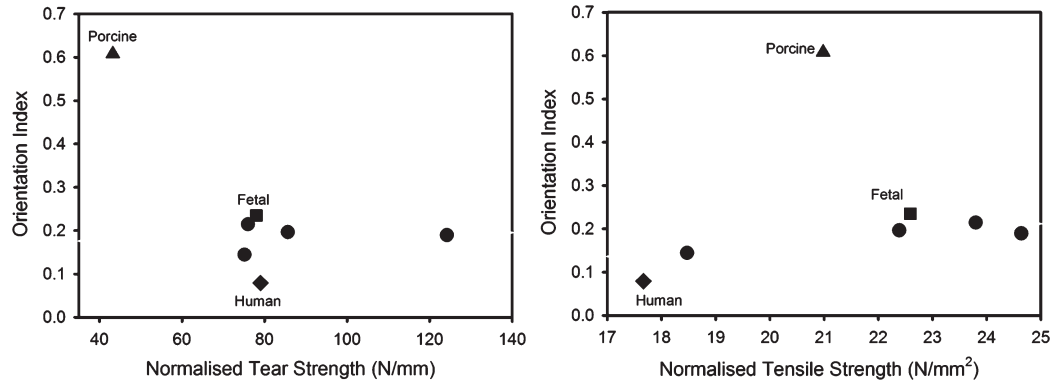

Figure 9. Tear (left) and tensile (right) strength and OI for ADM materials measured with the X-ray beam perpendicular to the samples. Unmarked points are bovine neonatal ADM.

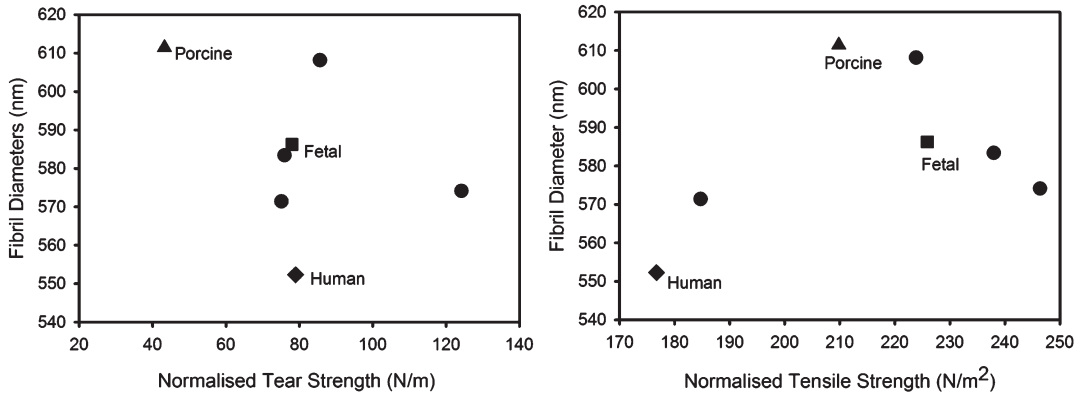

Figure 10. Tear strength and fibril diameter. Unmarked points are bovine neonatal ADM.

than older[8]). The thicker neonatal bovine materials have the next greatest strength, with the thinner neonatal bovine having a lower strength. The strength of these bovine materials is correlated with the OI measured edge-on (Figure 8) as it does in bovine and other leathers.[15,16] In the same strength range as the thinner bovine is the human ADM material, and the lowest strength material on a thickness-normalized basis is the porcine ADM. The strength of the human and porcine ADM material is consistent with the correlation of OI and strength in the bovine materials, so other factors are clearly also important for strength.

These materials derived from different species have largely similar properties and similar structures. There are some differences in strength and in thickness-normalized strength that may provide a preference for one of these materials over others in certain surgical applications. There are also differences in the porosity of the materials, which could be further investigated, quantified, and related to differences in the integration of the scaffold materials in vivo.

CONCLUSIONS

The study of strength and structure of a range of ADM materials has revealed insights into the differences between the materials and the relationship between the structure and some of the physical properties. Bovine ADM material is similar in strength to

DOI: 10.1021/acsbiomaterials.5b00310
ACS Biomater. Sci. Eng. 2015, 1, 1026−1038

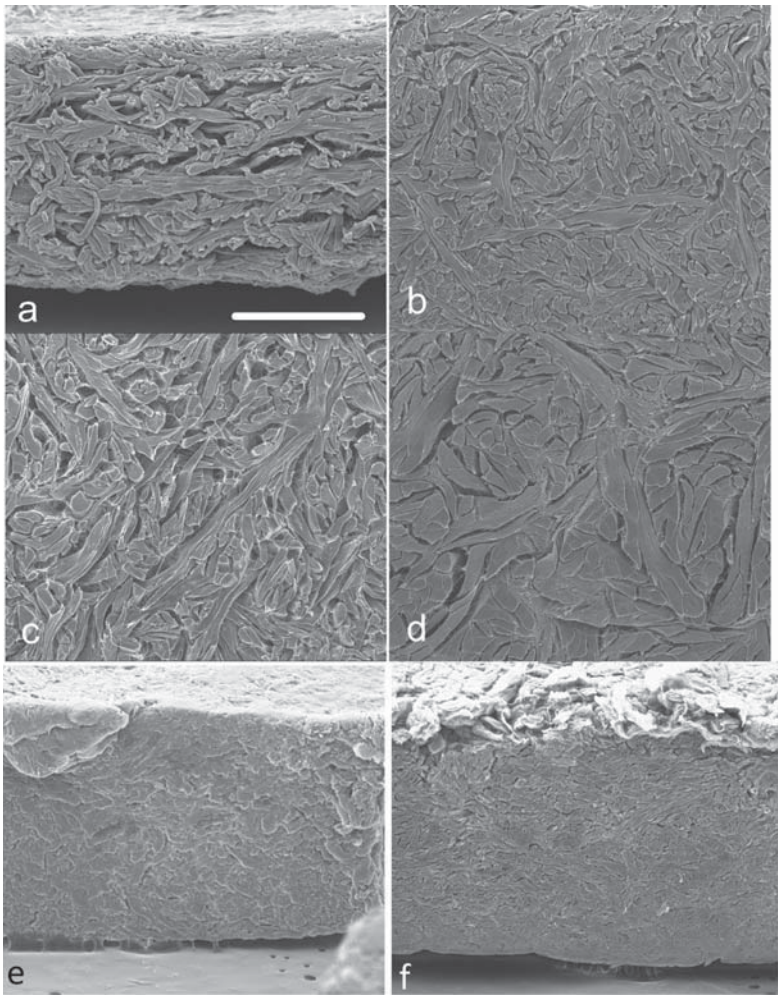

Figure 11. Scanning electron microscopy images through the thickness of the ADM materials: (a) fetal bovine; (b) neonatal bovine 2 mm thick; (c) neonatal bovine 3 mm thick; (d) neonatal bovine 4 mm thick; (e) porcine; (f) human. All at the same magnification; bar is 500 μm.

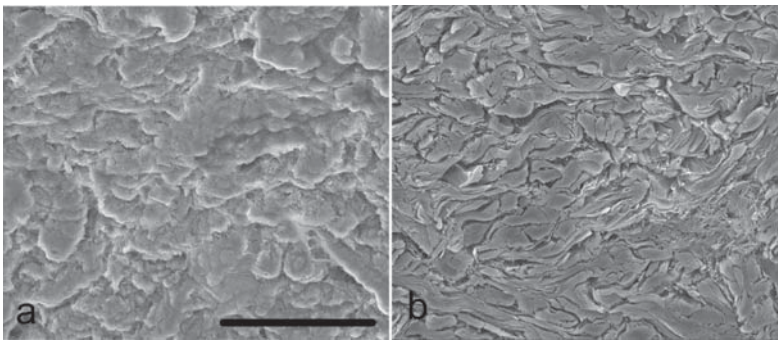

Figure 12. Scanning electron microscopy images at higher magnification through the thickness of the ADM materials: (a) porcine, (b) human. Both at the same magnification; bar is 200 μm.

or a little stronger than human ADM and is significantly stronger than porcine ADM. There is a wide variation in strength in bovine ADM materials and that variation is due to differences in collagen fibril orientation, with stronger materials having a more layered fibril structure. The human ADM material and the thinner (1.7, 2.0, and 3.0 mm) neonatal bovine materials are the most extensible (extensibility to 10 N/mm^2) while the porcine, fetal bovine and 4.0 mm neonatal bovine are the least extensible at this force. Bovine ADM materials have a more open structure than human or porcine ADM and we speculate (however without evidence) that this open structure might help with the integration of the ADM in vivo. The "weft/weave" structures of bovine, porcine and human ADM differ. The human material is the most isotropic, followed by bovine, whereas the porcine is the most anisotropic; these variations may affect the properties of the material in service, although this has not been studied in depth here. It has been shown that there are many similarities in the structures in the different materials but also some subtle

DOI: 10.1021/acsbiomaterials.5b00310
ACS Biomater. Sci. Eng. 2015, 1, 1026−1038

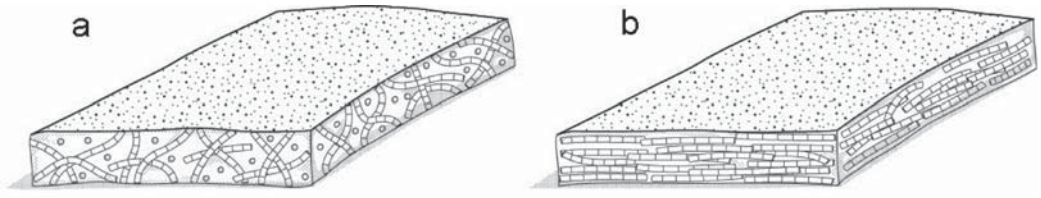

Figure 13. Illustration of the difference between ADM material that is (a) poorly oriented when measured with the X-ray beam edge-on; (b) highly oriented when measured with the X-ray beam edge-on.

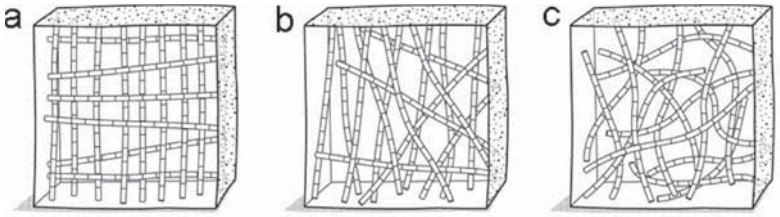

Figure 14. Illustration of the difference between ADM material that is (a) highly oriented in two orthogonal directions when measured with the X-ray beam perpendicular to the sample face, such as in porcine material; (b) partly oriented when measured with the X-ray beam perpendicular to the sample face, such as in bovine material; (c) largely isotropic when measured with the X-ray beam perpendicular to the sample face, such as in human material.

differences which affect physical properties and it may be that the differences in porosity are also important and worth investigating.

AUTHOR INFORMATION

Corresponding Author

*E-mail: r.haverkamp@massey.ac.nz.

Funding

The work was funded in part by the Australian Synchrotron and an unrestricted educational grant from TEI Biosciences.

Notes

The authors declare the following competing financial interest(s): Funding was obtained for this work under an unrestricted educational grant from TEI Biosciences.

ACKNOWLEDGMENTS

This research was undertaken on the SAXS/WAXS beamline at the Australian Synchrotron, Victoria, Australia. The Australian Synchrotron assisted with travel funding and accommodation. This work was supported by a grant from TEI Biosciences. Bret Jessee and Vladimir Russakovsky of TEI Biosciences provided the samples and the motivation for the work. Sue Hallas of Nelson assisted with editing the manuscript.

REFERENCES

(1) Lutolf, M. P.; Hubbell, J. A. Synthetic biomaterials as instructive extracellular microenvironments for morphogenesis in tissue engineering. *Nat. Biotechnol.* **2005**, *23* (1), 47−55.

(2) Badylak, S. F.; Freytes, D. O.; Gilbert, T. W. Extracellular matrix as a biological scaffold material: Structure and function. *Acta Biomater.* **2009**, *5* (1), 1−13.

(3) Meyers, M. A.; McKittrick, J.; Chen, P. Y. Structural biological materials: Critical mechanics-materials connections. *Science* **2013**, *339* (6121), 773−779.

(4) Wells, H. C.; Sizeland, K. H.; Kayed, H. R.; Kirby, N.; Hawley, A.; Mudie, S. T.; Haverkamp, R. G. Poisson's ratio of collagen fibrils measured by SAXS of strained bovine pericardium. *J. Appl. Phys.* **2015**, *117* (4), 044701.

(5) Yang, W.; Sherman, V. R.; Gludovatz, B.; Schaible, E.; Stewart, P.; Ritchie, R. O.; Meyers, M. A. On the tear resistance of skin. *Nat. Commun.* **2015**, *6*, 6649.

(6) Boote, C.; Kamma-Lorger, C. S.; Hayes, S.; Harris, J.; Burghammer, M.; Hiller, J.; Terrill, N. J.; Meek, K. M. Quantification of collagen organization in the peripheral human cornea at micron-scale resolution. *Biophys. J.* **2011**, *101* (1), 33−42.

(7) Sellaro, T. L.; Hildebrand, D.; Lu, Q. J.; Vyavahare, N.; Scott, M.; Sacks, M. S. Effects of collagen fiber orientation on the response of biologically derived soft tissue biomaterials to cyclic loading. *J. Biomed. Mater. Res., Part A* **2007**, *80A* (1), 194−205.

(8) Sizeland, K. H.; Wells, H. C.; Higgins, J. J.; Cunanan, C. M.; Kirby, N.; Hawley, A.; Haverkamp, R. G. Age dependent differences in collagen fibril orientation of glutaraldehyde fixed bovine pericardium. *BioMed Res. Int.* **2014**, *2014*, 189197.

(9) Liao, J.; Yang, L.; Grashow, J.; Sacks, M. S. Molecular orientation of collagen in intact planar connective tissues under biaxial stretch. *Acta Biomater.* **2005**, *1* (1), 45−54.

(10) Gilbert, T. W.; Wognum, S.; Joyce, E. M.; Freytes, D. O.; Sacks, M. S.; Badylak, S. F. Collagen fiber alignment and biaxial mechanical behavior of porcine urinary bladder derived extracellular matrix. *Biomaterials* **2008**, *29* (36), 4775−4782.

(11) Purslow, P. P.; Wess, T. J.; Hukins, D. W. L. Collagen orientation and molecular spacing during creep and stress-relaxation in soft connective tissues. *J. Exp. Biol.* **1998**, *201*, 135−142.

(12) Gasser, T. C. An irreversible constitutive model for fibrous soft biological tissue: A 3-D microfiber approach with demonstrative application to abdominal aortic aneurysms. *Acta Biomater.* **2011**, *7* (6), 2457−2466.

(13) Floden, E. W.; Malak, S.; Basil-Jones, M. M.; Negron, L.; Fisher, J. N.; Byrne, M.; Lun, S.; Dempsey, S. G.; Haverkamp, R. G.; Anderson, I.; Ward, B. R.; May, B. C. H.; et al. Biophysical characterization of ovine forestomach extracellular matrix biomaterials. *J. Biomed. Mater. Res., Part B* **2011**, *96B* (1), 67−75.

(14) Basil-Jones, M. M.; Edmonds, R. L.; Allsop, T. F.; Cooper, S. M.; Holmes, G.; Norris, G. E.; Cookson, D. J.; Kirby, N.; Haverkamp, R. G. Leather structure determination by small-angle X-ray scattering (SAXS): Cross sections of ovine and bovine leather. *J. Agric. Food Chem.* **2010**, *58* (9), 5286−5291.

(15) Basil-Jones, M. M.; Edmonds, R. L.; Cooper, S. M.; Haverkamp, R. G. Collagen fibril orientation in ovine and bovine leather affects strength: A small angle X-ray scattering (SAXS) study. *J. Agric. Food Chem.* **2011**, *59* (18), 9972−9979.

(16) Sizeland, K. H.; Basil-Jones, M. M.; Edmonds, R. L.; Cooper, S. M.; Kirby, N.; Hawley, A.; Haverkamp, R. G. Collagen alignment and leather strength for selected mammals. *J. Agric. Food Chem.* **2013**, *61* (4), 887−892.

DOI: 10.1021/acsbiomaterials.5b00310
ACS Biomater. Sci. Eng. 2015, 1, 1026−1038

(17) Sizeland, K. H.; Edmonds, R. L.; Basil -Jones, M. M.; Kirby, N.; Hawley, A.; Mudie, S.; Haverkamp, R. G. Changes to collagen structure during leather processing. *J. Agric. Food Chem.* **2015**, *63* (9), 2499−2505.
(18) James, V. J.; McConnell, J. F.; Capel, M. The D-spacing of collagen from mitral heart-valves changes with aging, but not with collagen type-III content. *Biochim. Biophys. Acta, Protein Struct. Mol. Enzymol.* **1991**, *1078* (1), 19−22.
(19) Scott, J. E.; Orford, C. R.; Hughes, E. W. Proteoglycan-collagen arrangements in developing rat tail tendon - an electron-microscopical and biochemical investigation. *Biochem. J.* **1981**, *195* (3), 573−584.
(20) Fang, M.; Goldstein, E. L.; Turner, A. S.; Les, C. M.; Orr, B. G.; Fisher, G. J.; Welch, K. B.; Rothman, E. D.; Banaszak Holl, M. M. Type I collagen D-spacing in fibril bundles of dermis, tendon, and bone: Bridging between nano- and micro-level tissue hierachy. *ACS Nano* **2012**, *6*, 9503−9514.
(21) Ripamonti, A.; Roveri, N.; Braga, D.; Hulmes, D. J. S.; Miller, A.; Timmins, P. A. Effects of pH and ionic-strength on the structure of collagen fibrils. *Biopolymers* **1980**, *19* (5), 965−975.
(22) Sizeland, K. H.; Wells, H. C.; Norris, G. E.; Edmonds, R. L.; Kirby, N.; Hawley, A.; Mudie, S.; Haverkamp, R. G. Collagen D-spacing and the effect of fat liquor addition. *J. Am. Leather Chem. Assoc.* **2015**, *110* (3), 66−71.
(23) Wess, T. J.; Orgel, J. P. Changes in collagen structure: drying, dehydrothermal treatment and relation to long term deterioration. *Thermochim. Acta* **2000**, *365* (1−2), 119−128.
(24) Masic, A.; Bertinetti, L.; Schuetz, R.; Chang, S.-W.; Metzger, T. H.; Buehler, M. J.; Fratzl, P. Osmotic pressure induced tensile forces in tendon collagen. *Nat. Commun.* **2015**, *6*, 5942.
(25) Gonzalez, A. D.; Gallant, M. A.; Burr, D. B.; Wallace, J. M. Multiscale analysis of morphology and mechanics in tail tendon from the ZDSD rat model of type 2 diabetes. *J. Biomech.* **2014**, *47*, 681−686.
(26) Balguid, A.; Driessen, N. J.; Mol, A.; Schmitz, J. P. J.; Verheyen, F.; Bouten, C. V. C.; Baaijens, F. P. T. Stress related collagen ultrastructure in human aortic valves - implications for tissue engineering. *J. Biomech.* **2008**, *41* (12), 2612−2617.
(27) Michna, H. Morphometric analysis of loading-induced changes in collagen-fibril populations in young tendons. *Cell Tissue Res.* **1984**, *236* (2), 465−470.
(28) Wells, H. C.; Edmonds, R. L.; Kirby, N.; Hawley, A.; Mudie, S. T.; Haverkamp, R. G. Collagen fibril diameter and leather strength. *J. Agric. Food Chem.* **2013**, *61* (47), 11524−11531.
(29) Parry, D. A. D.; Barnes, G. R. G.; Craig, A. S. Comparison of size distribution of collagen fibrils in connective tissues as a function of age and a possible relation between fibril size distribution and mechanical-properties. P. Roy. *Proc. R. Soc. London, Ser. B* **1978**, *203* (1152), 305−321.
(30) Cookson, D.; Kirby, N.; Knott, R.; Lee, M.; Schultz, D. Strategies for data collection and calibration with a pinhole-geometry SAXS instrument on a synchrotron beamline. *J. Synchrotron Radiat.* **2006**, *13*, 440−444.
(31) Ilavsky, J.; Jemian, P. R. Irena: tool suite for modeling and analysis of small-angle scattering. *J. Appl. Crystallogr.* **2009**, *42*, 347−353.
(32) Sacks, M. S.; Smith, D. B.; Hiester, E. D. A small angle light scattering device for planar connective tissue microstructural analysis. *Ann. Biomed. Eng.* **1997**, *25* (4), 678−689.
(33) Williams, J. M. V. IULTCS (IUP) test methods - Measurement of tear load-double edge tear. *J. Soc. Leather Technol. Ch.* **2000**, *84* (7), 327−329.
(34) Williams, J. M. V. IULTCS (IUP) test methods - Measurement of tensile strength and percentage elongation. *J. Soc. Leather Technol. Ch.* **2000**, *84* (7), 317−321.
(35) Clemens, M. W.; Selber, J. C.; Liu, J.; Adelman, D. M.; Baumann, D. P.; Garvey, P. B.; Butler, C. E. Bovine versus Porcine Acellular Dermal Matrix for Complex Abdominal Wall Reconstruction. *Plastic Reconstruc. Surg.* **2013**, *131* (1), 71−79.
(36) Russakovsky, V. *Personal communication*, 2015.
(37) Basil-Jones, M. M.; Edmonds, R. L.; Norris, G. E.; Haverkamp, R. G. Collagen fibril alignment and deformation during tensile strain of leather: A small-angle X-ray scattering study. *J. Agric. Food Chem.* **2012**, *60*, 1201−1208.
(38) Herchenhan, A.; Bayer, M. L.; Svensson, R. B.; Magnusson, S. P.; Kjaer, M. In vitro tendon tissue development from human fibroblasts demonstrates collagen fibril diameter growth associated with a rise in mechanical strength. *Dev. Dyn.* **2013**, *242* (1), 2−8.
(39) Bigi, A.; Ripamonti, A.; Roveri, N.; Jeronimidis, G.; Purslow, P. P. Collagen orientation by X-Ray pole figures and mechanical-properties of media carotid wall. *J. Mater. Sci.* **1981**, *16* (9), 2557−2562.
(40) Wolf, K.; Alexander, S.; Schacht, V.; Coussens, L. M.; von Andrian, U. H.; van Rheenen, J.; Deryugina, E.; Friedl, P. Collagen-based cell migration models in vitro and in vivo. *Semin. Cell Dev. Biol.* **2009**, *20* (8), 931−941.

DOI: 10.1021/acsbiomaterials.5b00310
ACS Biomater. Sci. Eng. 2015, 1, 1026−1038

Fatliquor Effects on Collagen Fibril Orientation and D-spacing in Leather During Tensile Strain

by

K. H. Sizeland,[†] G. Holmes,[§] R. L. Edmonds,[§] N. Kirby,[‡] A. Hawley,[‡] S. T. Mudie[‡] and R. G. Haverkamp[†]*

[†]*School of Engineering and Advanced Technology, Massey University*

Private Bag 11222, Palmerston North, New Zealand

[§]*Leather and Shoe Research Association,*

P.O. Box 8094, Palmerston North 4446, New Zealand

[‡]*Australian Synchrotron,*

800 Blackburn Road, Clayton, Melbourne, Australia

Abstract

Strength is a very important property of leather and is known to depend on the arrangement of the collagen fibrils within the material. The addition of fatliquor (penetrating oils) is an essential part of the manufacture of leather and enhances the strength and feel of leather. However, the mechanism by which fatliquor leads to increased strength is not understood. Here we use synchrotron based small angle X-ray scattering (SAXS) to monitor the collagen fibril rearrangement and internal strain of leather during tension. Differences in internal structural changes under strain with varying levels of fatliquor are investigated. It is found that when a strain of up to 40-70% was applied to leather, the orientation index (OI) of the collagen fibrils changed up to 21.8% and the d-spacing changed by up to 1.8% with no consistent differences at different levels of fatliquor. The extensibility of leather increases by 11.3% with as little as 2% fatliquor addition and the elastic modulus decreases with fatliquor addition but not in proportion to the amount of fatliquor. This change in extensibility is not reflected in differences in OI or d-spacing changes during strain. As reported previously, the fatliquor modifies the d-spacing of collagen. While fatliquor is traditionally considered to lubricate the fibers in leather, here the evidence suggests that this does not occur at the level of collagen fibrils. This provides an insight in the action of fatliquor in leather manufacture.

Introduction

The physical properties of leather result from a combination of the native characteristics of the skin or hide from which the leather is prepared and from the chemical and mechanical processing of leather manufacturing. Strength, flexibility, elasticity, and appearance are all important for the applications of leather. The major structural component of leather is type I collagen and it is the mechanical properties of the collagen fibrils [1-3] and the interactions between the fibrils [4-8] that make the major contribution to the physical properties of leather. Interactions between collagen fibrils in leather consist of hydrogen bonding, hydrophobic bonding, and cross-linking introduced by tanning with chromium salts or tannins. Cross-linking agents can alter the arrangement of collagen fibrils [8] and the mechanical properties of the material[9]

At a later stage in the processing of skins to leather, penetrating oils, known in the industry as fatliquor, are added to improve the feel of the leather and to increase the strength. It is believed that fatliquor acts to lubricate the fibers in leather. [10] Recently it has been shown that fatliquor penetrates to the level internal to collagen fibrils and alters the structure of the fibrils, increasing the d-spacing. [11] This is believed to be a result of shielding of the hydrophobic interaction between individual collagen molecules or tropocollagen units.

A powerful method to investigate the structure of collagen materials is small angle X–ray scattering (SAXS) that can provide detailed structural information on the microfibril orientation, d-spacing and the collagen fibril diameter in leather and other tissues. [12-17]

To understand the physical properties of leather, changes to the structure and arrangement of the collagen fibrils during mechanical strain has been investigated. [3,18-20] It has been found that with strain of the leather the collagen fibrils first re-orient and then stretch.

We wished to investigate the effect that fatliquor has on leather during mechanical strain. It is believed that fatliquor lubricates the fibers in leather and it has been shown that

*Corresponding author e-mail: r.haverkamp@massey.ac.nz

Manuscript received May 21, 2015, accepted for publication June 30, 2015.

fatliquor penetrates beyond the level of collagen fibrils, so does the fatliquor lubricate at the level of collagen fibrils?

EXPERIMENTAL

Ovine skins were obtained from 5-month-old, early season Romney cross lambs. Conventional beamhouse and tanning processes were used to generate leather. The skins were depilated using a caustic treatment comprising sodium sulfide and calcium hydroxide. The residual keratinaceous material was then removed in a 1.2% solution of sodium for 16 h at 20°C. The skins were then washed and treated with a proteolytic pancreatic enzyme (Tanzyme, Tryptec Biochemicals, Ltd.) at 0.1%, followed by pickling in a 2% sulfuric acid and 10% sodium chloride solution. The pickled skins were then pretanned using oxazolidine, degreased with an aqueous surfactant, and then tanned using chromium sulfate. The resulting "wet blue" was then retanned using a mimosa vegetable extract.

Fatliquoring was carried out using Lipsol EHF (Schill + Seilacher). This product contains a mixture of lanolin, bisulfited fish oil, and 2-methyl-2,4-pentanediol. Lanolin, or wool wax, consists primarily of long chain waxy esters and some hydrolysis and oxidation products of these esters. The fatliquor offered was 0–10% by weight of wet leather prior to drying and mechanical softening.

The fatliquor content of samples processed with offerings of 0-10% fatliquor was determined using standard method ISO 4048. Briefly, 10 g of ground leather was extracted with at least 30 changes of dichloromethane in a Soxhlet extraction apparatus. The extract was dried in an oven at 102°C for at least 4 h and the resulting grease was cooled in a desiccator and weighed.

Samples for synchrotron-based small angle X-ray scattering (SAXS) analysis were prepared by cutting strips of leather 1 × 30 mm from the official sampling position (OSP) [21] from skins processed to leather with 0, 2, 4, 6, 8, and 10% Lipsol EHF offered. Diffraction patterns were recorded on the Australian Synchrotron SAXS/WAXS beamline using a high-intensity undulator source. Each sample was mounted without tension in the X-ray beam to obtain scattering patterns from an edge-on direction. Measurements were made every 0.25 mm through the cross section from the grain to the corium. Energy resolution of 10^{-4} was obtained from a cryo-cooled Si (111) double-crystal monochromator, and the beam size [full width at half maximum (fwhm) focused at the sample] was 250 × 80 μm, with a total photon flux of about 2×10^{12} photons s^{-1}. All diffraction patterns were recorded with an X-ray energy of 11 keV using a Pilatus 1 M detector with an active area of 170 × 170 mm and a sample–detector distance of 3371 mm. Exposure time for diffraction patterns was 1 s, and data processing was carried out using the SAXS15ID software. [22]

A custom built stretching apparatus was built for in-situ small angle X-ray scattering (SAXS) measurements as described by Basil-Jones. [18] Each strip of leather was mounted without tension in the X-ray beam and measurements were made every 0.25 mm through the cross section to obtain scattering patterns through the full thickness of the leather. The sample was stretched by 1 mm and was maintained at this extension for 1 minute before diffraction patterns, force, and extension data were recorded. This process was repeated with the sample stretched a further 1 mm each time until the sample failed.

Orientation index (OI) is used to give a measure of the spread of microfibril orientation and can be any number within the range 0–1. An OI of 1 indicates anisotropic microfibrils or fibrils that are completely parallel to each other; an OI of 0 indicates isotropic microfibrils or fibrils that are completely randomly oriented. OI is defined as (90° – OA)/90° where OA is the azimuthal angle range that contains 50% of the microfibrils centered at 180° and is calculated for one of the most intense d-spacing peaks (at around 0.059–0.060 $Å^{-1}$) for every diffraction pattern. [1]

The d-spacing of collagen was determined for each spectrum from Bragg's Law by taking the central position of several collagen peaks, dividing these by the peak order (usually from $n = 5$ to $n = 10$) and averaging the resulting values.

Tear strengths of the crust leathers were tested using standard methods. [23] Samples were cut from the leather at the official sampling position (OSP). [21] The samples were then conditioned by holding at 20°C and 65% relative humidity for 24 hours then tested on an Instron tensile tester using jaws placed in a standard eye-shaped cutout. Stress and strain measurements were recorded on an Instron mechanical test system using a standard tensile strength test. [24]

RESULTS

Fatliquor Addition

The offer of fatliquor to the leather ranged up to 10% however the actual uptake of fatliquor was not quite the same as the offer. We therefore refer to the offer as the "nominal fatliquor". An analysis of the fat content of the fatliquored leather showed a higher fat content than the offer, because of some initial fat content in the leather, with a saturation occurring at 8% offer (Table I).

Scattering Patterns

The X-ray scattering patterns recorded for the leather samples show clear diffraction rings (Figure 1 a, b) which

are due to the collagen d-banding. The integrated intensity for these patterns shows these as well defined peaks from which the d-banding can be identified (Figure 1c, d). The variation in intensity with azimuthal angle (Figure 1e) can be used to calculate the orientation index of the collagen fibrils. It can be seen that when the leather is stretched the OI increases and a portion of the fibrils which are oriented in the direction of the strain become highly stretched with the d-spacing increasing substantially.

Tear Test

The tear force observed had an initial drop in the tear strength with the addition of a small amount of fatliquor followed by a general increase in tear strength with further fatliquor additions (Figure 2). Generally therefore leather is stronger when this fatliquor is present.

When the variation of d-spacing with strain is plotted it becomes apparent that the d-spacing increases with fatliquor

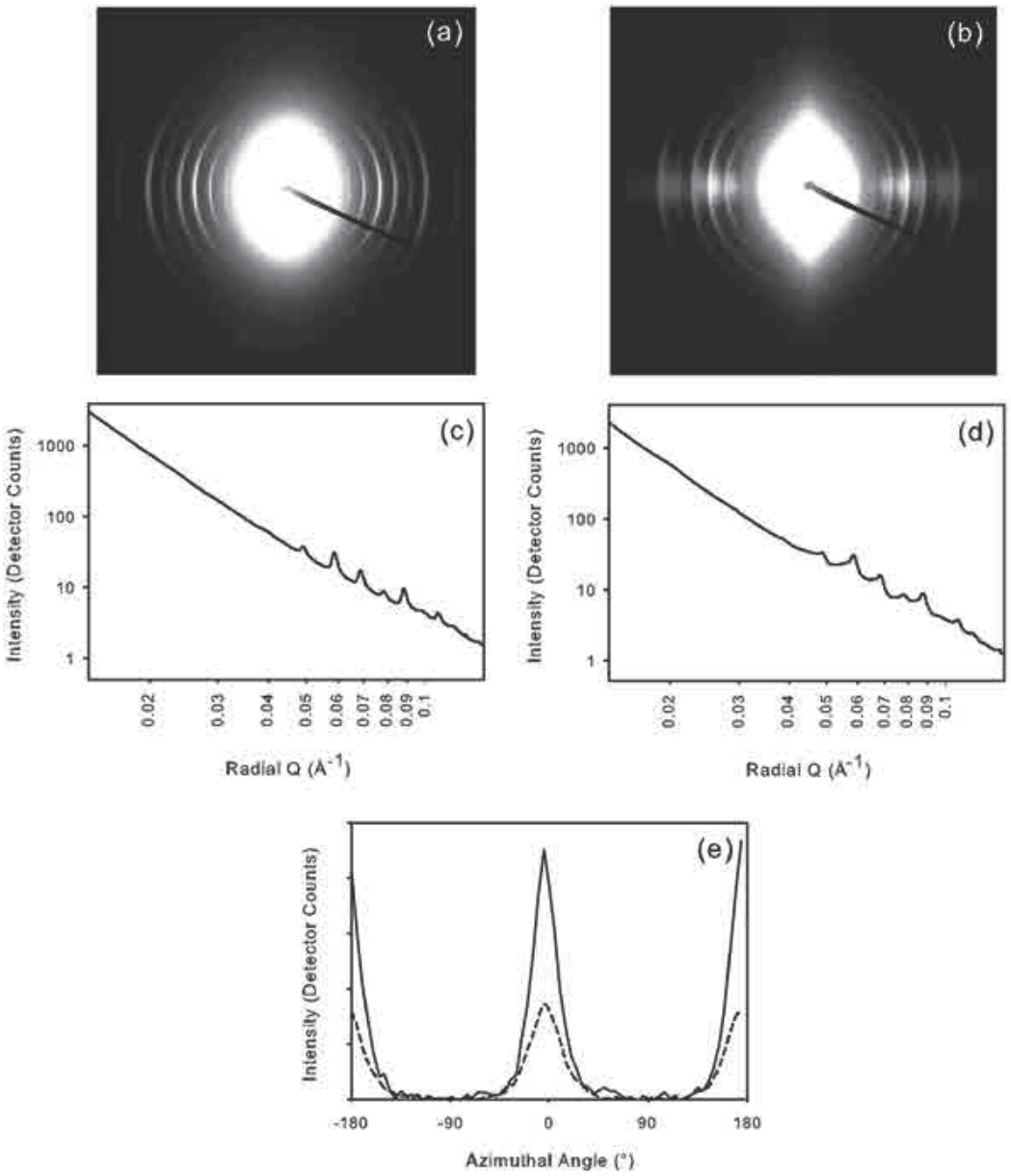

Figure 1. Example of SAXS of leather: (a) raw SAXS pattern static; (b) raw SAXS pattern after stretching; (c) integrated intensity profile of static sample; (d) integrated intensity profile of sample after stretching; (e) intensity variation with azimuthal angle for the 5th order diffraction peak (dotted line static, solid line stretched).

content (as reported elsewhere [11]) and increases with strain (as seen with ovine leather [18]) (Figure 3.). There is no difference between 8% and 10% fatliquor offered samples as these had saturated and had the same uptake of fatliquor.

Orientation Index

The OI increases with strain for all samples (Figure 4). No correlation was found between fatliquor and OI when the samples were not under tension (R^2 = 0.47, P = 0.13) (Figure 5a). Similarly, when stretched, after the increase in OI which happens for all samples, the OI measured at maximum strain before the samples broke does not correlate with fatliquor addition (R^2 = 0.08, P = 0.60) (Figure 5b).

TABLE I
Nominal addition of fatliquor and measured content of fat in leather samples.

Nominal Addition of Fatliquor (%)	Measured Fat Content (%)	Measured fatliquor added (%)
0	1.0	0.0
2	3.8	2.8
4	5.7	4.7
6	8.8	7.8
8	9.8	8.8
10	9.9	8.9

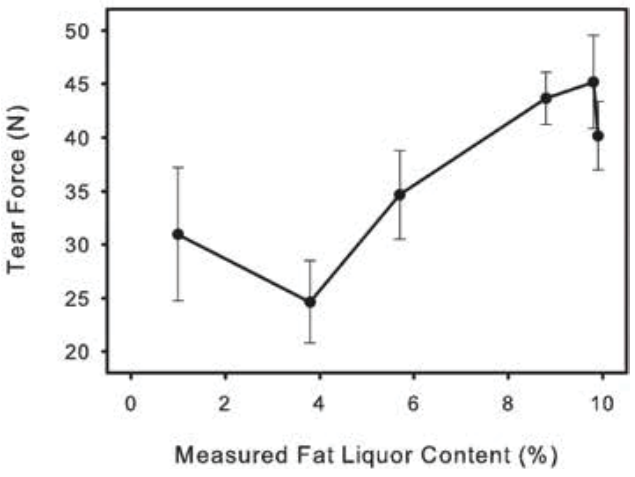

Figure 2. Tear force of leather with measured fatliquor content.

The samples with different fatliquor content do not all stretch the same amount. Therefore a plot of the change in d-spacing and OI at a strain of 0.4 is also shown (Figure 6). This provides a fair comparison between the changes that take place to fibril rearrangement and fibril extension under tension when different levels of fatliquor are present. This shows no trend when stretched with fatliquor content of the sample in either the amount that d-spacing changes or in the OI change with stretching (Figure 6).

Stress-strain

The stress-strain curves (Figure 7) show that the elasticity varies with fatliquor content. With fatliquor added, leather has

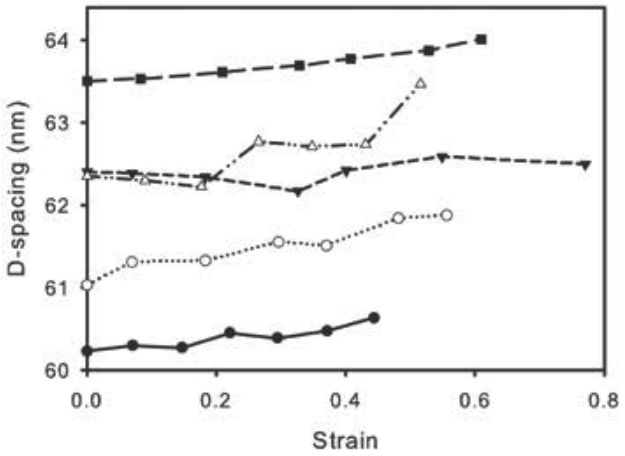

Figure 3. Variation in d-spacing with strain and fatliquor content: (●, _____) no fatliquor, (○, ·····) 2.8% fatliquor, (▼, – – – –) 4.7% fatliquor, (Δ, – ·· – ·· –) 7.8% fatliquor, (■, ———) 8.8% fatliquor.

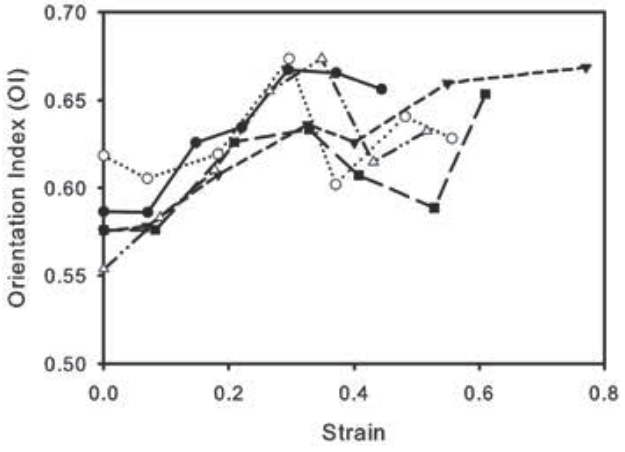

Figure 4. Variation in orientation index (OI) with strain and fatliquor content: (●, _____) no fatliquor, (○, ·····) 2.8% fatliquor, (▼, – – – –) 4.7% fatliquor, (Δ, – ·· – ·· –) 7.8% fatliquor, (■, ———) 8.8% fatliquor.

a longer region of low elastic modulus (stretchier material) before the leather starts to resist stretching. Full stress-strain curves for the small samples measured in-situ during X-ray analysis are shown in Figure 7a but these were small samples and must not be over-interpreted. Elastic modulus obtained from these curves show the initial drop in elastic modulus with an addition of a small amount of fatliquor followed by a general increase in elastic modulus with further fatliquor additions (Figure 7b). The total extensibility of the leather is also shown but does not follow an easily rationalized trend (Figure 7c).

OI of Cross Sections

The variation of OI through sections of leather with different amounts of fatliquor at different levels of strain (Figure 8) show the strain is taken up throughout the thickness of the leather and that this is similar with or without fatliquor added. There is no obviously different mechanism of responding to strain with or without fatliquor present.

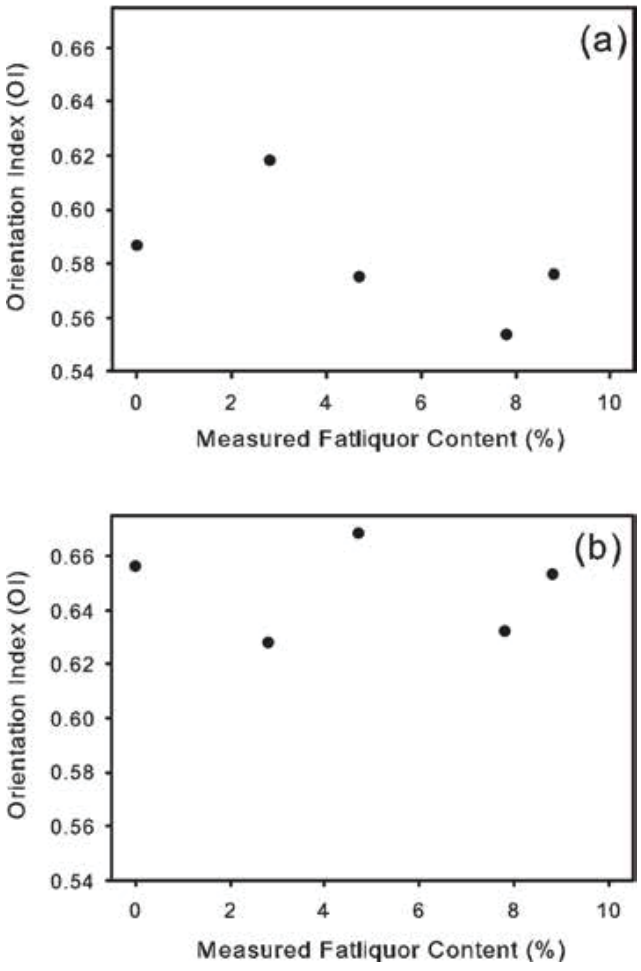

Figure 5. Variation of OI with measured fatliquor content (a) for unstrained leather; (b) for leather strained to Maximum, orientation is calculated by taking the average OI of the sample after each stretching increment (from no stretch up to the maximum amount stretched) and averaging these values.

DISCUSSION

While it can be seen that the fatliquor penetrates to the collagen fibrils and changes some aspect of the structure of the fibrils, the d-spacing, as reported elsewhere, [11] there does not appear to be any difference in the change in the orientation of the fibrils during strain with or without fatliquor. Therefore the rearrangement of fibrils in the leather is not greater with fatliquor added than without. In addition, the amount of force individual fibrils experience (evidenced by d-spacing change during stress) is not less with fatliquor than without.

If the fatliquor acted to lubricate the collagen fibrils so that they slide more easily past one another then it would be expected that the OI would change much more with strain when fatliquor is added because as the fibrils slide past each other they would be able to rearrange their positions to become more oriented in the direction of strain. If this is the mechanism of action of fatliquor then it would also be expected that once highly oriented the fibrils should be able to stretch more as they are oriented with the direction of force. Neither of these is seen, neither a greater change in OI nor a larger increase in d-spacing. Therefore, there is no evidence of lubrication of the collagen fibrils, even though we know that the fatliquor penetrates not just to the fibrils but also within the fibrils (as evidenced by the change in d-spacing).

From the stress-strain data, and as is well known already, fatliquor does improve the bulk properties of leather and increases the extensibility and decreases the elastic modulus of leather. Therefore fatliquor does have an effect on the leather. Since the lubrication by fatliquor does not appear to occur at the fibril level the mode of action may be lubrication between fibril bundles or fibers which is at a different scale to the fibrils.

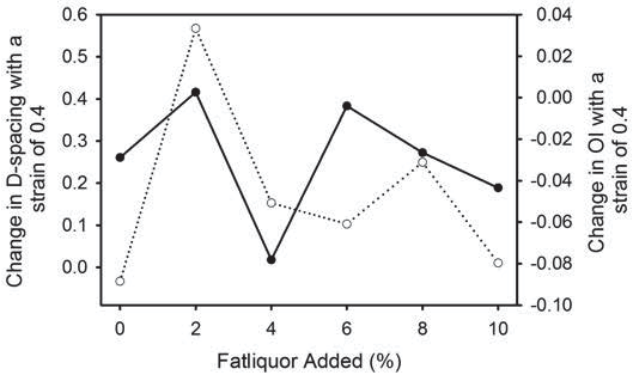

Figure 6. Change in OI and d-spacing upon strain to 0.4 for measured fatliquor contents: (●, _____) change in d-spacing, (○, ·····) change in OI.

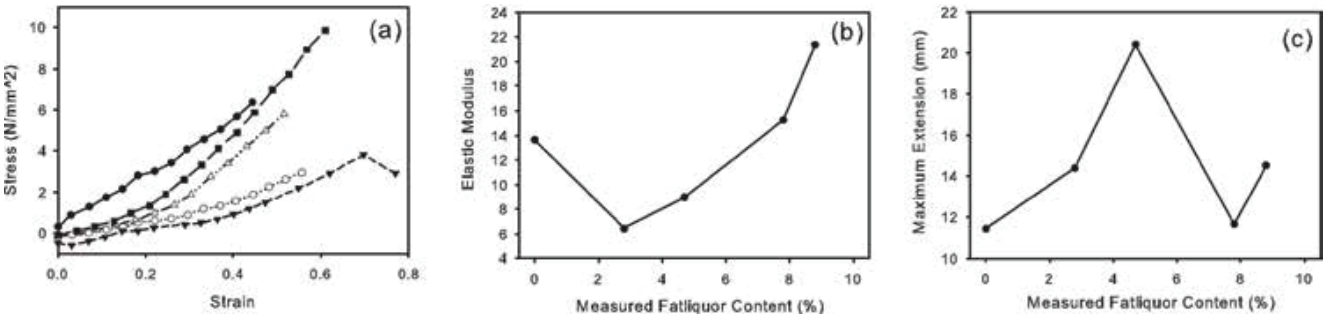

Figure 7. (a) Stress-strain on small leather samples recording during SAXS measurements: (●, _____) no fatliquor, (○, ·····) 2.8% fatliquor, (▼, – – – –) 4.7% fatliquor, (Δ, – ·· – ·· –) 7.8% fatliquor, (■, ———) 8.8% fatliquor; (b) Elastic modulus taken from curves in (a); (c) maximum extension of sample before break occurred versus measured fatliquor content.

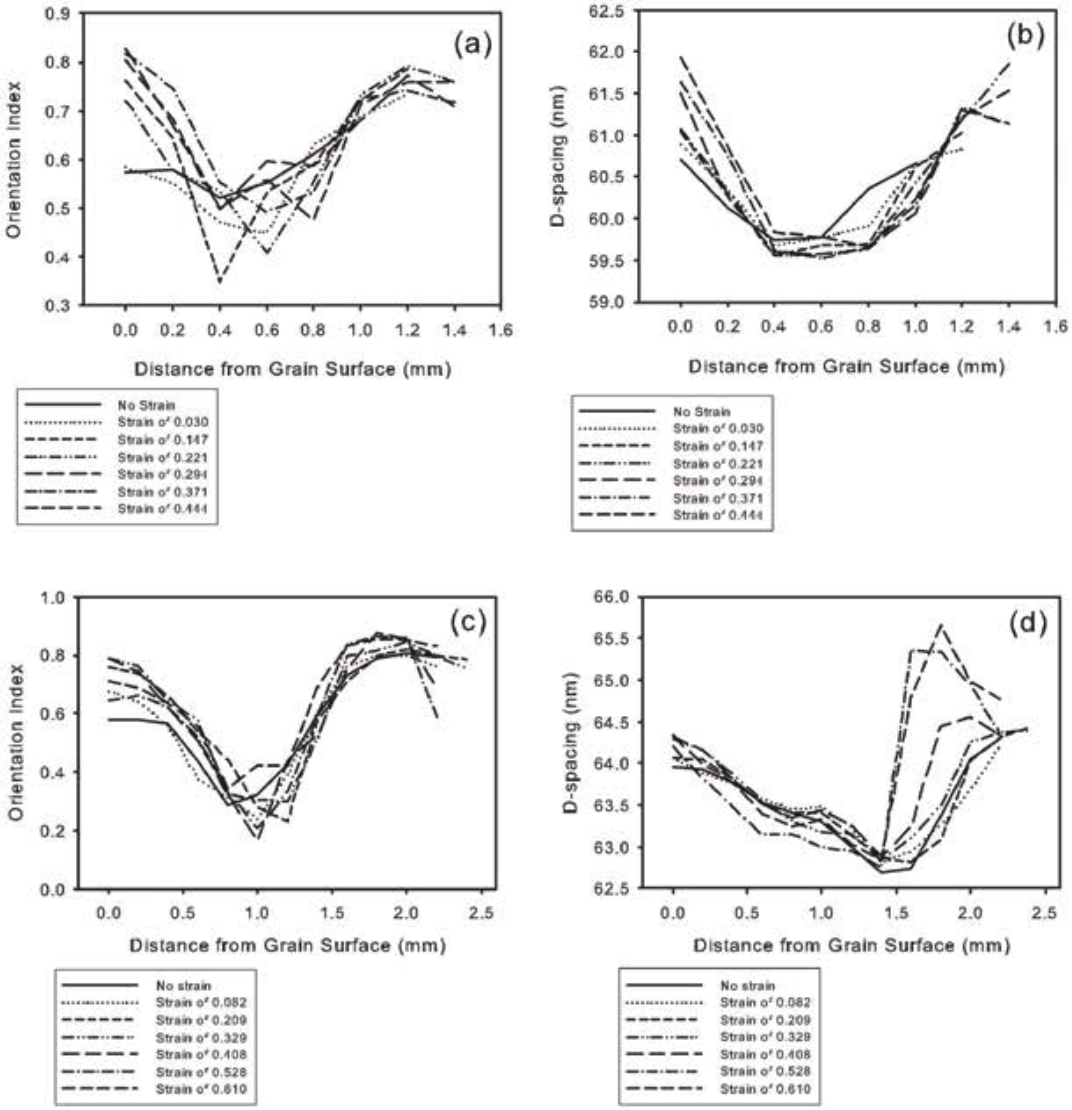

Figure 8. Cross sections of leather under strain. No fatliquor (a, b), 8.8% measured fatliquor content (c, d). Variation of OI with strain (a, c), variation of d-spacing with strain (b, d).

Leather takes up strain at a variety of scales, both within the fibril (d-spacing), between fibrils (OI) and at the fibril bundle and fiber level (possibly contributes also to OI). Fatliquor affects the larger scale processes such as drying of the leather and is the most important step in making soft leather. However, it was observed that the arrangement of fibers is mostly unaffected by fatliquor with no change in the spread of orientation.

CONCLUSIONS

Using small angle X-ray scattering to analyze leather, differences in collagen fibril orientation and d-spacing with different levels of fatliquor addition and at different levels of strain were investigated. Both the orientation index and d-spacing changed during strain however there were no consistent differences in these behaviors with different levels of fatliquor. While fatliquor is traditionally considered to lubricate the fibers in leather, here the evidence suggests that this does not occur at the level of collagen fibrils, even though there is evidence that the fatliquor penetrates to the level of the fibrils and changes the structure of the fibrils. We have been able to provide more knowledge on the mechanism of action of fatliquor to the elasticity of leather to inform the leather making process.

ACKNOWLEDGEMENTS

This research was undertaken on the SAXS/WAXS beamline at the Australian Synchrotron, Victoria, Australia. Sue Hallas of Nelson assisted with editing. This work was supported by the Ministry of Business, Innovation and Employment, New Zealand (Grant LSRX0801). The Australian Synchrotron provided travel funding and accommodation.

REFERENCES

1. Basil-Jones, M. M., Edmonds, R. L., Cooper, S. M., and Haverkamp, R. G.; Collagen fibril orientation in ovine and bovine leather affects strength: A small angle X-ray scattering (SAXS) study. *J. Agric. Food Chem.* **59**, 9972-9979, 2011.
2. Russell, A. E.; Stress-strain relationships in leather and the role of fiber structure. *J. Soc. Leather Technol. Chem.* **72**, 121-134, 1988.
3. Wells, H. C., Sizeland, K. H., Kayed, H. R., Kirby, N., Hawley, A., Mudie, S. T., and Haverkamp, R. G.; Poisson's Ratio of Collagen Fibrils Measured by SAXS of Strained Bovine Pericardium. *J. Appl. Phys.* **117**, 044701, 2015.
4. Chan, Y., Cox, G. M., Haverkamp, R. G., and Hill, J. M.; Mechanical model for a collagen fibril pair in extracellular matrix. *Eur. Biophys. J. Biophy. Lett.* **38**, 487-493, 2009.
5. Rabinovich, D.; Seeking soft leathers with a tight grain. *WORLD Leather* **14**, 27-32, 2001.
6. Deb Choudhury, S., Haverkamp, R. G., DasGupta, S., and Norris, G. E.; Effect of oxazolidine E on collagen fibril formation and stabilization of the collagen matrix. *J. Agric. Food Chem.* **55**, 6813-6822, 2007.
7. Michel, A.; Tanners' dilemma: Vertical fibre defect. *Leather International* **206**, 36-37, 2004.
8. Kayed, H. R., Sizeland, K. H., Kirby, N., Hawley, A., Mudie, S. T., and Haverkamp, R. G.; Collagen cross linking and fibril alignment in pericardium. *RSC Adv.* **5**, 3611-3618, 2015.
9 Makris, E. A., Responte, D. J., Paschos, N. K., Hu, J. C., and Athanasiou, K. A. ; Developing functional musculoskeletal tissues through hypoxia and lysyl oxidase-induced collagen cross-linking. *Proc. Natl. Acad. Sci. U. S. A.* **111**, E4832-E4841, 2014.
10. Bajza, Z., and Vreck, I. V.; Fatliquoring agent and drying temperature effects on leather properties. *J. Mater. Sci.* **36**, 5265-5270, 2001.
11. Sizeland, K. H., Edmonds, R. L., Basil-Jones, M. M., Kirby, N., Hawley, A., Mudie, S., and Haverkamp, R. G.; Changes to Collagen Structure during Leather Processing. *J. Agric. Food Chem.* **63**, 2499-2505, 2015.
12. Kronick, P. L., and Buechler, P. R.; Fiber orientation in calfskin by laser-light scattering or X-ray-diffraction and quantitative relation to mechanical-properties. *J. Am. Leather Chem. As.* **81**, 221-230, 1986.
13. Wells, H. C., Edmonds, R. L., Kirby, N., Hawley, A., Mudie, S. T., and Haverkamp, R. G.; Collagen Fibril Diameter and Leather Strength. *J. Agric. Food Chem.* **61**, 11524-11531, 2013.
14. Basil-Jones, M. M., Edmonds, R. L., Allsop, T. F., Cooper, S. M., Holmes, G., Norris, G. E., Cookson, D. J., Kirby, N., and Haverkamp, R. G.; Leather structure determination by small-angle X-ray scattering (SAXS): Cross sections of ovine and bovine leather. *J. Agric. Food Chem.* **58**, 5286-5291, 2010.
15. Sizeland, K. H., Basil-Jones, M. M., Edmonds, R. L., Cooper, S. M., Kirby, N., Hawley, A., and Haverkamp, R. G.; Collagen Orientation and Leather Strength for Selected Mammals. *J. Agric. Food Chem.* **61**, 887-892, 2013.
16. Kennedy, C. J., Hiller, J. C., Lammie, D., Drakopoulos, M., Vest, M., Cooper, M., Adderley, W. P., and Wess, T. J.; Microfocus X-ray diffraction of historical parchment reveals variations in structural features through parchment cross sections. *Nano Lett.* **4**, 1373-1380, 2004.
17. Goh, K. L., Hiller, J., Haston, J. L., Holmes, D. F., Kadler, K. E., Murdoch, A., Meakin, J. R., and Wess, T. J.; Analysis of collagen fibril diameter distribution in connective tissues using small-angle X-ray scattering. *BBA-Gen. Subjects* **1722**, 183-188, 2005.

18. Basil-Jones, M. M., Edmonds, R. L., Norris, G. E., and Haverkamp, R. G.; Collagen fibril alignment and deformation during tensile strain of leather: A SAXS study. *J. Agric. Food Chem.* **60**, 1201-1208, 2012.
19. Boote, C., Sturrock, E. J., Attenburrow, G. E., and Meek, K. M.; Psuedo-affine behaviour of collagen fibres during the uniaxial deformation of leather. *J. Mater. Sci.* **37**, 3651-3656, 2002.
20. Sturrock, E. J., Boote, C., Attenburrow, G. E., and Meek, K. M.; The effect of the biaxial stretching of leather on fibre orientation and tensile modulus. *J. Mater. Sci.* **39**, 2481-2486, 2004.
21. Williams, J. M. V.; IULTCS (IUP) test methods - Sampling. *J. Soc. Leather Technol. Chem.* **84**, 303-309, 2000.
22. Cookson, D., Kirby, N., Knott, R., Lee, M., and Schultz, D.; Strategies for data collection and calibration with a pinhole-geometry SAXS instrument on a synchrotron beamline. *J. Synchrotron Radiat.* **13**, 440-444, 2006.
23. Williams, J. M. V.; IULTCS (IUP) test methods - Measurement of tear load-double edge tear. *J. Soc. Leather Tech. Ch.* **84**, 327-329, 2000.
24. Williams, J. M. V.; IULTCS (IUP) test methods - Measurement of tensile strength and percentage elongation. *J. Soc. Leather Technol. Chem.* **84**, 317-321, 2000.

10.2 Appendix 2: Conference Papers

Sizeland, K. H., Basil-Jones, M. M., Edmonds, R. L., & Haverkamp, R. G. "Implications of Synchrotron Analysis for Leather Manufacturing", *Proceedings of the 63rd Annual Leather and Shoe Research Association conference,* (pp. 28-37), Wellington, New Zealand, 16th-17th August, 2012.

Sizeland, K. H., Basil-Jones, M. M., Norris, G. E., Edmonds, R. L. Kirby, N., Hawley, A., & Haverkamp, R. G. "Collagen Alignment and Leather Strength", *Proceedings of the International Union of Leather Technologists and Chemists Societies XXXII Congress,* (Paper 110), Istanbul, Turkey, 29th-31st May, 2013.

Haverkamp, R. G., Basil-Jones, M. M., **Sizeland, K. H.**, & Edmonds, R. L. "Synchrotron Studies of Leather Structure", *Proceedings of the International Union of Leather Technologists and Chemists Societies XXXII Congress,* (Paper 109), Istanbul, Turkey, 29th-31st May, 2013.

Sizeland, K. H., Edmonds, R. L., Norris, G. E., Kirby, N., Hawley, A., Mudie, S., & Haverkamp, R. G. (2014). "Modification of collagen d-spacing in skin", *Proceedings of the 28th International Federation of the Societies of Cosmetic Chemists Congress,* (pp. 1222-1235), Palais des Congrès, Paris, France, 27th-30th October, 2014.

Sizeland, K. H., Wells, H. C., Norris, G., Edmonds, R. L. & Haverkamp, R. G. "Collagen D-spacing Modification by Fat Liquor Addition". *Proceedings of the 65th Leather and Shoe Research Association Conference,* Wellington, New Zealand, 13th-14th August, 2014.

Wells, H., **Sizeland, K. H.**, Edmonds, R. L., Aitkenhead, W., Kappen, P., Glover, C., Johannessen, B., & Haverkamp, R. G. 2014. "Biochar and Other Solid Waste Minimisation Options". *Proceedings of the 65th Leather and Shoe Research Association Conference,* Wellington, New Zealand, 13th-14th August, 2014.

Implications of Synchrotron Analysis for Leather Manufacturing

Katie Sizeland[1], Richard Haverkamp[1], Melissa Basil-Jones[1], Richard Edmonds[2]

[1]School of Engineering and Advanced Technology, Massey University, Private Bag 11222, Palmerston North, New Zealand 4442; [2]Leather and Shoe Research Association of New Zealand, PO Box 8094, Palmerston North, New Zealand 4446.

Introduction

Leather, a material obtained through processing, is made up of two parallel planes that are mostly comprised of fibrous collagen. The strength and physical properties of leather are not solely reliant on the amount of collagen it contains. The strength is largely dependent on the arrangement of the collagen fibrils both within planes and the cross-over between planes. As it is a strong, flexible, water-resistant material leather is used in a wide variety of manufacturing applications including shoes, bags, furniture coverings, car interiors and airplane seat covers. However the leather used for these products is mostly bovine leather as it has a far greater strength than that of ovine leather. If the nanostructure of ovine leather was understood then the ability to manipulate processes in order to achieve ovine leather of higher strength may be realized. Synchrotron based techniques such as small angle X-ray scattering provide an ideal platform for nanostructure analysis of the fibrous collagen. Information regarding the structure and alignment of the collagen fibrils is provided by the small angle scattering pattern. This synchrotron technique allows us to determine why leather has the properties it does and how the fibril structure relates to the desirable attributes present. Following this, modifications can be configured to enhance the structure. The processing stages are able to be looked at in depth through the use of synchrotron techniques to discover how processing does change or could change the fibrous structure. Raw stock selection, raw stock performance prediction and breed enhancement can all be developed from the information obtained.

Experimental

The ovine pelts used were from 5 month old lambs. The bovine hides used were from 2−3 year old cattle. Leathers were generated with a variety of properties using conventional techniques. Specifically, the pelts were depilated using a caustic treatment comprising sodium sulfide (ranging from a slow-acting paint containing 160 g/L flake sodium sulfide to a quick-acting paint containing 200 g/L sodium sulfide) and a saturated solution of calcium hydroxide. Depilated slats were then processed to remove the residual wool in a solution of sodium sulfide ranging in concentration from 0.8 to 2.4% for 8−16 h at temperatures ranging from 16 to 24°C. After this treatment, the pelts were washed and treated with a proteolytic enzyme, either a bacterial enzyme (Tanzyme, Tryptec Biochemicals, Ltd.) or a pancreatic enzyme (Rohapon ANZ, Shamrock, Ltd.), at concentrations ranging from 0.025 to 0.1%, followed by pickling in a 2% sulfuric acid and 10% sodium chloride solution. The pickled pelts were then pretanned using oxazolidine, degreased with an aqueous surfactant, and then tanned using chromium sulfate. The resulting “wet blue” was then retanned using a mimosa vegetable extract and impregnated with lubricating oil prior to drying and mechanical softening. Tear strengths of the crust leathers were tested using standard methods (Williams 2000). In brief, samples (strips 1 ×50 mm) were cut from the leather at the official sampling positions (OSPs) (Williams 2000). parallel to the backbone. The bovine leather was shaved, resulting in samples approximately 1.3 mm thick, consisting, on average, of 34% grain and 66% corium. All samples were then conditioned by storing them at a constant temperature and humidity (20°C and 65% relative humidity, respectively) for 24 h, after which time they were tested on an Instron strength-testing device. A stretching apparatus was built as follows. A linear motor, Linmot PS01, 48×240/30×180-C (NTI AG, Switzerland), was mounted on a purpose-built frame with a custom-made clamp fitted to the end of the slider. The clamp was designed not to put a sharp point load on the leather (Figure 1). A L6D aluminum alloy OIML single-point loadcell (Hangzhou Wanto Precision Technology Co., Zhejiang, China) was attached to a second clamp that would hold the other end of the sample and was attached to the frame. Each leather sample was mounted horizontally between the clamps without tension and then moved into the X-ray beam. The sample was stretched in 1 mm increments until a force was registered by the loadcell. The slider was then moved back 1 mm, so that the sample was again not under tension, and spectra were recorded, with the sample being analyzed edge-on, parallel to the backbone, to allow the load to be correlated with tear strength (Basil-Jones, Edmonds et al. 2011). Measurements were made, depending upon the mounted orientation of the leather, either normal to the leather surface (flat) in a 0.5 mm grid of four points or edge-on at 0.10 mm intervals across

the sample from the grain to the corium (Basil-Jones, Edmonds et al. 2010). The sample was again stretched 1 mm and maintained at this extension for 1 min to stabilize, before SAXS spectra, the extension, and the force information was recorded. This process was repeated until the sample failed. Note that the flat samples were physically split into two layers, grain and corium, to produce two samples from each piece of leather, before diffraction patterns were recorded. Diffraction patterns were recorded on the Australian Synchrotron SAXS/WAXS beamline, using a high-intensity undulator source. Energy resolution of 10^{-4} is obtained from a cryo-cooled Si (111) double-crystal monochromator, and the beam size [full width at half maximum (fwhm) focused at the sample] was 250×80μm, with a total photon flux of about 2×10^{12} photons s^{-1}. All diffraction patterns were recorded with an X-ray energy of 11 keV using a Pilatus 1 M detector with an active area of 170×170 mm and a sample−detector distance of 3371 mm. Energy calibration used the absorption edge of zinc at 9.659 keV to set the zero angle of the monochromator. This results in energy calibration across the energy range used better than 5 eV and typically better than 2 eV. A diffraction peak of silver behenate is used to scale the camera length. The correct value of qis then calculated by trigonometry for each pixel in each diffraction image. Exposure time for diffraction patterns was 1 s, and data processing was carried out using the SAXS15ID software (Cookson, Kirby et al. 2006). No normalization was performed for changes in beam intensity. Orientation index (OI) is defined as (90°−OA)/90°, where OA is the minimum azimuthal angle range that contains 50% of the microfibrils centered at 180°. OI is used to give a measure of the spread of microfibril orientation (an OI of 1 indicates that the microfibrils are completely parallel to each other, and an OI of 0 indicates that the microfibrils are completely randomly oriented). The OI is calculated from the spread in azimuthal angle of the most intense d-spacing peak (at around 0.059−0.060 $Å^{-1}$) (Basil-Jones, Edmonds et al. 2011). The d spacing was determined for each spectrum from Bragg's law by averaging the central values of several collagen peaks (usually from n= 5 to 10).

Results and Discussion

Leather has many uses in a variety of different industries. The major commercial output capitalized on by bovine (cattle) leather is in the shoe industry. US$60 billion per year of shoes is traded internationally. Footwear requires strong leather. Ovine (sheep) leather has just half the strength of bovine leather. This results in ovine leather not meeting the strength requirements that would enable it to be used in the production of shoes. The project focuses on whether we can increase the strength of ovine leather consequently making it an applicable material for many more applications such as the manufacture of footwear. To do

this we need to determine what factors determine strength and other physical properties of the leather. The chemical composition is one aspect being explored; in particular the proteins, cross-links and fat content. In order to understand further what affects the strength of ovine leather, the nanostructure of the material is a major focus of the project. Leather is comprised of two layers, the grain and the corium (Figure 1). Both layers are being looked at with the protein structure, fibril size, bundle size, orientation and density all making up separate components of the investigation.

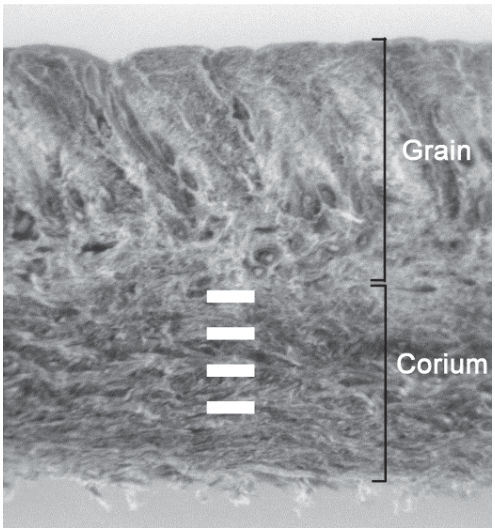

Figure 1: Magnified image of ovine leather displaying the grain and the corium layers (Basil-Jones, Edmonds et al. 2011). Images reprinted with permission from the Journal of Agricultural and Food Chemistry.

In order to investigate the fibrous nanostructure specific techniques are required. Synchrotron based technique small angle X-ray scattering has become a crucial part of the project. Figures 2 and 3 depict the beam line and analysis of leather samples in both a static state and during the stretching process. The stretching process performed on the samples was individual to this experiment. The data obtained from it has provided a huge insight into how the collagen fibrils react when tension is applied to the sample. Data was taken portraying how the reaction changes when a greater tension is applied to the sample thus providing information relating to structure change over time in proportion to the tension applied.

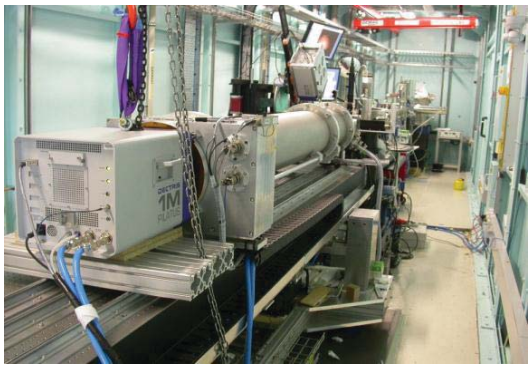

Figure 2: The small angle X-ray scattering beam line at the Australian Synchrotron.

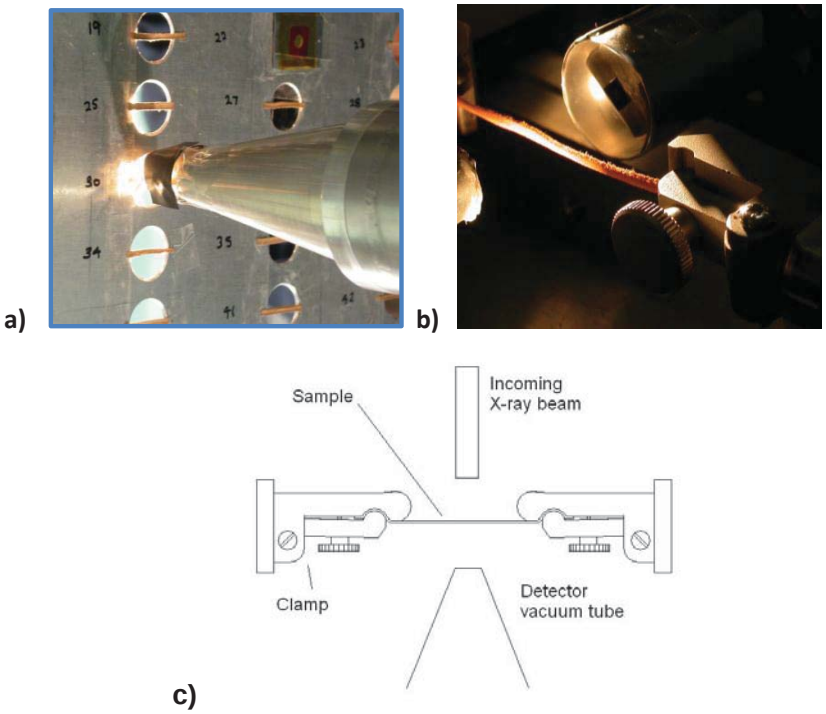

Figure 3: a) Static ovine leather samples being analysed on the small angle X-ray scattering beam line at the Australian Synchrotron, b) Ovine leather sample undergoing stretching during analysis by the small angle X-ray scattering beam line at the Australian Synchrotron, c) Experimental set up for stretching process (Basil-Jones, Edmonds et al. 2012). Images reprinted with permission from the Journal of Agricultural and Food Chemistry.

Information regarding the structure and alignment of the collagen fibrils is provided by the small angle scattering pattern obtained on the synchrotron beam line. Through a series of processing steps the orientation index and d spacing of the collagen fibrils can be obtained (Figure 4). Both of these values illustrate the fibrous collagen structure within the two layers of the leather and the cross over between them. Depending on the change in the d spacing

and orientation index numbers we are able to determine how the fibrils react to tension, whether they become more aligned and whether the individual fibres stretch or not.

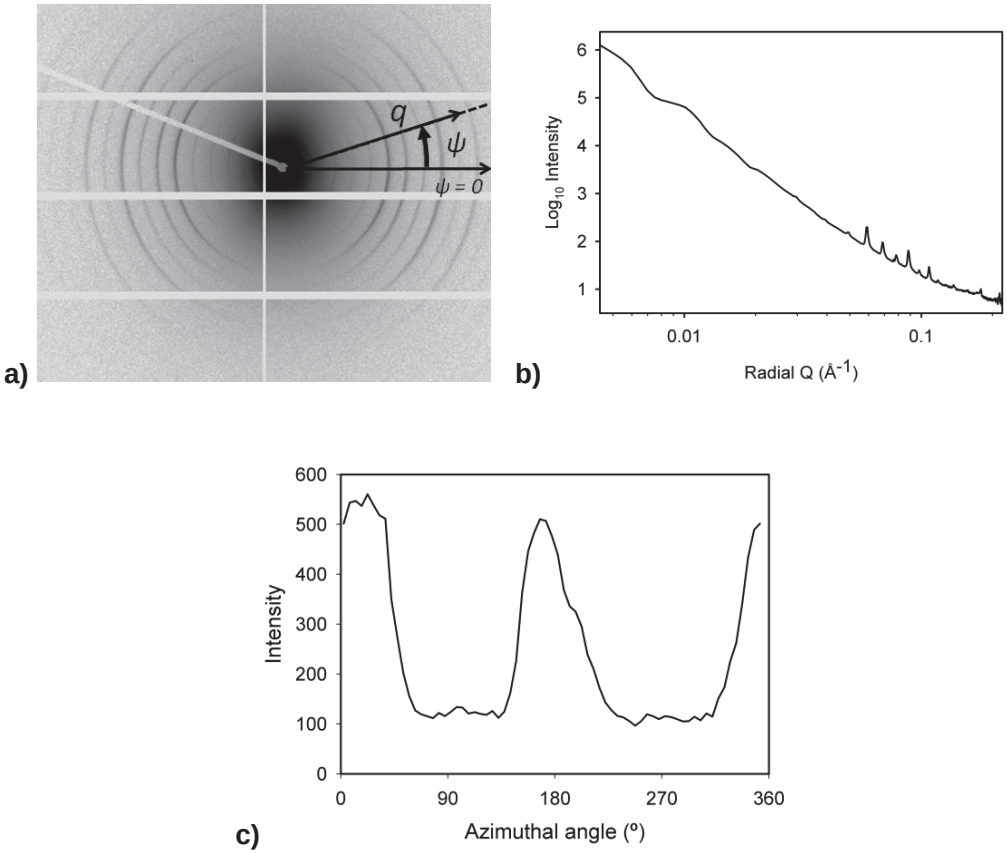

Figure 4: a) small angle scattering pattern obtained from the Australian synchrotron, (Basil-Jones, Edmonds et al. 2012), b) graph displaying collagen peaks obtained through data processing, (Basil-Jones, Edmonds et al. 2012), c) graph displaying azimuthal angle of a leather sample obtained through data processing. Images reprinted with permission from the Journal of Agricultural and Food Chemistry.

Leather samples analysed at the Australian Synchrotron were cut from leather skins in specific directions (Figure 5). With a full range of samples from all angles this ensured a clear three dimensional understanding of the collagen fibrils was obtained. Figure 5 refers to the sampling direction. “Backbone” indicates the direction of the animal backbone on the leather pelt. The edge on sample direction are in reference to the backbone as they are labeled parallel when cut parallel to the backbone and perpendicular when cut perpendicular to the backbone.

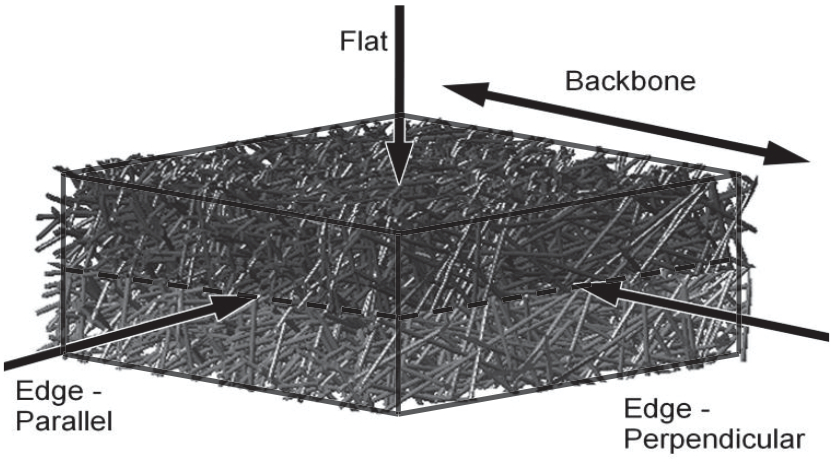

Figure 5: Sampling directions of ovine leather for analysis at the Australian Synchrotron (Basil-Jones, Edmonds et al. 2011). Image reprinted with permission from the Journal of Agricultural and Food Chemistry.

One of the main elements being investigated is the orientation index. This is a measurement that shows how aligned the collagen fibrils are. The orientation index measurement is given a value within the range of zero to one. An orientation index of zero shows that the fibrous structure is not at all aligned. Thus logically an orientation index of one would be a completely aligned structure.

The second major measurement under investigation is the d spacing. This is an internal measurement of the collagen fibrils. Each fibril is made up of five strands that are arranged in a staggered pattern (Figure 6b). The distance between one strand finishing and the next strand starting is referred to through the measurement called d spacing. With a lower d spacing value the strands will be tightly packed compared to a low d spacing value where the strand will be further away from each other. Images were taken using Atomic Force Microscopy (Figure 6a) that clearly display the bands formed by the staggered formation of the strands and the existence of the d spacing within the collagen fibrils.

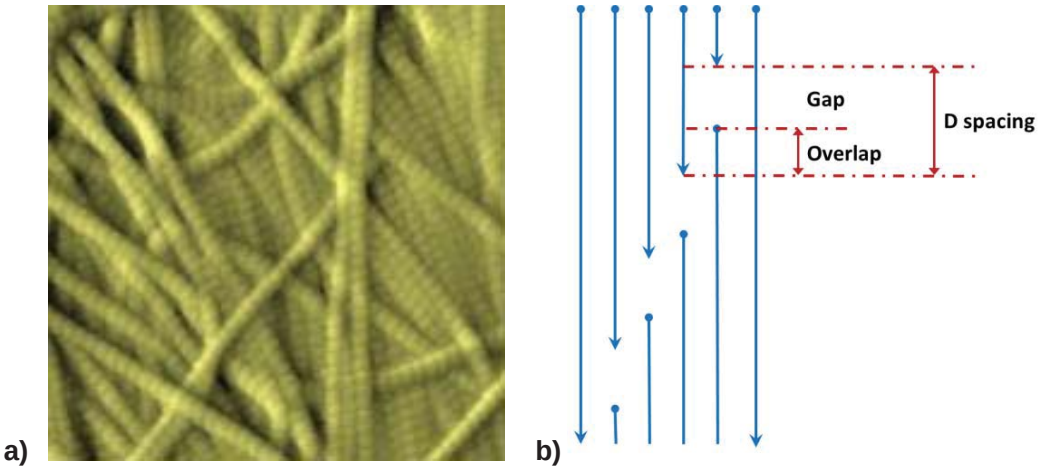

Figure 6: a) Atomic Force Microscopy image of collagen fibrils with clear definition enabling bands to be seen, b) Structure within a collagen fibril illustrating positions of d spacing bands.

To further understand how the nanostructure of leather affects its strength and physical properties a measurement specific to the tear strength of leather was required. This tear strength was measured using LASRA facilities (Figure 7) and consisted of making a hole of uniform shape and size in the leather sample and applying a pulling force by opening the two jaws inserted into the hole until a tear in the material occurred. The properties of the leather and how they change when tension is applied were characterized via an experiment completed at the Australian Synchrotron. Small angle X-ray scattering was performed on leather samples while they were undergoing a stretching process. From the data obtained the orientation index and d spacing of the samplings was acquired at every increment in the tension applied to the sample.

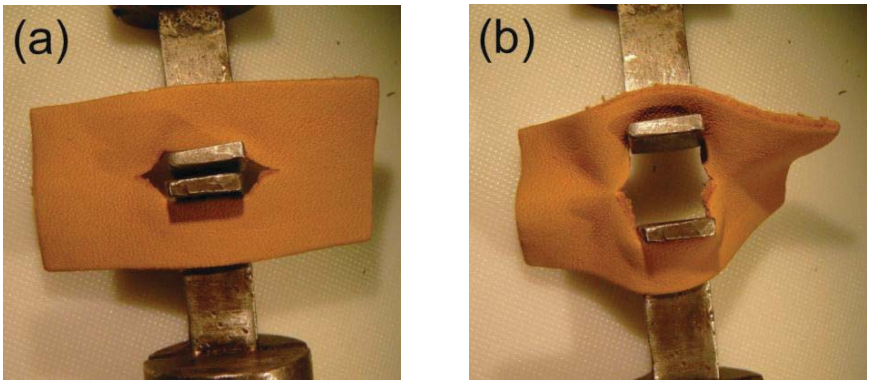

Figure 7: Tear strength testing procedure. a) Leather sample before tear strength test began, b) Leather sample during tear strength test.

Combining results from the LASRA tear strength tests and Australian Synchrotron data the structure-strength relationships could be evaluated. We determined that the orientation of the collagen fibrils within the leather samples correlates with strength.

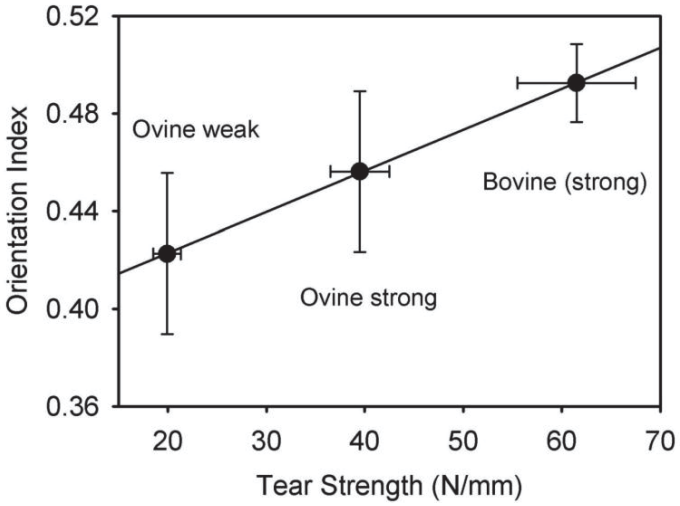

Figure 8: Structure-strength relationship displayed through combination of tear strength data and orientation indices (Basil-Jones, Edmonds et al. 2011). Image reprinted with permission from the Journal of Agricultural and Food Chemistry.

As seen in Figure 8 it is a strong relationship that clearly portrays the affect orientation has on the strength of the leather. This relationship proved that fibrils crossing over between the grain and the corium layers does not equate to stronger leather. It is rather the orientation within the planes of the leather that is the important orientation aspect to consider. Figure 9 illustrates what the collagen fibril arrangement would look like for a strong piece of leather highly orientated, Figure 9a) and a weak piece of leather (poorly orientated, Figure 9b).

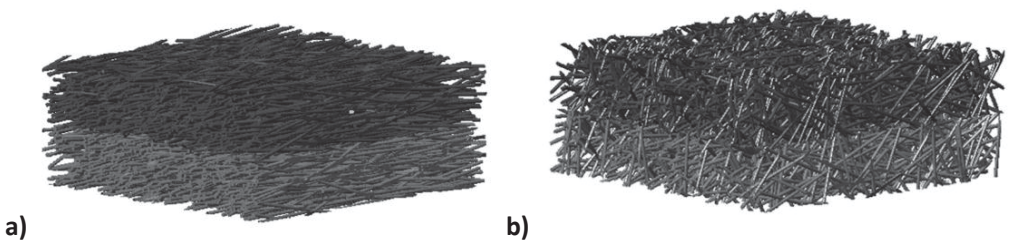

Figure 9: a) Strong leather; highly orientated collagen fibrils within planes, little cross over between planes, b) Weak leather; little orientation within planes, large number of fibrils crossing over between planes, (Basil-Jones, Edmonds et al. 2011). Images reprinted with permission from the Journal of Agricultural and Food Chemistry.

The orientation index has been analysed across the width of the leather with results proving that there is a difference between the grain and the corium layers (Figure 10). This work followed on from the establishment of a strength-structure relationship among ovine leather samples. As is shown in the graph below, the corium layer of leather is much stronger than the grain layer. Even in the magnified image of a leather sample we are able to view that the corium appears to have a higher level of orientation than the grain layer thus equating to the corium pertaining a higher strength.

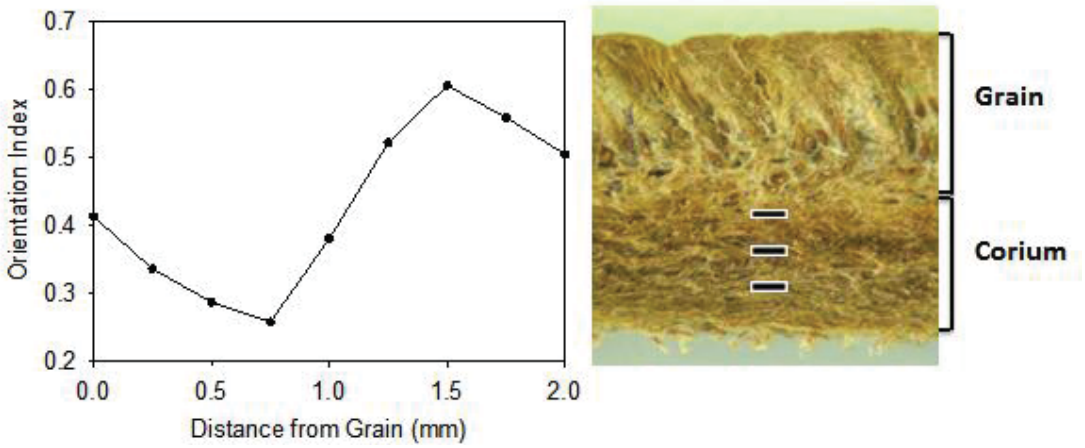

Figure 10: Orientation index displaying difference between grain and corium layers, (Basil-Jones, Edmonds et al. 2011). Images reprinted with permission from the Journal of Agricultural and Food Chemistry.

Through analysis of d spacing measurements the model through which leather stretches could be determined. From small angle X-ray spectroscopy patterns, d spacing values for the samples were obtained. When graphed against the strain applied to the samples it was conclusively found that the collagen fibrils first undergo alignment and second stretch (Figure 11). When a force is exerted on the leather sample, rather than stretching the fabric the tension is initially absorbed through the collagen fibrils become more highly aligned. The force pulls the fibres that are out of orientation into place resulting in the orientation index of the sample increasing. Subsequent to realignment, the individual collagen fibres take up the tension causing each fibril to stretch in length. This is seen through an increase in the d spacing. Very clearly portrayed below, this provides significant insight into the sequence of reactions of fibrous collagen material when tension is applied.

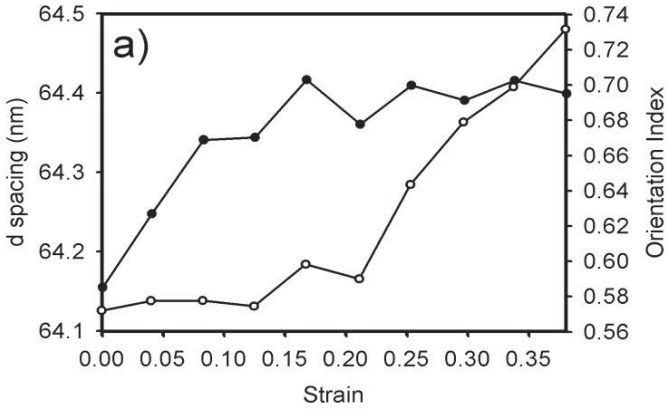

Figure 11: Orientation and d spacing changes in leather with applied strain. Closed circles: orientation index; open circles: d spacing (Basil-Jones, Edmonds et al. 2012). Image reprinted with permission from the Journal of Agricultural and Food Chemistry.

The response to strain was not found to be uniform across weak and strong leather. As seen in Figure 12a there is a large response variation among the fibrils in weak leather. The d spacing is not changed in a uniform manor. Comparatively, Figure 12b displays the far more uniform response to tension within strong leather samples. Weak leather has a lower orientation index indicating that the fibrils will be in a random orientation. Subsequently the first reaction to tension, the realignment of fibrils, will vary largely between samples. Hence a non-uniform reaction to the application of tension among weak leather samples is found. Alternatively strong leather has a high orientation index. Thus the ability of the leather to realign itself with the introduction of tension is far less. Ultimately, majority of the variability that would have otherwise been experienced is eliminated.

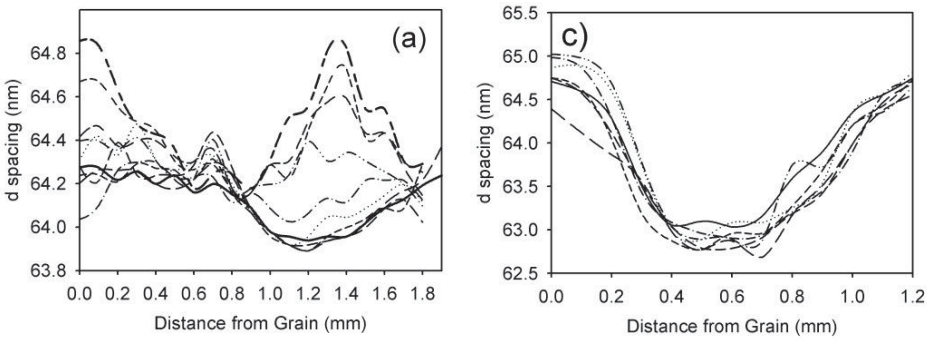

Figure 12: a) Strain response through the thickness of weak leather, b) Strain response through the thickness of strong leather, (Basil-Jones, Edmonds et al. 2012). Images reprinted with permission from the Journal of Agricultural and Food Chemistry.

Conclusion

A structure-strength relationship was found among ovine and bovine samples. It is now understood that the orientation of fibrils within planes correlates to the tear strength capabilities of the leather. The cross-over of fibrils between the grain and the corium is not a significant factor relative to strength. The two different layers that leather is comprised of have been analysed and orientation among them determined. The fibrous collagen within the corium has a higher orientation and as such is a stronger than the grain. Following investigation of leather samples when force is applied the reaction of the fibres to tension was analysed. We determined that the first response to tension is realignment of the fibrils seen through an increase in orientation indices. The second response is for the fibrils to stretch, identified through the increase in d spacing. This response sequence was found to be very uniform among strong leather samples but variable in weak leather samples. The findings are significant and can not only be advantageous within the leather industry but they provide insight that can be applied to the cosmetic, medical and biological industries also.

Acknowledgements

This work is part of a MSI/LASRA/Massey University consortium project. This research was undertaken on the SAXS/WAXS beamline at the Australian Synchrotron, Victoria, Australia.

References

Basil-Jones, M. M., R. L. Edmonds, et al. (2010). "Leather structure determination by small angle X-ray scattering (SAXS): cross sections of ovine and bovine leather." J. Agric. Food Chem. **59**(9): 5286-5291.

Basil-Jones, M. M., R. L. Edmonds, et al. (2011). "Collagen fibril orientation in ovine and bovine leather affects strength: A small angle X-ray scattering (SAXS) study." J. Agric. Food Chem. **59**(18): 9972-9979.

Basil-Jones, M. M., R. L. Edmonds, et al. (2012). "Collagen fibril alignment and deformation during tensile strain of leather: A SAXS study." J. Agric. Food Chem. **60**(5): 1201-1208.

Cookson, D., N. Kirby, et al. (2006). "Strategies for data collection and calibration with a pinhole-geometry SAXS instrument on a synchrotron beamline." J. Synchrotron Radiat. **13**: 440-444.

Williams, J. M. V. (2000). "IULTCS (IUP) test methods - Measurement of tear load-double edge tear." J. Soc. Leather Tech. Ch. **84**(7): 327-329.

Williams, J. M. V. (2000). "IULTCS (IUP) test methods - Sampling." J. Soc. Leather Tech. Ch. **84**(7): 303-309.

Collagen Alignment and Leather Strength

Katie Sizeland[1], Richard Haverkamp[1], Melissa M. Basil-Jones[1], Gillian E. Norris[1], Richard Edmonds[2].

[1]School of Engineering and Advanced Technology, Massey University, Private Bag 11222, Palmerston North 4442, New Zealand. [2]Institute of Fundamental Sciences, Massey University, Private Bag 11222, Palmerston North 4442, New Zealand. [3]Leather and Shoe Research Association, PO Box 8094, Hokowhitu, Palmerston North 4446, New Zealand.

k.h.sizeland@massey.ac.nz

Abstract

Leather strength is believed to be largely due to the fibrous collagen which makes up a major proportion of the material. However, the strength of leather is not proportional to the amount of collagen which it contains. The structure of collagen in the leather produced from a range of animals is investigated using synchrotron based small angle x-ray scattering. It is shown that the tear strength of leather depends upon the alignment of the collagen fibrils. Tear-resistant material has the fibrils contained within parallel planes with little cross-over between the top and bottom surfaces. For tear strengths in the range 20–110 N/mm^2 the orientation index ranges from 0.420–0.633 with a direct relationship between orientation index and strength. Greater alignment within the plane of the tissue results in stronger material. This study provides a valuable insight into the structural basis of strength in leather and the inherent differences between animal skins.

Keywords: Synchrotron, small angle X-ray scattering, collagen, orientation, strength

Introduction

Collagen is the main structural component of leather, skin (Fratzl 2008) and other materials such as medical scaffolds (Floden et al. 2010). The strength of these collagen materials is of crucial importance for each application. In a medical context, strength is a necessity for collagen-based extracellular matrix materials whilst a primary requirement for leather applications, such as shoes and

upholstery, is strength. Here we investigated the strength of collagen fibrils in leather and whether this corresponded with any physical properties of the material.

Leather, a material obtained through processing, is made up of two parallel planes that are mostly comprised of fibrous collagen. As a strong, flexible, water-resistant material, leather is used in a wide variety of manufacturing applications including shoes, bags, furniture coverings and car upholstery. However the leather used for these products is mostly bovine leather as it has a far greater strength than that of ovine leather. If the nanostructure of ovine leather was understood then the ability to manipulate processes in order to achieve ovine leather of higher strength may be realized.

In this experiment we analyse how the orientation of the collagen fibrils affects the strength of the leather. The amount of collagen present, the molecular structure of the collagen (□-spacing, collagen type), the nature of the cross-linking between collagen (Chan et al. 2009) and collagen bundle size are all factors previously considered as possibly contributing to the strength of collagen materials.

Synchrotron based technique small angle X-ray scattering (SAXS) provides an ideal platform for nanostructure analysis of the fibrous collagen. The small angle scattering pattern acquired provides information regarding the structure and alignment of the collagen fibrils. This synchrotron technique allows us to determine why leather has the properties it does and how the fibril structure relates to the desirable attributes present. Leather manufactured from different animals is able to be looked at in depth through the use of synchrotron techniques. The leather produced from the skin of different animals has varying strength values. Thus it is possible to compare the strength of each sample with the orientation of the collagen fibrils using SAXS data results.

A statistically significant relationship was found between tear strength and edge-on orientation in our recent study of ovine and bovine leathers of differing strengths (Basil-Jones et al. 2011). □e speculated that this trend may be of a more general nature among leather from various animal species. Thus to see if this relationship is more widely applicable among other animals, we have now measured fibril orientation in seven species of mammals. □e used SAXS at a modern synchrotron facility as it allows analysis of a small area (2□0 □ 80 μm). Therefore measurements of fibril orientation edge-on in tissues that are of limited thickness were able to be obtained.

Material and Methods

Leathers were generated using conventional techniques. Specifically fat and flesh was mechanically removed from the skin. Lime sulfide paint comprising of 140 g/L sodium sulfide, □0 g/L hydrated lime, and 23 g/L pre-gelled starch thickener was applied to the flesh side of the skin. The keratinaceous material was then removed after incubation of the skin at 20 □C for 16 hours. After this

treatment, the skin was washed and the pH was lowered to 8 with ammonium sulphate followed by the addition of Tanzyme, a commercial bate enzyme. The treated skin was then washed followed by pickling in 20□ sodium chloride and 2□ sulfuric acid. The pickled pelt was degreased using a non-ionic surfactant, neutralised using 8□ NaCl, 1□ disodium phthalate solution and 1□ formic acid, and tanned using chromium sulfate. The resulting wet-blue pelt was neutralised in 1□ sodium formate and 0.1□□ sodium bicarbonate for 1 hour and then washed. The pelt was retanned using Tanicor, a synthetic retanning agent, and Mimosa, a vegetable extract. Fat liquors were added prior to drying and mechanical softening.

Tear strengths were measured for all samples using standard methods (□illiams 2000a). In brief, samples were cut from the official sampling position (OSP) (□illiams 2000b). The samples were then conditioned at a constant temperature and humidity (20 □C and 6□□ relative humidity) for 24 h after which time they were then tested on an Instron strength-testing device.

Samples were prepared for SAXS analysis by cutting strips of leather of 1 □30 mm from the OSP. Each sample was mounted without tension in the X-ray beam in two directions□edge on so measurements could be taken through the thickness of the leather and flat on or normal to the surface of leather. Note that the flat samples were physically split into two layers, grain and corium, to produce two samples from each piece of leather, before diffraction patterns were recorded. For the edge-on samples measurements were made every 0.2□mm with the measurements moving from the corium to the grain. The flat-on samples were mounted with the uncut face of the leather directed toward the X-ray beam. Four measurements were made per sample in a rectangular grid. □iffraction patterns were recorded on the Australian Synchrotron SAXS/□ AXS beamline, using a high-intensity undulator source. Energy resolution of 10^{-4} was obtained from a cryo-cooled Si (111) double-crystal monochromator. The beam size □full width at half maximum (fwhm) focused at the sample was 2□0 □ 80 μm, with a total photon flux of about 2 □ 10^{12} photons s^{-1}. □iffraction patterns were recorded with an X-ray energy of 8 ke□ using a Pilatus 1M detector with an active area of 1□0 □ 1□0 mm and a sample-to-detector distance of 33□1 mm. Exposure time for the diffraction patterns was 1 s.

□ata processing was carried out using SAXS1□I□ software (Cookson et al. 2006). Orientation index (OI) is defined as (90° − OA)/90°, where OA is the minimum azimuthal angle range, centered at 180□, that contains □0□ of the microfibrils (Basil-Jones et al. 2010□Sacks et al. 199□). OI provides a measure of the spread of microfibril orientation. An OI approaching 1 indicates that the microfibrils are parallel to each other, whereas an OI of 0 indicates the microfibrils are randomly oriented. The OI is calculated from the spread in azimuthal angle of the most intense d-spacing peak (at around 0.059−0.060 $Å^{-1}$) (Basil-Jones et al. 2011). Each OI value presented here represents the average of 14−36 measurements of one sample. For edge-on mounted samples these measurements were taken at 0.2□mm intervals moving from the top of the corium to the bottom of the grain so that the whole

thickness of the sample was covered. For flat-on analyses, measurements were taken at a number of points in a grid pattern. For the sheep and cattle samples the averages are derived from 228, 249, and 16□measurements from 1□, 14,and 10 samples respectively and have been reported previously (Basil-Jones et al. 2011). The □-spacing was determined for each pattern by taking the central position of several of the collagen peaks, dividing these by the peak order (usually from n □ □to n □ 10), and averaging the resulting values.

Results and Discussion

Synchrotron based SAXS technique has become a crucial part of the project. The repeating fibril structure of collagen in the leather samples is represented by the SAXS pattern obtained on the beamline (Figure 1a). Each ring represents a collagen peak. Following integration, the collagen peaks become clearly distinguishable and the □ spacing can be determined (Figure 1b).

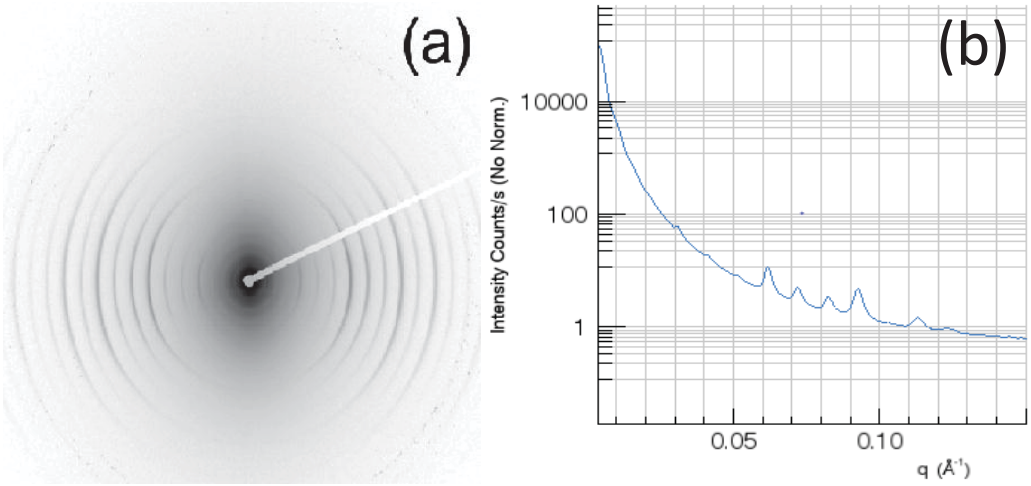

Figure 1. Leather analysis using SAXS (a) raw SAXS pattern. Reproduced from *J. Agric. Food Chem.* (2013) **61**, 88□-892 □ American Chemical Society□(b) integration of SAXS pattern.

Through a series of processing steps the orientation index (OI) of the collagen fibrils can be obtained. Both the □ spacing and the OI illustrate the fibrous collagen structure within the two layers of the leather and the cross over between them. Upon the application of stress the fibrils may become more aligned and the individual fibres may stretch. □ e are able to determine how the fibrils react to the tension by looking at the □ spacing and orientation index values.

The □ spacing for the samples analysed ranged from 62.8 to 6□3 nm. This variation was found across a large range of strength (Figure 2). □ e do not find any significant correlation between d spacing and strength.

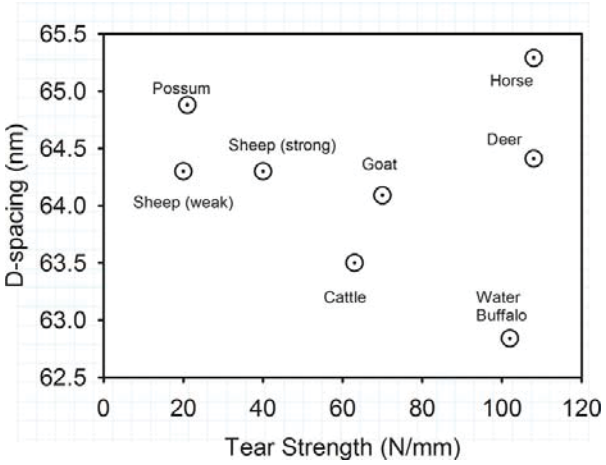

Figure 2. □ spacing and tear strength of collagen fibrils in leather for selected mammals. Reproduced from *J. Agric. Food Chem.* (2013) **61**, 88□-892 □ American Chemical Society.

Leather samples analysed at the Australian Synchrotron were cut from leather skins in specific directions. □ ith a full range of samples measured from all angles, a clear three dimensional understanding of the collagen fibrils was obtained. Figure 3 refers to the direction in which measurements were taken. “Backbone” indicates the direction of the animal backbone on the leather pelt. The edge on measurements taken span through the full thickness of the leather thus enabling the corium and grain layers and the crossover of fibrils between the layers to be analysed. The OI for these measurements conveys the degree to which the collagen fibrils are aligned within planes of the leather. The measurements taken normal to the surface portray the fibrils on the surface of the leather.

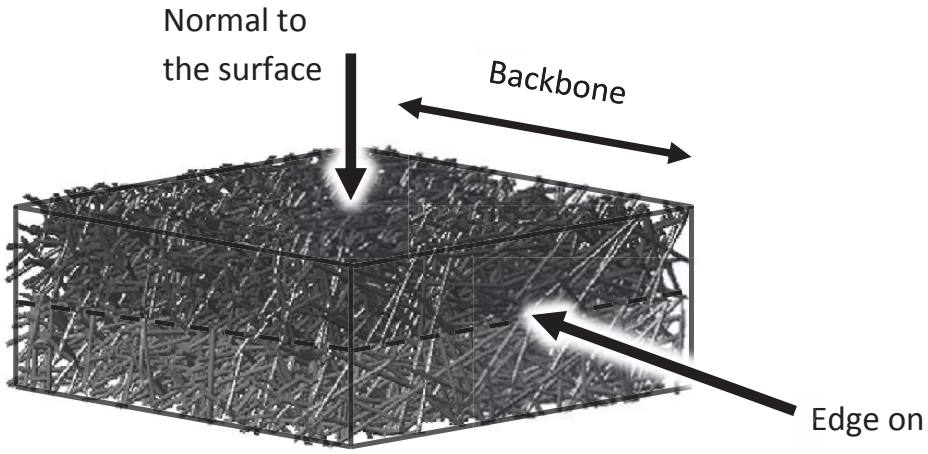

Figure 3. Measurement directions of leather samples used during analysis on the SAXS beamline at the Australian Synchrotron.

There is a large difference in OI between the measurements taken normal to the surface and measurements taken edge on. The OI numbers for the measurements normal to the surface are in the range of 0.18−0.35, with the exception of horse leather (Figure 4a). The edge-on measurements displayed OI values significantly higher (0.41−0.63) indicating the major component of fibril alignment is within the planes of the leather (Figure 4b) (Sizeland et al. 2013).

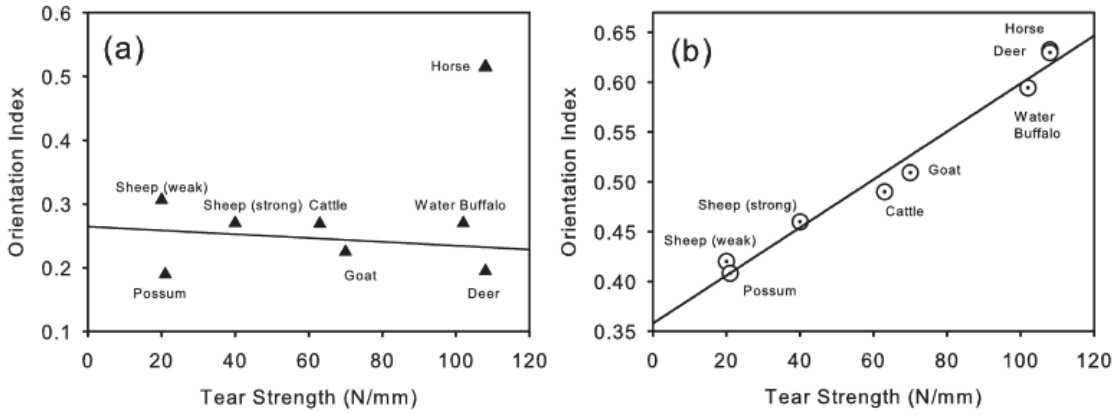

Figure 4. Orientation index and tear strength of collagen fibrils in leather for selected mammals (a) measured normal to the surface, (b) measured edge on. Reproduced from *J. Agric. Food Chem.* (2013) **61**, 88−892 © American Chemical Society.

We find a strong correlation between OI and tear strength for the edge on measurements. For the measurements taken normal to the surface of leather, we find little correlation if horse leather is excluded as an outlier. Therefore the tear strength of leather is relative to the planar alignment of the collagen fibrils.

 hen fibrils are not aligned within the planes but rather are aligned perpendicular to the planes, the fibres will not put up much resistance as they will be separated by any force applied (Figure a). This occurs in Hereford cattle (Amos 19 8 Kronick and Sacks 1991) and is known as vertical fibre defect. No samples with this defect were included in this study. hen there is a high degree of alignment of the fibres in the planes, maximum strength is obtained (Figure c). hen fibres are found to be anisotropic, strength will be greater than samples with vertical fibre defect as some of the fibrils will be more in line with the parallel planes of the leather.

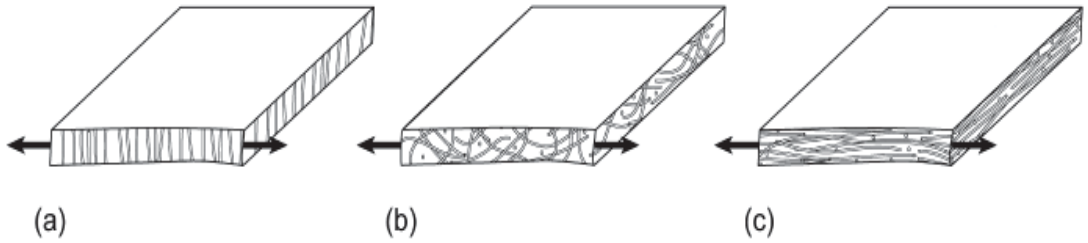

Figure 5. Relationship between OI of collagen fibrils and strength of skin. OI measured edge-on with orientation that results in leather that is (a) very weak (vertical fibre defect), (b) medium strength (low OI), or (c) strong (high OI). Arrow indicates direction of applied stress in tear measurements.

Reproduced from *J. Agric. Food Chem.* (2013) **61**, 88 892 American Chemical Society.

Tearing is used as the industry standard for leather strength. Tearing occurs at the two ends of a linear cut hole when looking normal to the surface of the leather (Figure 6). High OI values may indicate fibres running both parallel to (Figure 6a) and perpendicular to (Figure 6b) the hole. Strength will be low for samples with these structures as fibrils can be pulled apart along the shear lines with minimal force. Consequently it is expected that maximum strength will be associated with low OI indicating anisotropically arranged fibrils (Figure 6c).

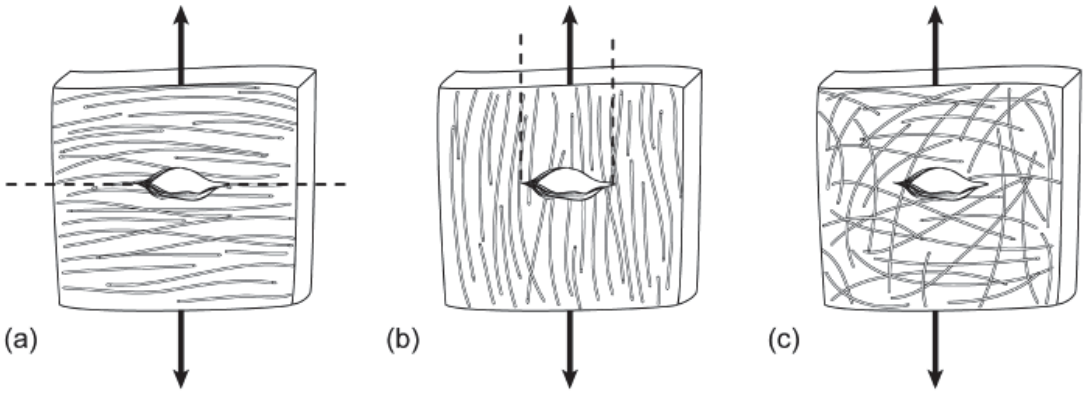

Figure 6. Relationship between OI of collagen fibrils and strength of skin. OI measured normal to the surface with orientation that results in leather that is (a) weak (high OI), (b) fairly weak (high OI), (c) strong in all directions. Arrow indicates direction of applied stress in tear measurements. □ashed lines represent probable lines of failure. Reproduced from *J. Agric. Food Chem.* (2013) **61**, 88□+892 □ American Chemical Society.

Conclusion

□ e investigated leather samples from a range of different mammals to develop an understanding of the structure-strength relationship. The correlation between tear strength and orientation of fibrils for edge on samples is remarkably quantitative. The strength range across which this relationship holds is much greater than has previously been demonstrated. This insight into collagen fibril structure may extend to tissues other than those studied here.

Acknowledgements

This research was undertaken on the SAXS/□ AXS beamline at the Australian Synchrotron, □ictoria, Australia. Assistance was provided with data collection and processing by □avid Cookson and Stephen Mudie at the Australian Synchrotron.

References

Amos, G.L., 19□8, □ertical fibre in relation to the properties of chrome side leather, J. Soc. Leather Tech. Ch., 42 □9-90p.

Basil-Jones, M.M., Edmonds, R.L., Allsop, T.F., Cooper, S.M., Holmes, G., Norris, G.E., Cookson, .J., Kirby, N.Haverkamp, R.G., 2010, Leather structure determination by small angle X-ray scattering (SAXS)cross sections of ovine and bovine leather, J. Agric. Food Chem., 8(9) 286-291p.

Basil-Jones, M.M., Edmonds, R.L., Cooper, S.M.Haverkamp, R.G., 2011, Collagen fibril orientation in ovine and bovine leather affects strength A small angle X-ray scattering (SAXS) study, J. Agric. Food Chem., 9(18) 992-999p.

Chan, ., Cox, G.M., Haverkamp, R.G.Hill, J.M., 2009, Mechanical model for a collagen fibril pair in extracellular matrix, Eur. Biophys. J., 38(4) 48-493p.

Cookson, ., Kirby, N., Knott, R., Lee, M.Schultz, ., 2006, Strategies for data collection and calibration with a pinhole-geometry SAXS instrument on a synchrotron beamline, J. Synchrotron Radiat., 13 440-444p.

Floden, E. ., Malak, S., Basil-Jones, M.M., Negron, L., Fisher, J.N., Byrne, M., Lun, S., empsey, S.G., Haverkamp, R.G., Anderson, I., ard, B.R.May, B.C.H., 2010, Biophysical characterization of ovine forestomach extracellular matrix biomaterials, J. Biomed. Mater. Res. B, 96B(1) 6-p.

Fratzl, P., Ed. 2008. Collagen Structure and mechanics. New ork, SpringerScience Business Media.

Kronick, P.L.Sacks, M.S., 1991, uantification of vertical-fiber defect in cattle hide by small-angle light-scattering, Connect. Tissue Res., 2(1) 1-13p.

Sacks, M.S., Smith, .B.Hiester, E.., 199, A small angle light scattering device for planar connective tissue microstructural analysis, Ann. Biomed. Eng., 2(4) 68-689p.

Sizeland, K.H., Haverkamp, R.G., Basil-Jones, M.M., Edmonds, R.L., Cooper, S.M., Kirby, N.Hawley, A., 2013, Collagen Alignment and Leather Strength for Selected Mammals, J. Agric. Food Chem., 61(4) 88□-892p.

□ illiams, J.M.□., 2000a, IULTCS (IUP) test methods - Measurement of tear load-double edge tear, J. Soc. Leather Tech. Ch., 84(□) 32□-329p.

□ illiams, J.M.□., 2000b, IULTCS (IUP) test methods - Sampling, J. Soc. Leather Tech. Ch., 84(□) 303-309p.

Synchrotron studies of leather structure

Richard G. Haverkamp[1], Melissa M. Basil-Jones[1], Katie H. Sizeland[1], Gillian E. Norris[2], Richard L. Edmonds[3].

[1]School of Engineering and Advanced Technology, Massey University, Private Bag 11222, Palmerston North 4442, New Zealand. [2]Institute of Fundamental Sciences, Massey University, Private Bag 11222, Palmerston North 4442, New Zealand. [3]Leather and Shoe Research Association, PO Box 8094, Hokowhitu, Palmerston North 4446, New Zealand.

r.haverkamp@massey.ac.nz

Abstract

The arrangement of collagen fibrils in leather is complex. Synchrotron based small angle X-ray scattering enables detailed structural information to be obtained. The variation in fibril orientation through cross sections of leather, and structural responses to dynamic loads between strong and weak leather were studied. Under tension, fibrils reorient at low strain then individual fibrils stretch at higher strain. In strong leather the load is taken up more uniformly across the thickness of leather compared with weak leather. This study provides an insight into the structural basis of strength in leather and the response of leather to stress.

Keywords: Synchrotron, Small angle x-ray scattering, orientation, strength

1. Introduction

The physical properties of leather depend upon the composition (proteins, fat, other components), the structural arrangement of these components and the chemical interactions between these components. Collagen is the main structural component of leather, responsible for its strength. Other molecular components, even at minor concentrations, can interact with collagen to affect the physical characteristics of leather. In particular, chemical cross-linking agents such as chromium salts or tannins link collagen fibrils and alter their mechanical properties and oils may act as lubricants of the

collagen matrix and alter the strength and suppleness of the leather. These components are fundamental to leather making.

Therefore, to understand leather, knowledge of the collagen fibril structure and arrangement is important. Measurement and an understanding of the variation of this structure with different processing methods, from different skins and hides, in good leather and defective leather, and during tension can contribute to the control of mechanical properties and to the art of leather manufacture.

The arrangement of collagen fibril structure in biological tissues has long been a subject of interest and has been investigated by a variety of methods. These methods include reflection anisotropy (Schofield et al. 2011), atomic force microscopy (Friedrichs et al. 200□), small angle light scattering (Billiar and Sacks 199□), confocal laser scattering (Jor et al. 2011), raman polarization microscopy (Falgayrac et al. 2010), anisotropic raman scattering (Janko et al. 2010), multiphoton microscopy (Lilledahl et al. 2011) and small angle X-ray scattering (SAXS) (Basil-Jones et al. 2010□Basil-Jones et al. 2011□Basil-Jones et al. 2012a□Boote et al. 2002□Kronick and Buechler 1986□Sizeland et al. 2013b).

It is recognized that defects in the collagen fibre arrangement can lead to poor quality leather with vertical fibre defect, a well know issue with some Hereford leather (□uivestein et al. 2000□Kronick and Sacks 1991).

X-ray diffraction is is a powerful technique for investigating material structures, giving information on long range structural order, with repeat distances in the order of 0.1 to 10 nm. It can be used for protein assemblages, such as collagen. For protein structures, small diffraction angles, θ, are measured, typically less than 10 degrees so that this X-ray diffraction technique is referred to as small angle X-ray scattering (SAXS). In SAXS the scattering momentum q is generally used rather than θ ($q = 4\pi sin\theta/\lambda$ where λ is the X-ray wavelength used) as it allows direct comparison of SAXS measured at different incident X-ray wavelengths. SAXS can provide information on macromolecules either in solution or in solid materials (Bernado et al. 200□□Tsutakawa et al. 200□) and has been used to investigate the structure of collagen (Cameron et al. 2002) and collagenous materials such as tendon (Sasaki and Odajima 1996a□Sasaki and Odajima 1996b)□bone (Burger et al. 2008□Cedola et al. 2006) and human articular cartilage (Mollenhauer et al. 2003). SAXS provides a quantitative measurement of both fibril orientation and the average d-spacing of collagen within the irradiated volume of sample.

SAXS can be performed on laboratory based instruments or on more synchrotron based instruments. The SAXS beam line at the Australian Synchrotron has several advantages over laboratory sources for characterization of leather. These are a focused beam (typically 250 x 80 μm) enabling detailed cross

sectional analysis of leather, very rapid sample collection, and very good signal to noise ratio due to the very high X-ray flux and very sensitive two dimensional detector. In addition the facility is staffed by scientists who are expert in their field and who maintain the facility at optimum performance and provide support to users. Access to the SAXS beamline is by competitive application. The facility operates 24 hours per day and experiments normally must be completed over a limited time, typically one or two days, so that very careful preparation is necessary prior to each experiment.

Here we describe the use of SAXS to understand the structure and arrangement of collagen fibrils in ovine and bovine leather and to derive the relationship between collagen structure and the physical characteristics, particularly strength, of leather.

2. Material and Methods

The methods have been described previously (Basil-Jones et al. 2012a).

Ovine pelts were from □-month-old, early season □black faced□ lambs, of breeds which may include Suffolk, South Suffolk and □orset □own. The bovine hides were from 2–3 year old cattle of a variety of breeds.

Leathers were generated with various properties by using a range of processing parameters both during the conventional beamhouse process and then during the conventional tanning of the pelts. Specifically, the pelts were depilated using a caustic treatment comprising sodium sulfide (ranging from a slow-acting paint containing 160 g/L flake sodium sulfide to a quick-acting paint containing 200 g/L sodium sulfide) and a saturated solution of calcium hydroxide. □epilated slats were then processed to remove the residual wool in a solution of sodium sulfide ranging in concentration from 0.8 to 2.4□ for 8–16 hours at temperatures ranging from 16 □C to 24 □C. After this treatment, the pelts were washed and treated with a proteolytic enzyme – either a bacterial enzyme (Tanzyme, Tryptec Biochemicals Ltd) or a pancreatic one (Rohapon ANZ, Shamrock Ltd) – at concentrations ranging from 0.02□□ to 0.1 □, followed by pickling in a 2□ sulfuric acid, 10□ sodium chloride solution. The pickled pelts were then pretanned using oxazolidine, degreased with an aqueous surfactant and before being tanned using chromium sulfate. The resulting “wet blue” was then retanned using a mimosa vegetable extract and impregnated with lubricating oil prior to drying and mechanical softening.

The tear strength of the crust leathers was tested using standard methods (□illiams 2000a).Samples (strips 1 x □0 mm) were cut from the leather at the official sampling positions (OSP) (□illiams

2000b), parallel to the backbone. The bovine leather was shaved to produce samples approximately 1.3 mm thick consisting, on average, of 34□ grain and 66□ corium. All samples were then conditioned by storage at a constant temperature and humidity (20□C and 6□□ relative humidity, respectively) for 24 hours, after which time they were tested using an Instron strength-testing device.

Leather samples were tested either statically or under load. Static samples were mounted on a plate containing up to 24 samples with sample changing taking place remotely (Figure 1, left).

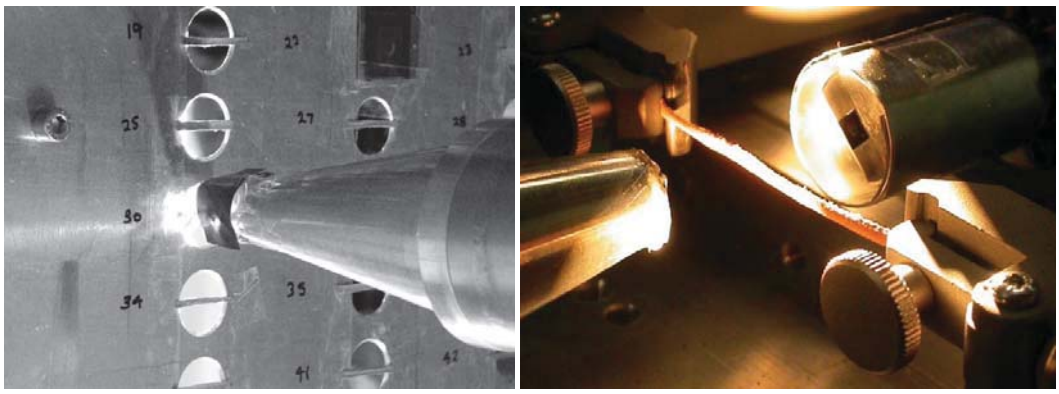

Figure 1. Sample mounting for SAXS measurements for left) static measurements. Reproduced from *J. Agric. Food Chem.* (2010) **58**, □286-□291 □ American Chemical Society□ right) measurement during stretching. Reproduced from *J. Agric. Food Chem.* (2012) **60**, 1201−1208 □ American Chemical Society.

For the samples under load, a stretching apparatus was built (Figure 1, right). A linear motor, Linmot PS01 – 48x240/30x180-C (NTI AG, Switzerland), was mounted on a purpose-built frame with a custom-made clamp fitted to the end of the slider. The clamp was designed so that the leather would not be subjected to a sharp point load. A L6□ Aluminum Alloy OIML single-point loadcell (Hangzhou □ anto Precision Technology Co., Zhejiang, China) was attached to second clamp that held the other end of the sample and was attached to the frame. Each leather sample was mounted horizontally between the clamps without tension and then moved into the X-ray beam. The sample was stretched in 1 mm increments until a force was registered by the loadcell. The slider was then moved back 1 mm to reduce the tension on the sample and diffraction patterns were recorded edge-on and parallel to the backbone. Measurements were made, depending on the mounted orientation of the leather, either normal to the leather surface (flat) in a 0.□mm grid of four points or edge-on at 0.10 to 0.20 mm intervals across the sample from the grain to the corium. The sample was stretched 1 mm, and maintained at this extension for 1 minute to stabilize, before a SAXS pattern was recorded. The extension and the force information were recorded. This process was repeated until the sample failed.

Note that the flat samples were physically split into two layers, grain and corium, resulting in the production of two samples from each piece of leather, before diffraction patterns were recorded.

□iffraction patterns were recorded on the Australian Synchrotron SAXS/□ AXS beamline, using a high-intensity undulator source. Energy resolution of 10^{-4} was obtained from a cryo-cooled Si (111) double-crystal monochromator to produce a beam size (F□ HM focused at the sample) of 2□0 x 80 μm, with a total photon flux of about 2 x 10^{12} ph.s^{-1}. All diffraction patterns were recorded with an X-ray energy of 11 ke□ (or 8 ke□) using a Pilatus 1M detector with an active area of 1□0 x 1□0 mm and a sample-to-detector distance of 33□1 mm. The absorption edge of zinc at 9.6□9 ke□ was used to calibrate the energy and to set the zero angle of the monochromator. This resulted in energy calibration across the energy range used being better than □ e□ and typically better than 2 e□. A diffraction peak of silver behenate was used to scale the camera length. The correct value of *q* is then calculated by trigonometry for each pixel in each diffraction image. Exposure time for diffraction patterns was 1 s and data processing was carried out using the SAXS1□I□ software (Cookson *et al.* 2006). No normalization was performed for changes in beam intensity.

3. Results and Discussion

The SAXS patterns recorded on leather show clearly the d-spacing and the orientation of the fibrils (Figure 2). The d-spacing is visible as a series of partial (or full) rings. The rings are of increasing diffraction order, so that the d-spacing can be calculated from any ring by dividing the space between rings by the order. In practice, the d-spacing is determined by averaging the central values of several collagen peaks (usually from n □ □to n □ 10). The orientation is apparent in the extent to which the collagen d-spacing diffraction rings extend around the full circle. This is quantified this by defining an orientation index (OI), which is defined as (90□– OA)/90□. The OA is the minimum azimuthal angle range that contains □0□ of the microfibrils centered at 180□. The OI is used to give a measure of the spread of microfibril orientation (an OI of 1 indicates the microfibrils are completely parallel to each other□an OI of 0 indicates the microfibrils are completely randomly oriented). The OI is calculated from the spread in azimuthal angle of one of the most intense d-spacing peaks (at around 0.0□9–0.060 □$^{-1}$).

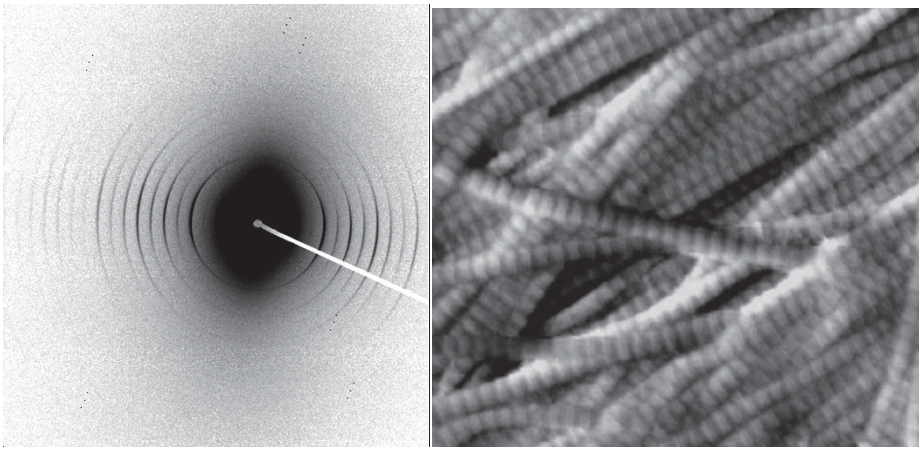

Figure 2. Left SAXS pattern of leather, showing the rings due to the d-banding of collagen. The orientation is apparent by the rings not extending around 360 Right An atomic force microscope image of bovine intestine, for an illustration of the structure of collagen fibrils to aid in understanding the SAXS pattern.

Selective information can be extracted from the SAXS pattern and represented in different forms. For example a radially integrated pattern can be plotted (losing the information on azimuthal variation) as in Figure 3 (left). The sharp peaks at higher q are due to the d-period, whereas the broader pattern at low q is due to the thickness of the collagen fibrils and the bundling of these fibrils. The variation in intensity with azimuthal angle can also be plotted. For example the variation in intensity at just one radial angle (corresponding to a d band) can be plotted as in Figure 3 (right) showing fibrils well aligned in the horizontal axis (0 – 180). An orientation profile can be obtained by taking just this portion of data for a series of measurements through the thickness of a piece of leather from grain to corium (Figure 4).

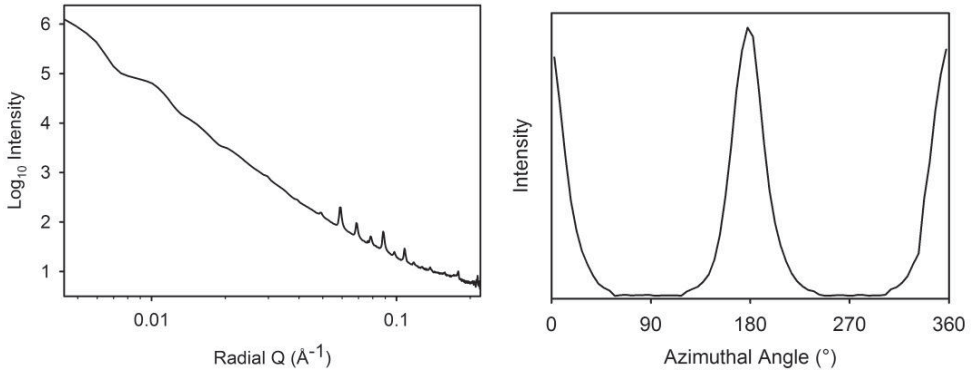

Figure 3. Left Radially integrated SAXS pattern with the sharp peaks due to the d-period visible Right Azimuthally integrated SAXS pattern at a radial angle corresponding with a d-period indicating fibril orientation.

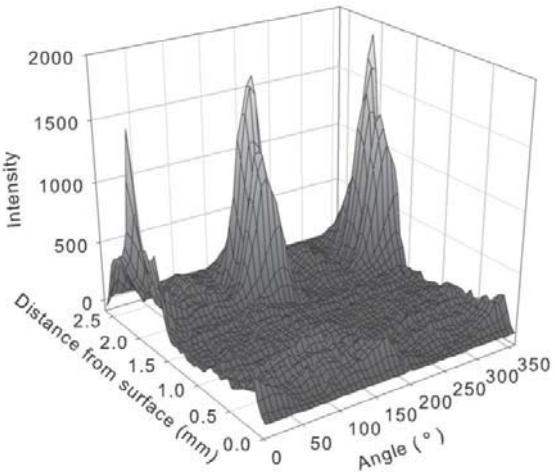

Figure 4. The Azimuthally integrated SAXS pattern through the thickness of ovine leather at the collagen d-spacing of around 0.0□9-0.06 □$^{-1}$. Reproduced from *J. Agric. Food Chem.* (2010) **58**, □286-□291 □ American Chemical Society.

□ ith these techniques it is possible to investigate the variation in d-spacing and fibril orientation through the thickness of leather, or at different positions in a piece of leather. For example, scanning through ovine and bovine leather a variation in d-spacing is observed with a lower d-period in the central region (Figure □, left). The OI also varies through the leather, with a lower OI in the grain and a higher OI in the corium. This difference in orientation is known from optical imaging, however, SAXS enables a more reliable quantification of the average fibril orientation.

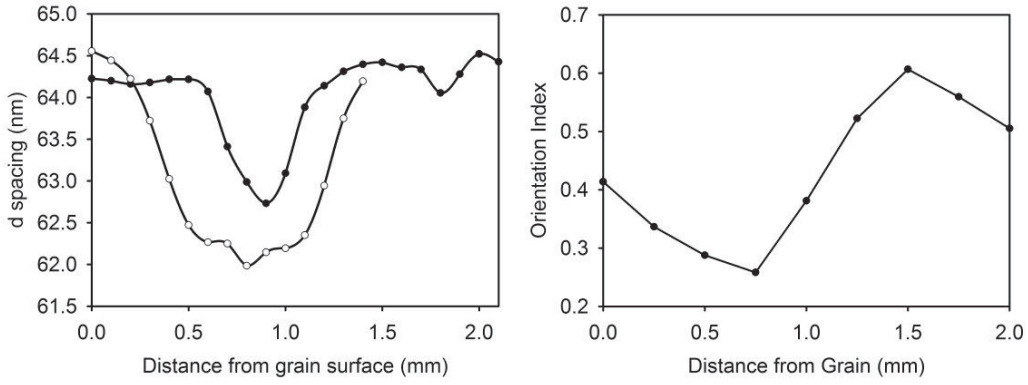

Figure 5. Left: □ariation in d-spacing through representative samples of (●) ovine and (○) bovine leathers. Right□Average orientation index across the thickness of ovine leather measured parallel to the backbone. An average of 24 leather samples (1 measurement per sample). Adapted from *J. Agric. Food Chem.* (2011) **59**, 99□2−99□9 □ American Chemical Society.

□ariations in d-period and OI for leathers of differing strength have been compared. There is not a strong correlation of d-period with strength (Basil-Jones et al. 2011□Sizeland et al. 2013b). There is however a good correlation of OI with strength (Basil-Jones et al. 2011□Sizeland et al. 2013a□ Sizeland et al. 2013b). A comparison of ovine leather grouped into weak and strong samples, and bovine leather which is stronger than the ovine leather, shows a significant correlation between average OI and strength (Figure 6). A regression line fitted to the averages of the three groups of data for OI and tear strength (low strength ovine□1 □samples, 228 analysis points□higher strength ovine□14 samples, 249 analysis points□and bovine□10 samples, 16□analysis points) has a slope of 1.□08 x 10^{-3} mm/N, r^2 □ 0.20, p □4.4□ x 10^{-}□. This relationship applies within a species (i.e. sheep) and is maintained between species (sheep and cattle). These measurements have recently been extended to hides from other mammals (Sizeland et al. 2013a□Sizeland et al. 2013b). The results obtained suggest that the relationship between fibril orientation and strength is a universal property of leather□strength is determined by fibril orientation, such that stronger leather has the fibrils arranged mostly parallel to the plane of the leather surface (low angle of weave), while weaker leather has more out-of-plane fibrils (higher angle of weave).

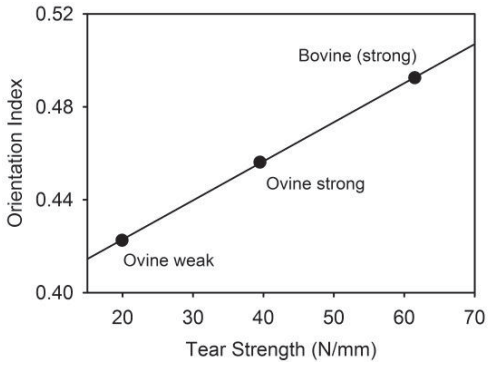

Figure 6. Orientation versus tear strength for the averages of each of the leather types measured through the edge parallel to the backbone. Adapted from *J. Agric. Food Chem.* (2011) **59**, 99□2−99□9 □ American Chemical Society.

Further information on the mechanical performance of leather can be obtained by stretching during SAXS measurements. It is observed that, under applied stress, the collagen fibrils in leather first rearrange to become more aligned (OI increases) before the fibrils stretch and the d-period increases (Figure □). The change in d-period can be used as an internal strain gauge, giving a measure of the strain experienced by individual fibrils.

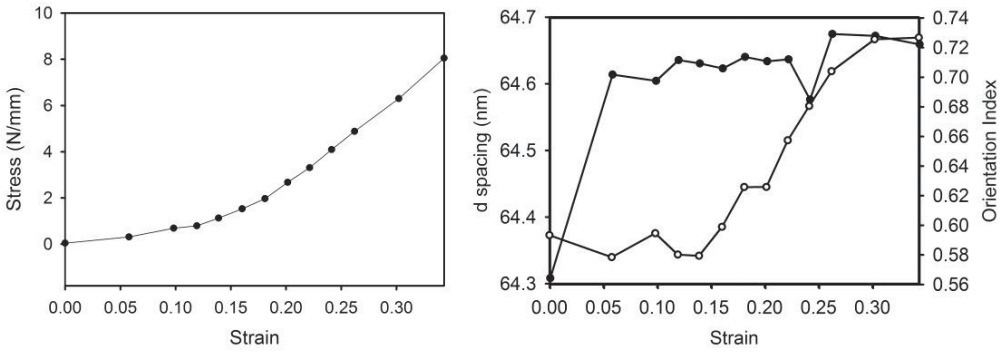

Figure 7. d-spacing and orientation versus strain measured edge-on, parallel to the backbone: (○) d spacing and (●) OI (parallel, OSP) for stronger ovine, 39 N/mm tear strength. Reproduced from *J. Agric. Food Chem.* (2012) **60**, 1201−1208 □ American Chemical Society.

It is also possible to monitor the variation in fibril orientation and d-spacing through the thickness of leather during strain. The stress that the collagen fibrils experience in different parts of the leather differs, as shown in Figure 8 where the fibrils in the centre of the corium and the surface of the grain of weak ovine leather undergo significantly more deformation that in the central region of the leather. There are differences in the deformation behaviour of weak and strong leather with strong leather tending to take up the stress over the full width of the leather and weak leather tending to have an uneven distribution of stress (Basil-Jones et al. 2012b).

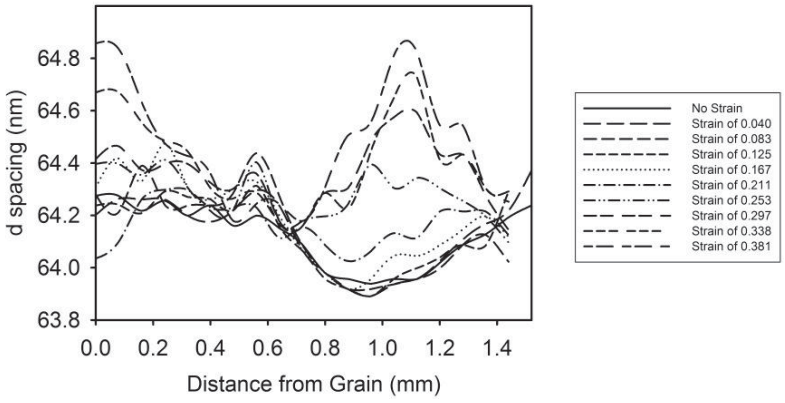

Figure 8. d spacing through the thickness of the leather and change in d spacing as a consequence of increasing strain, measured edge-on parallel to the backbone for weak ovine, 19 N/mm tear strength. Adapted from *J. Agric. Food Chem.* (2012) **60**, 1201−1208 □ American Chemical Society.

4. Conclusion

Synchrotron based small angle X-ray scattering has been shown to be a powerful technique for understanding the structure of leather. It provides information on fibril orientation and structure. Changes taking place during strain of the leather have been observed. These techniques have been used to study strength–structure relationships. It has been possible to show a correlation between strength and collagen fibril orientation, where leather that has fibrils more aligned in the plane of the leather is stronger. □uring tension, collagen fibrils first realign and then stretch. These methods can be extended to study the structure of leather during the stages of processing, with different tanning techniques and can enable the properties of leather obtained by different tanning procedures to be understood in terms of microstructure.

5. Acknowledgements

This research was undertaken on the SAXS/□ AXS beamline at the Australian Synchrotron, □ictoria, Australia. Nigel Kirby, Adrian Hawley and Stephen Mudie of the Australian Synchrotron are acknowledged for their contribution to this work. The NZ Synchrotron Group Ltd is acknowledged for travel funding. This work was supported by the Foundation for Research Science and Technology grant number LSRX0801.

6. References

Basil-Jones, M.M., Edmonds, R.L., Allsop, T.F., Cooper, S.M., Holmes, G., Norris, G.E., Cookson, D.J., Kirby, N.Haverkamp, R.G., 2010, Leather structure determination by small angle X-ray scattering (SAXS): cross sections of ovine and bovine leather, J. Agric. Food Chem., 58(9) 5286-5291p.

Basil-Jones, M.M., Edmonds, R.L., Cooper, S.M.Haverkamp, R.G., 2011, Collagen fibril orientation in ovine and bovine leather affects strength: A small angle X-ray scattering (SAXS) study, J. Agric. Food Chem., 59(18) 9972-9979p.

Basil-Jones, M.M., Edmonds, R.L., Norris, G.E.Haverkamp, R.G., 2012a, Collagen fibril alignment and deformation during tensile strain of leather: A SAXS study, J. Agric. Food Chem., 60(5) 1201-1208p.

Basil-Jones, M.M., Edmonds, R.L., Norris, G.E.Haverkamp, R.G., 2012b, Collagen Fibril Alignment and Deformation during Tensile Strain of Leather: A Small-Angle X-ray Scattering Study, J. Agric. Food Chem., 60(5) 1201-1208p.

Bernado, P., Mylonas, E., Petoukhov, M.V., Blackledge, M.Svergun, D.I., 2007, Structural characterization of flexible peoteins using small-angle X-ray scattering, J. Am. Chem. Soc., 129(17) 5656-5664p.

Billiar, K.L.Sacks, M.S., 1997, A method to quantify the fiber kinematics of planar tissues under biaxial stretch, J. Biomech., 30(7) 753-756p.

Boote, C., Sturrock, E.J., Attenburrow, G.E.Meek, K.M., 2002, Psuedo-affine behaviour of collagen fibres during the uniaxial deformation of leather, J. Mat. Sci., 37 3651-3656p.

Burger, C., Zhou, H.W., Sics, I., Hsiao, B.S., Chu, B., Graham, L.Glimcher, M.J., 2008, Small-angle X-ray scattering study of intramuscular fish bone: collagen fibril superstructure determined from equidistant meridional reflections, J. Appl. Crystallogr., 41 252-261p.

Cameron, G.J., Alberts, I.L., Laing, J.H.Wess, T.J., 2002, Structure of type I and type III heterotypic collagen fibrils: an x-ray diffaction study, J. Struct. Biol., 137 15-22p.

Cedola, A., Mastrogiacomo, M., Burghammer, M., Komlev, V., Giannoni, P., Favia, A., Cancedda, R., Rustichelli, F.Lagomarsino, S., 2006, Engineered bone from bone marrow stromal cells: A structural study by an advanced x-ray microdiffraction technique, Phys. Med. Biol., 51(6) N109-N116p.

Cookson, D., Kirby, N., Knott, R., Lee, M.Schultz, D., 2006, Strategies for data collection and calibration with a pinhole-geometry SAXS instrument on a synchrotron beamline, J. Synchrotron Radiat., 13 440-444p.

Duivestein, J., Pitchford, W., Bottema, C., Fassbender, R., Cusack, D., Meldrum, R.Leather, M., 2000, Detection of vertical fiber hide defect (VFHD) in Hereford cattle hides by biopsy, J. Am. Leather Chem. As., 95(3) 92-101p.

Falgayrac, G., Facq, S., Leroy, G., Cortet, B.Penel, G., 2010, New method for Raman investigation of the orientation of collagen fibrils and crystallites in the haversian system of bone, Appl. Spectrosc., 64(7) 775-780p.

Friedrichs, J., Taubenberger, A., Franz, C.M.Muller, D.J., 2007, Cellular remodelling of individual collagen fibrils visualized by time-lapse AFM, J. Mol. Biol., 372(3) 594-607p.

Janko, M., Davydovskaya, P., Bauer, M., Zink, A.Stark, R.W., 2010, Anisotropic Raman scattering in collagen bundles, Opt. Lett., 35(16) 2765-2767p.

Jor, J.W.Y., Nielsen, P.M.F., Nash, M.P.Hunter, P.J., 2011, Modelling collagen fibre orientation in porcine skin based upon confocal laser scanning microscopy, Skin Res. Technol., 17(2) 149-159p.

Kronick, P.L.Buechler, P.R., 1986, Fiber orientation in calfskin by laser-light scattering or X-ray-diffraction and quantitative relation to mechanical-properties, J. Am. Leather Chem. As., 81(7) 221-230p.

Kronick, P.L.Sacks, M.S., 1991, Quantification of vertical-fiber defect in cattle hide by small-angle light-scattering, Connect. Tissue Res., 27(1) 1-13p.

Lilledahl, M.B., Pierce, D.M., Ricken, T., Holzapfel, G.A.Davies, C.D., 2011, Structural analysis of articular cartilage using multiphoton microscopy: input for biomechanical modeling, IEEE T. Med. Imaging, 30(9) 1635-1648p.

Mollenhauer, J., Aurich, M., Muehleman, C., Khelashvilli, G.Irving, T.C., 2003, X-Ray Diffraction of the Molecular Substructure of Human Articular Cartilage, Connect. Tiss. Res., 44(5) 201-207p.

Sasaki, N.Odajima, S., 1996a, Elongation mechanisms of collagen fibils and force-strain relations of tendon at each level of structural hierarchy, J. Biomech., 29(9) 1131-1136p.

Sasaki, N.Odajima, S., 1996b, Stress-strain curve and youngs modulus of a collagen molecule as determined by the x-ray diffaction technique, J. Biomech., 29(5) 655-658p.

Schofield, A.L., Smith, C.I., Kearns, V.R., Martin, D.S., Farrell, T., Weightman, P.Williams, R.L., 2011, The use of reflection anisotropy spectroscopy to assess the alignment of collagen, J. Phys. D Appl. Phys., 44(33).

Sizeland, K.H., Basil-Jones, M.M., Edmonds, R.L., Cooper, S.M.Haverkamp, R.G., 2013a, Collagen Alignment and Leather Strength, IULTCS 2013, Istanbul, Turkey,

Sizeland, K.H., Haverkamp, R.G., Basil-Jones, M.M., Edmonds, R.L., Cooper, S.M., Kirby, N.Hawley, A., 2013b, Collagen Alignment and Leather Strength for Selected Mammals, J. Agric. Food Chem., 61(4) 887-892p.

Tsutakawa, S.E., Hura, G.L., Frankel, K.A., Cooper, P.K.Tainer, J.A., 2007, Structural analysis of flexible proteins in solution by small angle X-ray scattering combined with crystallography, J. Struct. Biol., 158(2) 214-223p.

Williams, J.M.V., 2000a, IULTCS (IUP) test methods - Measurement of leather softness, J. Soc. Leather Tech. Ch., 84(7) 377-379p.

Williams, J.M.V., 2000b, IULTCS (IUP) test methods - Measurement of tensile strength and percentage elongation, J. Soc. Leather Tech. Ch., 84(7) 317-321p.

Modification of Collagen □-spacing in Skin

K.H. Sizeland†, R.L. Edmonds§, G.E. Norris‡, N. Kirby⊥, A. Hawley⊥, S. Mudie⊥, R.G. Haverkamp□

□School of Engineering and Advanced Technology and the □Institute of Molecular Biosciences, Massey University, Palmerston North, New Zealand□□Leather and Shoe Research Association, Palmerston North, New Zealand□⊥Australian Synchrotron, 800 Blackburn Road, Clayton, Melbourne, Australia.

Short Summary

Oils and moisturisers are often added to skin in an attempt to create a smoother, more supple feel. Additives have been shown to modify the collagen fibrils of processed skin, extending the fibril length. If a similar process could take place in living skin it may improve the appearance and strength of skin. Synchrotron-based small angle X-ray scattering has been used to investigate the modification of the collagen structure by model compounds. These model compounds were chosen because of their opposite effects on protein solubility. Urea, which is an osmolyte, is often used to solubilise proteins and is commonly used in skin care products, while the amino acids proline and hydroxyproline are known to precipitate proteins. □ ith the addition of urea, proline and hydroxyproline, the □-spacing of the collagen fibrils increased and the orientation index decreased. □ e discuss how the model compounds may affect collagen structure by possibly manipulating the hydrogen bonding network. If the mechanisms for modification of the structure of collagen by fat liquors and other additives can be understood, insights may be gained that will lead to better comprehension of existing skin formulations and the development of new formulations based on more in-depth knowledge about the action of moisturisers and cosmetic products on living skin.

Keywords Collagen SAXS Orientation Tissue Skin Structure -spacing.

Introduction

Skin and the much desired smooth, wrinkle-free complexion of youthful skin is an important topic of study for cosmetic science. Collagen I is an important component of skin that contributes to its structure and appearance. In-situ modification of the structure of collagen may be an important component of the action of skin care cosmetics.

Hydrating or lubricating liquids and gels are added to skin products to achieve a strong, supple feel in both the cosmetics industry and the leather industry. In the leather making process, animal skin is converted to a durable, strong and supple material. As leather is the product of processed animal skin, the collagen fibre structure of this complex biomaterial is similar to that of living skin, as well as pericardium and some other tissues. Like skin, Type I collagen accounts for most of the complex architecture of leather, and it is this fibrous collagen network and the interactions occurring within it that can be held largely accountable for the physical attributes of leather (Russell, 1988, Rabinovich, 2001, Michel, 2004, Chan et al., 2009, Basil-Jones et al., 2011).

Fat liquoring is part of the manufacturing process of leather, whereby penetrating oils are added to achieve the high strength and soft, supple feel of the finished product. These additives have been shown to modify the collagen fibrils and extend the fibril length (Sizeland et al., 2013b). The cosmetic industry is founded on the desire of many women (and men) to protect their skin and to avoid the natural signs of aging through the topical application of moisturisers that contain natural oils, fats and other compounds designed to penetrate the dermis. hile there has been much research into the effects of urea, various

peptides and a number of oils and fats, little is known of how they affect the physical properties of skin at a molecular level.

In order to comprehend how fat liquor and other additives affect the architecture of collagen in skin, it is important to gain an understanding about the structure of collagen itself. A collagen molecule is a repeating amino acid sequence, Gly (glycine)-X-□, which forms an alpha helical polypeptide chain with a left-hand twist. The (Gly-X-□)^{n} repeating pattern is one of the distinctive features of collagen. A high proportion of the amino acids proline and hydroxyproline occupy the X and □ positions, respectively, with the most common triplet in collagen being Gly-Pro-Hyp, which accounts for about 10□ of the total sequence (Ramshaw et al., 1998). Three of collagen molecules twist together in a right-hand manner to form a triple helix, or tropocollagen. Hydrogen bonds between side-chains stabilise the tropocollagen quaternary structure along with some covalent crosslinks. Larger collagen fibrils are assembled from up to five tropocollagens. A part of the fibril contains four tropocollagen molecules and a part contains five, due to staggering of the tropocollagen molecules. This difference is responsible for the banding of collagen structures, visible with atomic force microscopy or transmitting electron microscopy, and is known as the □-spacing, which can be measured. □ ithin each fibril, the tropocollagen molecules are held together by crosslinks formed between lysine and allolysine as a result of the action of an enzyme lysyl oxidase. The □-spacing varies with tissue types, animal species (Sizeland et al., 2013a), age (James et al., 1991), mechanical stress (Basil-Jones et al., 2012) and chemical treatment (Ripamonti et al., 1980).

The arrangement of collagen fibrils may also vary, and one aspect that can be measured is the orientation and spread in orientation of the fibrils. The relationship between the

orientation of fibrils and the mechanical strength has been characterised (Fratzl and □ einkamer, 200□), and the correlation of strength with the orientation of collagen measured edge-on (alignment in-plane) has been shown in both bovine and ovine skin (Basil-Jones et al., 2011, Basil-Jones et al., 2012). This correlation extends across a range of mammal species with a strength range of over a factor of five (Sizeland et al., 2013a). There may also be a correlation between strength and fibril diameter (Parry et al., 19□8,□ ells et al., 2013).

Critical elements in maintaining the stability of macromolecular assemblies of collagen are the extensive, highly structured hydration shell and hydrogen bond networks around the collagen triple helices in which hydrogen bonds involving water form bridges between collagen fibrils (Bella et al., 1994, Naito et al., 1994, Bella et al., 199□).

Hydrogen bonding, both direct and water-mediated, plays a critical role in maintaining the stability of proteins such as collagen. The addition of dissolved amino acids to a protein may affect hydrogen bonding, depending on the amino acid added. If hydrogen bonds are modified, the triple helices and consequently the collagen fibril structure will be directly impacted.

It is standard practice to add fat liquors to skin during leather processing, however, the affect this has on the structure of collagen has only recently been investigated (Sizeland et al., 2013b). To better understand the influence of the penetrating oils on the molecular structure of collagen, the fibril orientation and axial periodicity of collagen fibrils have been quantified for samples processed with model compounds using synchrotron-based small angle X-ray scattering (SAXS). Three compounds were chosen□urea, known to solubilise proteins, and the amino acids proline and hydroxyproline, both known precipitators of proteins (Record et al., 2013). Here we report how the addition of urea, proline, and hydroxyproline affects the physical properties of ovine skin, in order to understand their effect at the structural level. In

addition, we compare the effects with that of lanolin, a compound used in many commercial skin preparations, which we have previously seen to modify collagen (Sizeland et al., 2013b). □ e hope to be able to extend this knowledge to the action of moisturisers and cosmetic products on living skin.

Methodology

Leather preparation

Ovine skin from the leather industry was used as a model material to investigate collagen modification by urea, hydroxyl-L-proline (Sigma-Aldrich), L-proline (Sigma-Aldrich) and lanolin (Sigma-Aldrich).

Ovine pelts were obtained from □-month-old, early season, New Zealand Romney cross lambs. The leather was generated using conventional beamhouse and tanning processes. Specifically, the skins were depilated using a caustic treatment comprising sodium sulfide and calcium hydroxide. The leather was then rotated in a drum for 16 hr at 20□C in a 1.2□ sodium sulfide solution to remove any residual keratinaceous material. The skins were next washed to remove the lime and treated with 0.1□ of a commercial bate enzyme (Tanzyme, Tryptec Biochemicals, Ltd.). They were then pickled in a 2□ sulfuric acid and 10□ sodium chloride solution. The pickled pelts were pre-tanned using oxazolidine, degreased with an aqueous surfactant, and tanned using chromium sulfate. Finally, a 3□ vegetable tanning material (mimosa, Tanac, Brazil) was used to re-tan the resulting □wet blue□.

In conventional beamhouse processing, fat liquors are added at this stage to the wet blue pelts prior to fixing with 0.□□ formic acid, washing, drying and mechanical softening. However, to make the samples for this study, the fat liquor was replaced with urea, L-proline and hydroxyl-L-proline at concentrations of 4□ and □2□ by weight of wet leather. Two

further samples were prepared□one with lanolin (Sigma) at a concentration of 8□ by weight of wet leather and one with no additives at all.

Synchrotron SAXS

The samples for SAXS analysis were cut from the official sampling position (OSP) (Williams, 2000) in strips 1 × 30 mm. Each sample was mounted without tension in the X-ray beam to obtain scattering patterns through the sample's full thickness. Each data point presented here (D-spacing, OI) is the average of 11-17 diffraction patterns recorded every 0.25 mm through the cross-section from the grain to the corium except the sample with no additives, which is the average of 6 patterns. Diffraction patterns were recorded on the Australian Synchrotron SAXS/WAXS beamline using a high-intensity undulator source. Energy resolution of 10^{-4} was obtained from a cryo-cooled Si (111), double-crystal monochromator, and the beam size (FWHM focused at the sample) was 250 × 80 μm, with a total photon flux of about 2×10^{12} photons s^{-1}. All diffraction patterns were recorded with an X-ray energy of 11 keV using a Pilatus 1 M detector with an active area of 170 × 170 mm and a sample-to-detector distance of 3371 mm. Exposure time for diffraction patterns was 1 s, and data processing was carried out using the SAXS15ID software (Cookson et al., 2006).

Orientation index

A measure of the spread in orientation of the microfibrils is given by the orientation index (OI), with an OI of 1 indicating the microfibrils are parallel to each other and an OI of 0 indicating the microfibrils are randomly oriented. OI is defined as (90° – OA)/90°, where OA is the minimum azimuthal angle range that contains 50% of the microfibrils. This measure is based on Sack's method for light scattering (Sacks et al., 1997) but converted to an index (Basil-Jones et al., 2011) using the spread in azimuthal angle of one or more Bragg peaks.

The peak used was typically the sixth order peak at approximately 0.055-0.059 □$^{-1}$ as it is one of the most intense D-spacing peaks. The peak area is measured, above a fitted baseline, at each azimuthal angle.

□□□□*acin*□

Bragg's □aw was used to determine the D-spacing of collagen for each diffraction pattern by taking the central position of several collagen peaks, dividing these by the peak order (usually from n □5 to n □10) and averaging the resulting values.

Results

SAXS patterns were obtained for the samples processed with no additives, with the model compounds (hydroxyproline, proline and urea) and with lanolin. Diffraction rings that occur due to the axial periodicity displayed by collagen were clearly visible in every spectrum (□igure 1a). The varying and non-uniform intensity around the azimuthal angle of the rings indicates the orientation of the fibrils. The integrated intensity of the scattering pattern can be plotted against □(□igure 1b), the azimuthal angle, and the D-spacing calculated using the position of the diffraction peaks.

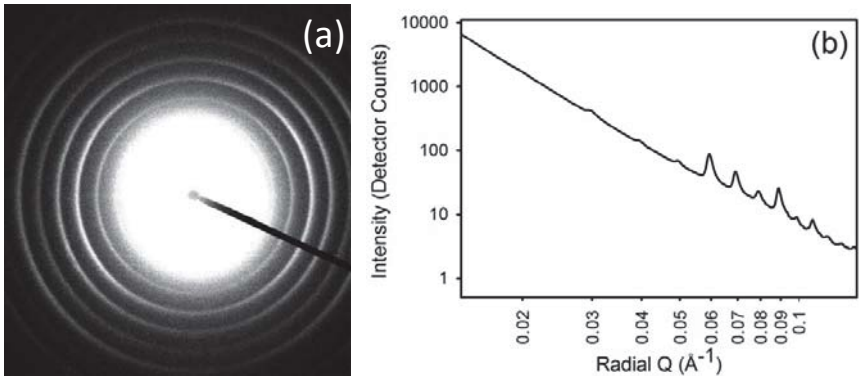

Figure 1. Example of SAXS of collagen□(a) raw SAXS pattern□(b) integrated intensity profile.

The addition of urea, proline and hydroxyproline all result in statistically significant increases in the D-spacing of collagen fibrils (□igure 2, for full statistics see Table 1). The D-spacing increased from 60.2 (σ □0.□2) nm for samples with no fat li□uor or additives up to maximums of 63.□(σ □0.25, P □3.□□x 10^{-11} at an alpha of 0.05) nm for urea. A D-spacing change occurred when 7.2% urea was added with an increase of 3.2 nm or 5.3%. The D-spacing of leather with □% lanolin was found to be 63.2 (0.50) nm, an increase of 3.0 nm.

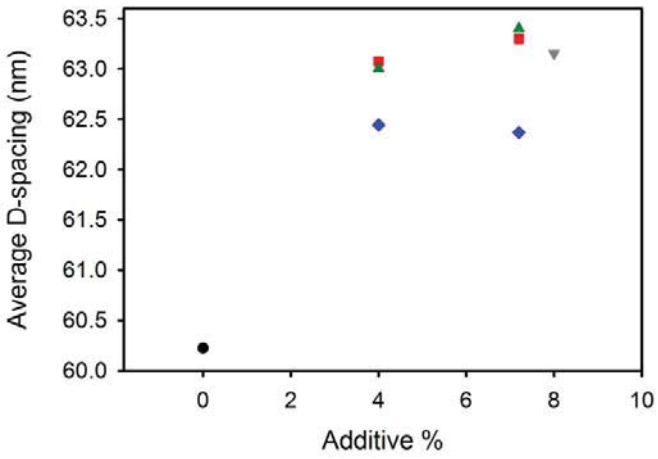

Figure 2. Collagen D-spacing versus additive percentage for processed skin□(●) no additives, (▼) lanolin, (♦) hydroxyproline, (■) proline, and (▲) urea. Each point is the average value taken from 11–17 scattering patterns, except the 0% sample, which is the average of 6 patterns.

The OI of the collagen fibrils decreased with the addition of the model compounds (□igure 3), with statistically significant decreases occurring with the addition of □% hydroxyproline, 7.2% hydroxyproline and □% urea. The OI decreased from 0.59 (σ □0.05) for samples with no fat li□uor or additives down to 0.□□(σ □0.12, P □0.0095 at an alpha of 0.05) for urea. The largest OI change occurred when □% urea was added, with a decrease of 0.15 nm or 25.3%. The OI of □% lanolin was found to be 0.69 (σ □0.06) which, in contrast to the other compounds, is an increase.

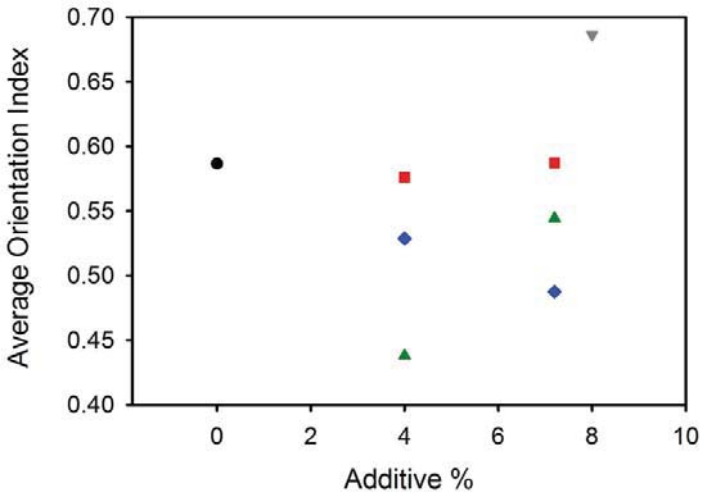

Figure 3. Collagen orientation index (OI) versus additive percentage for processed skin (●) no additives, (▼) lanolin, (♦) hydroxyproline, (■) proline, and (▲) urea. Each point is the average value taken from 11-17 scattering patterns, except the 0 % sample which is the average of 6 patterns.

	Orientation Index comparison				D-spacing comparison			
	Difference in values	Statistical Significance	*t* statistic	*P* value	Difference in values (nm)	Statistical Significance	*t* statistic	*P* value
0% to 4% hydroxyproline	-0.0580	Significant	2.33	0.0307	2.2182	Significant	-13.10	<0.0001
0% to 7.2% hydroxyproline	-0.0992	Significant	4.21	0.0004	2.1416	Significant	-10.54	<0.0001
0% to 4% proline	-0.0107	Not Significant	0.45	0.6600	2.8499	Significant	-18.31	<0.0001
0% to 7.2% proline	0.0005	Not Significant	-0.15	0.9880	3.0729	Significant	-20.48	<0.0001
0% to 4% urea	-0.1486	Significant	2.90	0.0095	2.7751	Significant	-18.79	<0.0001
0% to 7.2% urea	-0.0422	Not Significant	1.69	0.1120	3.1757	Significant	-19.72	<0.0001
0% to 8% lanolin	-0.0998	Significant	-3.36	0.0030	2.9274	Significant	-12.82	<0.0001

Table 1. Statistics for orientation index (OI) and D-spacing values when comparing samples

with no additives (0%) to samples with added model compounds. All *t*-tests were calculated using and alpha of 0.05.

Discussion

We found that urea changed the collagen fibril OI and D-spacing. □rea and other small organic compounds have a definitive use within skin care formulations. With this in mind, a way of predicting or outlining how such additives might alter the architecture of collagen would benefit the cosmetics industry hugely.

The observed D-spacing increase that the addition of the amino acids produces can be physically e□uated to a lengthening of the collagen fibrils. The mechanisms coming into play to attain such a lengthening may be due to alterations within the hydrogen bond network.

□ydrogen bonds are an important structural component of collagen. Two sets of interchain hydrogen bonds, one direct and one water-mediated, have been detected for a collagen-like peptide (□ramer et al., 1999). Both direct hydrogen bonds and water-mediated hydrogen bonds contribute to collagen stability.

□irstly, let us consider direct hydrogen bonds. The □-□ of glycine and the O□C of the residue in the X position on ad□acent polypeptide strands within every tropocollagen are linked by direct hydrogen bonds. There are also hydrogen bonds between the side-chains of the amino acids and main-chain atoms, as well as side-chain–side-chain hydrogen bonds. □rea is known to act by forming hydrogen bonds with peptide groups (□im et al., 2009). It is therefore possible that the increase in the tropocollagen unit length could be the result of urea breaking some □-bonds within the triple helix, resulting in looser coiling (Bella et al., 199□). This would result in an increase in D-spacing with the effect spread e□ually over both the gap and the overlap region of the fibril. Interestingly, lanolin had a similar effect. The D-spacing

values of collagen after addition of urea at 63.0 (σ □ 0.2□) nm at □% concentration and 63.□ (σ □ 0.25) nm at 7.2% concentration are similar to those of collagen samples made with □% lanolin, with a value of 63.2 (σ □ 0.50) nm. □anolin, a long-chain waxy ester, is likely to have a different mechanism based on its hydrophobic properties and its effect on water structure.

The effect of urea was expected, based on □im (P□AS 2009) and □ecord (□ecord et al., 2013). □owever, given the protein-precipitating properties of proline (□ecord et al., 2013), we expected proline and hydroxyproline to have the opposite effect, that of shortening the D-spacing. This we did not observe, but rather saw an extension of the D-spacing (Table 1).

□ow, let us turn to water-mediated hydrogen bonds. In the presence of hydrophobic molecules, water structure becomes ordered and the number of □-bonds is reduced. In the presence of polar molecules, the number of □-bonds also changes as the polar molecules compete with the water to interact with the tropocollagens. □ydrogen bonds mediated through water bridges within the tropocollagen structure may likewise be affected, resulting in a looser coiling of the triple helix and a concomitant increase in D-spacing.

In all samples treated with urea and hydroxyproline the OI of the collagen fibrils decreased (Table 1). As stated above, the OI indicates the spread in fibril orientation and has previously been found to be correlated with material strength (Basil-Jones et al., 2011). By contrast, lanolin increases the OI, showing that the addition of lanolin increases the alignment of the fibrils. These observations reflect the different nature of these two compounds, and a fundamental difference in their mode of activity. □rea exerts its influence through polar interactions, lanolin through hydrophobic interactions, both affecting water structure. □rea competes with water to make □-bonds with the peptide groups within the collagen structure, essentially affecting the hydration shell around the molecule, while lanolin orders the water around the molecule, also affecting the hydration shell. The effect within the fibril and

between fibrils is, however, different. □rea disrupts interactions between fibrils by breaking non-covalent bonds. It is likely that this will result in a decrease in the alignment of parts of or whole fibrils. Conversely, lanolin, because of its structure, can insert itself between fibres, trapping ordered water and allowing the fibres to slide over each other, to increase fibre alignment.

Conclusions

We conclude that the triple alpha helix structure of tropocollagen is modified by treatment with urea, hydroxyproline and lanolin, resulting in changes to the suppleness and strength of tanned skin (leather). □rea lengthens the D-spacing as predicted, while also significantly reducing the OI of the skin, which will impact on its robustness. While lanolin has the same effect on D-spacing, it has the opposite effect on the OI, significantly affecting the physical properties of the skin. □iven that lanolin is a ma□or component of most skin care formulations, understanding how it functions at a molecular level is important for the cosmetic industry. The D-spacing changes observed for added proline and hydroxyproline did not agree with our predictions. □urther investigations of the mechanisms of modification of collagen in skin by urea, proline, hydroxyproline, lanolin, and by extension other organic compounds, may lead to a better understanding of existing skin formulations and development of new formulations.

Acknowledgements

This research was undertaken on the SAXS/WAXS beamline at the Australian Synchrotron, Victoria, Australia. The □□ Synchrotron □roup □td is acknowledged for travel funding. The work was funded by a grant (□S□X0□01) from the Ministry of Business

Innovation and Employment in association with the □ew □ealand □eather and Shoe □esearch Association.

References

BASI□-JO□ES, M. M., EDMO□DS, □. □., COOPE□, S. M. □ □AVE□□AMP, □. □. 2011. Collagen fibril orientation in ovine and bovine leather affects strength□A small angle X-ray scattering (SAXS) study. □□*A□ric□□ood □he*□□59**,** 9972-9979.

BASI□-JO□ES, M. M., EDMO□DS, □. □., □O□□IS, □. E. □ □AVE□□AMP, □. □. 2012. Collagen □ibril Alignment and Deformation during Tensile Strain of □eather□A Small-Angle X-ray Scattering Study. □□*A□ric□□ood □he*□□60**,** 1201-120□.

BE□□A, J., B□ODS□□, B. □ BE□MA□, □. M. 1995. □ydration structure of a collagen peptide. *Str□ct□re*□**3,** □93-906.

BE□□A, J., EATO□, M., B□ODS□□, B. □ BE□MA□, □. M. 199□ Crystal-structure and molecular-structure of a collagen-like peptide at 1.9-□ngstrom resolution. *Science*□ **266,** 75-□1.

C□A□, □., COX, □. M., □AVE□□AMP, □. □. □ □I□□, J. M. 2009. Mechanical model for a collagen fibril pair in extracellular matrix. □□*r*□□*io□hy*□□□□□*io□hy*□□*ett*□□**3**□**,** □□7-□93.

COO□SO□, D., □I□B□, □., □□OTT, □., □EE, M. □ SC□□□T□, D. 2006. Strategies for data collection and calibration with a pinhole-geometry SAXS instrument on a synchrotron beamline. □□*Synchrotron □adiat*□□13**,** □□0-□□□.

□□AT□□, P. □ WEI□□AME□, □. 2007. □ature's hierarchical materials. □*ro*□□□*ater□Sci*□□ **52,** 1263-133□.

JAMES, V. J., MCCO□□E□□, J. □. □ CAPE□, M. 1991. The D-spacing of collagen from mitral heart-valves changes with aging, but not with collagen type-III content. □*iochi*□□□*io□hy*□□*Acta*□107□**,** 19-22.

□□AME□, □. □., BE□□A, J., MA□VI□□E, P., B□ODS□□, B. □ BE□MA□, □. M. 1999. Se□uence dependent conformational variations of collagen triple-helical structure. □*at□Str□ct□□io*□□6**,** □5□-57.

□IM, W. □., □OS□E□, J. □ E□□□A□DE□, S. W. 2009. □rea, but not guanidinium, destabilizes proteins by forming hydrogen bonds to the peptide group. □*roceedin□□o□ the □ationa□Acade□y o□Science□o□the □nited State□o□A□erica*□106**,** 2595-2600.

MIC□E□, A. 200□ Tanners□dilemma□Vertical fibre defect. □*eather □nternationa*□□206**,** 36-37.

□AITO, A., T□□I, S. □ SAITO, □. 199□ A high-resolution □-15 solid-state □M□-study of collagen and related polypeptides - the effect of hydration on formation of interchain hydrogen-bonds as the primary source of stability of the collagen-type triple-helix. □□*r*□□□□*ioche*□□□22□**,** 729-73□.

PA□□□, D. A. D., BA□□ES, □. □. □. □ C□AI□, A. S. 197□ Comparison of size distribution of collagen fibrils in connective tissues as a function of age and a possible relation between fibril size distribution and mechanical-properties. □□□*oy□Soc*□□□ □*io*□□*Sci*□□203**,** 305-321.

□ABI□OVIC□, D. 2001. Seeking soft leathers with a tight grain. □*O*□□□ □*eather*□1□**,** 27-32.

□AMS□AW, J. A. M., S□A□, □. □. □ B□ODS□□, B. 199□. □ly-X-□ tripeptide fre□uencies in collagen□A context for host-guest triple-helical peptides. *□o□rna□o□ Str□ct□ra□□io□o□y* 122**,** □6-91.
□ECO□D, M. T., □□I□□, E., PE□□AM, □. □ CAPP, M. 2013. Introductory □ecture□ Interpreting and predicting □ofmeister salt ion and solute effects on biopolymer and model processes using the solute partitioning model. *□araday □i□c□□ion□□* 160**,** 9-□□.
□IPAMO□TI, A., □OVE□I, □., B□A□A, D., □□□MES, D. J. S., MI□□E□, A. □ TIMMI□S, P. A. 19□0. Effects of p□ and ionic-strength on the structure of collagen fibrils. *□io□o□y□er□□* 19**,** 965-975.
□□SSE□□, A. E. 19□□. Stress-strain relationships in leather and the role of fiber structure. *□□ Soc□□eather □echno□□□he□□□* 72**,** 121-13□.
SAC□S, M. S., SMIT□, D. B. □ □IESTE□, E. D. 1997. A small angle light scattering device for planar connective tissue microstructural analysis. *Ann□□io□ed□□n□□□* 25**,** 67□-6□9.
SI□E□A□D, □. □., □AVE□□AMP, □. □., BASI□-JO□ES, M. M., EDMO□DS, □. □., COOPE□, S. M., □I□B□, □. □ □AW□E□, A. 2013a. Collagen Alignment and □eather Strength for Selected Mammals. *□□A□ric□□ood □he□□□* 61**,** □□7-□92.
SI□E□A□D, □. □., □O□□IS, □. E., EDMO□DS, □. □., □I□B□, □., □AW□E□, A. □ □AVE□□AMP, □. □. □ear. Polyol Modification of Collagen □ibril Axial Periodicity. *□n□* Australian Synchrotron □ser Meeting, 2013b Melbourne, Australia.
WE□□S, □. C., EDMO□DS, □. □., □I□B□, □., □AW□E□, A., M□DIE, S. T. □ □AVE□□AMP, □. □. 2013. Collagen □ibril Diameter and □eather Strength. *□□A□ric□ □ood □he□□□* 61**,** 1152□-11531.
WI□□IAMS, J. M. V. 2000. I□□TCS (I□P) test methods - Sampling. *□□Soc□□eather □echno□□□he□□□□* **,** 303-309.

Collagen D-spacing Modification by Fat Liquor Addition

Katie Sizeland†, Hannah Wells†, Gillian Norris‡, Richard Edmonds§, Richard Haverkamp†

†School of Engineering and Advanced Technology and ‡Institute of Molecular Biosciences, Massey University, Private Bag 11222, Palmerston North, New Zealand; §Leather and Shoe Research Association, Palmerston North 4442, New Zealand.

Introduction

The structure and strength of collagen fibre materials is of crucial importance in both the medical and textile industries. Collagen is the main structural component of skin (Fratzl, 2008); both in an unprocessed state and as leather following chemical and mechanical processing. Leather is a remarkable biomaterial that exhibits strength, flexibility and, durability. Leather is processed skin consisting mostly of collagen and it is produced on a large scale for shoes, clothing and upholstery, with high strength being a primary requirement for high-value applications. As such, the price of leather is based on its physical and aesthetic properties and these properties ultimately depend on the nanostructure of the collagen fibre network. Ovine leather is weaker than bovine leather, typically half the strength, making ovine leather a low-value product relative to bovine leather. If the strength of ovine leather could be increased, great value would be added to the New Zealand economy.

A collagen fibril contains multiple levels of structure. Collagen molecules are formed by a sequence of amino acids combining in a left-handed α helix. The tropocollagen molecule is formed when three collagen molecules are twisted together to form a right handed triple helix, or tropocollagen. Direct and water-mediated hydrogen bonds help stabilize the structure. Tropocollagens combine in an organized, manner to form fibrils that are characterized by a banded structure and display Bragg diffraction peaks. The banding pattern results from the staggered arrangement of the tropocollagen molecules and is referred to as the D-spacing. The extensive, highly structured hydration shell around the collagen triple helices, along with water bridges and covalent cross-links between tropocollagens are observed to be critical elements maintaining the macromolecular assemblies in which collagen molecules are involved.

In terms of microstructure, leather comprises two distinct layers: the ‘grain’ and the ‘corium’ that have significantly different structures. The D-spacing for stronger ovine and bovine leather has been shown to decrease at the interface between the corium and grain (Basil-Jones et al., 2012). While

changes in D-spacing have not been shown to correlate with strength in leather (Basil-Jones et al., 2011, Sizeland et al., 2013), D-spacing does vary with animal species (Sizeland et al., 2013), age (James et al., 1991, Scott et al., 1981), and chemical treatment (Scott et al., 1981, Ripamonti et al., 1980). It is also possible to observe changes in the D-spacing when leather is subjected to mechanical stress (Basil-Jones et al., 2012).

During the processing of skins and hides to leather, efforts are made to optimize the strength, flexibility and feel of leather. Adding penetrating oils, a process known as fat liquoring, is likely to improve both the flexibility and the texture of leather by lubricating the fibers to prevent adhesion between them (Bajza and Vreck, 2001). Little is known, however, about the effect of fat liquor on the molecular structure of the collagen fibrils.

Here we report a study of the effect of fat liquor on the nanostructure of leather. Once this is understood, the ability to manipulate leather processing in order to achieve improved aesthetic properties and strength may be realized.

Experimental

Ovine pelts were obtained from 5-month-old, early season New Zealand Romney cross lambs. Conventional beamhouse and tanning processes using an oxazolidine pretan, a chromium tan and a mimosa retan were used to generate leather. The fat liquor used was Lipsol EHF (Schill + Seilacher). This product contains a mixture of lanolin, bisulfited fish oil and 2-methyl-2,4-pentanediol. Lanolin, or wool wax, consists primarily of wax esters and some hydrolysis and oxidation products of these esters. The fat liquor was added in a ratio of 0–10% by weight of wet leather prior to drying and mechanical softening. One further sample was prepared with just the principal component of the fat liquor, lanolin (Sigma), at a concentration of 8% by weight of wet leather.

Samples for synchrotron-based small angle X-ray scattering (SAXS) analysis were prepared by cutting strips of leather 1 × 30 mm from the official sampling position (OSP) of the pelts. Diffraction patterns were recorded on the Australian Synchrotron SAXS/WAXS beamline with each sample mounted without tension in the X-ray beam to obtain scattering patterns from an edge-on direction. Measurements were made every 0.25 mm through the full thickness of the leather. Exposure time for diffraction patterns was 1 s, and data processing was carried out using the SAXS15ID software and the Irena software package running within Igor Pro.

The D-spacing of collagen was determined for each spectrum from Bragg's Law by taking the central position of several collagen peaks, dividing these by the peak order (usually from $n = 5$ to $n = 10$) and averaging the resulting values.

Fibril diameters were calculated by fitting the data at the wave vector Q, in the range of 0.01 – 0.04 $Å^{-1}$ and at an azimuthal angle which was 90° to the long axis of most of the collagen fibrils. The "cylinderAR" shape model with an arbitrary aspect ratio of 30 was used for all fitting.

The geometry of the hydrogen bonding in tropocollagen was determined using the software package Abalone (Agile Molecule) with the 9128 Da collagen-like peptide 1CAG from the protein databank.

Results

The SAXS patterns obtained for the different levels of fat liquor clearly show diffraction rings due to the axial periodicity of collagen (Figure 1a). Orientation of the collagen fibrils can be seen as the varying intensity of each of these rings around the azimuthal angle and the alignment at right angles to this of the central scattering region. From the integrated intensity of the whole scattering pattern (Figure 1b) the position of the diffraction peaks can be measured and from these the D-spacing is determined.

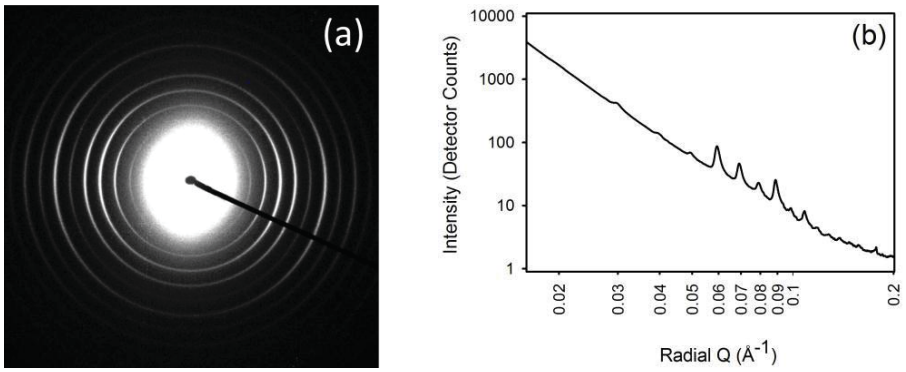

Figure 1. Example of SAXS of leather: (a) raw SAXS pattern; (b) integrated intensity profile.

The addition of fat liquor resulted in an increase in the D-spacing (standard deviation) from 60.2 (σ = 0.47) nm for samples with no fat liquor to 63.6 (σ = 0.43) nm for samples with 10% fat liquor (Figure 2). This is an increase of 3.4 nm or 5.6%. Despite structural differences in the corium and grain layers, the addition of fat liquor produced similar changes in D-spacing. There was a strong correlation between D-spacing and the percentage of fat liquor added as shown in Figure 2, where a linear slope of 0.34 nm/% fat liquor could be fitted to the data with an r^2 value of 0.93 (P = 0.0018 at an alpha of 0.05).

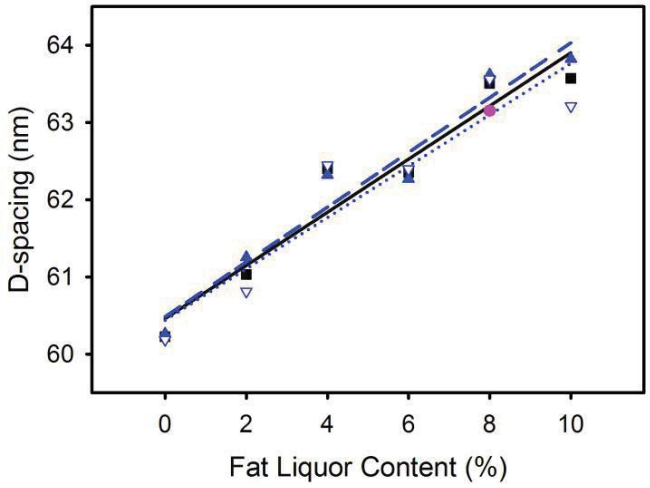

Figure 2. Collagen D-spacing versus fat liquor content for ovine leather: (▲, —— ——) corium, (▽, ····) grain, and (■, ——) average. Each point for the corium and grain is the average taken value from about 10 scattering patterns. Pure lanolin at 8% is shown in pink.

The one sample prepared with 8% lanolin rather than fat liquor had a D-spacing of 63.1 (σ = 0.39) nm, which falls on the regression line in Fig. 2. It is therefore possible that the change in D-spacing is could be caused by the lanolin content of the fat liquor.

An average fibril diameter of 56.8 (*n* = 106, σ = 1.3) nm was determined for the leather. There was no statistically significant change in fibril diameter with fat liquor addition.

Discussion

We found that the change in collagen D-spacing is proportional to the amount of fat liquor added, with a large change being observed when the greatest amount of fat liquor was added. The lanolin component of the fat liquor appears to be responsible for most or all of this change.

The observed change in D-spacing reflects a change in the length of the collagen fibrils. One mechanism that could result in longer collagen fibrils is by changing the way the fibrils are assembled. If there is a greater gap region between the tropocollagen molecules but they remain the same length then the D-spacing will increase. A second mechanism by which collagen fibrils might lengthen could result from an extension of the tropocollagen unit. This may be the consequence of a tighter coiling of the triple helix or an extension of critical H-bonds within the helix. Although these possibilities cannot be resolved from the results reported here, we can consider the plausibility of these mechanisms and suggest experimental work that might select between them.

A change in the length of a fibril by increasing the gap region could result from a change in the interaction between tropocollagens. The triple helices are surrounded by a highly structured cylinder of hydration. Lanolin, a main component of the fat liquor used, is hydrophobic and it may serve to remove some of the hydration cylinder and therefore alter the bonding between tropocollagens. Atomic force microscopy could be used to compare the ratio of the gap and overlap regions among leathers with different levels of fat liquor.

The second mechanism proposed suggests that the D-spacing increase is caused by an extension in the length of the tropocollagen molecule. This increased molecule length could be due to a change in length of the Hydrogen bonds either within the triple helix itself or between the tropocollagens that make up a fibril.

Firstly we will consider the change in length of the direct Hydrogen bonds within a tropocollagen. Direct Hydrogen bonds between glycine and hydroxyproline and between glycine and proline are present in every tropocollagen between adjacent polypeptide chains at an angle of 74º to the tropocollagens longitudinal axis. A lengthening of these bonds would result in an extension of the tropocollagen molecule and therefore an increase in the length of the collagen fibril and its axial periodicity. The observed increase in D-spacing of 5.6% (3.4 nm) would require a larger increase in the length of the Hydrogen bonds because the intra-tropocollagen bonds are not parallel to the long axis. Aligned at 74° from the long axis, a 20% increase in the bond length would be required to give the observed increase in D-spacing. With such a large increase in bond length required we would expect to see a significant increase in the fibril diameter.

Secondly we will consider the change in length of water-mediated Hydrogen bonds within a tropocollagen. Lanolin's hydrophobic nature may serve to exclude water. This would disrupt the water-mediated Hydrogen bonding between the collagen molecules in the triple helix. A shortening or disruption of these water mediated H-bonds would subsequently increase the twist of the tropocollagen helix which could in turn result in a longer (and perhaps thinner) tropocollagen and therefore a longer D-spacing in the fibril.

However, if an increase in tropocollagen length occurred by either of these mechanisms, we would expect to see an increase in the fibril diameter in the case of H-bond lengthening, or perhaps a small decrease in fibril diameter in the case of increased twist. The diameter was not observed to change and therefore these mechanisms are not supported.

Conclusion

In summary, we have investigated the structural changes of collagen within leather upon addition of varying amounts of fat liquor. We have shown that as we increased the amount of fat liquor, the D-spacing of the collagen fibrils increased, and that this could be due to the lanolin component of the fat liquor. This shows that fat liquor does more than just lubricate the fibers in leather; it actually alters the structure of the collagen fibrils. Alternative mechanisms for this increase in D-spacing have been discussed, including an increase in the gap region or an increase in the length of the tropocollagen triple helix.

Acknowledgements

This research was undertaken on the SAXS/WAXS beamline at the Australian Synchrotron, Victoria, Australia who also provided travel funding.

References

1. Bajza Z & Vreck IV: **Fatliquoring agent and drying temperature effects on leather properties.** *Journal of Materials Science* 2001, **36**:5265-5270

2. Basil-Jones MM, Edmonds RL, Cooper SM, & Haverkamp RG: **Collagen fibril orientation in ovine and bovine leather affects strength: A small angle X-ray scattering (SAXS) study**. *Journal of Agricultural and Food Chemistry* 2011, **59**:9972-9979

3. Basil-Jones MM, Edmonds RL, Norris GE, & Haverkamp RG: **Collagen fibril alignment and deformation during tensile strain of leather: A SAXS study.** *Journal of Agricultural and Food Chemistry* 2012, **60**:1201-1208

4. Bella J, Eaton M, Brodsky B, & Berman HM. **Crystal-structure and molecular-structure of a collagen-like peptide at 1.9-Ångstrom resolution.** *Science* 1994, **266:**75-81.

5. Fratzl P: **Collagen: Structure and mechanics.** *New York: SpringerScience+Business Media* 2008.

6. James VJ, McConnell JF, & Capel M: **The D-spacing of collagen from mitral heart-valves changes with aging, but not with collagen type-III content.** *Biochimica and Biophysica Acta* 1991, **1078**:19-22.

7. Ripamonti A, Roveri N, Braga D, Hulmes DJS, Miller A, & Timmins PA: **Effects of pH and ionic-strength on the structure of collagen fibrils.** *Biopolymers* 1980, **19**:965-975.

8. Scott JE, Orford CR, & Hughes EW: **Proteoglycan-collagen arrangements in developing rat tail tendon - an electron-microscopical and biochemical investigation.** *Biochemistry Journal* 1995, **19**:573-584.

9. Sizeland KH, Basil-Jones MM, Edmonds RL, Cooper SM, Kirby N, Hawley A, & Haverkamp RG: **Collagen Alignment and Leather Strength for Selected Mammals.** *Journal of Agricultural and Food Chemistry* 2013, **61**:887-892.

Forming Biochar from Leather Waste to Reduce Leaching of Chromium into the Environment

Hannah Wells, Massey University

H. C. Wells, K. H. Sizeland, R. L. Edmonds, W. Aitkenhead, P. Kappen, C. Glover, B. Johannessen, R.G. Haverkamp. Stabilized Chromium in Biochar from Leather Waste. ACS Sustainable Chem. Eng. **2014,** 2, 1864-1870.

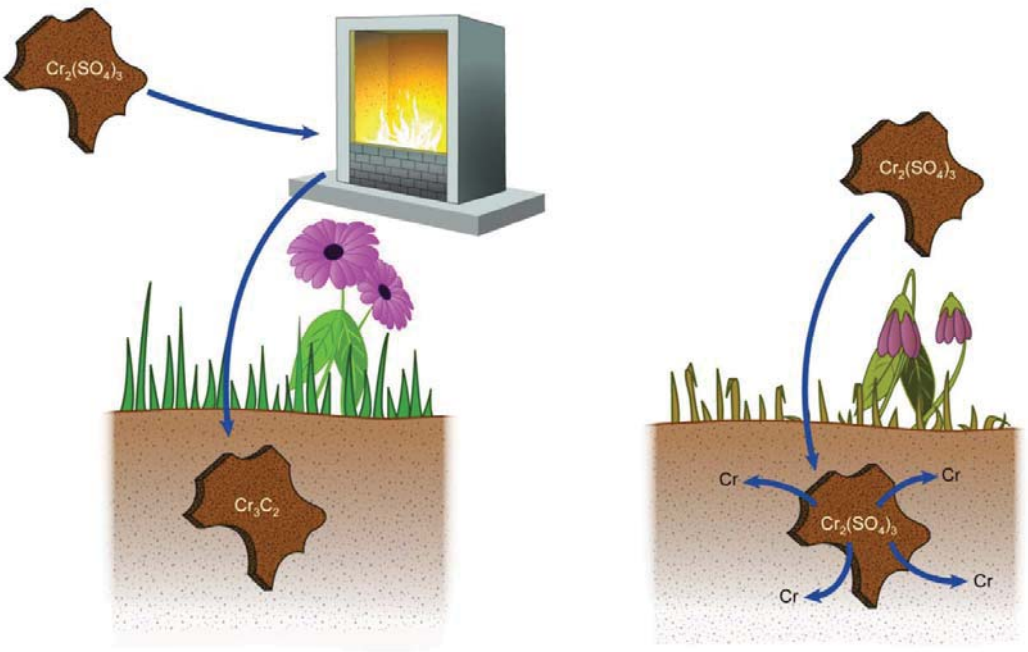

Introduction

Most leather is produced from skins and hides by tanning with chromium salts. Leather is used in upholstery (car and home), shoes and clothing but at the end of the life of these goods, the leather needs to be disposed of in an environmentally benign manner. Leather manufacture and production of goods from leather also produces leather scrap which requires disposal. Annual global leather production is about 6.8 million tonnes [1], around 80% of which contains Cr.

The main concern in the disposal of leather is the leaching from leather of Cr. Soluble Cr in a hexavalent oxidation state is considered to be undesirable in the environment [2, 3] and sites where Cr(VI) is present can require remediation [4].

Current and proposed leather disposal methods include: extraction of Cr before disposal [5-7]; disposal to wetlands for vegetation to absorb the Cr [8]; production of other reconstituted structural materials to bind the Cr in new products [9, 10]; and heating leather in an oxidizing environment to create a residue with soluble Cr [11, 12]. Cr contained in or on particulates from the burning of coal and biomass (in the presence of oxygen) can produce Cr(VI) [13]. Therefore, it is possible that burning leather may also generate Cr(VI), which is undesirable.

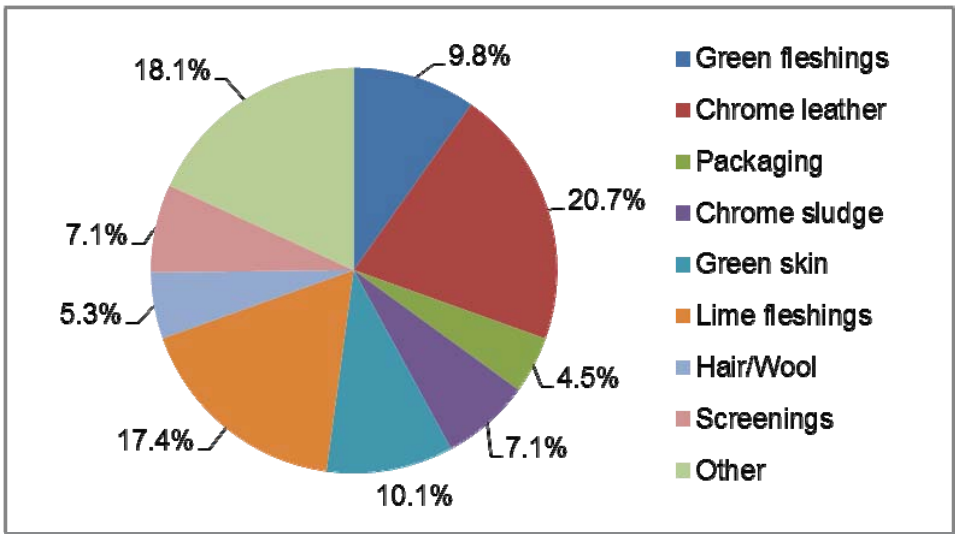

Figure 2: Breakdown of waste dumped in New Zealand landfills by the leather industry[29].

We have proposed that the production of biochar, carbonized organic matter, from waste leather may be a better alternative to other disposal methods[14]. Biochar is produced by heating organic matter in an oxygen deficient environment. The application of leather biochar is a way of sequestering carbon, thereby reducing the amount of carbon that may have otherwise become atmospheric CO_2. Biochar also has the demonstrated benefit of improving agricultural soil productivity[15]. Carbonized leather has previously been considered as a disposal option, with the suggestion of producing an activated carbon product for filtration applications [16-18].

Ideally, a leather biochar product could be produced that does not leach Cr. Exposing leather that has been "heat stablised" in a non-oxidising environment to leaching indicates that the material has a low solubility of Cr. Specifically, when leather was stablised at 350 °C or higher in a CO_2 environment, no soluble Cr is detected over a wide pH range in contrast to untreated, chrome-tanned leather [16]. It is also important that the Cr is resistant to oxidation, since both Cr oxidation and reduction between the Cr(III) and Cr(VI) couple [19] can occur in soils, depending on the nature and condition of the soils, and other factors that control the redox environment. This led to interest in the analysis of soils for the type of Cr contamination present [20, 21].

The chemical nature of Cr in leather has been characterised: Cr sulfate is used during tanning, and Cr bonds to the leather's collagen[22, 23] and is well dispersed. However, the form of Cr present in biochar is unknown, as are its stability and dispersion. In an earlier study of the leaching of leather after heat

treatment in a non-oxidising environment, the chemical state of the Cr was not determined, despite some interest in doing so[16].

The purpose of the work reported here is to investigate the speciation and structure of the Cr in biochar produced from chrome-tanned leather as a function of the heating conditions. We wish to confirm the earlier reports of decreased solubility of Cr from leather heated in a non-oxidising environment and determine that the samples we are studying for Cr speciation do in fact exhibit low Cr solubility. Developing and understanding of the nature of entrapment of Cr in leather biochar may enable us to predict the likely stability of the Cr in the char in the longer term. For the determination of the chemical speciation and structure of Cr, we use X-ray Absorption Spectroscopy (XAS) which is known to exhibit obvious spectral differences for different oxidation states and chemical environments.

Experimental

Standard, commercial chrome-tanned bovine leather was used for all experiments. The biochar was produced from leather by pyrolysis. Two pyrolysis reactors were used: a larger unit with no purge gas for the lower-temperature samples (up to 600 °C) and a smaller unit with the sample held under argon for higher-temperature samples (600–1000 °C). The temperatures were held for 1 hr before being cooled for analysis. Below is an overview of the experimental process carried out.

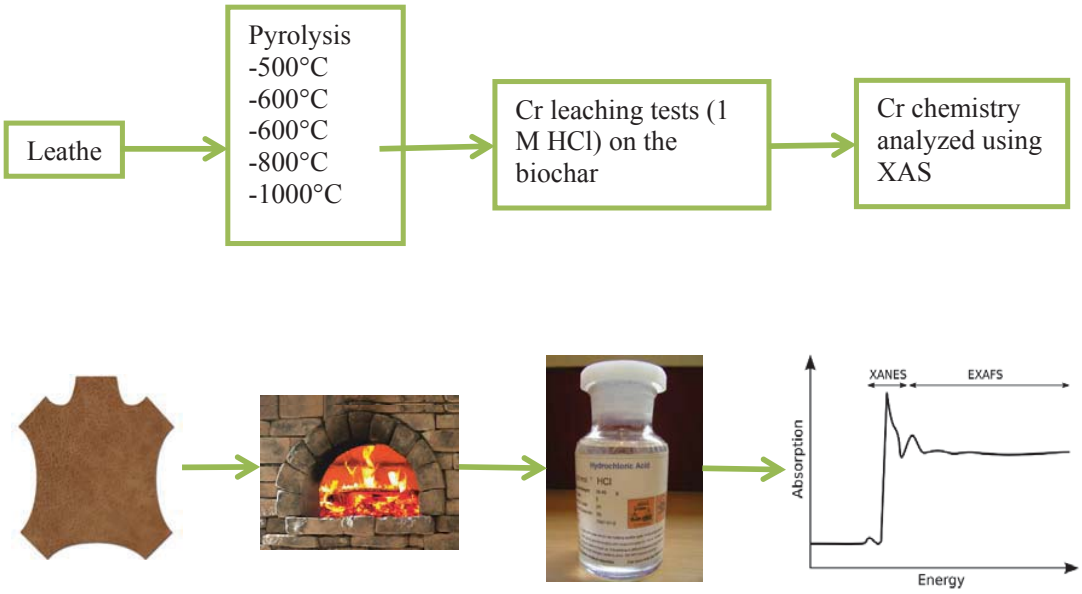

After pyrolysis, the char was measured for Cr content and leachable chromium. The Cr content of the char and leather samples was measured using a standard industry test method[24]. The leachable Cr was measured with duplicate samples of char (5 g) leached in 100 mL of 1 M HCl while shaken for 15 hours at room temperature. The Cr content of the aqueous HCl leachate was then assessed in duplicate with a Varian 220 SpectrAA using a standard industry test method[25].

XANES and EXAFS spectroscopic techniques were used to determine the chemical speciation and structure of the Cr in the leather and biochar samples from X-ray adsorption spectra recorded on the XAS beam line at the Australian synchrotron.

Results

We found that a small amount of Cr can be leached from leather that has not been heat treated (Table 1), as has been reported previously[16]. After heating of the leather, the leachability of Cr diminishes. At 600 °C where the leather is clearly char no leaching of Cr could be detected (Table 1). In an earlier leaching study it was found that at 350 °C the Cr was found no longer able to be leached from the heated leather[16].

Table 1. Initial chromium content and leachable chromium of leather and of biochar samples produced under various heat treatments. No leachable Cr was detected in biochar samples formed at 600 °C or above.

Sample	Initial % Cr (SD)	Leachable Cr, as % of initial Cr
Leather	0.99 (0.01)	2.45
300 °C*	2.60 (0.02)	0.69
600 °C*	7.39 (0.04)	0.0007
600 °C†	11.8 (0.8)	0.08
800 °C†	12.5 (0.1)	0.06
1000 °C†	15.4 (0.1)	0.03

*Larger reaction vessel. †Finely ground, from small reaction vessel.

X-ray absorption near edge structure (XANES) is a spectroscopic technique carried out on the XAS beam line, that is element specific and is local bonding sensitive. XANES was carried out on both the chrome leather and biochar samples. The XANES spectrum of chrome leather is very similar to that of $Cr_2(SO_4)_3.xH_2O$. This is the salt that is used in chrome tanning, so clearly some structural aspects of this salt are retained in the tanned leather. The XANES spectrum of the biochar indicated significant differences with each 200°C increase. As the treatment temperature increases, the amount of carbide increases. The calculated proportions of carbide and Cr sulfate (represented as the dry leather spectrum) are listed in Table 2.

Table 2. Chemical components of linear combination fitting to the XAS energy spectrum. Uncertainty in mol% Cr in $Cr_2(SO_4)_3.xH_2O$ and Cr_2C_3 is around ± 5 %.

	$Cr_2(SO_4)_3.xH_2O$ (mol % Cr)	Cr_2C_3 (mol % Cr)	R factor ($\times 10^{-4}$), χ^2
Biochar 500°C*	93	7	1.7, 0.027
Biochar 600°C*	77	23	3.4, 0.051

Biochar 600°C	59	41	5.6, 0.081
Biochar 800°C	35	65	5.8, 0.081
Biochar 1000°C	12	88	2.2, 0.031

*Larger reaction vessel.

Information about the structural environment of the Cr in the leather biochar is obtained from an analysis of the EXAFS range of the data acquired. The bond lengths obtained from the modelling of Fourier transform for EXAFS spectra of the biochar samples are given in table 3. The EXAFS analysis supports the XANES interpretation and confirms that Cr carbide is formed at higher temperatures.

Table 4. Bond lengths obtained from the modelling of Fourier transform of EXAFS spectra of leather biochar. Six scattering paths were combined for Cr-C, 12 paths for Cr-Cr in total (in two groups).

Sample	Cr-C (Å), coordination number	Cr-Cr (Å), coordination number	Cr-Cr (Å), coordination number
Biochar 800 °C	2.07, 3.6	2.58, 0.7	2.94, 3.0
Biochar 1000 °C	2.05, 1.7	2.70, 4.3	2.92, 1.8

Cr carbide is a very stable material, and is resistant to oxidation or reduction[26]. The charcoal or biochar matrix within which the Cr is contained is also known to be very stable in soils[27]. The addition of charcoal to soil enhances the agricultural productivity of the soil, for example in the traditional terra preta soils from South America[28] but also in more recent studies of soil productivity[15].

While we have found that using acid to produce biochar leachate does not remove Cr from the biochar, we have not performed long-term stability tests of the material in soil environments. These would be desirable to ensure the safety of the material for use in agricultural settings.

Conclusion

We have shown that there may an environmental benefit in making biochar from chrome-tanned leather waste. The char does not release Cr with acid leaching, unlike untreated leather. We have also shown that the Cr becomes chemically reduced by a carbothermic reaction on charing, at high temperatures forming Cr carbide. Cr carbide is an inherently stable compound and its stability is further enhanced by being highly dispersed in a stable carbon medium. Biochar has the added benefits of enhancing agricultural production from soil and providing long-term sequestration of carbon from the environment. This strategy may turn a large-scale, potentially troublesome waste into an economic resource.

References

1. Commodities and Trade Division, F. A. O., United Nations World statistical compendium for raw hides and skins, leather and leather footwear 1990-2011; Rome, 2012.

2. Gao, Y.; Xia, J., Chromium Contamination Accident in China: Viewing Environment Policy of China. Environmental Science & Technology **2011,** 45, (20), 8605-8606.

3. Izbicki, J. A.; Bullen, T. D.; Martin, P.; Schroth, B., Delta Chromium-53/52 isotopic composition of native and contaminated groundwater, Mojave Desert, USA. Applied Geochemistry **2012,** 27, (4), 841-853.

4. James, B. R., The challenge of remediating chromium-contaminated soil. Environmental Science & Technology **1996,** 30, (6), A248-A251.

5. Heidemann, E., Disposal and recycling of chrome-tanned materials. Journal of the American Leather Chemists Association **1991,** 86, (9), 331-333.

6. Cabeza, L. F.; Taylor, M. M.; DiMaio, G. L.; Brown, E. M.; Mermer, W. N.; Carrio, R.; Celma, P. J.; Cot, J., Processing of leather waste: pilot scale studies on chrome shavings. Isolation of potentially valuable protein products and chromium. Waste Management **1998,** 18, (3), 211-218.

7. Beltran-Prieto, J. C.; Veloz-Rodriguez, R.; Perez-Perez, M. C.; Navarrete-Bolanos, J. L.; Vazquez-Nava, E.; Jimenez-Islas, H.; Botello-Alvarez, J. E., Chromium recovery from solid leather waste by chemical treatment and optimisation by response surface methodology. Chemistry and Ecology **2012,** 28, (1), 89-102.

8. Dotro, G.; Castro, S.; Tujchneider, O.; Piovano, N.; Paris, M.; Faggi, A.; Palazolo, P.; Larsen, D.; Fitch, M., Performance of pilot-scale constructed wetlands for secondary treatment of chromium-bearing tannery wastewaters. Journal of Hazardous Materials **2012,** 239, 142-151.

9. Ashokkumar, M.; Thanikaivelan, P.; Krishnaraj, K.; Chandrasekaran, B., Transforming Chromium Containing Collagen Wastes Into Flexible Composite Sheets Using Cellulose Derivatives: Structural, Thermal, and Mechanical Investigations. Polymer Composites **2011,** 32, (6), 1009-1017.

10. Przepiorkowska, A.; Chronska, K.; Zaborski, M., Chrome-tanned leather shavings as a filler of butadiene-acrylonitrile rubber. Journal of Hazardous Materials **2007,** 141, (1), 252-257.

11. Erdem, M., Chromium recovery from chrome shaving generated in tanning process. Journal of Hazardous Materials **2006,** 129, (1-3), 143-146.

12. Tahiri, S.; Albizane, A.; Messaoudi, A.; Azzi, M.; Bennazha, J.; Younssi, S. A.; Bouhria, M., Thermal behaviour of chrome shavings and of sludges recovered after digestion of tanned solid wastes with calcium hydroxide. Waste Management **2007,** 27, (1), 89-95.

13. Stam, A. F.; Meij, R.; Winkel, H. T.; van Eijk, R. J.; Huggins, F. E.; Brem, G., Chromium Speciation in Coal and Biomass Co-Combustion Products. Environmental Science & Technology **2011,** 45, (6), 2450-2456.

14. Aitkenhead, W.; Edmonds, R. L., Biochar: A possibility for solid waste disposal. Leather International **2013,** 215, (4827), 28-30.

15. Chan, K. Y.; Van Zwieten, L.; Meszaros, I.; Downie, A.; Joseph, S., Agronomic values of greenwaste biochar as a soil amendment. Australian Journal of Soil Research **2007,** 45, (8), 629-634.

16. Erdem, M.; Ozverdi, A., Leaching behavior of chromium in chrome shaving generated in tanning process and its stabilization. Journal of Hazardous Materials **2008,** 156, (1-3), 51-55.

17. Oliveira, L. C. A.; Guerreiro, M. C.; Goncalves, M.; Oliveira, D. Q. L.; Costa, L. C. M., Preparation of activated carbon from leather waste: A new material containing small particle of chromium oxide. Materials Letters **2008,** 62, (21-22), 3710-3712.

18. Sekaran, G.; Shanmugasundaram, K. A.; Mariappan, M., Characterization and utilisation of buffing dust generated by the leather industry. Journal of Hazardous Materials **1998,** 63, (1), 53-68.

19. Brose, D. A.; James, B. R., Oxidation-Reduction Transformations of Chromium in Aerobic Soils and the Role of Electron-Shuttling Quinones. Environmental Science & Technology **2010,** 44, (24), 9438-9444.

20. Kappen, P.; Welter, E.; Beck, P. H.; McNamara, J. M.; Moroney, K. A.; Roe, G. M.; Read, A.; Pigram, P. J., Time-resolved XANES speciation studies of chromium on soils during simulated contamination. Talanta **2008,** 75, (5), 1284-1292.

21. Martin, R. R.; Naftel, S. J.; Sham, T. K.; Hart, B.; Powell, M. A., XANES of chromium in sludges used as soil ameliorants. Canadian Journal of Chemistry-Revue Canadienne De Chimie **2003,** 81, (2), 193-196.

22. Covington, A. D.; Lampard, G. S.; Menders, O.; Chadwick, A. V.; Rafeletos, G.; O'Brien, P., Extanded X-ray absorption fine structure sudies of the role of chromium in leather tanning. Polyhedron **2001,** 20, 461-466.

23. Reich, T.; Rossberg, A.; Hennig, C.; Reich, G., Characterization of chromium complexes in chrome tannins, leather, and gelatin using extended X-ray absorption fine structure (EXAFS) spectroscopy. Journal of the American Leather Chemists Association **2001,** 96, (4), 133-147.

24. ISO, Leather -- Chemical determination of chromic oxide content -- Part 1: Quantification by titration. In 2007; Vol. ISO 5398-1:2007 (IULTCS/IUC 8-1).

25. ISO, Leather -- Chemical determination of chromic oxide content -- Part 3: Quantification by atomic absorption spectrometry. **2007,** ISO 5398-3:2007 (IULTCS/IUC 8-3).

26. Sen, S.; Ozdemir, O.; Demirkiran, A. S.; Sen, U., Oxidation Kinetics of Chromium Carbide Coating Produced on AISI 1040 Steel by Thermo-Reactive Deposition Method During High Temperature in Air. In *Materials and Manufacturing Technologies Xiv*, Yigit, F.; Hashmi, M. S. J., Eds. 2012; Vol. 445, pp 649-654.

27. Schmidt, M. W. I.; Torn, M. S.; Abiven, S.; Dittmar, T.; Guggenberger, G.; Janssens, I. A.; Kleber, M.; Kogel-Knabner, I.; Lehmann, J.; Manning, D. A. C.; Nannipieri, P.; Rasse, D. P.; Weiner, S.; Trumbore, S. E., Persistence of soil organic matter as an ecosystem property. Nature 2011, 478, (7367), 49-56.

28. Glaser, B.; Haumaier, L.; Guggenberger, G.; Zech, W., The 'Terra Preta' phenomenon: a model for sustainable agriculture in the humid tropics. Naturwissenschaften 2001, 88, (1), 37-41.

29. Foster, N. Solid wastes survey and looking at options. In, Report of the 59th Annual LASRA Conference, Palmerston North, NZ: Leather and Shoe Research Association 2008, (59-68).

10.3 Appendix 3: Conference Presentations and Posters

Haverkamp, R. G., Basil-Jones, M. M., **Sizeland, K. H.**, & Edmonds, R. L. "Implications of Synchrotron Analysis for Leather Manufacturing", *Symposium conducted at 63rd Annual Leather and Shoe Research Association Conference*, Wellington, New Zealand, 16th-17th August, 2012.

Sizeland, K. H., Basil-Jones, M. M., Edmonds, R. L. & Haverkamp, R. G. "SAXS of Leather Reveals a Structural Basis for Strength", *Poster presented at the Australian Synchrotron Users Meeting,* Melbourne, Australia, 28th-29th November 2012.

Haverkamp, R. G., Basil-Jones, M. M., **Sizeland, K. H.**, & Edmonds, R. L. "SAXS Structural Studies of Collagen Materials", *Symposium conducted at the Australian Synchrotron Users Meeting*, Melbourne, Australia, 28th-29th November, 2012.

Poddar, D., Ainscough, E. W., Freeman, G. H., Ellis, A., Glover, C. J., Johannessen, B., **Sizeland, K. H.**, Singh, H., Haverkamp, R. G., & Jameson, G. "Preliminary characterization by XAS of Mn hyperaccumulated by probiotic Lactobacillus sp.", *Poster presented at the Australian Synchrotron Users Meeting,* Melbourne, Australia, 28th-29th November, 2012.

Sizeland, K. H., Basil-Jones, M. M., Norris, G. E., Edmonds, R. L., Kirby, N., Hawley, A., & Haverkamp, R. G. "Collagen Alignment and Leather Strength", *Poster presented at the International Union of Leather Technologists and Chemists Societies XXXII Congress*, Istanbul, Turkey, 28th-31st June, 2013.

Haverkamp, R. G., Basil-Jones, M. M., **Sizeland, K. H.**, & Edmonds, R. L. "Synchrotron Studies of Leather Structure", *Symposium conducted at the International Union of Leather Technologists and Chemists Societies XXXII Congress*, Istanbul, Turkey, 28th-31st June, 2013.

Sizeland, K. H., Basil-Jones, M. M., Norris, G. E., Edmonds, R. L., Kirby, N., Hawley, A., & Haverkamp, R. G. "Collagen Alignment and Leather Strength", *Poster presented at the 64th Annual Leather and Shoe Research Association Conference,* Wellington, New Zealand, 15th-16th August, 2013.

Sizeland, K. H., Norris, G. E., Edmonds, R. L. Kirby, N., Hawley, A., & Haverkamp, R. G. "Polyol Modification of Collagen Fibril Axial Periodicity", *Poster presented at the Australian Synchrotron Users Meeting,* Melbourne, Australia, 21st-22nd November, 2013.

Kayed, H. R., **Sizeland, K. H.**, Kirby, N., Hawley, A., Mudie, S., & Haverkamp, R. G. "Cross Linking Collagen Affects Fibril Orientation", *Poster presented at the Australian Synchrotron Users Meeting,* Melbourne, Australia, 21st-22nd November, 2013.

Sizeland, K. H., Norris, G. E., Edmonds, R. L., Kirby, N., Hawley, A., & Haverkamp, R. G. "Collagen Fibril Axial Periodicity and the Effects of Polyol Addition", *Poster presented at the 12th International Conference on Frontiers of Polymers and Advanced Materials*, Auckland, New Zealand, 8th-13th December, 2013.

Haverkamp, R. G., Wells, H. C., **Sizeland, K. H.**, Edmonds, R. L., Aitkenhead, W., Kappen, P., Glover, C., & Johannessen, B. "Biochar from Leather - the Fate of Chromium", *Symposium conducted at the 117th Society of Leather Technologists and Chemists Annual Conference*, Northampton, United Kingdom, 26th April, 2014.

Wells, H. C., **Sizeland, K. H.**, Edmonds, R. L., Kirby, N., Hawley, A., Mudie, S., & Haverkamp, R. G. "Poisson Ratio of Collagen Fibrils*", Poster presented at the 1st Matrix Biology Europe conference (XXIVth FECTS meeting)*, Rotterdam, Netherlands, 21st-24th June, 2014.

Sizeland, K. H., Wells, H., Norris, G. E., Edmonds, R. L., & Haverkamp, R. G. "Collagen D-spacing Modification by Fat Liquor Addition", *Symposium presented at the 65th Annual Leather and Shoe Research Association Conference,* Wellington, New Zealand, 13th-14th August, 2014.

Wells, H., **Sizeland, K. H.**, Edmonds, R. L., Aitkenhead, W., Kappen, P., Glover, C., Johannessen, B., & Haverkamp, R. G. "Biochar and Other Solid Waste Minimisation Options", *Symposium presented at the 65th Annual Leather and Shoe Research Association Conference*, Wellington, New Zealand, 13th-14th August, 2014.

Sizeland, K. H., Edmonds, R. L., Norris, G. E., Kirby, N., Hawley, A., Mudie, S. & Haverkamp, R. G. "Effects of Model Compounds on the Nanostructure of Skin",

Poster presented at the 65th Annual Leather and Shoe Research Association Conference, Wellington, New Zealand, 13th-14th August, 2014.

Sizeland, K. H., Edmonds, R. L., Norris, G. E., Kirby, N., Hawley, A., Mudie, S., & Haverkamp, R. G. "Modification of Collagen Structure in Skin", *Poster presented at the 28th International Federation of Societies of Cosmetic Chemists*, Palais des Congrès, Paris, France, 27th-30th October, 2014.

Sizeland, K. H., Basil-Jones, M. M., Edmonds, R. L., Kirby, N., Hawley, A., Mudie, S., & Haverkamp, R. G. "Changes to the Nanostructure of Collagen in Skin During Leather Processing", *Poster presented at the Australian Synchrotron Users Meeting*, Melbourne, Australia, 20th-21st November, 2014.

Sizeland, K. H., Edmonds, R. L., Kirby, N., Hawley, A., Mudie, S., & Haverkamp, R. G. "Chemical Processing and Leather Strength", *Poster presented at the Fourth International Conference on Multifunctional, Hybrid, and Nanomaterials*, Barcelona, Spain, 9th-13th March, 2015.

Haverkamp, R. G., **Sizeland, K. H.**, Wells, H. C., Kayed, H. R., Edmonds, R. L., Kirby, N., Hawley, A., & Mudie, S. "Strength in Collagen Biomaterials", *Poster presented at the Fourth International Conference on Multifunctional, Hybrid, and Nanomaterials*, Barcelona, Spain, 9th-13th March, 2015.

Wells, H. C., **Sizeland, K. H.**, Kayed, H. R., Kirby, N., Mudie, S., & Haverkamp, R. G. "Poisson Ratio of Collagen Fibrils Measured by SAXS", *Poster presented at the Fourth International Conference on Multifunctional, Hybrid, and Nanomaterials*, Barcelona, Spain, 9th-13th March, 2015.

Implications of Synchrotron Analysis for Leather Manufacturing

Haverkamp, R. G.[1], Basil-Jones, M. M.[1], Sizeland, K. H.[1], & Edmonds, R. L.[2]

[1]School of Engineering and Advanced Technology, Massey University, Palmerston North, New Zealand
[2]Leather and Shoe Research Association, Palmerston North, New Zealand

Leather, a material obtained through processing, is a strong, flexible, water-resistant material that is used in a wide variety of manufacturing applications including shoes, bags, furniture coverings, car interiors and airplane seat covers. If the nanostructure of ovine leather was understood then the ability to manipulate processes in order to achieve ovine leather of higher strength may be realized. Synchrotron based techniques such as small angle X-ray scattering provide an ideal platform for nanostructure analysis of the fibrous collagen. Information regarding the structure and alignment of the collagen fibrils is provided by the small angle scattering pattern. This synchrotron technique allows us to determine why leather has the properties it does and how the fibril structure relates to the desirable attributes present. Following this, modifications can be configured to enhance the structure. The findings are significant and can not only be advantageous within the leather industry but they provide insight that can be applied to the cosmetic, medical and biological industries also.

Symposium conducted at the 63rd Annual LASRA Conference, Wellington, New Zealand, 28th-29th November, 2012

SAXS of Leather Reveals a Structural Basis for Strength

Sizeland, K. H.,[1] Basil-Jones,[1] M. M., Edmonds,[2] R. L., & Haverkamp, R. G.[1]

[1]School of Engineering and Advanced Technology, Massey University, Palmerston North, New Zealand
[2]Leather and Shoe Research Association, Palmerston North, New Zealand

Leather is a processed material made from fibrous collagen. The physical properties of leather are due in large part to the arrangement of the collagen fibrils. We have used small angle X-ray scattering to characterize leather from seven species of animal with widely different mechanical properties. The two dimensional small angle scattering pattern provides information on the internal fibril structure and the fibril arrangement. It is shown that the strongest leather has fibrils which are highly aligned within parallel planes with few fibrils crossing between planes. Weak leather contains fibrils that are less aligned. Tear strengths for the selection of leathers fell in the range 20–110 N/mm^2 with orientation indices ranging from 0.420–0.633. There is a direct relationship between orientation index and strength. This understanding provides a new insight into structure – property relationships in leather and may be extended to other tissues for biological and medical applications.

Poster presented at the Australian Synchrotron Users Meeting, Melbourne, Australia, 28th-29th November, 2012

SAXS of Leather Reveals a Structural Basis for Strength

Katie H. Sizeland,[†] Melissa M. Basil-Jones,[†] Richard L. Edmonds,[§] and Richard G. Haverkamp.[†]

[†]School of Engineering and Advanced Technology, Massey University, Palmerston North, New Zealand 4442,
[§]Leather and Shoe Research Association, Palmerston North, New Zealand 4442.

Introduction

Leather, a material obtained from animal skin through processing, is made up of two layers, the corium and the grain, mostly comprised of fibrous collagen. Being a strong, flexible, water-resistant material, leather is used in a wide variety of manufacturing applications. Synchrotron based small angle X-ray scattering (SAXS) provides an ideal platform for nanostructure analysis of the fibrous collagen. This technique enables us to determine why leather has the properties it does and how the collagen structure relates to the desirable attributes. The focus of this work is to characterise the structure of leather, particularly the collagen structure and arrangement. Orientation indices allow us to determine the extent to which the fibres lie flat or traverse the thickness of the leather. We can see how this relates to the strength of the sample.

Experimental

Using the conventional beam house and tanning processes, leather pelts were prepared. Strips of leather 1mm thick and 50mm long were cut from the leather pelts of seven different animal species. SAXS diffraction patterns were recorded on the Australian Synchrotron SAXS/WAXS beamline, with a beam size of 250 × 80 μm and a total photon flux of 2×10^{12} photons s^{-1}. All diffraction patterns were recorded with an X-ray energy of 11keV using a Pilatus 1 M detector with an active area of 170x170 mm. The leather samples were mounted in the beam horizontally with a sample to detector distance of 3371mm and an exposure time for diffraction patterns of 1s. Sample stretching was carried out using a custom built machine. The leather sample was held in place by two clamps. The sample was stretched in 1mm increments with spectrum recorded after each increment until the sample failed.

Results and Discussion

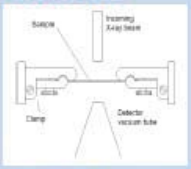

a]

b]

c]

Figure 1. a] Experimental set up for stretching process, **b]** static leather samples, **c]** stretched leather sample.

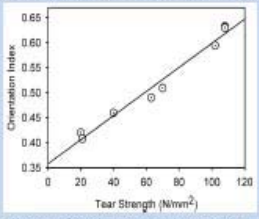

Figure 2. Collagen fibril orientation and tear strength for leather from different animals.

Results and Discussion cont.

The animals selected for analysis were sheep (selected weak), possum, sheep (selected strong), cattle, goat, water buffalo, deer and horse. Using the unique, custom built setup illustrated in Figure 1 the tear strength of all samples was successfully determined. The orientation index (OI), ranging from 0-1, provides a measure of alignment of the fibrils. An OI of 1 represents perfect alignment while 0 equates to an isotropic material. The tear strength results fell in the range of 20-110 N/mm with orientation indices of 0.420-0.633. A direct correlation was found when the two data sets were compared (Figure 2).

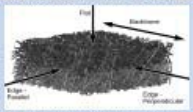

Figure 3. Sampling directions

Samples were analysed from two directions; flat on and edge on (Figure 3). This enabled us to determine any structure-property relationships present within the three dimensional structure of leather. The strong OI and tear strength relationship was found to be directly linked to the orientation of fibres within the corium and the grain. Figure 4 shows samples viewed edge-on illustrating the arrangement of fibrils in leather of varying strengths. It is the orientation in this plane that correlates most strongly with strength and highly aligned material being stronger. Figure 5 depicts the fibrous collagen orientation when viewed flat-on. In this direction an isotropic arrangement is desirable.

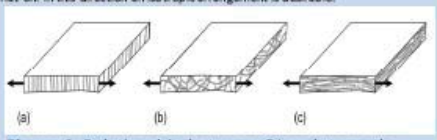

Figure 4. Relationship between OI and strength viewed edge-on. **a]** Weakest leather (vertical fibre defect), **b]** medium strength leather (low OI), **c]** Strong leather (high OI). Arrow indicates direction of applied strength for tear measurements.

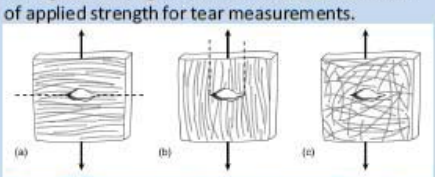

Figure 5. Relationship between OI and strength viewed flat-on. **a]** weak leather (high OI), **b]** fairly weak leather (high OI), **c]** strong leather. Arrow indicates direction of applied strength for tear measurements.

Conclusion

Our study reveals that the strongest leather contains fibrils that are highly aligned within planes with few collagen fibres crossing over between planes. Weak leather contains fibrils that are less aligned. Therefore there is a direct correlation between orientation index and strength.

Acknowledgements

Images reprinted with permission from the Journal of Agricultural and Food Chemistry. This research was supported by a grant from the Ministry of Business Innovation and Employment. This research was undertaken on the SAXS/WAXS beamline at the Australian Synchrotron, Victoria, Australia.

MASSEY UNIVERSITY
TE KUNENGA KI PŪREHUROA

Poster presented at the Australian Synchrotron Users Meeting, Melbourne, 28-29 November, 2012.

LASRA®

SAXS Structural Studies of Collagen Materials

Haverkamp, R. G.,[1] Basil-Jones,[1] M. M., Sizeland, K. H.,[1] & Edmonds[2] R. L.

[1]School of Engineering and Advanced Technology, Massey University, Palmerston North, New Zealand

[2]Leather and Shoe Research Association, Palmerston North, New Zealand

Fibrous collagen is the basis of leather and of tissues used in medical applications such as pericardium for heart valve repair. The structure of such materials contributes to their mechanical properties. We used small angle X-ray scattering to characterise the structure of fibrous collagen materials. The two dimensional small angle scattering pattern provides information on the internal fibril structure and the fibril arrangement. Leather of different strengths and juvenile and adult bovine pericardium for heart valve repair were characterized. The variation in fibril orientation through cross sections of tissue, structural responses to dynamic loads, and structural differences between strong and weak material were investigated. It was shown that greater collagen alignment leads to stronger material. Under tension fibrils reorient at low strain then individual fibrils stretch at higher strain. Processing treatments may affect the response of these tissues to strain. These studies provide an insight into the structural basis of strength in fibrous collagen materials and the behaviour of these materials under stress.

Poster presented at the Australian Synchrotron Users Meeting, Melbourne, Australia, 28th-29th November, 2012

Manganese in Shelf-Stable Probiotic Functional Foods: is it safe?

Poddar, D., Ainscough, E. W., Freeman, G. H., Ellis, A., Glover, C. J., Johannessen, B., Sizeland, K. H., Singh, H., Haverkamp, R. G., & Jameson. G. B.

Probiotics are live microorganisms which provide health benefits to the host upon consumption. The incorporation of these microorganisms into food products is a practical way of transferring this health benefit to the everyday consumer. Maintaining the viability of probiotics during processing, storage and gastrointestinal transit remains a challenge for researchers. These limitations can however be overcome by using suitable encapsulation strategies -- freeze drying, spray drying and fluidized bed drying -- used in this study. Probiotics of the genus lactobacillus have been found to accumulate manganese (Mn), which has been associated with superoxide dismutase (SOD) activity, thereby helping the bacteria to survive under conditions of low p□, high osmotic stress and temperature. The primary ob□ective of this study was to determine by X-ray absorption spectroscopy (XAS) the changes in Mn that occurred during storage of the encapsulated bacteria at 11%, 33% and 52% relative humidity (RH) at 25˚C for a period of 3 months, simulating conditions representing the □□ of food matrices. Secondly, it was also of interest to characterise the Mn bodies in the probiotic □□ □*araca*□*ei*□□inally, we were interested in any shifts in the oxidation state of Mn between live and dead bacteria and also bacteria harvested during different stages of growth, as other spectroscopies suggested changes occurred. The XAS findings (both XA□ES and EXA□S measurements) suggest there is no difference in the Mn among the encapsulated bacteria stored at different □□. The manganese XAS spectrum revealed no Mn^{3}□ compounds formed during storage, which could initiate □enton-type reactions, forming radical species. Preliminary analysis of the absorption edge and XA□ES region indicates that the spectra are well modelled by an approximately □0□20 mixture of manganese(II) phosphate and manganese(II) acetate, a possible proxy for manganese(II) interactions with Asp/□lu side chains of proteins. □urther to this, no change was observed in the manganese compounds present in live and dead bacteria. Bacterial accumulation of the manganese occurred between 6 to 12 hours of growth, supporting the results of previous studies. The increased accumulation of Mn during the

stationary phase could potentially be the reason why cells at this stage of growth can withstand harsher environmental conditions during storage, in comparison to other times during cell growth. In conclusion, the present study suggests that storage conditions and changes to bacterial viability of various probiotic encapsulates do not alter the oxidation state and speciation of Mn in a way that might be harmful for human consumption.

Poster presented at the Australian Synchrotron Users Meeting, Melbourne, Australia, 28th-29th November, 2012

Devastotra Poddar
Supervisors : Harjinder Singh, Geoff Jameson, Richard Haverkamp, Eric Ainscough, Shantanu Das and Jon Palmer

MASSEY UNIVERSITY

Riddet Institute
FOOD | INNOVATION | HEALTH

Stabilisation of probiotic lactobacilli under ambient storage

www.riddet.ac.nz
CENTRE OF RESEARCH EXCELLENCE

Introduction

Probiotics are live microorganisms which provide health benefits to the host upon consumption. The incorporation of these microorganisms into food products is a practical way of transferring health benefits to the everyday consumer. However, maintaining the viability of probiotics during processing, storage and gastrointestinal transit remains a challenge for researchers. These limitations, to some extent, can be overcome by using suitable encapsulation strategies -- freeze drying, spray drying and fluidized bed drying.

Objective

To understand the survival behaviour of the encapsulated probiotic *Lactobacillus paracasei* 431 (LAB), immobilized in a dairy matrix, during ambient storage (25°C).

Materials & Methods

- Stabilize *L.paracasei* in a dairy matrix by freeze drying, spray drying or fluidised bed drying

- Storage under controlled relative humidity (RH) 11.1, 33.3 and 52.5% at 25°C using saturated salt solutions
- Viability study-Plate count- log cfu/g
- Structural study of the protective bacterial matrix using Helium pycnometry and Scanning electron microscopy.
- X-Ray Diffraction (XRD) study of the encapsulated powders upon storage at controlled relative humidity conditions.
- Spectroscopic analysis to study the inherant protective mechanism of the bacteria during storage using Electron Spin Resonance (ESR) and X-ray Absorbtion Spectroscopy (XAS).

Results

Table 1 Moisture content of spray-dried, freeze-dried and fluidized bed dried Lactobacillus paracasei 431 powders stored at ambient under controlled relative humidity (± SD from three independent samplings)

Drying Technology	Moisture content before storage (%)	Water activity before equilibration	Storage (25°C) under controlled RH (LOW) (11.1%)	Storage (25°C) under controlled RH (MID) (33.3%)	Storage (25°C) under controlled RH (High) (52.5%)
Freeze dried	1.45±0.19	0.088	2.48±0.18	3.43±0.08	4.32±0.09
Spray dried	7.17±0.09	0.47	2.56±0.04	3.11±0.03	4.56±0.05
Fluidized bed dried	5.01±0.14	0.28	1.87±0.19	4.03±0.03	4.17±0.14

Acknowledgements: Riddet Institute, Australian Synchrotron, Monash University.

Bacterial survival study results upon storage under controlled RH to study the effectiveness of various drying techniques in providing protection

Upon storage under the same RH conditions, freeze drying produced less viable cells than spray drying and fluidized bed drying overall.

Structural difference in encapsulate

Freeze-dried powder had the highest bulk porosity of 77.5%, spray-dried and fluidised bed dried powders had similar bulk porosities of 51.5% and 50.3%, respectively.

X-ray diffraction to elucidate reason for observed difference

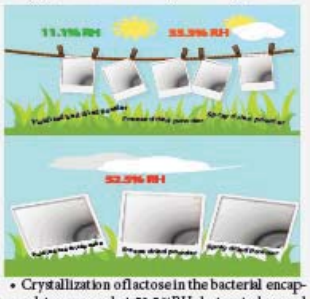

- Crystallization of lactose in the bacterial encapsulates occured at 52.5%RH, but not observed in lower RH, 11.1 and 33.3%.
- Fluidized bed dried matrix had different crystallization pattern at 52.5% RH.
- The crystallization in encapsulating matrix indicates increased molecular mobility due to the plasticization ability of water, at higher relative humidity, and thereby resulting in cell death.

Manganese (Mn) and lactobacillus

Mn has been associated with superoxide dismutase (SOD) activity, thereby helping the bacteria to survive under conditions of low pH, high osmotic stress and temperature. ESR was able to detect the Mn signals from *L. paracasei*. EDS and ICP-MS reconfirmed it.

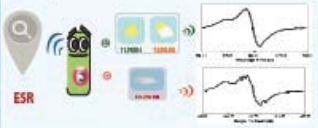

We observed a difference in ESR spectrum in the samples stored at higher relative humidity (except fluidized bed powder). This phenomenon concided well with the bacterial viability result. We hypothesized that upon storage under higher relative humidity the state of manganese changes from Mn^{2+} to Mn^{3+} and initiate Fenton-type reactions, forming radical species and resulting in bacterial death.

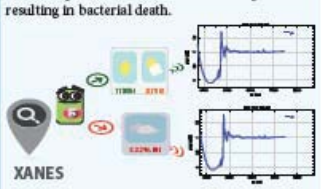

We carried out X-ray absorbsion spectroscopy (XANES) and observed that there was no change in the state of manganese in bacteria stored at higher and lower RH stored samples and the manganese present in the bacteria in the form of mixture of manganese(II) phosphate and manganese(II) acetate, possibly representing manganese(II) interactions with Asp/Glu side chains of proteins.

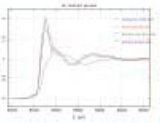

Discussion

ESR provided insights into the presence of water on the manganese concretions, with fluidized bed powder showing none even at high RH and this may be associated with the difference in crystal pattern observed in XRD and rigid structure, while powders from spray drying and freeze drying displayed water signals owing the porous structure and might be due to crystal water. XAS results provided the bulk material composition, while ESR was sensitive to to measure subtle changes in the surrounding environment of encapsulated bacteria, showing hyperfine splitting at higher relative humidity and none at lower RH.

Conclusion

Presence of water in the bacterial matrix and associated crystallization of lactose is the primary cause of death during storage.

Collagen Alignment and Leather Strength

Sizeland, K. H.,[1] Basil-Jones, M. M.,[1] Norris, G. E.,[2] Edmonds, R. L.,[3] Kirby, N.,[4] Hawley, A.,[4] & Haverkamp, R. G.[1]

[1]School of Engineering and Advanced Technology, Massey University, Palmerston North, New Zealand

[2]Institute of Fundamental Sciences, Massey University, Palmerston North, New Zealand

[3]Leather and Shoe Research Association, Palmerston North, New Zealand

[4]Australian Synchrotron, Melbourne, Australia

Leather strength is believed to be largely due to the fibrous collagen which makes up a major proportion of the material. However, the strength of leather depends on more than just the amount of collagen which it contains. The structure of collagen in the leather produced from a range of animals is investigated using synchrotron based small angle x-ray scattering. It is shown that the tear strength of leather depends upon the alignment of the collagen fibrils. Tear-resistant material has the fibrils contained within parallel planes with little cross-over between the top and bottom surfaces. For tear strengths in the range 20–110 N/mm^2 the orientation index ranges from 0.420–0.633 with a direct relationship between orientation index and strength. Greater alignment within the plane of the tissue results in stronger material. This study provides a valuable insight into the structural basis of strength in leather and the inherent differences between animal skins.

Poster presented at the International Union of Leather Technologists and Chemists Societies XXXII Congress, Istanbul, Turkey. 28th-31st June, 2013.

Collagen Alignment and Leather Strength

Katie H. Sizeland,[†] Melissa M. Basil-Jones,[†] Gillian E. Norris,[‡] Richard L. Edmonds,[§] Nigel Kirby,[¥] Adrian Hawley,[¥] and Richard G. Haverkamp.[†]

[†]School of Engineering and Advanced Technology, Massey University, Palmerston North, New Zealand 4442, [‡]Institute of Fundamental Sciences, Massey University, Private Bag 11222, Palmerston North 4442, New Zealand [§]Leather and Shoe Research Association, Palmerston North, New Zealand 4442, [¥]Australian Synchrotron, Clayton, Vic 3168, Australia.

Introduction

Leather, a material obtained from animal skin through processing, is made up of two layers, the corium and the grain, mostly comprised of fibrous collagen. Being a strong, flexible, water-resistant material, leather is used in a wide variety of manufacturing applications. Synchrotron based small angle X-ray scattering (SAXS) provides an ideal platform for nanostructure analysis of the fibrous collagen. This technique enables us to determine why leather has the properties it does and how the collagen structure relates to the desirable attributes. The focus of this work is to characterise the structure of leather, particularly the collagen structure and arrangement. Orientation indices allow us to determine the extent to which the fibres lie flat or traverse the thickness of the leather. We can see how this relates to the strength of the sample.

Experimental

Using the conventional beam house and tanning processes, leather pelts were prepared. Strips of leather 1mm thick and 50mm long were cut from the leather pelts of seven different animal species. SAXS diffraction patterns were recorded on the Australian Synchrotron SAXS/WAXS beamline, with a beam size of 250 × 80 µm and a total photon flux of 2×10^{12} photons s^{-1}. All diffraction patterns were recorded with an X-ray energy of 11keV using a Pilatus 1M detector with an active area of 170x170 mm. The leather samples were mounted in the beam horizontally with a sample to detector distance of 3371mm and an exposure time for diffraction patterns of 1s. Sample stretching was carried out using a custom built machine. The leather sample was held in place by two clamps. The sample was stretched in 1mm increments with spectrum recorded after each increment until the sample failed.

SAXS Analysis

The animals selected for analysis were sheep (selected weak), possum, sheep (selected strong), cattle, goat, water buffalo, deer and horse. Using the unique, custom built setup illustrated in Figure 1 the tear strength of all samples was successfully determined.

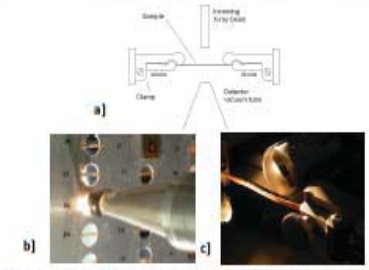

Figure 1. a] Experimental set up for stretching process, **b]** static leather samples, **c]** stretched leather sample.

Samples were analysed from two directions; flat on and edge on (Figure 2). This enabled us to determine any structure-property relationships present within the three dimensional structure of leather.

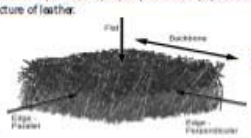

Figure 2. Sampling directions

Orientation Index and Tear Strength

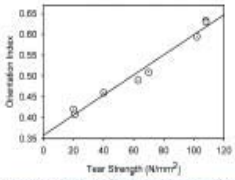

Figure 3. Collagen fibril orientation and tear strength for leather from different animals.

The orientation index (OI), ranging from 0-1, provides a measure of alignment of the fibrils. An OI of 1 represents perfect alignment while 0 equates to an isotropic material. The tear strength results fell in the range of 20-110 N/mm with orientation indices of 0.420-0.633. A direct correlation was found when the two data sets were compared (Figure 3).

Structure-Strength Relationship

The strong OI and tear strength relationship was found to be directly linked to the orientation of fibres within the corium and the grain. Figure 4 shows samples viewed edge-on illustrating the arrangement of fibrils in leather of varying strengths. It is the orientation in this plane that correlates most strongly with strength and highly aligned material being stronger. Figure 5 depicts the fibrous collagen orientation when viewed flat-on. In this direction anisotropic arrangement is desirable.

Figure 4. Relationship between OI and strength viewed edge-on. **a]** Weakest leather (vertical fibre defect), **b]** medium strength leather (low OI), **c]** Strong leather (high OI). Arrow indicates direction of applied strength for tear measurements.

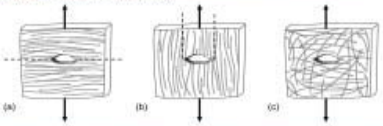

Figure 5. Relationship between OI and strength viewed flat-on. **a]** weak leather (high OI), **b]** fairly weak leather (high OI), **c]** strong leather. Arrow indicates direction of applied strength for tear measurements.

Conclusions

Our study reveals that the strongest leather contains fibrils that are highly aligned within planes with few collagen fibres crossing over between planes. Weak leather contains fibrils that are less aligned. Therefore there is a direct correlation between orientation index and strength

Acknowledgements

Images reprinted with permission from the Journal of Agricultural and Food Chemistry. This research was supported by a grant from the Ministry of Business Innovation and Employment. This research was undertaken on the SAXS/WAXS beamline at the Australian Synchrotron, Victoria, Australia.

MASSEY UNIVERSITY
TE KUNENGA KI PŪREHUROA

Poster presented at the International Union of Leather Technologists and Chemists Societies XXXII Congress, Istanbul, 28-31 May, 2013.

LASRA®

Synchrotron Studies of Leather Structure

Haverkamp, R. G.,[1] Basil-Jones, M. M.,[1] Sizeland, K. H.,[1] & Edmonds, R. L.[2]

[1]School of Engineering and Advanced Technology, Massey University, Palmerston North, New Zealand

[2]Leather and Shoe Research Association, Palmerston North, New Zealand

The arrangement of collagen fibrils in leather is complex. Synchrotron based small angle X-ray scattering enables detailed structural information to be obtained. The variation in fibril orientation through cross sections of leather, structural responses to dynamic loads, structural differences between strong and weak leather, and the structural changes during processing were all studied. Under tension fibrils reorient at low strain then individual fibrils stretch at higher strain. In strong leather the load is taken up more uniformly across the thickness of leather compared with weak leather of the same species. During processing to leather changes are observed in both fibril orientation and individual fibril structure. This study provides an insight into the structural basis of strength in leather and the response of leather to stress.

Symposium conducted at the International Union of Leather Technologists and Chemists Societies XXXII Congress, Istanbul, Turkey. 28th-31st June, 2013.

Collagen Alignment and Leather Strength

Sizeland, K. H.,[1] Basil-Jones,[1] M. M.,[1] Norris, G. E.,[2] Edmonds, R. L.,[3] Kirby, N.,[4] Hawley, A.,[4] & Haverkamp, R. G.[1]

[1]School of Engineering and Advanced Technology, Massey University, Palmerston North, New Zealand

[2]Institute of Fundamental Sciences, Massey University, Palmerston North, New Zealand

[3]Leather and Shoe Research Association, Palmerston North, New Zealand

[4]Australian Synchrotron, Melbourne, Australia

Leather, a material obtained from animal skin through processing, is made up of two layers, the corium and the grain, mostly comprised of fibrous collagen. Being a strong, flexible, water-resistant material, leather is used in a wide variety of manufacturing applications. The physical properties of leather are due in large part to the arrangement of the collagen fibrils. We have used small angle X-ray scattering to characterize leather from seven species of animal with widely different mechanical properties. The two dimensional small angle scattering pattern provides information on the internal fibril structure and the fibril arrangement. Our study reveals that the strongest leather contains fibrils that are highly aligned within planes with few collagen fibres crossing over between planes. Weak leather contains fibrils that are less aligned. Therefore there is a direct correlation between orientation index and strengthThis understanding provides a new insight into structure – property relationships in leather and may be extended to other tissues for biological and medical applications.

Poster presented at the 64th Annual LASRA Conference, Wellington, New Zealand, 15th-16th August, 2013

Collagen Alignment and Leather Strength

Katie H. Sizeland,[†] Melissa M. Basil-Jones,[†] Gillian E. Norris,[‡] Richard L. Edmonds,[§] Nigel Kirby,[¥] Adrian Hawley,[¥] and Richard G. Haverkamp.[†]

[†]School of Engineering and Advanced Technology, Massey University, Palmerston North, New Zealand 4442, [‡]Institute of Fundamental Sciences, Massey University, Private Bag 11222, Palmerston North 4442, New Zealand [§]Leather and Shoe Research Association, Palmerston North, New Zealand 4442, [¥]Australian Synchrotron, Clayton, Vic 3168, Australia.

Introduction

Leather, a material obtained from animal skin through processing, is made up of two layers, the corium and the grain, mostly comprised of fibrous collagen. Being a strong, flexible, water-resistant material, leather is used in a wide variety of manufacturing applications. Synchrotron based small angle X-ray scattering (SAXS) provides an ideal platform for nanostructure analysis of the fibrous collagen. This technique enables us to determine why leather has the properties it does and how the collagen structure relates to the desirable attributes. The focus of this work is to characterise the structure of leather, particularly the collagen structure and arrangement. Orientation indices allow us to determine the extent to which the fibres lie flat or traverse the thickness of the leather. We can see how this relates to the strength of the sample.

Experimental

Using the conventional beam house and tanning processes, leather pelts were prepared. Strips of leather 1mm thick and 50mm long were cut from the leather pelts of seven different animal species. SAXS diffraction patterns were recorded on the Australian Synchrotron SAXS/WAXS beamline, with a beam size of 250 × 80 µm and a total photon flux of 2×10^{12} photons s^{-1}. All diffraction patterns were recorded with an X-ray energy of 11keV using a Pilatus 1 M detector with an active area of 170x170 mm. The leather samples were mounted in the beam horizontally with a sample to detector distance of 3371mm and an exposure time for diffraction patterns of 1s. Sample stretching was carried out using a custom built machine. The leather sample was held in place by two clamps. The sample was stretched in 1mm increments with spectrum recorded after each increment until the sample failed.

SAXS Analysis

The animals selected for analysis were sheep (selected weak), possum, sheep (selected strong), cattle, goat, water buffalo, deer and horse. Using the unique, custom built setup illustrated in Figure 1 the tear strength of all samples was successfully determined.

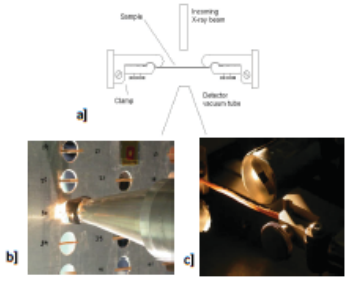

Figure 1. a] Experimental set up for stretching process, **b]** static leather samples, **c]** stretched leather sample.

Samples were analysed from two directions; flat on and edge on (Figure 2). This enabled us to determine any structure-property relationships present within the three dimensional structure of leather.

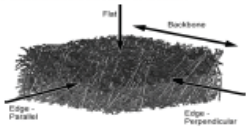

Figure 2. Sampling directions

Orientation Index and Tear Strength

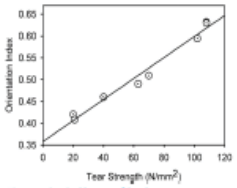

Figure 3. Collagen fibril orientation and tear strength for leather from different animals.

The orientation index (OI), ranging from 0-1, provides a measure of alignment of the fibrils. An OI of 1 represents perfect alignment while 0 equates to an isotropic material. The tear strength results fell in the range of 20-110 N/mm with orientation indices of 0.420-0.633. A direct correlation was found when the two data sets were compared (Figure 3).

Structure-Strength Relationship

The strong OI and tear strength relationship was found to be directly linked to the orientation of fibres within the corium and the grain. Figure 4 shows samples viewed edge-on illustrating the arrangement of fibrils in leather of varying strengths. It is the orientation in this plane that correlates most strongly with strength and highly aligned material being stronger. Figure 5 depicts the fibrous collagen orientation when viewed flat-on. In this direction an isotropic arrangement is desirable.

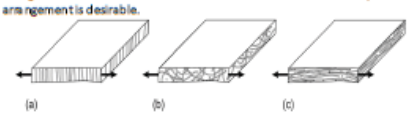

Figure 4. Relationship between OI and strength viewed edge-on. **a]** Weakest leather (vertical fibre defect), **b]** medium strength leather (low OI), **c]** Strong leather (high OI). Arrow indicates direction of applied strength for tear measurements.

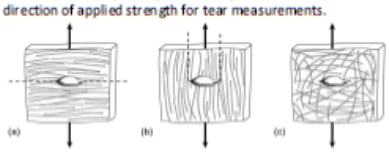

Figure 5. Relationship between OI and strength viewed flat-on. **a]** weak leather (high OI), **b]** fairly weak leather (high OI), **c]** strong leather. Arrow indicates direction of applied strength for tear measurements.

Conclusions

Our study reveals that the strongest leather contains fibrils that are highly aligned within planes with few collagen fibres crossing over between planes. Weak leather contains fibrils that are less aligned. Therefore there is a direct correlation between orientation index and strength

Acknowledgements

Images reprinted with permission from the Journal of Agricultural and Food Chemistry. This research was supported by a grant from the Ministry of Business Innovation and Employment. This research was undertaken on the SAXS/WAXS beamline at the Australian Synchrotron, Victoria, Australia.

MASSEY UNIVERSITY
TE KUNENGA KI PŪREHUROA

Poster presented at the International Union of Leather Technologists and Chemists Societies XXXII Congress, Istanbul, 28-31 May, 2013.

LASRA®

Polyol Modification of Collagen Fibril Axial Periodicity

Sizeland, K. H.,[1] Norris, G. E.,[2] Edmonds, R. L.,[3] Kirby, N.,[4] Hawley, A.,[4] Mudie, S.,[4] & Haverkamp, R. G.[1]

[1]School of Engineering and Advanced Technology, Massey University, Palmerston North, New Zealand
[2]Institute of Fundamental Sciences, Massey University, Palmerston North, New Zealand
[3]Leather and Shoe Research Association, Palmerston North, New Zealand
[4]Australian Synchrotron, Melbourne, Australia

Collagen I is the main structural protein for skin, tendons, pericardium and other tissues. A complex biomaterial, leather is largely composed of a web like network of collagen I fibrils. Penetrating oils are added in the preparation of leather. This process is known as fat-liquoring and is not only what gives leather its superior strength but imparts benefits to improve the leather texture. Synchrotron based technique small angle X-ray scattering provided an ideal platform for nanostructure analysis of leather. The structural changes were investigated, in particular D-spacing changes as a result of fat-liquoring. D spacing values of 60.2-63.8 nm were observed for samples with 0-10% fat liquor. This study shows that there is a large increase in D spacing as the amount of fat liquor added is increased. We propose that the dielectric environment of the collagen fibrils is diminished by displacing water with oils. This would result in a weakening of the hydrogen bonds that hold the tropocollagens in a triple alpha helix. The outcome of this is longer collagen fibrils with resulting increased D-banding. This understanding of the structural changes taking place within collagen to strengthen leather informs future processing developments. It could be supposed that a similar process takes place with the application of moisturisers to skin.

Poster presented at the Australian Synchrotron User Meeting, Melbourne, Australia, 21st-22nd November, 2013.

Polyol Modification of Collagen Fibril Axial Periodicity

K. H. Sizeland,[†] G. E. Norris,[‡] R. L. Edmonds,[§] N. Kirby,[¥] A. Hawley,[¥] and R. G. Haverkamp.[†]

[†]School of Engineering and Advanced Technology, Massey University, Palmerston North, New Zealand 4442, [‡]Institute of Fundamental Sciences, Massey University, Private Bag 11222, Palmerston North 4442, New Zealand [§]Leather and Shoe Research Association, Palmerston North, New Zealand 4442, [¥]Australian Synchrotron, Clayton, Vic 3168, Australia.

Introduction

Leather is a complex biomaterial largely composed of a network of collagen fibrils interlinked with natural and synthetic bonds. Penetrating polyol oils are added in the preparation of leather. This process is known as fat-liquoring and gives leather its superior strength and also improves the leather texture. However little is known about how the addition of fat liquor affects the structure of the collagen microfibrils. Synchrotron based small angle X-ray scattering (SAXS) provides an ideal platform for nanostructure analysis of the fibrous collagen. This technique enables us to investigate some of the characterising properties of leather thus providing insight into the collagen structure. As the axial packing of collagen is highly regular the periodicity or D spacing of the fibrils can be determined. The focus of this work is to ascertain the structural changes of collagen in leather that has been processed with different amounts of fat liquor and to attempt to understand how the added oil affects the nanostructure of leather and chemical environment of the collagen microfibrils.

Experimental

Using the conventional beam house and tanning processes, leather pelts were prepared. Samples of leather 1 × 30 mm were cut from leather pelts processed with 0, 2, 4, 6, 8, and 10% Lipsol EHF. SAXS diffraction patterns were recorded on the Australian Synchrotron SAXS/WAXS beamline, with a beam size of 250 × 80 µm and a total photon flux of 2×10^{12} photons s^{-1}. All diffraction patterns were recorded with an X-ray energy of 11 keV using a Pilatus 1 M detector with an active area of 170x170 mm. The leather samples were mounted without tension in the beam horizontally with a sample to detector distance of 3371 mm and an exposure time for diffraction patterns of 1s. Data processing was carried out using the SAXS15ID software. The D-spacing was determined for each spectrum from Bragg's Law by taking the central position of several collagen peaks, dividing these by the peak order (usually from n = 5 to n =10) and averaging the resulting values.

SAXS Analysis

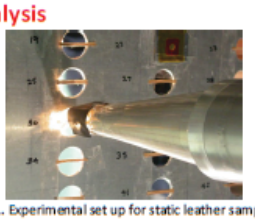

Figure 1. Experimental set up for static leather samples

The samples selected for analysis were processed with 0, 2, 4, 6, 8 and 10% of the fat liquor Lipsol EHF. Samples were mounted on a plate and analysed edge on (Figure 1). This enabled us to determine the structural properties through the full thickness of the leather. The collagen fibril structure of leather is represented by the rings in the SAXS images obtained. An example of a SAXS pattern is shown in Figure 2a. The intensity of the whole pattern is integrated (Figure 2b) allowing clear identification of each peak's position. From these the D-spacing is determined.

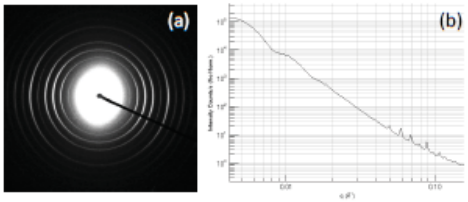

Figure 2. Example of SAXS analysis of leather: (a) raw SAXS pattern; (b) integrated intensity profile.

Fat Liquor Results

The D spacing provides an insight into the internal structure of the collagen fibrils. As depicted in Figure 4, the D spacing refers to the distance between the end of one triple helix and the start of another. It is inclusive of both the gap between fibres and the overlap region.
The D spacing results ranged from 60.2 nm for samples with no fat liquor added to 63.2 nm for samples with 10% fat liquor added. We find a remarkably strong correlation between D spacing and the fat liquor percentage (Figure 3) with a linear fit with a R^2 value of 0.93.

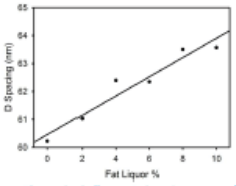

Figure 3. Collagen D Spacing versus fat liquor percentage for ovine leather.

D Spacing changes within the Collagen Fibres

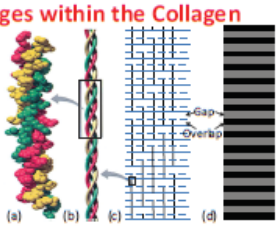

Figure 4. Hierarchical structure of collagen: (a-b) tropocollagens made up of three alpha helix polypeptide chains;(c-d) collagen molecules assembled into fibrils with a specific D banding sequence.

Collagen fibres are formed when a left hand twist combines protein residues to form an alpha helix. Three of these fibres coil together with a right hand twist to form a triple helix (tropocollagen). Larger fibrils are then assembled from multiple tropocollagens. Each fibril contains overlap between the tropocollagen units resulting in a banded structure.
Hydrogen bonding, either direct or water-mediated, plays a critical role in the collagen stabilisation, both within and between the tropocollagens. We propose that either the water-mediated hydrogen bonds between the C=O of glycine and N-H on other residues or possibly the hydroxyproline hydration stabilizing network are weakened by fat liquor polyol substitution. This results in an extended tropocollagen helix, which in turn increases the length of the collagen fibrils as measured by D-spacing. The exact mechanism, nature and position of this hydrogen bond modification is currently under investigation.

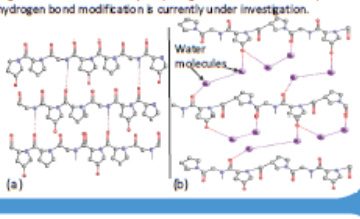

Figure 5. Hydrogen bonding patterns found in triple helix: (a) direct Glycine to residue hydrogen bonding; (b) water mediated hydrogen bonding.

Conclusions

We have investigated the structural changes of leather that occur within its network of collagen fibrils upon addition of varying amounts of fat liquor. We have shown that as the amount of fat liquor increases, the D-spacing of the collagen fibrils also increases. This has been explained as a result of the weakening intrafibrillar hydrogen bonding due to displacement or substitution.

Acknowledgements

This research was supported by a grant from the Ministry of Business Innovation and Employment. This research was undertaken on the SAXS/WAXS beamline at the Australian Synchrotron, Victoria, Australia.

MASSEY UNIVERSITY
TE KUNENGA KI PŪREHUROA

Poster presented at the Australian Synchrotron User Meeting, Melbourne, 21st- 22nd November, 2013.

LASRA®

Cross Linking Collagen Affects Fibril Orientation

Kayed, H. R.,[1] Sizeland, K. H.,[1] Kirby, N.,[2] Hawley, A.,[2] Mudie, S.,[2] & Haverkamp, R. G.[1]

[1]School of Engineering and Advanced Technology, Massey University, Palmerston North, New Zealand

[2]Australian Synchrotron, Melbourne, Australia

Bovine pericardium is treated with the cross linking agent glutaraldehyde before being used for heart valve repair in cardiovascular surgery. Glycosaminoglycan (GAG) cross links are inherent in pericardium and other collagen tissues. Further cross linking with glutaraldehyde has been reported to increase the mechanical properties of the tissue. Small angle X-ray scattering (SAXS) was used to characterise the nanostructure of a pericardium tissue with different degrees of cross linking to investigate the effect of cross links on pericardium structure. These different tissues were those with removed cross links; pericardium with natural cross links (GAGs); and pericardium with GAGs plus glutaraldehyde cross links. The integrated SAXS patterns of the pericardium under no tension were used to determine the alignment of fibrils within the tissue, reported as an orientation index (OI). Dramatic differences in fibril alignment with the degree of cross linking were found. Decreasing the cross linking increases the OI, and synthetically adding cross links decreases fibril orientation significantly. Pericardium with removed cross links, natural cross links and added glutaraldehyde cross links were found to have OI of 0.25, 0.54 and 0.77 respectively. We suggest progressive addition of cross links constrains the fibrils to form a random and more isotropic network.

Poster presented at the Australian Synchrotron User Meeting, Melbourne, Australia, 21st-22nd November, 2013.

Australian Synchrotron Users Meeting, Melbourne, Australia
21-22 November 2013

MASSEY UNIVERSITY
TE KUNENGA KI PŪREHIROA

Cross Linking Collagen Affects Fibril Orientation

Hanan R. Kayed[1], Katie H. Sizeland[1], Nigel Kirby[1], Adrian Hawley[1], Stephen Mudie[1], Richard G. Haverkamp[1]

[1] *School of Engineering and Advanced Technology, Massey University, Palmerston North, New Zealand*
[2] *Australian Synchrotron, Victoria, Australia*

1.0 Introduction

Bovine pericardium (BP) is a collagen rich fibrous tissue cross linked with glycosaminoglycans (GAGs). BP is treated with glutaraldehyde prior to use as heart valve replacements in cardiovascular surgeries to stabilise the tissue and reduce its immunogenicity. It is widely believed that glutaraldehyde further cross links collagen and is reported to increase its strength. Understanding the effects of cross links on BP tissue structure is vital in explaining their role on tissue properties which in turn influences their functionality. Small angle X-ray scattering (SAXS) was used to characterise the nanostructure of BP tissue with different degrees of cross linking to investigate the effect of these links on pericardium structure. This study uses SAXS to investigate specifically the alignment of collagen fibrils within BP, reported as an orientation index (OI).

2.0 Experimental Methods

2.1 Materials and Processing

This study considered fresh bull (Charolais Cross) pericardium in three different states:

4. Pericardium with removed cross links (chondroitinase ABC treated)
5. Pericardium with natural cross links (GAGs)
6. Pericardium with synthetically added cross links (glutaraldehyde treated)

Samples were processed as depicted in Figure 1.

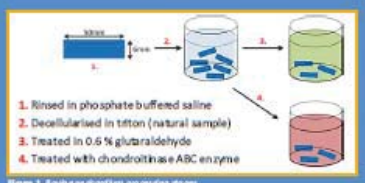

Figure 1. Bovine pericardium processing stages

2.2 SAXS

Hydrated samples were mounted between clamps with the sample flat aligned perpendicular to the X-ray beam (Figure 2 and 3). SAXS scattering patterns were recorded with an X-ray energy of 12 keV using a Pilatus 1 M detector with an active area of 170 x 170 mm and sample-to-detector distance of 3371 mm at the Australian Synchrotron SAXS/WAXS beamline. An X-ray beam size of 250 x 80 µm and total flux of 2 x 10^{11} ph.s^{-1} was used.

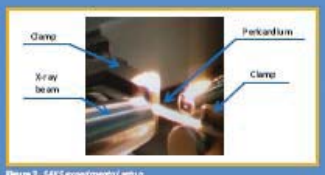

Figure 2. SAXS experimental setup

3.0 Results and Discussions

Representative X-ray scattering patterns are provided in Figure 3. Examination of these patterns alone reveals significant differences between the differently cross linked tissues; the glutaraldehyde treated pericardium shows even scattering around the diffraction ring (Figure 3a), so scattering is occurring from many directions, suggesting the fibrils are randomly aligned. The chondroitinase treated pericardium shows the other extreme where the Bragg diffraction bands only partially extend a full circle. This results from scattering in a limited angle range, implying higher fibril alignment.

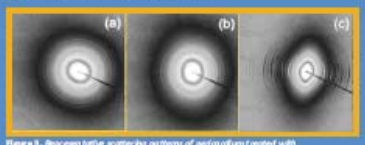

Figure 3. Representative scattering patterns of pericardium treated with (a) glutaraldehyde; (b) natural; (c) chondroitinase

Plotting the variation of intensity with azimuthal angle (Figure 4) is another way of demonstrating the fibril orientation distribution. The width of the peaks in Figure 4 equate to the widths of the diffraction bands in the X-ray scattering pattern so the broader the peak the more isotropic the tissue. From this plot the OI was calculated and falls within the range $0 \leq OI \geq 1$, where 1 corresponds to highly aligned fibrils and 0 indicates an isotropic material.

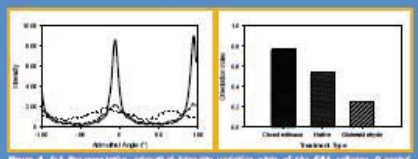

Figure 4. (a) Representative azimuthal intensity variation plots of the fifth collagen D-period diffraction peak for pericardium treated with, glutaraldehyde, natural, chondroitinase; b) Plot of the orientation index with pericardium treatment type

It was found that the OI of the glutaraldehyde, natural and chondroitinase treated pericardium are statistically significantly different at 0.225, 0.538 and 0.770 respectively. Therefore the degree of cross linking in collagenous tissues has a large role in fibril orientation and so nanostructure. Removal of natural GAG links (e.g. via enzyme digestion) causes higher fibril alignment and cross link addition (e.g. via glutaraldehyde treatment) results in a network structure.

We suggest that the natural tendency of fibrils is to align, as did the 'free' fibrils consequent to GAG removal, whilst the addition of synthetic cross links progressively constrains the collagen fibrils into a random network structure.

4.0 Conclusion

Our SAXS experiment on pericardium tissues has highlighted the importance of the role of cross links, both natural and synthetic in the resulting tissue structure, specifically in terms of collagen fibril orientation. This cross linking-fibril alignment relationship is likely to have implications on the mechanical properties of pericardium and this knowledge could potentially be used in the biomedical industry for the preparation and development of new biomaterials.

5.0 Acknowledgements

This research was undertaken on the SAXS/WAXS beamline at the Australian Synchrotron, Victoria, Australia. The NZ Synchrotron Group Ltd is acknowledged for travel funding. Melissa Basil-Jones of Massey University assisted with data collection. John Shannon supplied the pericardium.

Collagen Fibril Axial Periodicity and the Effects of Polyol Addition

Sizeland, K. H.,[1] Norris, G. E.,[2] Edmonds, R. L.,[3] Kirby, N.,[4] Hawley, A.,[4] & Haverkamp, R. G.[1]

[1]School of Engineering and Advanced Technology, Massey University, Palmerston North, New Zealand

[2]Institute of Fundamental Sciences, Massey University, Palmerston North, New Zealand

[3]Leather and Shoe Research Association, Palmerston North, New Zealand

[4]Australian Synchrotron, Melbourne, Australia

Collagen I is the main structural protein for skin, tendons and other tissues and is the material leather is largely composed of. In the preparation of leather penetrating oils are added. This process is known as fat-liquoring and is what gives leather its superior strength and improves the leather texture. Synchrotron based technique small angle X-ray scattering provided an ideal platform for nanostructure analysis of leather. The structural changes were investigated, in particular D-spacing changes as a result of fat-liquoring. D spacing values of 60.2-63.8 nm were observed for samples with 0-10% fat liquor. This study shows that there is a large increase in D spacing as the amount of fat liquor added is increased. We propose that diminishing the dielectric environment of the collagen fibrils by displacing water with oils results in a weakening of the hydrogen bonding that holds the tropocollagen in a triple alpha helix. The outcome of this is longer collagen fibrils with resulting increased D-banding. This understanding of the structural changes taking place within collagen to strengthen leather informs future processing developments. It could be supposed that a similar process takes place with the application of moisturisers to skin.

Poster presented at the 12th International Conference on Frontiers of Polymers and Advanced Materials, Auckland, New Zealand, 8th-13th December, 2013.

Collagen Fibril Axial Periodicity and the Effects of Polyol Addition

K. H. Sizeland,[†] G. E. Norris,[‡] R. L. Edmonds,[§] N. Kirby,[¥] A. Hawley,[¥] and R. G. Haverkamp.[†]

[†]School of Engineering and Advanced Technology, Massey University, Palmerston North, New Zealand 4442, [‡]Institute of Fundamental Sciences, Massey University, Private Bag 11222, Palmerston North 4442, New Zealand [§]Leather and Shoe Research Association, Palmerston North, New Zealand 4442, [¥]Australian Synchrotron, Clayton, Vic 3168, Australia.

Introduction

Leather is a complex biomaterial largely composed of a network of collagen fibrils interlinked with natural and synthetic bonds. Penetrating polyol oils are added in the preparation of leather. This process is known as fat-liquoring and gives leather its superior strength and also improves the leather texture. However little is known about how the addition of fat liquor affects the structure of the collagen microfibrils. Synchrotron based small angle X-ray scattering (SAXS) provides an ideal platform for nanostructure analysis of the fibrous collagen. This technique enables us to investigate some of the characterising properties of leather thus providing insight into the collagen structure. As the axial packing of collagen is highly regular the periodicity or D spacing of the fibrils can be determined. The focus of this work is to ascertain the structural changes of collagen in leather that has been processed with different amounts of fat liquor and to attempt to understand how the added oil affects the nanostructure of leather and chemical environment of the collagen microfibrils.

Experimental

Using the conventional beam house and tanning processes, leather pelts were prepared. Samples of leather 1 × 30 mm were cut from leather pelts processed with 0, 2, 4, 6, 8, and 10% Lipsol EHF. SAXS diffraction patterns were recorded on the Australian Synchrotron SAXS/WAXS beamline, with a beam size of 250 × 80 µm and a total photon flux of 2×10^{12} photons s^{-1}. All diffraction patterns were recorded with an X-ray energy of 11 keV using a Pilatus 1 M detector with an active area of 170x170 mm. The leather samples were mounted without tension in the beam horizontally with a sample to detector distance of 3371mm and an exposure time for diffraction patterns of 1s. Data processing was carried out using the SAXS15ID software. The D-spacing was determined for each spectrum from Bragg's Law by taking the central position of several collagen peaks, dividing these by the peak order (usually from n = 5 to n =10) and averaging the resulting values.

SAXS Analysis

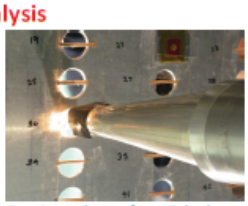

Figure 1. Experimental set up for static leather samples

The samples selected for analysis were processed with 0, 2, 4, 6, 8 and 10% of the fat liquor Lipsol EHF. Samples were mounted on a plate and analysed edge on (Figure 1). This enabled us to determine the structural properties through the full thickness of the leather. The collagen fibril structure of leather is represented by the rings in the SAXS images obtained. An example of a SAXS pattern is shown in Figure 2a. The intensity of the whole pattern is integrated (Figure 2b) allowing clear identification of each peak's position. From these the D-spacing is determined.

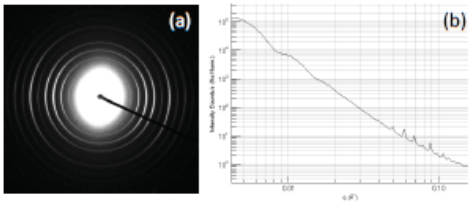

Figure 2. Example of SAXS analysis of leather: (a) raw SAXS pattern; (b) integrated intensity profile.

Fat Liquor Results

The D spacing provides an insight into the internal structure of the collagen fibrils. As depicted in Figure 4, the D spacing refers to the distance between the end of one triple helix and the start of another. It is inclusive of both the gap between fibres and the overlap region.

The D spacing results ranged from 60.2 nm for samples with no fat liquor added to 63.2 nm for samples with 10% fat liquor added. We find a remarkably strong correlation between D spacing and the fat liquor percentage (Figure 3) with a linear fit with a R^2 value of 0.93.

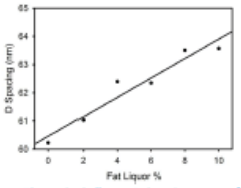

Figure 3. Collagen D Spacing versus fat liquor percentage for ovine leather.

D Spacing changes within the Collagen Fibres

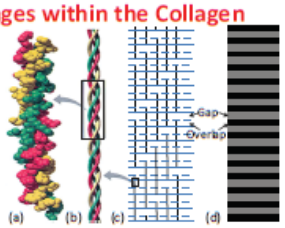

Figure 4. Hierarchical structure of collagen: (a-b) tropocollagens made up of three alpha helix polypeptide chains;(c-d) collagen molecules assembled into fibrils with a specific D banding sequence.

Collagen fibres are formed when a left hand twist combines protein residues to form an alpha helix. Three of these fibres coil together with a right hand twist to form a triple helix (tropocollagen). Larger fibrils are then assembled from multiple tropocollagens. Each fibril contains overlap between the tropocollagen units resulting in a banded structure.

Hydrogen bonding, either direct or water-mediated, plays a critical role in the collagen stabilisation, both within and between the tropocollagens. We propose that either the water-mediated hydrogen bonds between the C=O of glycine and N-H on other residues or possibly the hydroxyproline hydration stabilizing network are weakened by fat liquor polyol substitution. This results in an extended tropocollagen helix, which in turn increases the length of the collagen fibrils as measured by D-spacing. The exact mechanism, nature and position of this hydrogen bond modification is currently under investigation.

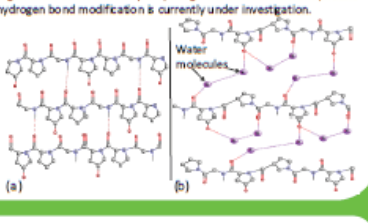

Figure 5. Hydrogen bonding patterns found in triple helix: (a) direct Glycine to residue hydrogen bonding; (b) water mediated hydrogen bonding.

Conclusions

We have investigated the structural changes of leather that occur within its network of collagen fibrils upon addition of varying amounts of fat liquor. We have shown that as the amount of fat liquor increases, the D-spacing of the collagen fibrils also increases. This has been explained as a result of the weakening intrafibrillar hydrogen bonding due to displacement or substitution.

Acknowledgements

This research was supported by a grant from the Ministry of Business Innovation and Employment. This research was undertaken on the SAXS/WAXS beamline at the Australian Synchrotron, Victoria, Australia.

MASSEY UNIVERSITY
TE KUNENGA KI PŪREHUROA

Poster presented at the 12th International Conference on Frontiers of Polymers and Advanced Materials, Auckland 8th-13th December, 2013.

LASRA®

The Fate of Chromium - Biochar from Leather

Wells, H. C.,[1] Sizeland, K. H.,[1] Edmonds, R. E.,[2] Aitkenhead, W.,[2] Kappen, P.,[3] Glover, C.,[3] Johannessen, B.,[3] & Haverkamp, R. G.[1]

[1]School of Engineering and Advanced Technology, Massey University, Palmerston North, New Zealand

[2] Leather and Shoe Research Association, Palmerston North, New Zealand

[3]Australian Synchrotron, Melbourne, Australia

Disposal of chrome-tanned leather waste provides an environmental challenge, with land-based methods risking leaching of chromium into the environment. We investigate the production of biochar from leather as an alternative means to dispose of leather
waste. Chrome-tanned leather is heated at 500–1000 °C in an environment excluding oxygen to form biochar. The char is leached in 1 M HCl for 15 h, and the leachate is analyzed for Cr to confirm that Cr does not leach from char formed at or above 600 °C. The char is analyzed by X-ray absorption spectroscopy (XAS) for chemical state and structure. X-ray absorption near edge structure (XANES) analysis shows that the leather and biochar contain Cr as a mixture of Cr sulfate and Cr carbide, with the proportion of Cr as carbide increasing from 0% for untreated leather to 88% for char formed at 1000 °C. Modeling of the extended X-ray absorption fine structure (EXAFS) spectra shows that the atomic near-range structure is consistent with that of chromium carbide for the high-temperature samples. Biochar produced from chrome-tanned leather waste contains highly dispersed chromium present as a stable, carbide-like structure (provided sufficiently high temperatures are used). This material, rather than being an environmental problem, may be used for soil remediation and carbon sequestration.

Symposium presented at the Society of Leather Technologists and Chemists Conference, Northampton, United Kingdom, 26th April, 2014.

Poisson Ratio of Collagen Fibrils

Wells, H. C.,[1] Sizeland, K. H.,[1] Edmonds, R. E.,[2] Kirby, N.,[3] Hawley, A.,[3] Mudie, S.,[3] & Haverkamp, R. G.[1]

[1]School of Engineering and Advanced Technology, Massey University, Palmerston North, New Zealand

[2]Leather and Shoe Research Association, Palmerston North, New Zealand

[3]Australian Synchrotron, Melbourne, Australia

The main structural component of skin and tendons is type I collagen. These tissues are elastic and deform reversibly under stress. The mechanical properties of individual collagen fibrils contribute to the mechanical properties of the tissues which they comprise. We have used synchrotron based small angle X-ray scattering to investigate the deformation of collagen fibrils during stress in pericardium. Fibril diameter is calculated from the scattering pattern and fibril elongation is calculated from the diffraction peaks resulting from the d-spacing. As collagen fibrils are stretched their density increases. We are able to determine the poisson ratio for collagen fibrils. This knowledge may be incorporated into models of the macrolevel behaviour of tissues.

Poster presented at the 1st Matrix Biology Europe Conference, Rotterdam, Netherlands, 21st-24th June 2014.

Poisson Ratio of Collagen Fibrils

Hannah C. Wells[1], Hanan R. Kayed[1], Katie H. Sizeland[1], R. L. Edmonds[2], Nigel Kirby[3], Adrian Hawley[3], Stephen T. Mudie[3], Richard G. Haverkamp[1].

[1]School of Engineering and Advanced Technology, Massey University, Private Bag 11222, Palmerston North, New Zealand 4442. [2]Leather and Shoe Research Association, Private Bag, Palmerston North, New Zealand 4442. [3]Australian Synchrotron, 800 Blackburn Road, Melbourne, Australia.

Abstract

Tendon, skin and skin products are all primarily made up of collagen type I. In order to understand the mechanical performance of these materials, we must understand the mechanical performance of collagen fibrils that make up the materials. Here, a study has been carried out using synchrotron based small angled X-ray scattering (SAXS) on bovine pericardium under strain. From the SAXS patterns recorded the changes in d-spacing, which is a measure of fibril extension, and the changes in fibril diameter were measured.

The pericardium tissue was strained to 7.3%. The Poisson ratio of the collagen fibrils was calculated as the ratio of the collagen fibril length extension to width contraction, corrected for a rod shape. This was found to be 1.9 for a fibril strain of 0 to 7.3%, or 1.1 for the measurements taken after initial fibril straightening.

The calculated Poisson ratio indicates that the volume of individual collagen fibrils decrease with an increase in strain. This is unlike many engineering materials and may help to explain some of the unique properties of collagen-based materials, and also may be useful to incorporate into models of tissue performance.

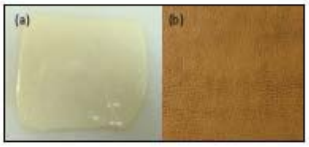

Figure 1. Samples of skin products, primarily comprised of type I collagen (a) Stratiflex extracellular matrix scaffolds for surgical applications and (b) leather

Introduction

A number of studies have been carried out on collagenous materials to determine their behaviour and mechanical performance. For example, in tendon a Poisson ratio of 0.8 was measured under compression[1] and for spinal dura mater under uniaxial tension, a Poisson ratio in the range of 0.5 - 1.6[2].

The mechanical properties of collagenous materials can be affected by the arrangement and orientation of the collagen fibrils, fibril diameter [3, 4], the amount of crimp, the extent to which the fibrils slide over each other, and cross linking [5,6,7]. In leather, the reorientation of fibrils is the most significant mechanism for taking up strain[8,9].

In the work presented here, the change in structure of individual fibrils in type I collagen during strain have been investigated using small angled X-ray scattering (SAXS).

Methods and Materials

Fresh bull pericardium was collected and kept wet in PBS while diffraction patterns were recorded at room temperature. Samples were stretched in 1 mm increments, and maintained at each extension for one minute each time before the SAXS spectra, the extension and the force data was all recorded. This was carried out until the sample broke.

Diffraction patterns were recorded on the Australian Synchrotron SAXS/WAXS beamline. D-spacing and orientation index (OI) were calculated using the SAXS1SID software. Fibril diameters were determined using Irena software running within Igor Pro. D-spacing was calculated from the centre position of the 9th order diffraction peak, taken in the azimuthal range 45° to 135°. The OI is a measure of fibril alignment where 1 indicates parallel fibrils and 0 indicates isotropic orientation.

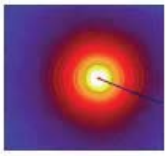

Figure 2. An example of the SAXS scattering pattern of pericardium.

Results

Clear, well-defined SAXS diffraction patterns were collected from the pericardium samples (Figure 2). A stress-strain curve was recorded from the in-situ stretching (Figure 3). The maximum strain before break was 7.3%.

From the unstrained state to the maximum strain, the d-spacing increases from 66.13 nm to 69.12 nm and the OI increases from 0.53 to 0.75 before plateauing at 0.8 after initial fibril straightening. Fibril diameter decreases from 62.1nm to 55.4nm (Figure 4).

The Poisson ratio of the individual collagen fibrils is expressed as the ratio of fibril diameter to d-spacing spacing extension under cumulative strain. For the pericardium tested here, a strain of 0.073 caused a 2.99 nm increase in d-spacing (4.52 %) and a 6.7 nm decrease in fibril diameter (10.8%). This gives a Poisson ratio of 1.9 or 1.1 for the measurements taken after initial fibril straightening.

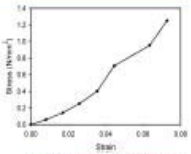

Figure 3. Stress-strain curve recorded during SAXS measurements.

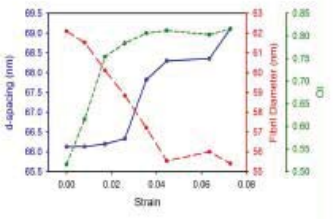

Figure 4. Changes in d-spacing (solid, blue), fibril diameter (long dash, red) and OI (short dash, green) with strain.

Discussion

A clear inverse relationship is observed between the d-spacing and fibril diameter of the collagen fibrils in pericardium as it is stretched. The d-spacing increases and the fibril diameter decreases. Two stages in the strain behaviour of pericardium are observed. In the first stage, up to a strain of around 0.02, we see a decrease in fibril diameter with a large increase in OI, and a small increase in d-spacing. This indicates the removal of crimp and re-orientation of fibrils[11] is taking up most of the strain in the initial stages of stretching.

The second stage involves no significant change in OI but the d-spacing increases substantially, suggesting the fibrils are now being stretched. The changes in fibril diameter and d-spacing during strain in the pericardium tissue gave a Poisson ratio of 1.9. This Poisson ratio suggests a large decrease in volume with increasing strain. This is an unusual property - isotropic materials have a Poisson ratio of 0.5 to -1. The large reduction in fibril diameter during strain, that gives this high Poisson ratio, could be a result of tighter packing of tropocollagen molecules that make up the fibrils.

Conclusions

In this study we have used synchrotron based small angled X-ray scattering to measure the fibril diameter change and fibril extension of collagen in bovine pericardium under strain. From this information we were able to calculate the Poisson ratio for collagen fibrils and found that the volume of collagen fibrils decreases under strain. This information has given some insight into the behaviour of collagen and also could be useful to improve models of the behaviour of collagen-based materials by providing more realistic behaviour of the fibril responses.

Acknowledgements

This research was undertaken on the SAXS/WAXS beamline at the Australian Synchrotron, Victoria, Australia. The NZ Synchrotron Group Ltd is acknowledged for travel funding. This work was supported by the Ministry of Innovation, Business and Employment grants LSRX0801 and LSRX1202.

Contact

Hannah Wells
Massey University
New Zealand
Email: h.c.wells@massey.ac.nz

References

1. Cheng, V. W. T.; Screen, H. R. C., The micro-structural strain response of tendon. Journal of Materials Science 2007, 42, (21), 8957-8965.
2. Persson, C.; Davis, S.; Healey, R.; Summers, J. L.; Hall, R. M., Poisson's Ratio and Strain Rate Dependency of the Constitutive Behavior of Spinal Dura Mater. Annals of Biomedical Engineering 2008, 36, (3), 475-483.
3. Parry, D. A. D.; Barnes, G. R. G.; Craig, A. S., Comparison of size distribution of collagen fibrils in connective tissues as a function of age and a possible relation between fibril size distribution and mechanical properties. P Roy Soc B-Biol Sci 1978, 203, (1152), 305-321.
4. Wells, H. C.; Clements, R. L.; Kirby, N.; Hawley, A.; Mudie, S. T.; Haverkamp, R. G., Collagen Fibril Diameter and Leather Strength. J Agric Food Chem 2010, 58, (8), 5124-5130.
5. Gibb, A. M.; Scott, J. E., Tensile response to tensile stress - an ultrastructural investigation of collagen - proteoglycan interactions in stressed tendon. J Anat 1985, 142, 357-370.
6. Haverkamp, R. G.; Williams, M. A. K.; Scott, J. E., Stretching single molecules of connective tissue glycans to hundreds their shape-maintaining lengths. Biomacromolecules 2005, 6, (3), 1310-1316.
7. Vergari, M. P. E.; Hulmes, D. J. S.; Meadows, R., Nanoscale morphological classification of collagen fibrils. Nanotechnology 2008, 19, (18).
8. Buchanan, M. M.; Edmonds, R. L.; Hurst, G. G.; Haverkamp, R. G., Collagen fibril alignment and deformation during tensile strain of leather: A SAXS study. J Agric Food Chem 2012, 60, (6), 1505-1510.
9. Sizeland, K. H.; Haverkamp, R. G.; Hall Jones, M. M.; Simmons, R. L.; Cooper, S. M.; Kirby, N.; Hawley, A., Collagen Alignment and Leather Strength for Selected Mammals. J Agric Food Chem 2018, 66, (4), 887-893.

Collagen D-spacing Modification by Fat Liquor Addition

Sizeland, K. H.,[1] Wells, H. C.,[1] Norris, G. E.,[2] Edmonds, R. E.,[3] & Haverkamp, R. G.[1]

[1]School of Engineering and Advanced Technology, Massey University, Palmerston North, New Zealand

[2]Institute of Fundamental Sciences, Massey University, Palmerston North, New Zealand

[3]Leather and Shoe Research Association, Palmerston North, New Zealand

Collagen is the main structural component of skin, both in an unprocessed state and as leather following chemical and mechanical processing. Leather is a remarkable biomaterial that exhibits strength, flexibility and, durability. Leather is processed skin consisting mostly of collagen and it is produced on a large scale for shoes, clothing and upholstery, with high strength being a primary requirement for high-value applications.

During the processing of skins and hides to leather, efforts are made to optimize the strength, flexibility and feel of leather. Adding penetrating oils, a process known as fat liquoring, is likely to improve both the flexibility and the texture of leather by lubricating the fibers to prevent adhesion between them. Little is known, however, about the effect of fat liquor on the molecular structure of the collagen fibrils. We have investigated the structural changes of collagen within leather upon addition of varying amounts of fat liquor. We have shown that as we increased the amount of fat liquor, the D-spacing of the collagen fibrils increased, and that this could be due to the lanolin component of the fat liquor. This shows that fat liquor does more than just lubricate the fibers in leather; it actually alters the structure of the collagen fibrils. Alternative mechanisms for this increase in D-spacing have been discussed, including an increase in the gap region or an increase in the length of the tropocollagen triple helix.

Symposium presented at the 65th LASRA Conference, Wellington, New Zealand, 14th-15th August 2014.

Forming Biochar from Leather Waste to Reduce Leaching of Chromium into the Environment

Wells, H. C.,[1] Sizeland, K. H.,[1] Edmonds, R. E.,[2] Aitkenhead, W.,[2] Kappen, P.,[3] Glover, C.,[3] Johannessen, B.,[3] & Haverkamp, R. G.[1]

[1]School of Engineering and Advanced Technology, Massey University, Palmerston North, New Zealand

[2]Leather and Shoe Research Association, Palmerston North, New Zealand

[3]Australian Synchrotron, Melbourne, Australia

Most leather is produced from skins and hides by tanning with chromium salts. Leather is used in upholstery, shoes and clothing but at the end of the life of these goods, the leather needs to be disposed of in an environmentally benign manner. 80% of the annual global leather production contains Cr. The main concern in the disposal of leather is the leaching from leather of Cr. Soluble Cr in a hexavalent oxidation state is considered to be undesirable in the environment and sites where Cr (VI) is present can require remediation. The chemical speciation and structure of Cr, was determined using X-ray Absorption Spectroscopy. We have shown that there may an environmental benefit in making biochar from chrome-tanned leather waste. The char does not release Cr with acid leaching, unlike untreated leather. We have also shown that the Cr becomes chemically reduced by a carbothermic reaction on charing, at high temperatures forming Cr carbide. Biochar has the added benefits of enhancing agricultural production from soil and providing long-term sequestration of carbon from the environment. This strategy may turn a large-scale, potentially troublesome waste into an economic resource.

Symposium presented at the 65th LASRA Conference, Wellington, New Zealand, 14th-15th August 2014.

Effect of Model Compounds on Nanostructure of Skin

Sizeland, K. H.,[1] Edmonds, R. E.,[2] Norris, G. E.,[3] Kirby, N.,[4] Hawley, A.,[4] Mudie, S.,[4] & Haverkamp, R. G.[1]

[1]School of Engineering and Advanced Technology, Massey University, Palmerston North, New Zealand
[2]Leather and Shoe Research Association, Palmerston North, New Zealand
[3]Institute of Fundamental Sciences, Massey University, Palmerston North, New Zealand
[4]Australian Synchrotron, Melbourne, Australia

Type I collagen is an important component of skin and leather that contributes to its structure and appearance. To achieve the high strength and soft, supple feel of leather, penetrating oils are added to leather during processing. These additives have been shown to increase the collagen D-spacing. The appearance and strength of skin may improve if a similar process could take place in living skin. The purpose of this work is to better understand the mechanism of the action of these penetrating oils on the molecular structure of collagen through the use of model compounds. These model compounds include; urea, which is known as a solubiliser of proteins, and hydroxyproline, which is known as a precipitator of proteins, these compounds being at either end of the Hoffmeister series. Small angle X-ray scattering was used to measure the changes in the D-spacing of collagen. Urea and the lanolin based fat liquor increased the collagen D-spacing while hydroxyproline decreased the D-spacing. The hydrogen bonds which maintain the triple alpha helix structure of tropocollagen are affected by these additives. An understanding of the mechanisms of modification of collagen in skin by lanolin, urea, and hydroxyproline may lead to a better understanding of existing skin formulations and development of new formulations.

Poster presented at the 65th Annual LASRA Conference, Wellington, New Zealand, 14th-15th August, 2014.

Effects of Model Compounds on the Nanostructure of Skin

K. H. Sizeland,[†] R. L. Edmonds,[§] G. E. Norris,[‡] N. Kirby, [¥] A. Hawley,[¥] S. Mudie,[¥] and R. G. Haverkamp.[†]

[†]School of Engineering and Advanced Technology, Massey University, Palmerston North, New Zealand 4442, [‡]Institute of Fundamental Sciences, Massey University, Private Bag 11222, Palmerston North 4442, New Zealand [§]Leather and Shoe Research Association, Palmerston North, New Zealand 4442, [¥]Australian Synchrotron, Clayton, Vic 3168, Australia.

Introduction

Collagen I is an important component of skin that contributes to its structure and appearance. In-situ modification of the structure of collagen may be an important component of the action of skin care cosmetics. Oils and moisturisers are often added to skin in an attempt to create a smoother, more supple feel. They have been shown to modify the collagen fibrils of processed skin, extending the fibril length. If a similar process could take place in living skin it may improve the appearance and strength of skin. The fibril orientation and axial periodicity of collagen fibrils have been quantified for samples processed with model compounds to better understand the influence of the penetrating oils on the molecular structure of collagen. Model compounds were chosen because of their opposite effects on protein solubility. Urea, which is an osmolyte, is often used to solubilise proteins and is commonly used in skin care products, while the amino acids proline and hydroxyproline are known to precipitate proteins.

Experimental

Ovine skin from the leather industry was used as a model material to investigate collagen modification. Using conventional beam house and tanning processes, skin was processed to leather. Samples of leather were cut from pelts processed with urea, L-proline and hydroxyl-L-proline at concentrations of 4% and 7.2%. Samples were also prepared with lanolin at 8% and with no fat liquor. Small angle X-ray scattering (SAXS) diffraction patterns were recorded on the Australian Synchrotron SAXS/WAXS beamline, with a beam size of 250 × 80 µm, a total photon flux of 2×10^{11} photons s^{-1} and an X-ray energy of 11keV using a Pilatus 1 M detector with an active area of 170 × 170 mm. The leather samples were mounted without tension in the beam horizontally with a sample to detector distance of 3371mm and the exposure time for diffraction patterns was 1s. Data processing was carried out using SAXS1SID software. For each diffraction pattern the D-spacing was determined from Bragg's Law and the orientation index (OI) was calculated based on Sack's method for light scattering but converted to an index.

SAXS Analysis

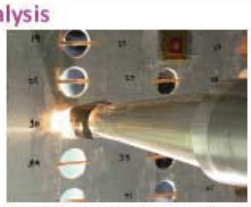

Figure 1. Experimental set up for static leather samples

Samples were mounted on a plate and analysed edge on (Figure 1). This enabled us to determine the structural properties through the full thickness of the sample. The collagen fibril structure is represented by the rings in the SAXS diffraction patterns. An example of a SAXS pattern is shown in Figure 2a. The intensity of the whole pattern is integrated (Figure 2b) allowing clear identification of each peak's position. From these the D-spacing is determined. OI is calculated using the sixth order peak at approximately 0.055-0.059 Å^{-1}. The peak area is measured, above a fitted baseline, at each azimuthal angle.

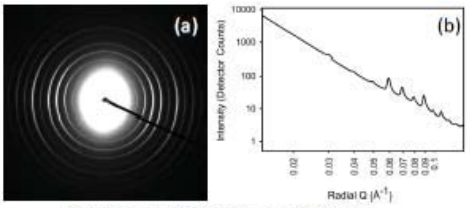

Figure 2. Example of SAXS analysis of leather: (a) raw SAXS pattern; (b) integrated intensity profile.

D-spacing

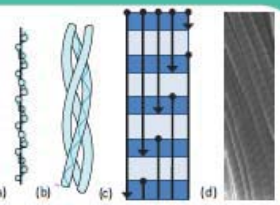

Figure 3. Hierarchical structure of collagen: (a) alpha helical polypeptide chains; (b) triple helix; (c-d) collagen molecules assembled into fibrils with a specific D banding sequence.

Collagen fibres are formed when a left hand twist combines protein residues to form an alpha helix. Three of these fibres coil together with a right hand twist to form a triple helix (tropocollagen). Larger fibrils are then assembled from multiple tropocollagens. Each fibril contains overlap between the tropocollagen units resulting in a banded structure (Figure 3). Hydrogen bonding, either direct or water-mediated, plays a critical role in the stabilisation of collagen, both within and between the tropocollagens. The mechanisms coming into play to get the increase in D-spacing observed here may be due to alterations within the hydrogen bonding network. Urea forms hydrogen bonds with peptide groups so it is therefore possible that the increase in length could be the result of urea breaking H-bonds within the triple helix, resulting in looser coiling. The number of water-mediated hydrogen bonds decreases in the presence of hydrophobic molecules (order water structure) and polar molecules (compete with water molecules to interact with the tropocollagens). As such there may be a looser coiling of the triple helix and consequently an increase in D-spacing.

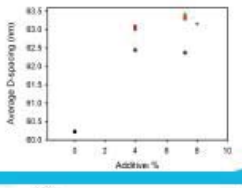

Figure 4. D-spacing versus additive percentage for processed skin: (●) no additives, (▼) lanolin, (♦) hydroxyproline, (■) proline, and (▲) urea.

Orientation Index

The OI indicates the spread in fibril orientation and has previously been found to be correlated with material strength. Urea exerts its influence through polar interactions and lanolin through hydrophobic interactions, both affecting water structure. Urea competes with water to interact with the tropocollagens thus disrupting non-covalent bonds between fibrils likely resulting in a decrease in the alignment of fibrils. Lanolin, a long chain waxy ester, can insert itself between fibrils, trapping ordered water and allowing fibrils to slide over one another thus increasing the orientation of the fibrils.

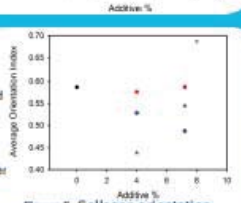

Figure 5. Collagen orientation index (OI) versus additive percentage for processed skin: (●) no additives, (▼) lanolin, (♦) hydroxyproline, (■) proline, and (▲) urea.

Conclusions

The structure of collagen is modified by the model compounds, resulting in changes to the suppleness and strength of tanned skin. Given that lanolin is a major component of most skin care formulations, understanding how it functions at a molecular level is important for the cosmetic industry. Further investigations of the mechanisms of modification of collagen in skin by urea, proline, hydroxyproline, lanolin, and by extension other organic compounds, may lead to a better understanding of existing skin formulations and development of new formulations.

Acknowledgements

This research was supported by a grant from the Ministry of Business Innovation and Employment. This research was undertaken on the SAXS/WAXS beamline at the Australian Synchrotron, Victoria, Australia.

MASSEY UNIVERSITY
TE KUNENGA KI PŪREHUROA

Poster presented at the 65th Annual LASRA Conference, Wellington, 14th-15th August, 2014.

LASRA®

Modification of Collagen D-spacing in Skin

Sizeland, K. H.,[1] Edmonds, R. E.,[2] Norris, G. E.,[3] Kirby, N.,[4] Hawley, A.,[4] Mudie, S.,[4] & Haverkamp, R. G.[1]

[1]School of Engineering and Advanced Technology, Massey University, Palmerston North, New Zealand
[2]Leather and Shoe Research Association, Palmerston North, New Zealand
[3]Institute of Fundamental Sciences, Massey University, Palmerston North, New Zealand
[4]Australian Synchrotron, Melbourne, Australia

An important component of skin that contributes to its structure and appearance is the network of type I collagen. In the leather making process animal skin is converted to a durable, strong and supple material. To achieve the high strength and soft, supple feel of leather, penetrating oils are added to leather during processing, known as fat liquoring. These additives have been shown to modify the collagen fibrils, extending the fibril length and increasing the collagen volume. If a similar process could take place in living skin it may improve the appearance and strength of skin. The purpose of this work is to better understand the mechanism of the action of these penetrating oils on the molecular structure of collagen through the use of model compounds. These model compounds include; urea, which is known as a solubiliser of proteins, and hydroxyproline, which is known as a precipitator of proteins, these compounds being at either end of the Hoffmeister series. Urea is commonly used in skin care formulations, as is lanolin which is a component of the fat liquor used here. We have used ovine hide from the leather industry as a model material for collagen modification experiments. Crust leather was impregnated with urea, hydroxyproline, lanoline or the fat liquor Lipsol EHF (Schill+Seilacher) which contains bisulfited oils and lanoline. Small angle X-ray scattering patterns were recorded on the SAXS/WAXWS beam line at the Australian Synchrotron. Changes in the collagen structure by these additives were measured including the axial periodicity, or D-spacing, which is measured from the

diffraction peaks. When urea or lanolin based fat liquor is added to leather, the collagen D-spacing increases. This results in longer collagen molecules with greater total volume. When hydroxyproline is added to leather, the D-spacing decreases resulting in shorter collagen molecules of lesser volume. In accordance with the Hoffmeister theory, urea weakens hydrogen bonding while hydroxyproline enhances hydrogen bonding. In collagen, we conclude that the hydrogen bonds between the glycine residue and the hydroxyproline or proline residues, which maintain the triple alpha helix structure of tropocollagen, are affected by these additives. Hydrogen bonding in collagen tissues can be modified by selection of compounds from the Hoffmeister series. This can result in changes to the suppleness and strength of the tissues. Some of the physical property changes may be due to the changes in collagen molecule volume. An understanding of the mechanisms of modification of collagen in skin by lanolin, urea and hydroxyproline and by extension other organic compounds may lead to a better understanding of existing skin formulations and development of new formulations.

Poster presented at the 28th IFSCC Conference, Paris, France, 27th-30th October 2014.

Modification of Collagen Structure in Skin

K.H. Sizeland,[†] R.L. Edmonds,[§] G.E. Norris,[‡] N.Kirby,[¥] A.Hawley,[¥] S. Mudie,[¥] and R.G. Haverkamp.[†]

[†]School of Engineering and Advanced Technology, Massey University, Palmerston North, New Zealand 4442, [‡]Institute of Fundamental Sciences, Massey University, Private Bag 11222, Palmerston North 4442, New Zealand [§]Leather and Shoe Research Association, Palmerston North, New Zealand 4442, [¥]Australian Synchrotron, Clayton, Vic 3168, Australia.

Introduction

Collagen I is an important component of skin that contributes to its structure and appearance. In-situ modification of the structure of collagen may be an important component of the action of skin care cosmetics. Oils and moisturisers are often added to skin in an attempt to create a smoother, more supple feel. They have been shown to modify the collagen fibrils of processed skin, extending the fibril length. If a similar process could take place in living skin it may improve the appearance and strength of skin. The fibril orientation and axial periodicity of collagen fibrils have been quantified for samples processed with model compounds to better understand the influence of the penetrating oils on the molecular structure of collagen. Model compounds were chosen because of their opposite effects on protein solubility. Urea, which is an osmolyte, is often used to solubilise proteins and is commonly used in skin care products, while the amino acids proline and hydroxyproline are known to precipitate proteins.

Experimental

Ovine skin from the leather industry was used as a model material to investigate collagen modification. Using conventional beam house and tanning processes, skin was processed to leather. Samples of leather were cut from pelts processed with urea, L-proline and hydroxyl-L-proline at concentrations of 4% and 7.2%. Samples were also prepared with lanolin at 8% and with no fat liquor. Small angle X-ray scattering (SAXS) diffraction patterns were recorded on the Australian Synchrotron SAXS/WAXS beamline, with a beam size of 250 × 80 µm, a total photon flux of 2 × 1012 photons s-1 and an X-ray energy of 11keV using a Pilatus 1 M detector with an active area of 170 × 170 mm. The leather samples were mounted without tension in the beam horizontally with a sample to detector distance of 337mm and the exposure time for diffraction patterns was 1s. Data processing was carried out using SAXSISO software. For each diffraction pattern the D-spacing was determined from Bragg's Law and the orientation index (OI) was calculated based on Sack's method for light scattering but converted to an index.

SAXS Analysis

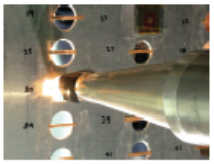

Figure 1. *Experimental set up for static leather samples.*

Samples were mounted on a plate and analysed edge on (Figure 1). This enabled us to determine the structural properties through the full thickness of the sample. The collagen fibril structure is represented by the rings in the SAXS diffraction patterns. An example of a SAXS pattern is shown in Figure 2a. The intensity of the whole pattern is integrated (Figure 2b) allowing clear identification of each peak's position. From these the D-spacing is determined. OI is calculated using the sixth order peak at approximately 0.055-0.059 Å-1. The peak area is measured, above a fitted baseline, at each azimuthal angle.

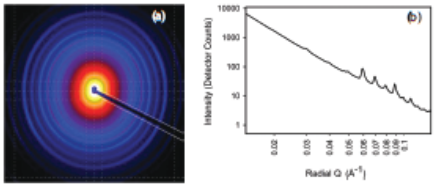

Figure 2. Example of SAXS analysis of leather: (a) raw SAXS pattern; (b) integrated intensity profile.

D-spacing

Collagen fibres are formed when a left hand twist combines protein residues to form an alpha helix. Three of these fibres coil together with a right hand twist to form a triple helix (tropocollagen). Larger fibrils are then assembled from multiple tropocollagens. Each fibril contains overlap between the tropocollagen units resulting in a banded structure (Figure 3). Hydrogen bonding, either direct or water-mediated, plays a critical role in the stabilisation of collagen, both within and between the tropocollagens. The mechanisms coming into play to get the increase in D-spacing observed here may be due to alterations within the hydrogen bonding network. Urea forms hydrogen bonds with peptide groups so it is therefore possible that the increase in length could be the result of urea breaking H-bonds within the triple helix, resulting in looser coiling. The number of water-mediated hydrogen bonds decreases in the presence of hydrophobic molecules (order water structure) and polar molecules (compete with water molecules to interact with the tropocollagens). As such there may be a looser coiling of the triple helix and consequently an increase in D-spacing.

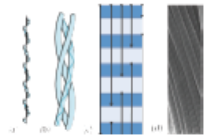

Figure 3. Hierarchical structure of collagen: (a) alpha helical polypeptide chains; (b) triple helix; (c-d) collagen molecules assembled into fibrils with a specific D banding sequence.

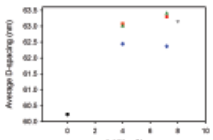

Figure 4. D-spacing versus additive percentage for processed skin: (●) no additives, (▼) lanolin, (◆) hydroxyproline, (■) proline, and (▲) urea.

Orientation Index

The OI indicates the spread in fibril orientation and has previously been found to be correlated with material strength. Urea exerts its influence through polar interactions and lanolin through hydrophobic interactions, both affecting water structure. Urea competes with water to interact with the tropocollagens thus disrupting non-covalent bonds between fibrils likely resulting in a decrease in the alignment of fibrils. Lanolin, a long-chain waxy ester, can insert itself between fibrils, trapping ordered water and allowing fibrils to slide over one another thus increasing the orientation of the fibrils.

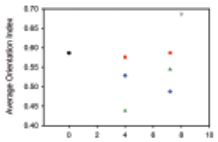

Figure 5. Collagen orientation index (OI) versus additive percentage for processed skin: (●) no additives, (▼) lanolin, (◆) hydroxyproline, (■) proline, and (▲) urea.

Conclusions

The structure of collagen is modified by the model compounds, resulting in changes to the suppleness and strength of tanned skin. Given that lanolin is a major component of most skin care formulations, understanding how it functions at a molecular level is important for the cosmetic industry. Further investigations of the mechanisms of modification of collagen in skin by urea, proline, hydroxyproline, lanolin, and by extension other organic compounds, may lead to a better understanding of existing skin formulations and development of new formulations.

Acknowledgements

This research was supported by a grant from the Ministry of Business Innovation and Employment. This research was undertaken on the SAXS/WAXS beamline at the Australian Synchrotron, Victoria, Australia.

Poster presented at the 28th Congress of the International Federation of Societies of Cosmetic Chemists, Paris, 27th-30th October, 2014.

Changes to the Nanostructure of Collagen in Skin During Leather Processing

Sizeland, K. H.,[1] Basil-Jones, M. M.,[1] Edmonds, R. E.,[2] Kirby, N.,[3] Hawley, A.,[3] Mudie, S.,[3] & Haverkamp, R. G.[1]

[1]School of Engineering and Advanced Technology, Massey University, Palmerston North, New Zealand

[2]Leather and Shoe Research Association, Palmerston North, New Zealand

[3]Australian Synchrotron, Melbourne, Australia

Leather is a complex biomaterial largely composed of collagen fibrils. As skins are processed to produce leather, chemical and physical changes take place that affect the physical properties of the material. The structural foundation of these changes at the collagen fibril level is not fully understood and formed the basis of this investigation. Synchrotron-based small-angle X-ray scattering was used to quantify fibril orientation and D-spacing through eight stages of processing from fresh green ovine skins to staked dry crust leather. Both these structural aspects were found to change with processing. At a higher pH, both D-spacing and the fibril orientation index are lower. The elastic modulus also changes with high salt concentrations and low pH conditions associated with materials that have a low elastic modulus. This study shows that there are structural changes taking place during the processing of skin to leather. It is proposed the change in D-spacing is due to pH affecting the H-bonding within the tropocollagen unit and the decrease in OI is due to the relaxation of tension in the fibrils enabling the collagen fibrils to bend or distort more. This understanding informs the influence of the chemistry at different stages of processing on the development of the final physical characteristics of leather. By understanding the structural changes of collagen that occur when skin is subjected to chemical and mechanical treatments, it may be possible to modify some of these processing steps to alter the final properties of leather

Poster presented at the ASUM Meeting, Melbourne, Australia, 20th-21st November 2014.

Changes to the Nanostructure of Collagen in Skin During Leather Processing

K.H. Sizeland,[†] M.M. Basil-Jones,[†] R.L. Edmonds,[§] N. Kirby,[Y] A. Hawley,[Y] S. Mudie,[Y] and R.G. Haverkamp.[†]

[†]School of Engineering and Advanced Technology, Massey University, Palmerston North, New Zealand 4442, Massey University, Private Bag 11222, Palmerston North 4442, New Zealand [§]Leather and Shoe Research Association, Palmerston North, New Zealand 4442, [Y]Australian Synchrotron, Clayton, Vic 3168, Australia.

Introduction

Leather is a complex biomaterial largely composed of collagen fibrils. The leather making process preserves skins to stop decomposition and provides a strong, flexible material.

Chemical and physical changes take place during the process that affect the strength and other physical properties of the material. Each of the chemical treatments alters the composition of the original skin, for example, extracting components from the native skin or adding components such as cross-linking agents. It is well known that the chemistry of the collagen changes during these processes but it is possible the collagen structure is also effected. Determining if any structural changes occur at the collagen fibril level formed the basis of this investigation.

Experimental

Using conventional beam house and tanning processes, skin was processed to leather. Samples of leather were cut from pelts at each of the following eight stages: fresh green, salted, pickled, pretanned, wet blue, retanned, dry crust and dry crust staked. Small angle X-ray scattering (SAXS) diffraction patterns were recorded on the Australian Synchrotron SAXS/WAXS beamline, with a beam size of 250 × 80 µm, a total photon flux of 2×10^{13} photons s^{-1} and an X-ray energy of 11keV using a Pilatus 1 M detector with an active area of 170 × 170 mm. The leather samples were mounted in a custom built stretching apparatus with a sample to detector distance of 337mm. SAXS patterns were taken through the full thickness of the sample with exposure times of 1s. The force and extension information was logged. The sample was stretched by 1 mm and was maintained at this extension for 1 minute before patterns were recorded. This process was repeated with the sample stretched a further 1 mm each time until the sample failed. Data processing was carried out using scatterBrain Analysis software. For each diffraction pattern the D-spacing was determined from Bragg's Law. The orientation index (OI) is defined as (90° - OA)/90° where OA is the azimuthal angle range that contains 50% of the microfibrils centered at 180°.

SAXS Analysis

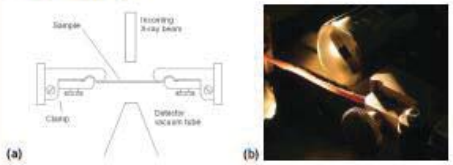

Figure 1.
Experimental set up for leather samples: (a) birds eye view of stretching apparatus; (b) edge on leather sample as positioned in beamline.

Samples were mounted on in the stretching apparatus and analysed edge on (Fig. 1). This enabled us to determine the structural properties through the full thickness of the sample. The collagen fibril structure is represented by the rings in the SAXS diffraction patterns. An example of a SAXS pattern is shown in Fig. 2a. The intensity of the whole pattern is integrated (Fig. 2b) allowing clear identification of each peak's position. From these the D-spacing is determined. OI is calculated using the sixth order peak at approximately 0.055-0.060 Å-1. The peak area is measured, above a fitted baseline, at each azimuthal angle.

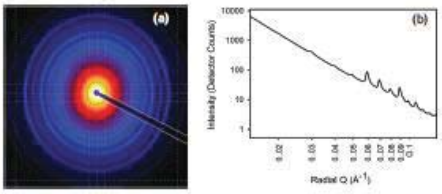

Figure 2. *Example of SAXS analysis of leather: (a) raw SAXS patterns; (b) integrated intensity profile.*

Orientation Index

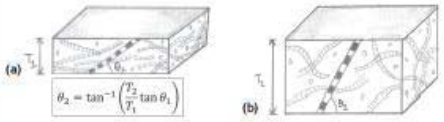

Figure 3. *Change in fibril angle with change in thickness of the leather: (a) thinner material, smaller angle; (b) thicker material, larger angle.*

The OI changed throughout the different stages and appeared to form two groups, one of the dry samples and one of the wet samples. Both groups' OIs decreased when the thickness increased. During the processing of skins to leather the thickness of the material changes substantially. If the collagen fibrils are not lying flat then as the thickness of the leather increases the angle of these fibrils to the plane of leather will increase (Fig. 3). This will cause a change in OI. A model was developed to account for the thickness changes. This enabled us to determine how much of the change in OI is due just to the change in thickness and how much is due to other factors. The recalculated OI now reflects any underlying structural changes that take place during the chemical and mechanical processing of skin through to leather. After the correction, the stages appear to be in two or three groups (Fig. 4). There is the group of dry samples that now seems to split into two groups with salted skin having an OI of 0.62 and the other three dry samples having an OI of about 0.67. The wet samples are in another group with a higher OI (around 0.8) that decreases with thickness.

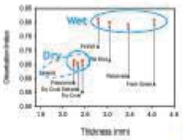

Figure 4. *Orientation Index versus thickness of the leather for different stages of processing: (▲) OI calculated from the SAXS data; (■) OI adjusted for the thickness of the sample.*

Mechanical Stretching

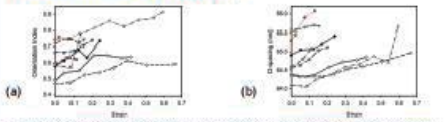

Figure 5. *Changes in collagen fibril (a) OI, and (b) D-spacing as samples of partially processed skin are stretched: (●, ——) Fresh green, (●, ·····) salted, (▽, – – – –) pickled, (▲, – " – " –) pretanned, (■, — —) wet blue, (■, – ' – ' –) retanned, (◆, ——) dry crust, (◆, ——) dry crust staked.*

There is an increase in OI when the samples undergo stretching (Fig. 5a) as the collagen fibrils realign in the direction of the applied force. We also find an increase in D-spacing as the skin or leather samples are stretched (Fig. 5b). This increase in D-spacing indicates the stress is being transferred to the individual fibrils causing their length to increase. There is no obvious difference in the rate at which the OI and D-spacing increase at each of the different processing stages. This indicates that when tension is applied, collagen reacts through the same basic structural mechanisms. Natural and synthetic crosslinks do not change the structural response.

Conclusions

We have found that the changes in OI throughout the processing of skin to leather are not a fundamental redistribution of fibrils, but rather are due to thickness differences and hydration. We have been able to model thickness changes but do not yet understand the wet/dry differences.

Acknowledgements

This research was supported by a grant from the Ministry of Business Innovation and Employment. This research was undertaken on the SAXS/WAXS beamline at the Australian Synchrotron, Victoria, Australia.

MASSEY UNIVERSITY
TE KUNENGA KI PURETUMU
UNIVERSITY OF NEW ZEALAND

Ministry of Business, Innovation & Employment

Poster presented at the Australian Synchrotron User Meeting, Melbourne, 20th-21st November, 2014

LASRA

Chemical Processing and Leather Strength

Sizeland, K. H.,[1] Edmonds, R. E.,[2] Kirby, N.,[3] Hawley, A.,[3] Mudie, S.,[3] & Haverkamp, R. G.[1]

[1]School of Engineering and Advanced Technology, Massey University, Palmerston North, New Zealand

[2]Leather and Shoe Research Association, Palmerston North, New Zealand

[3]Australian Synchrotron, Melbourne, Australia

Leather is a complex biomaterial largely composed of a network of collagen fibrils where a high strength material and a soft, supple feel are sought after qualities. The physical properties of leather are partly dictated by the arrangement and structure of the collagen fibrils. If we can determine how the structure adapts and changes throughout the chemical and mechanical processes skin undertakes to transform into leather, the final physical properties of the material may be able to be manipulated. Synchrotron based small angle X-ray scattering (SAXS) was used to quantify the orientation of the fibrils and the D-spacing through eight stages of processing from fresh green ovine skins to staked dry crust leather. The modification of collagen structure by fat liquoring with 0-10% was also investigated. Both the D-spacing and the fibril orientation index (OI) changed throughout the processing stages. The D-spacing of collagen changed by 6% from 60.2 nm with no fat liquor added to 63.6 nm with 10% fat liquor added. The thickness was found to vary between the samples from the different processing stages. The effect on the OI of the collagen fibrils resulting from thickness changes was calculated. After this correction was made, the main difference in OI is due to the hydration state of the material with dry materials being less oriented than wet. Mechanisms for the extension of fibrils reflected by the increase in D-spacing are discussed. These results provide a greater understanding of the leather manufacturing process and the structural changes it instigates. This insight has the ability to advance leather processing to maximise physical properties of the finished material. As collagen has medical and cosmetic applications, an

understanding on how the structure of collagen changes under chemical and mechanical stresses is also relevant to these industries.

Poster presented at the 4th International Multifunctional, Hybrid, and Nanomaterials, Barcelona, Spain, 9th-13th March 2015.

Chemical Processing and Leather Strength

Katie H. Sizeland[1], Richard L. Edmonds[2], Nigel Kirby[3], Adrian Hawley[3], Stephen Mudie[3], and Richard G. Haverkamp[1]

[1]School of Engineering and Advanced Technology, Massey University, Palmerston North, New Zealand 4442, Massey University, Private Bag 11222, Palmerston North 4442, New Zealand [2]Leather and Shoe Research Association, Palmerston North, New Zealand 4442, [3]Australian Synchrotron, Clayton, Vic 3168, Australia.

Introduction

Leather is a complex biomaterial largely composed of a network of collagen fibrils. A high strength material and a soft, supple feel are sought after qualities and are a requirement for many of the high value applications of leather. These important physical properties of leather are partly dictated by the arrangement and structure of the collagen fibrils. In the manufacture of leather, chemical and physical changes take place that affect the strength and other physical properties of the material. The changes to the chemical environment during these processes have been investigated but it is possible the physical structure of collagen is also effected. Determining if any structural changes occur at the collagen fibril level formed the basis of this investigation. We investigated the structure of collagen in samples taken throughout the processing of skin to leather. We also analysed the structure of leather samples produced using varying amounts of fat liquor.

Experimental

Using conventional beam house and tanning processes, skin was processed to leather. Samples of leather were cut from pelts at each of the following eight stages: fresh green, salted, pickled, pretanned, wet blue, retanned, dry crust and dry crust staked. Samples were cut from finished leathers processed using no fat liquor, and using increasing amounts of the fat liquor Lipsol EHF (2%, 4%, 6%, 8%, and 10%). Small angle X-ray scattering (SAXS) diffraction patterns were recorded on the Australian Synchrotron SAXS/WAXS beamline, with a beam size of 250 × 80 µm, a total photon flux of 2×10^{12} photons s^{-1} and an X-ray energy of 11 keV using a Pilatus 1 M detector with an active area of 170 × 170 mm. Data processing was carried out using scatterBrain Analysis software. For each diffraction pattern the D spacing was determined from Bragg's Law. The orientation index (OI) is defined as (90° − OA)/90° where OA is the azimuthal angle range that contains 50% of the microfibrils centered at 180°.

SAXS Analysis

Figure 1. Leather samples mounted on a plate with wet samples in between two pieces of kapton tape.

Samples were mounted on a plate with wet samples sandwiched between kapton tape and scans were taken through the full thickness of the sample (Fig. 1). The collagen fibril structure is represented by the rings in the SAXS diffraction patterns (Fig. 2a). The intensity of the whole pattern is integrated (Fig. 2b) allowing clear identification of each peak's position. From these the D spacing is determined. OI is calculated using the sixth order peak at approximately 0.055-0.060 Å^{-1}. The peak area is measured, above a fitted baseline, at each azimuthal angle.

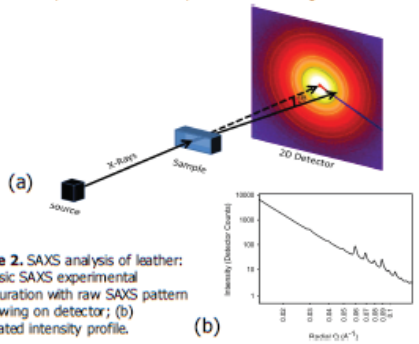

Figure 2. SAXS analysis of leather: (a) Basic SAXS experimental configuration with raw SAXS pattern at showing on detector; (b) integrated intensity profile.

Fat Liquor Results

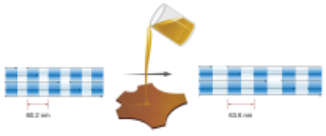

Figure 3. Increase in collagen D spacing with fat liquor addition.

The D spacing refers to the distance between the end of one triple helix and the start of another. It is inclusive of both the gap between fibres and the overlap region. The D spacing results ranged from 60.2 nm for samples with no fat liquor to 63.2 nm for samples with 10% fat liquor added (Fig. 3). We find a remarkably strong correlation between D spacing and the fat liquor addition (Fig. 4) with a linear fit with a R^2 value of 0.93. The mechanisms for this increase in D spacing could be an increase in the gap region or an increase in the length of the tropocollagen triple helix.

Figure 4. Collagen D spacing versus fat liquor percentage for ovine leather.

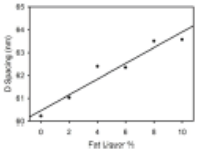

Processing Stages Results

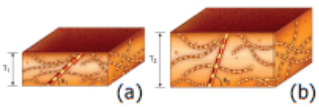

Figure 5. Change in fibril angle with the change in thickness: (a) thinner material, smaller angle; (b) thicker material, larger angle.

The OI changed throughout the processing stages and appeared to form two groups, one of the dry samples and one of the wet samples. During the processing of skins to leather the thickness of the material changes substantially. If the collagen fibrils are not lying flat then as the thickness of the leather increases the angle of these fibrils to the plane of leather will increase (Fig. 5). This will cause a change in OI. A model was developed to account for the thickness. This eliminated the OI change that is due to the change in thickness. As such the recalculated OI now reflects any underlying structural changes that take place. After the correction, the stages appear to be in two or three groups (Fig. 6). There is the group of dry samples that now seems to split into two groups with salted skin having an OI of 0.62 and the other three dry samples having an OI of about 0.67. The wet samples are in another group with a higher OI (around 0.8) that decreases with thickness.

Figure 6. Orientation Index versus thickness of the leather for different stages of processing: (▲) OI calculated from the SAXS data; (■) OI adjusted for the thickness of the sample.

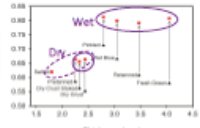

Conclusions

We have shown that fat liquor does not just lubricate fibres in leather, but alters the collagen structure. We have also shown that the changes in OI throughout the processing of skin to leather are not a fundamental redistribution of fibrils, but rather are due to thickness differences and hydration. Both findings will inform future developments so processes can be manipulated to maximise the final strength of the biomaterial.

Acknowledgements

This research was supported by a grant from the Ministry of Business, Innovation, and Employment. This research was undertaken on the SAXS/WAXS beamline at the Australian Synchrotron, Victoria, Australia.

MASSEY UNIVERSITY TE KUNENGA KI PŪREHUROA

Ministry of Business, Innovation & Employment

Poster presented at the Fourth International Conference on Multifunctional, Hybrid and Nanomaterials, Barcelona, 9th-13th March 2015.

LASRA®

Strength in Collagen Biomaterials

Sizeland, K. H.,[1] Wells, H. C.,[1] Kayed, H. R.,[1] Edmonds, R. E.,[2] Kirby, N.,[3] Hawley, A.,[3] Mudie, S.,[3] & Haverkamp, R. G.[1]

[1]School of Engineering and Advanced Technology, Massey University, Palmerston North, New Zealand

[2]Leather and Shoe Research Association, Palmerston North, New Zealand

[3]Australian Synchrotron, Melbourne, Australia

Natural collagen materials are used in industrial and medical applications; for example leather for shoes and garments, and extra cellular matrix materials for surgical scaffolds. For most applications the strength of the material is a critical performance property. Therefore, an improved understanding of how the structure of these natural and processed materials relates to strength is needed. A range of collagen based materials have been characterised using synchrotron based small angle X-ray scattering (SAXS). The distribution of collagen fibril orientation in a material can be determined from this technique. In leather, fibril orientation in the plane of the leather was found to correlate strongly with the tear strength of the leather. Highly aligned collagen fibrils lead to stronger leather. This is explained by a structural model. Mechanisms of nanostructural response to strain in leather, medical scaffold material and pericardium were also investigated by these techniques. Collagen fibrils rearrange and then stretch but these behaviours are governed by a number of factors and the response can be altered by chemical and physical treatments. A better understanding of the structure and strain characteristics of collagen biomaterials has resulted and this enables the design of stronger materials for industrial and medical applications.

Poster presented at the 4th International Multifunctional, Hybrid, and Nanomaterials, Barcelona, Spain, 9th-13th March 2015.

Strength in Collagen Biomaterials

Katie H. Sizeland[1], Hannah Wells[1], Hanan Kayed[1], Richard L. Edmonds[2], Nigel Kirby[3], Adrian Hawley[3], Stephen Mudie[3], and Richard G. Haverkamp[1].

[1]School of Engineering and Advanced Technology, Massey University, Palmerston North, New Zealand 4442, Massey University, Private Bag 11222, Palmerston North 4442, New Zealand [2]Leather and Shoe Research Association, Palmerston North, New Zealand 4442, [3]Australian Synchrotron, Clayton, Vic 3168, Australia.

Introduction

Collagen I assembles with a complex hierarchical structure and forms the basis of many structural components in animals such as skin, pericardium, and other tissues. The network of collagen fibrils plays a definitive role in the overall physical properties of these biomaterials. By characterising some of the structural features of collagen we can gain a better understanding of how collagen reacts to different chemical and mechanical processes. This knowledge would inform future developments and may enable us to manipulate processes to maximise a material's final physical properties. This has formed the basis of our research where we have utilised small angle X-ray scattering (SAXS) to characterise the collagen structures in pericardium, leather, and surgical scaffold materials.

SAXS Analysis

SAXS provides a wealth of useful information that may be used to characterise and compare leathers, skin, and connective tissue. Samples were analysed either statically or under strain. SAXS produces diffraction patterns (Fig. 1a) and the collagen fibril structure is represented by the rings in these patterns. The intensity of the whole pattern is integrated (Fig. 1b) allowing clear identification of each peak's position. From these the d spacing is determined. The orientation index (OI) is calculated from the spread in azimuthal angle around a d-spacing peak, generally we used the sixth order peak at approximately 0.055-0.060 Å^{-1}. The peak area is measured, above a fitted baseline, at each azimuthal angle. These results were analysed and in some experiments were compared with strain, stress and tensile strength results.

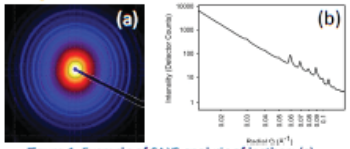

Figure 1. Example of SAXS analysis of leather: (a) raw SAXS pattern; (b) integrated intensity profile.

Pericardium

Heart valve leaflets can be replaced percutaneously with bovine pericardium using adult or neonatal pericardium. The mechanical strength and performance of the material are important properties for a long life in service. Pericardium is a fibrous collagen extracellular matrix similar to skin and other tissues. Neonatal pericardium was found to have a higher modulus of elasticity (83.7 MPa) to adult pericardium (33.5 MPa), a higher tensile strength (32.9 MPa) to adult pericardium (19.1 MPa). The collagen fibrils were found to be far more aligned in neonatal pericardium (OI = 0.78) than in adult pericardium (OI = 0.62) (Fig. 2).

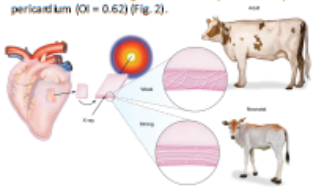

Figure 2. Pericardium, the outside sac of the heart; a weaker material with less aligned fibrils for adult tissue and a stronger material with more aligned fibrils for neonatal tissue.

To achieve high strength, it is thought that the structure of collagen materials requires cross linking of the fibrils to restrict them from sliding past one another. We analysed the structural effects of natural cross linking by glycosaminoglycan (GAG), synthetic cross linking by glutaraldehyde, and the removal of all cross links by chondroitinase ABC. Alignment of the fibrils was found to be affected with the OI of native pericardium (0.19) and the chondroitinase ABC treated pericardium (0.21) being higher than the glutaraldehyde treated pericardium (0.12) (Fig. 3).

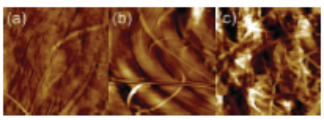

Figure 3. Atomic force microscopy images for (a) native pericardium; (b) chondroitinase ABC treated pericardium; (c) glutaraldehyde treated pericardium.

Leather

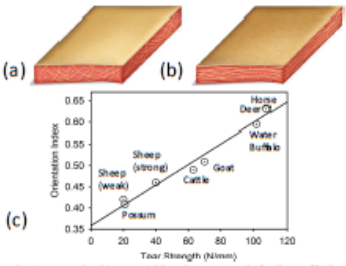

Figure 4. OI of collagen fibrils in edge on ovine leather: (a) low OI, weaker material; (b) high OI, stronger material; (c) Collagen fibril orientation and tear strength for leather from different animals.

Leather is a complex biomaterial largely composed of collagen fibrils which are partly responsible for the material's physical properties. Used in a wide variety of applications, the physical properties exhibited are of importance for both strength and aesthetic reasons. Using SAXS, it has been shown that the fibril orientation strongly correlates with strength in ovine leather; stronger leather has a high OI and weaker leather has a low OI (Fig. 4a and 4b). This correlation was shown to exist across a range of different animals (Fig. 4c). When subjected to strain it has been shown that initially fibres reorient to become more aligned (as seen by an increase in OI) (Fig. 5). Then as the strain increases it is taken up by the individual fibrils (as seen by the d-spacing increase).

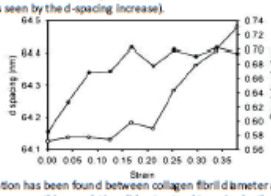

Figure 5. d spacing and OI versus strain measured edge-on for ovine leather: (o) d spacing; (•) OI.

A correlation has been found between collagen fibril diameter and tear strength in bovine leather, however this correlation did not extend to ovine leather or across a selection of other animal leathers. Samples were analysed throughout the processing of skin to leather and it was found that the changes in OI are not a fundamental redistribution of fibrils, but rather are due to thickness differences and hydration with a wet sample having a higher OI than a dry sample. A correlation was also found between the amount of fat liquor used in the production of leather and the d spacing such that as the amount of fat liquor increases, the d-spacing of the collagen fibrils also increases.

Surgical Scaffolds

Biomaterials are an implantable mesh that stimulates, supports, and hosts cell colonisation of a tissue leading to regeneration. The surgical scaffold must be engineered with suitable biophysical properties to allow for clinical use. An ovine forestomach matrix (Fig. 6) was analysed and determined to retain the native collagen architecture which in turn imparted excellent biophysical properties to this surgical scaffold.

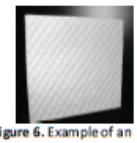

Figure 6. Example of an OFM scaffold material.

Conclusions

We have found SAXS to be a particularly suitable method for the structural analysis of collagen I in a number of biomaterials. We have successfully determined the OI and d spacing of collagen in a number of different experiments and have been able to link these structural features to the strength of the materials too. We hope these findings will lead to the development of processes to maximise the final strength of the material. We plan to continue with our SAXS-based collagen research in the future.

Acknowledgements

This research was supported by grants from the Ministry of Business Innovation and Employment. This research was undertaken on the SAXS/WAXS beamline at the Australian Synchrotron, Victoria, Australia.

MASSEY UNIVERSITY TE KUNENGA KI PŪREHUROA

Ministry of Business, Innovation & Employment

Poster presented at the Fourth International Conference on Multifunctional, Hybrid and Nanomaterials, Barcelona, 9th-13th March 2015.

LASRA®

Poisson Ratio of Collagen Fibrils Measured by SAXS

Wells, H. C.,[1] Sizeland, K. H.,[1] Kayed, H. R.,[1] Kirby, N.,[2] Hawley, A.,[2] Mudie, S.,[2] & Haverkamp, R. G.[1]

[1]School of Engineering and Advanced Technology, Massey University, Palmerston North, New Zealand

[2]Australian Synchrotron, Melbourne, Australia

Tendon, skin and skin products are primarily composed of the fibrous protein, type I collagen. Collagen provides strength and stability in biological tissues and therefore the structure and mechanical properties of collagen are important in understanding the overall behaviour of the tissues. While the bulk tissues themselves have been well characterized in terms of mechanical properties, little is known about the mechanical properties of the individual collagen fibrils. To determine the behaviour of collagen fibrils we have carried out an investigation using synchrotron based small angle X-ray scattering (SAXS) on bovine pericardium under stress. From the SAXS diffraction patterns the fibril diameter is calculated and the fibril elongation is calculated from the diffraction peaks that result from the collagen d-spacing. The tissue is strained 0.25 (25%) with a corresponding strain in the collagen fibrils of 0.045 observed. There are two stages in the collagen fibril structure that we observe while increasing strain. The first stage, at low strain (up to about 0.09) we observe a decrease in fibril diameter, a small increase in d-spacing and a large increase in OI. During this initial stage, the strain is taken up by the reorientation of fibrils and removal of crimp in the fibrils. The second stage involves only a small change in OI but the d-spacing increases significantly and the fibril diameter decreases. This indicates there is an increase in stress on each of the individual fibrils during this stage. At a tissue strain above 0.15 the fibrils continue to be stretched however the fibrils no longer decrease in diameter. We are able to determine the ratio of collagen fibril width contraction to length extension, or Poisson ratio, for collagen fibrils from the changes in fibril

diameter and d-spacing observed. The Poisson ratio, corrected for a rod shape, can be calculated using the equation:

$$v' = -\frac{\sqrt{\pi}/2(\frac{\Delta D}{D})}{\Delta L/L}$$

Poster presented at the 4th International Multifunctional, Hybrid, and Nanomaterials, Barcelona, Spain, 9th-13th March 2015.

Poisson Ratio of Collagen Fibrils Measured by SAXS

Hannah C. Wells[1], Katie H. Sizeland[1], Hanan R. Kayed[1], Nigel Kirby[2], Adrian Hawley[2], Stephen T. Mudie[2], Richard G. Haverkamp[1].

[1]School of Engineering and Advanced Technology, Massey University, Private Bag 11222, Palmerston North, New Zealand 4442; [2]Australian Synchrotron, 800 Blackburn Road, Melbourne, Australia.

Fourth International Conference on Multifunctional, Hybrid and Nanomaterials
9-13th March 2015, Sitges, Spain

Introduction

Type I collagen is the main structural protein of tendon, skin and skin products, providing strength and stability in these biological tissues. The mechanical properties of collagen-based tissues are fundamental to their natural and industrial uses. While the bulk materials have been widely studied, the mechanical properties of the individual collagen fibers that make up these materials have not.

Here we look at the Poisson ratio (ν) of collagen fibrils to characterize the collagen fibril structure and performance in tissue during tension. Previous studies on the bulk tissues have given Poisson ratio values greater than 0.5, indicating the volume of the tissue decreases as it is strained.

We have determined the behavior of collagen fibrils when stress is applied using synchrotron based small angle X-ray scattering (SAXS). Bovine pericardium was used as a collagen source, which was strained up to 25% during data collection.

Methods

SAXS Analysis

Bull pericardium was used as the collagen source for analysis using SAXS. The pericardium was kept fresh in PBS buffer while diffraction patterns were recorded on the SAXS/WAXS beam line at the Australian Synchrotron. The samples were stretch in 1 mm increments and were maintained at each position for one minute before SAXS spectra, the extension and the force was all recorded. This was repeated for each sample, until the sample broke.

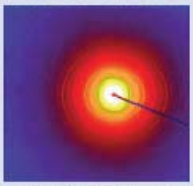

Figure 1. An example of a SAXS diffraction pattern of pericardium

From the recorded diffraction patterns the d-spacing and orientation index (OI) were determined using saxs15ID software, and the fibril diameters were determined using Irena software running with Igor Pro. The d-spacing is a measure of fibril extension, the OI is a measure of fibril alignment in the bulk material.

Calculating Poisson's Ratio

The Poisson's ratio, ν, is the ratio of transverse strain to longitudinal strain in the loading direction and is calculated from the equation:

$$\nu = \frac{\left(\frac{\Delta W}{W}\right)}{\Delta L / L}$$

Where W is the width of a cube or bar, and L is the length of a cube or bar.

The Poisson ratio for collagen fibrils can be expressed as the ratio of fibril diameter to d-spacing extension under cumulative strain. Since ν is defined for a cube, we corrected the ratio by $\sqrt{\pi}/2$.Therefore, the equation for the Poisson ratio of collagen fibrils becomes:

$$\nu' = \frac{\sqrt{\pi}/2\left(\frac{\Delta D}{D}\right)}{\Delta L / L}$$

Where *D* is the fibril diameter and *L* is the d-spacing or fibril extension.

Collagen Structure During Tension

The tissue was strained up to 25%. We observed two stages in the structural changes at the collagen fibril level during strain.

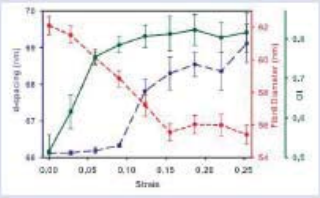

Figure 2. Changes in d-spacing (blue), fibril diameter (red), and orientation index (OI) of the collagen fibrils in pericardium as strain is increased.

In the first stage (up to strain of 0.09), we notice a decrease in the collagen fibril diameter with a small increase in d-spacing and a large increase in OI. During this phase of strain, most of the strain is taken up by the reorientation of the individual fibrils within the tissue.

The second stage of strain (above 0.09) there is little change in OI, however the d-spacing begins to increase and the fibril diameter decreases. This indicates the stress is now mostly on the individual collagen fibrils. At a strain above 0.15, the fibrils continue to stretch however the change in fibril diameter plateaus.

Poisson's Ratio

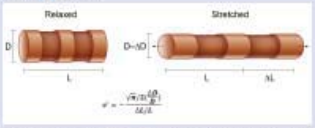

From an unstrained state to maximum strain before rupture, the d-spacing with the fibrils increased 4.5%. The fibril diameter decreased 10.8%. From the changes in d-spacing and fibril diameter, the Poisson's ratio was calculated to be 2.1±0.7 when the tissue is strained up to 25%.

The high Poisson's ratio indicates a volume decrease in the fibrils as the tissue is strained. This could help to explain some of the unique properties of collagen based materials. The high Poisson ration could be explained by tighter packing within the fibril under strain, where there could be compression of hydrogen bonding within the fibril, micro fibril or tropocollagen.

Conclusion

Synchrotron based SAXS has been used as a useful tool for characterizing the structure of individual collagen fibrils within pericardium tissue, as strain is applied to the tissue. From the SAXS diffraction patterns, the collagen d-spacing (or fibril extension), fibril diameter and orientation of the fibrils was determined and used to calculate the Poisson's ratio of collagen of 2.1 ± 0.7.

Previous studies on collagen based bulk materials have given $\nu > 0.5$ and here we have provided experimental evidence that the individual collagen fibrils may also have $\nu' > 0.5$. This suggests that this property of collagen fibrils may contribute to the bulk properties of tissues.

Acknowledgements

This research was carried out on the SAXS/WAXS beamline at the Australian Synchrotron, Victoria, Australia. The NZ Synchrotron Group Ltd is acknowledged for travel funding. This work was supported by the Ministry of Innovation, Business and Employment grants LSRX0801 and LSRX1301.

MASSEY UNIVERSITY
GRADUATE RESEARCH SCHOOL

STATEMENT OF CONTRIBUTION TO DOCTORAL THESIS CONTAINING PUBLICATIONS

(To appear at the end of each thesis chapter/section/appendix submitted as an article/paper or collected as an appendix at the end of the thesis)

We, the candidate and the candidate's Principal Supervisor, certify that all co-authors have consented to their work being included in the thesis and they have accepted the candidate's contribution as indicated below in the *Statement of Originality*.

Name of Candidate: Katie Sizeland

Name/Title of Principal Supervisor: Prof. Richard Haverkamp

Name of Published Research Output and full reference:
Sizeland, K.H., Basil-Jones, M.M., Edmonds, R.L., Cooper, S.M., Kirby, N., (2013). Collagen Orientation and Leather Strength for Selected Mammals. Journal of Agricultural and Food Chemistry, 61(4), 887-892.

In which Chapter is the Published Work:

Please indicate either:

- The percentage of the Published Work that was contributed by the candidate: 80%
  and / or
- Describe the contribution that the candidate has made to the Published Work:

Candidate's Signature — Date: 7/3/2015

Principal Supervisor's signature — Date: 7/3/15

GRS Version 3– 16 September 2011

MASSEY UNIVERSITY
GRADUATE RESEARCH SCHOOL

STATEMENT OF CONTRIBUTION TO DOCTORAL THESIS CONTAINING PUBLICATIONS

(To appear at the end of each thesis chapter/section/appendix submitted as an article/paper or collected as an appendix at the end of the thesis)

We, the candidate and the candidate's Principal Supervisor, certify that all co-authors have consented to their work being included in the thesis and they have accepted the candidate's contribution as indicated below in the *Statement of Originality*.

Name of Candidate: Katie Sizeland

Name/Title of Principal Supervisor: Prof. Richard Haverkamp

Name of Published Research Output and full reference:
Sizeland, K.H., Wells, H.C., Norris, G.E., Edmonds, R.L., Kirby, N., Hawley, A., Mudie, S.T., Haverkamp, R.G., (2015). Collagen D-spacing and the Effect of Fat Liquor Addition. Journal of the American Leather Chemists Association, 110(3), 66-71.

In which Chapter is the Published Work:

Please indicate either:

- The percentage of the Published Work that was contributed by the candidate: 90 %

  and / or
- Describe the contribution that the candidate has made to the Published Work:

Candidate's Signature — 7/3/2015 Date

Principal Supervisor's signature — 7/8/15 Date

GRS Version 3– 16 September 2011

MASSEY UNIVERSITY
GRADUATE RESEARCH SCHOOL

STATEMENT OF CONTRIBUTION TO DOCTORAL THESIS CONTAINING PUBLICATIONS

(To appear at the end of each thesis chapter/section/appendix submitted as an article/paper or collected as an appendix at the end of the thesis)

We, the candidate and the candidate's Principal Supervisor, certify that all co-authors have consented to their work being included in the thesis and they have accepted the candidate's contribution as indicated below in the *Statement of Originality*.

Name of Candidate: Katie Sizeland

Name/Title of Principal Supervisor: Prof. Richard Haverkamp

Name of Published Research Output and full reference:
Sizeland, K.H., Edmonds, R.L., Basil-Jones, M.M., Kirby, N., Hawley, A., Mudie, S.T., Haverkamp, R.G., (2015). Changes to Collagen Structure during Leather Processing. Journal of Agricultural and Food Chemistry

In which Chapter is the Published Work:

Please indicate either:

- The percentage of the Published Work that was contributed by the candidate: 85 %

  and / or
- Describe the contribution that the candidate has made to the Published Work:

Candidate's Signature — Date: 7/3/2015

Principal Supervisor's signature — Date: 7/3/15

GRS Version 3– 16 September 2011

MASSEY UNIVERSITY
GRADUATE RESEARCH SCHOOL

STATEMENT OF CONTRIBUTION TO DOCTORAL THESIS CONTAINING PUBLICATIONS

(To appear at the end of each thesis chapter/section/appendix submitted as an article/paper or collected as an appendix at the end of the thesis)

We, the candidate and the candidate's Principal Supervisor, certify that all co-authors have consented to their work being included in the thesis and they have accepted the candidate's contribution as indicated below in the *Statement of Originality*.

Name of Candidate: Katie Sizeland

Name/Title of Principal Supervisor: Prof. Richard Haverkamp

Name of Published Research Output and full reference:

Sizeland, K.H., Wells, H.C., Higgins, J., Cunanan, C.M., Kirby, N., Hawley, A., Mudie, S.T., Haverkamp, R.G., (2014). Age Dependent Differences in Collagen Alignment of Glutaraldehyde Fixed Bovine Pericardium. Biomed Research Internation

In which Chapter is the Published Work:

Please indicate either:

- The percentage of the Published Work that was contributed by the candidate: 85%

  and / or
- Describe the contribution that the candidate has made to the Published Work:

Candidate's Signature

7/3/2015
Date

Principal Supervisor's signature

7/3/15
Date

MASSEY UNIVERSITY
GRADUATE RESEARCH SCHOOL

STATEMENT OF CONTRIBUTION TO DOCTORAL THESIS CONTAINING PUBLICATIONS

(To appear at the end of each thesis chapter/section/appendix submitted as an article/paper or collected as an appendix at the end of the thesis)

We, the candidate and the candidate's Principal Supervisor, certify that all co-authors have consented to their work being included in the thesis and they have accepted the candidate's contribution as indicated below in the *Statement of Originality*.

Name of Candidate: Katie Sizeland

Name/Title of Principal Supervisor: Prof. Richard Haverkamp

Name of Published Research Output and full reference:
Sizeland, K.H., Wells, H.C., Basil-Jones, m.m., Edmonds, R.L., Haverkamp, R.G. (2014). Leather Nanostructure and Performance. International Leather Maker, 30-34.

In which Chapter is the Published Work:

Please indicate either:

- The percentage of the Published Work that was contributed by the candidate:
  and / or
- Describe the contribution that the candidate has made to the Published Work: ~~Data~~ Collected data of some ~~all~~ samples at the Australian Synchroton, prepared samples for analysis, prepared graphs for paper and assisting with paper editing.

Candidate's Signature — 7/3/2015 Date

Principal Supervisor's signature — 7/3/15 Date

MASSEY UNIVERSITY
GRADUATE RESEARCH SCHOOL

STATEMENT OF CONTRIBUTION TO DOCTORAL THESIS CONTAINING PUBLICATIONS

(To appear at the end of each thesis chapter/section/appendix submitted as an article/paper or collected as an appendix at the end of the thesis)

We, the candidate and the candidate's Principal Supervisor, certify that all co-authors have consented to their work being included in the thesis and they have accepted the candidate's contribution as indicated below in the *Statement of Originality*.

Name of Candidate: Katie Sizeland

Name/Title of Principal Supervisor: Prof. Richard Haverkamp

Name of Published Research Output and full reference:
Wells, H.C., Sizeland, K.H., Edmonds, R.L., Aitkenhead W., Kappen, P., Glover, C., Johannessen, B., Haverkamp, R.G., (2014). Stabilising Chromium from Leather Waste in Biochar. ACS Sustainable Chemistry and Engineering, 2(7), 1864 -1870.

In which Chapter is the Published Work:

Please indicate either:

- The percentage of the Published Work that was contributed by the candidate:
  and / or
- Describe the contribution that the candidate has made to the Published Work: Assisted with beamtime on the SAXS beamline at the Australian synchrotron, assisted with sample prepartion.

Candidate's Signature — Date: 7/3/2015

Principal Supervisor's signature — Date: 7/3/15

GRS Version 3– 16 September 2011

MASSEY UNIVERSITY
GRADUATE RESEARCH SCHOOL

STATEMENT OF CONTRIBUTION TO DOCTORAL THESIS CONTAINING PUBLICATIONS

(To appear at the end of each thesis chapter/section/appendix submitted as an article/paper or collected as an appendix at the end of the thesis)

We, the candidate and the candidate's Principal Supervisor, certify that all co-authors have consented to their work being included in the thesis and they have accepted the candidate's contribution as indicated below in the *Statement of Originality*.

Name of Candidate: Katie Sizeland

Name/Title of Principal Supervisor: Prof. Richard Haverkamp

Name of Published Research Output and full reference:
Kayed, H.R., Sizeland, K.H., Kirby, N., Hawley, A., Mudie, S.T., Haverkamp, R.G., (2015). Collagen Cross Linking and Fibril Alignment in Pericardium. RSC Advances, 5(5), 3611 - 3618.

In which Chapter is the Published Work:

Please indicate either:

- The percentage of the Published Work that was contributed by the candidate:
  and / or
- Describe the contribution that the candidate has made to the Published Work: Assisted with sample ~~prepp~~ preparation and beamtime for collection of data at the Australian Synchrotron. Assisted with sample preparation and image collection for microscopic imaging. Transfered knowledge on sample processing.

Candidate's Signature — 7/3/2015 Date

Principal Supervisor's signature — 7/3/15 Date

MASSEY UNIVERSITY
GRADUATE RESEARCH SCHOOL

STATEMENT OF CONTRIBUTION TO DOCTORAL THESIS CONTAINING PUBLICATIONS

(To appear at the end of each thesis chapter/section/appendix submitted as an article/paper or collected as an appendix at the end of the thesis)

We, the candidate and the candidate's Principal Supervisor, certify that all co-authors have consented to their work being included in the thesis and they have accepted the candidate's contribution as indicated below in the *Statement of Originality*.

Name of Candidate: Katie Sizeland

Name/Title of Principal Supervisor: Prof. Richard Haverkamp

Name of Published Research Output and full reference:
Wells, H.C., Sizeland, K.H., Kayed, H.R., Kirby, N., Hawley, A., Mudie, S.T., Haverkamp, R.G., (2015). Poisson's Ratio of Collagen Fibrils Measured by Small Angle X-Ray Scattering of Strained Bovine Pericardium. Journal of Applied Physics, 117(4).

In which Chapter is the Published Work:

Please indicate either:

- The percentage of the Published Work that was contributed by the candidate:
  and / or
- Describe the contribution that the candidate has made to the Published Work: Assisted with sample preparation and data collection on SAXS beamline at Australian Synchrotron. Transfered knowledge on sample processing.

Candidate's Signature — 7/3/2015 Date

Principal Supervisor's signature — 7/3/15 Date

GRS Version 3– 16 September 2011

Chapter 11: References

AMOS, G. L. 1958. Vertical fibre in relation to the properties of chrome side leather. *Journal of the Society of Leather Technologists and Chemists,* 42**,** 79-90.

AUSTRALIAN SYNCHROTRON. How is Synchrotron Light Created? Melbourne: Australian Synchrotron; 2015; Available from: http://www.synchrotron.org.au/synchrotron-science/how-is-synchrotron-light-created.

BAJZA, Z. & VRECK, I. V. 2001. Fatliquoring agent and drying temperature effects on leather properties. *Journal of Material Science,* 36**,** 5265-5270.

BAGENAL, F. *13: Light.* Astrophysical & Planetary Sciences Department, University of Colorado, Boulder; Available from: http://lasp.colorado.edu/~bagenal/1010/SESSIONS/13.Light.html.

BARLOW, J. R. 1975. Scanning Electron-Microscopy of Hides, Skins and Leather. *Journal of the American Leather Chemists Association,* 70**,** 114-128.

BASIL-JONES, M. M., EDMONDS, R. L., ALLSOP, T. F., COOPER, S. M., HOLMES, G., NORRIS, G. E., COOKSON, D. J., KIRBY, N. & HAVERKAMP, R. G. 2010. Leather structure determination by small-angle X-ray scattering (SAXS): Cross sections of ovine and bovine leather. *Journal of Agricultural and Food Chemistry,* 58**,** 5286-5291.

BASIL-JONES, M. M., EDMONDS, R. L., COOPER, S. M. & HAVERKAMP, R. G. 2011. Collagen fibril orientation in ovine and bovine leather affects strength: A small angle X-ray scattering (SAXS) study. *Journal of Agricultural and Food Chemistry,* 59**,** 9972-9979.

BASIL-JONES, M. M., EDMONDS, R. L., COOPER, S. M., KIRBY, N., HAWLEY, A. & HAVERKAMP, R. G. 2013. Collagen Fibril Orientation and Tear Strength across Ovine Skins. *Journal of Agricultural and Food Chemistry,* 61**,** 12327-12332.

BASIL-JONES, M. M., EDMONDS, R. L., NORRIS, G. E. & HAVERKAMP, R. G. 2012b. Collagen Fibril Alignment and Deformation during Tensile Strain of Leather: A Small-Angle X-ray Scattering Study. *Journal of Agricultural and Food Chemistry,* 60**,** 1201-1208.

BAVINTON, J. H., PETERS, D. E. & STEPHENS, L. J. 1987. A Comparative Morphology of Kangaroo and Bovine Leathers. *Journal of the American Leather Chemists Association,* 82**,** 197-199.

BEAR, R. S. 1944. X-ray, diffraction studies on protein fibers I The large fiber-axis period of collagen. *Journal of the American Chemical Society,* 66**,** 1297-1305.

BELLA, J., BRODSKY, B. & BERMAN, H. M. 1995. Hydration structure of a collagen peptide. *Structure,* 3**,** 893-906.

BELLA, J., EATON, M., BRODSKY, B. & BERMAN, H. M. 1994a. Crystal-structure and molecular-structure of a collagen-like peptide at 1.9-Ångstrom resolution. *Science,* 266**,** 75-81.

BELLA, J., BRODSKY, B. & BERMAN, H. M. 1995. Hydration structure of a collagen peptide. *Structure,* 3**,** 893-906.

BERISIO, R., VITAGLIANO, L., MAZZARELLA, L. & ZAGARI, A. 2001. Crystal structure of a collagen-like polypeptide with repeating sequence Pro-Hyp-Gly at 1.4 angstrom resolution: Implications for collagen hydration. *Biopolymers,* 56**,** 8-13.

BERNADO, P., MYLONAS, E., PETOUKHOV, M. V., BLACKLEDGE, M. & SVERGUN, D. I. 2007. Structural characterization of flexible proteins using small-angle X-ray scattering. *Journal of the American Chemical Society,* 129**,** 5656-5664.

BIGI, A., RIPAMONTI, A., ROVERI, N., JERONIMIDIS, G. & PURSLOW, P. P. 1981. Collagen orientation by X-Ray pole figures and mechanical-properties of media carotid wall. *Journal of Materials Science,* 16**,** 2557-2562.

BILLIAR, K. L. & SACKS, M. S. 1997. A method to quantify the fiber kinematics of planar tissues under biaxial stretch. *Journal of Biomechanics,* 30**,** 753-756.

BOOTE, C., KAMMA-LORGER, C. S., HAYES, S., HARRIS, J., BURGHAMMER, M., HILLER, J., TERRILL, N. J. & MEEK, K. M. 2011. Quantification of collagen organization in the peripheral human cornea at micron-scale resolution. *Biophysical Journal,* 101**,** 33-42.

BOOTE, C., STURROCK, E. J., ATTENBURROW, G. E. & MEEK, K. M. 2002. Psuedo-affine behaviour of collagen fibres during the uniaxial deformation of leather. *Journal of Materials Science,* 37**,** 3651-3656.

BRAU, J. *Synchrotron Radiation.* Oregon: University of Oregon; 2015; Available from: http://pages.uoregon.edu/jimbrau/BrauImNew/Chap24/6th/24_35Figurea-F.jpg.

BRODSKY, B., EIKENBERRY, E. F. & CASSIDY, K. 1980. An unusual collagen periodicity in skin. *Biochimica et Biophysica Acta,* 621**,** 162-166.

BULO, R. E., SIGGEL, L., MOLNAR, F. & WEISS, H. 2007. Modeling of bovine Type-I collagen fibrils: Interaction with pickling and retanning agents. *Macromolecular Bioscience,* 7**,** 234-240.

BURGER, C., HSIAO, B. S. & CHU, B. 2010. Preferred Orientation in Polymer Fibre Scattering. *Journal of Macromolecular Science, Part C: Polymer Reviews,* 50**,** 91-111.

BURGER, C., LIU, L. Z., HSIAO, B. S., CHU, B., HANSON, J., HORI, T. & GLIMCHER, M. J. 2001. Synchrotron SAXS/WAXS study of the composite nature of bone. *Polymeric Materials: Science and Engineering,* 84**,** 169-170.

BURGER, C., ZHOU, H.-W., SICS, I., HSIAO, B. S., CHU, B., GRAHAM, L. & GLIMCHER, M. J. 2008a. Small-angle X-ray scattering study of intramuscular fish bone: Collagen fibril superstructure determined from equidistant meridional reflections. *Journal of Applied Crystallography.* 41**,** 252-261.

BURGER, C., ZHOU, H.-W., WANG, H., SICS, I., HSIAO, B. S., CHU, B., GRAHAM, L. & GLIMCHER, M. J. 2008b. Lateral Packing of Mineral Crystals in Bone Collagen Fibrils. *Biophysical Journal,* 95**,** 1985-1992.

BURJANADZE, T. V. 1992. Thermodynamic Substantiation of Water-Bridged Collagen Structure. *Biopolymers,* 32**,** 941-949.

CHAN, Y., COX, G. M., HAVERKAMP, R. G. & HILL, J. M. 2009. Mechanical model for a collagen fibril pair in extracellular matrix. *European Biophysics Journal with Biophysics Letters,* 38**,** 487-493.

COOKSON, D., KIRBY, N., KNOTT, R., LEE, M. & SCHULTZ, D. 2006. Strategies for data collection and calibration with a pinhole-geometry SAXS instrument on a synchrotron beamline. *Journal of Synchrotron Radiation,* 13**,** 440-444.

DEB CHOUDHURY, S., HAVERKAMP, R. G., DASGUPTA, S. & NORRIS, G. E. 2007. Effect of oxazolidine E on collagen fibril formation and stabilization of the collagen matrix. *Journal of Agricultural and Food Chemistry.* 55**,** 6813-6822.

GOH, K. L., HILLER, J., HASTON, J. L., HOLMES, D. F., KADLER, K. E., MURDOCH, A., MEAKIN, J. R. & WESS, T. J. 2005. Analysis of collagen fibril diameter distribution in connective tissues using small-angle X-ray scattering. *Biochimica Et Biophysica Acta-General Subjects,* 1722**,** 183-188.

CAMERON, G. J., ALBERTS, I. L., LAING, J. H. & WESS, T. J. 2002. Structure of type I and type III heterotypic collagen fibrils: an x-ray diffaction study. *Journal of Structural Biology,* 137**,** 15-22.

CEDOLA, A., MASTROGIACOMO, M., BURGHAMMER, M., KOMLEV, V., GIANNONI, P., FAVIA, A., CANCEDDA, R., RUSTICHELLI, F. & LAGOMARSINO, S. 2006. Engineered bone from bone marrow stromal cells: A structural study by an advanced x-ray microdiffraction technique. *Physics in Medicine and Biology,* 51**,** N109-N116.

CEDOLA, A., MASTROGIACOMO, M., LAGOMARSINO, S., CANCEDDA, R., GIANNINI, C., GUAGLIARDI, A., LADISA, M., BURGHAMMER, M., RUSTICHELLI, F. & KOMLEV, V. 2007. Orientation of mineral crystals by collagen fibers during in vivo bone engineering: An X-ray diffraction imaging study. *Spectrochimica Acta B-Atomic Spectroscopy,* 62**,** 642-647.

CHAN, Y., COX, G. M., HAVERKAMP, R. G. & HILL, J. M. 2009a. Mechanical model for a collagen fibril pair in extracellular matrix. *European Biophysics Journal with Biophysics Letters,* 38**,** 487-493.

CHRISTOPHERS, E. 1971. CELLULAR ARCHITECTURE OF STRATUM CORNEUM. *Journal of Investigative Dermatology,* 56**,** 165-&.

CIFERRI, A. 2008. Charge-dependent and charge-independent contributions to ion-protein interaction. *Biopolymers,* 89**,** 700-709.

COMMODITIES AND TRADE DIVISION, F. A. O., UNITED NATIONS 2010. World statistical compendium for raw hides and skins, leather and leather footwear 1990-2009. Rome.

COOKSON, D., KIRBY, N., KNOTT, R., LEE, M. & SCHULTZ, D. 2006. Strategies for data collection and calibration with a pinhole-geometry SAXS instrument on a synchrotron beamline. *Journal of Synchrotron Radiation,* 13**,** 440-444.

COVINGTON, A. D. 1997. Modern tanning chemistry. *Chemical Society Reviews,* 26**,** 111-126.

CRANFORD, S. W. & BUEHLER, M. J. 2013. Critical cross-linking to mechanically couple polyelectrolytes and flexible molecules. *Soft Matter,* 9**,** 1076-1090.

CRIBIER, A., ELTCHANINOFF, H., TRON, C., BASH, A., BORENSTEIN, N., BAUER, E., DERUMEAUX, G., PONTIER, G., LABORDE, F. & LEON, M. B. 2003. Percutaneous artificial cardiac valves: from animal experimentation to the first human implantation in a case of calcified aortic stenosis. *Archives Des Maladies Du Coeur Et Des Vaisseaux,* 96**,** 645-652.

CSISZAR, K. 2001. Lysyl oxidases: A novel multifunctional amine oxidase family. *Progress in Nucleic Acid Research and Molecular Biology, Vol 70,* 70**,** 1-32.

CUQ, M. H., PALEVODY, C. & DELMAS, M. 2000. Fundamental study of cross-linking of collagen with chrome tanning agents in traditional and Cr.A.B processes. *Journal of the Society of Leather Technologists and Chemists,* 83**,** 233-238.

DEB CHOUDHURY, S., HAVERKAMP, R. G., DASGUPTA, S. & NORRIS, G. E. 2007. Effect of oxazolidine E on collagen fibril formation and stabilization of the collagen matrix. *Journal of Agricultural and Food Chemistry,* 55**,** 6813-6822.

DI LULLO, G. A., SWEENEY, S. M., KORKKO, J., ALA-KOKKO, L. & SAN ANTONIO, J. D. 2002. Mapping the ligand-binding sites and disease-associated mutations on the most abundant protein in the human, type I collagen. *Journal of Biological Chemistry,* 277**,** 4223-4231.

ECKERT, M. 2012. Max von Laue and the discovery of X-ray diffraction in 1912. *Annalen Der Physik,* 524**,** A83-A85.

EDMONDS, R. L., CHOUDHURY, S. D., HAVERKAMP, R. G., BIRTLES, M., ALLSOP, T. F. & NORRIS, G. E. 2008. Using proteomics, immunohistology, and atomic force microscopy to characterize surface damage to lambskins observed after enzymatic dewooling. *Journal of Agricultural and Food Chemistry,* 56**,** 7934-7941.

ELDER, F. R., GUREWITSCH, A. M., LANGMUIR, R. V. & POLLOCK, H. C. 1947. RADIATION FROM ELECTRONS IN A SYNCHROTRON. *Physical Review,* 71**,** 829-830.

EMSLEY, J., KNIGHT, C. G., FARNDALE, R. W., BARNES, M. J. & LIDDINGTON, R. C. 2000. Structural basis of collagen recognition by integrin alpha 2 beta 1. *Cell,* 101**,** 47-56.

ENGEL, J., CHEN, H. T., PROCKOP, D. J. & KLUMP, H. 1977. Triple Helix Reversible Coil Conversion of Collagen-Like Polytripeptides in Aqueous and Non-Aqueous Solvents - Comparison of Thermodynamic Parameters and Binding of Water to (L-pro-L-pro-gly)N and (L-pro-L-hyp-gly)N. *Biopolymers,* 16**,** 601-622.

EWALD, P. P. 1962. *Fifty years of X-ray diffraction: Dedicated to the International Union of Crystallography on the occasion of the commemoration meeting in Munich, July 1962,* Utrecht, International Union of Crystallography by A. Oosthoek's Uitgeversmij.

FALGAYRAC, G., FACQ, S., LEROY, G., CORTET, B. & PENEL, G. 2010. New method for Raman investigation of the orientation of collagen fibrils and crystallites in the haversian system of bone. *Applied Spectroscopy,* 64**,** 775-780.

FANG, M., GOLDSTEIN, E. L., TURNER, A. S., LES, C. M., BRADFORD, G. O., FISHER, G. J., WELCH, K. B., ROTHMAN, E. D. & BANASZAK HOLL, M. M. 2012. Type I Collagen DiSpacing in Fibril Bundles of Dermis, Tendon, and Bone: Bridging between Nano- and Micro-Level Tissue Hierachy. *ACS Nano,* 6**,** 9503-9514.

FANG, M., GOLDSTEIN, E. L., TURNER, A. S., LES, C. M., BRADFORD, G. O., FISHER, G. J., WELCH, K. B., ROTHMAN, E. D. & BANASZAK HOLL, M. M. 2012. Type I Collagen DiSpacing in Fibril Bundles of Dermis, Tendon, and Bone: Bridging between Nano- and Micro-Level Tissue Hierachy. *ACS Nano,* 6**,** 9503-9514.

FESSEL, G. & SNEDEKER, J. G. 2011. Equivalent stiffness after glycosaminoglycan depletion in tendon - an ultra-structural finite element model and corresponding experiments. *Journal of Theoretical Biology,* 268**,** 77-83.

FLODEN, E. W., MALAK, S., BASIL-JONES, M. M., NEGRON, L., FISHER, J. N., BYRNE, M., LUN, S., DEMPSEY, S. G., HAVERKAMP, R. G., ANDERSON, I., WARD, B. R. & MAY, B. C. H. 2010. Biophysical characterization of ovine forestomach extracellular matrix biomaterials. *Journal of Biomedical Materials Research B,* 96B**,** 67-75.

FOLKHARD, W., GEERCKEN, W., KNORZER, E., NEMETSCHEK-GANSLER, H., NEMETSCHEK, T. & KOCH, M. H. J. 1987b. Quantitative analysis of the molecular sliding mechanism in native tendon collagen - time-resolved dynamic studies using synchrotron radiation. *International Journal of Biological Macromolecules,* 9**,** 169-175.

FOLKHARD, W., GEERCKEN, W., KNORZER, E., MOSLER, E., NEMETSCHEK-GANSLER, H., NEMETSCHEK, T. & KOCH, M. H. J. 1987a. Structural dynamic of native tendon collagen. *Journal of Molecular Biology,* 193**,** 405-407.

FRANCHI, M., TRIRE, A., QUARANTA, M., ORSINI, E. & OTTANI, V. 2007. Collagen structure of tendon relates to function. *Scientific World Journal,* 7**,** 404-420.

FRANDSON, R. D., WILKE, W. L. & FAILS, A. D. 2013. *Anatomy and Physiology of Farm Animals*, Wiley.

FRASER, R. D. B., MACRAE, T. P. & SUZUKI, E. 1979. *The molecular and fibrillar structure of collagen*. *In:* PARRY, D. A. D. & CREAMER, L. K., 1979. eds. Fourth International Conference on Fibrous Proteins, Palmerston North, New Zealand. Academic Press Inc., 179-206.

FRATZL, P. (ed.) 2008. *Collagen: Structure and mechanics,* New York: SpringerScience+Business Media.

FRATZL, P. & DAXER, A. 1993. Structural Transformation of Collagen Fibrils in Corneal Stroma During Drying: An X-ray Scattering Study. *Biophysical Journal,* 64**,** 1210-1214.

FRATZL, P., FRATZL-ZELMAN, N. & KLAUSHOFER, K. 1993. Collagen packing and mineralization: an x-ray scattering inverstigation of turkey leg tendon. *Biophysical Journal,* 64**,** 260-266.

FRATZL, P., JAKOB, H. F., RINNERTHALER, S., ROSCHGER, P. & KLAUSHOFER, K. 1997. Position-resolved small-angle X-ray scattering of complex biological materials. *Journal of Applied Crystallography,* 30**,** 765-769.

FRATZL, P. & WEINKAMER, R. 2007. Nature's hierarchical materials. *Progress in Materials Science,* 52**,** 1263-1334.

FRIEDRICHS, J., TAUBENBERGER, A., FRANZ, C. M. & MULLER, D. J. 2007. Cellular remodelling of individual collagen fibrils visualized by time-lapse AFM. *Journal of Molecular Biology,* 372**,** 594-607.

GAJDA, M. J., ZAPIEN, D. M., UCHIKAWA, E. & DOCK-BREGEON, A. C. 2013. Modeling the Structure of RNA Molecules with Small-Angle X-Ray Scattering Data. *Plos One,* 8.

GASSER, T. C. 2011. An irreversible constitutive model for fibrous soft biological tissue: A 3-D microfiber approach with demonstrative application to abdominal aortic aneurysms. *Acta Biomaterialia,* 7**,** 2457-2466.

GAUTIERI, A., VESENTINI, S., REDAELLI, A. & BUEHLER, M. J. 2011. Hierarchical Structure and Nanomechanics of Collagen Microfibrils from the Atomistic Scale Up. *Nano Letters,* 11**,** 757-766.

GILBERT, T. W., WOGNUM, S., JOYCE, E. M., FREYTES, D. O., SACKS, M. S. & BADYLAK, S. F. 2008. Collagen fiber alignment and biaxial mechanical behavior of porcine urinary bladder derived extracellular matrix. *Biomaterials,* 29**,** 4775-4782.

GLATTER, O. & KRATKY, O. 1982. *Small Angle X-ray Scattering,* London, Academic Press Inc. .

GONZALEZ, A. D., GALLANT, M. A., BURR, D. B. & WALLACE, J. M. 2014. Multiscale analysis of morphology and mechanics in tail tendon from the ZDSD rat model of type 2 diabetes. *Jouranl of Biomechanics,* 47**,** 681-686.

GRANT, C. A., BROCKWELL, D. J., RADFORD, S. E. & THOMSON, N. H. 2009. Tuning the Elastic Modulus of Hydrated Collagen Fibrils. *Biophysical Journal,* 97**,** 2985-2992.

GUSTAVSON, K. H. 1956. *The chemistry and reactivity of collagen*, Academic Press.

HAINES, B. M. 1984. The Skin Before Tannage - Procters View and Now. *Journal of the Society of Leather Technologists and Chemists,* 68**,** 57-70.

HELSETH, D. L. & VEIS, A. 1981. Collagen Self-Assembly Invitro - Differentiating Specific Telopeptide-Dependent Interactions Using Selective Enzyme Modification and the Addition of Free Amino Telopeptide. *Jouranl of Biological Chemistry,* 256**,** 7118-7128.

ILAVSKY, J. & JEMIAN, P. R. 2009. Irena: tool suite for modeling and analysis of small-angle scattering. *Journal of Applied Crystallography,* 42**,** 347-353.

JAMES, V., DELBRIDGE, L., MCLENNAN, S. V. & YUE, D. K. 1991a. Use of X-Ray Diffraction in Study of Human Diabetic and Aging Collagen. *Diabetes,* 40**,** 391-394.

JAMES, V. J., MCCONNELL, J. F. & CAPEL, M. 1991b. The D-spacing of collagen from mitral heart-valves changes with aging, but not with collagen type-III content. *Biochimica Biophysica Acta,* 1078**,** 19-22.

JANKO, M., DAVYDOVSKAYA, P., BAUER, M., ZINK, A. & STARK, R. W. 2010. Anisotropic Raman scattering in collagen bundles. *Optics Letters,* 35**,** 2765-2767.

JOBSIS, P. D., ASHIKAGA, H., WEN, H., ROTHSTEIN, E. C., HORVATH, K. A., MCVEIGH, E. R. & BALABAN, R. S. 2007. The visceral pericardium: macromolecular structure and contribution to passive mechanical properties of the left ventricle. *American Journal of Physiology-Heart Circulatory Physiology,* 293**,** H3379-H3387.

JOR, J. W. Y., NIELSEN, P. M. F., NASH, M. P. & HUNTER, P. J. 2011. Modelling collagen fibre orientation in porcine skin based upon confocal laser scanning microscopy. *Skin Resesearch and Technology,* 17**,** 149-159.

JOYCE, E. M., LIAO, J., SCHOEN, F. J., MAYER, J. E. & SACKS, M. S. 2009. Functional collagen fiber architecture of the pulmonary heart valve cusp. *Annals of Thoracic Surgery,* 87**,** 1240-1249.

KAMMA-LORGER, C. S., BOOTE, C., HAYES, S., MOGER, J., BURGHAMMER, M., KNUPP, C., QUANTOCK, A. J., SORENSEN, T., DI COLA, E., WHITE, N., YOUNG, R. D. & MEEK, K. M. 2010. Collagen and mature elastic fibre organisation as a function of depth in the human cornea and limbus. *Journal of Structural Biology,* 169**,** 424-430.

KAR, K., IBRAR, S., NANDA, V., GETZ, T. M., KUNAPULI, S. P. & BRODSKY, B. 2009. Aromatic Interactions Promote Self-Association of Collagen Triple-Helical Peptides to Higher-Order Structures. *Biochemistry,* 48**,** 7959-7968.

KARAMANOS, N., GULLBERG, D., PARASKEVI, H., SCHAEFER, L., TENNI, R., THEOCHARIS, A. & WINBERG, J. O. 2012. *Extracellular Matrix: Pathobiology and Signaling*, De Gruyter.

KAYED, H. R., SIZELAND, K. H., KIRBY, N., HAWLEY, A., MUDIE, S. T. & HAVERKAMP, R. G. 2015a. Collagen cross linking and fibril alignment in pericardium. *RSC Advances,* 5**,** 3611-3618.

KENNEDY, C. J., HILLER, J. C., LAMMIE, D., DRAKOPOULOS, M., VEST, M., COOPER, M., ADDERLEY, W. P. & WESS, T. J. 2004. Microfocus X-ray diffraction of historical parchment reveals variations in structural features through parchment cross sections. *Nano Letters,* 4**,** 1373-1380.

KEMP, A. D., HARDING, C. C., CABRAL, W. A., MARINI, J. C. & WALLACE, J. M. 2012. Effects of tissue hydration on nanoscale structural morphology and mechanics of individual Type I collagen fibrils in the Brtl mouse model of Osteogenesis Imperfecta. *Journal of Structural Biology,* 180**,** 428-438.

KIELTY, C. M. & SHUTTLEWORTH, C. A. 1997. Microfibrillar elements of the dermal matrix. *Microscopy Research and Technique,* 38**,** 413-427.

KRAMER, R. Z., BELLA, J., BRODSKY, B. & BERMAN, H. M. 2001. The crystal and molecular structure of a collagen-like peptide with a biologically relevant sequence. *Journal of Molecular Biology,* 311**,** 131-147.

KRAMER, R. Z., BELLA, J., MAYVILLE, P., BRODSKY, B. & BERMAN, H. M. 1999. Sequence dependent conformational variations of collagen triple-helical structure. *Nature Structural Biology,* 6**,** 454-457.

KRAMER, R. Z., VENUGOPAL, M. G., BELLA, J., MAYVILLE, P., BRODSKY, B. & BERMAN, H. M. 2000. Staggered molecular packing in crystals of a collagen-like peptide with a single charged pair. *Journal of Molecular Biology,* 301**,** 1191-1205.

KRONICK, P. L. & BUECHLER, P. R. 1986. Fiber orientation in calfskin by laser-light scattering or X-ray-diffraction and quantitative relation to mechanical-properties. *Journal of the American Leather Chemists Association,* 81**,** 221-230.

KRONICK, P. L. & SACKS, M. S. 1991. Quantification of vertical-fiber defect in cattle hide by small-angle light-scattering. *Connective Tissue Research,* 27**,** 1-13.

KUCHARZ, E. J. 2011. *The Collagens: Biochemistry and Pathophysiology*, Springer Berlin Heidelberg.

LIAO, J., YANG, L., GRASHOW, J. & SACKS, M. S. 2005. Molecular orientation of collagen in intact planar connective tissues under biaxial stretch. *Acta Biomaterialia,* 1**,** 45-54.

LIAO, J., YANG, L., GRASHOW, J. & SACKS, M. S. 2007. The relation between collagen fibril kinematics and mechanical properties in the mitral valve anterior leaflet. *Journal of Biomechanical Engineering,* 129**,** 78-87.

LILLEDAHL, M. B., PIERCE, D. M., RICKEN, T., HOLZAPFEL, G. A. & DAVIES, C. D. 2011. Structural analysis of articular cartilage using multiphoton microscopy: input for biomechanical modeling. *IEEE Transaction on Medical Imaging,* 30**,** 1635-1648.

LIM, W. K., ROSGEN, J. & ENGLANDER, S. W. 2009. Urea, but not guanidinium, destabilizes proteins by forming hydrogen bonds to the peptide group. *Proceedings of the National Academy of Sciences of the United States of America,* 106**,** 2595-2600.

LINDEMAN, J. H. N., ASHCROFT, B. A., BEENAKKER, J. W. M., VAN ES, M., KOEKKOEK, N. B. R., PRINS, F. A., TIELEMANS, J. F., ABDUL-HUSSIEN, H., BANK, R. A. & OOSTERKAMP, T. H. 2010. Distinct defects in collagen microarchitecture underlie vessel-wall failure in advanced abdominal aneurysms and aneurysms in Marfan syndrome. *Proceedings of the National Academy of Sciences of the United States of America,* 107**,** 862-865.

MAXWELL, C. A., WESS, T. J. & KENNEDY, C. J. 2006. X-Ray Diffraction Study into the Effects of Liming on the Structure of Collagen. *Biomacromolecules,* 7**,** 2321-2326.

MAYNES, R. 2012. *Structure and function of Collagen types*, Elsevier Science.

MCGUIRE, N. 2003. SAXS Education. *Today's Chemist at work***,** 17-18.

MEEK, K. M., CHAPMAN, J. A. & HARDCASTLE, R. A. 1979. STAINING PATTERN OF COLLAGEN FIBRILS - IMPROVED CORRELATION WITH SEQUENCE DATA. *Journal of Biological Chemistry,* 254**,** 710-714.

MICHEL, A. 2004. Tanners' dilemma: Vertical fibre defect. *Leather International,* 206**,** 36-37.

MIRNAJAFI, A., RAYMER, J., SCOTT, M. J. & SACKS, M. S. 2005. The effects of collagen fiber orientation on the flexural properties of pericardial heterograft biomaterials. *Biomaterials,* 26**,** 795-804.

MIRNAJAFI, A., ZUBIATE, B. & SACKS, M. S. 2010. Effects of cyclic flexural fatigue on porcine bioprosthetic heart valve heterograft biomaterials. *Journal of Biomedical Materials Research Part A,* 94A**,** 205-213.

MISOF, K., RAPP, G. & FRATZL, P. 1997. A new molecular model for collagen elasticity based on synchrotron x-ray scattering evidence. *Biophysical Journal,* 72**,** 1376-1381.

MOLLENHAUER, J., AURICH, M., MUEHLEMAN, C., KHELASHVILLI, G. & IRVING, T. C. 2003. X-Ray Diffraction of the Molecular Substructure of Human Articular Cartilage. *Connective Tissue Research,* 44**,** 201-207.

MOLLENHAUER, J., AURICH, M. E., ZHONG, Z., MUEHLEMAN, C., COLE, A. A., HASNAH, M., OLTULU, O., KUETTNER, K. E., MARGULIS, A. & CHAPMAN, L. D. 2002. Diffraction-Enhanced X-ray Imaging of Articular Cartilage. *Osteoarthritis and Cartilage,* 10**,** 163-171.

MONASH UNIVERSITY. *Australian Synchrotron breaks new ground.* Melbourne: Monash University; 2010; Available from: http://adm.monash.edu/records-archives/archives/memo-archive/2004-2007/stories/20080305/synchrotron.html.

MONTAGNA, W. & PARAKKAL, P. F. 1974. *The structure and function of skin*, Academic Press.

NAITO, A., TUZI, S. & SAITO, H. 1994. A high-resolution N-15 solid-state NMR-study of collagen and related polypeptides - the effect of hydration on formation of interchain hydrogen-bonds as the primary source of stability of the collagen-type triple-helix. *European Journal of Biochemistry,* 224**,** 729-734.

NARHI, T., SIITONEN, U., LEHTO, L. J., HYTTINEN, M. M., AROKOSKI, J. P. A., BRAMA, P. A., JURVELIN, J. S., HELMINEN, H. J. & JULKUNEN, P. 2011. Minor influence of lifelong voluntary exercise on composition, structure, and incidence of osteoarthritis in tibial articular cartilage of mice compared with major effects caused by growth, maturation, and aging. *Connective Tissue Research,* 52**,** 380-392.

NOBELPRIZE.ORG. 2014. *All Nobel Prizes in Physics* [Online]. Nobel Media AB 2014. Available: http://www.nobelprize.org/nobel_prizes/physics/laureates/

NORRIS, M. & SIEGFRIED, D. R. 2011. *Anatomy and Physiology For Dummies*, Wiley.

NWAEJIKE, N. & ASCIONE, R. 2011. Mitral Valve Repair for Disruptive Acute Endocarditis: Extensive Replacement of Posterior Leaflet with Bovine Pericardium. *Journal of Cardiac Surgery,* 26**,** 31-33.

OIKAWA, D., NAKANISHI, T., NAKAMURA, Y., YAMAMOTO, T., YAMAGUCHI, A., SHIBA, N., IWAMOTO, H., TACHIBANA, T. & FURUSE, M. 2005. Modification of skin composition by conjugated linoleic acid alone or with combination of other fatty acids in mice. *British Journal of Nutrition,* 94**,** 275-281.

OKUYAMA, K., ARNOTT, S., TAKAYANAGI, M. & KAKUDO, M. 1981. CRYSTAL AND MOLECULAR-STRUCTURE OF A COLLAGEN-LIKE POLYPEPTIDE (PRO-PRO-GLY)10. *Journal of Molecular Biology,* 152**,** 427-443.

OLSEN, L. O. & JEMEC, G. B. E. 1993. THE INFLUENCE OF WATER, GLYCERIN, PARAFFIN OIL AND ETHANOL ON SKIN MECHANICS. *Acta Dermato-Venereologica,* 73**,** 404-406.

ORGEL, J., MILLER, A., IRVING, T. C., FISCHETTI, R. F., HAMMERSLEY, A. P. & WESS, T. J. 2001. The in situ supermolecular structure of type I collagen. *Structure,* 9**,** 1061-1069.

OTTANI, V., RASPANTI, M. & RUGGERI, A. 2001. Collagen structure and functional implications. *Micron,* 32**,** 252-260.

OXLUND, B. S., ORTOFT, G., BRUEL, A., DANIELSEN, C. C., OXLUND, H. & ULDBJERG, N. 2010. Cervical collagen and biomechanical strength in non-pregnant women with a history of cervical insufficiency. *Reproductive Biology and Endocrinology,* 8**,** 92.

PAEZ, J. M. G., SANMARTIN, A. C., HERRERO, E. J., MILLAN, I., CORDON, A., ROCHA, A., MAESTRO, M., BURGOS, R., TELLEZ, G. & CASTILLO-OLIVARES, J. L. 2006.

Durability of a cardiac valve leaflet made of calf pericardium: Fatigue and energy consumption. *Journal of Biomedical Materials Research Part A,* 77A**,** 839-849.

PAN, M., HEINECKE, G., BERNARDO, S., TSUI, C. & LEVITT, J. 2013. Urea: a comprehensive review of the clinical literature. *Dermatology online journal,* 19**,** 20392.

PARRY, D. A. D. & SQUIRE, J. M. 2005. *Fibrous Proteins: Coiled-coils, Collagen and Elastomers*, Elsevier.

PARRY, D. A. D., BARNES, G. R. G. & CRAIG, A. S. 1978. COMPARISON OF SIZE DISTRIBUTION OF COLLAGEN FIBRILS IN CONNECTIVE TISSUES AS A FUNCTION OF AGE AND A POSSIBLE RELATION BETWEEN FIBRIL SIZE DISTRIBUTION AND MECHANICAL-PROPERTIES. *Proceedings of the Royal Society Series B-Biological Sciences,* 203**,** 305-321.

PETOUKHOV, M. V. & SVERGUN, D. I. 2006. Joint use of small-angle X-ray and neutron scattering to study biological macromolecules in solution. *European Biophysics Journal with Biophysics Letters,* 35**,** 567-576.

PICU, R. C. 2011. Mechanics of random fiber networks-a review. *Soft Matter,* 7**,** 6768-6785.

PRICE, R. I., LEES, S. & KIRSCHNER, D. A. 1997. X-ray diffraction analysis of tendon collagen at ambient and cryogenic temperatures: Role of hydration. *International Journal of Biological Macromolecules,* 20**,** 23-33.

PROCKOP, D. J. & FERTALA, A. 1998. The collagen fibril: The almost crystalline structure. *Journal of Structural Biology,* 122**,** 111-118.

PURSLOW, P. P., WESS, T. J. & HUKINS, D. W. L. 1998. Collagen orientation and molecular spacing during creep and stress-relaxation in soft connective tissues. *Journal of Experimental Biology,* 201**,** 135-142.

PUTNAM, C. D., HAMMEL, M., HURA, G. L. & TAINER, J. A. 2007. X-ray solution scattering (SAXS) combined with crystallography and computation: defining

accurate macromolecular structures, conformations and assemblies in solution. *Quarterly Reviews of Biophysics,* 40**,** 191-285.

PUXKANDL, R., ZIZAK, I., PARIS, O., KECKES, J., TESCH, W., BERNSTORFF, S., PURSLOW, P. & FRATZL, P. 2002. Viscoelastic properties of collagen: synchrotron radiation investigations and structural model. *Philosophical Transactions of the Royal Society,* 357**,** 191-197.

RABINOVICH, D. 2001. Seeking soft leathers with a tight grain. *WORLD Leather,* 14**,** 27-32.

RAMSHAW, J. A. M., SHAH, N. K. & BRODSKY, B. 1998. Gly-X-Y tripeptide frequencies in collagen: A context for host-guest triple-helical peptides. *Journal of Structural Biology,* 122**,** 86-91.

RAWLINGS, A. V. & LOMBARD, K. J. 2012. A review on the extensive skin benefits of mineral oil. *International Journal of Cosmetic Science,* 34**,** 511-518.

RECORD, M. T., GUINN, E., PEGRAM, L. & CAPP, M. 2013. Introductory Lecture: Interpreting and predicting Hofmeister salt ion and solute effects on biopolymer and model processes using the solute partitioning model. *Faraday Discussions,* 160**,** 9-44.

REDAELLI, A., VESENTINI, S., SONCINI, M., VENA, P., MANTERO, S. & MONTEVECCHI, F. M. 2003. Possible role of decorin glycosaminoglycans in fibril to fibril force transfer in relative mature tendons - a computational study from molecular to microstructural level. *Journal of Biomechanics,* 36**,** 1555-1569.

REICH, G., BRADT, J., MERTIG, M., POMPE, W. & TAEGER, T. 1999. Scanning probe microscopy a useful tool in leather research. *Journal of the Society of Leather Technologists and Chemists,* 82**,** 11-14.

REIMERS, W. 2007. *Neutrons and synchrotron radiation in engineering materials science : from fundamentals to superior materials characterization,* Weinheim; Chichester, Wiley-VCH ; John Wiley [distributor].

REISER, K., MCCORMICK, R. J. & RUCKER, R. B. 1992. ENZYMATIC AND NONENZYMATIC CROSS-LINKING OF COLLAGEN AND ELASTIN. *Faseb Journal,* 6**,** 2439-2449.

RICH, A. & CRICK, F. C. H. 1961. The Molecular Structure of Collagen. *Journal of Molecular Biology***,** 483-506.

RIPAMONTI, A., ROVERI, N., BRAGA, D., HULMES, D. J. S., MILLER, A. & TIMMINS, P. A. 1980. Effects of pH and ionic-strength on the structure of collagen fibrils. *Biopolymers,* 19**,** 965-975.

ROSENBLOOM, J., HARSCH, M. & JIMENEZ, S. 1973. Hydroxyproline Content Determines Denaturation Temperature of Chick Tendon Collagen. *Archives of Biochemistry and Biophysics,* 158**,** 478-484.

RUSSELL, A. E. 1988. Stress-strain relationships in leather and the role of fiber structure. *Journal of the Society of Leather Technologists and Chemists,* 72**,** 121-134.

SACKS, M. S., SMITH, D. B. & HIESTER, E. D. 1997. A small angle light scattering device for planar connective tissue microstructural analysis. *Annals of Biomedical Engineering,* 25**,** 678-689.

SASAKI, N. & ODAJIMA, S. 1996a. Elongation mechanism of collagen fibrils and force-strain relations of tendon at each level of structural hierarchy. *Journal of Biomechanics,* 29**,** 1131-1136.

SASAKI, N. & ODAJIMA, S. 1996b. Stress-strain curve and youngs modulus of a collagen molecule as determined by the x-ray diffaction technique. *Journal of Biomechanics,* 29**,** 655-658.

SASAKI, N., SHUKUNAMI, N., MATSUSHIMA, N. & IZUMI, Y. 1999. Time-resolved x-ray diffraction from tendon collagen during creep using synchrotron radiation. *Journal of Biomechanics,* 32**,** 285-292.

SCHOFIELD, A. L., SMITH, C. I., KEARNS, V. R., MARTIN, D. S., FARRELL, T., WEIGHTMAN, P. & WILLIAMS, R. L. 2011. The use of reflection anisotropy

spectroscopy to assess the alignment of collagen. *Journal of Physics D-Applied Physics,* 44.

SCOTT, J. E., ORFORD, C. R. & HUGHES, E. W. 1981. Proteoglycan-collagen arrangements in developing rat tail tendon - an electron-microscopical and biochemical investigation. *Biochemical Journal,* 195**,** 573-584.

SEGAL, D. M. 1969. POLYMERS OF TRIPEPTIDES AS COLLAGEN MODELS .7. SYNTHESIS AND SOLUTION PROPERTIES OF 4 COLLAGEN-LIKE POLYHEXAPEPTIDES. *Journal of Molecular Biology,* 43**,** 497-&.

SELLARO, T. L., HILDEBRAND, D., LU, Q. J., VYAVAHARE, N., SCOTT, M. & SACKS, M. S. 2007. Effects of collagen fiber orientation on the response of biologically derived soft tissue biomaterials to cyclic loading. *Journal of Biomedical Materials Research B,* 80A**,** 194-205.

SIZELAND, K. H., HAVERKAMP, R. G., BASIL-JONES, M. M., EDMONDS, R. L., COOPER, S. M., KIRBY, N. & HAWLEY, A. 2013. Collagen Alignment and Leather Strength for Selected Mammals. *Journal of Agricultural and Food Chemistry,* 61**,** 887-892.

SIZELAND, K. H., EDMONDS, R. L., BASIL-JONES, M. M., KIRBY, N., HAWLEY, A., MUDIE, S. & HAVERKAMP, R. G. 2015. Changes to Collagen Structure during Leather Processing. *Journal of Agricultural and Food Chemistry,* 63**,** 2499-2505.

SIZELAND, K. H., WELLS, H. C., HIGGINS, J. J., CUNANAN, C. M., KIRBY, N., HAWLEY, A. & HAVERKAMP, R. G. 2014. Age Dependant Differences in Collagen Fibril Orientation of Glutaraldehyde Fixed Bovine Pericardium. *BioMed Research International,* 2014**,** 189197.

SIZELAND, K. H., WELLS, H. C., NORRIS, G. E., EDMONDS, R. L., KIRBY, N., HAWLEY, A., MUDIE, S. & HAVERKAMP, R. G. 2015. Collagen D-spacing and the Effect of Fat Liquor Addition. *Journal of the American Leather Chemists Association,* 110**,** 66-71.

SIZELAND, K. H., EDMONDS, R. L., NORRIS, G. E., KIRBY, N., HAWLEY, A., MUDIE, S. & HAVERKAMP, R. G. 2014. Modification of collagen D-spacing in skin. *28th IFSCC Congress.* Palais des Congrès, Paris.

SKEDROS, J. G., DAYTON, M. R., SYBROWSKY, C. L., BLOEBAUM, R. D. & BACHUS, K. N. 2006. The influence of collagen fiber orientation and other histocompositional characteristics on the mechanical properties of equine cortical bone. *Journal of Experimental Biology,* 209**,** 3025-3042.

STAMOV, D. R. & POMPE, T. 2012. Structure and function of ECM-inspired composite collagen type I scaffolds. *Soft Matter,* 8**,** 10200-10212.

STOK, K. & OLOYEDE, A. 2003. A qualitative analysis of crack propagation in articular cartilage at varying rates of tensile loading. *Connective Tissue Research,* 44**,** 109-120.

STURROCK, E. J., BOOTE, C., ATTENBURROW, G. E. & MEEK, K. M. 2004. The effect of the biaxial stretching of leather on fibre orientation and tensile modulus. *Journal of Materials Science,* 39**,** 2481-2486.

SUZUKI, E., FRASER, R. D. B. & MACRAE, T. P. 1980. Role of hydroxyproline in the stabilization of the collagen molecule via water-molecules. *International Journal of Biological Macromolecules,* 2**,** 54-56.

SVERGUN, D. I. & KOCH, M. H. J. 2003. Small-angle scattering studies of biological macromolecules in solution. *Reports on Progress in Physics,* 66**,** 1735-1782.

SWEENEY, S. M., ORGEL, J. P., FERTALA, A., MCAULIFFE, J. D., TURNER, K. R., DI LULLO, G. A., CHEN, S., ANTIPOVA, O., PERUMAL, S., ALA-KOKKO, L., FORLINO, A., CABRAL, W. A., BARNES, A. M., MARINI, J. C. & ANTONIO, J. D. S. 2008. Candidate cell and matrix interaction domains on the collagen fibril, the predominant protein of vertebrates. *Journal of Biological Chemistry,* 283**,** 21187-21197.

SYNCHROTRON, A. 2014. An Introduction to the Australian Synchrotron. *In:* SYNCHROTRON, A. (ed.). Melbourne.

THOMAS, J. M. P. D. 1990. *Selections and reflections: the legacy of Sir Lawrence Bragg,* London, The Royal Institute of Great Britain.

THORSTENSEN, T. C. 1993. *Practical Leather Technology*, Krieger Publishing Company.

TORTORA, G. J. & DERRICKSON, B. H. 2010. *Principles of Anatomy and Physiology, 13th Edition*, Wiley Global Education.

TSUTAKAWA, S. E., HURA, G. L., FRANKEL, K. A., COOPER, P. K. & TAINER, J. A. 2007. Structural analysis of flexible proteins in solution by small angle X-ray scattering combined with crystallography. *Journal of Structural Biology,* 158**,** 214-223.

USHA, R. & RAMASAMI, T. 1999. Influence of Hydrogen Bond, Hydrophobic and Electrovalent Salt Linkages on the Transition Temperature, Enthalpy and Activation Energy in Rat Tail Tendon (RTT) Collagen Fibre. *Thermochimica Acta,* 338**,** 17-25.

WAUGH, A. & GRANT, A. 2006. *Ross & Wilson Anatomy and Physiology in Health and Illness*, Elsevier Health Sciences UK.

WELLS, H. C., EDMONDS, R. L., KIRBY, N., HAWLEY, A., MUDIE, S. T. & HAVERKAMP, R. G. 2013. Collagen Fibril Diameter and Leather Strength. *Journal of Agricultural and Food Chemistry,* 61**,** 11524-11531.

WELLS, H. C., SIZELAND, K. H., KAYED, H. R., KIRBY, N., HAWLEY, A., MUDIE, S. T. & HAVERKAMP, R. G. 2015b. Poisson's ratio of collagen fibrils measured by small angle X-ray scattering of strained bovine pericardium. *Journal of Applied Physics,* 117**,** 044701.

WESS, T. J., PURSLOW, P. P. & KIELTY, C. M. 1998. X-ray diffraction studies of fibrillin-rich microfibrils: Effects of tissue extension on axial and lateral packing. *Journal of Structural Biology,* 122**,** 123-127.

WESS, T. J. & ORGEL, J. P. 2000. Changes in collagen structure: drying, dehydrothermal treatment and relation to long term deterioration. *Thermochimica Acta,* 365**,** 119-128.

WILLIAMS, J. M. V. 2000a. IULTCS (IUP) test methods - Measurement of tear load-double edge tear. *Journal of the Society of Leather Technologists and Chemists,* 84**,** 327-329.

WILLIAMS, J. M. V. 2000b. IULTCS (IUP) test methods - Sampling. *Journal of the Society of Leather Technologists and Chemists,* 84**,** 303-309.

WILKINSON, S. J. & HUKINS, D. W. L. 1999. Determination of collagen fibril structure and orientation in connective tissues by X-ray diffraction. *Radiation Physics and Chemistry,* 56**,** 197-204.

ZAIDI, Z. & LANIGAN, S. W. 2010. *Dermatology in Clinical Practice*, Springer.

ZANABONI, G., ROSSI, A., ONANA, A. M. T. & TENNI, R. 2000. Stability and Networks of Hydrogen Bonds of Collagen Triple Helical Structure: Influence of pH and Chaotropic Nature of Three Anions. *Matrix Biology,* 19**,** 511-520.

ZIMMERMANN, E. A., SCHAIBLE, E., BALE, H., BARTH, H. D., TANG, S. Y., REICHERT, P., BUSSE, B., ALLISTON, T., AGER, J. W. & RITCHIE, R. O. 2011. Age-related changes in the plasticity and toughness of human cortical bone at multiple length scales. *Proceedings of the National Academy of Sciences of the United States of America,* 108**,** 14416-14421.

ZOU, Q., HABERMANN-ROTTINGHAUS, S. M. & MURPHY, K. P. 1998. Urea effects on protein stability: Hydrogen bonding and the hydrophobic effect. *Proteins: Structure, Function, and Bioinformatics,* 31**,** 107-115.